UNIVERSITAT DE BARCELONA

Novel multi-target directed ligands as drug candidates against Alzheimer's disease

Francisco Javier Pérez Areales

Facultad de Farmacia y Ciencias de la Alimentación

Departamento de Farmacología, Toxicología y Química Terapéutica

Unidad de Química Farmacéutica

NOVEL MULTI-TARGET DIRECTED LIGANDS AS DRUG CANDIDATES AGAINST ALZHEIMER'S DISEASE

Francisco Javier Pérez Areales

Barcelona, 2017

UNIVERSITAT DE BARCELONA

Facultad de Farmacia y Ciencias de la Alimentación

Programa de doctorado:

Química Orgánica Experimental e Industrial

NOVEL MULTI-TARGET DIRECTED LIGANDS AS DRUG CANDIDATES AGAINST ALZHEIMER'S DISEASE

Memoria presentada por Francisco Javier Pérez Areales para optar al título de Doctor por la Universitat de Barcelona

Director y tutor:

Dr. Diego Muñoz-Torrero López-Ibarra

Doctorando:

Francisco Javier Pérez Areales

Barcelona, 2017

El trabajo experimental recogido en esta memoria ha sido realizado en el Laboratorio de Química Farmacéutica de la Facultad de Farmacia de la Universidad de Barcelona bajo la dirección del doctor Diego Muñoz-Torrero.

La presente Tesis Doctoral ha sido posible gracias a la concesión de una beca de Ayudas para la contratación de personal investigador novel (FI-DGR2014), otorgada por la *Generalitat de Catalunya* a través de la *Agència de Gestió d'Ajuts Universitaris i de Recerca*.

El presente trabajo ha sido financiado por el *Ministerio de Ciencia e Innovación* (CTQ2011-22433), el *Ministerio de Economía y Competitividad / FEDER* (SAF2014-57094-R) y la *Generalitat de Catalunya* (2009SGR1396 y 2014SGR52).

Summary

Alzheimer's disease (AD) is the main neurodegenerative disorder and one of the most important health-care problems worldwide, because of its high prevalence and personal and economic impact. To aggravate this situation, current treatments are only symptomatic, but do not prevent, halt, or delay the disease progression. In the light of the multiple mechanisms involved in its pathogenesis, such as dysfunction of cholinergic and glutamatergic neurotransmitter systems, amyloid and tau pathologies, or oxidative stress, among others, the traditional medicinal chemistry approach of developing drugs based on the reductionist pattern of "one molecule-one target" is being increasingly perceived as ineffective. Alternatively, the so-called multitarget directed ligands (MTDLs), which consist of molecules designed to hit simultaneously different key targets of the complex pathological network, are emerging as a more realistic option to confront the disease. In this context, the purpose of the present PhD Thesis was the design, synthesis and biological evaluation of four novel families of compounds, endowed with multi-target profile, as drug candidates for the treatment of AD: 1) firstly, a family of shogaol–huprine hybrids, with purported dual antioxidant and anticholinesterase activity, with those activities to be imparted by their shogaol-derived and huprine moieties, respectively, and with β-amyloid and tau anti-aggregating activity likely arising from the planar aromatic moieties of their two constituting units; 2) secondly, a second generation of rhein–huprine hybrids designed by modification of the huprine aromatic ring of the lead compound of a previous generation of compounds, developed in our group, to explore the effect of pyridinic ring basicity on the different biological activities, with the hope of identifying an optimized hybrid with favorable activity profile on cholinesterases, β-secretase 1, β-amyloid and tau aggregation, and free radicals, and with reduced basicity, and, hence, with expectable better bioavailability; 3) thirdly, a family of CR-6–tacrine hybrids, which was designed to achieve a dual site binding within both acetylcholinesterase and β-secretase 1, apart from antioxidant activity, by combining a unit of the potent acetylcholinesterase inhibitor 6-chlorotacrine with a moiety derived from CR-6, a potent antioxidant; and 4) finally, a class of benzoadamantane–tacrine hybrids intented to act as acetylcholinesterase inhibitors and NMDA receptor antagonists, to combat neurodegeneration as well as improve memory and cognition. A crucial property for central nervous system drugs, the blood–brain permeability, was additionally assessed for all the abovementioned compounds.

Abbreviations

Aβ	β-amyloid peptide
$A\beta_{40}$	β-amyloid peptide 1–40
$A\beta_{42}$	β-amyloid peptide 1–42
AβDP	Aβ-degrading protease
ABTS	2,2′-Azinobis-(3-ethylbenzothiazoline-6-sulfonic acid)
AC	Antioxidant capacity
ACh	Acetylcholine
AChE	Acetylcholinesterase
AChEI	Acetylcholinesterase inhibitor
AD	Alzheimer's disease
AMPA	*α*-Amino-3-hydroxy-5-methyl-4-isoxazolepropionic acid
ApoE	Apolipoprotein E
APP	Amyloid precursor protein
ATCh	Acetylthiocholine
ATD	Amino-terminal domain
BACE1	β-secretase; β-site amyloid precursor protein cleaving enzyme 1
BBB	Blood–brain barrier
BCh	Butyrylcholine
BChE	Butyrylcholinesterase
bcl-2	B-cell lymphoma 2
Boc	*tert*-butoxycarbonyl
BS1	Binding site 1 (BACE1)
BS2	Binding site 2 (BACE1)
CAS	Catalytic anionic site
CCSD	Coupled cluster Slater determinant
Cdk5	Cyclin-dependent kinase 5
ChAT	Choline acetyltransferase
CNS	Central nervous system

DAST	Diethylaminosulfur trifluoride
DIBAL-H	Diisobutylaluminum hydride
DIMCARB	Dimethylammonium dimethyl carbamate
DMF	*N*,*N*-Dimethylformamide
DMSO	Dimethyl sulfoxide
DPPH	2,2-Diphenyl-1-picrylhydrazyl
EAAT	Excitatory amino acid transporter
EDC	1-Ethyl-3-(3-dimethylaminopropyl)carbodiimide
EphB2	Ephrin type-B receptor 2
Et	Ethyl
EtOAc	Ethyl acetate
F–C	Folin–Ciocalteu
GAE	Gallic acid equivalent
G protein	Guanine nucleotide-binding protein
GSK-3β	Glycogen synthase kinase 3β
*h*BACE1	Human β-secretase
*h*AChE	Human acetylcholinesterase
*h*BChE	Human butyrylcholinesterase
HOBt	1-Hydroxybenzotriazole
IgG1	Immunoglobulin G 1
IL-6	Interleukin 6
K_M	Michaelis-Menten constant
LBD	Ligand-binding domain
LTD	Long-term depression
LTP	Long-term potentiation
mAb	Monoclonal antibody
mAChR	Muscarinic acetylcholine receptor
MCM	Multiple-compound medication
Me	Methyl
MEM	2-Methoxyethoxymethyl ether

MMT	Multiple-medication therapy
MP2	Møller–Plesset perturbation second order
Ms	Mesyl
MTDL	Multi-target directed ligand
nAChR	Nicotinic acetylcholine receptor
NFTs	Neurofibrillary tangles
NMDA	*N*-Methyl-D-aspartate
PAMPA	Parallel artificial membrane permeability assay
PAS	Peripheral anionic site
P-gp	P-glycoprotein
PHF	Paired helical filaments
PSD-95	Post synaptic density protein-95
PSEN	Presenilin
PS1	Presenilin 1
p3	β-amyloid peptide 17–40/42
QM	Quantum mechanics
Red-Al	Sodium bis(2-methoxyethoxy)aluminumhydride
RNS	Reactive nitrogen species
ROS	Reactive oxygen species
SAPK	Stress-activated protein kinases
sAPPα	Secreted amyloid precursor protein-alpha form
sAPPβ	Secreted amyloid precursor protein-beta form
tau	Tubulin-associated unit
THF	Tetrahydrofuran
Th-S	Thioflavin-S
TLC	Thin-layer chromatography
TMD	Transmembrane domain
TP	Total phenolics
TNFα	Tumor necrosis factor alpha
Ts	Tosyl

Table of contents

CHAPTER 1

Introduction

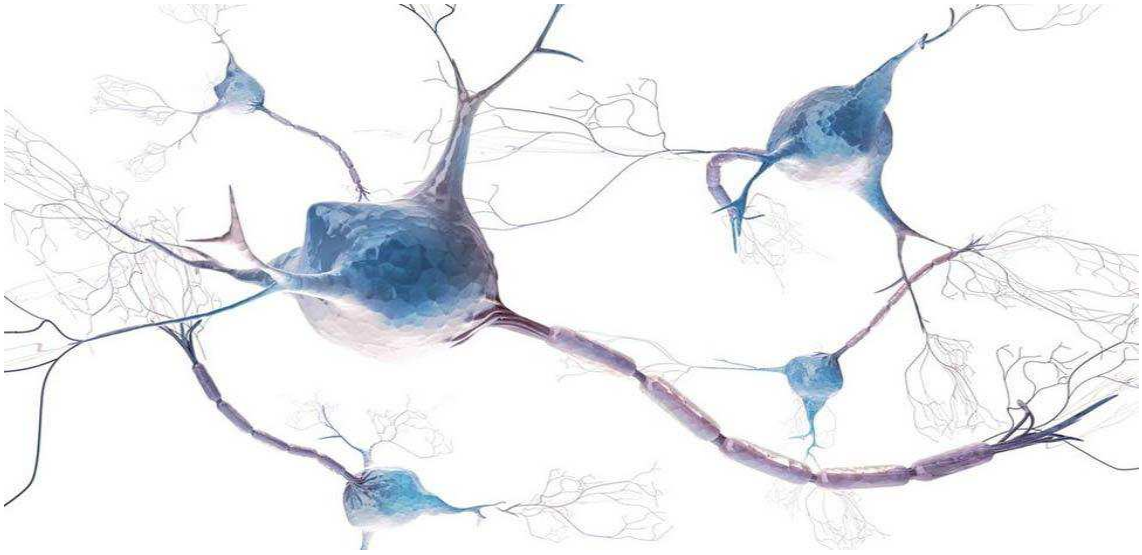

Image source: Alzheimer's Disease Genetics Consortium. University of Pennsylvania, School of Medicine (*www.adgenetics.org*)

1.1 Dementia and Alzheimer's disease

Nowadays, 47 million people live with dementia worldwide, but this number is estimated to increase to more than 131 million by 2050, as populations age. Dementia also has a huge economic impact, with a total estimated worldwide cost of US$ 818 billion, which will become a trillion dollars by 2018.[1]

Alzheimer's Disease (AD) represents the main type of neurodegenerative disorder and one of the most important health-care problems in developed countries, which is characterized by inexorably progressive deterioration in cognitive ability and capacity for independent living.[2] The most common symptom pattern begins with a gradually worsening ability to remember new information. This symptom occurs because the first neurons to die and malfunction are usually neurons in brain regions involved in forming new memories. Apathy and depression are also often early symptoms. As neurons in other parts of the brain malfunction and die, individuals experience other difficulties, which may include impaired judgment, disorientation, confusion, behavior changes, and difficulty speaking, swallowing, and walking. In the final stages of the disease, patients lose their ability to communicate, to recognize loved ones, and become bed-bound. When individuals experience difficulty moving because of AD, they are more vulnerable to infections, which are often a contributing factor to the death of people with AD.[3]

This dementia-type memory related disorder is mainly related to age, so the majority of cases are of later onset and do not follow Mendelian inheritance, despite showing significant heritability (up to 76%), what makes AD a genetically complex and heterogeneous disorder.[4] Thus far, four genes have been definitively implicated in the etiology of AD. Mutations of the genes encoding amyloid precursor protein (APP) and presenilin 1 and 2 (PSEN1, PSEN2) cause rare, Mendelian forms of the disease (familial AD), usually with an early onset. However, in the most common form of the disease (sporadic AD), only apolipoprotein E (ApoE) has been

[1] M. Prince, A. Comas-Herrera, M. Knapp, M. Guerchet, M. Karagiannidou. *World Alzheimer Report 2016: Improving healthcare for people living with dementia.* Alzheimer's Disease International **2016**.
[2] M. Prince, R. Bryce, E. Albanese, A. Wimo, W. Ribeiro, C. P. Ferri. *Alzheimer's & Dementia* **2013**, *9*, 63.
[3] a) Alzheimer's Association. *Alzheimer's & Dementia* **2015**, *11*, 332. b) Alzheimer's Association. *Alzheimer's & Dementia* **2013**, *9*, 208.
[4] D. Avramopoulos. *Genome Medicine* **2009**, *1*, 3.

established unequivocally as a susceptibility gene.[4-7] Aiming to identify new AD loci, several genome-wide association studies have identified strong evidence for AD risk association to ApoE, whereas have found less convincing evidence implicating other genes.[5,6]

1.2 Pathogenesis of Alzheimer's disease

AD was first diagnosed in 1907 by Dr. Alois Alzheimer, who described the occurrence of neurotic plaques and a tangle of fibrils on autopsy in the cerebral cortex of a 56-year-old woman having dementia, which are the only histopathological signs of the disease.[8] However, it was 70 years thereafter when AD was recognized as the most common cause of dementia.[9] Since then, intensive research efforts have aimed to decipher the mechanism of AD progression without success.

Therefore, the etiology of AD is still incompletely understood, and as aforementioned, the unique neuropathological events clearly defined are the senile plaques and neurofibrillary tangles (NFTs) (**Figure 1.1**) in the medial temporal lobe structures and cortical areas of the brain, together with a degeneration of the neurons and synapses.[5,10] These structures are mainly composed of β-amyloid peptide (Aβ) and hyperphosphorylated tau (tubulin-associated unit) protein, respectively, and may be observed about 10 to 15 years before symptoms appear. As there is little known about the sequence of molecular mechanisms, it remains unclear which of them occurs first, or even whether or not they are at the root of the pathogenesis of the disease.[10] Several pathogenic mechanisms that underlie these changes have been studied, including Aβ aggregation and deposition with senile plaque development, tau hyperphosphorylation with tangle formation, neurovascular dysfunction, and other mechanisms

[5] K. Blennow, M. J. de Leon, H. Zetterberg. *Lancet* **2006**, *368*, 387.
[6] L. Bertram, M. B. McQueen, K. Mullin, D. Blacker, R. E. Tanzi. *Nat. Genet.* **2007**, *39*, 17.
[7] D. Harold, R. Abraham, P. Hollingworth, R. Sims, A. Gerrish, M. L. Hamshere, J. S. Pahwa, V. Moskvina, K. Dowzell, A. Williams, N. Jones, C. Thomas, A. Stretton, A. R. Morgan, S. Lovestone, J. Powell, P. Proitsi, M. K. Lupton, C. Brayne, D. C. Rubinsztein *et al. Nat. Genet.* **2009**, *41*, 1088.
[8] a) A. Alzheimer. *Allgemeine Zeitschrift für Psychiatrie and Psychisch-Gerichtliche Medizin* **1907**, *64*, 146. b) A. Rainulf, H. Stelzma, N. Schnitzlein, F. R. Murtagh. *Clin. Anat.* **1995**, *8*, 429.
[9] R. Katzman. *Arch. Neurol.* **1976**, *33*, 217.
[10] P. Nelson, I. Alafuzoff, E. Bigio, C. Bouras, H. Braak, N. Cairns, R. Castellani, B. Crain, P. Davies. *J. Neuropathol. Exp. Neurol.* **2012**, *71*, 362.

such as cell-cycle abnormalities, inflammatory processes, oxidative stress, and mitochondrial dysfunction, which has resulted in different hypotheses about the pathogenesis of the disease.[5]

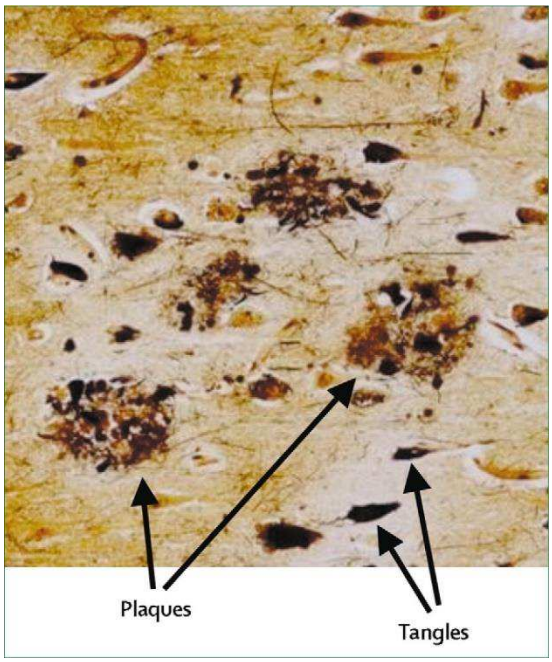

Figure 1.1: Senile plaques and neurofibrillary tangles in the cerebral cortex of AD patients. Plaques are extracellular deposits of Aβ surrounded by dystrophic neurites, reactive astrocytes, and microglia, whereas tangles are intracellular aggregates composed of a hyperphosphorylated form of the microtubule-associated protein tau. (Image source: K. Blennow, M. J. de Leon, H. Zetterberg. *Lancet* **2006**, *368*, 387).

1.2.1 Amyloid hypothesis

This model, also referred to as "amyloid cascade hypothesis", postulates that neurodegeneration in AD is caused by Aβ plaques formation and its extracellular accumulation in various areas of the brain. It was first described 26 years ago, becoming the dominant theory of AD pathogenesis and guiding the development of potential treatments during last years.[11-14] This hypothesis establishes that AD is caused by an imbalance between Aβ production and clearance, resulting in increased amounts of Aβ in various forms such as monomers, oligomers, insoluble fibrils, and plaques in the central nervous system (CNS) (**Figure 1.2**). High levels of Aβ

[11] J. Hardy, D. Allsop. *Trends Pharm. Sci.* **1991**, *12*, 383.
[12] D. J. Selkoe. *Neuron.* **1991**, *6*, 487.
[13] J. Hardy, D. J. Selkoe. *Science* **2002**, *297*, 353.
[14] D. J. Selkoe, J. Hardy. *EMBO Mol. Med.* **2016**, *8*, 595.

then initiate a cascade of events culminating in neuronal damage and death manifesting as progressive clinical dementia of AD.[11-15]

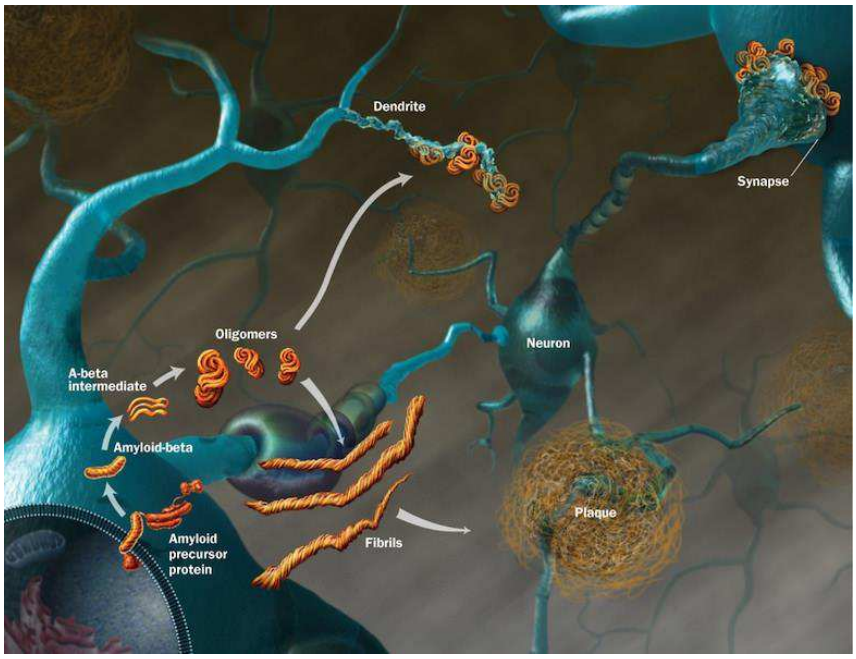

Figure 1.2: Schematic representation of Aβ peptide aggregation into oligomers, and eventually, fibrils and plaques. Also shown where these aggregates are located. (Image source: Nutrition Review: https://nutritionreview.org/).

Thus, the amyloid hypothesis deals with an alteration in the metabolism of the APP, which has been implicated as a regulator of synapse formation and function,[16] and neural activity, plasticity and memory.[17] In healthy brains, this transmembrane glycoprotein is broken-down by sequential cleavage through α- and γ-secretase, giving soluble, even neuroprotective, fragments.[18] However, the cleavage through the sequential action of β-secretase (BACE1) and γ-secretase, results in a polypeptide (39–43 amino acid length), Aβ, which is highly insoluble and shows strong tendency to aggregate (**Figure 1.3**).[19]

[15] K. G. Mawuenyega, W. Sigurdson, V. Ovod, L. Munsell, T. Kasten, J. C. Morris, K. E. Yarasheski, R. J. Bateman. *Science* **2010**, *330*, 1774.
[16] C. Priller, T. Bauer, G. Mitteregger, B. Krebs, H. A. Kretzschmar, J. Herms. *J. Neurosci.* **2006**, *26*, 7212.
[17] P. R. Turner, K. O'Connor, W. P. Tate, W. C. Abraham. *Prog. Neurobiol.* **2003**, *70*, 1.
[18] J. Näslund, A. Schierhorn, U. Hellman, L. Lannfelt, D. Roses, L. O. Tjernberg, J. Silberring, S. E. Gandy, B. Winblad, P. Greengard. *PNAS* **1994**, *91*, 8378.
[19] H. F. Kung. *ACS Med. Chem. Lett.* **2012**, *3*, 265.

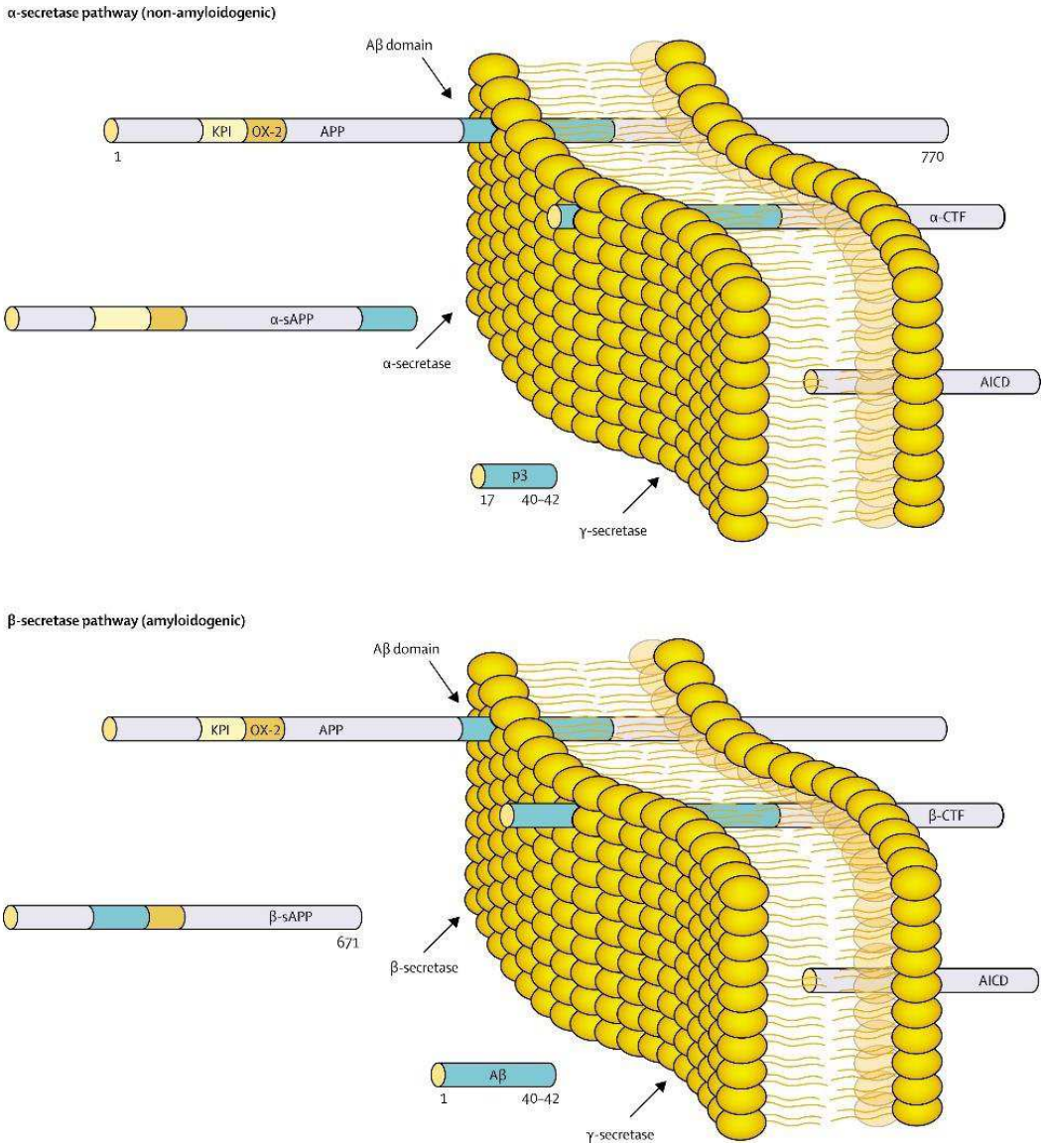

Figure 1.3: The amyloidogenic and non-amyloidogenic cleavage pathway of APP. The non-amyloidogenic pathway involves the consecutive cleavage by α- and γ-secretase, affording two soluble fragments, sAPPα (a fragment composed of 83 amino acids with neuroprotective properties) and p3. The amyloidogenic pathway implies the consecutive cleavage by β- and γ-secretase, giving sAPPβ (a 99-amino acid soluble fragment) and Aβ (a highly insoluble fragment). (Image source: K. Blennow, M. J. de Leon, H. Zetterberg. *Lancet* **2006**, *368*, 387).

The amyloidogenic pathway is increased in AD patients, resulting in a sustained imbalance between production and clearance of Aβ fragments.[15] Of those Aβ species, two principal isoforms are increased in AD, $A\beta_{40}$ and $A\beta_{42}$. The former is more abundant, however, $A\beta_{42}$ is the most fibrillogenic.[20] $A\beta_{42}$ auto-assembly can result in insoluble fibrils that are deposited in amyloid plaques or in soluble oligomers, which are potent neurotoxins that target

[20] I. W. Hamley. *Chem. Rev.* **2012**, *112*, 5147.

and disrupt particular synapses,[21] alter intracellular Ca^{2+} levels, restrain mitochondrial activity and activate the inflammatory processes,[22] triggering a cascade of neurotoxic events that lead to a widespread neuronal degeneration (**Figure 1.4**).[11-15]

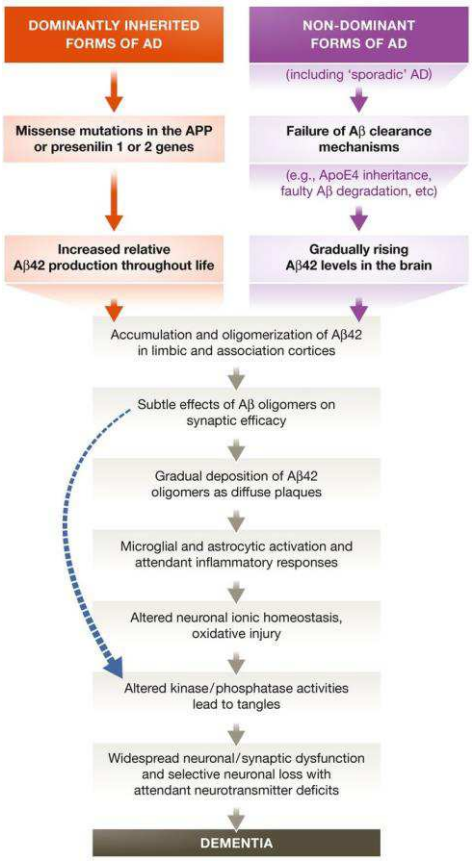

Figure 1.4: The sequence of major pathogenic events leading to AD proposed by the amyloid cascade hypothesis. The curved blue arrow indicates that Aβ oligomers may directly injure the synapses and neurites of brain neurons, in addition to activating microglia and astrocytes. (Image source: D. J. Selkoe, J. Hardy. *EMBO Mol. Med.* **2016**, *8*, 595).

Nevertheless, there are some limitations of the amyloid cascade hypothesis. According to this hypothesis, deposition of Aβ represents the initial pathological trigger and the first neurotoxic step, whereas soluble Aβ oligomers are thought to induce synaptic damage,[21] resulting in NFT formation, neuronal death and ultimately dementia.[13] Thus, amyloid removal by immunization should protect against Aβ-mediated neurotoxicity and preserve cognitive

[21] S. T. Ferreira, W. L. Klein. *Neurobiol. Learn Mem.* **2011**, *96*, 529.
[22] M. T. Heneka, M. J. Carson, J. El Khoury, G. E. Landreth, F. Brosseron, D. L. Feinstein, A. H. Jacobs, T. Wyss-Coray, J. Vitorica, R. M. Ransohoff, K. Herrup, S. A. Frautschy, B. Finsen, G. C. Brown, A. Verkhratsky, K. Yamanaka, J. Koistinaho, E. Latz, A. Halle, G. C. Petzold *et al. Lancet Neurol.* **2015**, *14*, 388.

function,[23] what is not clearly this scenario. Moreover, the amyloid cascade hypothesis does not explain the poor temporal correlation between appearance and accumulation of Aβ in the brain and the onset of disease symptoms.[24] Furthermore, the current hypothesis is not anatomically consistent with the fact that areas with the highest amyloid deposition do not correspond to areas most affected by NFT formation, and subsequent loss of synapses and neurons.[24,25] In this context, tau pathology correlates much more closely with neuronal loss, both spatially and temporally, than amyloid plaques.[26]

1.2.2 Tau hypothesis

Another hallmark of the disease is NFTs formation, which directly involves a key microtubule-associated protein, tau, which stabilizes the microtubules in the axon of neurons. Thus, tau protein is associated with efficient axonal transport, which is deregulated in AD patients.[27] In AD, it is thought that Aβ interacts with the signaling pathways regulating tau protein phosphorylation by increasing kinase activity, namely Cdk5 and GSK-3β in this case.[28] The hyperphosphorylated tau (the distorted protein) detach from the microtubules, so that the skeleton of the neuron axon dissociates and it is no longer maintained. Defective tau proteins assemble to form paired helical filaments (PHF) inside the neuron, which are composed of two strands of filament twisted around one another, and the abnormal accumulation of these tau filaments results in NFTs formation. Without the cytoskeleton, neurons degenerate, and connections between neurons are lost, what eventually leads to apoptosis due to the loss of function (**Figure 1.5**).[28]

[23] C. Haass, D. J. Selkoe. *Nat. Rev. Mol. Cell Biol.* **2007**, *8*, 101.
[24] E. S. Musiek, D. M. Holtzman. *Nat. Neurosci.* **2015**, *18*, 800.
[25] E. Giacobini, G. Gold. *Nat. Rev. Neurol*. **2013**, *9*, 677.
[26] A. Serrano-Pozo, M. P. Frosch, E. Masliah, B. T. Hyman. *Cold Spring Harb. Perspect. Med.* **2011**, *1*, a006189.
[27] L. Buée, T. Bussière, V. Buée-Scherrer, A. Delacourte, P. R. Hof. *Brain Res. Rev.* **2000**, *33*, 95.
[28] a) V. M.-Y. Lee, M. Goedert, J. Q. Trojanowski. *Annu. Rev. Neurosci.* **2001**, *24*, 1121. b) K. Iqbal, A. del C. Alonso, S. Chen, M. O. Chohan, E. El-Akkad, C.-X. Gong, S. Khatoon, B. Li, F. Liu, A. Rahman, H. Tanimukai, I. Grundke-Iqbal. *Biochim. Biophys. Acta* **2005**, *1739*, 198.

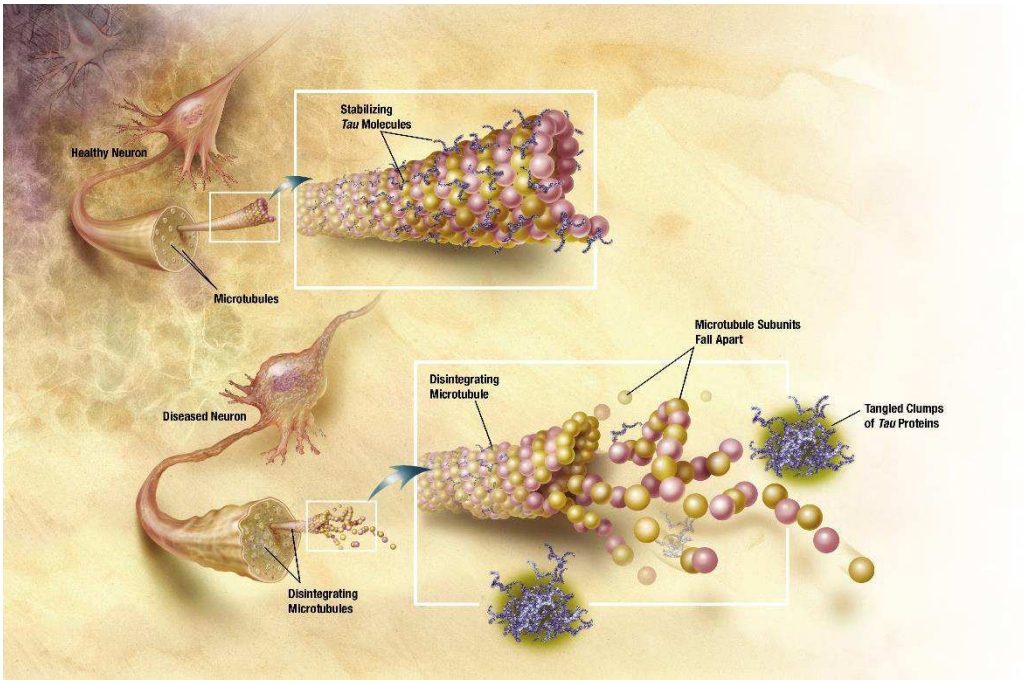

Figure 1.5: Scheme of the physiological function of tau protein (up), and the pathological hyperphosphorylation of tau followed by microtubules disintegration and NFTs formation (bellow) (Image source: National Institute on Aging: https://www.nia.nih.gov/).

1.2.3 Cholinergic hypothesis

Another common feature in AD patients is a cholinergic dysfunction. In 1974, memory was related to the cholinergic system and was age dependent,[29] and two years later, a link between the clinical symptoms of the disease and specific cholinergic deficits in the brains of people with AD was discovered by Dr. Peter Davies.[30] These findings led to the postulation of the "cholinergic hypothesis", which proposed that degeneration of cholinergic neurons in the basal of forebrain and the associated loss of cholinergic neurotransmission in the cerebral cortex and other areas contributed significantly to the deterioration in cognitive function, perception, comprehension, reasoning, and short-term memory, observed in patients with AD.[31,32]

[29] D. A. Drachman, J. Leavitt. *Arch. Neurol.* **1974**, *30*, 113.
[30] a) P. Davies, A. J. F. Maloney. *Lancet* **1976**, *2*, 1403. b) D. M. Bowen, C.B. Smith, P. White, A. N. Davison. *Brain* **1976**, *99*, 459.
[31] R. Bartus, R. Dean, B. Beer, A. Lippa. *Science* **1982**, *217*, 408.
[32] P. Francis, A. Palmer, M. Snape, G. Wilcock. *J. Neurol. Neurosurg. Psychiatry* **1999**, *66*, 137.

Abnormal acetylcholine (ACh) neurotransmission is caused by dysregulation at different levels of synapses: firstly, a deficit in ACh synthesis due to a reduced expression of the enzyme choline acetyltransferase (ChAT); secondly, a decreased availability of ACh in synapse, because of high-affinity choline uptake and reduced ACh release; thirdly, a reduced ACh metabolism by acetylcholinesterase (AChE); and fourthly, a loss of nicotinic ACh receptors (nAChRs), responsible for action potential transmission to the postsynaptic neuron, by a decrease in binding parameters, but not muscarinic ACh receptors (mAChRs), which activate G protein signaling pathway (**Figure 1.6**).[32,33]

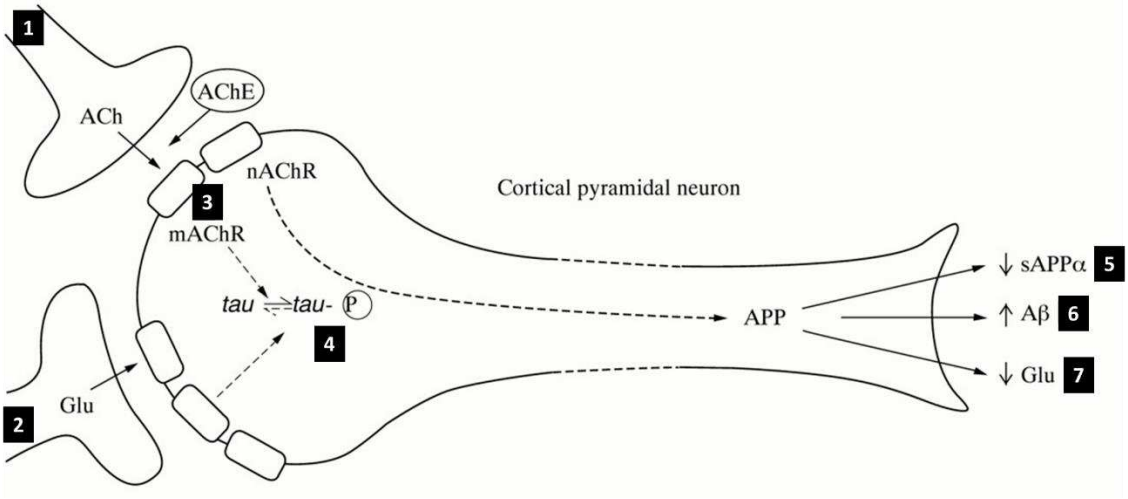

Figure 1.6: Schematic diagram of a neuron representing alterations in neurotransmission in AD. (1) reduced cortical cholinergic innervation; (2) reduced corticocortical glutamatergic neurotransmission due to neuron or synapse loss; (3) reduced coupling of mAChR to second messenger system; (4) shift of tau to the hyperphosphorylated state; (5) reduced secretion of soluble APP; (6) increased production of Aβ; (7) decreased glutamate production. It is hypothesized that these changes give rise to the clinical symptoms of AD and contribute to the spread of pathology (Image source: P. T. Francis, A. M. Palmer, M. Snape *et al. J. Neurol. Neurosurg. Psychiatry* **1999**, *66*, 137).

1.2.4 Oxidative stress hypothesis

Oxidative stress is defined as a marked imbalance between the reactive oxygen species (ROS) and its removal by the antioxidant system.[34] During aging, the endogenous antioxidant system progressively decays, and an increasing body of evidence supports the involvement of oxidative stress in different pathologies, such as cancer, cardiovascular, and neurodegenerative

[33] G. Benzi, A. Moretti. *Eur. J. Pharmacol.* **1998**, *346*, 1.
[34] B. Halliwell. *Drug & Aging* **2001**, *18*, 685.

diseases. In AD, oxidative damage in cellular structures is an event that precedes the appearance of other pathological hallmarks of the disease, such as senile plaques and neurofibrillary tangles, which suggests an early involvement of oxidative stress in the pathogenesis and progression of AD.[35,36] Brain is particularly susceptible to oxidative stress because of the high oxygen consumption rate, rich in unsaturated lipids, and a relatively high abundance of redox-capable transition metal ions and a relatively low availability of antioxidant enzymes compared with other organs.[37]

ROS and reactive nitrogen species (RNS) are products of normal cellular metabolism, and are recognized for playing a dual role as both deleterious and beneficial species. Beneficial effects of reactive species occur at low to moderate concentrations and involve physiological roles through the activation of a number of cellular signaling pathways. The harmful effect of free radicals causing potential biological damage, called oxidative stress (for ROS) and nitrosative stress (for RNS), occurs in biological systems when there is an overproduction of ROS/RNS on one side and a deficiency of enzymatic and non-enzymatic antioxidants on the other. In other words, oxidative stress results from the metabolic reactions that use oxygen and represents a disturbance in the equilibrium between pro-oxidant/antioxidant status in living organisms. The excessive production of reactive species can damage cellular lipids, proteins, or nucleic acids, altering their normal function. The source of oxidative stress in AD is metals, which play a major catalytic role in the production of free radicals, especially iron, copper and zinc [36,38]

1.2.5 Glutamate hypothesis

Glutamate is the major excitatory neurotransmitter in the nervous system throughout the brain and spinal cord in neurons and glia.[39] At the hippocampus, the glutamatergic neurotransmitter system is responsible for the synaptic plasticity and long-term memory

[35] M. Ansari, S. Scheff. *J. Neuropathol. Exp. Neurol.* **2010**, *69*, 155.
[36] P. Moreira, M. Santos, C. Oliveira, J. Shenk, A. Nunomura, M. Smith, X. Zhu, G. Perry. *CNS Neurol. Disord. – Drug Targets* **2008**, *7*, 3.
[37] F. Gu, M. Zhu, J. Shi, Y. Hu, Z. Zhao. *Neurosci. Lett.* **2008**, *440*, 44.
[38] M. Rosini, E. Simoni, A. Milelli, A. Minarini, C. Melchiorre. *J. Med. Chem.* **2014**, *57*, 2821.
[39] B. Moghaddam, D. Javitt. *Neuropsychopharmacology Rev.* **2012**, *37*, 4.

(learning), through a phenomenon called long-term potentiation (LTP).[40] Two different glutamate-gated ion channels are involved in a LTP, the *α*-amino-3-hydroxy-5-methyl-4-isoxazolepropionic acid (AMPA) receptor, permeable to Na^+, and the *N*-methyl-D-aspartate (NMDA) receptor, mainly permeable to Ca^{2+}, although only the NMDA receptor is the final responsible for the LTP. It is required a high frequency action potential, bringing about glutamate release, which binds to both AMPA (it opens due to fast activation/inactivation kinetics) and NMDA (it remains close, blocked by a Mg^{2+} ion, and with slow ligand-gated kinetics) receptors. AMPA channels allow Na^+ influx, triggering a post-synaptic depolarization that must reach a threshold to repeal Mg^{2+} from the NMDA channel, enabling Ca^{2+} influx, and the corresponding LTP through several signalling pathways (**Figure 1.7**).[41]

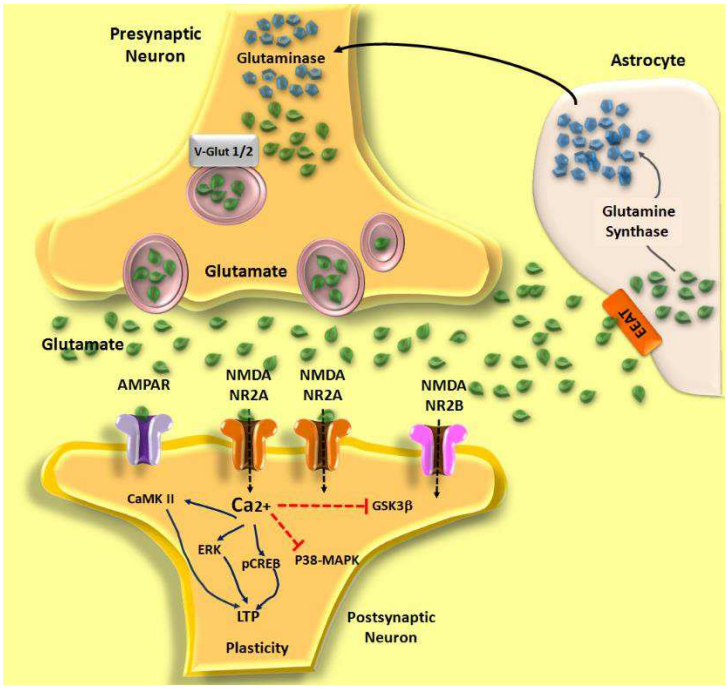

Figure 1.7: Scheme of glutamatergic transmission in normal brain. Glutamate released from presynaptic terminals acts through the activation of glutamate receptors located at the postsynaptic terminal. The interaction between glutamate and NMDA receptor favors the activation of several metabolic pathways, which are responsible for anabolic activation with subsequent activation of LTP mechanisms. Glutamate excess is transported via the excitatory amino acid transporter (EAAT) into astrocytes, where is transformed into glutamine by the enzyme glutamine synthase. Subsequently, glutamine is converted into glutamate by glutaminase and packaged into vesicles through specific transporters (Image source: V. Campos-Peña, M. A. Meraz-Ríos. *Neurochemistry*, *InTechOpen*, **2014**).

[40] T. Takeuchi, A. Duszkiewicz, R. Morris. *Phil. Trans. R. Soc. B* **2014**, *369*, 20130288.
[41] C. Tabone, M. Ramaswami. *Neuron* **2012**, *74*, 767.

The maintenance of low extracellular concentrations of glutamate is essential for CNS functions. However, in AD patients an overactivation of the NMDA receptors takes place, which may be attributable to several factors, such as the fact that glutamate is not properly cleared and is inappropriately released.[42] Under these conditions, neurons become depolarized and the Mg^{2+} blockade of the NMDA receptor channel can be lifted, what triggers the pathological influx of Ca^{2+}, so the ionic homeostasis disruption. The prolonged Ca^{2+} overload leads first to loss of synaptic function, then to synaptotoxicity, and ultimately to cell death, which correlates with the loss of memory function and learning ability in AD patients. Last process is the so-called "excitotoxicity", defined as cell death caused by the toxicity of an excessive action of excitatory amino acids, such as glutamate.[43]

1.2.6 Other hypotheses

- *Neuroinflammation hypothesis*: In the brain, glial cells, including astrocytes and microglia, undergo activation under pro-inflammatory conditions by increasing the production of inflammatory cytokines in the CNS, which becomes deleterious and leads to progressive tissue damage in degenerative diseases.[44] In AD pathology, it has been reported that microglia are activated by Aβ oligomers to produce cytokines, chemokines, and neurotoxins that contribute to neuronal degeneration by initiating a series of cellular events, which are able to elicit an immune response. Moreover, Aβ deposition in parenchyma and blood vessels has been described to trigger microglial migration and mediation of inflammatory response against the aggregates, thus inducing the production of nitric oxide, ROS and pro-inflammatory cytokines, which eventually may promote neuronal death.[45]

- *Calcium hypothesis*: Ca^{2+} acts as a vital intracellular messenger in the brain, important for synaptic transmission, neuronal development, and plasticity in neurons by manipulating the cytoskeleton and associated proteins. The long-term, slightly raised cytosolic Ca^{2+} levels and

[42] H. Wei, C. Dobkin, A. Sheikh, M. Malik, W. T. Brown, X. Li. *PLoS ONE* **2012**, *7*, e36981.
[43] M. Parsons, L. Raymond. *Neuron* **2014**, *82*, 279.
[44] I. Morales, L. Guzmán-Martínez, C. Cerda-Troncoso, G. A. Farías, R. B. Maccioni. *Front. Cell. Neurosci.* **2014**, *8*, 112.
[45] M. Kitazawa, D. Cheng, F. LaFerla. *J. Neurochem.* **2009**, *108*, 1550.

disturbances in Ca^{2+} homeostasis correspond to the neuronal devastation and promote the generation of free radicals and ROS.[46]

- *Biometal dyshomeostasis*: Some studies in AD have described an increase in the levels of oxidative stress reflected by a deregulated content of metals iron, copper, and zinc in the brain of patients. Redox-active metals, especially Fe^{2+} and Cu^{2+}, are capable of stimulating free radical formation via the Fenton reaction, thereby increasing protein and DNA oxidation and enhancing lipid peroxidation.[47] Metal cations have also been reported to mediate Aβ toxicity in AD.[48] The Aβ peptide itself has been shown to be a strong redox-active catalyst able to produce ROS in presence of copper or iron, which, in turn, are enriched in the amyloid cores of senile plaques.[49] Metal ions may also interact with Aβ promoting its self-aggregation,[49] and tau hyperphosphorylation by inducing aggregation upon tau interaction with Aβ .[50]

- *Mitochondrial cascade hypothesis*: This hypothesis maintains that gene inheritance defines an individual baseline mitochondrial function, inherited and environmental factors determine rates at which mitochondrial function changes over time, and baseline mitochondrial function and mitochondrial change rates influence AD chronology. Mitochondrial function affects APP expression, APP processing, or Aβ accumulation.[51,52]

- *Neurovascular hypothesis*: In contrast to traditional neuron-centric views of AD, this theory postulates that neurovascular dysfunction contributes to cognitive decline and neurodegeneration, suggesting a blood–brain barrier (BBB) dysfunction associated with the accumulation of several vasculotoxic and neurotoxic molecules within brain parenchyma, a reduction in cerebral blood flow, and hypoxia. Thus, it postulates that faulty clearance of Aβ across the BBB, aberrant angiogenesis and senescence of the cerebrovascular system could

[46] L. Bojarski, J. Herms, J. Kuznicki. *Neurochem. Int.* **2008**, *52*, 621.
[47] M. Khalil, C. Teunissen, C. Langkammer. *Mult. Scler. Int.* **2011**, 606807.
[48] J. Duce, A. Tsatsanis, M. Cater, S. James, E. Robb, K. Wikhe, S. L. Leong, K. Perez, T. Johanssen, M. Greenough, H.-H. Cho, D. Galatis, R. Moir, C. Masters, C. McLean, R. Tanzi, R. Cappai, K. Barnham, G. Ciccotosto, J. Rogers, A. Bush. *Cell* **2010**, *142*, 857.
[49] X. Huang, M. Cuajungco, C. Atwood, M. Hartshorn, J. Tyndall, G. Hanson, K. Stokes, M. Leopold, G. Multhaup, L. Goldstein, R. Scarpa, A. Saunders, J. Lim, R. Moir, C. Glabe, E. Bowden, C. Masters, D. Fairlie, R. Tanzi, A. Bush. *J. Biol. Chem.* **1999**, *274*, 37111.
[50] A. Yamamoto, R.-W. Shin, K. Hasegawa, H. Naiki, H. Sato, F. Yoshimasu, T. Kitamoto. *J. Neurochem.* **2002**, *82*, 1137.
[51] R. Swerdlow, S. Khan. *Med. Hypotheses* **2004**, *63*, 8.
[52] R. Swerdlow, J. Burns, S. Khan. *Biochim. Biophys. Acta* **2014**, *1842*, 1219.

initiate neurovascular uncoupling, vessel regression, brain hypoperfusion and neurovascular inflammation. Ultimately, this would lead to BBB compromise, to chemical imbalance in the neuronal environment and to synaptic and neuronal dysfunction, injury and loss.[53,54]

1.3 Pathological network of Alzheimer's disease

In light of the aforementioned various complex mechanisms, it becomes evident the multifactorial nature of AD pathogenesis, which makes it extremely challenging to find an efficient treatment against this disease. Moreover, an extra problem relies on the ability of the disease for finding alternative pathways through which it continues developing, meaning that we must understand AD as a *pathological network*, where several key proteins and neural pathways are interconnected, even though some of these connections have not been elucidated yet.

From this perspective, none of the explained hypotheses should be exclusive, and an important first step in understanding how AD network organization influences the onset and course of disease is the generation of a comprehensive map of the connectivity between different pathways (**Figure 1.8**).

[53] B. Zlokovic. *Nat. Rev. Neurosci*. **2014**, *12*, 723.
[54] B. Zlokovic. *Trends Neurosci.* **2005**, *28*, 202.

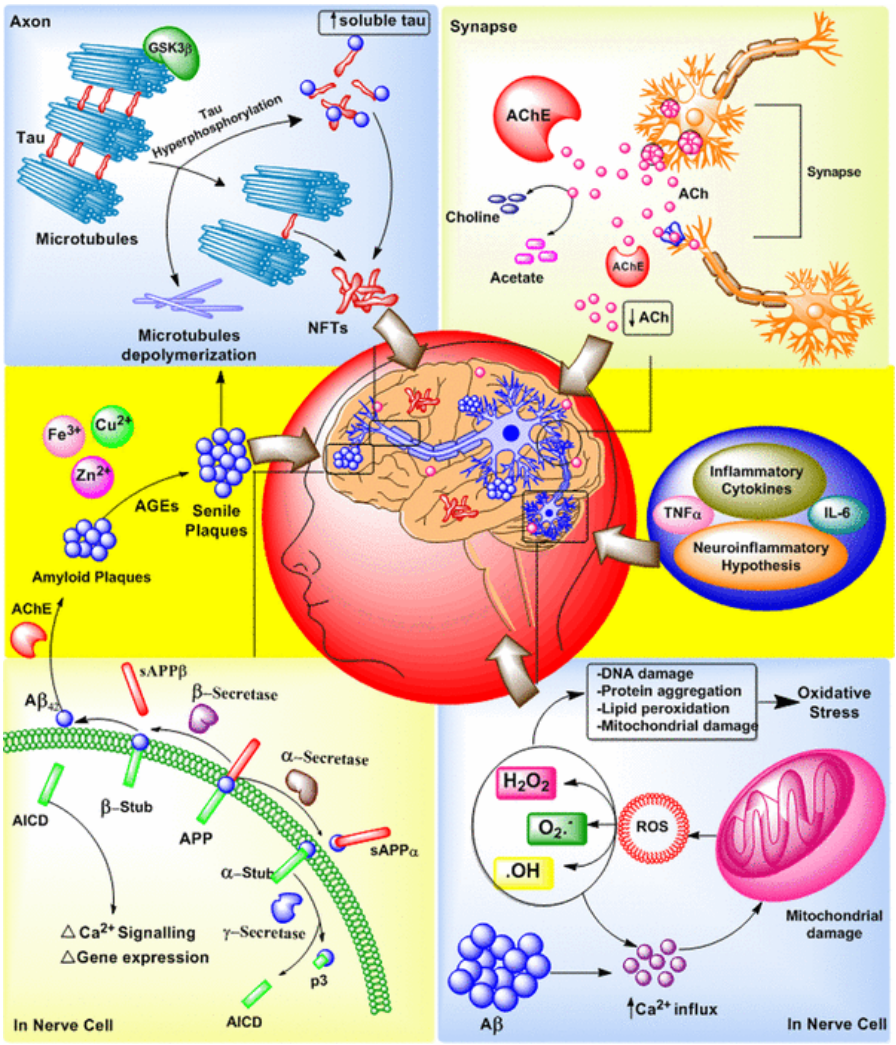

Figure 1.8: Map of the pathological network of AD. Only the main pathways are represented (Image source: M. Singh, M. Kaur, N. Chadha *et al*. *Mol. Divers.* **2016**, *20*, 271).

The main actors proposed by the amyloid cascade hypothesis, either Aβ oligomers or plaques, might be considered to play a central role in the network connections (**Figure 1.9**). Aβ might exert its neurotoxic effects through a variety of ways, including disruption of mitochondrial function via binding to Aβ-binding alcohol dehydrogenase protein,[55] induction of apoptotic genes through inhibition of Wnt[56] and insulin[57]signalling pathways, formation of ion

[55] J. Lustbader, M. Cirilli, C. Lin, H. W. Xu, K. Takuma, N. Wang, C. Caspersen, X. Chen, S. Pollak, M. Chaney, F. Trinchese, S. Liu, F. Gunn-Moore, L.-F. Lue, D. Walker, P. Kuppusamy, Z. Zewier, O. Arancio, D. Stern, S. S. Yan,H. Wu. *Science* **2004**, *304*, 448.
[56] A. Caricasole, A. Copani, A. Caruso, F. Caraci, L. Iacovelli, M. A. Sortino, G. C. Terstappen, F. Nicoletti. *Trends Pharm. Sci.* **2003**, *24*, 233.
[57] L. Xie, E. Helmerhorst, K. Taddei, B. Plewright, W. v. Bronswijk, R. Martins. *J. Neurosci.* **2002**, *22*, RC221.

channels,[58] stimulation of the stress-activated protein kinases (SAPK) pathway[59] or activation of microglia cells leading to the expression of proinflammatory genes, an increase in ROS, and eventual neuronal toxicity and death.[60]

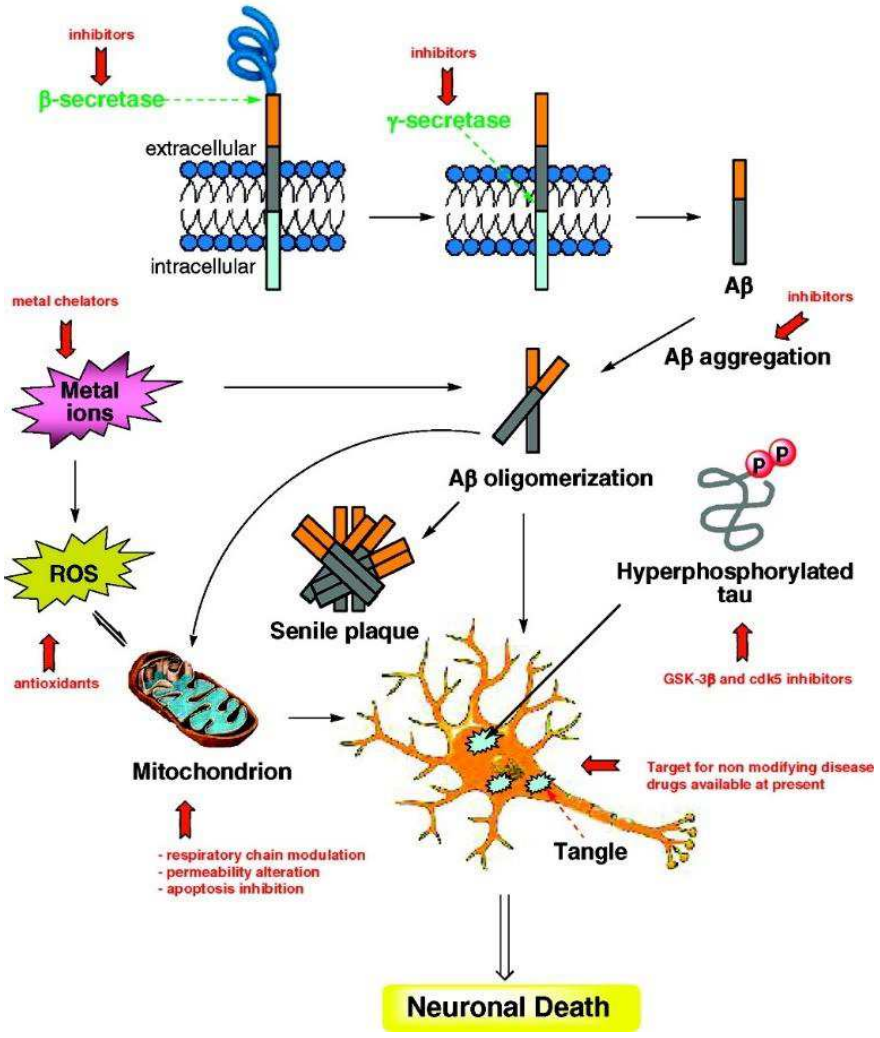

Figure 1.9: Possible molecular causes of neuronal death and protective mechanisms of Aβ-related pathogenesis in AD (Image source: A. Cavalli, M. L. Bolognesi, A. Minarini *et al*. *J. Med. Chem*. **2008**, *51*, 347).

In the present PhD Thesis, the most relevant pathway connections that have been addressed are those related with the amyloid pathology, oxidative stress, and cholinergic and glutamatergic neurotransmitter systems.

[58] B. Kagana, Y. Hirakura, R. Azimov, R. Azimova, M.-C. Lin. *Peptides* **2002**, *23*, 1311.
[59] E. Tamagno, M. Parola, M. Guglielmotto, G. Santoro, P. Bardini, L. Marra, M. Tabaton, O. Danni. *Free Radic. Biol. Med.* **2003**, *35*, 45.
[60] M. Bamberger, G. Landreth. *Microsc. Res. Tech.* **2001**, *54*, 59.

1.3.1 Connection between amyloid and tau hypotheses

Some studies suggest a toxic alliance of Aβ and tau in AD,[24] such as Aβ synaptotoxicity mediated by tau, whereby Aβ-promoted endogenous hyperphosphorylation of tau leads to decreased microtubule binding[61] and missorting of tau from the axon into the somatodendritic compartment by retrograde axonal transport.[62] A conformational change occurs in some parts of the unfolded tau protein, and this transition leads to tau aggregation in the form of intracellular filamentous inclusions.[63]

1.3.2 Connection between amyloid and cholinergic hypotheses

Today, both hypotheses are the most accepted throughout the research community, therefore they have been the most studied, which has led to the identification of several points of connection between them, such as:

- Selective activation of M1/M3-mAChRs and nAChRs modulates APP processing by favoring the non-amyloidogenic pathway, thereby preventing Aβ fibril formation.[64]

- Activation of α7 nAChRs may contribute to the degradation and clearance of Aβ.[64]

- Reactive astrocytes and activated microglia associated with senile plaques produce some pro-inflammatory cytokines that have been shown to selectively degenerate cholinergic basal forebrain cells, upregulate APP expression, stimulate the amyloidogenic route of APP processing, and may also promote the activity and expression of AChE.[64]

A highly relevant finding was the co-localization of Aβ in senile plaques with the enzymes AChE and butyrylcholinesterase (BChE) in AD patients,[64,65] as well as the ability of AChE to affect APP processing, which suggested a link between APP metabolism and cholinergic neurotransmission.[64] Then, AChE was found to promote the aggregation of Aβ forming a

[61] T. Maas, J. Eidenmüller, R. Brandt. *J. Biol. Chem.* **2000**, *275*, 15733.
[62] X. Li, Y. Kumar, H. Zempel, E.-M. Mandelkow, J. Biernat, E. Mandelkow. *EMBO J.* **2011**, *30*, 4825.
[63] F. Hernández, J. Avila. *Cell. Mol. Life Sci.* **2007**, *64*, 2219.
[64] R. Schliebs. *Neurochem. Res.* **2005**, *30*, 895.
[65] M. A. Moran, E. J. Mufson, P. Gomez-Ramos. *Acta Neuropathol.* **1993**, *85*, 362.

complex with the growing fibrils (complex AChE-Aβ),[66] which induces alterations in some of the enzyme properties and increases the neurotoxicity of fibrils.[67,68] These findings provided strong evidence for an important role of AChE in amyloid deposition. Further studies about the interaction indicated that Aβ binds a hydrophobic environment at the *peripheral anionic site* (PAS) of the enzyme (**Figure 1.10**),[64,66,69,70] which is a secondary interaction region located at the mouth of the catalytic gorge of AChE, and responsible for early binding to the neurotransmitter ACh and its directioning towards the *catalytic anionic site* (CAS).[71] This fact led to the suggestion that inhibition of the PAS of AChE might represent a potential strategy to avoid Aβ aggregation.[72] On the other side, Aβ induced enhancement of AChE through the action Aβ on α7 nAChRs, pointing out that the local increase in AChE around senile plaques in AD may also be a result of a direct action of Aβ on α7 nAChRs located on terminals around senile plaques.[73]

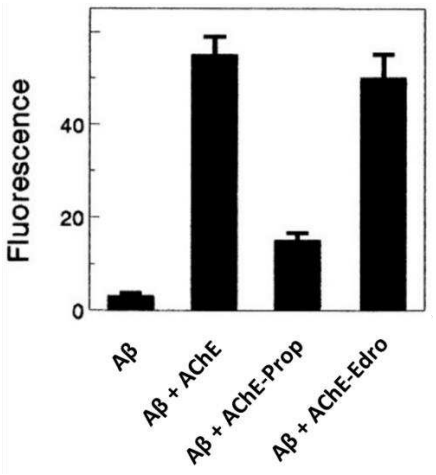

Figure 1.10: Aβ aggregation results in different conditions. Left (as reference): Aβ alone; Aβ and AChE. Right (in the presence of ligands): propidium (a specific PAS-binding inhibitor), 75% inhibition; edrophonium (CAS-binding ligand), no inhibition (Image source: N. Inestrosa, A. Alvarez, C. Pérez *et al*. *Neuron* **1996**, *16*, 881).

[66] N. Inestrosa, A. Alvarez, C. Pérez, R. Moreno, M. Vicente, C. Linker, O. Casanueva, C. Soto, J. Garrido. *Neuron* **1996**, *16*, 881.
[67] A. Alvarez, R. Alarcón, C. Opazo, E. O. Campos, F. J. Muñoz, F. H. Calderón, F. Dajas, M. K. Gentry, B. P. Doctor, F. G. De Mello, N. Inestrosa. *J. Neurosci.* **1998**, *18*, 3213.
[68] A. Reyes, M. Chacon, M. Dinamarca, W. Cerpa, C. Morgan, N. Inestrosa. *Am. J. Pathol.* **2004**, *164*, 2163.
[69] N. Inestrosa, R. Alarcón. *J. Physiol.-Paris* **1998**, *92*, 341.
[70] A. Alvarez, C. Opazo, R. Alarcón, J. Garrido, N. Inestrosa. *J. Mol. Biol.* **1997**, *272*, 348.
[71] J. L. Sussman, M. Harel, F. Frolow, C. Oefner, A. Goldman, L. Toker, I. Silman. *Science* **1991**, *253*, 872.
[72] R. Fuentealba, G. Farias, J. Scheu, M. Bronfman, M. Marzolo, N. Inestrosa. *Brain Res. Rev.* **2004**, *47*, 275.
[73] L. Fodero, S. Mok, D. Losic, L. Martin, M. Aguilar, C. Barrow, B. Livett, D. Small. *J. Neurochem.* **2004**, *88*, 1186.

1.3.3 Connection between amyloid and glutamate hypotheses

One robust effect of Aβ on synapses is the induction of depression of glutamatergic synaptic transmission in hippocampal pyramidal neurons, triggering the loss of function. The mechanisms involved are (**Figure 1.11**): (a) short oligomers of Aβ (25-35 amino acids) show moderate affinity for the agonist recognition sites of the NMDA receptor;[74] (b) $A\beta_{42}$ oligomers may bind postsynaptic anchoring proteins like PSD-95, which indirectly affect NMDA receptors;[75] (c) both pathways bring about a tonic overactivation of NMDA receptors by driving an abnormal conformation of the receptor, where the Mg^{2+} blockade function is no longer effective. In turn, synaptic "noise" rises, impairing detection of the relevant synaptic signal required for learning or plasticity;[74-76] (d) Aβ binds EphB2, a surface tyrosine kinase that binds the NMDA receptor, leading to EphB2 degradation, then to the loss of NMDA receptor function and reduced LTP;[77] (e) the level of NMDA receptor activation may control the effect on Aβ production, i.e. low levels of NMDA receptor activation increase Aβ production, whereas higher levels of NMDA receptor activation reduce Aβ production.[78]

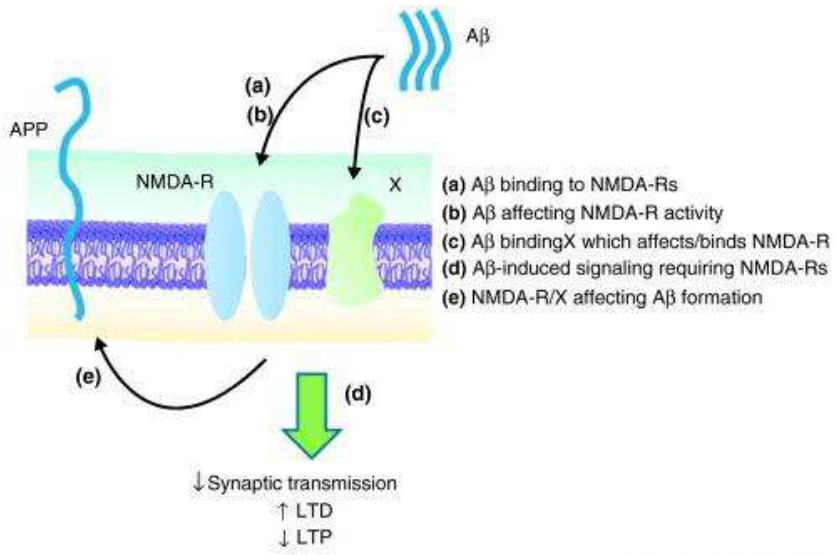

Figure 1.11: Several potential roles for NMDA receptors in the effects of Aβ are depicted. (Image source: R. Malinow. *Curr. Opin. Neurol.* **2012**, *22*, 559).

[74] D. Venkitaramani, J. Chin, W. Netzer, G. Gouras, S. Lesne, R. Malinow, P. Lombroso. *J. Neurosci.* **2007**, *27*, 11832.
[75] F. De Felice, P. Velasco, M. Lambert, K. Viola, S. Fernandez, S. Ferreira, L. Klein. *J. Biol. Chem.* **2007**, *282*, 11590.
[76] W. Danysz, C. G. Parsons. *Br. J. Pharmacol.* **2012**, *167*, 324.
[77] R. Malinow. *Curr Opin Neurobiol.* **2012**, *22*, 559.
[78] D. Verges, J. Restivo, W. Goebel, D. Holtzman, J. Cirrito. *J. Neurosci.* **2011**, *31*, 11328.

1.4 Current treatments and trends against Alzheimer's disease

At present, the therapeutic arsenal against AD is dominated by a group of drugs which are mainly based on the "cholinergic hypothesis" and aimed at re-establishing functional cholinergic neurotransmission. Only five drugs have been approved for use in AD, of which four of them are acetylcholinesterase inhibitors (AChEIs),[79] so fitting within indirect-acting cholinomimetic drugs, and one is a NMDA receptor uncompetitive antagonist.[80]

1.4.1 Acetylcholinesterase inhibition

1.4.1.1 Acetylcholinestarase

Human AChE (*h*AChE) is a 583 amino acid enzyme, additionally provided with a 31 residue signal peptide. The hydrolysis of ACh (**1**) takes place inside the catalytic site of the enzyme, the CAS, localized at the bottom of a 20 Å length gorge (**Figure 1.12**). The CAS is constituted by a catalytic triad, which consists of residues Ser203-His447-Glu334 that are responsible for the neurotransmitter hydrolysis, and a neighbouring anionic hydrophobic site (Trp86-Glu202-Tyr337-Tyr341-Phe338), which stabilizes the positive charge of the quaternary ammonium group of ACh by cation-π interactions and allows to position its ester group in a proper orientation to face the CAS. Moreover, as previously mentioned, a second AChE binding site is the PAS, a larger region rich in aromatic residues, which is located at the mouth of this narrow gorge and is responsible for the early binding and guiding of the substrate towards the CAS (**Figure 1.13**).[71,81]

[79] P. Anand, B. Singh. *Arch. Pharm. Res.* **2013**, *36*, 375.
[80] J. Kemp, R. McKernan. *Nat. Neurosci.* **2002**, *5*, 1039.
[81] H. Dvir, I. Silman, M. Harel, T. L. Rosenberry, J. Sussman. *Chem. Biol. Interact.* **2010**, *187*, 10.

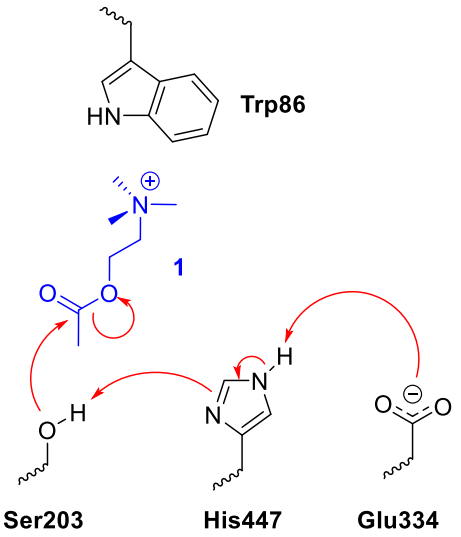

Figure 1.12: Schematic representation of the hydrolytic degradation of ACh (**1**) by the catalytic triad in the CAS of AChE.

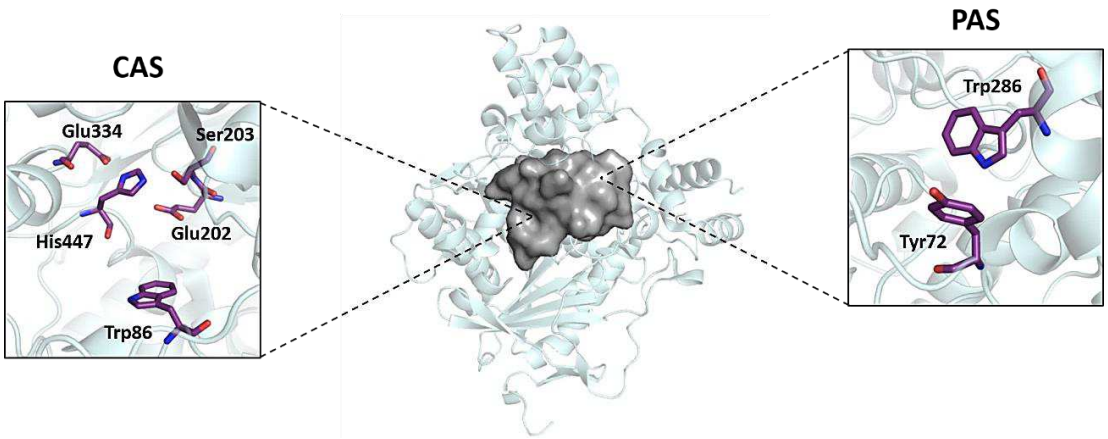

Figure 1.13: X-ray structure of *h*AChE (PDB ID: 3LII) with details of the CAS and the PAS.

1.4.1.2 Butyrylcholinestarase

It is worthy to comment that there are two major classes of enzymes responsible for ACh degradation, AChE and BChE, which are mainly present in the central and peripheral nervous systems, respectively, although not exclusively. Functionally, both enzymes hydrolyze ACh efficiently, but at different rates. BChE hydrolyzes butyrylcholine (BCh) at rates faster than

ACh, while AChE degrades BCh much more slowly than ACh.[82,83] In healthy brains, AChE hydrolyses the majority of ACh whereas BChE plays a secondary role. However, in AD patients, the activity of brain AChE is decreased, whilst the levels of BChE in the hippocampus and temporal cortex are increased. Thus, BChE gains significance as AD progresses partly compensating for the lack of AChE.[84]

1.4.1.3 Commercialized acetylcholinesterase inhibitors

The four commercialized anti-Alzheimer drugs acting as AChEIs are tacrine, **2** (marketed in 1993, **Figure 1.14**),[85,86] donepezil, **3** (marketed in 1996),[87] rivastigmine, **4** (marketed in 2000),[88] and galantamine, **5** (marketed in 2001),[89] although tacrine was withdrawn from the market after showing hepatotoxicity issues.[90] Tacrine, donepezil and galantamine are reversible AChEIs, whilst rivastigmine is considered a pseudoirreversible AChEI, since it contains a carbamate group that reacts with Ser203, leading to a carbamoylated AChE, whose activity is slowly recovered after hydrolysis of the formed serine carbamate group. All of them increase the levels of ACh at synapses by avoiding its degradation, therefore achieving a stabilization of the cognitive function at a steady level during at least the first year of treatment in about 50% patients.[91] Some studies were carried out to clarify what determines whether or not patient is responsive to treatments, and reported that patients with pronounced medial temporal lobe atrophy are less likely to respond to donepezil,[92] whereas other studies have tested the difference between ApoE ε4 allele carriers and non-carriers, having found no statistically significant effect on cognitive response to donepezil treatment between both genotypes.[93]

---

[82] W. Krall, J. Sramek, N. Cutler. *Ann. Pharmacother.* **1999**, *33*, 441.
[83] L. Savini, A. Gaeta, C. Fattorusso, B. Catalanotti, G. Campiani, L. Chiasserini, C. Pellerano, E. Novellino, D. McKissic, A. Saxena. *J. Med. Chem.* **2003**, *46*, 1.
[84] G. Reid, N. Chilukuri, S. Darvesh. *Neuroscience* **2013**, *234*, 53.
[85] K. Davis, L. Thai, E. Gamzu, C. Davis, R. Woolson, S. Gracon, D. Drachman, L. Schneider, P. Whitehouse, T. Hoover *et al. N. Engl. J. Med.* **1992**, *327*, 1253.
[86] M. Knapp, D. Knopman, P. Solomon, W. Pendlebury, C. Davis, S. Gracon. *JAMA* **1994**, *271*, 985.
[87] H. Sugimoto, Y. Iimura, Y. Yamanishi, K. Yamatsu. *J. Med. Chem.* **1996**, *38*, 4821.
[88] R. Polinsky. *Clin. Therap.* **1998**, *20*, 634.
[89] J. Sramek, E. Frackiewicz, N. Cutler. *Exp. Opin. Invest. Drugs* **2000**, *9*, 2393.
[90] P. Camps, D. Muñoz-Torrero. *Mini Rev. Med. Chem.* **2002**, *2*, 11.
[91] E. Giacobini. *Pharmacol. Res.* **2004**, *50*, 433.
[92] P. Connelly, N. Prentice, K. Fowler. *J. Neurol. Neurosurg. Psychiatry* **2005**, *76*, 320.
[93] J. Waring, Q. Tang, W. Robieson, D. King, U. Das, J. Dubow, S. Dutta, G. Marek, L. M. Gault. *J. Alzheimers Dis.* **2015**, *47*, 137.

The analysis of the X-ray structures of the commercialized AChEIs in complex with AChE pointed out that while tacrine, **2**, rivastigmine, **4**, and galantamine, **5**, clearly interact within the active site of the enzyme, donepezil, **3**, exhibits a dual binding mode of interaction,[94] expanding on the whole length of the gorge and achieving a simultaneous interaction with both the CAS and the PAS (**Figure 1.14**).

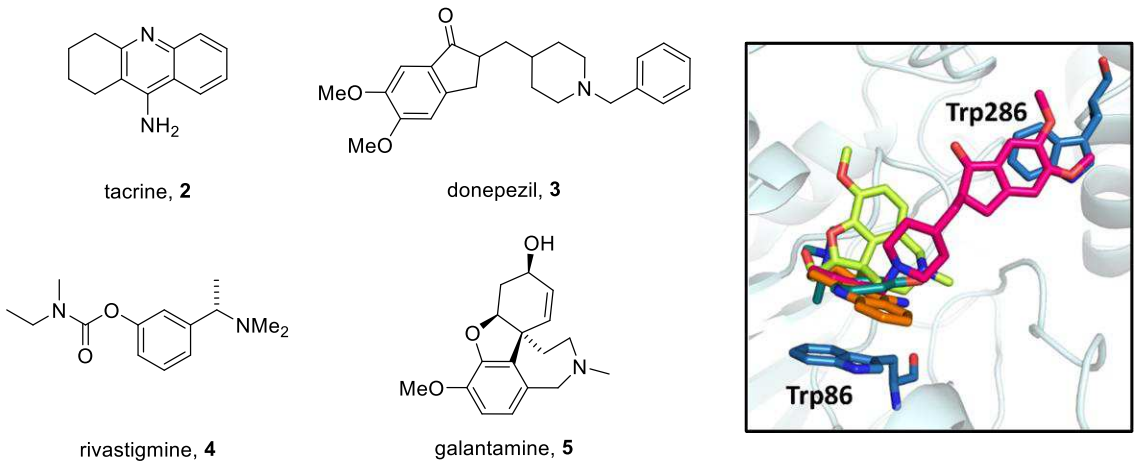

Figure 1.14: Left: structure of the four commercialized AChEIs. Right: Binding mode in the gorge of AChE: tacrine, **2** (orange, PDB ID: 1ACJ); donepezil, **3** (magenta, PDB ID: 1EVE); rivastigmine, **4** (green, PDB ID: 1GQR); and galantamine, **5** (yellow, PDB ID: 4EY6).

In addition to their ability to inhibit AChE, these drugs have shown a plethora of neuroprotective effects associated with their administration. This fact challenges the prevailing view of these compounds just as palliative drugs and suggests their potential efficacy in the frame of a disease-modifying therapeutic approach. Indeed, it has been reported that AChEIs display effects such as positive allosteric modulation of α7 nAChRs,[95] blockade of the glutamate-induced excitotoxicity through antagonism of NMDA receptors,[96] overexpression of the antiapoptotic protein bcl-2 following stimulation of α7 and α4β2 nAChRs,[96] mobilization of calcium pools from the intracellular endoplasmic reticulum following activation of α1 receptors,[96] upregulation of the neuroprotective splice variants of AChE,[96] and interference in Aβ formation and aggregation.[96]

[94] E. Giacobini. *Neurochem. Res.* **2000**, *25*, 1185.
[95] S. Buckingham, A. Jones, L. Brown, D. Sattelle. *Pharmacol. Rev.* **2009**, *61*, 39.
[96] D. Muñoz-Torrero. *Curr. Med. Chem.* **2008**, *15*, 2433.

1.4.2 NMDA receptor antagonism

1.4.2.1 NMDA receptor

This type of ionotropic glutamate receptor is a heterotetramer mainly composed of two copies each of GluN1 and GluN2, which are activated upon concurrent binding of glycine or D-serine to GluN1 and L-glutamate to GluN2, and relief of a magnesium blockade of the ion channel pore by membrane depolarization.[97,98] Opening of NMDA receptor channels results in an influx of Ca^{2+} ions, although the channel is also permeable to Na^{+} and K^{+}, which triggers signal transduction cascades that control the strength of neural connectivity or neuroplasticity.[98] Thus, for the permeation of Ca^{2+} ions two conditions are needed: activation by endogenous ligands, and depolarization of the neuron by prior activation of AMPA receptors, whose gating kinetics are much faster than NMDA receptor kinetics, which allows to control the postsynaptic Ca^{2+} levels in physiological conditions.

The overall structure of the NMDA receptor shows two extracellular domains, the amino-terminal domain (ATD) and the ligand-binding domain (LBD), and a transmembrane domain (TMD, **Figure 1.15**). The ATD contributes to control the opening/closing rate and contains allosteric modulator binding sites, such as zinc (in GluN2A and 2B), ifenprodil (GluN2B) and several poliamines (GluN2B).[99] The LBD contains binding sites of Mg^{2+}, glycine and glutamate. The TMD comprises the architecture of the pore (**Figure 1.16**), and the carboxy termini are associated to intracellular proteins that trigger signaling pathways.[97,98]

[97] C.H. Lee, W. Lü, J. C. Michel, A. Goehring, J. Du, X. Song, E. Gouaux. *Nature* **2014**, *511*, 191.
[98] E. Karakas, H. Furukawa. *Science* **2014**, *344*, 992.
[99] H. Yuan, K. Hansen, K. Vance, K. Ogden, S. Traynelis. *J. Neurosci.* **2009**, *29*, 12045.

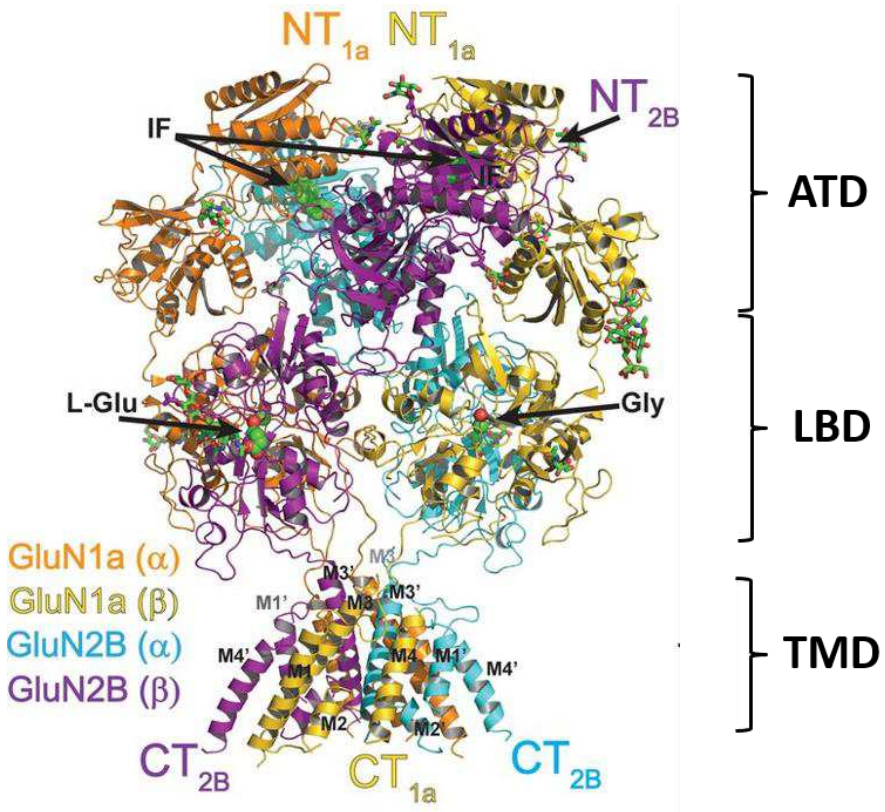

Figure 1.15: Overall structure of heterotetrameric GluN1a-GluN2B NMDA receptor. GluN1a and GluN2B subunits, labeled as GluN1a (α), GluN1a (β), GluN2B (α), GluN2B (β) are colored in orange, yellow, cyan, and purple, respectively. The amino (NT) and carboxy (CT) termini are located on top and bottom, respectively. Ifenprodil (IF), located at the GluN1a-GluN2B ATD heterodimer interfaces, and agonists, glycine (Gly) and L-glutamate (L-Glu), lodged at the LBD clamshells, are shown in green spheres (Image source: E. Karakas, H. Furukawa. *Science* **2014**, *344*, 992).

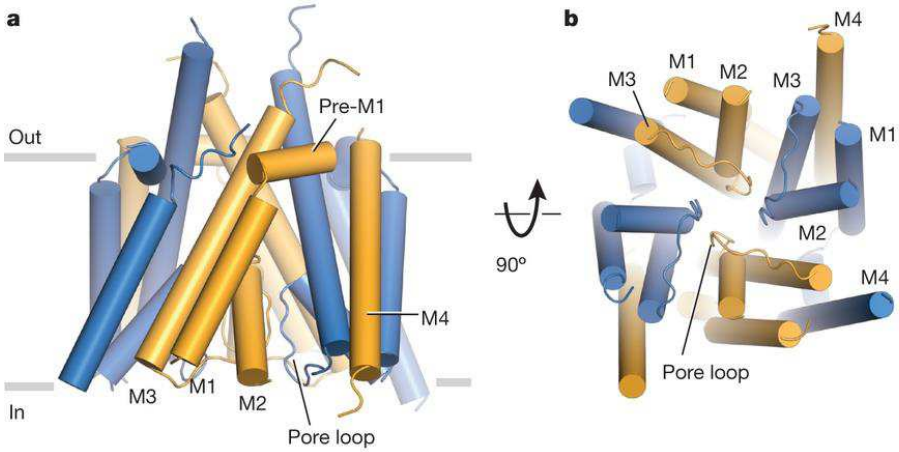

Figure 1.16: View of the TMD (a) parallel to the membrane and (b) along the pore axis, from the cytoplasmic side of the membrane. GluN1 and GluN2B subunits are shown in blue and orange, respectively (Image source: C.-H. Lee, W. Lü, J. C. Michel *et al*. *Nature* **2014**, *511*, 191).

1.4.2.2 Commercialized NMDA receptor antagonist

The currently commercialized NMDA receptor antagonist is memantine, **6** (**Figure 1.17**), and was marketed in 2002.[100] Memantine is approved for use in moderate to severe AD and is thought to function by preferentially blocking open NMDA channels by means of an uncompetitive-antagonist mechanism, and hence, a balance between open and closed channels can be achieved by adjusting dosage.[101] The interaction between NMDA receptors and memantine is reversible, and its affinity depends on the state of the receptor, so when channel is open memantine is able to block it, while in channel close state it has little or no ability to block it.[102] This critical feature, known as *partial trapping*, allows the inhibition only in pathological conditions, when NMDA receptors are overactivated, but still allows NMDA receptors activation to maintain physiological transmission. Thus, memantine blocks the neurotoxicity of glutamate in AD without interfering with physiological conditions.

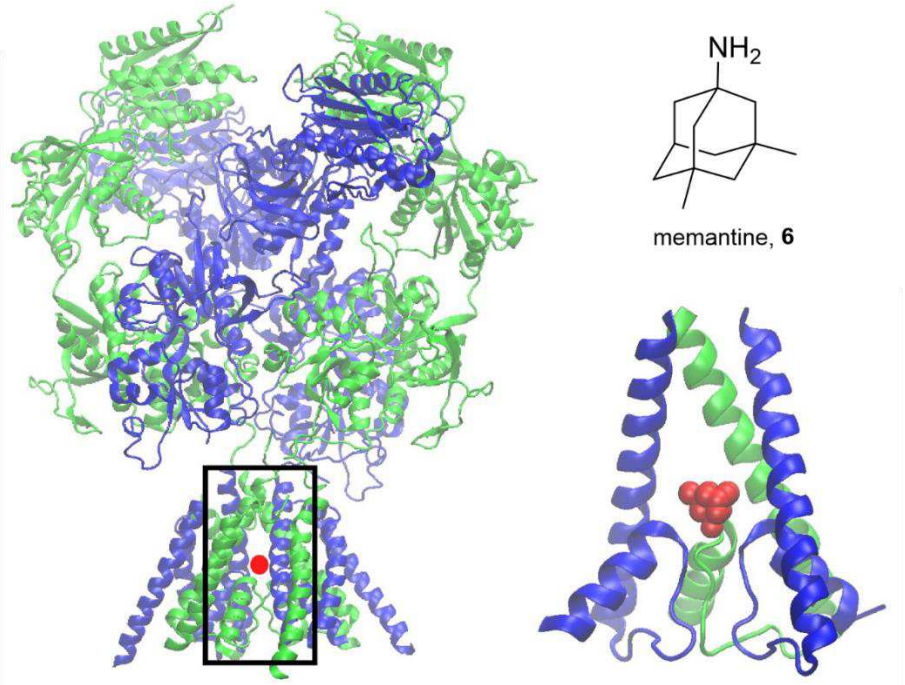

Figure 1.17: NMDA channel blocked by memantine. Left: General view of the channel, with a red dot at the likely approximate location of the binding site of memantine (PDB ID: 4TLM). Right: On top, the structure of memantine (**6**). At the bottom, pore blocked by memantine (red spheres). GluN1 subunits are shown in green and GluN2 subunits in blue (Image source: J. Johnson, N. Glasgow, N. Povysheva. *Curr. Opin. Pharmacol.* **2015**, *20*, 54).

[100] S. Lipton. *Nature* **2004**, *428*, 473.
[101] C. Parsons, A. Stöffler, W. Danysz. *Neuropharmacol.* **2007**, *53*, 699.
[102] J. Johnson, N. Glasgow, N. Povysheva. *Curr. Opin. Pharmacol.* **2015**, *20*, 54.

Memantine is a low- to moderate-affinity uncompetitive NMDA receptor antagonist with strong voltage-dependency and rapid blocking and unblocking kinetics. This voltage-dependence mechanism of memantine may be explained because its binding site in the receptor overlaps with the Mg^{2+} binding site, so a post-synaptic depolarization that forces Mg^{2+} to leave the channel is required for memantine action. Thus, memantine acts as a physical blocker of the channel (**Figure 1.17**).[102] Regarding the particular kinetic behavior of this compound, memantine is able to differentiate between pathological and physiological depolarizations thanks to that crucial property.[76] More precisely, it is believed that memantine is placed with the charged nitrogen pointing inside the cell, near the critical channel asparagine residues. However, the excellent affinity of memantine is explained by the presence of hydrophobic binding pockets in the binding site for the two methyl groups of memantine. The removal of these two groups, leading to *amantadine*, or the addition of a third methyl group diminishes affinity.[103]

In addition to the aforementioned effect restoring a proper glutamatergic transmission, memantine confers neuroprotective effects by avoiding the aforementioned connection between Aβ and NMDA receptors.[76] Under physiological conditions, synaptic plasticity depends on a sufficiently strong synaptic signal, however, in AD, Aβ oligomers are also able to overactivate NMDA receptors by interacting with anchoring protein complexes that modify NMDA receptor structure, so that Mg^{2+} is no longer effective to play its "filtering" function. In turn, synaptic noise rises, impairing detection of the sufficiently strong synaptic signals, leading to synaptotoxicity. In this case, memantine is able to perform as a more effective filter than Mg^{2+}, blocking pathological signals at glutamatergic synapses, and thereby allowing detection of the relevant synaptic signals, restoring the synaptic plasticity (**Figure 1.18**).[76]

[103] W. Limapichat, W. Yu, E. Branigan, H. Lester, D. Dougherty. *ACS Chem. Neurosci.* **2013**, *4*, 255.

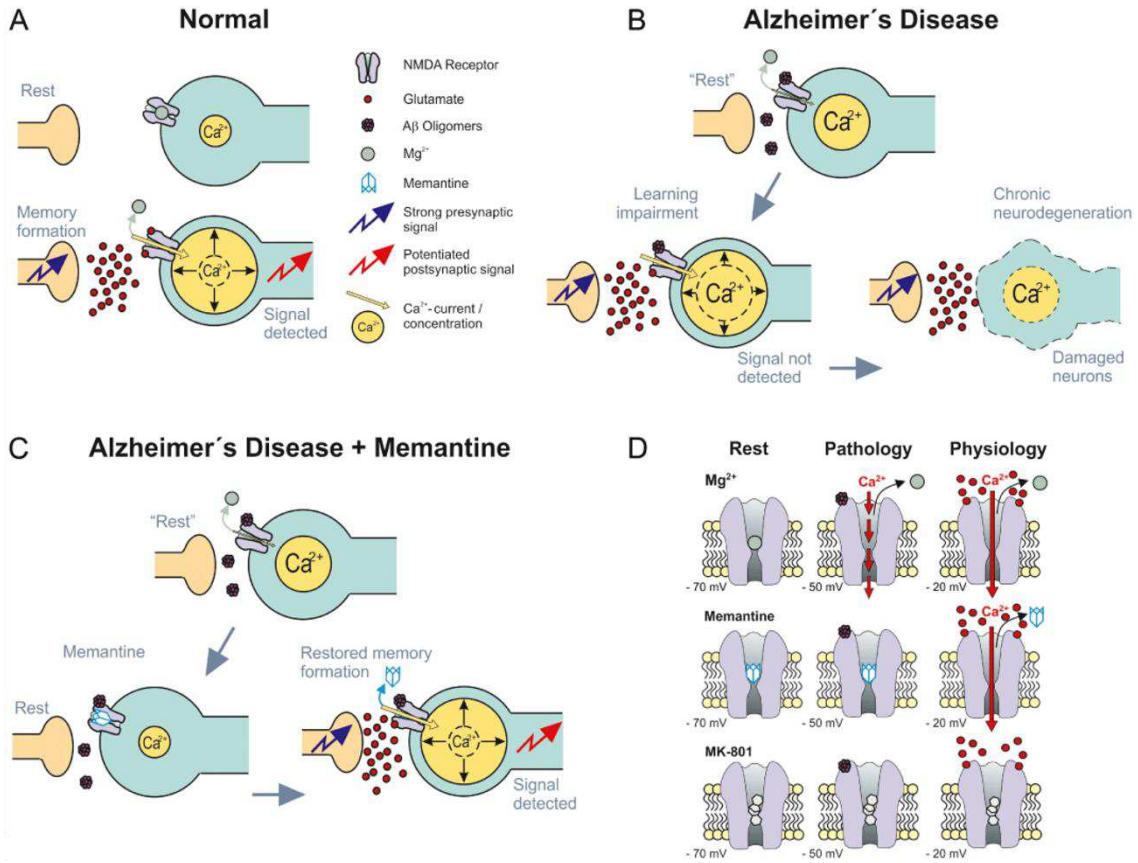

Figure 1.18: Schematic illustration of the glutamatergic system involving the NMDA receptor and Aβ oligomers. (A) Normal physiological transmission with dependence on a relevant synaptic signal. (B) In AD, there is a sustained activation of the NMDA receptors by Aβ, which leads to the rise of the synaptic noise, then impaired detection of relevant synaptic signals. (C) Synaptic plasticity recovered by antagonism with memantine. (D) Schematic illustration of how the fast unblocking kinetics of memantine allow to differentiate between physiological and pathological activation of NMDA receptors. Under resting therapeutic conditions (i.e. −70 mV, left), all occupy the NMDA receptor channel. Both Mg^{2+} and memantine are able to leave the NMDA receptor channel upon strong synaptic depolarization (−20 mV, right), whereas the slow potent blocker MK-801 remains trapped. However, memantine, in contrast to Mg^{2+}, does not leave the channel so easily upon moderate prolonged depolarization (−50 mV, centre) during chronic excitotoxic insults caused by soluble Aβ oligomers (Image source: W. Danysz, C. G. Parsons. *Br. J. Pharmacol.* **2012**, *167*, 324).

1.4.3 Trends in drug discovery for the treatment of Alzheimer's disease

An important number of potential biological targets have emerged as a consequence of the awareness of the complex and multifactorial pathogenesis of AD. Herein, the targets that are being mostly considered for the design of compounds with potential to modify the natural course of AD will be discussed.

1.4.3.1 Aβ-directed strategies

In view of the role of Aβ in AD pathogenesis, the development of Aβ-directed agents has been actively pursued during the last decades, especially compounds that modulate Aβ production by inhibiting β- or γ-secretases. However, so far none of the Aβ-targeted drugs has shown statistically significant benefits on its pre-specified endpoints clinical trials.[14]

Modulation of Aβ production

The γ-secretase complex is known to cleave up to 50 different type 1 transmembrane protein substrates besides APP, so the identification of a selective and specific inhibitor for only APP processing represents a tremendous drug-development challenge. The only γ-secretase inhibitor to reach phase III testing was *semagacestat*, a small-molecule γ-secretase inhibitor, which not only failed to achieve endpoints related to slowing disease progression but also appeared to have worsened some symptoms.[104] *Avagacestat*, another γ-secretase inhibitor that reached phase II study, caused serious adverse events such as cerebral microbleeds, dose-dependent glycosuria, and non-melanoma skin cancer.[105] Currently in phase II trials, *EVP-0962* is a γ-secretase modulator that reduces the production of $A\beta_{42}$ by shifting the APP cleavage toward the production of shorter and less toxic Aβ peptides.

The β-site APP cleaving enzyme 1 (BACE1 or β-secretase) has become the favored target in the pursuit of Aβ-centered therapeutics,[106] because it is the first enzyme to cleave APP and plays a crucial role in the generation of Aβ. BACE1 is a 501-amino acid transmembrane aspartic acid protease, related to the pepsin family, with two aspartic acid residues, Asp32 and Asp228, responsible for the hydrolytic cleavage within a hydrophilic 20 Å long cavity that form the active site of the enzyme. The binding cleft is characterized for being partially covered by a highly flexible antiparallel hairpin-loop, referred to as the "flap", which guides the entrance of the

[104] R. Doody, R. Raman, M. Farlow, T. Iwatsubo, B. Vellas, S. Joffe, K. Kieburtz, F. He, X. Sun, R. G. Thomas, P. S. Aisen *et al. N. Engl. J. Med.* **2013**, *369*, 341.
[105] V. Coric, C. v. Dyck, S. Salloway, N. Andreasen, M. Brody, R. Richter, H. Soininen, S. Thein, T. Shiovitz, G. Pilcher, S. Colby, L. Rollin, R. Dockens, C. Pachai, E. Portelius, U. Andreasson, K. Blennow, H. Soares, C. Albright, H. Feldman, R. Berman. *Arch. Neurol.* **2012**, *69*, 1430.
[106] A. Ghosh, H. Osswald. *Chem. Soc. Rev.* **2014**, *43*, 6765.

substrate into the catalytic site, enabling the adoption of a reactive conformation suitable for hydrolysis (**Figure 1.19**).[107]

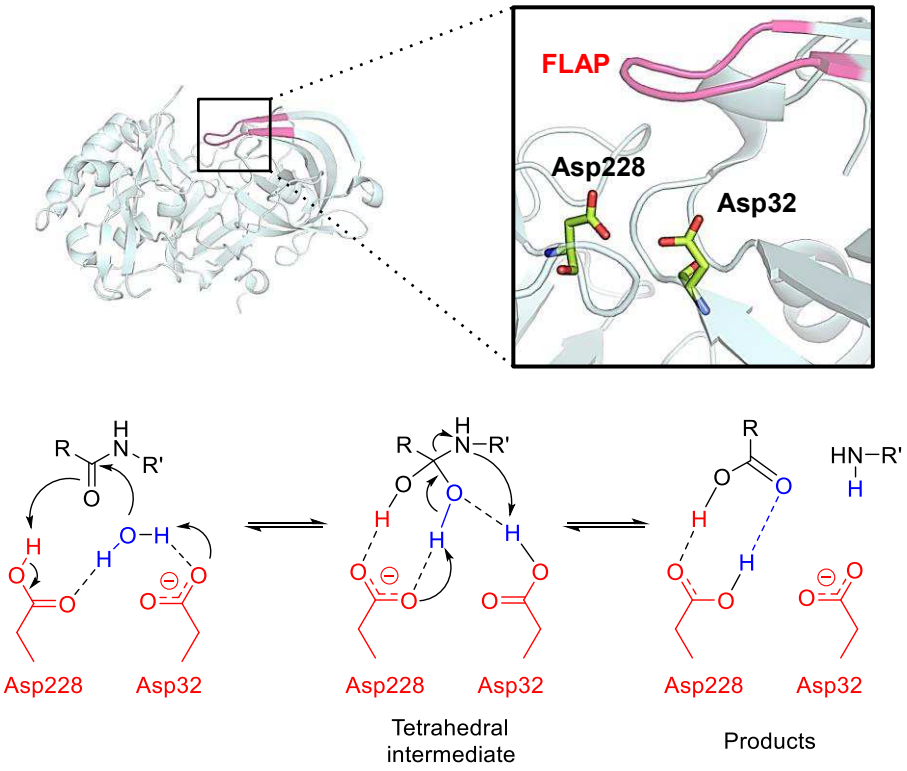

Figure 1.19: On the top: structure of BACE1 (PDB ID: 1SGZ) with the details of the catalytic anionic dyad and the "flap". At the bottom: hydrolytic reaction performed by BACE1.

The first generation of BACE1 inhibitors, such as *BI 1181181*, comprised non-cleavable peptide-based transition-state analogs, and they failed because of low oral bioavailability and low BBB penetration.[108,109] Second-generation BACE1 inhibitors, such as *RG7129*, *LY2811376* or *LY2886721*, were supposed to be more lipophilic and to cross plasma and endosomal membranes to reach the BACE1 active site, however, many of them failed in advanced-phase clinical trials because of liver toxicity.[108,109] More recently, potent third-generation small-molecule BACE1 inhibitors have shown satisfactory pharmacokinetics and provided encouraging clinical data in ongoing studies: in phase II, *E2609*; in phase II/III, *AZD3293, CNP520* and *JNJ-54861911*; in phase III, *verubecestat*. [108,109]

[107] L. Hong, J. Tang. *Biochemistry* **2004**, *43*, 4689.
[108] B. Winblad, P. Amouyel, S. Andrieu, C. Ballard, C. Brayne, H. Brodaty, A. Cedazo-Minguez, B. Dubois, D. Edvardsson, H. Feldman, L. Fratiglioni, G. B. Frisoni, S. Gauthier, J. Georges, C. Graff, K. Iqbal, F. Jessen, G. Johansson, L. Jönsson, M. Kivipelto *et al. Lancet Neurol.* **2016**, *15*, 455.
[109] V. Graham, A. Bonito-Oliva, T. Sakmar. *Annu. Rev. Med.* **2017**, *68*, 413.

Immunotherapy to increase Aβ clearance

Numerous peptidases and proteinases, known as Aβ-degrading proteases (AβDPs), affect Aβ levels. In patients with AD, increased Aβ levels may be caused not only by elevated production, but also by reduced degradation.[15,110] In this context, passive immunization therapies with systemic infusion of monoclonal antibodies (mAbs) directed to Aβ have been developed, with this approach showing the potential to prevent oligomerization and fibril formation[111] and to dissolve Aβ aggregates.[112] Despite their low BBB penetration, mAbs provide high specificity and affinity toward their antigen, low toxicity, and good plasma pharmacokinetics. *Bapineuzumab*, which reached phase III clinical trials, is a humanized mouse IgG1 mAb that binds an *N*-terminal epitope ($Aβ_{1–5}$), whose effects interestingly depend on ApoE4 genotype, showing no improvement and developing severe vasogenic edema in ApoE4-carriers, while the drug seemed to be safe and well tolerated in non-ApoE4 carriers. A derivative of *bapineuzumab*, *AAB-003*, is currently in phase I trials.[108,109] *Solanezumab* is a mAb against the central epitope of Aβ ($Aβ_{16–24}$), which confers a more promising safety profile. *Solanezumab* binds to soluble monomers and reduces $Aβ_{42}$. Phase III trials are ongoing to confirm *solanezumab* efficacy as a disease-modifying agent and possible disease-prevention agent.[108,109] Unlike *solanezumab*, *gantenerumab*, which is currently in phase III, moderately binds monomers and oligomers, and potently binds to and degrades fibrils.[113] Finally, produced through a "reverse translational medicine" approach, *aducanumab* is a fully human IgG1 mAb that selectively targets and dose-dependently reduces Aβ deposition and slows cognitive decline, and is currently in a phase III trial.[114]

[110] D. Selkoe. *Neuron* **2001**, *32*, 177.
[111] D. Frenkel, O. Katz, B. Solomon. *PNAS* **2000**, *97*, 11455.
[112] J. Legleiter, D. Czilli, B. Gitter, R. DeMattos, D. Holtzman, T. Kowalewski. *J. Mol. Biol.* **2004**, *335*, 997.
[113] B. Bohrmann, K. Baumann, J. Benz, F. Gerber, W. Huber, F. Knoflach, J. Messer, K. Oroszlan, R. Rauchenberger, W.F. Richter, C. Rothe, M. Urban, M. Bardroff, M. Winter, C. Nordstedt, H. Loetscher. *J. Alzheimers Dis.* **2012**, *28*, 49.
[114] J. Sevigny, P. Chiao, T. Bussière, P. H. Weinreb, L. Williams, M. Maier, R. Dunstan, S. Salloway, T. Chen, Y. Ling, J. O'Gorman, F. Qian, M. Arastu, M. Li, S. Chollate, M. Brennan, O. Quintero-Monzon, R. Scannevin, M. Arnold, T. Engber. *Nature* **2016**, *537*, 50.

1.4.3.2 Tau-directed strategies

Tau aggregation occurs through a nucleation-dependent elongation mechanism.[115] In fact, tau may adopt stable seed structures, displaying prion-like characteristics.[116,117] Prevention of tau aggregation regardless of phosphorylation, in which a large number of kinases is involved (then low selectivity), is a promising therapeutic approach. *TRx0237*, a methylene blue derivative, has shown to disrupt the aggregation of tau, thereby reducing oxidative stress, preventing mitochondrial damage, and preserving cognitive function,[118,119] and is currently in a phase III trial.[108,109]

Active immunization against phosphorylated tau is a viable approach for eliciting the activation of the immune system and production of high-affinity antibodies against the target. Two active immunization vaccines, *AADvac-1* and *ACI-35*, are currently in clinical trials.[120,121] There are also a number of passive immunization trials in progress, which target hyperphosphorylated tau, conformations of tau, fragments of tau, and/or total tau.[122]

1.4.3.3 Oxidative stress-directed strategies

Natural antioxidants, such as vitamins E, C, and carotenoids, phytochemicals and synthetic compounds, are well known to confer neuroprotection in AD.[38,123] Recently, a drug

[115] M. v. Bergen, P. Friedhoff, J. Biernat, J. Heberle, E.-M. Mandelkow, E. Mandelkow. *PNAS* **2000**, *97*, 5129.
[116] F. Clavaguera, J. Hench, I. Lavenir, G. Schweighauser, S. Frank, M. Goedert, M. Tolnay. *Acta Neuropathol.* **2014**, *127*, 299.
[117] D. Sanders, S. Kaufman, S. DeVos, A. Sharma, H. Mirbaha, A. Li, S. Barker, A. Foley, J. Thorpe, L. Serpell, T. Miller, L. Grinberg, W. Seeley, M. Diamond. *Neuron* **2014**, *82*, 1271.
[118] K. Hochgräfe, A. Sydow, D. Matenia, D. Cadinu, S. Könen, O. Petrova, M. Pickhardt, P. Goll, F. Morellini, E. Mandelkow, E.-M. Mandelkow. *Acta Neuropathol. Commun.* **2015**, *3*, 25.
[119] T. Baddeley, J. McCaffrey, J. Storey, J. Cheung, V. Melis, D. Horsley, C. Harrington, C. Wischik. *J. Pharmacol. Exp. Ther.* **2015**, *352*, 110.
[120] C. Theunis, N. Crespo-Biel, V. Gafner, M. Pihlgren, M. P. López-Deber, P. Reis, D. Hickman, O. Adolfsson, N. Chuard, D. M. Ndao, P. Borghgraef, H. Devijver, F. v. Leuven, A. Pfeifer, A. Muhs. *PLoS ONE* **2013**, *8*, e72301.
[121] E. Kontsekova, N. Zilka, B. Kovacech, P. Novak, M. Novak. *Alzheimers Res. Ther.* **2014**, *6*, 44.
[122] J. T. Pedersen, E. Sigurdsson. *Trends Mol. Med.* **2015**, *21*, 394.
[123] M. Valko, D. Leibfritz, J. Moncola, M. Cronin, M. Mazura, J. Telser. *Int. J. Biochem. Cell. Biol.* **2007**, *39*, 44.

candidate combining vitamin E with memantine has completed phase III trials,[124] and also a phase III study of vitamin E with selenium is currently ongoing. Some ubiquitous antioxidants like flavonoids, rutin and carotenoids have also shown neuroprotective effect in experimental models of AD.[125] Melatonin is another potent antioxidant currently in phase II trials, and a novel melatonin agonist, *Neu-P11*, has shown to reduce neuronal loss and to improve memory in rats.[126,127]

1.5 Multi-target directed ligand strategy

In light of the various complex mechanisms involved in the pathological network of AD, the classic medicinal chemistry paradigm of developing drugs based on the reductionist pattern of "one molecule-one target" has met with very limited success, highlighting the need of a more comprehensive pharmacological approach to obtain effective outcomes.

In this context, some pharmacological approaches are available to overcome the lack of efficacy associated with the use of single target drugs against multifactorial diseases as AD. The most commonly used in general pharmacotherapy, referred to as *multiple-medication therapy* (MMT), consists of combining several drugs with different action mechanisms. However, this approach might be disadvantageous for patients with compliance problems, such as AD patients, and is associated with bioavailability, pharmacokinetics and metabolism issues, such as potential drug-drug interactions.[128,129] An alternative approach may be the use of a *multiple-compound medication* (MCM), also called "single-pill drug combination", which implies the incorporation of different drugs into the same formulation in order to simplify dosing regimens and improve patient compliance, but it still maintains the other problems.[128,129]

---

[124] M. Dysken, P. Guarino, J. Vertrees, S. Asthana, M. Sano, M. Llorente, M. Pallaki, S. Love, G. Schellenberg, R. McCarten, J. Malphurs, S. Prieto, P. Chen, D. Loreck, S. Carney, G. Trapp, R. Bakshi, J. Mintzer, J. Heidebrink, A. Vidal-Cardona. *Alzheimers Dement.* **2014**, *10*, 36.
[125] H. Javed, M. M. Khan, A. Ahmad, K. Vaibhav, M. E. Ahmad, A. Khan, M. Ashafaq, F. Islam, M. S. Siddiqui, M. M. Safhi. *Neuroscience* **2012**, *210*, 340.
[126] D. Cardinali, A. Furio, L. Brusco. *Curr. Neuropharmacol.* **2010**, *8*, 218.
[127] M. She, X. Deng, Z. Guo, M. Laudon, Z. Hu, D. Liao, X. Hu, Y. Luo, Q. Shen, Z. Su, W. Yin. *Pharmacol. Res.* **2009**, *59*, 248.
[128] A. Cavalli, M. L. Bolognesi, A. Minarini, M. Rosini, V. Tumiatti, M. Recanatini, C. Melchiorre. *J. Med. Chem.* **2008**, *51*, 347.
[129] B. Schmitt, T. Bernhardt, H.-J. Moeller, I. Heuser, L. Frölich. *CNS Drugs* **2004**, *18*, 827.

Finally, a third strategy has emerged on the basis of the assumption that a single compound may be able to hit multiple targets, which clearly has inherent advantages over MMT or MCM, facilitating the management of multifactorial diseases. This approach is the so-called *multi-target directed ligand* therapy (MTDL, **Figure 1.20**) or simply "polypharmacology", and shows advantages such as easier pharmacokinetics for ADME profile optimization, improved efficacy due to synergistic effects arising from the simultaneous modulation of several targets, and improved safety by decreasing potential side effects and preventing the risk of drug-drug interactions.[128,130,131] Nevertheless, this approach must face up important challenges at the early stages of drug discovery, since a multi-target directed compound must recognize multiple targets with comparable or balanced affinities, but also potential drug promiscuity might arise from off-target effects, which renders their design a challenging task.[132,133] In any case, new hopes for the treatment of AD and other multifactorial diseases, such as cancer or depression, have arisen related to this new approach, encouraged by recent findings on already existing drugs that have been retrospectively found to be multi-target, i.e. clozapine,[133] galantamine[95,134] or donepezile.[95,133]

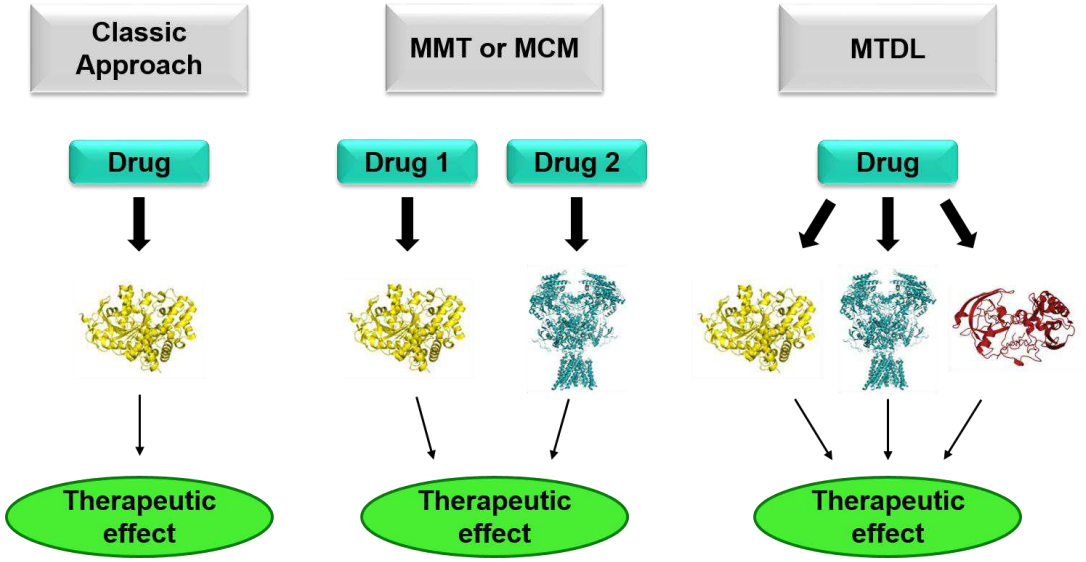

Figure 1.20: Different approaches leading to the discovery of new therapies. Left: one-molecule-one-target strategy. Centre: multiple-medication therapy (MMT); in case of multiple-compound medication (MCM), both drugs applied in the same pill. Right: multi-target directed ligand (MTDL) approach.

[130] R. Morphy, Z. Rankovic. *J. Med. Chem.* **2005**, *48*, 6523.
[131] D. Muñoz-Torrero. *Curr. Med. Chem.* **2013**, *20*, 1621.
[132] E. Viayna, I. Sola, O. Di Pietro, D. Muñoz-Torrero. **2013**, *20*, 1623.
[133] A. Anighoro, J. Bajorath, G. Rastelli. *J. Med. Chem.* **2014**, *57*, 7874.
[134] T. Kihara, H. Sawada, T. Nakamizo, R. Kanki, H. Yamashita, A. Maelicke, S. Shimohama. *Biochem. Biophys. Res. Commun.* **2004**, *325*, 976.

1.6 Precedent work in our research group

In the past decade many academic research groups, including ours, have developed a large number of MTDLs in the search of potential drug candidates for the sough-after disease-modifying treatment of AD. In the following section, some of the most recent work of our group in this field will be discussed.

MTDLs can be rationally designed through the molecular assembly of distinct pharmacophore moieties from identified bioactive molecules, where each drug entity has conserved the potential to interact with its specific site on the target.[135] A recent example of MTDL hybrid molecules developed in our research group are the levetiracetam–huprine and levetiracetam–tacrine hybrids, developed as part of Dr. Irene Sola's PhD Thesis.[136] Evidence derived from population-based and observational studies shows that AD is associated with a substantially increased risk of seizures and epilepsy.[137] In this context, a levetiracetam (**7**, **Figure 1.21**) moiety, a marketed antiepileptic drug that effectively suppresses epileptiform activity in mouse models of AD,[138] was combined with either a huprine Y (**8**) or a tacrine (**2**) fragment, both highly potent AChE inhibitors.[136]

In agreement with the design rationale, the levetiracetam-based hybrid **10** retained the potent anticholinesterase activity of the parent huprine and led to a statistically significant reduction of the incidence of epileptic seizures in a mouse model of AD. Indeed, this compound exhibited a very promising multi-target profile, encompassing a dual nanomolar *h*AChE and human BChE (*h*BChE) *in vitro* inhibition, moderately potent dual $A\beta_{42}$ and tau antiaggregating effect in a cell-based assay, as well as a reduction of the incidence of epileptic seizures, amyloid load, and neuroinflammation, and a cognition enhancing effect in transgenic APP/PS1 mice.[136]

[135] M. Decker. *Curr. Med. Chem.* **2011**, *18*, 1464.
[136] I. Sola, E. Aso, D. Frattini, I. López-González, A. Espargaró, R. Sabaté, O. Di Pietro, F. J. Luque, M. V. Clos, I. Ferrer, D. Muñoz-Torrero. *J. Med. Chem.* **2015**, *58*, 6018.
[137] D. d. C. Miranda, S. M. D. Brucki. *Dement. Neuropsychol.* **2014**, *8*, 66.
[138] J.-Q. Shi, B.-R. Wang, Y.-Y. Tian, J. Xu, L. Gao, S.-L. Zhao, T. Jiang, H.-G. Xie, Y.-D. Zhang. *CNS Neurosci. Ther.* **2013**, *19*, 871.

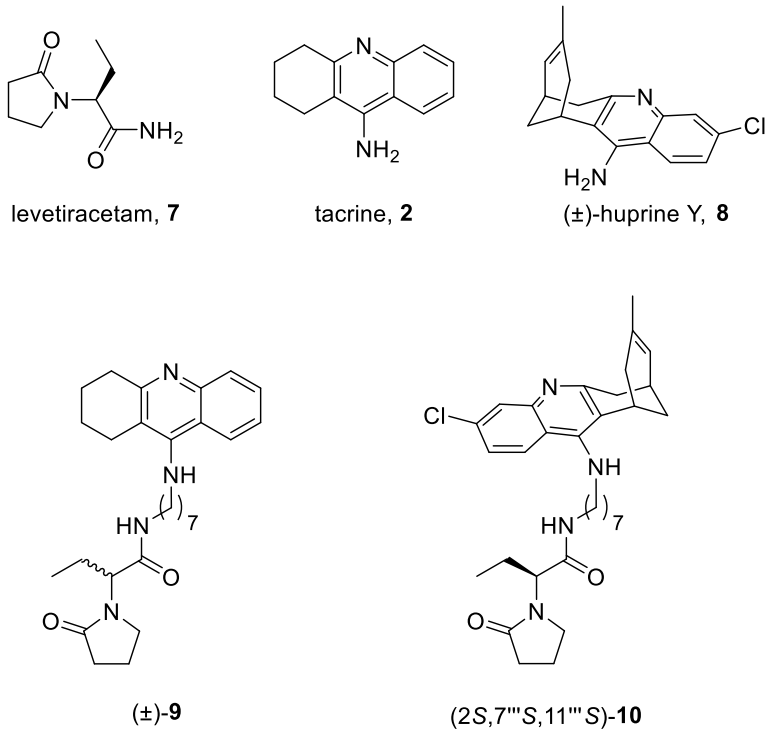

Figure 1.21: Relevant structures for this work on levetiracetam–tacrine (**9**) and levetiracetam–huprine (**10**) hybrids, and their parent pharmacophoric structures.

Because the PAS of AChE promotes Aβ aggregation,[66] inhibitors that simultaneously block both the PAS and the CAS of AChE emerged some years ago as a particular approach to derive multi-target therapies, inasmuch as these compounds should be endowed with potent inhibitory activity against both AChE and Aβ aggregation. An attractive example of a rational design of dual binding AChE inhibitors was developed in a project that was part of Dr. Ornella Di Pietro's PhD Thesis and of my own MSc's work. This work resulted in a series of compounds that consisted of a CAS interacting unit, derived from a well validated AChE inhibitor, linked by means of a tether of suitable length to a PAS interacting unit.

Firstly, Dr. Di Pietro carried out the optimization of a PAS binding motif, structurally related to the prototype of PAS binding AChEI propidium (**11**, **Figure 1.22**). This optimization process successfully led to the nanomolar PAS binding ligand **12**, a 1,2,3,4-tetrahydrobenzo[*h*][1,6]naphthyridine.[139]

[139] O. Di Pietro, E. Viayna, E. Vicente-García, M. Bartolini, R. Ramón, J. Juárez-Jiménez, M. V. Clos, B. Pérez, V. Andrisano, F. J. Luque, R. Lavilla, D. Muñoz-Torrero. *Eur. J. Med. Chem.* **2014**, *73*, 141.

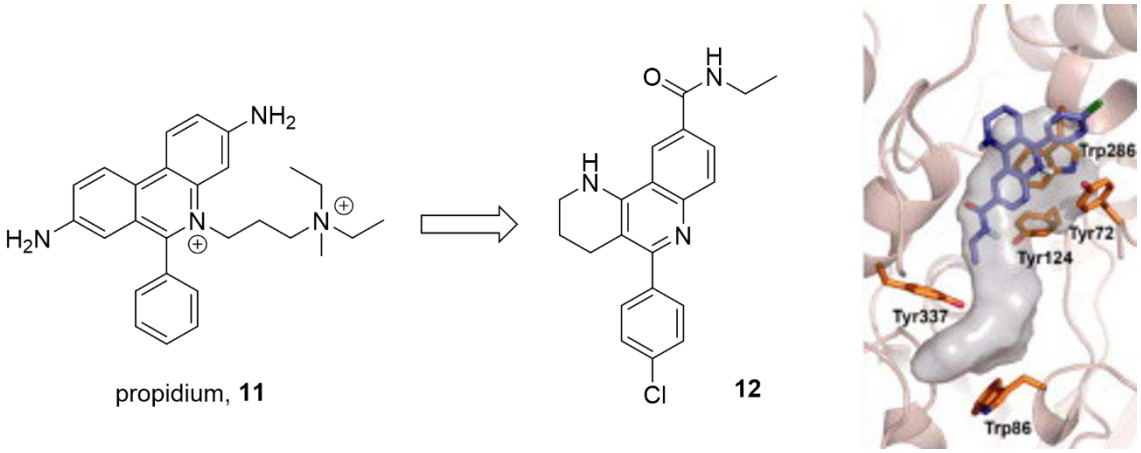

Figure 1.22: Left: Propidium, **11**, and the developed benzonaphthyridine **12**. Right: representation of the binding mode of compound **12** to the PAS of AChE (Image source: O. Di Pietro, E. Viayna, E. Vicente-García, *et al*. *Eur. J. Med. Chem.* **2014**, *73*, 141).

Afterwards, we performed the development of a hybrid that combined the PAS binding pharmacophore of **12** with a unit of the well-known CAS binding ligand 6-chlorotacrine (**13**, optimized derivative of tacrine, **2**), a highly potent AChEI, through a 3-methylene linker, predicted by previous computational studies to be the most suitable to achieve a dual binding mode within AChE (**Figure 1.23**).[140]

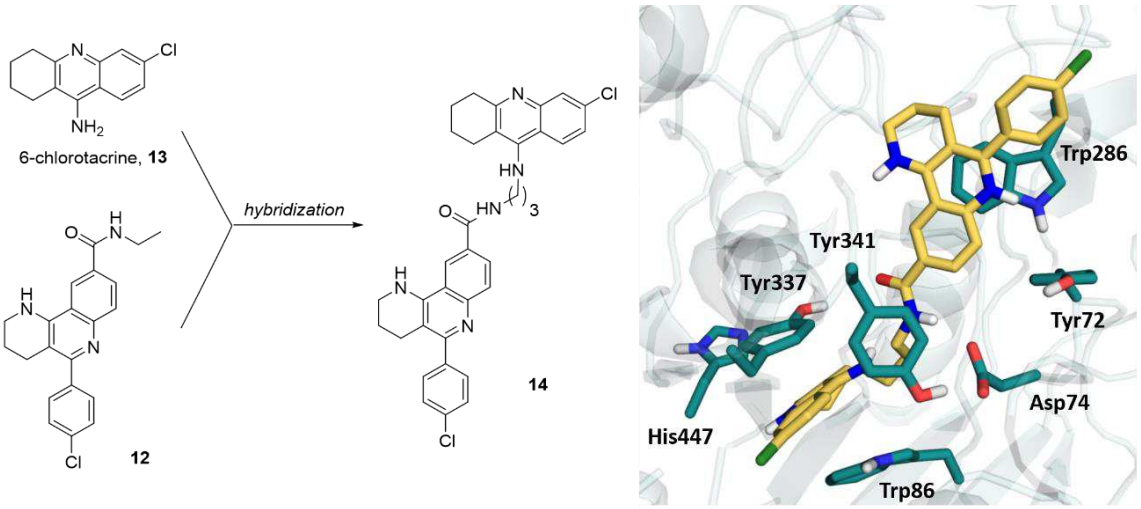

Figure 1.23: Left: Development of the hybrid benzonaphthyridine–6-chlorotacrine **14**. Right: representation of the binding mode of compound **14** within AChE (Image source: O. Di Pietro, F. J. Pérez-Areales, J. Juárez-Jiménez, *et al*. *Eur. J. Med. Chem.* **2014**, *84*, 107).

[140] O. Di Pietro, F. J. Pérez-Areales, J. Juárez-Jiménez, A. Espargaró, M. V. Clos, B. Pérez, R. Lavilla, R. Sabaté, F. J. Luque, D. Muñoz-Torrero. *Eur. J. Med. Chem.* **2014**, *84*, 107.

As expected by the rational design, compound **14** seemed to hit AChE in a dual binding mode. Beyond our expectations, this compound displayed a surprisingly high inhibitory activity against *h*AChE *in vitro* (IC_{50} = 0.006 nM), being 1000-fold more potent than reference compound 6-chlorotacrine (**13**, IC_{50} = 5.9 nM). Additionally, **14** was found to moderatately inhibit *h*BChE, and $A\beta_{42}$ and tau aggregation, thereby constituting an interesting MTDL.[140]

CHAPTER 2

Objectives

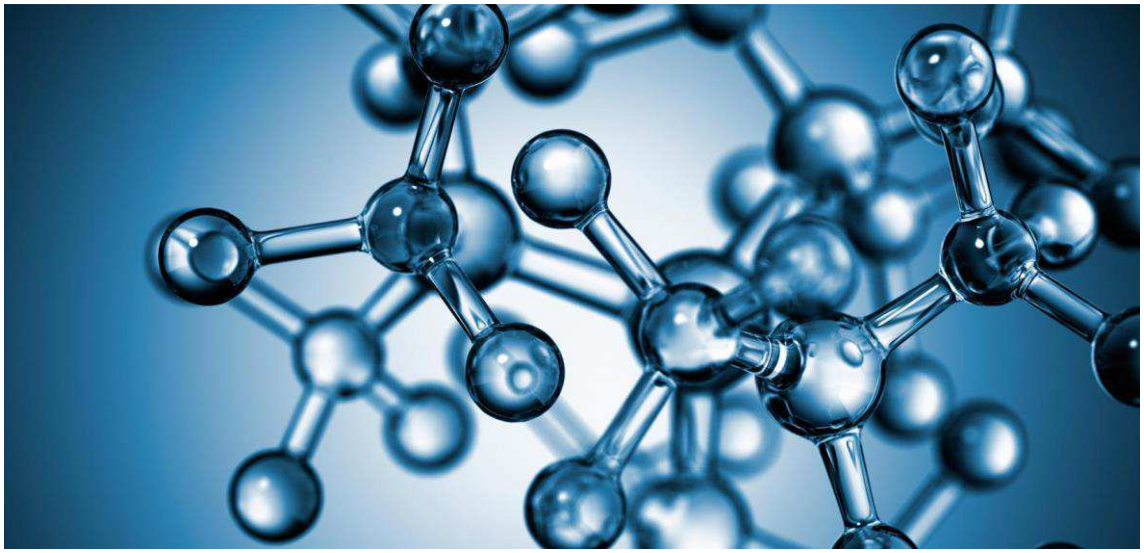

Image source: Danish Diabetes Academy (*www.danishdiabetesacademy.dk*)

2.1 Shogaol–huprine hybrids: design, synthesis and biological evaluation

Taking into account the multifactorial nature of AD and the potential of the MTDLs to derive efficacious anti-AD therapies, the first purpose of this PhD Thesis work involved a short series of hybrid compounds, the shogaol–huprine hybrids (general structure **I**, **Figure 2.1**), which were designed as dual antioxidant and anticholinesterase agents, with those activities to be imparted by their shogaol-derived and huprine moieties, respectively. The initial work of this project was carried out in the context of Dr. Carles Galdeano's PhD Thesis, but the target compounds could not be obtained likely due to stability issues. In this work, we slightly re-designed the structure of the shogaol-based moiety, in order to confer higher stability to the final compounds, and the synthetic pathway.

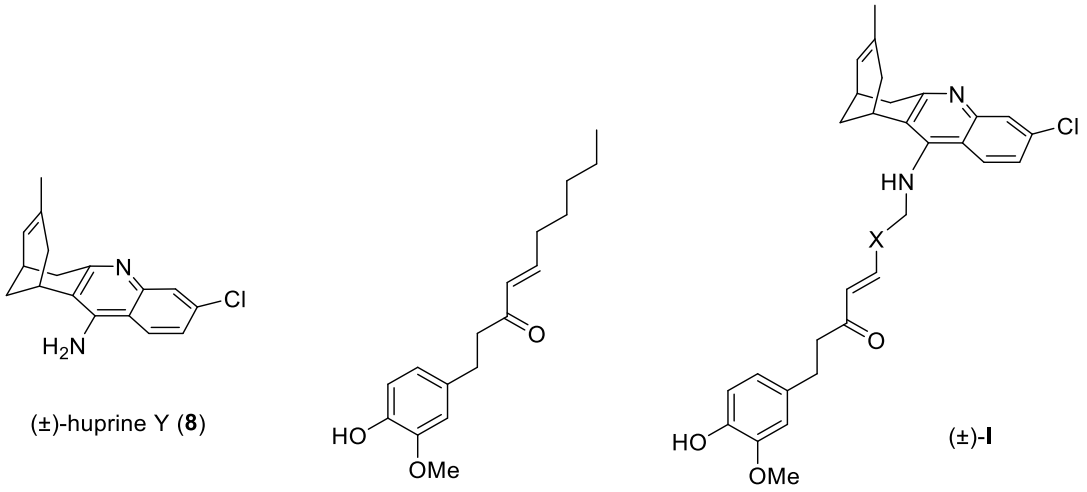

Figure 2.1: Structures of huprine Y, **8**, [6]-shogaol, **15**, and general structure of shogaol–huprine hybrids (**I**).

The preparation of the oligomethylene-linked hybrid was envisioned by a sequence that involved the initial preparation of the shogaol moiety through a Mannich-type condensation reaction, and the huprine moiety through an alkylation with 5-bromo-1-pentene, followed by a cross metathesis reaction between both units.

For the synthesis of the *p*-phenylene-linked hybrid, the reductive alkylation of racemic huprine Y with *p*-cyanobenzaldehyde was planned, followed by the reduction of the nitrile to the corresponding aldehyde, and a final Mannich-type condensation of the aldehyde with vanillin acetone.

2.2 Rhein–modified huprine hybrids: design, synthesis and biological evaluation

Rhein–huprine hybrids were recently developed in the context of the PhD works of Drs. Elisabet Viayna and Irene Sola, as a novel class of MTDLs with a very interesting *in vitro* and *in vivo* multi-target anti-Alzheimer profile. Among the multiple biological effects of the lead compound **16** (**Figure 2.2**), a high potency against human BACE1 (*h*BACE1, IC_{50} = 120 nM) stood out, even though this trait was not specifically pursued when these compounds were designed.[141] Herein, we envisaged the synthesis of a second generation of rhein–huprine hybrids (general structure **II**), designed by modification of the huprine aromatic ring of the lead **16**. The design of these novel analogs aimed at exploring the effect of pyridinic ring basicity on the different biological activities, with the hope of identifying an optimized hybrid with favorable multi-target activity profile and reduced basicity, and, hence, with expectable better bioavailability.

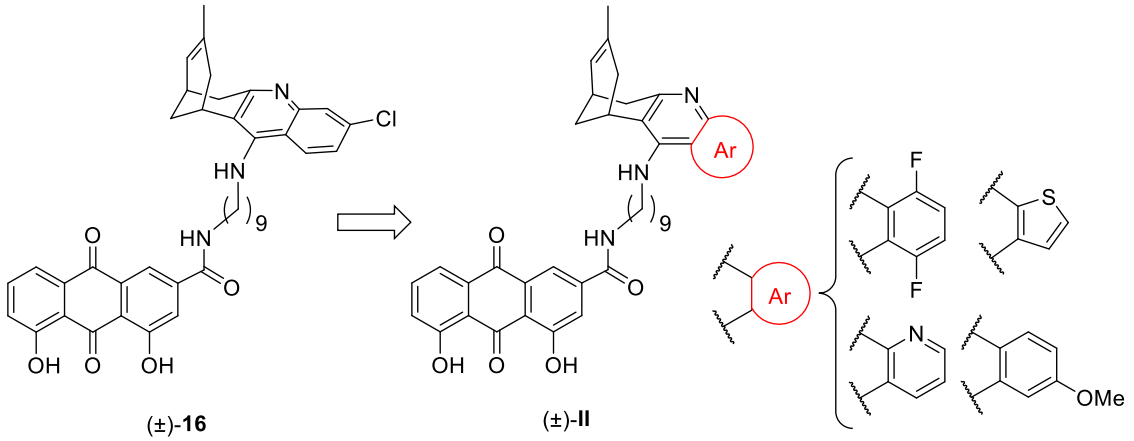

Figure 2.2: Structure of the lead compound from the first generation of rhein–huprine hybrids, **16**, and the general structure of the purposed second generation (**II**).

Firstly, the modified huprines were to be prepared through the methodology developed by Prof. Pelayo Camps,[142] which involved a Friedländer reaction between 7-methylbicyclo[3.3.1]non-6-en-3-one and the appropriate aminonitrile. Next, the preparation of hybrids was envisaged using a general methodology, which comprised, as previously

[141] E. Viayna, I. Sola, M. Bartolini, A. De Simone, C. Tapia-Rojas, F. G. Serrano, R. Sabaté, J. Juárez-Jiménez, B. Pérez, F. J. Luque, V. Andrisano, M. V. Clos, N. C. Inestrosa, D. Muñoz-Torrero. *J. Med. Chem.* **2014**, *57*, 2549.
[142] P. Camps, R. El Achab, M. Font-Bardia, D. Görbig, J. Morral, D. Muñoz-Torrero, X. Solans, M. Simon. *Tetrahedron* **1996**, *52*, 5867.

described,[141] the alkylation of the racemic modified huprines with 9-bromononanenitrile, followed by a reduction to the corresponding aminononylhuprines, and the final acylation with rhein.

2.3 CR-6–tacrine hybrids: design, synthesis and biological evaluation

Given the pivotal role of BACE1 and oxidative stress in AD, and considering the previous knowledge about AChEIs in our research group, we envisioned a new family of compounds to be prepared in a collaborative work with Dr. María Garrido, from the group of Prof. Àngel Messeguer (*Instituto de Química Avanzada de Cataluña*, IQAC-CSIC), with extensive knowledge in the development of antioxidants. This family was designed to achieve a dual site binding within both AChE and BACE1, apart from antioxidant activity, by combining a unit of the potent AChEI 6-chlorotacrine (**13**) with a moiety derived from CR-6 (**17**, **Figure 2.3**), a potent antioxidant developed in Prof. Àngel Messeguer's group,[143] through a tether of the proper length (general structure **III**).

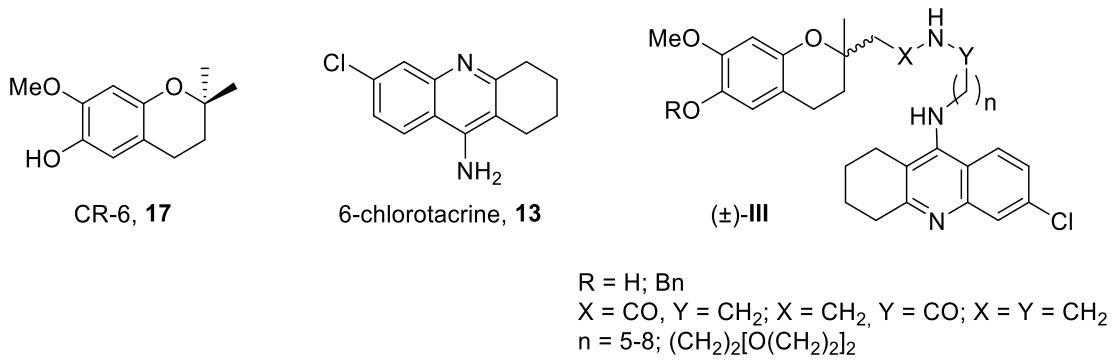

Figure 2.3: Structures of CR-6 (**17**) and 6-chlorotacrine (**13**), and the general structure of the novel family of CR-6–tacrine hybrids (**III**).

The synthesis of a first series of CR-6–tacrine hybrids was envisaged by amide coupling of a carboxylic acid derived from CR-6 and ω-aminoalkyltacrines, which were to be prepared by nucleophilic aromatic substitution of 6,9-dichloro-1,2,3,4-tetrahydroacridine with the corresponding diamines. The synthesis of a second series of inverse amides was envisaged by

[143] L. Vázquez-Jiménez, M. Garrido, M. Miceli, E. Prats, A. Ferrer-Montiel, M. Teixidó, C. Jimeno, A. Messeguer. *Eur. J. Med. Chem.* **2016**, *123*, 788.

coupling of a primary amine derived from CR-6 and ω-carboxyalkyltacrines, which were to be prepared by nucleophilic substitution of ω-bromoalkanenitriles with 6-chlorotacrine, followed by hydrolysis to the corresponding carboxylic acid. The synthesis of a third series of hybrids bearing a basic secondary amino group within the linker, was envisaged by nucleophilic substitution of a tosylate derived from CR-6 with ω-aminoalkyltacrines.

2.4 Benzoadamantane–tacrine hybrids: design, synthesis and biological evaluation

The combination of pharmacophores that enable modulation of glutamatergic and cholinergic systems has not been very intensively explored so far, even though a few examples of MTDLs with this profile exist. In particular, this approach involves the combination of a NMDA receptor antagonist moiety, to combat neurodegeneration, with an AChE inhibitor moiety, to improve memory and cognition. Taking advantage of our knowledge about AChE inhibitors, a collaborative work was planned with the group of Dr. Santiago Vázquez (*Universitat de Barcelona*), which has a wide expertise on the synthesis of adamantane-like scaffolds, some of them endowed with potent NMDA antagonistic activity. Benzopolycyclic amine **18** (**Figure 2.4**), which was developed in the context of Dr. Elena Valverde's PhD Thesis[144] and displayed an IC_{50} value for NMDA antagonism (1.93 μM) in the same range of memantine (1.5 μM), was chosen as the NMDA antagonist moiety to construct a new family of hybrids (general structures **IV** and **V**) blended with 6-chlorotacrine (**13**) by an appropriate linker to achieve a dual binding site within AChE.

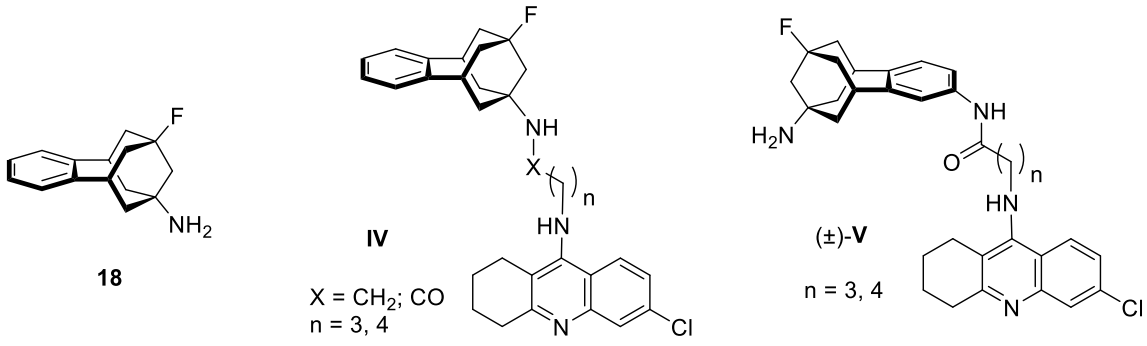

Figure 2.4: Structure of benzoadamantane **18**, and the general structure of the two series of hybrids **IV** and **V**.

[144] E. Valverde, F. X. Sureda, S. Vázquez. *Bioorg. Med. Chem.* **2014**, *22*, 2678.

The synthesis of the intermediate benzoadamantane **18** was planned as described in the PhD Thesis of Dr. Elena Valverde.[144] The preparation of the series **IV** was envisaged by direct acylation of the benzoadamantane **18** with the corresponding ω-carboxyalkyltacrines (prepared as described in section **2.3**), followed by the eventual reduction of the resulting amide to the secondary amine. The synthesis of the series of general structure **V** was envisaged through a more laborious synthetic pathway, due to the complexity of the aniline-derived benzoadamantane intermediate, with the aliphatic amine protected as a chloroacetamide, which was to be prepared as described in the PhD Thesis of Dr. Marta Barniol,[145] and then acylated with the corresponding ω-carboxyalkyltacrine, and deprotected.

[145] M. Barniol-Xicota, A. Escandell, E. Valverde, E. Julián, E. Torrents, S. Vázquez. *Bioorg. Med. Chem.* **2015**, *23*, 290.

CHAPTER 3

Shogaol–huprine hybrids

Zingiber officinale (ginger)

Image source: B and T World Seeds' Botanical Glossary (*www.b-and-t-world-seeds.com*)

3.1 Background

3.1.1 Huprines as AChE inhibitors

In 1998, Prof. Pelayo Camps and Dr. Diego Muñoz-Torrero developed a novel class of AChEIs called huprines, which turned out to be among the most potent reversible AChEIs reported so far.[146-148] They were designed by conjunctive approaches using as templates two well-known CAS inhibitors, namely tacrine (**2**), the first marketed anti-Alzheimer drug, and (–)-huperzine A (**19**, **Figure 3.1**), an alkaloid isolated from *Huperzia serrata* with potent AChE inhibitory activity that is commercialized as a nutraceutical in the USA.[148] More than thirty different huprines were designed, synthesized and pharmacologically tested. The most active huprines prepared to date are the so-called (–)-huprine Y, (–)-**8**, and (–)-huprine X, (–)-**20**, which are, in racemic form, up to 640- and 810-fold more potent human AChE inhibitors than the parent compounds tacrine and (–)-huperzine A, respectively.[148]

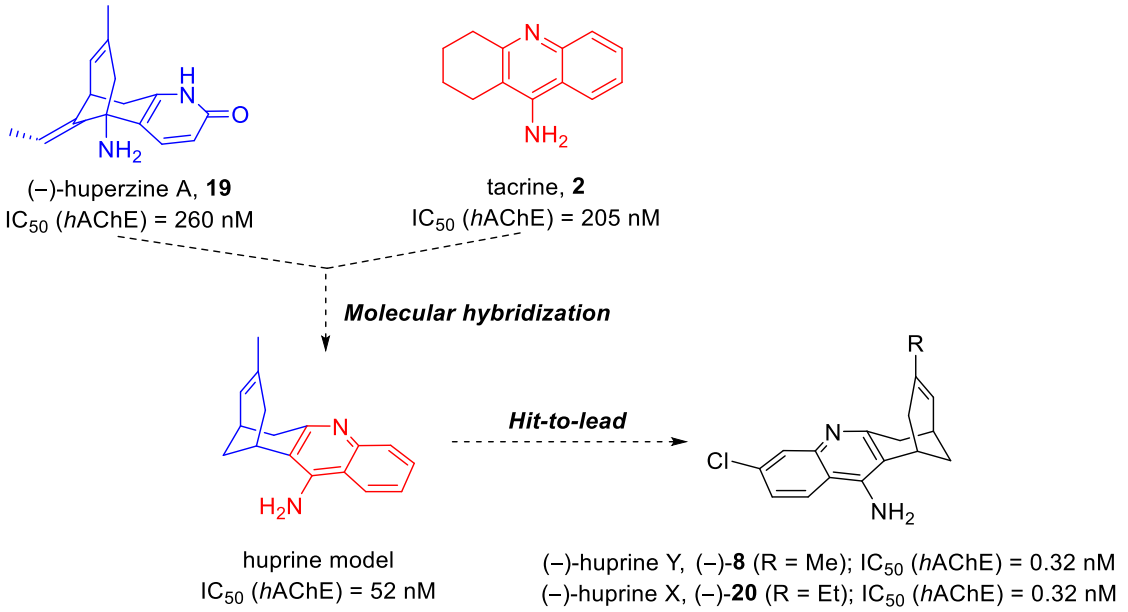

Figure 3.1: Development of huprines.

[146] A. Badia, J. E. Baños, P. Camps, J. Contreras, D. M. Görbig, D. Muñoz-Torrero, M. Simón, N. M. Vivas. *Bioorg. Med. Chem.* **1998**, *6*, 427.
[147] P. Camps, R. El Achab, D. Görbig, J. Morral, D. Muñoz-Torrero, A. Badia, J. E. Baños, N. M. Vivas, X. Barril, M. Orozco, F. J. Luque. *J. Med. Chem.* **1999**, *42*, 3227.
[148] D. Muñoz-Torrero, P. Camps. *Exp. Op. Drug Disc.* **2008**, *3*, 65.

3.1.2 Shogaols as antioxidant agents

[6]-Shogaol (**15**, **Figure 3.2**) is one of the major bioactive constituents of ginger (*Zingiber officinale*), a plant widely used in the Chinese traditional medicine. It has been reported that [6]-shogaol displays potent antioxidant and anti-inflammatory activities due to its enone moiety.[149] Interestingly, [6]-shogaol enhances antioxidant defense mechanisms in both cell cultures and in mice[150] and counteracts the hydrogen peroxide-induced increase of ROS in an *in vitro* model of hippocampal cholinergic neurons.[151]

3.1.3 Precedents in our research group

As mentioned in the objectives, a short series of shogaol–huprine hybrids was first attempted to be synthesized without success in the context of Dr. Carles Galdeano's PhD Thesis (**Scheme 3.1**).

[149] S. Dugasani, M. R. Pichika, V. D. Nadarajah, M. K. Balijepalli, S. Tandra, J. N. Korlakunta. *J. Ethnopharmacol.* **2010**, *127*, 515.
[150] M.-J. Bak, S. Ok, M. Jun, W.-S. Jeong. *Molecules* **2012**, *17*, 8037.
[151] S. Shim, J. Kwon. *Food Chem. Toxicol.* **2012**, *50*, 1454.

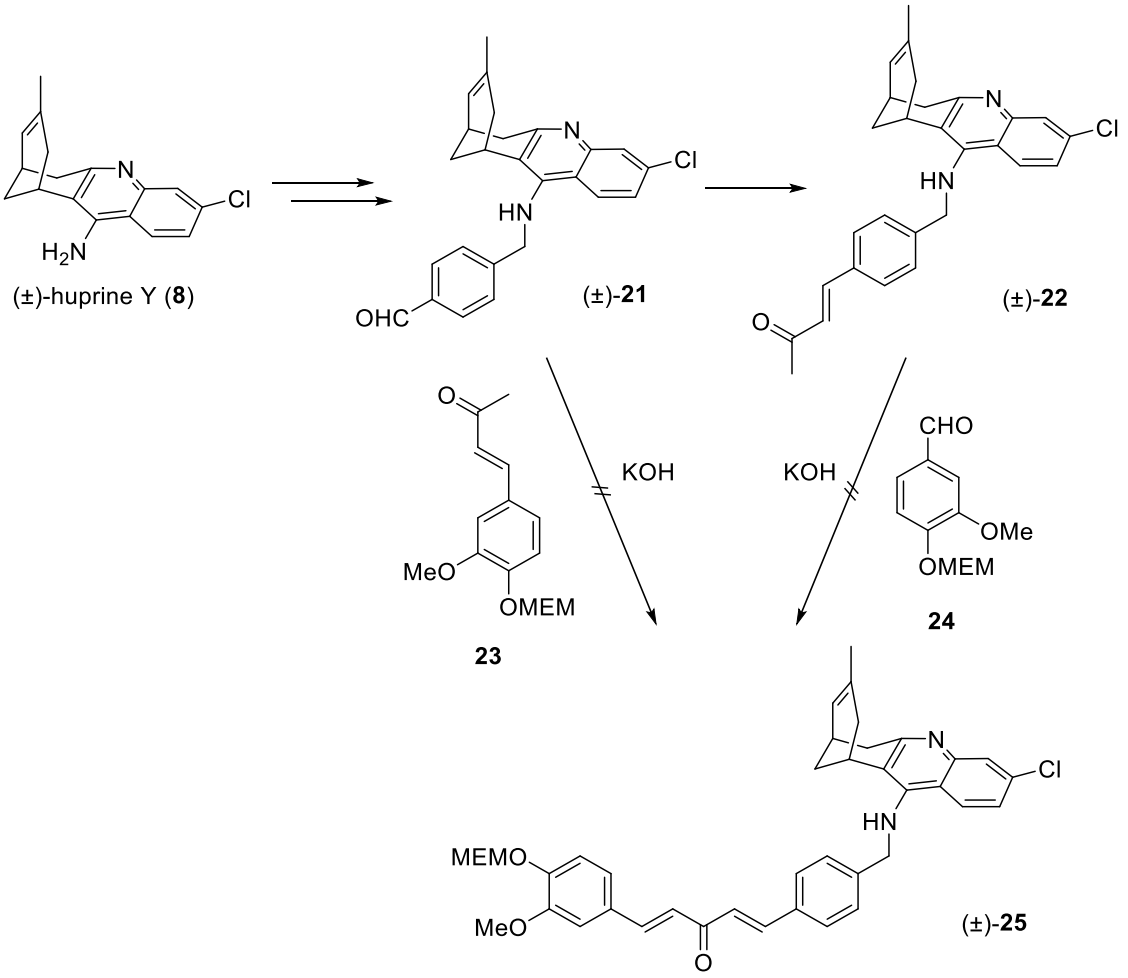

Scheme 3.1

3.2 Design of shogaol–huprine hybrids

Keeping in mind the aforementioned pathway, we decided to increase the stability of the desired hybrid by removing the double Michael acceptor moiety, namely the double bond included in the shogaol unit, given the fact that is not part of the original molecule of [6]-shogaol (**15**). The inclusion of this double bond in the initially purposed hybrid pretended to increase both $A\beta_{42}$ and tau anti-aggregating properties, which highly depend on the presence of flat conjugated systems in the molecule. The mentioned change should not affect the multi-target profile of the compound, with regard to the expected dual antioxidant and anticholinesterase activities, to be conferred by shogaol and huprine moieties, respectively.

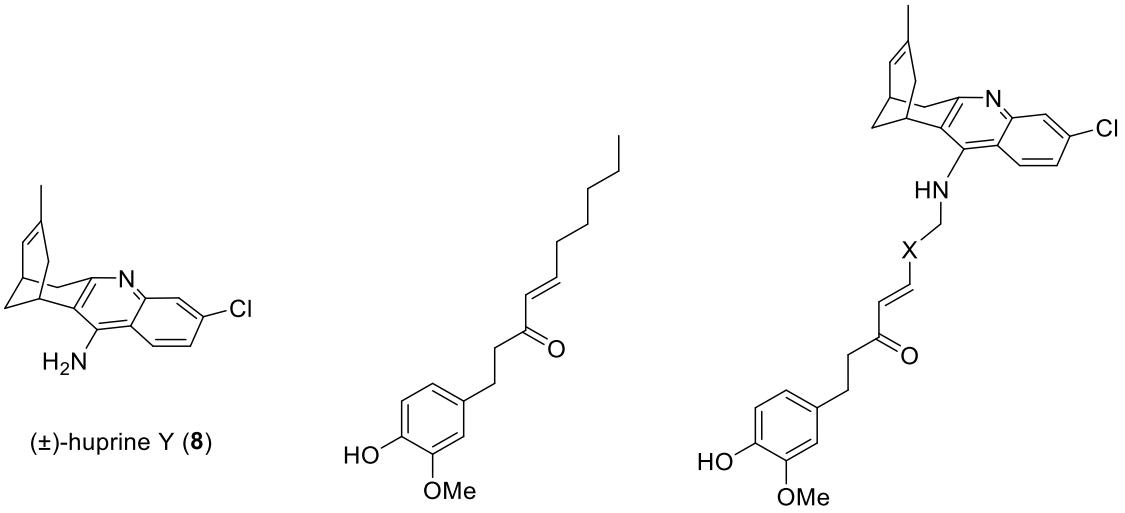

(±)-huprine Y (**8**)

[6]-shogaol (**15**)

X = $(CH_2)_2$, (±)-**26**
X = *p*-phenylene, (±)-**27**

Figure 3.2: Parent compounds, huprine Y (**8**) and [6]-shogaol (**15**), and purposed shogaol–huprine hybrids (**26** and **27**).

Dr. F. Javier Luque's group (*Universitat de Barcelona*) carried out molecular modeling studies to select the optimal tether length for the interaction of the hybrids within AChE, and taking into account that the antioxidant activity of shogaols seems to reside in the α,β-unsaturated ketone, apart from the phenolic ring, irrespective of the alkyl chain length.[149] To this end, a series of hybrids differing in the number of methylene units present between the huprine and shogaol units were subjected to docking calculations in three different *h*AChE models. A preferential binding to the *h*AChE model in which Trp286 retains the orientation found in the AChE–propidium complex (PDB ID: 1N5R) in conjunction with a chain of eight carbon atoms for the linker in the shogaol–huprine hybrids (compound (±)-**26**, **Figure 3.2**) was found. This chain length should enable the simultaneous binding to both the CAS and the PAS of *h*AChE, which are separated by a distance of approximately 14 Å.[81] Thus, the huprine unit was located in the pocket defined by residues Trp86 and Tyr337 in the CAS, forming a direct hydrogen-bond contact with the carbonyl oxygen of His447. On the other hand, the phenolic ring stacked against Trp286 in the PAS (**Figure 3.3A**). Nevertheless, the flexibility conferred by the polymethylene linker in hybrid **26** leads to different arrangements of the tether in the midgorge region, because the carbonyl group present in the tether is capable of forming hydrogen bonds with either Tyr124 or Tyr72.

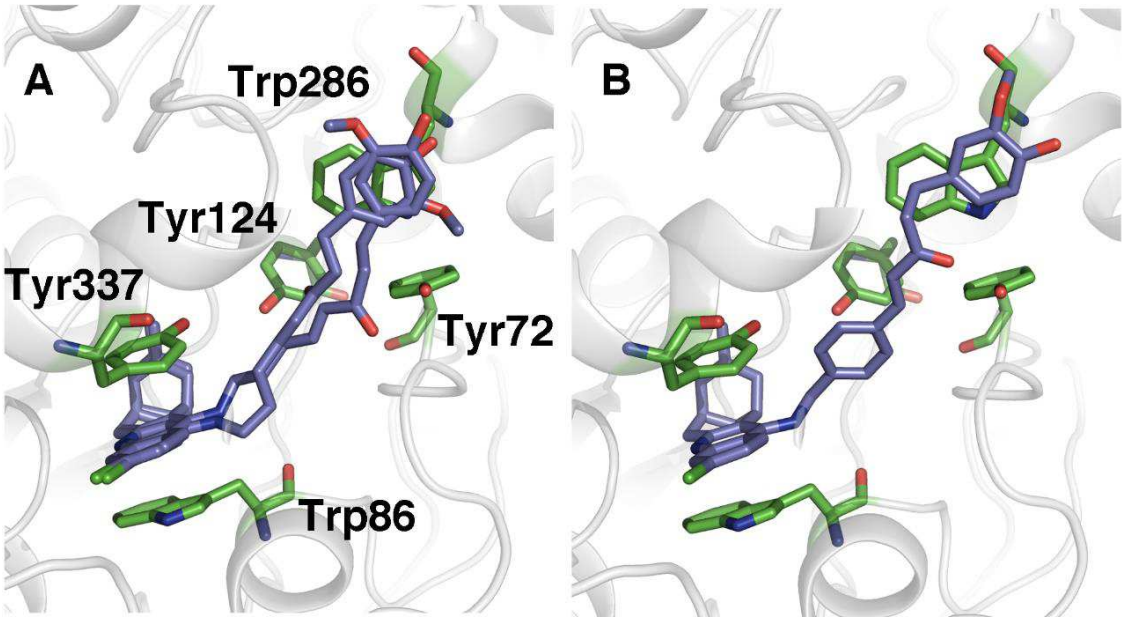

Figure 3.3: Structural detail of the predicted binding mode of the shogaol–huprine hybrids (A) (–)-**26** and (B) (–)-**27** to *h*AChE according to docking calculations.

We also explored the potential effect of introducing a benzene ring conjugated with the α,β-unsaturated ketone (compound (±)-**27**, **Figure 3.2**). This structural change did not alter the ability of the compound to stack against Trp86 and Trp286 in the CAS and PAS, respectively (**Figure 3.3B**). In contrast to **26**, however, most of the docked poses clustered into a single orientation characterized by a hydrogen bond of the carbonyl unit and Tyr72. Overall, the introduction of the benzene ring conjugated with the enone did not appear to be detrimental for the binding mode of the compound within AChE, while, as previously mentioned, it might be valuable to improve the pharmacological profile by targeting the $A\beta_{42}$ and tau aggregation.

3.3 Synthesis of shogaol–huprine hybrids

3.3.1 Synthesis of hybrid 26

We envisaged the synthesis of the oligomethylene-linked hybrid **26** through a cross metathesis between enone **28** and alkene **29** (**Scheme 3.2**).

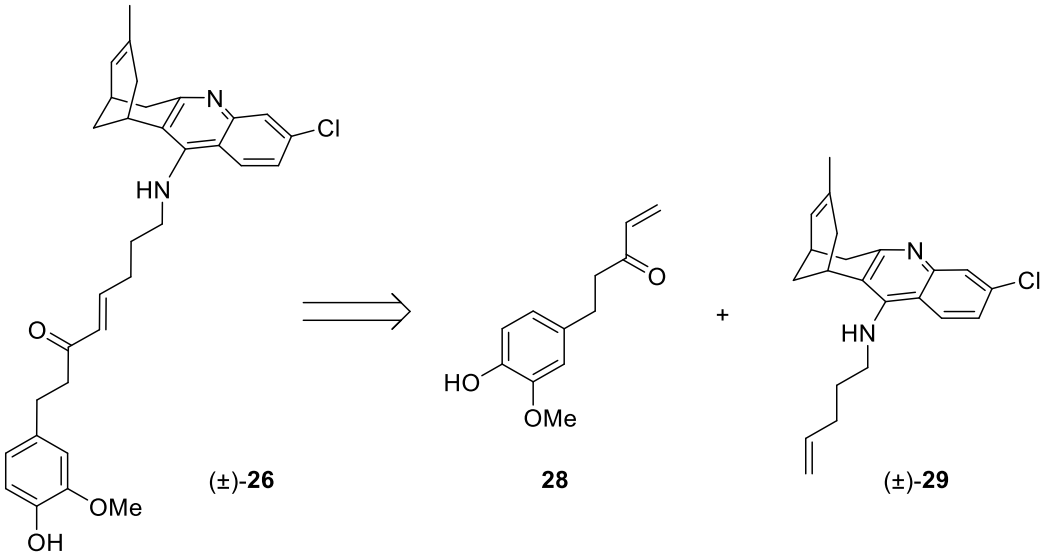

Scheme 3.2

Then, we first proceeded to synthesize enone **28** through a dimethylammonium dimethyl carbamate (DIMCARB)-mediated Mannich-type condensation.[152] Unfortunately, this condensation between vanillylacetone, **30**, and formaldehyde did not work. Further attempts with analogous acetaldehyde in different conditions were also performed without success (**Scheme 3.3**).

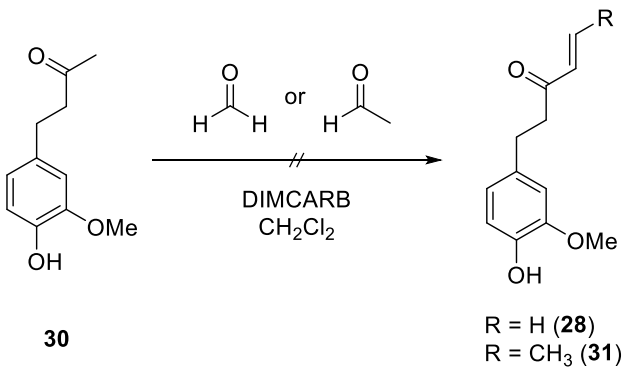

Scheme 3.3

Taking previous issues into account, we re-planned the synthetic pathway by preparing the intermediate 1-(4-hydroxy-3-methoxyphenyl)oct-4-en-3-one, **33**, through the mentioned DIMCARB-mediated Mannich-type condensation (detailed mechanism in **Scheme 3.4**).[152] Thus, we treated under inert conditions a solution of vanillylacetone, **30**, in DIMCARB, which acted as both solvent and catalyst, dropwise using a syringe pump for 10 h with butyraldehyde, **32**. The

[152] N. Mase, N. Kitagawa, K. Takabe. *Synlett* **2010**, *1*, 93.

resulting mixture was stirred at room temperature for 2 days and afforded the desired enone **33** ([4]-shogaol),[152] after silica gel column chromatography purification in 42% yield.

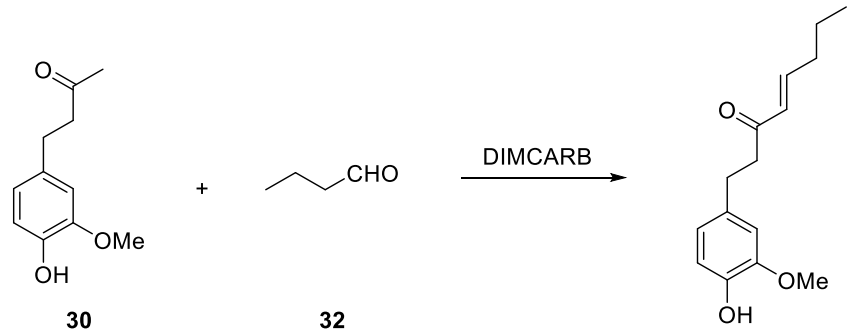

30 **32** **33** (42%)

DIMCARB-mediated Mannich-type condensation mechanism:

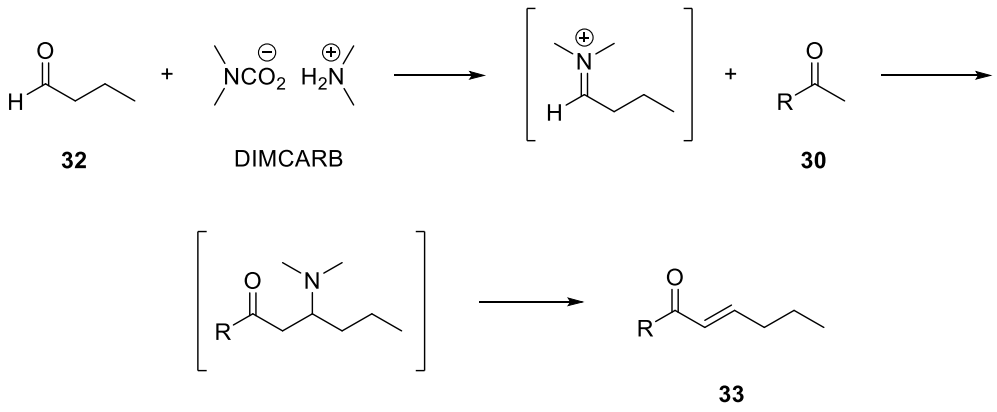

32 DIMCARB **30** **33**

Scheme 3.4

Concurrently, the initial alkylation of racemic huprine Y, **8**, with 5-bromo-1-pentene was carried out in the presence of KOH and anhydrous DMSO at room temperature overnight, affording the desired alkenylhuprine **29** in 30% yield, after silica gel column chromatography purification (**Scheme 3.5**).

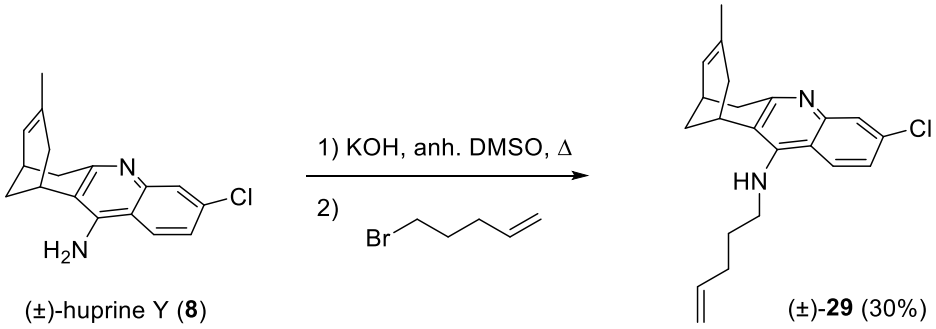

(±)-huprine Y (**8**) (±)-**29** (30%)

Scheme 3.5

Subsequent cross metathesis reaction between the alkenylhuprine **29** and enone **33**, using the Hoveyda–Grubbs second generation catalyst in the presence of *p*-benzoquinone and under reflux for 3 days, afforded hybrid **26** in 15% yield, after two consecutive tedious silica gel column chromatography purifications (**Scheme 3.6**). The observation in the ^{1}H NMR spectrum of **26** of a coupling constant of 15.6 Hz in the signals of the two enone olefin protons was clearly indicative of the *E* configuration of its carbon–carbon double bond.

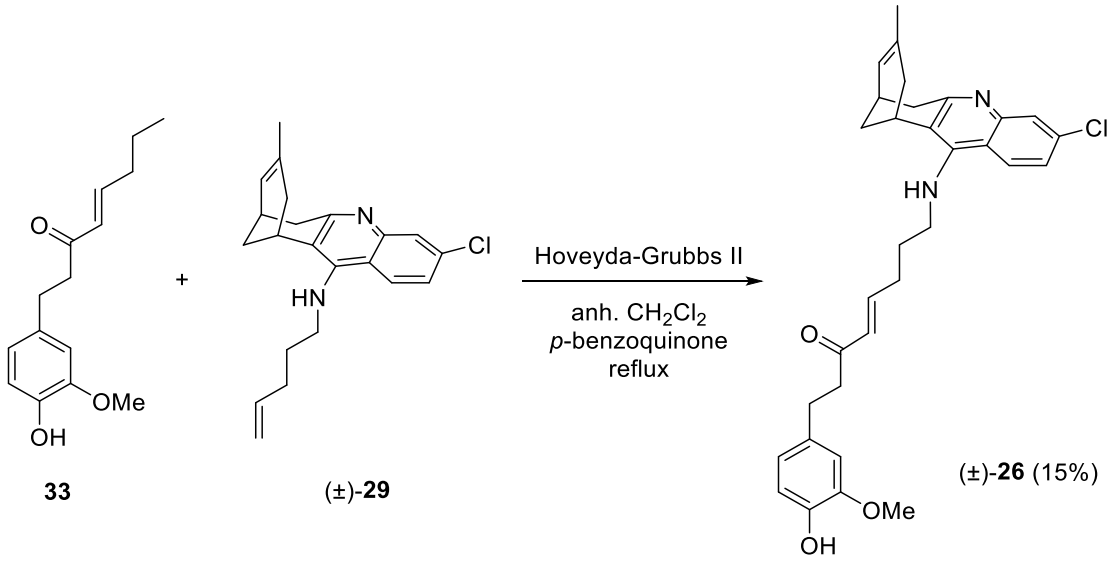

Scheme 3.6

3.3.2 Synthesis of hybrid 27

For the preparation of the *p*-phenylene-linked hybrid **27**, we started synthesizing the aldehyde intermediate **21**. Firstly, alkylation of huprine Y, **8**, with *p*-cyanobenzaldehyde in the presence of freshly distilled morpholine, in toluene under reflux for 2 days, provided, after a silica gel column chromatography purification, the desired imine **34** in 37% yield (**Scheme 3.7**), which was subsequently reduced with $NaCNBH_3$ in glacial AcOH for 3 h at 0 ^{o}C. Silica gel column chromatography purification was needed to obtain the desired amine **35** in 45% yield. Then, amine **35** was quantitatively reduced with DIBAL-H in anhydrous toluene at 0 ^{o}C overnight, to give the desired aldehyde **21**.

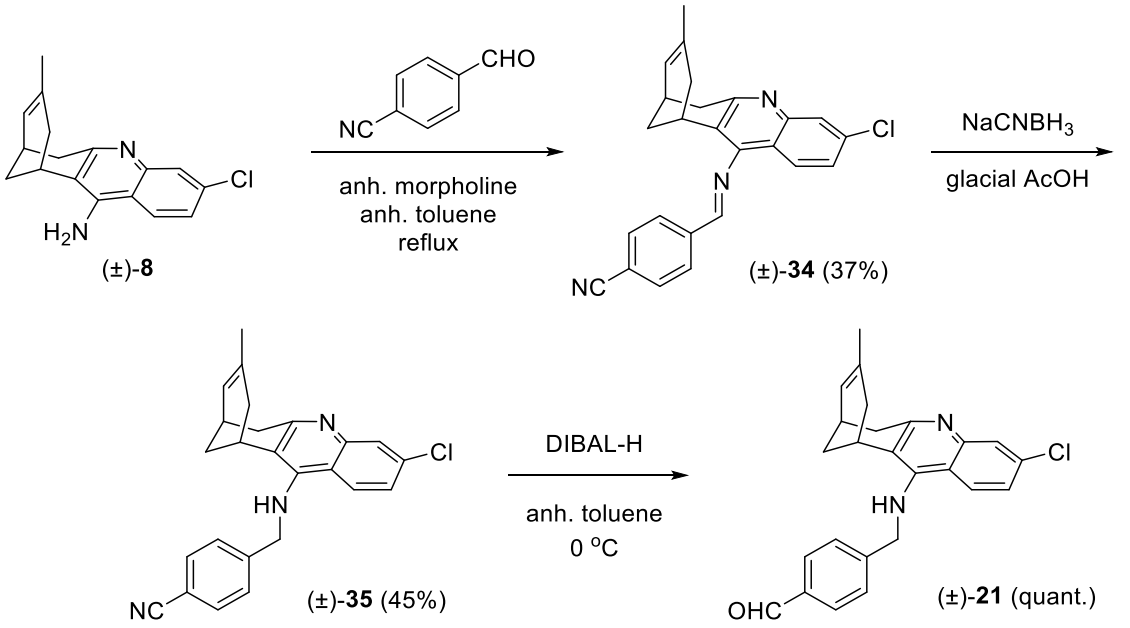

Scheme 3.7

Finally, we carried out another Mannich-type condensation of aldehyde **21** with vanillylacetone, **30**, at 80 °C overnight in a closed vessel, promoted by DIMCARB, which after three consecutive silica gel column chromatography purifications of the resulting reaction crude, gave the desired hybrid **27** in 13% isolated yield. Of note, byproduct **36**, bearing a dimethylaminomethyl substituent at position 3 of the phenolic ring, was also isolated in 15% yield (**Scheme 3.8**).

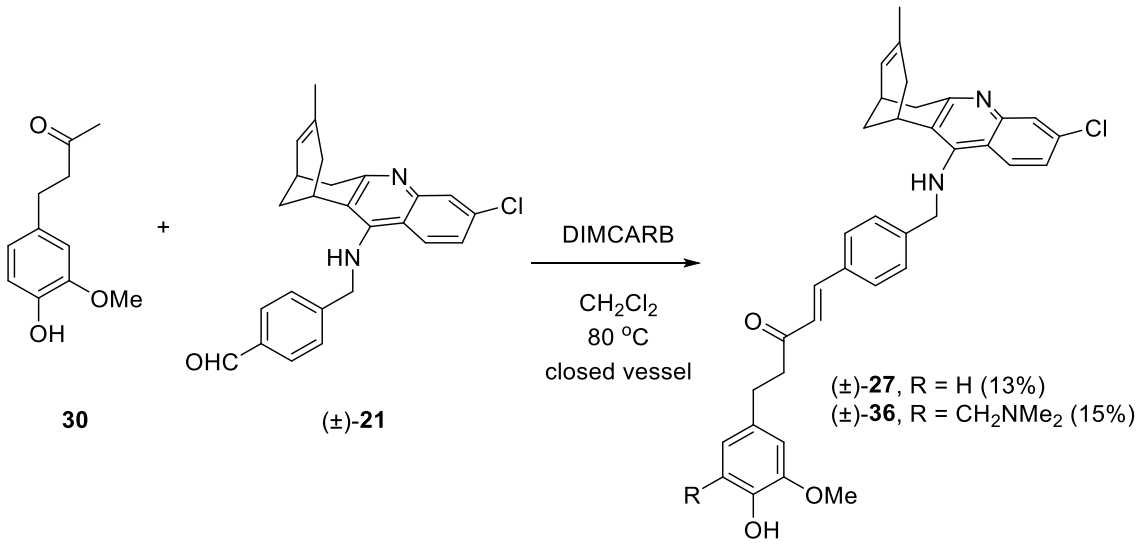

Scheme 3.8

The structural similarity of compound **36** with hybrid **27** and the fact that the presence of an aliphatic amino group in **36**, protonatable at physiological pH, might enhance the interaction of the phenolic moiety with the AChE PAS aromatic residues (mainly Trp286) prompted us to subject also compound **36** to biological evaluation.

3.4 Pharmacological evaluation of shogaol–huprine hybrids

3.4.1 Cholinesterase inhibitory activity

The evaluation of the anticholinesterase activities was carried out by Dr. Victòria Clos's group (*Universitat Autònoma de Barcelona*). The inhibitory activity of the hybrids **26**, **27** and **36** against recombinant *h*AChE and serum *h*BChE was evaluated by the method of Ellman *et al.*,[153] and compared with that of the parent racemic huprine Y, **8**,[154] and [4]-shogaol, **33**, under the same assay conditions (**Table 3.1**).

The shogaol–huprine hybrids are very potent inhibitors of *h*AChE, with IC_{50} values in the low nanomolar range (7–21 nM), being much more potent than the parent [4]-shogaol (28% inhibition at 10 μM), but less potent than huprine Y. The most potent hybrid was compound **26**, which is indeed the most genuine shogaol–huprine hybrid, as it formally results from merging the structure of [4]-shogaol and huprine Y. Hybrid **26** is however only 3-fold more potent than analogs **27** and **36**, bearing a benzene ring conjugated with the shogaol enone group. The presence of an additional basic nitrogen atom at the phenolic ring in hybrid **36** has no influence on the *h*AChE inhibitory activity, with this compound displaying equipotent activity to hybrid **27**.

[153] G. L. Ellman, K. D. Courtney, V. Andres Jr., R. M. Featherstone. *Biochem. Pharmacol.* **1961**, *7*, 88.
[154] C. Galdeano, E. Viayna, I. Sola, X. Formosa, P. Camps, A. Badia, M. V. Clos, J. Relat, M. Ratia, M. Bartolini, F. Mancini, V. Andrisano, M. Salmona, C. Minguillón, G. C. González-Muñoz, M. I. Rodríguez-Franco, A. Bidon-Chanal, F. J. Luque, D. Muñoz-Torrero. *J. Med. Chem.* **2012**, *55*, 661.

Table 3.1: *h*AChE and *h*BChE inhibitory activities of [4]-shogaol (**33**), and the hydrochloride salts of (±)-huprine Y (**8**), and the hybrids (±)-**26**, (±)-**27** and (±)-**36**.

Compound	*h*AChE[a] IC_{50} (nM)	*h*BChE[a] IC_{50} (nM)
(±)-**26**·HCl	6.7 ± 0.1	982 ± 190
(±)-**27**·HCl	18.3 ± 2.0	742 ± 74
(±)-**36**·2HCl	21.1 ± 1.9	181 ± 27
(±)-huprine Y·HCl	0.7 ± 0.3[b]	175 ± 6[b]
[4]-shogaol	[c]	[d]

[a] IC_{50} inhibitory concentration (nM) of human recombinant AChE and human serum BChE. IC_{50} values are expressed as mean ± standard error of the mean (SEM) of at least four experiments, each performed in duplicate.
[b] Data from Ref. 153.
[c] 28% inhibition at 10 µM.
[d] 6% inhibition at 10 µM.

The parent huprine Y exhibits a potent *h*BChE inhibitory activity, even though it is selective against *h*AChE (250-fold). Conversely, the parent [4]-shogaol (**33**) is essentially inactive for *h*BChE inhibition (6% inhibition at 10 µM). Like huprine Y, the shogaol–huprine hybrids turned out to be potent inhibitors of *h*BChE (submicromolar IC_{50} values) and selective towards *h*AChE (selectivity factors of 9–147) The structural features leading to higher *h*BChE inhibitory activity were just the opposite as for *h*AChE inhibition, thereby the hybrids bearing the benzene ring conjugated with the shogaol enone moiety were the most potent. Interestingly, the presence of the amino group at the phenolic ring had a significant influence on this activity, hybrid **36** being 5- and 4-fold more potent *h*BChE inhibitor than **26** and **27**, respectively, and equipotent to huprine Y. This fact might be caused by interaction with the Asp70 and Tyr332, which are located at the lip of the active site gorge, and whose function is to guide down positively charged substrates such as BCh or ACh.[155]

[155] P. Masson, W. Xie, M. T. Froment, V. Levitsky, P. L. Fortier, C. Albaret, O. Lockridge. *Biochim. Biophys. Acta* **1999**, *1433*, 281.

3.4.2 Antioxidant activity

Antioxidant activity assays were performed by Dr. Rosa Lamuela-Raventós's group (*Universitat de Barcelona*). For the evaluation of the putative beneficial effects of the shogaol–huprine hybrids against oxidative stress, their antioxidant capacity (AC) and that of the parent huprine Y and [4]-shogaol was assessed using an $ABTS^{\cdot+}$ radical decolorization assay, the DPPH assay and the Folin–Ciocalteu (F–C) assay as a measure of total phenolics (TP).[156] Gallic acid, a naturally occurring phenolic acid, and trolox, a water-soluble analog of vitamin E, with well-established antioxidant activities were also evaluated as positive standards. The results were calculated as trolox equivalents (μmol Trolox / μmol tested compound) for the $ABTS^{\cdot+}$ and DPPH assays, and as mg of gallic acid equivalents (GAE) / g sample for the F–C assay (**Table 3.2**).

The shogaol–huprine hybrids exhibited a potent antioxidant activity in the $ABTS^{\cdot+}$ and DPPH assays (3–12 trolox eq.), as well as in the TP assay. The order of antioxidant potencies was **36** > **27** > **26**, with the sole exception of the DPPH assay, where hybrid **36** was surprisingly less potent than their analogs, albeit still being 3-fold more potent than trolox. As compared with the reference compounds, the hybrids were less potent antioxidant agents than the parent [4]-shogaol, **33**, and gallic acid, but more potent than huprine Y, **8**, the latter strikingly displaying a remarkable potency, especially in the $ABTS^{\cdot+}$ and DPPH assays (1–2.6 trolox eq.). Thus, even though the shogaol phenolic ring and the enone group and, to a minor extent, the huprine moiety of these hybrids must impart antioxidant activity, the presence in the linker of the benzene ring conjugated with the shogaol enone group as well as the dimethylaminomethyl group at the shogaol phenolic ring of **36** seemed to be beneficial for antioxidant activity. Overall, the potent antioxidant activity of the shogaol–huprine hybrids constitutes a very valuable complement to their potent anticholinesterase inhibitory activities in the context of a MTDL anti-Alzheimer treatment.

[156] R. L. Prior, X. Wu, K. Schaich. *J. Agric. Food Chem.* **2005**, *53*, 4290.

Table 3.2: Antioxidant activity of [4]-shogaol (**33**), and the hydrochloride salts of (±)-huprine Y (**8**), and the hybrids (±)-**26**, (±)-**27** and (±)-**36**.

Compound	ABTS$^{\cdot+}$[a] (trolox eq.)	DPPH[a] (trolox eq.)	TP[a] (mg GAE / g sample)
(±)-**26**·HCl	7.6 ± 0.6	6.6 ± 0.5	29.8 ± 2.6
(±)-**27**·HCl	10.5 ± 0.6	8.8 ± 0.7	50.0 ± 2.4
(±)-**36**·2HCl	11.8 ± 0.5	2.8 ± 0.1	68.8 ± 4.3
(±)-huprine Y·HCl	2.6 ± 0.2	1.0 ± 0.01	10.2 ± 1.3
[4]-shogaol	26.2 ± 0.2	12.2 ± 0.2	384 ± 25
gallic acid	18.6 ± 0.1	10.3 ± 0.04	1033 ± 25

[a] Antioxidant capacity measured through ABTS$^{\cdot+}$, DPPH, or total polyphenols. Values are expressed as mean ± SEM of three experiments.

3.4.3 Aβ$_{42}$ and tau anti-aggregating activity

Some classes of AChE inhibitors, especially dual binding site inhibitors, are often endowed with Aβ anti-aggregating properties,[157] which arise either from blockade of the AChE PAS (blockade of AChE-induced Aβ aggregation)[66] or from a direct interaction with Aβ (blockade of spontaneous Aβ aggregation), in the latter case likely due to the presence of aromatic planar moieties in the inhibitors as mentioned in the design section in this chapter. In this case, only the spontaneous anti-aggregating potencies are determined, thereby in the absence of AChE. The protein anti-aggregating assays were carried out by Dr. Raimon Sabaté's group (*Universitat de Barcelona*). The methodology consisted of overexpression of amyloid-prone proteins in *E. coli* through a methodology previously described by his group. The extent of aggregation of those proteins can be monitored measuring the variations of the fluorescence of Thioflavin-S (Th-S).[158]

The same order of potencies against both Aβ$_{42}$ and tau aggregation were found for the three shogaol–huprine hybrids (**Table 3.3**), which supports the existence of common mechanisms behind the aggregation of different amyloidogenic proteins and the likelihood of

[157] E. Viayna, R. Sabaté, D. Muñoz-Torrero. *Curr. Top. Med. Chem.* **2013**, *13*, 1820.
[158] S. Pouplana, A. Espargaró, C. Galdeano, E. Viayna, I. Sola, S. Ventura, D. Muñoz-Torrero, R. Sabaté. *Curr. Med. Chem.* **2014**, *21*, 1152.

common treatments against different amyloidogenic diseases.[159] For this particular family of compounds, the $A\beta_{42}$ and tau anti-aggregating activities were in the ranges 39–71% and 35–51%, respectively, using a 10 μM concentration of the hybrids, with these compounds being clearly more potent than the parent huprine Y and [4]-shogaol, **33** (about 10% inhibition at 10 μM). The order of potencies among the hybrids for both activities was **27** > **36** > **26**, as expected and in agreement with the beneficial effect of the additional benzene ring in hybrids **27** and **36**. The presence of several aromatic moieties with extended π-conjugated systems seems to play an important role for the anti-aggregating activities. On the other hand, the presence of the dimethylaminomethyl group in the phenolic ring of **36** was rather detrimental for these activities. Overall, hybrids **27** and **36** emerge as moderately potent $A\beta_{42}$ and tau anti-aggregating agents, with IC_{50} values that must be in the low micromolar range.

Table 3.3: $A\beta_{42}$ and tau anti-aggregating activities of [4]-shogaol (**33**), and the hydrochloride salts of (±)-huprine Y (**8**), and the hybrids (±)-**26**, (±)-**27** and (±)-**36**.

Compound	$A\beta_{42}$ aggregation[a] (% inh. at 10 μM)	tau aggregation[a] (% inh. at 10 μM)
(±)-**26**·HCl	39.3 ± 2.8	35.2 ± 2.3
(±)-**27**·HCl	70.6 ± 4.3	51.0 ± 1.9
(±)-**36**·2HCl	53.9 ± 4.4	40.1 ± 2.4
(±)-huprine Y·HCl	8.9 ± 1.3	7.6 ± 3.4
[4]-shogaol	10.5 ± 0.8	9.2 ± 0.7

[a] % of inhibition of $A\beta_{42}$ and tau protein aggregation at 10 μM in intact *E. coli* cells. Values are expressed as mean ± SEM of four independent experiments.

3.4.4 In vitro BBB permeation assay

In order to demonstrate the ability of the shogaol–huprine hybrids to cross the BBB and access the CNS, which is obviously a necessary condition for CNS drugs, Dr. Belén Pérez (*Universitat Autònoma de Barcelona*) applied the parallel artificial membrane permeability assay

[159] H.-Y. Zhang. *Biochem. Biophys. Res. Commun.* **2006**, *351*, 578.

(PAMPA)-BBB assay, a well-established *in vitro* test that uses an artificial membrane model.[160] Previous results from *in vitro*, *ex vivo*, and *in vivo* studies have shown that huprine Y and several classes of huprine-based hybrid compounds can readily cross the BBB, leading to central effects.[141,154,161,162] Conversely, phenolic antioxidants usually have low bioavailabilities and inherent difficulties to cross the BBB,[163] thereby making it imperative the assessment of the ability of the shogaol–huprine hybrids to enter the brain. The *in vitro* permeability (P_e) of the shogaol–huprine hybrids, the parent compounds huprine Y and [4]-shogaol, **33**, was determined (**Table 3.4**).

Regarding the limits established for BBB permeation,[160] compounds with P_e (10^{-6} cm s^{-1}) > 5.2 would be expected to have high BBB permeation (CNS+) and compounds with P_e (10^{-6} cm s^{-1}) < 2.1 would have low BBB permeation (CNS–). The three shogaol–huprine hybrids, like the parent huprine Y and [4]-shogaol, were predicted to be able to cross the BBB, as their P_e values were above the threshold for high BBB permeation, which should enable them to reach their multiple CNS targets. Notwithstanding the apparent brain permeability of the shogaol–huprine hybrids, it would remain to be determined whether other pharmacokinetic properties are so favorable, especially taking into account the known phase II metabolic liability of polyphenolic compounds.[164,165]

[160] L. Di, E. Kerns, K. Fan, O. McConnell, G. Carter. *Eur. J. Med. Chem.* **2003**, *38*, 223.
[161] P. Camps, R. El Achab, J. Morral, D. Muñoz-Torrero, A. Badia, J. E. Baños, N. M. Vivas, X. Barril, M. Orozco, F. Javier Luque. *J. Med. Chem.* **2000**, *43*, 4657.
[162] M. Hedberg, M. V. Clos, M. Ratia, D. Gonzalez, C. U. Lithner, P. Camps, D. Muñoz-Torrero, A. Badia, L. Giménez-Llort, A. Nordberg. *Neurodegener. Dis.* **2010**, *7*, 379.
[163] J. Teixeira, T. Silva, P. B. Andrade, F. Borges. *Curr. Med. Chem.* **2013**, *20*, 2939.
[164] A. Mattarei, M. Azzolini, M. Carraro, N. Sassi, M. Zoratti, C. Paradisi, L. Biasutto. *Mol. Pharmaceutics* **2013**, *10*, 2781.
[165] S. Barnes, J. Prasain, T. D'Alessandro, A. Arabshahi, N. Botting, M. A. Lila, G. Jackson, E. M. Janleb, C. M. Weaver. *Food Funct.* **2011**, *2*, 235.

Table 3.4: Permeability results from the PAMPA-BBB assay of [4]-shogaol (**33**), and the hydrochloride salts of (±)-huprine Y (**8**), and the hybrids (±)-**26**, (±)-**27** and (±)-**36**.

Compound	P_e (10^{-6} cm s^{-1})[a]	Prediction
(±)-**26**·HCl	11.7 ± 0.4	CNS+
(±)-**27**·HCl	6.5 ± 0.8	CNS+
(±)-**36**·2HCl	8.4 ± 1.3	CNS+
(±)-huprine Y·HCl	21.9 ± 1.2	CNS+
[4]-shogaol	14.7 ± 0.5	CNS+

[a] Permeability values from the PAMPA-BBB assay. Values are expressed as the mean ± SD of three independent experiments.

CHAPTER 4

Rhein–modified huprine hybrids

Rheum rhabarbarum (Rhubarb)

Image source: Vladimír Motyčka. Botanická fotogalerie (*www.botanickafotogalerie.cz*)

4.1 Background

4.1.1 First generation of rhein–huprine hybrids

The design of these hybrids had its origin in the finding that compounds sharing a core structure of hydroxyanthraquinones displayed tau anti-aggregating properties *in vitro* with IC_{50} values in the low micromolar range.[166,167] The structurally related compound rhein, (**37**, **Figure 4.1**), is a natural product found in the traditional Chinese herbal medicine rhubarb (*Rheum rhabarbarum*), which is well tolerated in humans.[168] Accordingly, in the context of Drs. Elisabet Viayna and Irene Sola's PhD Theses, the first generation of rhein–huprine hybrids was prepared and biologically tested. These compounds combined a unit of rhein, which we found to display moderately potent $A\beta_{42}$ and tau anti-aggregating activity, and a unit of the potent AChE inhibitor huprine Y, with the lead compound being (±)-**16**.[141,169]

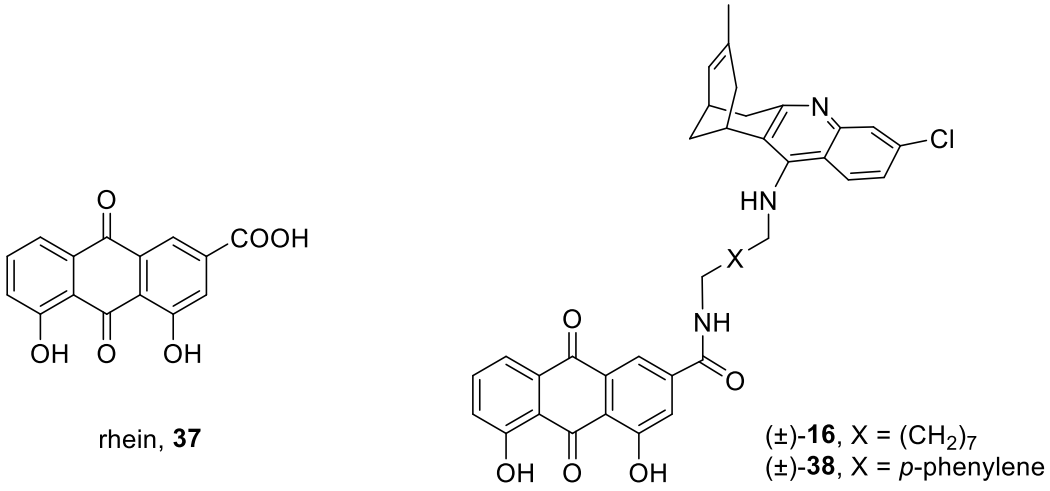

Figure 4.1: Rhein, **37**, the lead compound of the first generation of rhein–huprine hybrids, (±)-**16**, and the *p*-phenylene-linked analog (±)-**38**.

[166] M. Pickhardt, Z. Gazova, M. v. Bergen, I. Khlistunova, Y. Wang, A. Hascher, E.-M. Mandelkow, J. Biernat, E. Mandelkow. *J. Biol. Chem.* **2005**, *280*, 3628.
[167] B. Bulic, M. Pickhardt, B. Schmidt, E.-M. Mandelkow, H. Waldmann, E. Mandelkow. *Angew. Chem. Int. Ed.* **2009**, *48*, 1740.
[168] X. Yang, G. Sun, C. Yang, B. Wang. *ChemMedChem* **2011**, *6*, 2294.
[169] F. G. Serrano, C. Tapia-Rojas, F. J. Carvajal, P. Cisternas, E. Viayna, I. Sola, D. Muñoz-Torrero, N. C. Inestrosa. *Curr. Alzheimer Res.* **2016**, *13*, 1017.

These hybrids were endowed with a very interesting *in vitro* and *in vivo* multi-target profile, especially compound **16**, which displayed cholinergic activity through inhibition of human cholinesterases (*h*AChE, IC_{50} = 3.60 nM; and *h*BChE, IC_{50} = 620 nM) and $A\beta_{42}$ and tau anti-aggregating activity (48% and 30% inhibition at 10 μM, respectively). Surprisingly, the lead compound **16** was found to be a potent inhibitor of *h*BACE1 (IC_{50} = 120 nM), which led to a significant Aβ lowering effect in a transgenic mouse model of AD (APP/PS1 mice).[141,169] As expected, molecular modeling studies suggested that the potent inhibitory activity of these hybrids against *h*AChE stems from a dual binding mode within the enzyme (**Figure 4.2**).[141]

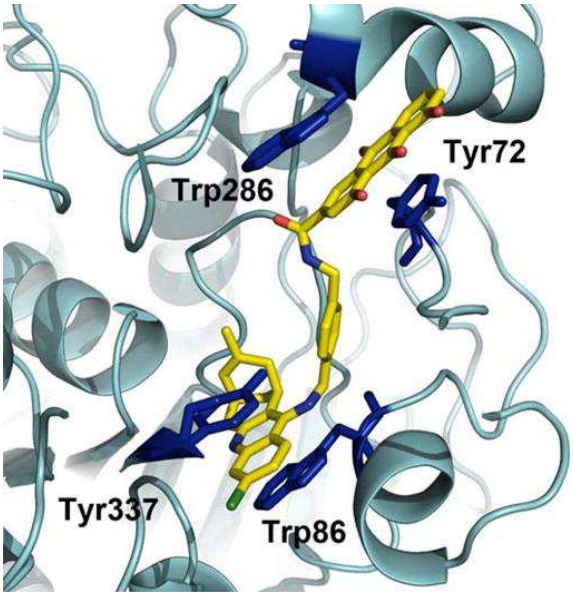

Figure 4.2: Binding mode of the *p*-phenylene-linked rhein–huprine hybrid (–)-**38**, a less flexible analog of **16**, within *h*AChE. This compound was chosen due to the limited number of rotatable bonds as compared with **16** (Image source: E. Viayna, I. Sola, M. Bartolini *et al*. *J. Med. Chem.* **2014**, *57*, 2549).

4.1.2 Further computational studies within BACE1

As discussed in sections **1.2.1** and **1.4.3.1**, BACE1 is the enzyme involved in the first and rate limiting step of Aβ formation from the APP cleavage, which has made BACE1 the focus of very intensive research efforts. However, BACE1 has proven to be a difficult target, mainly due to its intrinsic flexibility, involving large domain motions.[170]

[170] S. Patel, L. Vuillard, A. Cleasby, C. Murray, J. Yon. *J. Mol. Biol.* **2004**, *343*, 407.

Given the unexpected high potency against BACE1 exhibited by compound **16**, it was worthwhile to carry out molecular dynamics studies to shed light on the binding mode within BACE1. In a first step, this was accomplished by examining the druggable pockets present in the enzyme in order to determine their ability to accommodate the huprine and hydroxyanthraquinone moieties. Two druggable pockets, namely BS1, which encompasses the catalytic site, and BS2, which includes unexplored subsites, were found to be suitable for binding of the huprine and hydroxyanthraquinone moieties present in hybrids (**Figure 4.3**). Furthermore, the distance between huprine and hydroxyanthraquinone in these pockets was comprised between 7 and 11 Å, thus satisfying the geometrical criteria required for the tether in the rhein−huprine hybrids. Accordingly, docking of (±)-**38**, a more rigid *p*-phenylene-linked analog of **16**, was performed by exploring the volume defined by both BS1 and BS2 sites. Even though this *p*-phenylene-linked rhein–huprine hybrid was not the most potent of the series (IC_{50} = 2 μM), it was chosen for the molecular modeling studies due to the limited number of rotatable bonds, which thus makes it easier to perform a more exhaustive exploration of the binding mode. Calculations suggested a clear dual binding mode, in which the huprine moiety is accommodated at the BS1 pocket, and the hydroxyanthraquinone moiety fills the BS2 site (**Figure 4.3**). The huprine moiety remains tightly bound to BS1 in all cases, as expected from the electrostatic stabilization between the protonated aminoquinoline system and the catalytic dyad (Asp32 and Asp228), whereas the bicyclic system of the huprine moiety fills a hydrophobic pocket near the catalytic dyad. On the other hand, the hydroxyanthraquinone moiety in (+)-**38** (for the sake of simplicity, only this enantiomer is explained) exhibits a common binding mode, which involves the electrostatic interaction with Lys321, hydrogen bonds with the backbone of Phe322 and the side chain of Asn233, and hydrophobic contacts with Val309 (**Figure 4.3**). On the basis of these findings, it is reasonable to expect that the larger flexibility afforded by the linker in **16** will facilitate a proper accommodation to both BS1 and BS2 in BACE1, thus explaining the increase in BACE1 inhibitory activity. Overall, this analysis suggested that BS2 might be exploited to find novel moieties, leading to enhanced binding affinity and hence to hybrid compounds with more potent inhibitory activity against BACE1.[141]

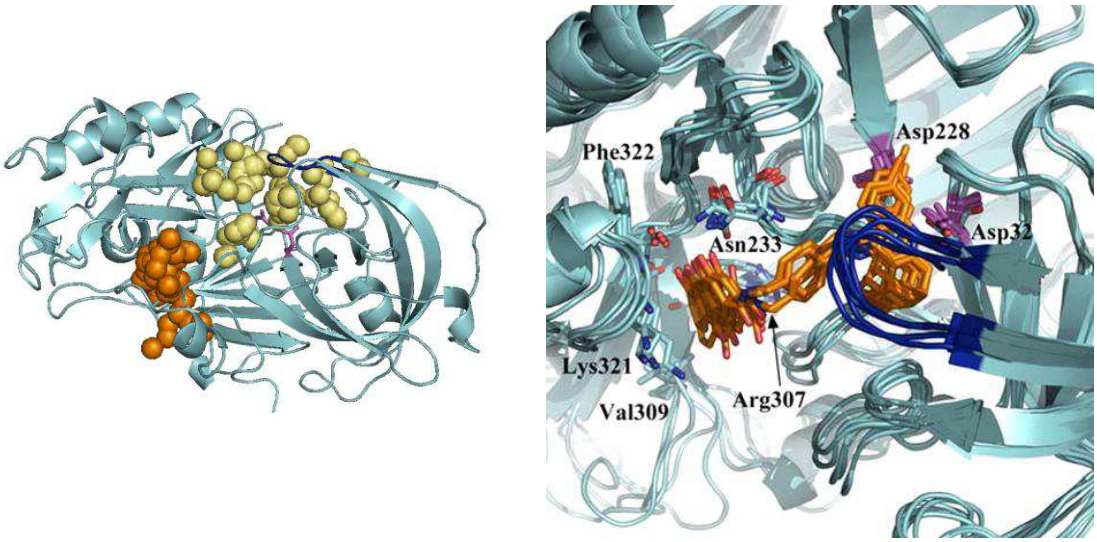

Figure 4.3: Left: representation of the two druggable pockets, namely BS1 (yellow spheres), which encompasses the catalytic site and is shaped by the "flap" (shown in blue), and BS2 (orange spheres), an unexplored secondary site within BACE1. Right: superposition of four independent molecular dynamic simulations of hybrid (+)-**38** bound to BACE1 (Image source: E. Viayna, I. Sola, M. Bartolini *et al*. *J. Med. Chem.* **2014**, *57*, 2549).

4.2 Design of the second generation of rhein–huprine hybrids

According to the predicted binding mode of the rhein–huprine hybrid **38**, the huprine moiety of **16**, protonated at physiological pH, would interact at the catalytic site of both AChE and BACE1. In AChE, it enables cation-π interactions, apart from π-stacking, with the indole ring of Trp86 and the benzene ring of Tyr337 and hydrogen bonding with the His447 carbonyl oxygen, while in BACE1 it might be involved in a salt bridge with the Asp32 and Asp228 residues of the catalytic dyad. The basicity of the huprine moiety of **16** is therefore crucial for AChE and BACE1 inhibition. However, in general, high basicity has been associated with poor permeation through biological membranes and P-glycoprotein (P-gp)-mediated efflux.[171,172] Indeed, reduction of the basicity of amidine-based BACE1 inhibitors has been successfully used to ameliorate oral bioavailability and CNS distribution.[173] The experimentally determined pK_a value of huprine X, a

[171] Z. Rankovic. *J. Med. Chem.* **2015**, *58*, 2584.
[172] T. Ginman, J. Viklund, J. Malmström, J. Blid, R. Emond, R. Forsblom, A. Johansson, A. Kers, F. Lake, F. Sehgelmeble, K. J. Sterky, M. Bergh, A. Lindgren, P. Johansson, F. Jeppsson, J. Fälting, Y. Gravenfors, F. Rahm. *J. Med. Chem.* **2013**, *56*, 4181.
[173] F. Rombouts, G. Tresadern, O. Delgado, C. Martínez-Lamenca, M. v. Gool, A. García-Molina, S. Alonso de Diego, D. Oehlrich, H. Prokopcova, J. M. Alonso, N. Austin, H. Borghys, S. v. Brandt, M. Surkyn, M. De Cleyn, A. Vos, R. Alexander, G. Macdonald, D. Moechars, H. Gijsen, A. Trabanco. *J. Med. Chem.* **2015**, *58*, 8216.

9-ethyl analog of huprine Y, is 8.9,[174] which compares well with the pK_a values reported for some cyclic amidines.[173] Thus, we assumed that huprine Y and its derivatives, such as the rhein–huprine hybrid **16**, should have a similar pK_a, and hence, they should be prevalently protonated at physiological pH and might suffer at some extent from permeability or P-gp efflux issues. In the case of BACE1, the optimal balance between the relevant properties of enzymatic potency, cellular potency, passive permeability and P-gp mediated efflux, has been reported for compounds with pK_a values between 7 and 7.5.[175]

In this context, a second generation of rhein–huprine hybrids was designed using as a template the lead compound **16** by structural modification of its huprine moiety, with the aim of exploring the effect on biological activities of reducing the basicity of the pyridine nitrogen, and with the prospect of identifying a novel analog with favorable multi-target activity profile and reduced basicity, which might result in a better bioavailability. Thus, we envisaged the replacement of the chlorobenzene ring of the huprine Y moiety of hybrid **16** by other aromatic or heteroaromatic rings. We made a selection on the basis of the calculated pK_a values of the corresponding modified huprines, using MarvinSketch 16.2.15 software, and taking into account the commercial availability of the necessary 2-aminonitriles. In this way, three modified huprines (**39a-c**, **Figure 4.4**) were selected. Furthermore, the modified huprine **39d** was selected to explore the effect of increased basicity.

Afterwards, with the aim of obtaining more accurate pK_a values of the modified huprine moieties, high-level quantum mechanical (QM) computations were carried by the group of Dr. F. Javier Luque (*Universitat de Barcelona*). Calculations were performed both for the unsubstituted monomeric modified huprines **39a-d** as well as for their corresponding derivatives methylated at the exocyclic primary amino group, which was considered to take into account the effect of the methylenic linker of the hybrids (**Table 4.1**). We found that methylation of the primary amino group consistently led to a reduction of one unit of the calculated pK_a value.

[174] P. Camps, B. Cusack, W. D. Mallender, R. El Achab, J. Morral, D. Muñoz-Torrero, T. L. Rosenberry. *Mol. Pharmacol.* **2000**, *57*, 409.
[175] A. Lerchner, R. Machauer, C. Betschart, S. Veenstra, H. Rueeger, C. McCarthy, M. Tintelnot-Blomley, A.-L. Jaton, S. Rabe, S. Desrayaud, A. Enz, M. Staufenbiel, P. Paganetti, J.-M. Rondeau, U. Neumann. *Bioorg. Med. Chem. Lett.* **2010**, *20*, 603.

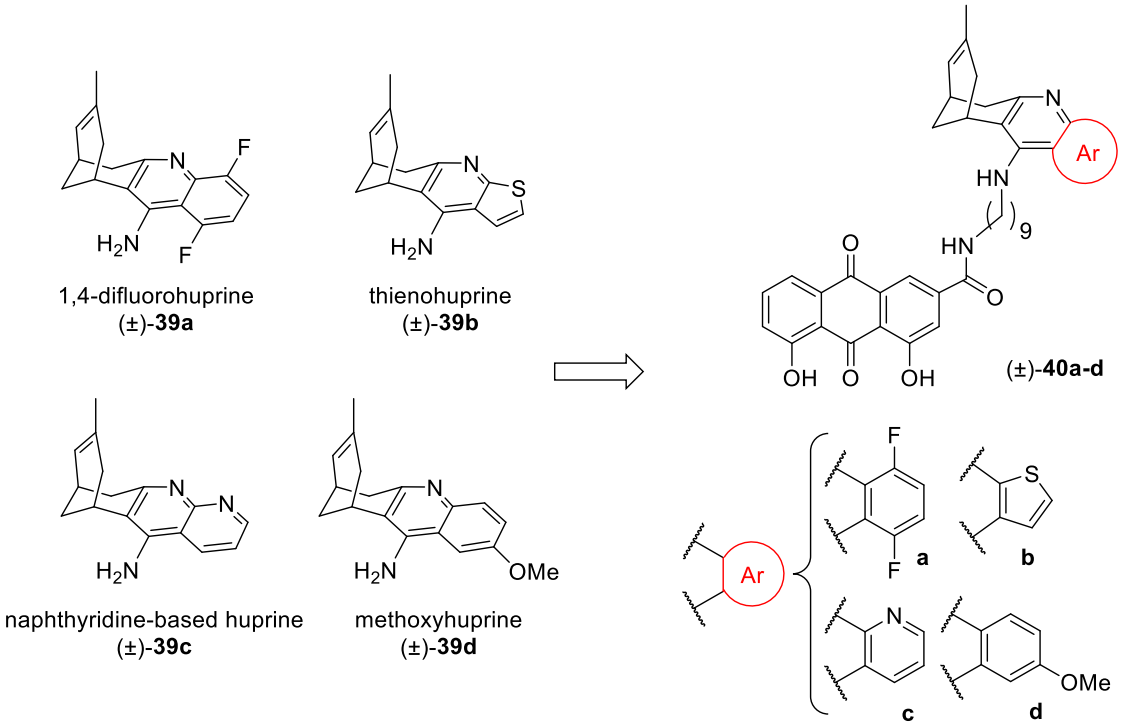

Figure 4.4: Selected modified huprines with various basicities (**39a-d**), and their corresponding rhein–huprine hybrids (**40a-d**).

Table 4.1: Calculated pK_a values of selected compounds determined from high-level QM calculations.

Compound	R	pK_a (QM)[a]
Huprine Y	H	9.5
	CH_3	8.2
39a	H	7.8
	CH_3	7.0
39b	H	7.6
	CH_3	6.7
39c	H	10.1
	CH_3	9.2
39d	H	10.1
	CH_3	8.8

[a] The pK_a values were estimated from high-level QM computations, which combine MP2 calculations with extrapolation to complete basis set effects, higher-order electron correlation effects at the CCSD level, and solvation effects through continuum solvation models.

Using this protocol, two of the selected compounds were predicted to be into the desired range of pK_a values (**39a** and **39b**), thereby with reduced basicity compared to huprine Y, while the other two selected compounds were predicted to be slightly more basic than huprine Y (**39d**, and surprisingly **39c**). Regardless of the different ranges of the calculated pK_a values, all the novel rhein–huprine hybrids **40a**-**d** (**Figure 4.4**) should be protonated in the acidic endosomal compartments (pH 4.5–6.5) where BACE1 localizes and is optimally active,[176-178] so that they should retain the ability to establish a salt bridge with the aspartate residues of the catalytic dyad of BACE1. Likewise, at physiological pH and at the experimental conditions for evaluation of the AChE inhibitory activity (pH 8.0), the most basic huprines **39c** and **39d** and the corresponding hybrids **40c** and **40d** should be mostly protonated, which should have positive implications regarding AChE inhibition but might lead to membrane permeability issues or P-gp efflux liability. In contrast, the least basic huprines **39a** and **39b** and the hybrids **40a** and **40b** should predominate in the neutral form in both conditions, which might be detrimental for AChE inhibition but favorable for tissue distribution.

4.3 Synthesis of rhein–modified huprine hybrids

For the preparation of the distinct modified huprine derivatives, we first needed to prepare the intermediate enone **48**, through the synthetic procedure developed by the group of Prof. Pelayo Camps (**Scheme 4.1**).[142,146,147] The synthetic route consisted of a first acidic hydrolysis of the diacetal **41** to give malondialdehyde, **42**, which subsequently reacted with 2 equivalents of dimethyl 1,3-acetonedicarboxylate, **43**, in the presence of NaOH in MeOH, the so-called Weiss-Cook condensation, affording the tetraester **44** in 41% overall yield. Later on, the tetraester **44** was subjected to acidic hydrolysis followed by decarboxylation to give diketone **45** in 70% yield, which was then treated with 1 equivalent of MeLi in anhydrous THF at 0 ^{o}C to provide oxaadamantanol **46** in 99% yield, followed by the transformation to the corresponding mesylate, **47**, in quantitative yield after reacting with MsCl in the presence of Et_3N at -10 ^{o}C. Finally, silica gel mediated fragmentation of mesylate **47** provided the desired intermediate enone **48** in 85% yield, after silica gel column chromatography purification.

[176] A. Sorkin, M. von Zastrow. *Nat. Rev. Mol. Cell Biol.* **2002**, *3*, 600.
[177] X. Zhang, W. Song. *Alzheimers Res. Ther.* **2013**, *5*, 46.
[178] V. Hook, T. Toneff, W. Aaron, S. Yasothornsrikul, R. Bundey, T. Reisine. *J. Neurochem.* **2002**, *81*, 237.

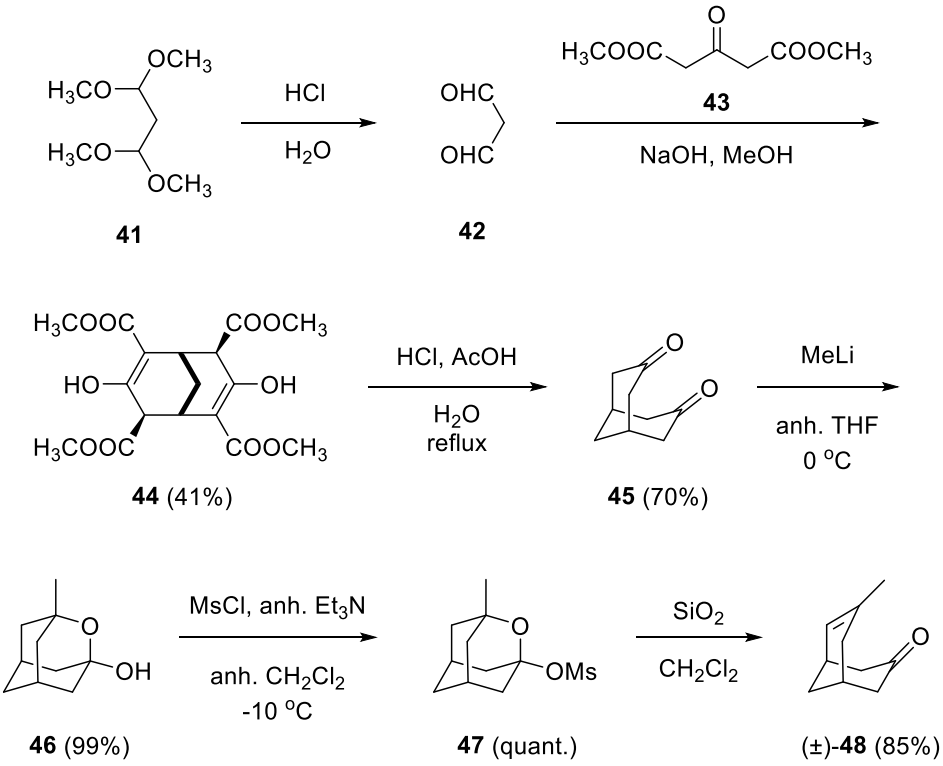

Scheme 4.1

The following synthetic step comprised a Friedländer condensation of enone **48** with the adequate aminonitrile **49a-d** in 1,2-dichloroethane under reflux and $AlCl_3$ catalysis, to afford the known huprine **39c**,[179] and the novel huprines **39a**, **39b** and **39d**, in moderate to good yields (37–80% yield) after silica gel column chromatography purification (**Scheme 4.2**). Of note, the synthesis of **40d** was carried out by Dr. Nibal Betari, from the group of Prof. Vincenzo Tumiatti (*Università di Bologna*), during her research placement in our laboratory.

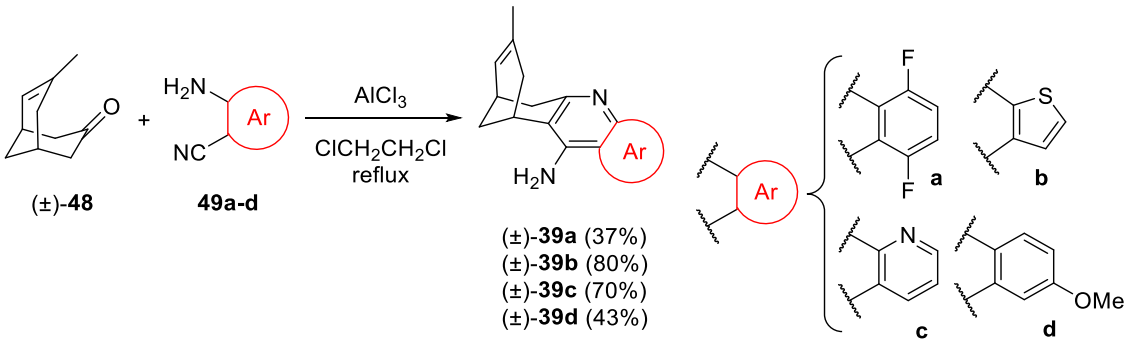

Scheme 4.2

[179] C. Ronco, G. Sorin, F. Nachon, R. Foucault, L. Jean, A. Romieu, P.-Y. Renard. *Bioorg. Med. Chem.* **2009**, *17*, 4523.

Alkylation of the modified huprines **39a-d** with 9-bromononanenitrile, **50c**, in the presence of KOH in DMSO at room temperature overnight, led to nitriles **51a-d** after column chromatography purification in moderate to good yields (29–82%, **Scheme 4.3**). It should be noted that 9-bromononanenitrile, **50c**, is not commercially available, consequently it had to be prepared by reaction between 1,8-dibromooctane and NaCN, and purified by a tedious micro-distillation process from a mixture with unreacted dibromoalkane and di-reacted byproduct.

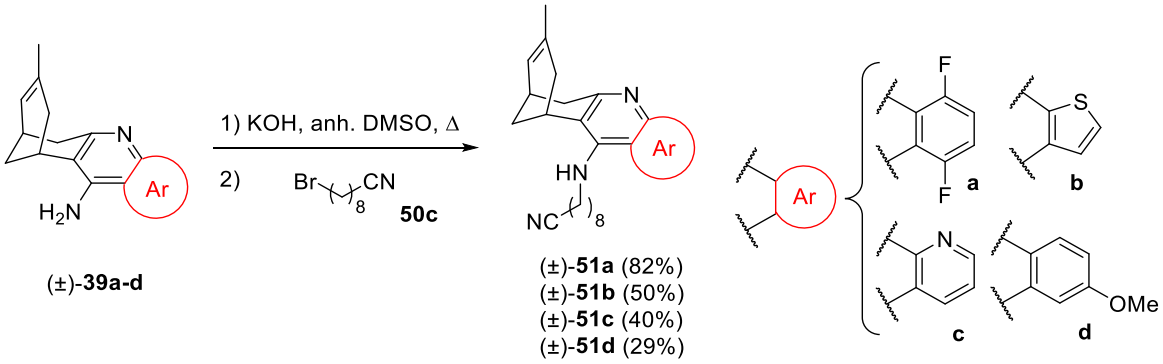

Scheme 4.3

Afterwards, nitriles **51a-d** were reduced by treatment with $LiAlH_4$ in Et_2O at room temperature overnight, to afford the corresponding aminononylhuprines **52a-d** in moderate to high yield without the need of further purification (**Scheme 4.4**), except in the case of **52c**, which had to be purified by tedious silica gel column chromatography to separate it from a byproduct that seemed to arise from the reduction of the aromatic ring.

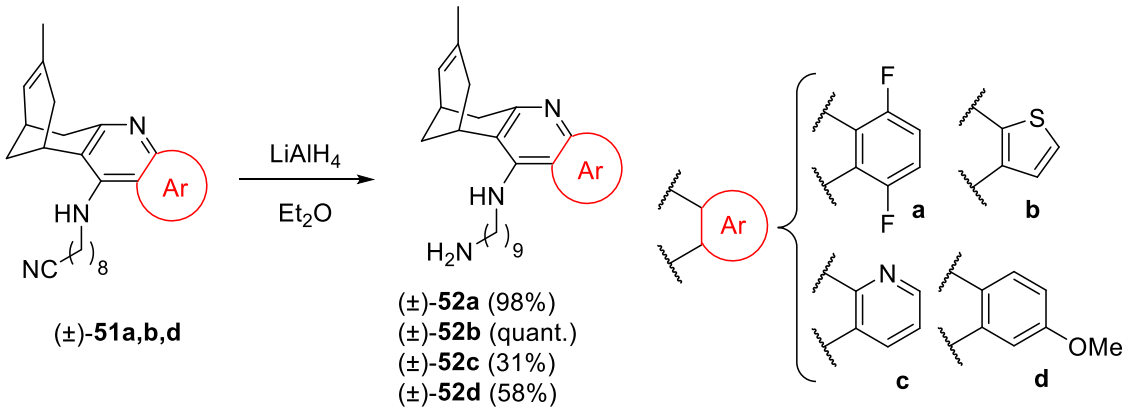

Scheme 4.4

Final coupling reaction between rhein, **37**, and the corresponding primary amines **52a-d** was performed in the presence of EDC, HOBt, and Et_3N in a mixture EtOAc / DMF at room

temperature for 24 h, to provide the target rhein–huprine hybrids **40a-d** in good yields (45–90%, **Scheme 4.5**).

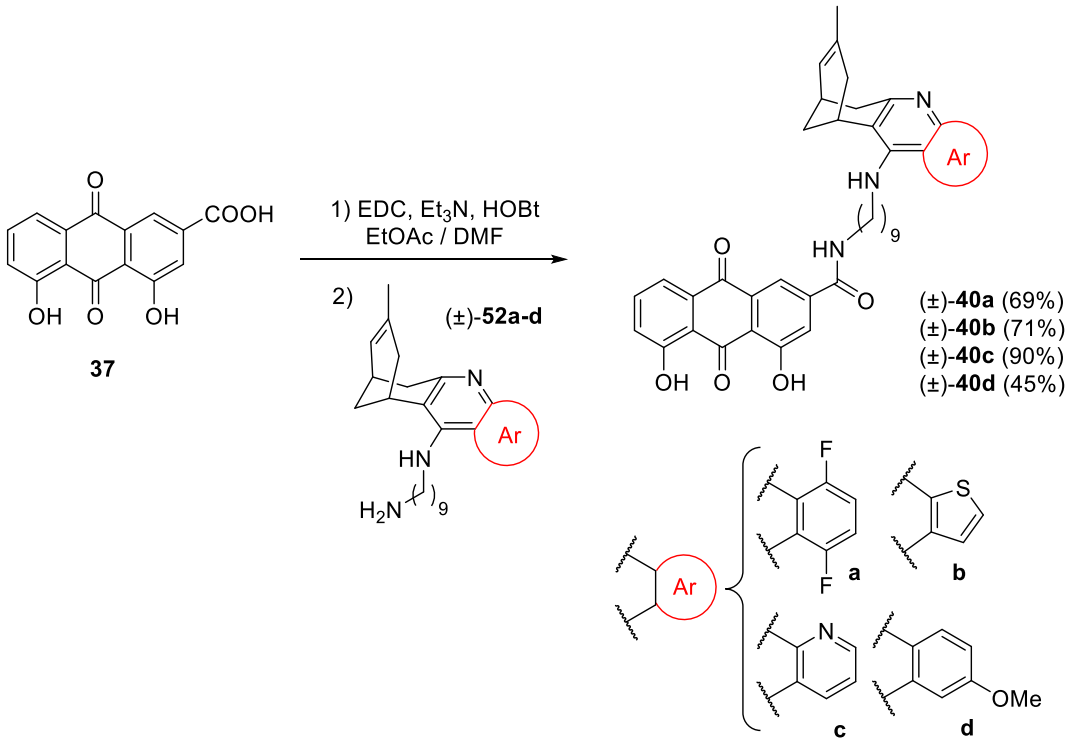

Scheme 4.5

4.4 Biology and molecular modeling studies of the rhein–modified huprine hybrids

4.4.1 Cholinesterase inhibitory activity

The anticholinesterase activities were evaluated by Dr. Manuela Bartolini (*Università di Bologna*). The inhibitory activity of the four modified huprines, **39a-d**, and their corresponding hybrids, **40a-d**, against recombinant *h*AChE and serum *h*BChE was evaluated by the method of Ellman *et al.*,[153] and compared with that of the parent racemic huprine Y, **8**, and rhein, **37**, and the lead compound of the first generation of hybrids **16**,[141] under the same assay conditions (**Table 4.2**).

It is well-known that replacement of the chlorine atom at position 3 of huprine Y by other substituents at the benzene ring[147,148] or replacement of the chlorobenzene ring of huprine

Y by different heteroaromatic systems[179] are detrimental for the AChE inhibitory activity. Even though a lower AChE inhibitory activity of the modified huprines **39a**-**d** and the corresponding rhein–huprine hybrids **40a**-**d**, compared with huprine Y and the lead rhein–huprine hybrid **16**, might have been anticipated, this should lead to a more balanced multi-target profile in the novel hybrids. In the event, modified huprines **39a**-**d** and rhein–huprine hybrids **40a**-**d** were clearly less potent *h*AChE inhibitors than huprine Y and **16**, with IC_{50} values in the submicromolar to low micromolar range in most cases. The most potent hybrid of the new series was the naphthyridine derivative **40c**, which displayed a still potent *h*AChE inhibitory activity (IC_{50} = 180 nM).

Table 4.2: *h*AChE and *h*BChE inhibitory activities of rhein (**37**), and the hydrochloride salts of the modified huprines (±)-**39a**-**d**, and the rhein–huprine hybrids (±)-**40a**-**d**, (±)-huprine Y (**8**) and the lead compound (±)-**16**.

Compound	*h*AChE[a] IC_{50} (μM)	*h*BChE[a] IC_{50} (μM)
(±)-**39a**·HCl	1.25 ± 0.17	1.68 ± 0.14
(±)-**39b**·HCl	2.61 ± 0.17	0.53 ± 0.05
(±)-**39c**·HCl	0.66 ± 0.04	0.21 ± 0.01
(±)-**39d**·HCl	5.16 ± 0.44	2.90 ± 0.02
(±)-**40a**·HCl	18.5 ± 1.5	> 10[b]
(±)-**40b**·HCl	> 10[c]	40.8 ± 8.9
(±)-**40c**·HCl	0.18 ± 0.01	2.55 ± 0.26
(±)-**40d**·HCl	1.40 ± 0.24	100 ± 9
rhein	> 10[d]	17.0 ± 4.22[d]
(±)-huprine Y·HCl	0.001 ± 0.00005[d]	0.18 ± 0.01[d]
(±)-**16**·HCl	0.004 ± 0.0002[d]	0.62 ± 0.02[d]

[a] IC_{50} inhibitory concentration (μM) of recombinant *h*AChE and serum *h*BChE. Values are expressed as mean ± standard error of the mean (SEM) of at least three experiments, each performed in duplicate.
[b] 22.5% inhibition at 10 μM.
[c] 15.2% inhibition at 15 μM.
[d] Data from Ref. 141.

As previously mentioned, the presence of a net positive charge at the quinoline nitrogen atom of the huprine moiety is a key feature that mediate binding to the CAS of AChE due to the formation of a hydrogen bond interaction between that protonated nitrogen and the carbonyl group of His447. Furthermore, the positive charge is stabilized by the formation of cation-π interactions with the electron density of the indole ring of Trp86 and the benzene ring of Tyr337. Accordingly, the most basic rhein–huprine hybrids, **40c** (calculated pK_a = 9.2) and **40d** (calculated pK_a = 8.8), which should be mostly protonated under the experimental conditions (pH = 8), are clearly more potent than the least basic hybrids, **40a** (calculated pK_a = 7.0) and **40b** (calculated pK_a = 6.7), which will probably be mostly in the neutral form.

The lower inhibitory potency of hybrids **40c** and **40d** compared to the lead **16** may be ascribed to specific interactions in the binding site. In particular, for hybrid **40d**, if we assume that the methoxyquinoline system binds the AChE catalytic site with the usual pattern of intermolecular interactions of huprines, the presence of the methoxy group would lead to a steric clash with the indole ring of Trp439, which might decrease the anticholinesterase activity compared with hybrid **16**. However, no apparent steric conflict can be observed at first sight for the naphthyridine derivative (**40c**). For this reason, group of Dr. F. Javier Luque (*Universitat de Barcelona*) studied the role of secondary interactions in its binding within *h*AChE by means of QM computations using reduced models of the binding site. The reduced activity of **40c** compared with **16** might be attributed to the absence of the chlorine atom present at position 3 of huprine Y, which fills a hydrophobic pocket formed by Pro446, Trp439, and Met443, as well as to unfavorable secondary interactions with the lone pair of His447 carbonyl oxygen (**Figure 4.5**). This oxygen atom forms a hydrogen bond with the protonated nitrogen of huprine Y (distance of 2.8 Å), an interaction that is stabilized with the favorable secondary interaction with the C–H bond at position 4 (distance of 3.4 Å). However, replacement of the chloroquinoline moiety of huprine Y by a naphthyridine system should weaken the binding due to the electrostatic repulsion between the lone pairs of the nitrogen atom and of the His447 carbonyl oxygen. Indeed, QM calculations point out that the interaction energy (corrected for basis set superposition effects) is estimated to be 3.3 kcal/mol less favorable for the naphthyridine analog compared to huprine Y. Of note, the desolvation cost is also predicted to be larger for the naphthyridine derivative, as noted in the fact that the change in water → octanol solvation free energy ($\Delta G_{wat \rightarrow oct}$) is disfavored by 1.7 kcal/mol for the naphthyridine moiety.

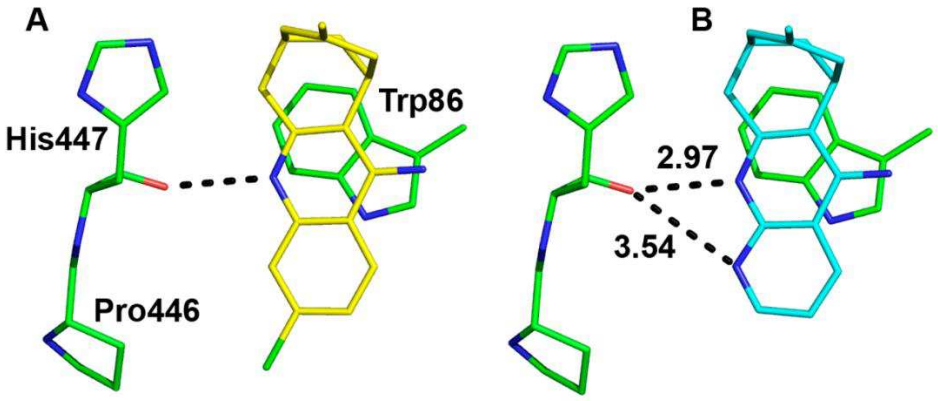

Figure 4.5: Representation of selected key interactions that modulate the binding of (A) huprine Y (carbon atoms in yellow) and (B) huprine **39c** (carbon atoms in blue) to the CAS of AChE (distances in Å).

Furthermore, kinetic studies were carried out to determine the mechanism of *h*AChE inhibition of **40c**, the most potent compound of the novel series. Lineweaver-Burk plot depicted decreased maximum reaction velocity (V_{max}) and increased Michaelis-Menten constant (K_M) with increasing inhibitor concentrations, which confirmed that **40c** acted as a mixed-type inhibitor of *h*AChE. This result was in agreement with those previously found for the lead compound **16**[141] and for structurally related rhein–tacrine hybrids[180]. The inhibitor dissociation constant (K_i) and the dissociation constant for the enzyme–substrate–inhibitor complex (K'_i) were estimated to be 0.130 µM and 0.237 µM, respectively (**Figure 4.6**).

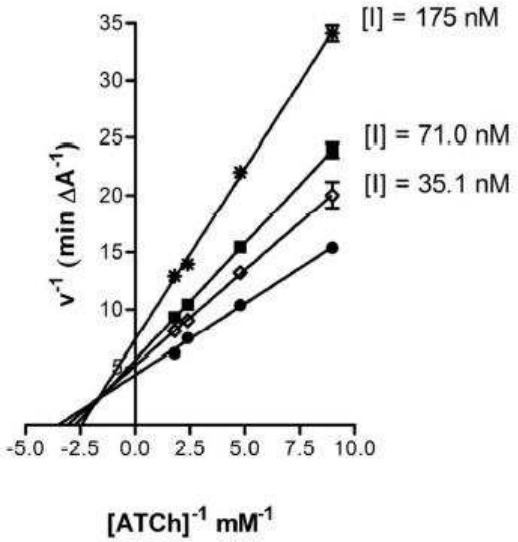

Figure 4.6: Mechanism of *h*AChE inhibition by **40c**. Overlaid Lineweaver–Burk reciprocal plots showing the variation of the initial velocity (v) as a function of increasing substrate acetylthiocholine (ATCh) concentrations in the absence and in the presence of increasing concentrations of **40c**.

[180] S.-Y. Li, N. Jiang, S.-S. Xie, K. Wang, X.-B. Wang, L.-Y. Kong. *Org. Biomol. Chem.* **2014**, *12*, 801.

Unlike most huprines developed so far, which are selective for AChE over BChE inhibition, huprines **39b**, **39c**, and **39d** were 2-5-fold more potent against *h*BChE than against *h*AChE, whereas **39a** was roughly equipotent for both enzymes. This effect might be attributed to the absence in the modified huprines of the chlorine atom present at position 3 of huprine Y. This chlorine atom of huprine Y is crucial for the inhibitory activity against *h*AChE by filling a hydrophobic pocket, but detrimental for the inhibitory activity against *h*BChE due to the steric hindrance with Met437. Thus, the absence of a chlorine atom in the modified huprines abolishes its positive effect on *h*AChE inhibitory activity and the negative effect on *h*BChE inhibitory activity, with which the novel compounds are either equipotent for both enzymes or even selective towards *h*BChE. In contrast, hybrids **40a**-**d** were selective for *h*AChE inhibition, as they displayed micromolar IC_{50} values against *h*BChE (**Table 4.2**). Again, hybrid **40c** was the most potent of the series against *h*BChE, with a one-digit micromolar potency (IC_{50} = 2.55 μM).

4.4.2 BACE1 inhibitory activity

The evaluation of the BACE1 inhibitory activity of the novel hybrids was performed by the group of Dr. Vincenza Andrisano (*Università di Bologna*) and turned out to be troublesome, due to interferences in fluorescence emission of these compounds at concentrations above 1 or 5 μM, which precluded the determination of IC_{50} values.

Regardless these technical problems, we managed to measure some BACE1 inhibitory activity for hybrids **40a** (22% inhibition at 1 μM) and **40b** (34% inhibition at 80 nM), whereas **40c** and **40d** seemed to be essentially inactive (**Table 4.3**). Gratifyingly, in the case of the most potent hybrid, **40b**, an interesting IC_{50} value of 490 nM was extrapolated from some percentages of inhibition measured in the range from 4 nM to 80 nM.

Table 4.3: *h*BACE1 inhibitory activities of rhein (**37**), and the hydrochloride salts of the rhein–huprine hybrids (±)-**40a**-**d**, (±)-huprine Y (**8**) and the lead compound (±)-**16**.

Compound	*h*BACE1 (% inhibition)[a] or IC_{50} (μM)[b]
(±)-**40a**·HCl	22.0 ± 0.01%
(±)-**40b**·HCl	0.49 ± 0.08
(±)-**40c**·HCl	na[c]
(±)-**40d**·HCl	nd[d]
rhein	na[c]
(±)-huprine Y·HCl	14%[e]
(±)-**16**·HCl	0.12 ± 0.09[f]

[a] % inhibition at 1 μM.
[b] IC_{50} inhibitory concentration (μM) of human BACE1. Values are expressed as mean ± standard error of the mean (SEM) of at least three experiments, each performed in duplicate.
[c] Not active.
[d] Not detectable.
[e] 14% Inhibition at 5 μM.
[f] Data from Ref. 141.

As previously mentioned, all the novel rhein–huprine hybrids must be protonated at the acidic pH adopted in experimental assays for the evaluation of BACE1 inhibitory activity, which mimics the acidic conditions of the endosomal compartments where BACE1 localizes. Therefore, the decrease in inhibitory potency relative to the lead hybrid **16** may be ascribed to specific interactions formed at the binding site. In this regard, the lower inhibitory potency, relative to the lead **16**, of the most potent compound of the novel series, **40b**, likely arises from unfavorable electrostatic interactions with the catalytic dyad. With the aim of clarifying these interactions, group of Dr. F. Javier Luque (*Universitat de Barcelona*) performed QM computations using reduced models of the binding site, involving interactions by means of electrostatic stabilization between the protonated nitrogen atom and the catalytic dyad formed by Asp32 (deprotonated) and Asp228 (protonated), which are hydrogen bonded. Replacement of the fused benzene ring in huprine Y by a thiophene ring led to unfavorable secondary interactions with the carboxylate oxygens (**Figure 4.7**), as the interaction energy of **40b** is destabilized relative to the binding of the two enantiomeric forms of huprine Y (by 0.6 and 2.8 kcal/mol). In addition, desolvation of

40b is predicted to be slightly disfavored relative to **16**, as the $\Delta G_{wat \rightarrow oct}$ value is estimated to be 1 kcal/mol lower for this latter compound.

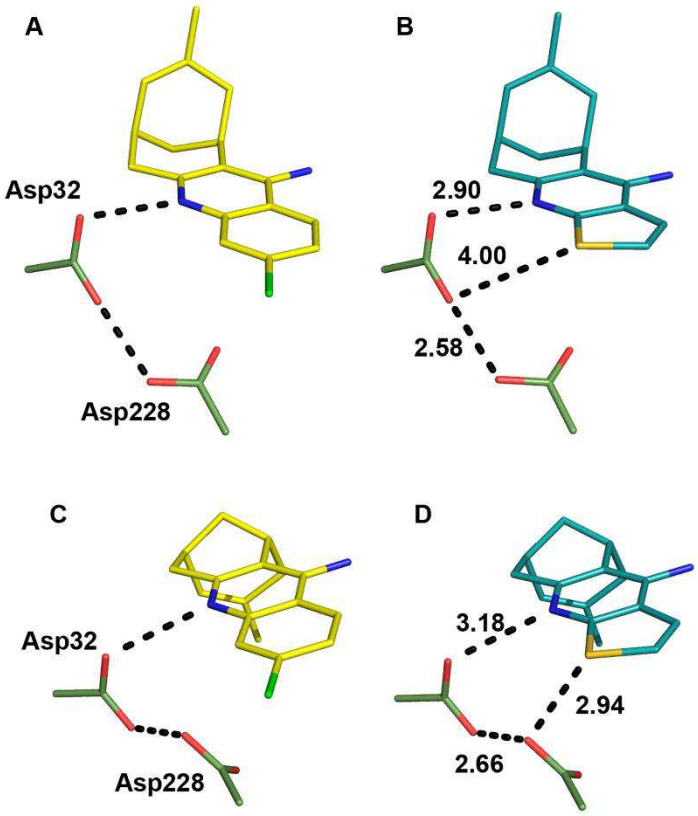

Figure 4.7: Representation of selected key interactions that modulate the binding of (A, C) huprine Y (carbon atoms in yellow) and (B, D) huprine **39b** (carbon atoms in blue) to the catalytic site of BACE1, taking into account the distinct arrangements of the two enantiomeric forms (distances in Å).

4.4.3 Aβ$_{42}$ and tau anti-aggregating activity

The inhibitory activity of the novel rhein–huprine hybrids and the monomeric huprines against the aggregation of Aβ$_{42}$ and tau was assessed by Dr. Raimon Sabaté's group (*Universitat de Barcelona*) in *E. coli* cells (**Table 4.4**).[158]

The novel rhein–huprine hybrids retained the Aβ$_{42}$ anti-aggregating activity of the lead compound **16** and showed slightly increased tau anti-aggregating potency, with percentages of inhibition of Aβ$_{42}$ and tau aggregation in the ranges 24-46% and 26-52%, respectively, using a concentration 10 μM of the hybrids. The most potent Aβ$_{42}$ (**40c**, 46.2% inhibition) and tau (**40d**,

52.4% inhibition) anti-aggregating compounds of the series display IC_{50} values close to 10 μM. As expected, the monomers of the modified huprines **39a**-**d** were essentially inactive, as we had previously found for huprine Y and structurally related compounds such as tacrine and 6-chlorotacrine.[136,140,141,181]

Table 4.4: $A\beta_{42}$ and tau anti-aggregating activities of rhein (**37**), and the hydrochloride salts of the modified huprines (±)-**39a**-**d**, the rhein–huprine hybrids (±)-**40a**-**d**, (±)-huprine Y (**8**) and the lead compound (±)-**16**.

Compound	$A\beta_{42}$ aggregation[a] (% inh. at 10 μM)	tau aggregation[a] (% inh. at 10 μM)
(±)-**39a**·HCl	1.1 ± 5.0	7.7 ± 2.9
(±)-**39b**·HCl	-3.7 ± 0.9	2.6 ± 3.6
(±)-**39c**·HCl	1.0 ± 3.9	3.6 ± 1.8
(±)-**39d**·HCl	-5.4 ± 2.1	12.8 ± 4.5
(±)-**40a**·HCl	36.2 ± 2.5	26.4 ± 1.7
(±)-**40b**·HCl	23.9 ± 1.1	40.7 ± 2.2
(±)-**40c**·HCl	46.2 ± 3.9	34.2 ± 1.9
(±)-**40d**·HCl	40.0 ± 2.7	52.4 ± 1.9
rhein	49.9 ± 6.4	40.8 ± 0.7
(±)-huprine Y·HCl	8.9 ± 1.3	7.6 ± 3.4
(±)-**16**·HCl	47.9 ± 14.5	29.6 ± 8.5

[a] % of inhibition of $A\beta_{42}$ and tau protein aggregation at 10 μM in intact *E. coli* cells. Values are expressed as mean ± SEM of four independent experiments.

4.4.4 Antioxidant activity

Because of the presence of phenolic groups in the rhein moiety of hybrids **40a**-**d** we inferred that they might display antioxidant activity. Indeed, it has been recently reported that

[181] F. J. Pérez-Areales, O. Di Pietro, A. Espargaró, A. Vallverdú-Queralt, C. Galdeano, I. M. Ragusa, E. Viayna, C. Guillou, M. V. Clos, B. Pérez, R. Sabaté, R. M. Lamuela-Raventós, F. J. Luque, D. Muñoz-Torrero. *Bioorg. Med. Chem.* **2014**, *22*, 5298.

rhein exhibits antioxidant properties by decreasing ROS production,[182] and also displaying ROS and radical scavenging activity.[183] Thus, the putative antioxidant activity of the novel rhein–huprine hybrids **40a**-**d**, the modified huprines **39a**-**d**, and rhein, **37**, was assessed through the $ABTS^{\cdot+}$, DPPH, and TP assays, using gallic acid and trolox as reference compounds (**Table 4.5**). These assays were performed by Dr. Rosa Lamuela-Raventós's group (*Universitat de Barcelona*).

As expected, rhein and huprines **39a**-**d** displayed a remarkable antioxidant activity, which was especially evident in the $ABTS^{\cdot+}$ and DPPH assays (3–6 trolox eq.). Very interestingly, the rhein-huprine hybrids **40a**-**d** showed a very potent antioxidant activity, with these compounds being 10–22-fold and 12–13-fold more potent than trolox in the $ABTS^{\cdot+}$ and DPPH assays, respectively, and slightly more potent than gallic acid.

Table 4.5: Antioxidant activity of rhein (**37**), gallic acid, and the hydrochloride salts of the modified huprines (±)-**39a**-**d**, the rhein–huprine hybrids (±)-**40a**-**d**, and (±)-huprine Y (**8**).

Compound	$ABTS^{\cdot+}$[a] (trolox eq.)	DPPH[a] (trolox eq.)	TP[a] (mg GAE / g sample)
(±)-**39a**·HCl	5.1 ± 0.3	6.0 ± 0.2	37.7 ± 3.9
(±)-**39b**·HCl	4.8 ± 0.4	3.9 ± 0.3	152 ± 5.7
(±)-**39c**·HCl	3.9 ± 0.8	5.5 ± 0.3	34.1 ± 0.7
(±)-**39d**·HCl	5.0 ± 0.2	2.6 ± 0.1	90.1 ± 6.2
(±)-**40a**·HCl	11.8 ± 0.6	13.4 ± 0.6	41.3 ± 4.0
(±)-**40b**·HCl	20.7 ± 2.5	12.4 ± 0.4	99.9 ± 5.0
(±)-**40c**·HCl	10.4 ± 0.9	12.7 ± 0.4	37.9 ± 3.2
(±)-**40d**·HCl	21.6 ± 1.2	12.4 ± 1.0	10.7 ± 1.2
rhein	4.0 ± 0.2	5.8 ± 0.3	29.5 ± 2.0
(±)-huprine Y·HCl	2.6 ± 0.2	1.0 ± 0.1	10.2 ± 1.3
gallic acid	12.5 ± 0.4	9.7 ± 0.4	1004 ± 3.1

[a] Antioxidant capacity measured through $ABTS^{\cdot+}$, DPPH, or total polyphenols. Values are expressed as mean ± SEM of three experiments.

[182] Y. Wang, X. Fan, T. Tang, R. Fan, C. Zhang, Z. Huang, W. Peng, P. Gan, X. Xiong, W. Huang, X. Huang. *Sci Rep.* **2016**, *30*, 37098.
[183] F. Vargas, Y. Díaz, K. Carbonell. *Pharm. Biol.* **2004**, *42*, 342.

4.4.5 In vitro BBB permeation assay

Like for the previous family of compounds, Dr. Belén Pérez (*Universitat Autònoma de Barcelona*) was responsible for assessing the brain permeation of the novel rhein–huprine hybrids through the PAMPA-BBB assay (**Table 4.6**).[160] Even though the relatively high molecular weight of compounds resulting from molecular hybridization might compromise their ability to cross membranes, good oral bioavailability and/or brain permeability in mice have been found in the first generation of rhein–huprine hybrids[141,169] and other structurally related families of huprine-based hybrids with similar molecular weights.[154,161,181]

From the correlation obtained by comparing the experimental and reported *in* vitro permeability P_e values of fourteen reference drugs and the limits established for BBB permeation,[160] the threshold for high BBB permeation (CNS+) was set at P_e (10^{-6} cm s^{-1}) > 5.1. P_e values over this threshold were obtained for all the novel rhein–huprine hybrids, so that all of them should be able to cross BBB and reach their multiple targets at the CNS.

Table 4.6: Permeabilities from the PAMPA-BBB assay of rhein (**37**), and the hydrochloride salts of the modified huprines (±)-**39a**-**d**, the rhein–huprine hybrids (±)-**40a**-**d**, (±)-huprine Y (**8**) and the lead (±)-**16**.

Compound	P_e (10^{-6} cm s^{-1})[a]	Prediction
(±)-**39a**·HCl	10.6 ± 0.8	CNS+
(±)-**39b**·HCl	18.6 ± 1.4	CNS+
(±)-**39c**·HCl	11.6 ± 1.4	CNS+
(±)-**39d**·HCl	16.8 ± 1.3	CNS+
(±)-**40a**·HCl	9.1 ± 0.1	CNS+
(±)-**40b**·HCl	8.4 ± 0.8	CNS+
(±)-**40c**·HCl	10.5 ± 0.8	CNS+
(±)-**40d**·HCl	10.4 ± 0.8	CNS+
rhein	2.7 ± 0.1	CNS+/–
(±)-huprine Y·HCl	23.8 ± 2.7	CNS+
(±)-**16**·HCl	21.5 ± 0.7	CNS+

[a] Permeability values from the PAMPA-BBB assay. Values are expressed as the mean ± SD of three independent experiments.

CHAPTER 5

CR-6–tacrine hybrids

Helianthus annuus (sunflower)

Image source: Bruce Fritz. US Department of Agriculture

5.1 Background

Vitamin E encompasses a group of natural antioxidant compounds, namely a mixture of tocopherols and tocotrienols. This mixture includes four different tocopherols depending on the substitutions on the aromatic ring of the chromane scaffold (**53-56**, **Figure 5.1**), with α- and γ-tocopherols being those with highest antioxidant potency.[184] However, the great pharmaceutical limitation of these compounds is their low BBB permeability. In this context, the group of Prof. Àngel Messeguer (*Instituto de Química Avanzada de Cataluña*, IQAC-CSIC) discovered 3,4-dihydro-6-hydroxy-7-methoxy-2,2-dimethyl-1(2*H*)-benzopyran (CR-6, **17**), as the most potent antioxidant of a collection of simple 1(2*H*)-benzopyran analogs of tocopherols that exhibited an inhibitory effect on lipid peroxidation.[185-187]

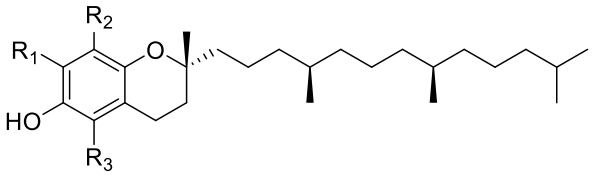

Vitamin E

α: $R_1 = R_2 = R_3 = CH_3$ (**53**) γ: $R_1 = R_2 = CH_3$, R_3 = H (**55**)

β: R_1 = H, $R_2 = R_3 = CH_3$ (**54**) δ: $R_1 = R_3 = CH_3$, R_2 = H (**56**)

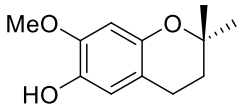

CR-6, **17**

Figure 5.1: CR-6, **17**, and the parent tocopherols (**53-56**).

The presence of a hydroxyl group at position 6 is the most important structural feature in these compounds, accounting for the elicited antioxidant protection, due to their high ability to neutralize reactive radical species (**Figure 5.2**).[188] Moreover, CR-6 contains two non-substituted and highly activated aromatic positions (C5 and C8) capable of reacting with RNS,[188,189] which led to consider this antioxidant compound as a γ-tocopherol analog.

[184] R. Brigelius-Flohé, M. G. Traber. *FASEB J.* **1999**, *13*, 1145.
[185] J. Irurre, J. Casas, I. Ramos, A. Messeguer. *Bioorg. Med. Chem.* **1993**, *1*, 219.
[186] J. Casas, G. Gorchs, F. Sánchez-Baeza, P. Teixidor, A. Messeguer. *J. Agric. Food Chem.* **1992**, *40*, 585.
[187] S. Yenes, J. Commandeur, N. Vermeulen, A. Messeguer. *Chem. Res. Toxicol.* **2004**, *17*, 904.
[188] G. W. Burton, K. U. Ingold. *Acc. Chem. Res.* **1986**, *19*, 194.
[189] C. Montoliu, M. Llansola, R. Sáez, S. Yenes, A. Messeguer, V. Felipo. *Biochem. Pharmacol.* **1999**, *58*, 255.

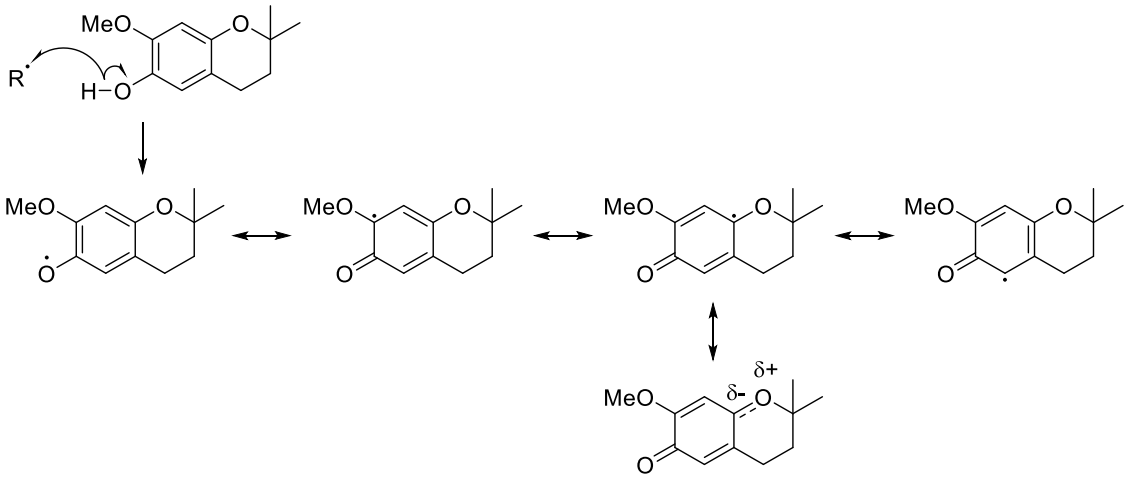

Figure 5.2: Stabilization of phenoxyl CR-6 radical by resonance after neutralizing a free radical.

Furthermore, *in vivo* assays with animal models demonstrated potential applications of CR-6, such as reducing the oxidative stress induced by apoptosis in ocular diseases,[190] or acting as neuroprotective agent by reducing oxidative damage after an ischemia/reperfusion process.[191,192]

5.2 Design of CR-6–tacrine hybrids

In the light of the above-mentioned attributes, we considered the potential interest of incorporating a CR-6 moiety as part of MTDLs against AD. Thus, we envisioned a novel family of compounds featuring a CR-6 (**17**) moiety connected to an AChE inhibitor fragment, 6-chlorotacrine (**13**), which was selected for its synthetic simplicity relative to huprine. The linkage between both units was envisaged through a tether chain containing amide or amine functionalities (general structure **III**, **Figure 5.3**).

[190] N. Sanvicens, V. Gómez-Vicente, A. Messeguer, T. G. Cotter. *J. Neurochem.* **2006**, *98*, 735.
[191] F. Jiménez-Altayó, L. Caracuel, F. J. Pérez-Asensio, S. Martínez-Revelles, A. Messeguer, A. M. Planas, E. Vila. *J. Pharm. Exp. Ther.* **2009**, *331*, 429.
[192] F. Pérez-Asensio, X. de la Rosa, F. Jiménez-Altayó, R. Gorina, E. Martínez, À. Messeguer, E. Vila, À. Chamorro, A. M. Planas. *J. Cereb. Blood Flow Metab.* **2010**, *30*, 638.

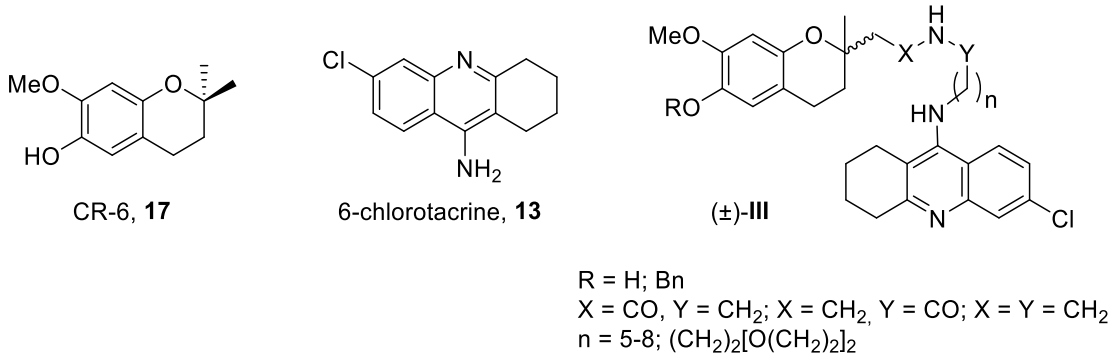

Figure 5.3: Structures of CR-6 (**17**) and 6-chlorotacrine (**13**), and general structure of the CR-6–tacrine hybrids (**III**).

6-Chlorotacrine (**13**) is a well-known highly potent AChE inhibitor, which has been commonly used by our research group in MTDL hybrids.[136,140,193-195] This compound, which will be protonated at physiological pH, tightly binds the CAS of AChE through cation-π and π-π stacking interactions with the indole ring of Trp86 and the benzene ring of Tyr337, hydrogen bonding between the protonated acridine nitrogen atom and the carbonyl oxygen of His447, and hydrophobic interactions by the chlorine atom, which fills a hydrophobic pocket formed by Pro446, Trp439, and Met443. Concomitant to this interaction of the 6-chlorotacrine unit at the CAS, we might expect a dual binding mode of the CR-6–tacrine hybrids within AChE, since CR-6 moiety should stablish some additional interactions with the PAS, such as π-π stacking interactions with the aromatic PAS residues Trp286 and Tyr72, or hydrogen binding due to the presence of three oxygen atoms. Moreover, the amide or secondary amine functions integrated in the linker might enable further interactions with midgorge residues.

On the other hand, in the light of our experience in BACE1 inhibition and according to the binding mode proposed for the first generation of rhein–huprine hybrids (**Section 4.1**),[141] whereby the huprine moiety is accommodated at the BS1 pocket (corresponding to the catalytic dyad consisting of two aspartic acid residues), and the hydroxyanthraquinone unit fills the

[193] P. Camps, X. Formosa, C. Galdeano, T. Gómez, D. Muñoz-Torrero, L. Ramírez, E. Viayna, E. Gómez, N. Isambert, R. Lavilla, A. Badia, M. V. Clos, M. Bartolini, F. Mancini, V. Andrisano, A. Bidon-Chanal, Ó. Huertas, T. Dafni, F. J. Luque. *Chem. Biol. Interact.* **2010**, *187*, 411.
[194] P. Camps, X. Formosa, C. Galdeano, D. Muñoz-Torrero, L. Ramírez, E. Gómez, N. Isambert, R. Lavilla, A. Badia, M. V. Clos, M. Bartolini, F. Mancini, V. Andrisano, M. P. Arce, M. I. Rodríguez-Franco, O. Huertas, T. Dafni, F. J. Luque. *J. Med. Chem.* **2009**, *52*, 5365.
[195] P. Camps, X. Formosa, C. Galdeano, T. Gómez, D. Muñoz-Torrero, M. Scarpellini, E. Viayna, A. Badia, M. V. Clos, A. Camins, M. Pallàs, M. Bartolini, F. Mancini, V. Andrisano, J. Estelrich, M. Lizondo, A. Bidon-Chanal, F. J. Luque. *J. Med. Chem.* **2008**, *51*, 3588.

unexplored BS2 site, we hypothesized that the 6-chlorotacrine scaffold of the target CR-6–tacrine hybrids might fit into the BS1 pocket in a similar mode to huprine. Thus, the 6-chlorotacrine unit, protonated at the acidic cellular compartments where BACE1 localizes, might interact through electrostatic interactions with the aspartate residues of the catalytic dyad of BACE1 (Asp32 and Asp228). Concomitant interactions might be established at the BS2 pocket by the CR-6 moiety, which shares with rhein the presence of a phenolic system.

In this context, we selected several linkers aiming to explore the potential dual binding mode within BACE1. Thus, we considered as optimal a polymethylenic tether of 12 atoms length, in order to preserve the same separation between fragments as that of the lead compound of rhein–huprine hybrids (**Section 4.1**).[141] Interestingly, that tether length should perfectly allow the dual binding mode within AChE as well. Apart from the hybrids with the selected tether length, the synthesis of one atom longer and shorter homologs was also planned to better delineate the optimal linker lenght, as well as some analogs bearing ethylene glycol units within the linker to increase aqueous solubility and ameliorate physicochemical and pharmacokinetic properties.

5.3 Synthesis of the CR-6–tacrine hybrids

The simplified retrosynthetic route to the target hybrids is depicted in **Scheme 5.1**.

As part of this collaborative project, Dr. María Garrido (*Instituto de Química Avanzada de Cataluña*, IQAC-CSIC) prepared the three CR-6 intermediate compounds (**58**, **61**, and **64**), following the synthetic methodologies previously reported by the research group of Prof. Àngel Messeguer.[143]

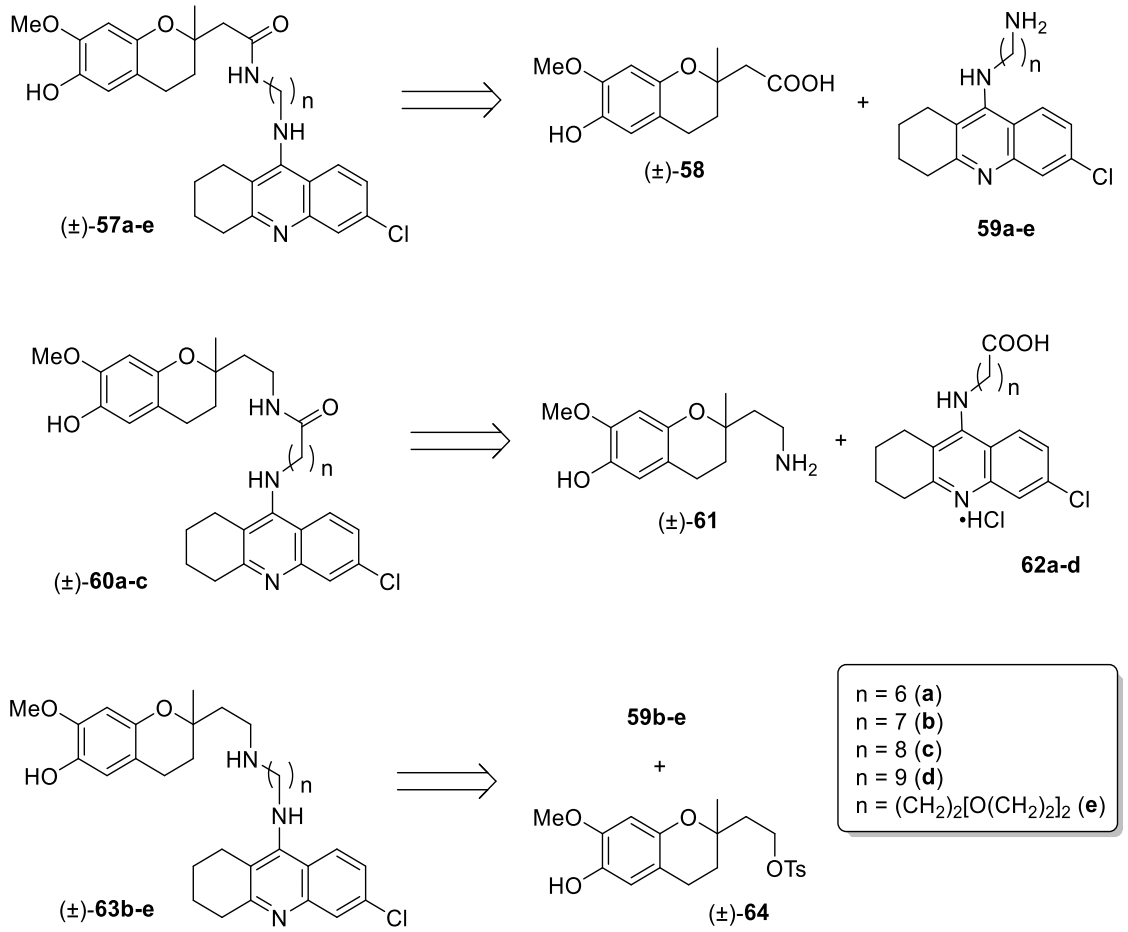

Scheme 5.1

5.3.1 Synthesis of the series of amides 57

For the preparation of this series of amides, we started synthetizing the required intermediates **59a-e** through a procedure widely used by our research group,[136,140,193-195] which was first described in 1999.[196] The first step involved the formation of the 6,9-dichlorotacrine **67**, which was obtained in 81% yield by Friedländer condensation of cyclohexanone, **66**, with the anthranilic acid **65** under reflux for 2 h in the presence of $POCl_3$ (**Scheme 5.2**).

[196] P. Carlier, Y. F. Han, E. Chow, C. Li, H. Wang, T. X. Lieu, H. S. Wong, Y.-P. Pang. *Bioorg. Med. Chem.* **1999**, *7*, 351.

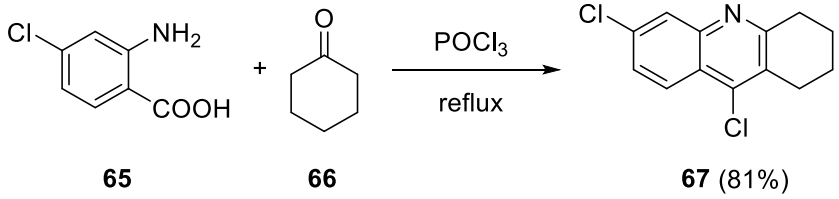

65 **66** **67** (81%)

Scheme 5.2

Afterwards, we carried out the amination of compound **67** with the corresponding diamine, **68a-e**, under reflux of 1-pentanol for 24 h, to provide, after silica gel column chromatography purification, the aminoalkyltacrines **59a-d** in moderate yields (**Scheme 5.3**). An alternative methodology had to be applied in the case of **59e**, because the boiling point of the necessary diamine **68e** was lower than the reaction temperature. In that case, the reaction was performed in a closed vessel, affording the target aminoalkyltacrine **59e** in higher yield (77%) than those obtained for **59a-d**. This operational improvement was then assessed for **59c**, confirming the increased reaction yield from 43% to 69%.

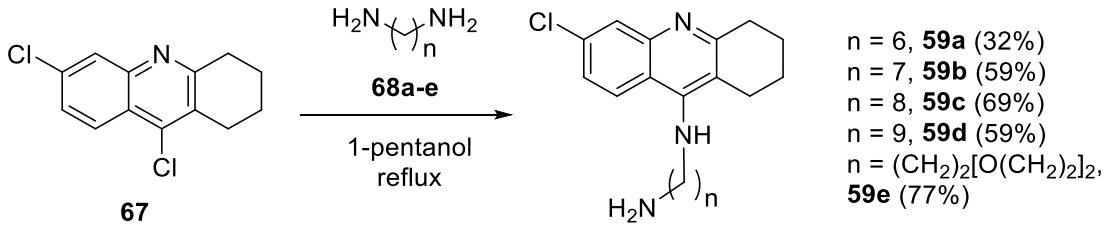

Scheme 5.3

Subsequently, the amide coupling reactions between the *O*-benzyl-protected CR-6-derived carboxylic acid **69** and the primary amines **59a-d** were performed in the presence of EDC, Et_3N, and HOBt, in a mixture EtOAc / DMF at room temperature for 24 h, to provide the benzylated CR-6–tacrine hybrids **70a-d** in excellent yields (83–100%), after silica gel column chromatography purification (**Scheme 5.4**). Final deprotection of the phenolic group of the target hybrids, which was carried out by Dr. María Garrido, involved a hydrogenation reaction under Pd/C catalysis at 1 atm overnight. Despite the mild reaction conditions, the desired *O*-debenzylation at the CR-6 moiety was accompanied by dechlorination at the tacrine unit. In any case, both the benzylated hybrids **70a-d**, and the debenzylated and dechlorinated hybrids **71a-d**, were subjected to the same biological evaluation as other target compounds.

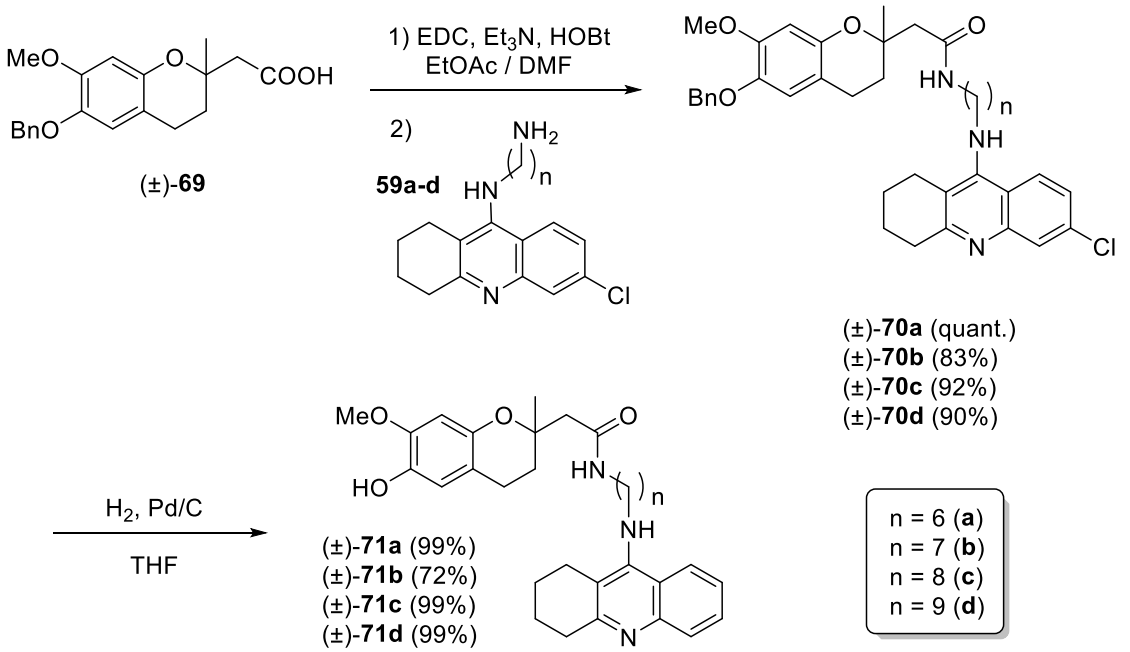

Scheme 5.4

In the light of the results observed in the deprotection reaction of the benzylated hybrids **70a-d**, the synthesis of the target hybrids **57a-d** was alternatively envisaged starting from the unprotected CR-6 carboxylic acid derivative **58**. Gratifyingly, hybrids **57a-d** were obtained in high yields, without observing the formation of *O*-acylated byproducts (**Scheme 5.5**).

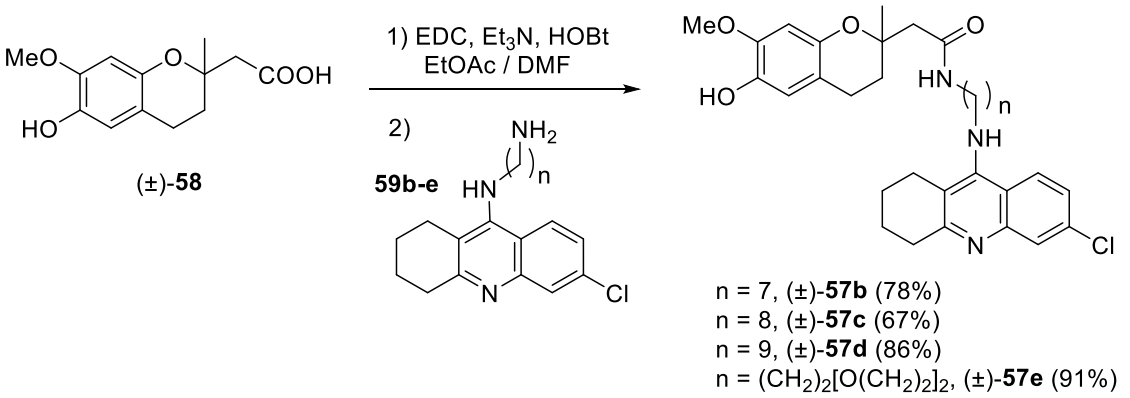

Scheme 5.5

5.3.2 Synthesis of the series of inverse amides 60

The first step involved the Friedländer condensation of cyclohexanone, **66**, with the aminobenzonitrile **72** in 1,2-dichloroethane under reflux for 18 h in the presence of $AlCl_3$, providing 6-chlorotacrine, **13**, in quantitative yield (**Scheme 5.6**).

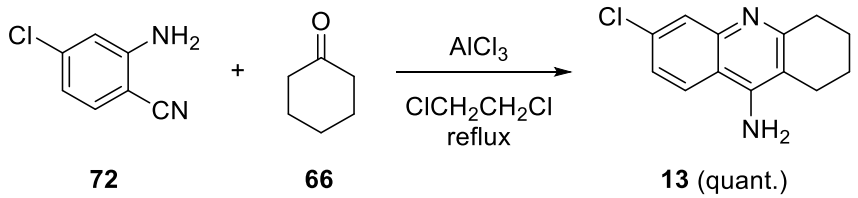

72 **66** **13** (quant.)

Scheme 5.6

Alkylation of 6-chlorotacrine, **13**, with the corresponding ω-bromoalkanenitrile, **50a-c**, in the presence of KOH in DMSO at room temperature overnight, led to nitriles **73a**-**c**, after silica gel column chromatography purification, in good yields (65–86%, **Scheme 5.7**). Of note, compounds **73a-c** were evaluated as anti-trypanosomal agents in the context of Dr. Irene Sola's PhD Thesis work, and the results included in a publication.[197] It should be pointed out that 8- and 9-bromoalkanenitrile, **50b** and **50c**, are not commercially available, so that they had to be synthesized by reaction between the corresponding α,ω-dibromoalkane and NaCN, and purified by a tedious micro-distillation process from a mixture with unreacted dibromoalkane and the alkanedicarbonitrile byproduct.

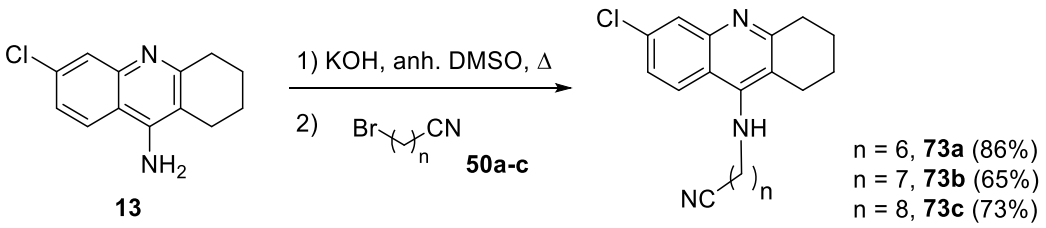

13

Scheme 5.7

Later on, hydrolysis of nitriles **73a-c** led to the corresponding carboxylic acids **62a-c**, which were obtained as hydrochloride salts and used in the following step without further purification (**Scheme 5.8**). Then, the amide coupling reactions between the CR-6-derived

[197] I. Sola, A. Artigas, M. C. Taylor, F. J. Pérez-Areales, E. Viayna, M. V. Clos, B. Pérez, C. Wright, J. Kelly, D. Muñoz-Torrero. *Bioorg. Med. Chem.* **2016**, *24*, 5162.

primary amine **61** and the carboxylic acids **62a-c** were carried out in the presence of EDC, Et_3N, and HOBt in a mixture EtOAc / DMF at room temperature for 24 h, to give the CR-6–tacrine inverse amides **60a-c** in good yields (52–87%) after silica gel column chromatography purification.

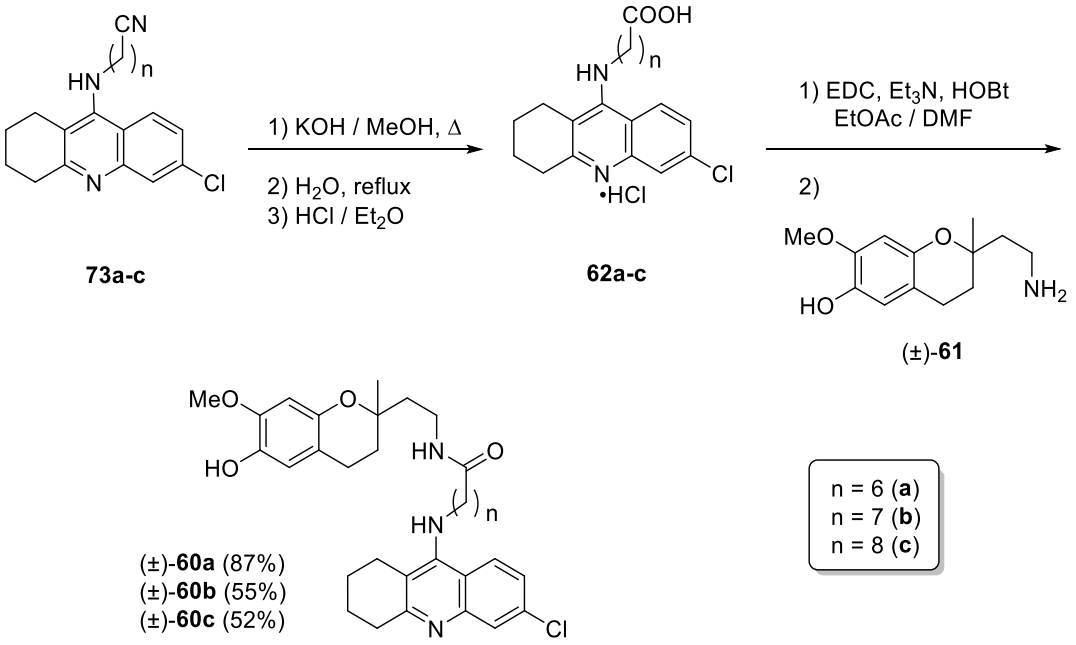

73a-c **62a-c** (±)-**61**

Scheme 5.8

5.3.3 Synthesis of the series of secondary amines 63

The synthesis of the last series of compounds was carried out by direct nucleophilic substitution of the previously synthesized intermediate primary amines **59b-e** over the CR-6-derived tosylate **64**, in the presence of Et_3N, in acetonitrile under reflux for 48 h, to provide, after the subsequent column chromatography purification, the desired hybrids in low to moderate yields (24–59%, **Scheme 5.9**).

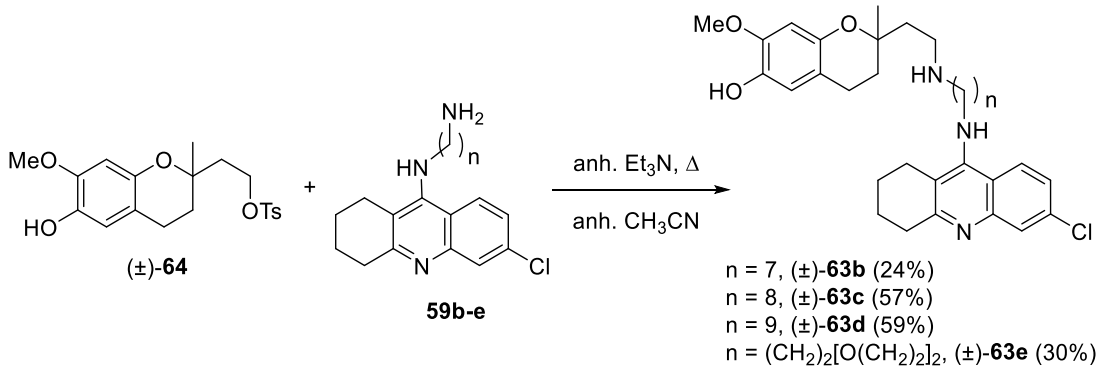

Scheme 5.9

5.4 Biological characterization of CR-6–tacrine hybrids

5.4.1 Cholinesterase inhibitory activity

The inhibitory activity toward human cholinesterases was evaluated by Dr. Manuela Bartolini (*Università di Bologna*). The anticholinesterase activity of the hybrids **70a-d**, **71a-d**, **57b-e**, **60a-c** and **63b-e** was assessed by the method of Ellman *et al.*[153] using recombinant *h*AChE and serum *h*BChE, and compared with that of the parent 6-chlorotacrine, **13**, and CR-6 derivatives **58** and **61**, under the same assay conditions (**Table 5.1**).

These results enabled us to delineate the structure-activity relationships in this structural class, which agree in general terms with the previous knowledge about AChE and BChE inhibition, and with the rational design. Firstly, the presence of the benzyl group at the CR-6 moiety resulted detrimental for the AChE inhibitory activity, as benzylated amides **70b-d** (7.0–11.0 nM) are slightly less potent than deprotected amides **57b-d** (2.1–5.4 nM), which might be caused by some steric hindrance in the interaction with the PAS of AChE. However, both series of compounds are endowed with a very high AChE inhibitory potency. Conversely, the benzylated amides **70b-d** are 2-6-fold more potent BChE inhibitors than deprotected amides **57b-d**. As expected, we can appreciate by comparison of the tacrine-based hybrids **71a-d** (57.8–275 nM) and 6-chlorotacrine-based hybrids **57b-d** (2.1–5.4 nM) that the presence of a chlorine atom at position 6 of the tacrine unit is critical for the inhibition of AChE, as a result of additional interactions within a hydrophobic pocket close to the CAS. Conversely, the absence of this chlorine atom led to a strongly enhanced inhibition of BChE (4.3–5.4 nM for **71a-d** in comparison

with 79–170 nM for **57b-d**). It is known that the presence of the chlorine atom at the tacrine unit is detrimental for the BChE inhibitory activity because of a steric class with Met437. On the other hand, the presence of ethylene glycol units within the linker, which might lead to better physicochemical properties, affects negatively both anti-cholinesterase activities, thus **57e** and **63e** are 13- and 69-fold less potent AChE inhibitors and 11- and 13-fold less potent BChE inhibitors than their homologous oligomethylene-linked compounds **57c** and **63c**, with equivalent tether length. Amides **57b-d** turned out to be slightly more potent toward both AChE (2.1–5.4 nM) and BChE (79–170 nM) than inverse amides **60a-c** (3.8–8.0 nM and 102–187 nM), which suggests a slightly different accommodation within both enzymes to enable some interactions with midgorge residues. Finally, the series of aliphatic amines **63b-d** showed a surprisingly increased potency against both AChE (0.12–0.44 nM) and BChE (13.4–18.3 nM), exhibiting picomolar and low nanomolar IC_{50} values, respectively. Because the secondary amine of the linker will be mainly protonated at physiological pH, it could stablish additional electrostatic and cation-π interactions with midgorge residues, which could account for their high potency. Overall, with the sole exception of compound **57e**, all the CR-6–tacrine hybrids of the three initially planned series, containing a 6-chlorotacrine unit, were more potent AChE and BChE inhibitors than the parent compounds 6-chlorotacrine, and the CR-6-derived compounds **58** and **61**, which might be ascribed to a dual site binding of the hybrids within AChE and BChE, in agreement with their rational design. The lead compound with regard to the anti-cholinesterase activies, **63c** (IC_{50} *h*AChE = 0.121 nM; IC_{50} *h*BChE = 13.4 nM), is 120- and almost one million-fold more potent *h*AChE inhibitor than 6-chlorotacrine and the amine **61**, respectively, and 40- and 2000-fold more potent *h*BChE inhibitor than these parent compounds.

Table 5.1: *h*AChE and *h*BChE inhibitory activities of the CR-6-derived carboxylic acid (±)-**58**, and the hydrochloride salts of the amides (±)-**57b-e**, the inverse amides (±)-**60a-c**, the amines (±)-**63b-e**, the benzylated amides (±)-**70a-d**, the tacrine-based amides (±)-**71a-d**, 6-chlorotacrine (**13**), and the CR-6-derived amine (±)-**61**.

Compound	*h*AChE[a] IC_{50} (nM)	*h*BChE[a] IC_{50} (nM)
(±)-**70a**·HCl	11.0 ± 0.6	201 ± 11
(±)-**70b**·HCl	6.99 ± 0.35	51.0 ± 1.8
(±)-**70c**·HCl	10.4 ± 0.6	100 ± 5
(±)-**70d**·HCl	7.89 ± 0.42	30.6 ± 2.2
(±)-**71a**·HCl	275 ± 38	4.99 ± 0.36
(±)-**71b**·HCl	111 ± 5	4.28 ± 0.31
(±)-**71c**·HCl	69.8 ± 6.4	5.33 ± 0.49
(±)-**71d**·HCl	57.8 ± 4.8	5.36 ± 0.24
(±)-**57b**·HCl	5.43 ± 0.27	79.1 ± 3.7
(±)-**57c**·HCl	3.69 ± 0.19	170 ± 9
(±)-**57d**·HCl	2.05 ± 0.11	168 ± 5
(±)-**57e**·HCl	47.9 ± 2.5	1840 ± 130
(±)-**60a**·HCl	3.80 ± 0.24	102 ± 8
(±)-**60b**·HCl	7.94 ± 0.31	187 ± 7
(±)-**60c**·HCl	6.23 ± 0.36	148 ± 4
(±)-**63b**·2HCl	0.442 ± 0.039	17.4 ± 1.6
(±)-**63c**·2HCl	0.121 ± 0.004	13.4 ± 0.9
(±)-**63d**·2HCl	0.272 ± 0.021	18.3 ± 0.4
(±)-**63e**·2HCl	8.35 ± 0.51	180 ± 9
(±)-**58** (CR-6-COOH)	na[b]	na[b]
(±)-**61**·HCl (CR-6-NH_2)	101000 ± 9000	23200 ± 1100
13·HCl (6-chlorotacrine)	14.5 ± 0.9	505 ± 28

[a] IC_{50} inhibitory concentration (nM) of human recombinant AChE and human serum BChE. Values are expressed as mean ± standard error of the mean (SEM) of at least three experiments, each performed in duplicate.
[b] Not active at 100 µM.

To gain further insight into the structural basis of the high AChE and BChE inhibitory activity for compound **63c**, the binding mode to both enzymes was explored by means of molecular dynamics simulations, which were carried out by the group of Dr. F. Javier Luque (*Universitat de Barcelona*). These studies showed a complex network of interactions with the residues along the catalytic gorge of *h*AChE (**Figure 5.4**). As expected, the 6-chlorotacrine moiety was tightly bound in the CAS due to the cation-π interactions with the indole and phenol rings of Trp86 and Tyr337, respectively, and the hydrogen bond between the protonated quinolinic nitrogen atom and the carbonyl oxygen of His447. However, the distribution of the CR-6 moiety differed clearly for both enantiomers of **63c**, being in (*R*)-**63c** firmly stacked against Trp286, but not in (*S*)-**63c**. The most remarkable finding concerned the salt bridge formed by the protonated secondary amino group in the linker with Asp74, which likely contributed to a great extent to the surprisingly high potency displayed by hybrid **63c**.

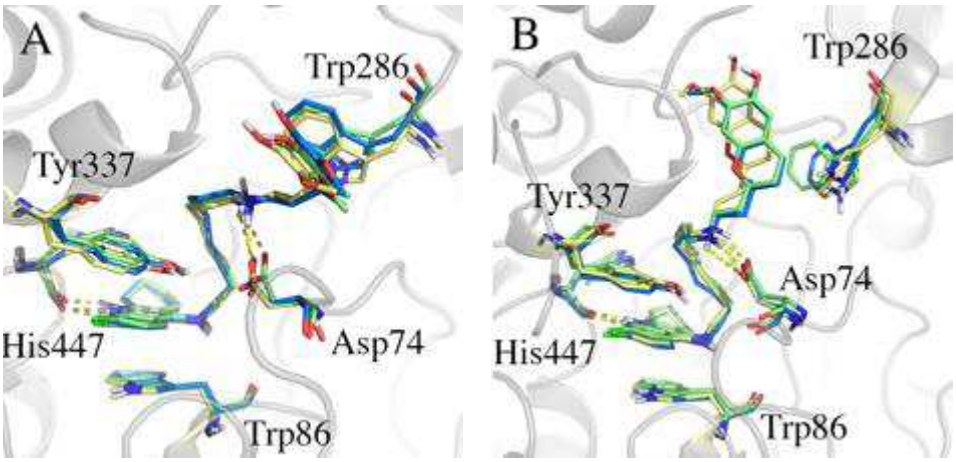

Figure 5.4: Representation of the binding mode of the hybrids (A) (*R*)-**63c** and (B) (*S*)-**63c** within *h*AChE. The residues involved in interactions are shown (PDB ID: 1Q83).

Regarding the binding mode within BChE (**Figure 5.5**), the molecular dynamics simulations showed that the 6-chlorotacrine moiety was bound in the CAS, stacked between Trp82 and His438, and forming a hydrogen bond between the protonated quinolinic nitrogen atom and the carbonyl oxygen of His438. We could also observe the steric hindrance of the chlorine atom at the tacrine unit with Met437. As observed in AChE, the distribution of the CR-6 moiety differed for both enantiomers of **63c**. Hydrogen bonding between the protonated secondary amino group within the linker and the carbonyl group of Gln119 or Pro285 was observed for both enantiomers.

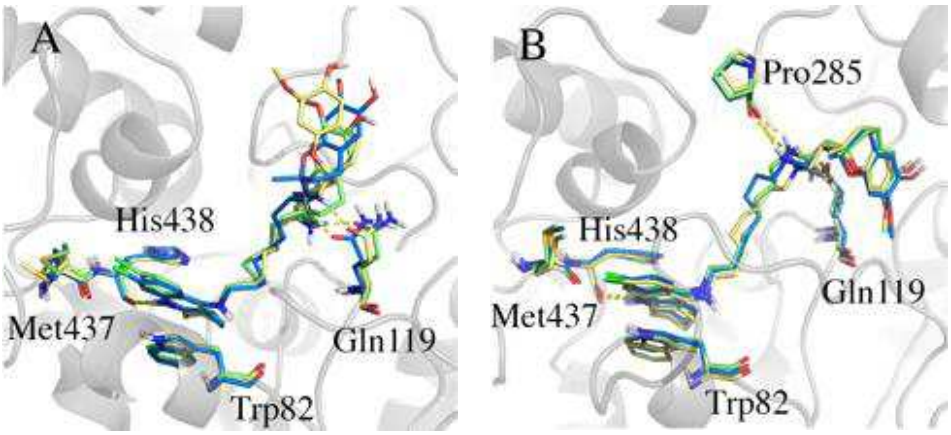

Figure 5.5: Representation of the binding mode of the hybrids (A) (*R*)-**63c** and (B) (*S*)-**63c** within *h*BChE. The residues involved in interactions are shown (PDB ID: 5K5E).

To shed light on the mechanism of action of this novel structural class on *h*AChE, a kinetics study was carried out with the most potent compound, **63c**. The Lineweaver-Burk plot depicted decreased maximum reaction velocity (V_{max}) and increased Michaelis-Menten constant (K_M) with increasing inhibitor concentrations, which is indicative of a mixed-type inhibition of the AChE-mediated acetylthiocholine hydrolysis by **63c**. The inhibitor constant (K_i) and the dissociation constant for the enzyme–substrate–inhibitor complex (K'_i) were estimated to be 0.132 nM and 0.258 nM, respectively (**Figure 5.6**).

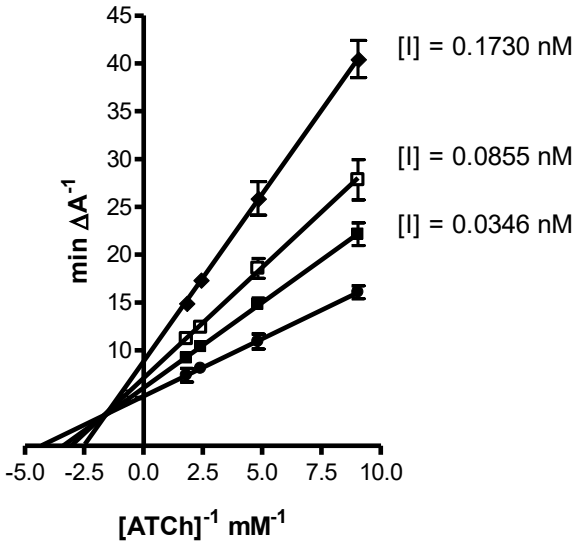

Figure 5.6: Mechanism of *h*AChE inhibition by **63c**. Overlaid Lineweaver-Burk plot reciprocal plots showing the variation of the initial velocity (v) as a function of increasing substrate acetylthiocholine (ATCh) concentrations in the absence and in the presence of increasing concentrations of **63c**.

To confirm the dual binding mode of **63c** within AChE predicted by the molecular dynamics simulations, propidium displacement studies were performed by Dr. Manuela Bartolini (*Università di Bologna*). The obtained dissociation constant (K_D = 2.03 ± 0.09 μM), albeit being 3-fold higher than that of the specific PAS inhibitor propidium (K_D = 0.7 μM), supported the interaction of **63c** with the PAS of AChE, and hence, its dual site binding (**Figure 5.7**).

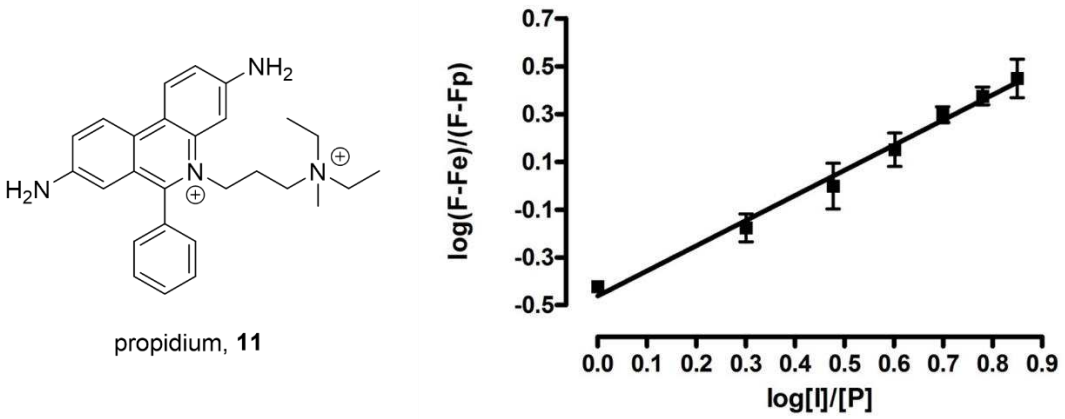

Figure 5.7: Left: structure of propidium (**11**). Right: propidium displacement studies with **63c**. Determination of K_D value from the antilog of the Y-intercept value. *P* stands for propidium iodide; *I* stands for tested inhibitor; *Fe* is the initial fluorescence intensity when enzyme sites are saturated with *P*; *Fp* is the fluorescence intensity when propidium is completely displaced from the enzyme; *F* denotes the fluorescence intensity after adding a determined amount of displacing agent during the experiment.

5.4.2 BACE1 inhibitory activity

The assessment of the BACE1 inhibitory activity of this family of hybrids was carried out by the group of Dr. Vincenza Andrisano (*Università di Bologna*). Unfortunately, it was not possible to determine IC_{50} values due to interferences in fluorescence emission of these compounds at high concentrations. Alternatively, the percentages of inhibition of BACE1 by the novel CR-6–tacrine hybrids and reference compounds were determined at a single concentration of 5 μM, as a preliminary assessment of this activity (**Table 5.2**).

Most hybrids featuring an amide functionality within the linker displayed BACE1 inhibitory activity, whereas the hybrids bearing a secondary amino group in the linker turned out to be inactive. As we had found in the rhein–huprine hybrids, the BACE1 inhibitory activity of the CR-6–tacrine hybrids was significantly influenced by the linker length. Indeed, the most potent compounds were the benzylated amide **70c** (54% inhibition at 5 μM) and the amide **57c**

(42% inhibition at 5 µM), featuring the same linker with 12 atoms in total. These compounds should have an IC_{50} value around 5 µM, i.e. they can be considered moderately potent BACE1 inhibitors.

Table 5.2: *h*BACE1 inhibitory activities of the hydrochloride salts of the amides (±)-**57b-e**, the inverse amides (±)-**60a-c**, the amines (±)-**63b-e**, the benzylated amides (±)-**70a-d**, the tacrine-based amides (±)-**71a-d** and 6-chlorotacrine (**13**).

Compound	*h*BACE1 (% inhibition)[a]
(±)-**70a**·HCl	24.94
(±)-**70b**·HCl	18.06
(±)-**70c**·HCl	54.02
(±)-**70d**·HCl	nd[b]
(±)-**71a**·HCl	28.46
(±)-**71b**·HCl	27.70
(±)-**71c**·HCl	11.91
(±)-**71d**·HCl	6.83
(±)-**57b**·HCl	na[c]
(±)-**57c**·HCl	42.06
(±)-**57d**·HCl	17.98
(±)-**57e**·HCl	na[c]
(±)-**60a**·HCl	31.03
(±)-**60b**·HCl	11.81
(±)-**60c**·HCl	na[c]
(±)-**63b**·2HCl	na[c]
(±)-**63c**·2HCl	na[c]
(±)-**63d**·2HCl	nd[b]
(±)-**63e**·2HCl	9.08
13·HCl (6-chlorotacrine)	na[c]

[a] % inhibition at 5 µM.
[b] Not detectable.
[c] Not active.

5.4.3 Aβ$_{42}$ and tau anti-aggregating activity

The inhibitory activity of the novel CR-6–tacrine hybrids against the self-aggregation of $A\beta_{42}$ and tau was tested by Dr. Raimon Sabaté's group (*Universitat de Barcelona*) in *E. coli* cells using the Th-S fluorometric assay (**Table 5.3**).[158]

The amides **57b-e**, the inverse amides **60a-c**, and the tacrine-based amides **71a-d** were found to be only weakly active as $A\beta_{42}$ and tau anti-aggregating agents, exhibiting percentages of inhibition in the range 7–11%, 6–11%, and 8–17%, respectively ($A\beta_{42}$), and 8–15%, 4–18%, and 3–13%, respectively (tau) at a concentration of 10 μM, whereas the reference compounds 6-chlorotacrine (**13**), **58** and **61** were found to be inactive, as expected. Interestingly, the series of benzylated amides and secondary amines elicited moderately potent $A\beta_{42}$ and tau anti-aggregating activity, which was clearly dependent on the length of the linker. Thus, the $A\beta_{42}$ anti-aggregating activity of the amines increased in the order **63b** (n = 7; 18% inhibition) < **63c** (n = 8; 28% inhibition) < **63d** (n = 9; 34% inhibition). Likewise, their tau anti-aggregating activity increased in the order **63b** (n = 7; 29% inhibition) < **63c** (n = 8; 35% inhibition) < **63d** (n = 9; 48% inhibition). The presence of ethylenedioxy units in the linker of the amine **63e** led to a drop in both $A\beta_{42}$ (10% inhibition) and tau (18% inhibition) anti-aggregating activity relative to amine **63c**, with an equivalent tether length. The same trend regarding the influence of the length of the linker was found for the benzylated amides, where the $A\beta_{42}$ and tau anti-aggregating activities increased in the order **70a** (n = 6; 4% and 13% inhibition for $A\beta_{42}$ and tau, respectively) < **70b** (n = 7; 8% and 21% inhibition) < **70c** (n = 8; 24% and 40% inhibition) < **70d** (n = 9; 42% and 55% inhibition). Therefore, molecular hybridization of compounds completely devoid of $A\beta_{42}$ and tau anti-aggregating activity results in some hybrid compounds with moderately potent anti-aggregating effects. In particular, the longest homologs of the amines and benzylated amides series, **63d** and **70d**, must have IC_{50} values around 10 μM for both $A\beta_{42}$ and tau anti-aggregating activity.

Table 5.3: $A\beta_{42}$ and tau anti-aggregating activities of the CR-6-derived carboxylic acid (±)-**58**, and the hydrochloride salts of the amides (±)-**57b-e**, the inverse amides (±)-**60a-c**, the amines (±)-**63b-e**, the benzylated amides (±)-**70a-d**, the tacrine-based amides (±)-**71a-d**, 6-chlorotacrine (**13**), and the CR-6-derived amine (±)-**61**.

Compound	$A\beta_{42}$ aggregation[a] (% inh. at 10 µM)	tau aggregation[a] (% inh. at 10 µM)
(±)-**70a**·HCl	4.4 ± 3.0	12.9 ± 3.5
(±)-**70b**·HCl	8.2 ± 2.6	20.8 ± 2.5
(±)-**70c**·HCl	24.4 ± 2.9	40.4 ± 2.8
(±)-**70d**·HCl	41.8 ± 2.5	55.2 ± 2.1
(±)-**71a**·HCl	8.4 ± 2.5	7.5 ± 1.7
(±)-**71b**·HCl	8.7 ± 2.4	2.6 ± 1.3
(±)-**71c**·HCl	17.4 ± 3.8	9.2 ± 3.1
(±)-**71d**·HCl	16.4 ± 3.6	12.7 ± 2.1
(±)-**57b**·HCl	8.7 ± 3.1	8.3 ± 1.3
(±)-**57c**·HCl	7.5 ± 2.0	15.0 ± 2.1
(±)-**57d**·HCl	11.2 ± 3.1	12.6 ± 3.3
(±)-**57e**·HCl	6.5 ± 2.8	10.7 ± 2.0
(±)-**60a**·HCl	6.3 ± 3.0	4.5 ± 2.6
(±)-**60b**·HCl	6.4 ± 3.0	12.5 ± 2.1
(±)-**60c**·HCl	11.0 ± 2.5	18.5 ± 3.1
(±)-**63b**·2HCl	17.9 ± 4.0	29.0 ± 3.2
(±)-**63c**·2HCl	27.9 ± 3.3	35.5 ± 2.8
(±)-**63d**·2HCl	34.0 ± 2.8	48.2 ± 2.9
(±)-**63e**·2HCl	9.8 ± 1.4	17.6 ± 3.3
(±)-**58** (CR-6-COOH)	2.2 ± 2.3	0.5 ± 1.5
(±)-**61**·HCl (CR-6-NH_2)	2.6 ± 1.4	0.9 ± 1.5
13·HCl (6-chlorotacrine)	0.1 ± 0.6	0.7 ± 2.7

[a] % of inhibition of $A\beta_{42}$ and tau protein aggregation at 10 µM in intact *E. coli* cells. Values are expressed as mean ± SEM of four independent experiments.

5.4.4 Antioxidant activity

The antioxidant activity of the CR-6–tacrine hybrids was assessed through the free radical DPPH assay, which was carried out by Dr. María Garrido as part of this collaborative project (**Table 5.4**).

As expected, the benzylated amides **70a-d** were devoid of antioxidant activity, due to the absence of an available phenolic group, which confers the radical scavenging property. Conversely, because of the presence of a phenol-containing CR-6-derived moiety in the structure of the CR-6–tacrine hybrids, these compounds exhibited good antioxidant activity, being roughly equipotent to CR-6 (**17**), trolox (commonly used as reference compound in antioxidant activity assays), and both the CR-6-derived carboxylic acid **58** and amine **61**. Of note, the amine **63c** was the most potent antioxidant compound (IC_{50} = 6.9 μM), being 2-fold more potent than the reference compounds CR-6 and trolox.

Table 5.4: Antioxidant activity of trolox, CR-6 (**17**), and the CR-6-derived carboxylic acid (±)-**58**, and the hydrochloride salts of the amides (±)-**57b-e**, the inverse amides (±)-**60a-c**, the amines (±)-**63b-e**, the benzylated amides (±)-**70a-d**, the tacrine-based amides (±)-**71a-d**, 6-chlorotacrine (**13**), and the CR-6-derived amine (±)-**61**.

Compound	DPPH[a] IC_{50} (µM)
(±)-**70a**·HCl	ni[b]
(±)-**70b**·HCl	ni[b]
(±)-**70c**·HCl	ni[b]
(±)-**70d**·HCl	ni[b]
(±)-**71a**·HCl	22.9 ± 6.7
(±)-**71b**·HCl	13.6 ± 5.6
(±)-**71c**·HCl	19.4 ± 6.6
(±)-**71d**·HCl	14.7 ± 4.9
(±)-**57b**·HCl	15.2 ± 5.6
(±)-**57c**·HCl	19.1 ± 5.6
(±)-**57d**·HCl	13.4 ± 5.1
(±)-**57e**·HCl	16.8 ± 5.0
(±)-**60a**·HCl	8.9 ± 1.6
(±)-**60b**·HCl	15.1 ± 2.3
(±)-**60c**·HCl	13.1 ± 2.9
(±)-**63b**·2HCl	16.5 ± 3.7
(±)-**63c**·2HCl	6.9 ± 1.6
(±)-**63d**·2HCl	18.5 ± 1.7
(±)-**63e**·2HCl	17.8 ± 5.8
(±)-**58** (CR-6-COOH)	14.9 ± 2.5
(±)-**61**·HCl (CR-6-NH_2)	14.0 ± 3.3
13·HCl (6-chlorotacrine)	ni[b]
17 (CR-6)	17.4 ± 5.7
trolox	15.7 ± 0.9[c]

[a] IC_{50} values for free radical DPPH assay. Values are expressed as mean ± SD of one representative experiment performed in triplicate.
[b] No inhibition.
[c] Data from Ref. 143.

5.4.5 In vitro BBB permeation assay

Like for the previous families of compounds, the PAMPA-BBB assay[160] was performed by Dr. Belén Pérez (*Universitat Autònoma de Barcelona*) to predict the brain permeation of the novel CR-6–tacrine hybrids (**Table 5.5**).

From the correlation obtained by comparing the experimental and reported *in vitro* permeability (P_e) values of fourteen reference drugs and the limits established for BBB permeation,[160] the threshold for high BBB permeation (CNS+) was set at P_e (10^{-6} cm s^{-1}) > 5.157, compounds of low BBB permeation (CNS–) at P_e (10^{-6} cm s^{-1}) < 2.006, and compounds of uncertain BBB permeation (CNS+/–) 5.157 > P_e (10^{-6} cm s^{-1}) > 2.006. With regard to the parent compounds, the relatively polar CR-6-derived carboxylic acid **58** and amine **61** were predicted not to be able to cross the BBB, whereas the lipophilic 6-chlorotacrine displayed a high permeability value, well above the limit established for high BBB permeation. Intermediate permeability values between those of 6-chlorotacrine and the CR-6-derived parent compounds were found for the novel CR-6–tacrine hybrids. In general, the predicted permeabilities of the hybrids increased with factors that lead to increased lipophilicity as increased tether length and the presence of a benzyl group in the benzylated amides, while they decreased with factors that increased polarity such as the presence of ethylenedioxy units within the linker. Notwithstanding these trends, P_e values over the CNS+ threshold were obtained for all the novel CR-6–tacrine hybrids, with the sole exception of the tacrine-based hybrid **71a**, so that all of them should be able to cross BBB and reach their multiple targets at the CNS.

Table 5.5: Permeability results from the PAMPA-BBB assay of the CR-6-derived-carboxylic acid (±)-**58**, and the hydrochloride salts of the amides (±)-**57b-e**, the inverse amides (±)-**60a-c**, the amines (±)-**63b-e**, the benzylated amides (±)-**70a-d**, the tacrine-based amides (±)-**71a-d**, 6-chlorotacrine (**13**), and the CR-6-derived amine (±)-**61**.

Compound	P_e (10^{-6} cm s^{-1})[a]	Prediction
(±)-**70a**·HCl	10.8 ± 1.0	CNS+
(±)-**70b**·HCl	11.5 ± 0.5	CNS+
(±)-**70c**·HCl	12.3 ± 0.2	CNS+
(±)-**70d**·HCl	10.4 ± 0.7	CNS+
(±)-**71a**·HCl	4.3 ± 0.3	CNS+/–
(±)-**71b**·HCl	6.6 ± 0.8	CNS+
(±)-**71c**·HCl	7.3 ± 0.9	CNS+
(±)-**71d**·HCl	8.9 ± 0.5	CNS+
(±)-**57b**·HCl	9.7 ± 0.7	CNS+
(±)-**57c**·HCl	9.6 ± 0.6	CNS+
(±)-**57d**·HCl	8.2 ± 0.5	CNS+
(±)-**57e**·HCl	7.0 ± 0.2	CNS+
(±)-**60a**·HCl	7.8 ± 0.2	CNS+
(±)-**60b**·HCl	8.3 ± 1.3	CNS+
(±)-**60c**·HCl	8.7 ± 0.8	CNS+
(±)-**63b**·2HCl	10.4 ± 0.2	CNS+
(±)-**63c**·2HCl	12.5 ± 0.6	CNS+
(±)-**63d**·2HCl	10.1 ± 1.3	CNS+
(±)-**63e**·2HCl	9.7 ± 0.6	CNS+
(±)-**58** (CR-6-COOH)	0.4 ± 0.02	CNS–
(±)-**61**·HCl (CR-6-NH_2)	1.0 ± 0.05	CNS–
13·HCl (6-chlorotacrine)	26.1 ± 0.6	CNS+

[a] Permeability values from the PAMPA-BBB assay. Values are expressed as the mean ± SD of three experiments, each performed in triplicate.

5.4.6 In vivo assays

In the light of the outstanding multi-target profile exhibited by some compounds of this structural class, further studies have been scheduled in collaboration with the group of Drs. Isidre Ferrer and Ester Aso (*Institut d'Investigació Biomèdica de Bellvitge*), namely *in vivo* assays in APP/PS1 transgenic mice, a well-established mouse model of AD.

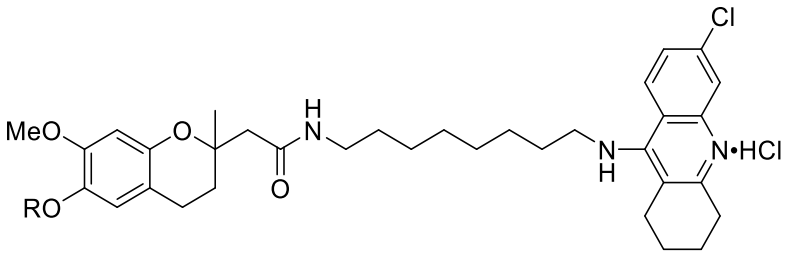

(±)-**57c**, R = H
(±)-**70c**, R = Bn

Figure 5.8: Structures of the selected CR-6–tacrine hybrids for *in vivo* assays, (±)-**70c** and (±)-**57c**.

The benzylated amide **70c** and its homologous deprotected counterpart **57c** (**Figure 5.8**) have been selected for the *in vivo* studies, in light of their complementary pharmacological profile (**Table 5.6**). These compounds display good potency against *h*AChE, *h*BChE and *h*BACE1. However, **70c** is a moderately potent $A\beta_{42}$ and tau anti-aggregating inhibitor, but inactive as antioxidant because the benzyl group is masking the phenolic OH group, whereas **57c** is essentially the opposite, being devoid of anti-aggregating activity, but displaying a potent antioxidant effect. Of note, **70c** might be converted into **57c** after a phase I metabolic *O*-dealkylation reaction in liver. Since both compounds are predicted to cross the BBB, we could speculate that administration of **70c** could afford a sustained combined multi-target activity profile afforded by **70c** itself and/or its potential metabolite **57c**.

Table 5.6: Summary of the biological activities of the selected compounds.

Compound	**(±)-70c**	**(±)-57c**
***h*AChE** IC_{50} (nM)	10.4 ± 0.6	3.69 ± 0.19
***h*BChE** IC_{50} (nM)	100 ± 5	170 ± 9
***h*BACE1** (% inh. at 5 µM)	54.02	42.06
$A\beta_{42}$ aggregation (% inh. at 10 µM)	24.4 ± 2.9	7.5 ± 2.0
tau aggregation (% inh. at 10 µM)	40.4 ± 2.8	15.0 ± 2.1
DPPH IC_{50} (µM)	*no inhibition*	19.1 ± 5.6
P_e (prediction)	12.3 ± 0.2 (CNS+)	9.6 ± 0.6 (CNS+)

CHAPTER 6

Benzoadamantane–tacrine hybrids

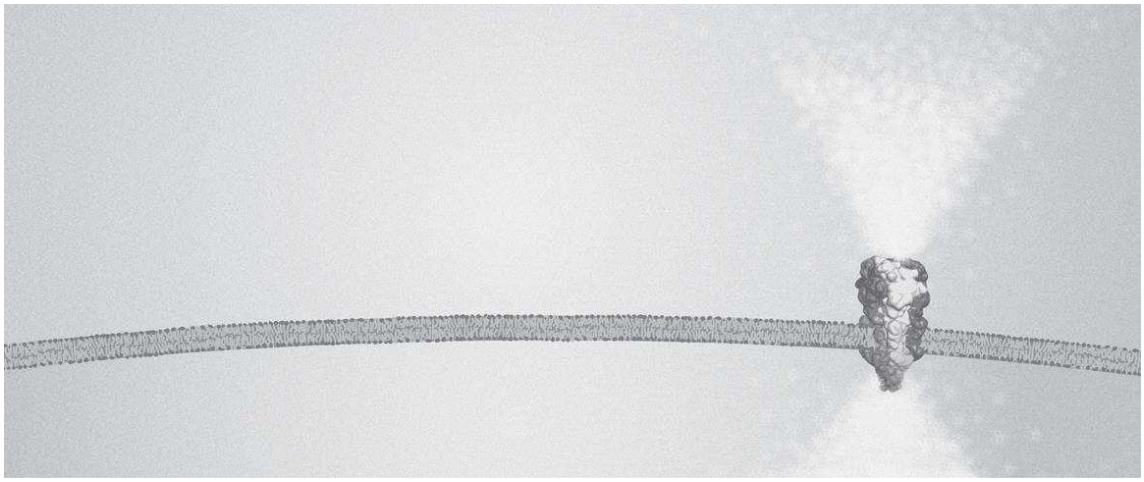

Image source: daCosta]:[lab, University of Ottawa. (*www.dacosta.net*)

6.1 Background

Even though both AChE inhibitors and NMDA receptor antagonists are the unique type of marketed anti-Alzheimer drugs, their combination in MTDLs has been barely explored.[198,199] The main family of compounds involving this specific multi-target profile combined pharmacophoric moieties of the marketed drugs galantamine and memantine. The corresponding hybrid compounds were endowed with low nanomolar and low micromolar IC_{50} values against AChE and NMDA receptor, respectively, and also showed neuroprotective effects.[200] These interesting results prompted us to envision the design of the novel family of benzoadamantane–tacrine hybrids described in this chapter, with the aim of integrating the symptomatic relief resulting from AChE inhibition and the neuroprotective action of NMDA receptor antagonism.

Over the last years, the group of Dr. Santiago Vazquez (*Universitat de Barcelona*) has intensively pursued the development of polycyclic amines able to block the NMDA receptor. Dr. Elena Valverde has recently optimized, during her PhD work, a benzoadamantane scaffold with that purpose, namely the benzopolycyclic amine **18** (**Figure 6.1**), which displayed an IC_{50} value (1.9 μM) in the same range of memantine, **6** (1.5 μM).[144] Later on, and taking account of the deleterious effect elicited by substitution on the amino group of memantine derivatives,[144] Dr. Marta Barniol functionalized the aromatic ring of **18** with an additional primary amino group (**74**, IC_{50} = 39 μM),[145] which could be used as the linkage position with the tacrine moiety, while leaving intact the aliphatic amino group, essential for NMDA antagonistic activity.

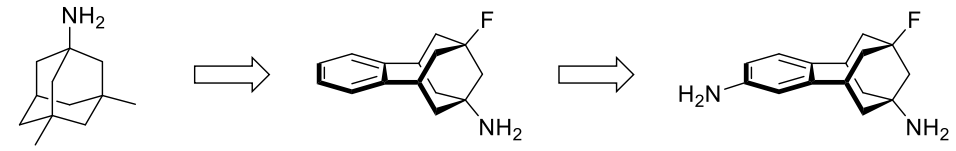

memantine, **6** **18** (±)-**74**

Figure 6.1: Structures of memantine, **6**, and benzohomoadamantanes **18** and **74**.

[198] a) V. Tumiatti, A. Minarini, M. L. Bolognesi, A. Milelli, M. Rosini, C. Melchiorre. *Curr. Med. Chem.* **2010**, *17*, 1825. b) A. Minarini, A. Milelli, E. Simoni, M. Rosini, M. L. Bolognesi, C. Marchetti, V. Tumiatti. *Curr. Top. Med. Chem.* **2013**, *13*, 1771.
[199] M. Rosini, E. Simoni, A. Minarini, C. Melchiorre. *Neurochem. Res.* **2014**, *39*, 1914.
[200] E. Simoni, S. Daniele, G. Bottegoni, D. Pizzirani, M. L. Trincavelli, L. Goldoni, G. Tarozzo, A. Reggiani, C. Martini, D. Piomelli, C. Melchiorre, M. Rosini, A. Cavalli. *J. Med. Chem.* **2012**, *55*, 9708.

As mentioned in the introduction (**Section 1.4.2.2**), it is believed that memantine is placed in the channel pore with the charged nitrogen pointing inside the cell, near the critical channel asparagine residues, while the two methyl groups fill two hydrophobic pockets in the binding site (**Figure 6.2**).[103] Indeed, this proposed binding mode agrees with the loss of potency arising from *N*-substitutions.

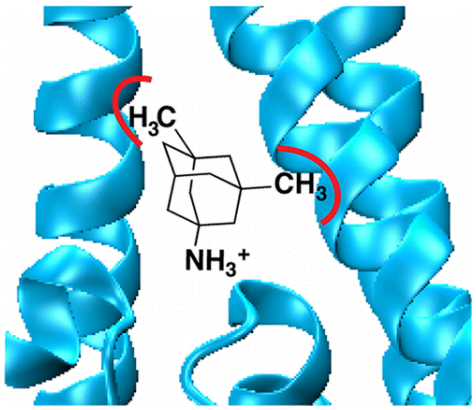

Figure 6.2: Predicted binding mode for memantine, **6**, inside the NMDA channel pore (Image source: W. Limapichat, W. Y. Yu, E. Branigan *et al*. *ACS Chem. Neurosci.* **2013**, *4*, 255).

6.2 Design of benzoadamantane–tacrine hybrids

In this context, we envisaged the combination of the well-known AChE inhibitor 6-chlorotacrine (**13**), with a benzohomoadamantane moiety (for the sake of simplicity, the shorter term *benzoadamantane* will be used from now on) with reported NMDA antagonistic properties. Two series of hybrids were designed, differing in the linkage position at the benzoadamantane moiety. Firstly, we envisaged the linkage from the amino group of benzoadamantane **18**, in analogy with the previously reported family of memantine–galantamine hybrids, which exhibited an interesting NMDA receptor antagonist activity[200] despite being substituted at the amino group (general structure **IV**, **Figure 6.3**). Secondly, we planned the linkage from the aniline amino group of the benzoadamantane **74**, to keep the aliphatic amino group unsubstituted, which should allow the hybrids to retain the binding mode predicted for memantine(general structure **V**).

For the choice of the tether length, we envisioned a dual binding mode within AChE. This goal prompted us to select an appropriate spacer of 6 or 7 atoms between both

pharmacophoric fragments to cover the 16 Å distance between Trp86 in the CAS, where the 6-chlorotacrine fragment binds, and Trp286, the main residue in the PAS involved in ligand-interactions. The coupling between both units was envisaged by means of an amide functionality.

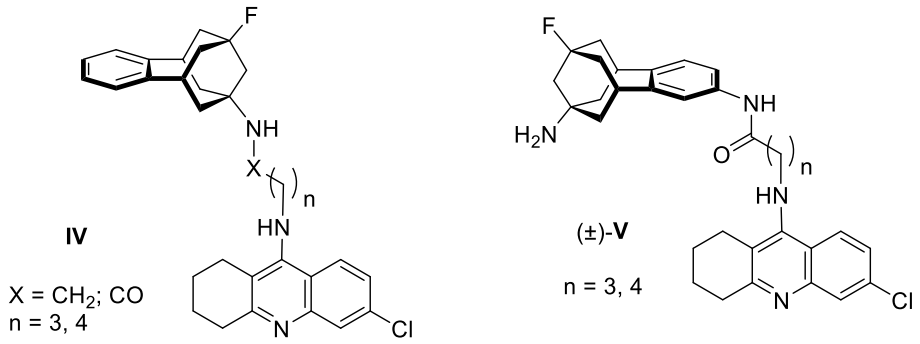

Figure 6.3: General structure of the two series of benzoadamantane–tacrine hybrids (**IV** and **V**).

The 6-chlorotacrine moiety of these hybrids, which will be protonated at physiological pH, was expected to tightly bind the CAS of AChE by means of cation-π and π-π stacking interactions with the indole ring of Trp86 and the benzene ring of Tyr337, hydrogen bonding between the protonated acridine nitrogen atom and the carbonyl oxygen of His447, and hydrophobic interactions by the chlorine atom, which should fill a hydrophobic pocket formed by Pro446, Trp439, and Met443. Moreover, we might expect simultaneous interactions of the benzoadamantane moiety with the PAS of AChE, where the benzene ring could stablish π-π stacking interactions with the aromatic PAS residues Trp286 and Tyr72, and, additionally, in series **V**, the protonated aliphatic amino group could enable cation-π interactions with the indole group of Trp286. Furthermore, additional interactions in the PAS and/or the midgorge residues might be expected for both series of hybrids.

6.3 Synthesis of the benzoadamantane–tacrine hybrids

The retrosynthetic pathway is depicted in **Scheme 6.1**.

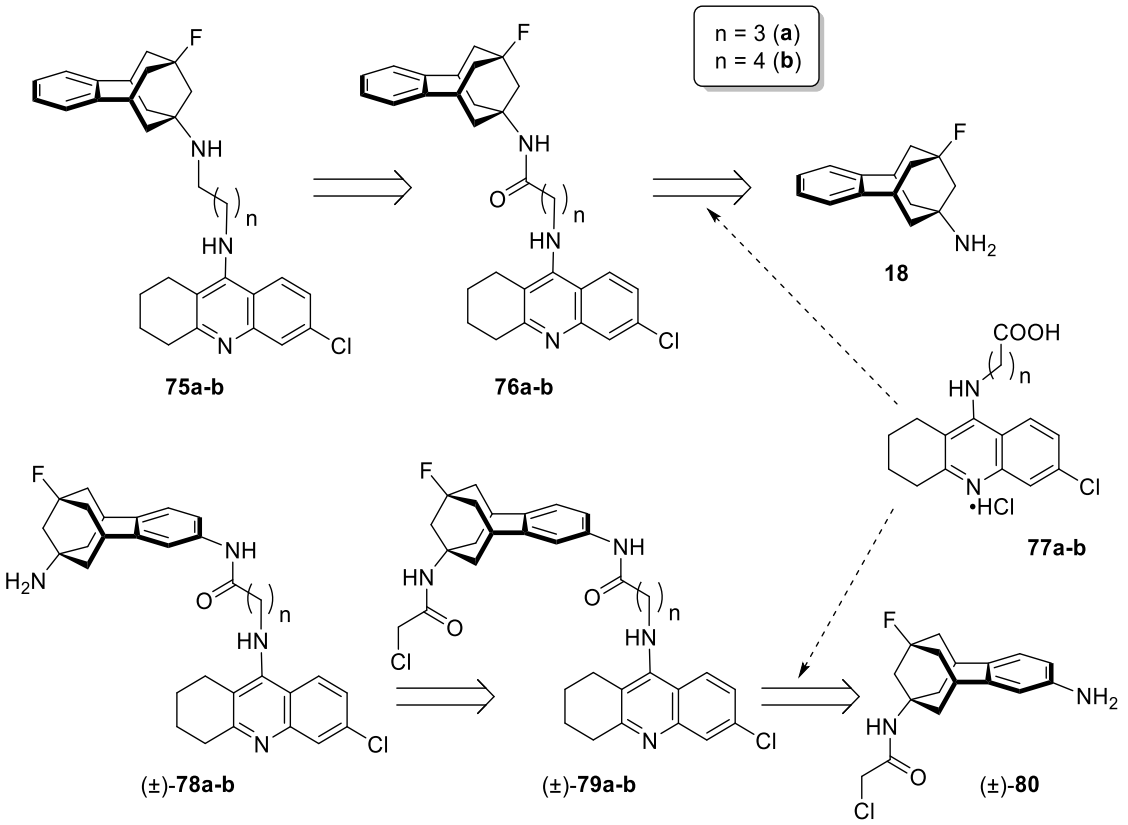

Scheme 6.1

It must be noted that this project was originally carried out in collaboration with Dr. Marta Barniol, who was responsible for the synthesis of both benzoadamantane derivatives, **18** and **80**. However, eventual complications precluded the synthesis of these hybrids in the last steps, so that both compounds, **18** and **80**, had to be re-synthesized, first by myself together with the graduated Erasmus student Deborah Pivetta, and then again, with slight structural modifications, by the PhD student Andreea L. Turcu.

6.3.1 Synthesis of the benzoadamantane scaffold 18

The preparation of adamantane-like intermediate **18** was carried out by following a described procedure (**Scheme 6.2**).[144]

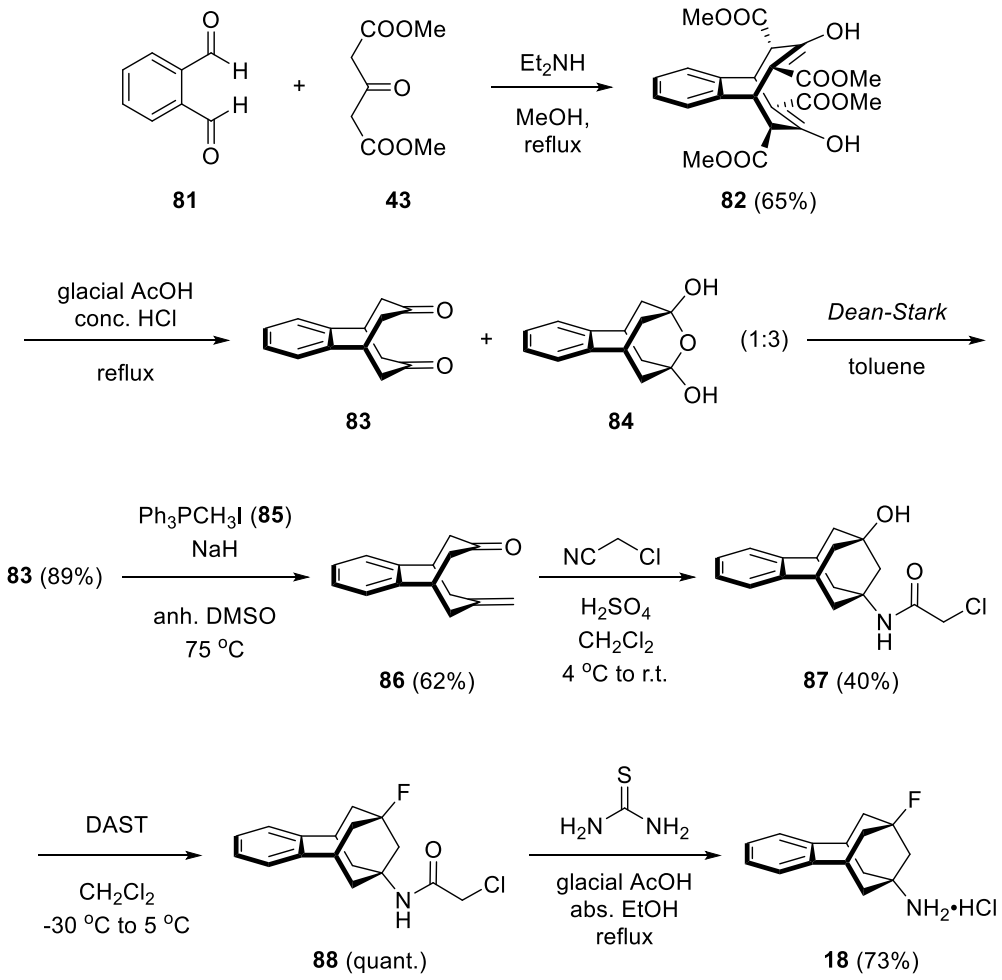

Scheme 6.2

The synthetic route comprised an initial Weiss-Cook condensation reaction between phthaldialdehyde, **81**, and 2 equivalents of dimethyl 1,3-acetonedicarboxylate, **43**, in the presence of Et_2NH and MeOH, to provide the tetraester intermediate **82** in 65% yield. Later on, the tetraester **82** was subjected to acidic hydrolysis followed by spontaneous decarboxylation to give a mixture of diketone **83** and its hydrate **84** in a ratio 1:3. Heating of this mixture in toluene under reflux using a Dean-Stark apparatus afforded pure diketone **83** in 89% overall yield. Wittig reaction of the phosphorus ylide generated from methyltriphenylphosphonium iodide with one of the ketone groups of diketone **83** afforded enone **86**. The byproduct formed in the latter reaction, phosphine oxide, was removed by packing the reaction crude in silica gel followed by extraction with an appropriate mixture of petroleum ether and diethyl ether, obtaining the mono-Wittig reaction product **86** in 62% yield. The synthesis continued with a Prins-Ritter transannular cyclization with chloroacetonitrile in the presence of sulfuric acid, to afford, after aluminum oxide column chromatography, the chloroacetamide **87** in 40% yield,

which was then treated with the fluorinating agent (diethylamino)sulfur trifluoride (DAST) to provide in quantitative yield the key fluorinated derivative **88**, a common intermediate for both benzoadamantane scaffolds **18** and **80**. In this case, **18** was prepared by removing the chloroacetamide group using thiourea and glacial acetic acid in absolute ethanol, giving the desired amine in 73% yield.

6.3.2 Synthesis of the tacrine-derived intermediates

The preparation of intermediates **77a-b** started with the alkylation of 6-chlorotacrine, **13**, with the corresponding ω-bromoalkanenitrile, **89a-b**, in the presence of KOH and DMSO at room temperature overnight (**Scheme 6.3**), a procedure commonly used in our research group and previously described for compounds **73a-c**. By applying this methodology, cyanoalkyltacrine **90b** was obtained in 64% yield, whereas compound **90a** was not observed in the resulting reaction crude.

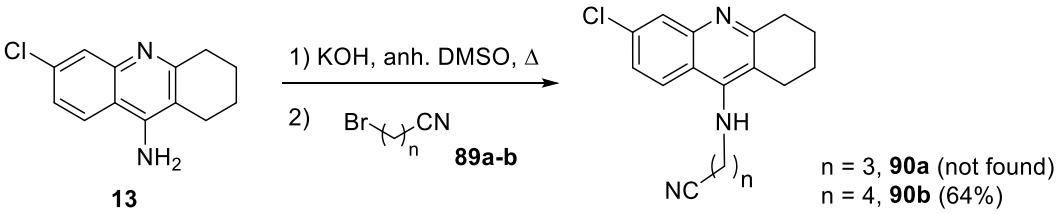

Scheme 6.3

Therefore, some modifications in the methodology were attempted for the synthesis of **90a**. The addition of catalytic amounts of potassium iodide to facilitate the nucleophilic substitution reaction was fruitless (**Scheme 6.4**). We speculated that the higher acidity of the α-cyano position in **89a** relative to **89b**, due to the closer proximity of the halogen atom, might trigger undesired reactions, such as polymerization. Taking account of this assumption, we attempted the alkylation reaction using a weaker base (potassium carbonate) using some reported conditions,[201,202] even though our exocyclic amine was less nucleophilic than the amines described in those manuscripts. Unfortunately, exclusively starting material was found in the control TLC after 2 days under reflux.

[201] V. N. Devegowda, S. H. Seo, A. N. Pae, G. Nam, K. Il Choi. *Bull. Korean Chem. Soc.* **2012**, *33*, 647.
[202] R. A. Gardner, M. Belting, K. Svensson, O. Phanstiel. *J. Med. Chem.* **2007**, *50,* 308.

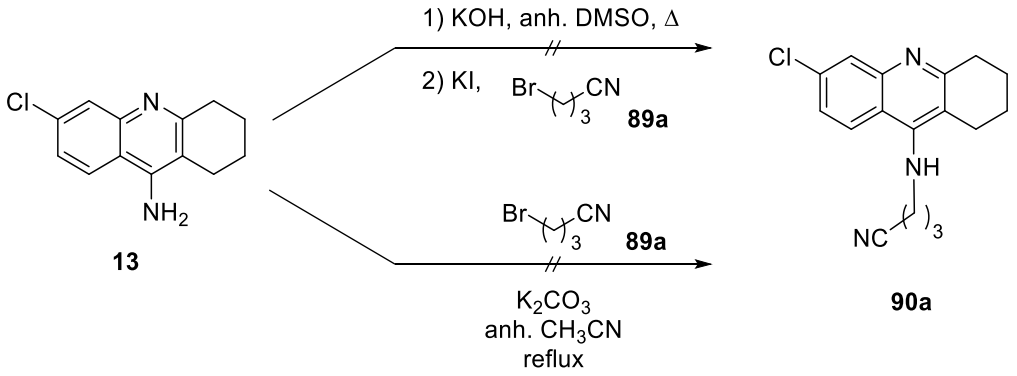

Scheme 6.4

In the light of these results, we decided to design a new synthetic route, which started with the amination of the 6,9-dichloroacridine derivative **67** with 3-aminopropan-1-ol, **91**, to afford the alcohol **92** in 94% yield (**Scheme 6.5**).[195,203,204] Subsequently, mesylate **93** was formed in quantitative yield by treating the alcohol **92** with methanesulfonyl chloride in the presence of Et_3N,[195] and reacted with NaCN in DMF, to afford the desired cyanoalkyltacrine **90a** in 98% yield[205] (92% overall yield from **67**).

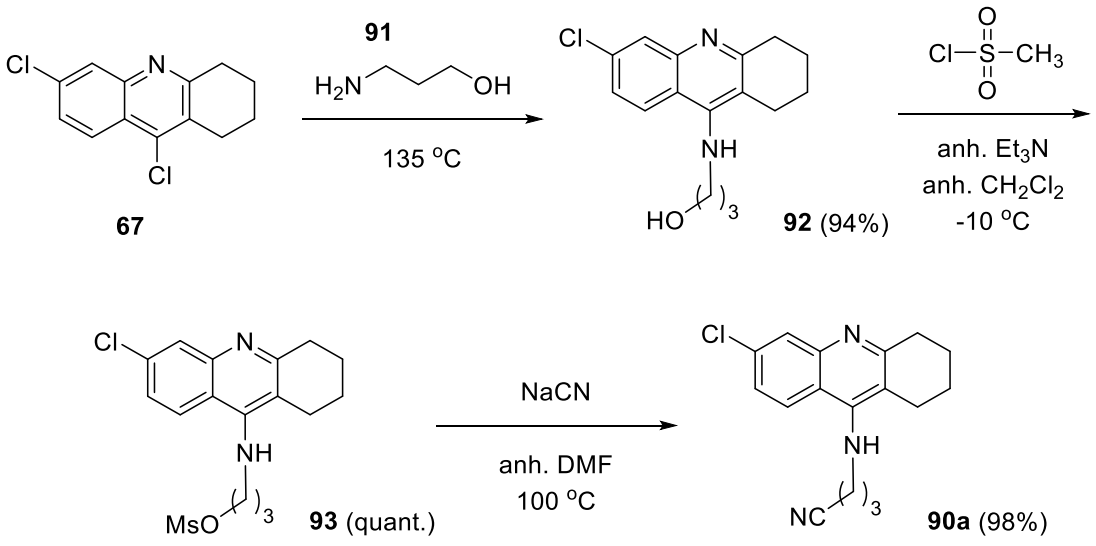

Scheme 6.5

[203] S. Burgess, A. Selzer, J. Kelly, M. Smilkstein, M. Riscoe, D. Peyton. *J. Med. Chem.* **2006**, *49,* 5623.
[204] K. Starčević, D. Pešić, A. Toplak, G. Landek, S. Alihodžić, E. Herreros, S. Ferrer, R. Spaventi, M. Perć. *Eur. J. Med. Chem.* **2012**, *49*, 365.
[205] M. de Souza, K. Pais, C. Kaiser, M. Peralta, M. Ferreira, M. Lourenço. *Bioorg. Med. Chem.* **2009**, *17*, 1474.

6.3.3 Synthesis of hybrids 76 and 75

Afterwards, hydrolysis of nitriles **90a-b** led to the corresponding quinoline carboxylic acids **77a-b**, which were obtained as hydrochloride salts and used in the following step without further purification (**Scheme 6.6**). Then, the amide coupling reactions between the benzoadamantanamine **18** and the carboxylic acids **77a-b** were carried out in the presence of EDC, HOBt, and Et_3N in a mixture EtOAc / DMF at room temperature for 24 h, giving the amides **76a-b** in 40 and 75% yield, respectively, after silica gel column chromatography purification.

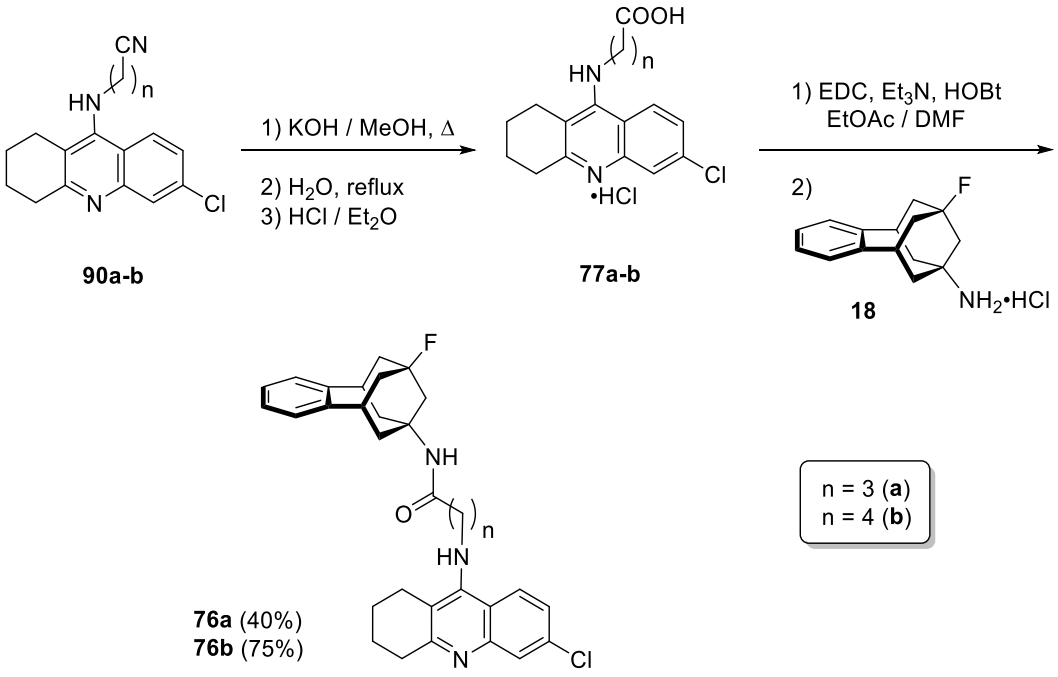

Scheme 6.6

For the last step of this synthetic pathway, as shown in the retrosynthesis (**Scheme 6.1**), we envisaged the reduction of the amides **76a-b** to the amines **75a-b**, which turned out to be a difficult task. Treatment of **76a** and **76b** with borane in THF at room temperature overnight afforded the target amine hybrids **75a-b** in low yields (**Scheme 6.7**).

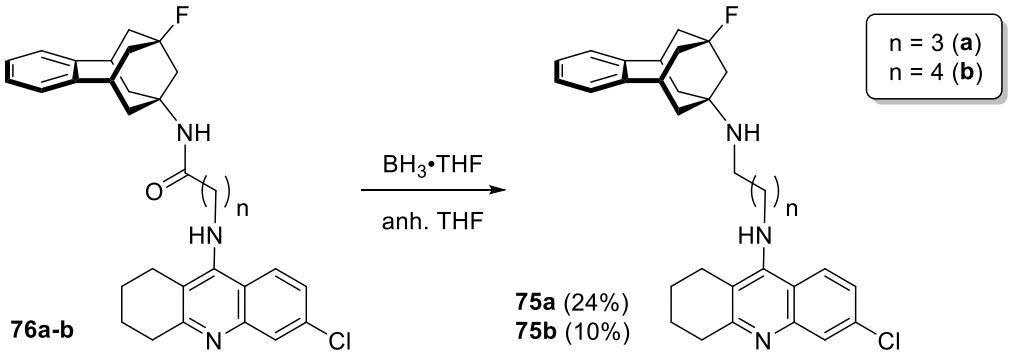

Scheme 6.7

These results prompted us to explore other reducing agents, such as lithium borohydride,[206] lithium aluminum hydride[207] and Red-Al, in several conditions. All reductions were attempted over **76b**, since it had been obtained a larger amount than the shorter homolog **76a**. Nevertheless, none of the performed reductions was successful (**Scheme 6.8**).

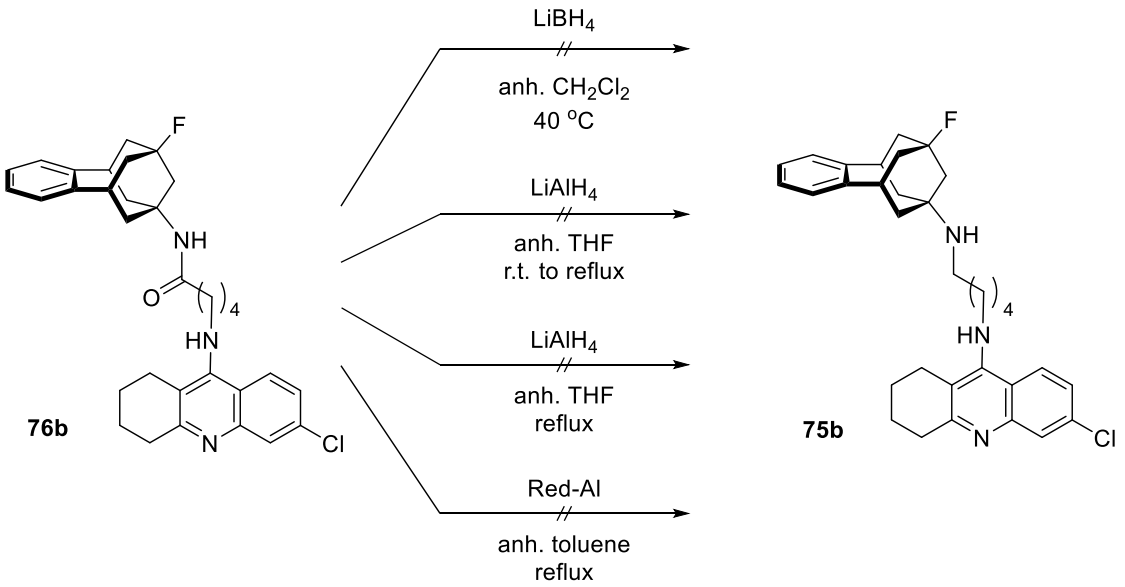

Scheme 6.8

At this point, a new synthetic approach was envisaged to get access to amines **75a-b**, which involved a nucleophilic substitution of tacrine-based mesylates **94a-b** with amine **18** (**Scheme 6.9**).

[206] U. Larsen, M, Begtrup, L. Martiny. *J. Labelled Comp. Radiopharm.* **2005**, *48*, 429.
[207] S. Seto, K. Yumoto, K. Okada, Y. Asahina, A. Iwane, M. Iwago, R. Terasawa, K. Shreder, K. Murakami, Y. Kohno. *Bioorg. Med. Chem.* **2012**, *20*, 1188.

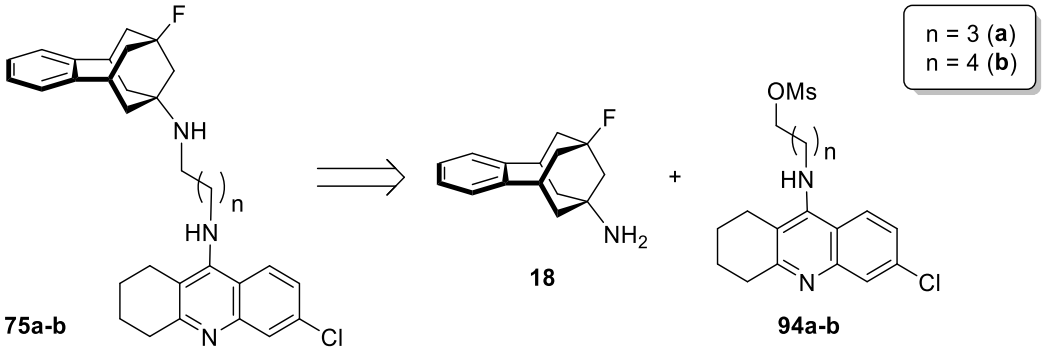

Scheme 6.9

The preparation of mesylates **94a-b** was planned as previously described for mesylate **93** (**Scheme 6.5**). Thus, alkylation of the 6,9-dichloroacridine derivative **67** with the corresponding aminoalcohol **95a-b** afforded the alcohols **96a-b** in quantitative and 40% yield, respectively (**Scheme 6.10**).[203,204,208] Mesylate **94b** was formed in quantitative yield by treating alcohol **96b** with methanesulfonyl chloride in the presence of Et_3N,[195] while mesylate **94a** was not found in the corresponding reaction crude, because it spontaneously underwent a cyclization reaction to pyrrolidine **97**.

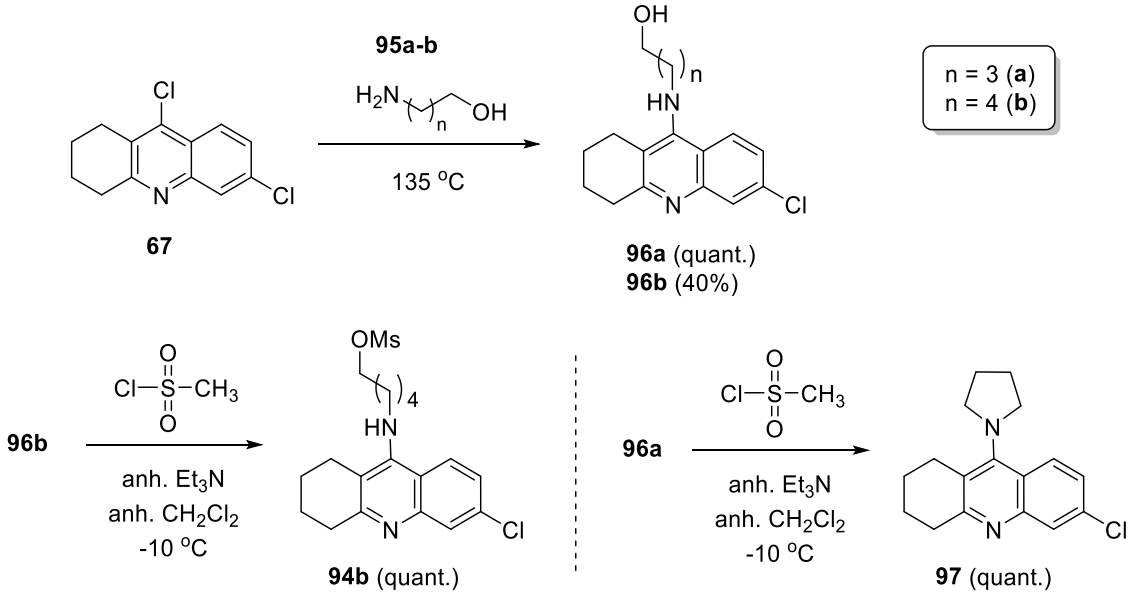

Scheme 6.10

[208] T. Eckroat, K. Green, R. Reed, J. Bornstein, S. Garneau-Tsodikova. *Bioorg. Med. Chem.* **2013**, *21*, 3614.

Reaction of amine **18** with mesylate **94b** in basic conditions at 80 °C afforded a complex mixture of compounds, from which the chloroderivative **98** and a mixture of alcohol **96b** and the target amine **75b** were isolated after silica gel column chromatography purification (**Scheme 6.11**). Unfortunately, different attempts to isolate the target hybrid **75b** from its mixture with **96b**, including crystallization or two more consecutive column chromatography purification processes, were unsuccessful.

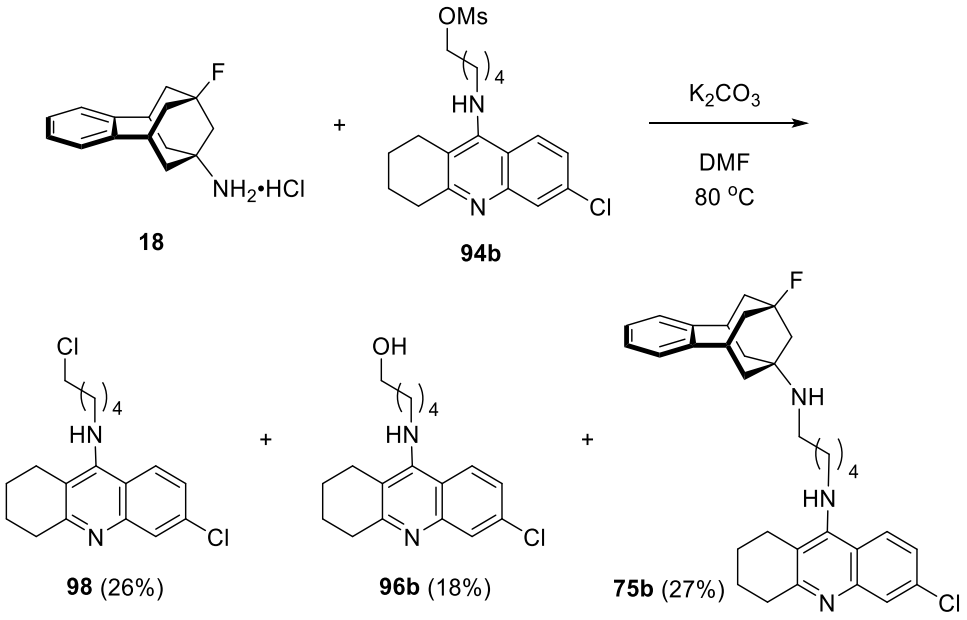

Scheme 6.11

In light of these results, an alternative synthetic pathway was planned for the preparation of hybrids **75a-b**, whose retrosynthesis is depicted below (**Scheme 6.12**).

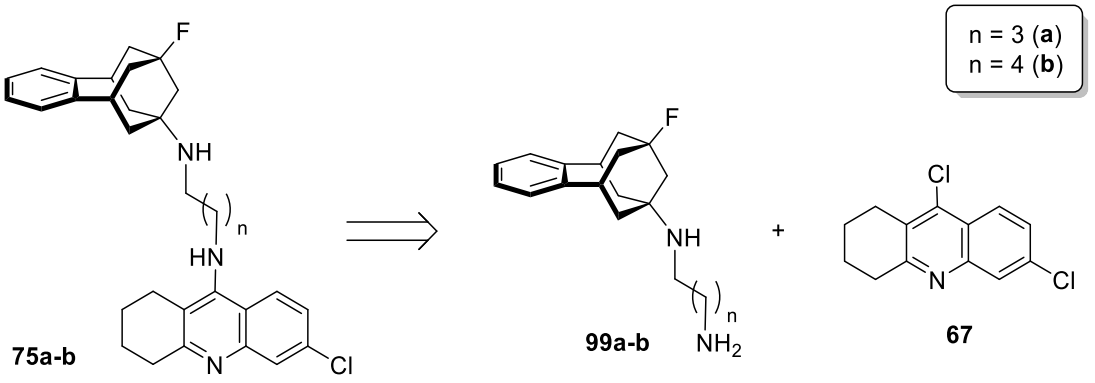

Scheme 6.12

We first proceeded to prepare the intermediate **99b** by alkylation of benzoadamantane **18** with 5-bromovaleronitrile, **89b**, in the presence of potassium carbonate at 80 °C,[200] which afforded the nitrile **100b** in 61% yield, after silica gel column chromatography purification. The attempted reduction of nitrile **100b** with lithium aluminum hydride did not afford the desired amine **99b**, but the byproducts **86** and **101** (**Scheme 6.13**). We hypothesized that these byproducts might arise from a retro-Prins reaction initiated by deprotonation of the secondary amine and involving the departure of fluoride as a leaving group, to form a bicyclic enimine that could be reduced to the enamine **101** or hydrolyzed to the enone **86** during the aqueous work-up.

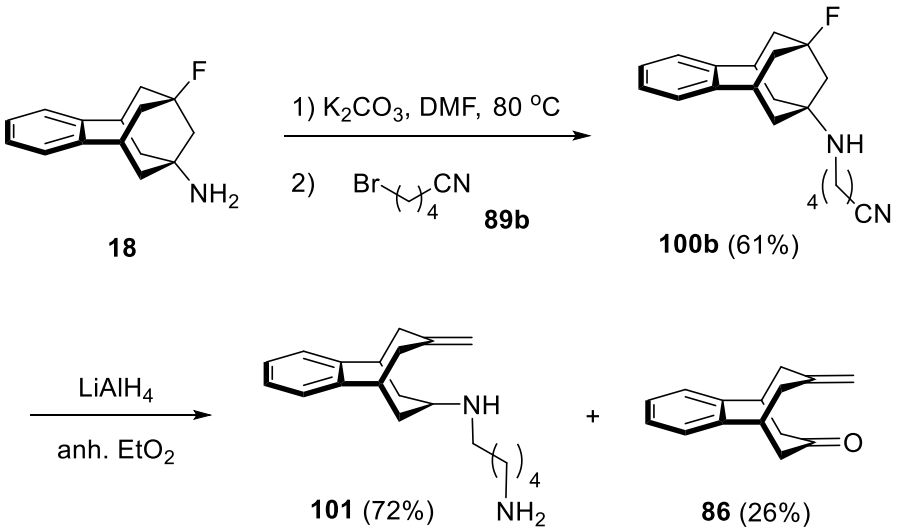

Scheme 6.13

Finally, we managed to perform the whole biological evaluation of hybrids **75a-b** with the low amount obtained after the reduction of **76a-b** with borane (**Scheme 6.7**).

6.3.4 Synthesis of the benzoadamantane scaffold 80

For the preparation of hybrids **78a-b**, we first needed the adamantane-like intermediate **80**, whose synthesis was envisaged starting from the previously synthesized intermediate **88**. Treatment of **88** with glacial acetic acid and nitric acid, in the presence of acetic anhydride at room temperature for 24 h, afforded regioselectively the nitroderivative **102** (**Scheme 6.14**). This compound was subsequently subjected to a hydrogenation reaction under mild conditions,

likely providing the desired benzoadamantane derivative **80**, which, unfortunately, underwent a polymerization reaction, so that **80** could not be isolated from the reaction crude.

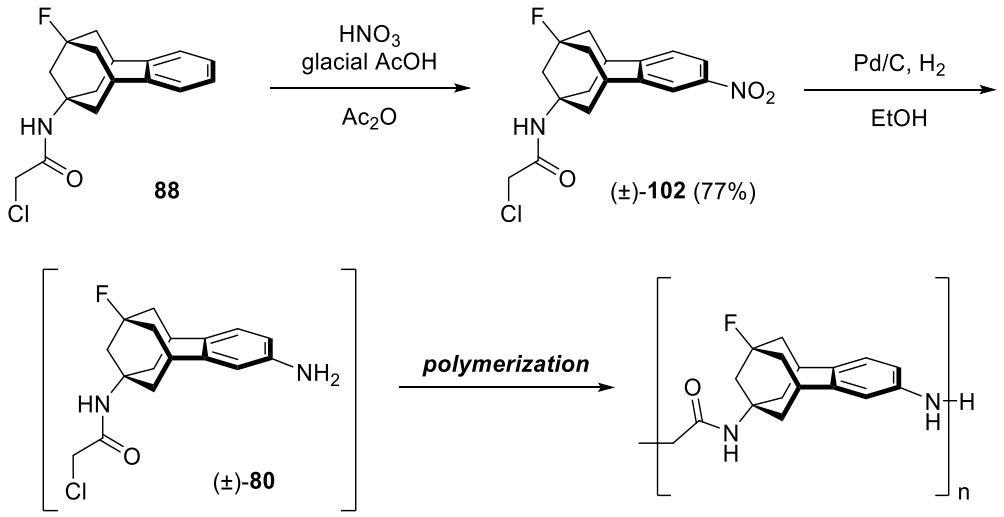

Scheme 6.14

Alternatively, we envisioned a new pathway to get access to the target hybrids **78a-b**. Then, in the context of Andreea L. Turcu's PhD Thesis work, intermediate **88** was re-synthesized and the new route was subsequently applied, consisting of consecutive nitration, removal of chloroacetamide group, addition of *tert*-butoxycarbonyl (Boc) protecting group, and hydrogenation, to afford the amine **105** (**Scheme 6.15**), which was used for the amide coupling reactions with the corresponding tacrine-derived carboxylic acid.

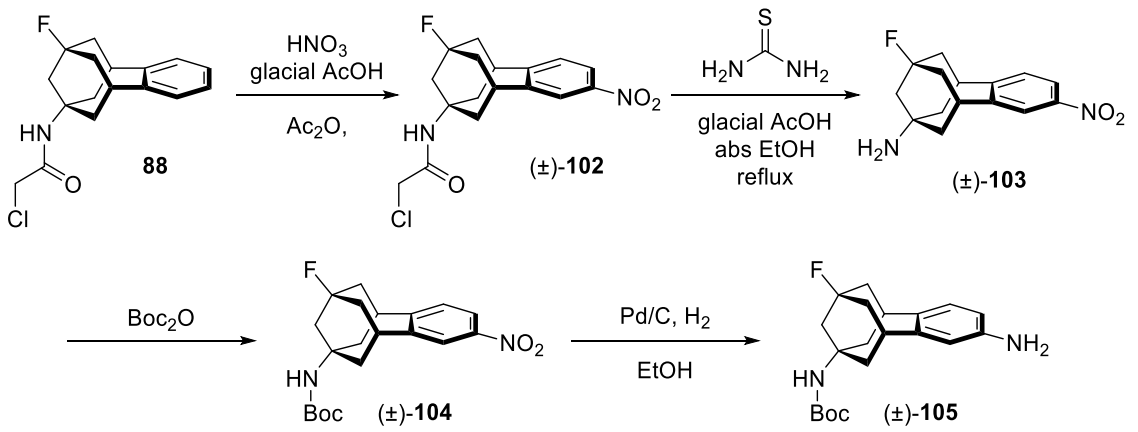

Scheme 6.15

6.3.5 Synthesis of the series of hybrids 78

Fot the next step, hydrolysis of the nitriles **90a-b** was performed, leading to the corresponding quinoline carboxylic acids **77a-b**, which were obtained as hydrochloride salts and used in the following step without further purification (**Scheme 6.16**). The amide coupling reactions between the benzoadamantane **105** and the carboxylic acids **77a-b** were carried out in the presence of EDC, HOBt, and Et_3N in a mixture EtOAc / DMF at room temperature for 24 h, giving, after silica gel column chromatography purification, slightly impure amides **106a-b**. After removal of the Boc protecting group of **106a-b** by treatment with HCl in dioxane at room temperature for 24 h, followed by silica gel column chromatography purification of the resulting crudes, pure hybrids **78a-b** were isolated in moderate yields.

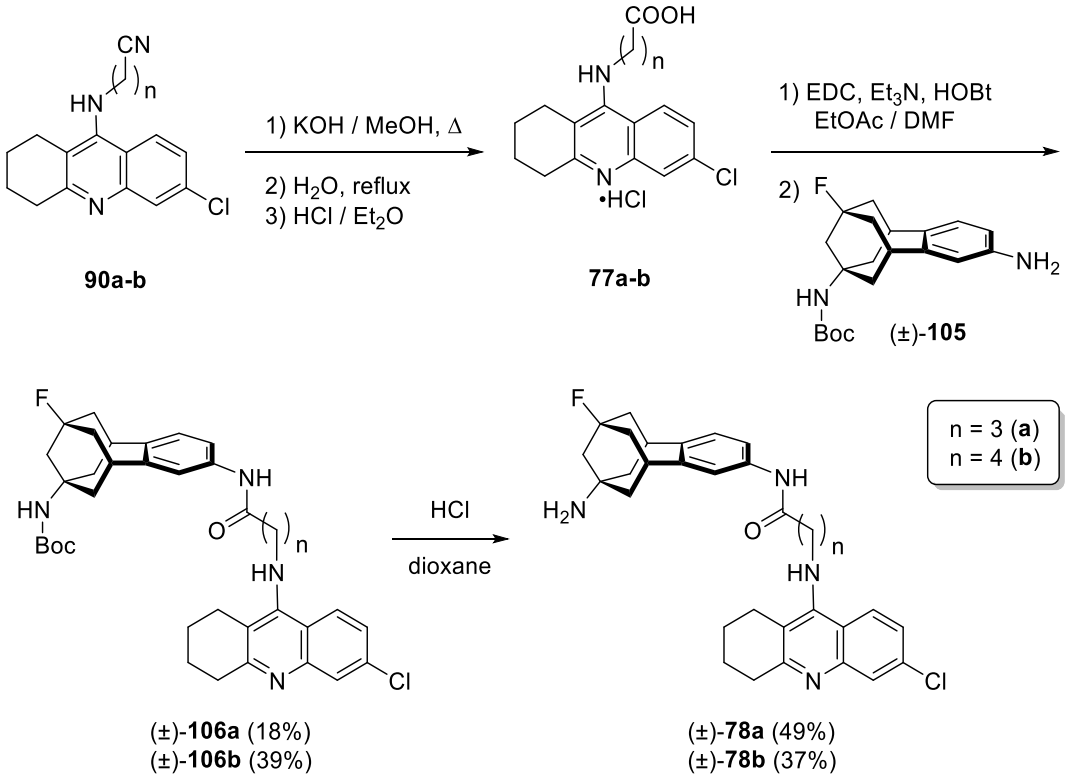

Scheme 6.16

6.4 Biological characterization of benzoadamantane–tacrine hybrids

6.4.1 Cholinesterase inhibitory activity

The inhibitory activity of the hybrids **76a-b**, **75a-b** and **78a-b** toward human cholinesterases was evaluated by Dr. Manuela Bartolini (*Università di Bologna*), through the method of Ellman *et al.*[153] using recombinant *h*AChE and serum *h*BChE (**Table 6.1**).

All the novel benzoadamantane–tacrine hybrids turned out to be more potent hAChE inhibitors than the parent compound 6-chlorotacrine, exhibiting IC_{50} values in the 1–2 nM to subnanomolar range, thereby highlighting the success of the hybridization strategy. In the first series of hybrids, i.e. those linked at the aliphatic amino group of the benzoadamantane scaffold, no differences in *h*AChE inhibitory potency were found between amides **76a-b** and amines **75a-b**, likely reflecting that the putative binding of these compounds with the PAS of AChE is mainly driven by hydrophobic or π-stacking interactions of the benzoadamantane moiety, but not by cation-π interactions in the case of amines **75a-b**, which should be protonated at physiological pH (and at the pH at which the Ellman assay is performed, pH = 8), whereas the chlorotacrine moiety should be firmly bound to the CAS of AChE. Also, neither in the amides **76a-b** nor in the amines **75a-b** differences in *h*AChE inhibitory potency were found between the shorter and the longer homolog, even though it should be kept in mind that they differ in only one methylene. Conversely, a significantly different *h*AChE inhibitory potency was found for the two anilides, with the longer homolog **78b** being 7.5-fold more potent than the shorter counterpart. This result is suggestive of an important influence of the tether length of the anilides on the binding mode within *h*AChE. Anilide **78b** is also 4-fold more potent than amide **76b** and amine **75b**, which might be ascribed to a different binding mode at the PAS of AChE, where anilide **78b** might establish additional cation-π interactions through its protonated aliphatic primary amine. Thus, anilide **78b** emerges as an extremely potent *h*AChE inhibitor (IC_{50} = 0.335 nM), 43-fold more potent than the high affinity CAS inhibitor 6-chlorotacrine.

Table 6.1: *h*AChE and *h*BChE inhibitory activities of the hydrochloride salts of the amides **76a-b**, the amines **75a-b**, the anilides (±)-**78a-b**, and 6-chlorotacrine (**13**).

Compound	*h*AChE[a] IC_{50} (nM)	*h*BChE[a] IC_{50} (nM)
76a·HCl	1.44 ± 0.07	2320 ± 110
76b·HCl	1.30 ± 0.08	32360 ± 160
75a·HCl	1.96 ± 0.08	1060 ± 50
75b·HCl	1.44 ± 0.06	211 ± 7
(±)-**78a**·2HCl	2.50 ± 0.53	20.8 ± 3.8
(±)-**78b**·2HCl	0.335 ± 0.031	491 ± 37
13·HCl (6-chlorotacrine)	14.5 ± 0.9	505 ± 28

[a] IC_{50} inhibitory concentration (nM) of recombinant *h*AChE and serum *h*BChE. Values are expressed as mean ± standard error of the mean (SEM) of at least three experiments, each performed in duplicate.

Like the parent 6-chlorotacrine, the novel benzoadamantane–tacrine hybrids were less potent for *h*BChE than for *h*AChE inhibition, and, hence, selective toward *h*AChE over *h*BChE, with selectivity indices in the range 1500–25000 for the amides **76a-b**, 150–500 for the amines **75a-b**, and 10–1500 for the anilides **78a-b**. The tether length seemed to have an important influence on the *h*BChE inhibitory activity, leading to large differences in potency between the homolog pairs **76a** / **76b**, **75a** / **75b**, and **78a** / **78b**, but without showing a general trend. Of note, one of the hybrids, the anilide **78a**, exhibits a very potent *h*BChE inhibitory activity (IC_{50} = 20.8 nM), being 24-fold more potent than the parent compound 6-chlorotacrine.

6.4.2 NMDA receptor antagonist activity

The assessment of the NMDA receptor antagonistic activity of the benzoadamantane–tacrine hybrids is being carried out by Dr. Francesc X. Sureda (*Universitat Rovira i Virgili*) and is turning out to be troublesome, due to the low solubility of the compounds from certain

concentrations. The assay consists of measuring the effect of the hybrids on the increase in intracellular calcium evoked by glutamate on rat cultured cerebellar granule neurons.[209]

So far, IC_{50} values of 14.5 and 51.6 μM have been determined for the amides **76a** and **76b**, respectively (**Figure 6.4**). However, it has not been possible to determine the IC_{50} values of amines **75a-b**, and the evaluation of the anilides **78a-b** is in progress, so that no structure-activity relationship data can be discussed at this point regarding the NMDA antagonistic activity of the novel benzoadamantane–tacrine hybrids. Nevertheless, the significant activity found for the amide **76a** and the expectation of a more potent activity for the series of anilides **78a-b**, in which the aliphatic amino group is unsubstituted like in memantine and other potent NMDA antagonists developed in the group of Dr. Santiago Vázquez (*Universitat de Barcelona*), make us being optimistic about an important contribution of the NMDA antagonistic activity in the multi-target biological profile of the novel hybrids.

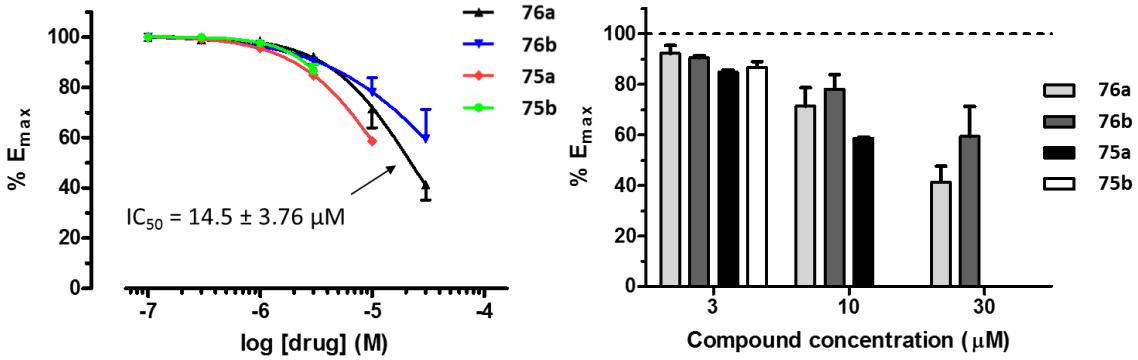

Figure 6.4: Inhibitory effect of the amides **76a-b** and the amines **75a-b** on NMDA-induced calcium increases in cultured cerebellar granule neurons. Data shown are means of at least three separate experiments carried out on three different batches of cultured cells, at 100 μM of NMDA in the presence of 10 μM glycine.

6.4.3 Aβ$_{42}$ and tau anti-aggregating activity

The inhibitory activity of the novel hybrids against the self-aggregation of $A\beta_{42}$ and tau was tested by Dr. Raimon Sabaté's group (*Universitat de Barcelona*) using *E. coli* cells (**Table 6.2**).[158]

[209] E. Torres, M. D. Duque, M. López-Querol, M. Taylor, L. Naesens, C. Mae, L. Pinto, F. Sureda, J. Kelly, S. Vázquez. *Bioorg. Med. Chem.* **2012**, *20*, 942.

Unlike other tacrine- or huprine-based hybrids developed in our group, the novel benzoadamantane–tacrine hybrids were essentially devoid of $A\beta_{42}$ anti-aggregating activity and were only weakly active against tau aggregation. The other previously developed tacrine- or huprine-based hybrids, which had exhibited potent or moderately potent $A\beta_{42}$ and tau anti-aggregating activity, featured a second planar extended aromatic moiety apart from the tacrine or huprine moiety. Maybe the bicyclic benzoadamantane system of the benzoadamantane–tacrine hybrids sterically hampers a proper contribution of the benzene ring to the global interaction with the amyloidogenic proteins.

Table 6.2: $A\beta_{42}$ and tau anti-aggregating activities of the hydrochloride salts of the amides **76a-b**, the amines **75a-b**, the anilides (±)-**78a-b**, and 6-chlorotacrine (**13**).

Compound	$A\beta_{42}$ aggregation[a] (% inh. at 10 µM)	tau aggregation[a] (% inh. at 10 µM)
76a·HCl	4.7 ± 1.8	10.2 ± 2.4
76b·HCl	9.0 ± 1.2	12.6 ± 2.7
75a·HCl	8.4 ± 2.2	22.0 ± 2.7
75b·HCl	12.3 ± 2.6	20.7 ± 2.4
(±)-**78a**·2HCl	-3.4 ± 1.4	6.9 ± 3.9
(±)-**78b**·2HCl	-5.1 ± 4.0	22.9 ± 5.0
13·HCl (6-chlorotacrine)	0.1 ± 0.6	0.7 ± 2.7

[a] % of inhibition of $A\beta_{42}$ and tau protein aggregation at 10 µM in intact *E. coli* cells. Values are expressed as mean ± SEM of four independent experiments.

6.4.4 In vitro BBB permeation assay

The ability to cross the BBB was predicted through the PAMPA-BBB assay,[160] which was performed by Dr. Belén Pérez (*Universitat Autònoma de Barcelona*, **Table 6.3**).

From the correlation obtained by comparing the experimental and reported *in vitro* permeability (P_e) values of fourteen reference drugs and the limits established for BBB permeation,[160] the threshold for high BBB permeation (CNS+) was set at P_e (10^{-6} cm s^{-1}) > 5.157, compounds of low BBB permeation (CNS–) at P_e (10^{-6} cm s^{-1}) < 2.006, and compounds of

uncertain BBB permeation (CNS+/–) 5.157 > P_e (10^{-6} cm s^{-1}) > 2.006. P_e values over the CNS+ threshold were obtained for hybrids **76a-b** and **75a-b**, whereas for anilides **78a-b** an uncertain permeation was predicted.

Table 6.3: Permeability results from the PAMPA-BBB assay of the hydrochloride salts of the amides **76a-b**, the amines **75a-b**, the anilides (±)-**78a-b**, and 6-chlorotacrine (**13**).

Compound	P_e (10^{-6} cm s^{-1})[a]	Prediction
76a·HCl	9.8 ± 0.9	CNS+
76b·HCl	9.0 ± 0.5	CNS+
75a·HCl	6.3 ± 0.1	CNS+
75b·HCl	6.5 ± 0.3	CNS+
(±)-**78a**·2HCl	2.7 ± 0.6	CNS+/–
(±)-**78b**·2HCl	3.1 ± 0.7	CNS+/–
13·HCl (6-chlorotacrine)	26.1 ± 0.6	CNS+

[a] Permeability values from the PAMPA-BBB assay. Values are expressed as the mean ± SD of three experiments, each performed in triplicate.

We are currently awaiting the remaining results of the NMDA antagonistic activity, to decide whether further biological characterization should be done for one of the novel benzoadamantane–tacrine hybrids.

CHAPTER 7

Conclusions

Image source: *Insights in Clinical Pharmacology*, Open Access Open Peer Review (*www.oprscience.com*)

7.1 Shogaol–huprine hybrids

The first objective of this PhD Thesis work consisted of the preparation of a class of shogaol–huprine hybrids, which were designed as dual antioxidant and anticholinesterase agents, with those activities to be imparted by their shogaol-derived and huprine moieties, respectively. Additionally, we inferred that these compounds might exhibit Aβ and tau anti-aggregating activity due to the presence of flat conjugated systems in their structure. This project pretended to complete a previous unsuccessful work of our research group. Therefore, we slightly re-designed the structure of the target shogaol-based moiety, so that the hybrids would be endowed with higher stability. The target hybrids were prepared through sequences that involved a Mannich-type condensation for **26**, and a cross metathesis reaction for **27** and **36**, as key reactions. These compounds were biologically evaluated, and turned out to be potent inhibitors of *h*AChE and *h*BChE, in agreement with the predicted dual site binding in both enzymes. Additionally, these compounds showed high antioxidant activity due to the shogaol moiety, and good anti-aggregating properties against $A\beta_{42}$ and tau proteins, especially **27** and **36** because of the presence of the aromatic ring in the linker. The three target compounds exhibited well-balanced activities, and were also predicted to cross the BBB, which makes them interesting lead compounds to treat AD. This work resulted in a publication in *Bioorg. Med. Chem.*[181]

7.2 Rhein–modified huprine hybrids

With regard to the second objective of this PhD Thesis, second-generation rhein–huprine hybrids were synthesized, fully characterised and pharmacologically assessed. These compounds derived from a family of MTDLs recently developed in our group, with a very interesting *in vitro* and *in vivo* multi-target anti-Alzheimer profile. The design strategy focused on the modification of the huprine aromatic ring of the lead compound of the first generation, with the aim of exploring the effect of pyridinic ring basicity on the different biological activities, while concurrently improving the bioavailability. In this context, we first prepared the intermediate **48**, which was subjected to Friedländer reactions with the corresponding aminonitriles, to afford the desired modified huprines **39a-d**. Secondly, rhein–modified hybrids **40a-d** were accessed through consecutive alkylation of **39a-d**, reduction of the resulting nitriles

to the primary amines, and acylation with rhein. We have found that these compounds displayed lower *h*AChE and *h*BACE1 inhibitory activities, which were the main enzymatic targets, than the first-generation lead compound, even though they displayed on average increased potencies towards $A\beta_{42}$ and tau aggregation. Additionally, we demonstrated for the first time that these hybrids are endowed with a potent antioxidant activity, as we expected because of their phenolic groups. Also, they were predicted to cross the BBB and be able to penetrate into the CNS. Overall, hybrid **40b** exhibited an interesting multitarget profile, with moderately potent $A\beta_{42}$ and tau anti-aggregating activity, potent antioxidant activity, and submicromolar *h*BACE-1 inhibitory activity. Of note, due to its lower basicity, it should be mostly in neutral form at physiological pH, which might allow it to circumvent some potential membrane permeability and P-gp efflux issues that are associated with highly basic compounds. This work has been accepted for publication in *Fut. Med. Chem*.[210]

7.3 CR-6–tacrine hybrids

Regarding the third objective in this PhD Thesis, a new family of CR-6–tacrine hybrids was designed and synthesized to interact in a dual binding site manner within AChE and BACE1, and to exhibit antioxidant properties. Three series of CR-6–tacrine hybrids, i.e. **70a-d**, **71a-d** and **57b-e**, were prepared by amide coupling of a carboxylic acid derived from CR-6 and ω-aminoalkyltacrines. The synthesis of the series of inverse amides **60a-c** was performed by coupling of a primary amine derived from CR-6 and carboxyalkyltacrines. And finally, the series of hybrids **63b-e**, bearing a basic secondary amino group within the linker, was prepared by nucleophilic substitution of a tosylate derived from CR-6 with ω-aminoalkyltacrines. Secondary amines **63b-d** displayed subnanomolar and low nanomolar IC_{50} values against *h*AChE and *h*BChE, respectively, but also the rest of hybrids were found to be potent inhibitors of these enzymes. Additional studies demonstrated dual binding site inhibition of *h*AChE for the most potent hybrid **63c**. The BACE1 inhibitory activity of these compounds was found to be clearly dependent on the length of the linker, being amide **57c** and its homologous benzylated amide **70c** the most potent, with IC_{50} values about 5 μM. Overall, all the family of CR-6–tacrine hybrids were

[210] F. J. Pérez-Areales, N. Betari, A. Viayna, C. Pont, A. Espargaró, M. Bartolini, A. De Simone, J. F. Rinaldi Alvarenga, B. Pérez, R. Sabate, R. M. Lamuela-Raventós, V. Andrisano, F. J. Luque, D. Muñoz-Torrero. *Fut. Med. Chem.* **2017**, in press.

endowed with significant $A\beta_{42}$ and tau anti-aggregating and antioxidant activities, and they were predicted to be able to cross the BBB. Because of their multi-target pharmacological profile, the benzylated amide **70c**, and its homologous deprotected **57c**, have been selected for *in vivo* assays in APP/PS1 transgenic mice.

7.4 Benzoadamantane–tacrine hybrids

Finally, a class of benzoadamantane–tacrine hybrids was designed and synthesized by the combination of a NMDA receptor antagonist pharmacophore with an AChE inhibitor moiety, through oligomethylenic linkers of two different lengths, pursuing a dual site binding within AChE. We first prepared the intermediate benzoadamantane **18**, which was coupled with the corresponding carboxytacrine to afford amides **76a-b**, which were eventually reduced to amines **75a-b**. The preparation of the series of anilides **78a-b** was carried out through coupling reaction between the Boc-protected intermediate **105** and the corresponding carboxytacrine, followed by a deprotection reaction. The three series of compounds resulted to be highly potent inhibitors of *h*AChE (1.30–1.96 nM), especially amide **78b** with an IC_{50} value in the subnanomolar range. The hybrids **76a-b** and **75a-b** displayed some NMDA receptor antagonistic activity, even though solubility issues did not allow their full characterization, whereas assay for hybrids **78a-b** is in progress. Concerning $A\beta_{42}$ and tau aggregation inhibition, these compounds were essentially inactive against $A\beta_{42}$ aggregation, and weak to moderate towards tau aggregation. Compounds **76a-b** and **75a-b** were also predicted to cross the BBB, while anilides **78a-b** showed uncertain BBB permeation. Overall, all compounds exhibited a good MTDL profile against AD, so that further studies might be carried out once we obtain the final report of NMDA receptor antagonist activities.

CHAPTER 8

Experimental part

Image source: Department of Chemistry, University of Carleton (*www.carleton.ca/chemistry*)

General Methods

Melting points were determined in open capillary tubes with a MFB 59510M Gallenkamp.

NMR spectra were carried out at *Centres Científics i Tecnològics de la Universitat de Barcelona* (CCiTUB) using 300 MHz ^{1}H / 75.4 MHz ^{13}C NMR spectra, 400 MHz ^{1}H / 100.6 MHz ^{13}C NMR spectra, and 500MHz ^{1}H / 125.7 MHz ^{13}C NMR spectra were recorded on Varian Gemini 300, Varian Mercury 400, and Varian Inova 500 spectrometers, respectively. The chemical shifts are reported in ppm (δ scale) relative to solvent peak, and coupling constants are reported in Hertz (Hz). Assignments given for the NMR spectra of the new compounds have been carried out on the basis of DEPT, COSY ^{1}H / ^{1}H (standard procedures), and COSY ^{1}H / ^{13}C (gHSQC and gHMBC sequences) experiments. The used abbreviations were: s, singlet; d, doublet; t, triplet; q, quadruplet; m, multiplet; or combinations thereof.

IR spectra were run on FTIR Perkin-Elmer Spectrum RX I spectrophotometer using potassium bromide (KBr) or sodium chloride (NaCl) pellets, or attenuated total reflectance (ATR) technique. Absorption values are expressed as wavenumbers (cm^{-1}); only significant absorption bands are given.

Column chromatography was performed on silica gel 60 Å (35–70 mesh, SDS, ref 2000027), or on aluminum oxide, neutral, 60 Å (50–200 µm, Brockmann I). Thin-layer chromatography was performed with aluminum-backed sheets with silica gel 60 F_{254} (Merck, ref 1.05554), or aluminum oxide 60 Å (Sigma-Aldrich, ref 06408-25EA), and spots were visualized with UV light, 1% aqueous solution of $KMnO_4$ and/or Dragendorff reagent.

The accurate mass analyses were carried out at *Unitat d'Espectrometria de Masses dels Centres Científics i Tecnològics de la Universitat de Barcelona* (CCiTUB) using Electrospray ionization (ESI-TOF MS) technique in an Agilent Technologies spectrophotometer.

Solvent purification was carried out following the procedures described in: Perrin, D. D.; Armarego, W. L. F. *Purification of Laboratory Chemicals*, 4th Edition, Butterworth-Heinemann: Oxford, 1996.

The HPLC measurements of the rhein–modified-huprine family were performed using an HPLC Waters Alliance HT apparatus comprising a pump (Edwards RV12) with degasser, an autosampler, a diode array detector and a column as specified below. The reverse phase HPLC determinations were carried out on a YMC-Pack ODS-AQ column (50 × 4.6 mm, DS. 3 μm, 12 nm). CH_3CN / H_2O mixture containing 0.1% formic acid at 1.6 mL/min were used as mobile phase. A gradient method from 5% to 100% of CH_3CN in 3.5 min at 50 ^oC was used in all cases.

The HPLC analysis of the CR-6–tacrine family was performed with a Hewlett-Packard Series 1100 modular system with an UV detector 1315A. A reverse-phase Kromasil 100C_{18} (150 mm × 4.6 mm, 5 mm) column was used to elute compounds. CH_3CN / H_2O mixtures containing 0.1% TFA at 1 mL/min were used as mobile phase and monitoring wavelength was set at 220 and 254 nm. A gradient method from 20% to 100% of CH_3CN in 20 min was used in all cases.

Log P values were calculated using *Molinspiration Property Calculation Service* software from www.molinspiration.com.

Analytical samples of all the compounds prepared in this PhD Thesis work were dried at 65 ^oC / 2 Torr for at least 48 h (standard conditions). All the new compounds which were subjected to pharmacological evaluation possessed a purity ≥ 95% as evidenced by their analytical data, if possible.

Attempted preparation of 5-(4-hydroxy-3-methoxyphenyl)pent-1-en-3-one, 28

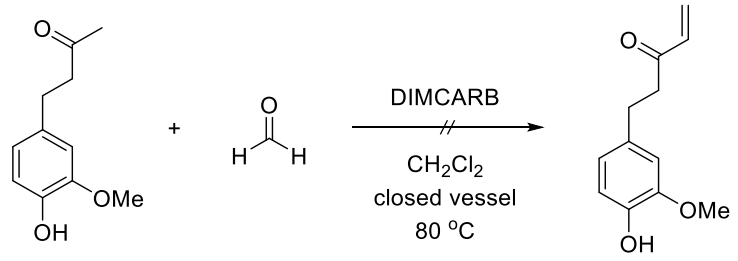

30 **28**

In a 25 mL closed vessel provided with a magnetic stirrer, a solution of vanililacetone, **30**, (1.50 g, 7.72 mmol) in dimethylammonium dimethyl carbamate (DIMCARB, 0.99 mL, 1.04 g, 7.72 mmol) was prepared, and treated with a solution of formaldehyde (37% aq. sol., 1.73 mL, 23.2 mmol) in CH_2Cl_2 (10 mL), then stirred at 80 °C overnight. The resulting mixture was treated with 10% HCl aq. sol. (50 mL) and extracted with CH_2Cl_2 (4 × 30 mL). The combined organic layers were dried over anhydrous Na_2SO_4, filtered and concentrated under reduced pressure, but no desired product was found.

Attempted preparation of 1-(4-hydroxy-3-methoxyphenyl)hex-4-en-3-one, 31

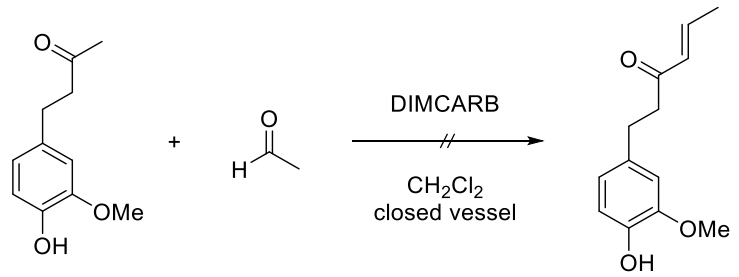

30 **31**

In a double necked 25 mL round-bottomed flask provided with an inert atmosphere and a magnetic stirrer, a solution of vanililacetone, **30**, (1.50 g, 7.72 mmol) in dimethylammonium dimethyl carbamate (DIMCARB, 4.84 mL, 5.08 g, 37.8 mmol) was prepared, and treated dropwise using a syringe pump for 10 hours with acetaldehyde (1.31 mL, 1.02 g, 23.2 mmol), and stirred at room temperature for 2 days. The resulting mixture was treated with 10% HCl aq. sol. (450 mL) and extracted with CH_2Cl_2 (4 × 300 mL). The combined organic layers were dried over anhydrous Na_2SO_4, filtered and concentrated under reduced pressure, but no desired product was found.

Preparation of 1-(4-hydroxy-3-methoxyphenyl)oct-4-en-3-one, 33

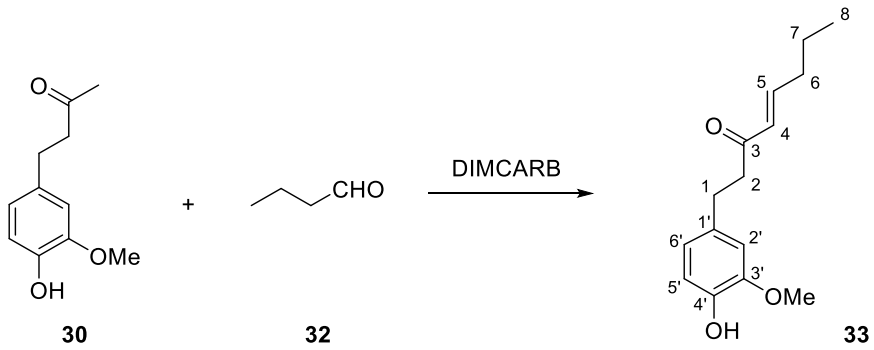

30 **32** **33**

In a 25 mL round-bottomed flask provided with a magnetic stirrer and an inert atmosphere, a solution of vanililacetone, **30**, (1.50 g, 7.72 mmol) in dimethylammonium dimethyl carbamate (DIMCARB, 4.84 mL, 5.08 g, 37.9 mmol) was prepared, and treated dropwise using a syringe pump for 10 hours with butirylaldehyde (2.09 mL, 1.67 g, 23.2 mmol). The resulting mixture was stirred at room temperature for 2 days, then treated with 10% HCl aq. sol. (100 mL) and extracted with CH_2Cl_2 (3 × 100 mL). The combined organic layers were dried over anhydrous Na_2SO_4, filtered and concentrated under reduced pressure to give a yellow oil (2.09 g), which was subjected to column chromatography purification [silica gel 35−70 μm (120 g); Ø = 5 cm; #1–13, 500 mL, hexane; #14–20, 500 mL, hexane / EtOAc 95:5; #21–52, 2.5 L, hexane / EtOAc 90:10; #53–57, 500 mL, hexane / EtOAc 80:20; #58–62, 500 mL, hexane / EtOAc 70:30; #63–67, 500 mL, EtOAc], to provide the desired enone **33** (#36–52, 799 mg, 42% yield) as a yellow oil.

R_f = 0.32 (silica gel, 10 cm, hexane / EtOAc 70:30).

IR (KBr) *v*: 3404 (O–H st), 1663, 1626, 1514 (C=O, Ar–C–C, Ar–C–N st) cm^{-1}.

^{1}H NMR (400 MHz, $CDCl_3$) δ: 0.93 (t, *J* = 7.6 Hz, 3H, 8-CH_3), 1.48 (m, *J* = 7.6 Hz, 2H, 7-H_2), 2.18 (dq, *J* = 7.6 Hz, *J'* = 1.6 Hz, 2H, 6-H_2), 2.78–2.89 (complex signal, 4H, 1-H_2 and 2-H_2), 3.87 (s, 3H, 3'-OCH_3), 5.47 (broad s, 1H, 4'-OH), 6.09 (dt, *J* = 16.0 Hz, *J'* = 1.6 Hz, 1H, 4-H), 6.68 (dd, *J* = 8.0 Hz, *J'* = 2.0 Hz, 1H, 6'-H), 6.71 (d, *J* = 2.0 Hz, 1H, 2'-H), 6.81 (dt, *J* = 15.6 Hz, *J'* = 6.8 Hz, 1H, 5-H), 6.82 (d, *J* = 7.6 Hz, 1H, 5'-H).

^{13}C NMR (100.6 MHz, $CDCl_3$) δ: 13.7 (CH_3), 21.3 (CH_2), 29.9 (CH_2), 34.5 (CH_2), 42.0 (CH_2), 55.9 (CH_3), 111.1 (CH), 114.3 (CH), 120.8 (CH), 130.5 (CH), 133.2 (C), 143.9 (C), 146.4 (C), 147.5 (CH), 199.8 (C).

Preparation of (±)-3-Chloro-6,7,10,11-tetrahydro-9-methyl-12-(4-pentenyl)-7,11-methanocycloocta[*b*]quinoline, (±)-29

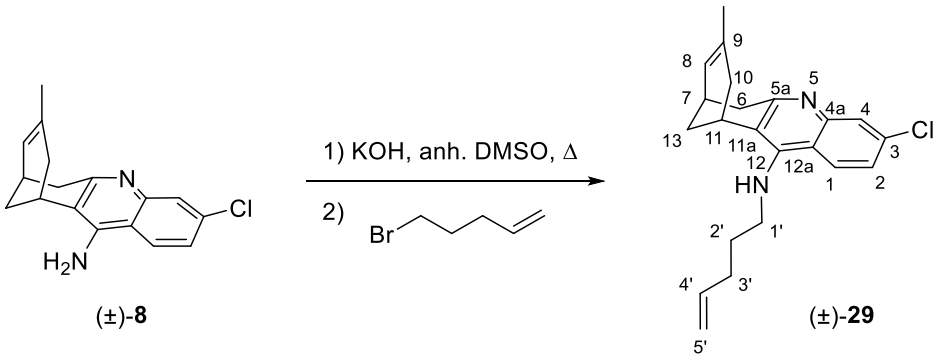

(±)-**8** (±)-**29**

In a triple necked 50 mL round-bottomed flask provided with an inert atmosphere, a magnetic stirrer, and 4 Å molecular sieves, a suspension of (±)-huprine Y, **8** (1.50 g, 5.27 mmol) and finely powdered NaOH (420 mg, 10.5 mmol) in anhydrous DMSO (15 mL) was prepared. The resulting suspension was stirred, heating every 10 minutes with a heat gun for 1 hour, and at room temperature one more hour, then treated with 5-bromo-1-pentene (0.69 mL, 868 mg, 5.82 mmol). The reaction mixture was stirred at room temperature overnight, then diluted with 5 N NaOH aq. sol. (250 mL), and extracted with EtOAc (3 × 300 mL). The combined organic layers were washed with water (3 × 200 mL), dried with anhydrous Na_2SO_4, filtered and evaporated under reduced pressure to give a yellow oil (1.54 g), which was purified by column chromatography [silica gel 35−70 μm (100 g); Ø = 5 cm; #1–165, 5.3 L, CH_2Cl_2 / 50% aq. NH_4OH 100:0.4; #166, 200 mL, CH_2Cl_2 / MeOH / 50% aq. NH_4OH 95:5:0.4], to provide the desired alkene (±)-**29** (#84–156, 562 mg, 30% yield) as a yellow oil.

R_f = 0.63 (silica gel, 10 cm, CH_2Cl_2 / MeOH / 50% aq. NH_4OH 90:10:1).

Analytical sample of (±)-29·HCl

In a 25 mL round-bottomed flask, (±)-**29** (106 mg, 0.30 mmol) was dissolved in CH_2Cl_2 (10 mL), filtered through a PTFE filter (0.2 μm), treated with HCl / MeOH (0.75 N, 1.2 mL), evaporated *in vacuo*, and washed with pentane (3 × 2 mL), giving, after drying in standard conditions, **29**·HCl (110 mg) as a yellow solid.

Melting point: 128–129 °C (CH_2Cl_2 / MeOH 89:11).

IR (KBr) *v*: 3500–2500 (max. at 3226, 3111, 3049, 3004, 2925, 2854, 2717, N–H, $^+$N–H, C–H st), 1717, 1699, 1684, 1669, 1629, 1582, 1569, 1560 (Ar–C–C, Ar–C–N st) cm^{-1}.

^{1}H NMR (400 MHz, CD_3OD) δ: 1.57 (s, 3H, 9-CH_3), 1.91–2.02 (complex signal, 4H, 13-H_{syn}, 10-H_{endo} and 2′-H_2), 2.08 (dm, J = 12.8 Hz, 1H, 13-H_{anti}), 2.10 (dt, J = J' = 7.2 Hz, 3′-H_2), 2.56 (dd, J = 17.6 Hz, J' = 4.8 Hz, 1H, 10-H_{exo}), 2.76 (m, 1H, 7-H), 2.89 (d, J = 17.6 Hz, 1H, 6-H_{endo}), 3.21 (dd, J = 17.6 Hz, J' = 5.2 Hz, 1H, 6-H_{exo}), 3.48 (m, 1H, 11-H), 3.99 (dt, J = J' = 6.8 Hz, 2H, 1′-H_2), 4.86 (s, NH and $^+$NH), 5.00 (ddt, J = 10.4 Hz, J' = J'' = 1.6 Hz, 1H, 5′-H_A), 5.04 (ddt, J = 17.2 Hz, J' = J'' = 1.6 Hz, 1H, 5′-H_B), 5.57 (br d, J = 4.8 Hz, 1H, 8-H), 5.86 (ddt, J = 17.2 Hz, J' = 10.4, J'' = 6.8 Hz, 1H, 4′-H), 7.52 (d, J = 9.6 Hz, 1H, 2-H), 7.80 (s, 1H, 4-H), 8.36 (d, J = 9.6 Hz, 1H, 1-H).

^{13}C NMR (100.6 MHz, CD_3OD) δ: 23.5 (CH_3, 9-CH_3), 27.2 (CH, C11), 27.8 (CH, C7), 29.3 (CH_2, C13), 30.5 (CH_2), 31.9 (CH_2) (C2′ and C3′), 36.0 (CH_2, C6), 36.2 (CH_2, C10), 50.9 (CH_2, C1′), 115.6 (C, C12a), 116.3 (CH_2, C5′), 117.9 (C, C11a), 119.1 (CH, C4), 125.1 (CH, C8), 126.6 (CH, C2), 129.4 (CH, C1), 134.5 (C, C9), 138.4 (CH, C4′), 140.1 (C, C3), 140.9 (C, C4a), 151.3 (C, C5a), 156.9 (C, C12).

HRMS (ESI):

Calculated for ($C_{22}H_{25}{}^{35}ClN_2$ + H^+):	353.1779
Found:	353.1777

Preparation of (±)-8-[(3-Chloro-6,7,10,11-tetrahydro-9-methyl-7,11-methanocycloocta[*b*]quinolin-12-yl)amino]-1-(4-hydroxy-3-methoxyphenyl)oct-4-en-3-one, (±)-26

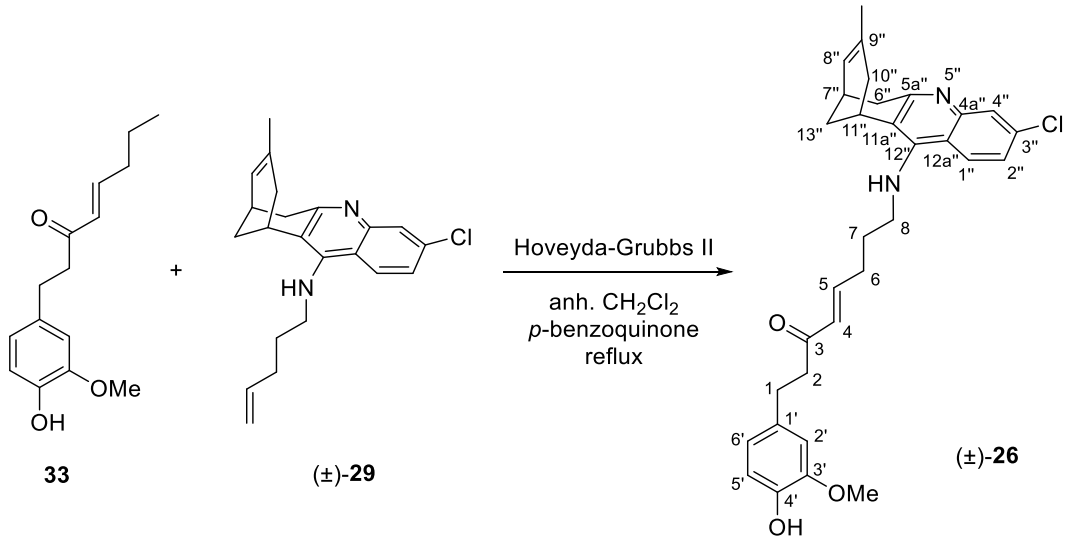

In a triple necked 100 mL round-bottomed flask provided with an inert atmosphere, a magnetic stirrer and a refrigerant, a solution of alkene (±)-**29** (725 mg, 2.05 mmol) in anhydrous CH_2Cl_2 (28.4 mL) was prepared, then treated with enone **33** (765 mg, 3.08 mmol), *p*-benzoquinone (21 mg, 0.19 mmol) and Hoveyda–Grubbs 2nd generation catalyst (65 mg, 0.10 mmol), and stirred under reflux for 3 days. The resulting mixture was directly purified by column chromatography [silica gel 35−70 µm (105 g); Ø = 5 cm; #1–43, 2.5 L, CH_2Cl_2 / 50% aq. NH_4OH 100:0.4; #44–57, 500 mL, CH_2Cl_2 / MeOH / 50% aq. NH_4OH 99.9:0.1:0.4; #58–66, 300 mL, CH_2Cl_2 / MeOH / 50% aq. NH_4OH 99.8:0.2:0.4; #67–74, 200 mL, CH_2Cl_2 / MeOH / 50% aq. NH_4OH 99.7:0.3:0.4; #75–82, 200 mL, CH_2Cl_2 / MeOH / 50% aq. NH_4OH 99.5:0.5:0.4; #83–89, 200 mL, CH_2Cl_2 / MeOH / 50% aq. NH_4OH 99.2:0.8:0.4; #90–94, 200 mL, CH_2Cl_2 / MeOH / 50% aq. NH_4OH 99:1:0.4; #95–104, 200 mL, CH_2Cl_2 / MeOH / NH_4OH 98.5:1.5:0.4; #105–187, 1.45 L, CH_2Cl_2 / MeOH / 50% aq. NH_4OH 98:2:0.4; #188–201, 200 mL, CH_2Cl_2 / MeOH / 50% aq. NH_4OH 95:5:0.4; #202–219, 200 mL, CH_2Cl_2 / MeOH / 50% aq. NH_4OH 90:10:0.4], to provide a mixture that included the desired compound (±)-**26** (#127–162, 640 mg), which was again subjected to column chromatography purification [silica gel 35−70 µm (25 g); Ø = 3 cm; #1–8, 300 mL, hexane; #9–45, 1.25 L, hexane / EtOAc 90:10; #46–53, 250 mL, hexane / EtOAc 85:15; #54–76, 750 mL, hexane / EtOAc 80:20; #77–83, 250 mL, hexane / EtOAc 70:30; #84–98, 250 mL, hexane / EtOAc

60:40; #99–108, 750 mL, hexane / EtOAc 50:50; #109–112, 350 mL, EtOAc], to afford the desired alkene (±)-**26** (#86–106, 158 mg, 15% yield) as a pale yellow solid.

R_f = 0.72 (silica gel, 10 cm, CH_2Cl_2 / MeOH / 50% aq. NH_4OH 90:10:1).

Analytical sample of (±)-26

An aliquot amount of (±)-**26** (100 mg, 0.18 mmol) was subjected to preparative thin layer chromatography, then washed with pentane (3 × 2 mL), affording, after drying in standard conditions, (±)-**26** (30 mg) as a pale yellow solid.

Melting point: 69–71 °C.

IR (ATR) *v*: 3352 (O–H, N–H st), 1666, 1660, 1632, 1603, 1572, 1556, 1514 (C=O, Ar–C–C, Ar–C–N st) cm^{-1}.

^{1}H NMR (400 MHz, $CDCl_3$) δ: 1.51 (s, 3H, 9″-CH_3), 1.78 (broad d, J = 16.4 Hz, 1H, 10″-H_{endo}), 1.86 (tt, J = J' = 6.8 Hz, 2H, 7-H_2), 1.92 (dm, J = 12.0 Hz, 1H, 13″-H_{syn}), 2.05 (dm, J = 12.0 Hz, 1H, 13″-H_{anti}), 2.33 (dtd, J = J' = 6.8 Hz, J'' = 1.6 Hz, 2H, 6-H_2), 2.54 (dm, J = 16.4 Hz, 1H, 10″-H_{exo}), 2.74 (m, 1H, 7″-H), 2.78–2.89 (complex signal, 4H, 1-H_2, 2-H_2), 3.01 (broad d, J = 17.6 Hz, 1H, 6″-H_{endo}), 3.15 (dd, J = 17.6 Hz, J' = 5.2 Hz, 1H, 6″-H_{exo}), 3.29 (m, 1H, 11″-H), 3.46 (m, 2H, 8-H_2), 3.86 (s, 3H, 3′-OCH_3), 5.54 (broad d, J = 4.4 Hz, 1H, 8″-H), 6.11 (dt, J = 15.6 Hz, J' = 1.6 Hz, 1H, 4-H), 6.67 (dd, J = 8.0 Hz, J' = 2.0 Hz, 1H, 6′-H), 6.70 (d, J = 2.0 Hz, 1H, 2′-H), 6.80 (dt, J = 15.6 Hz, J' = 6.8 Hz, 1H, 5-H), 6.82 (d, J = 8.0 Hz, 1H, 5′-H), 7.27 (dd, J = 8.8 Hz, J' = 2.0 Hz, 1H, 2″-H), 7.87 (d, J = 8.8 Hz, 1H, 1″-H), 7.89 (d, J = 2.0 Hz, 1H, 4″-H).

^{13}C NMR (100.6 MHz, CD_3OD) δ: 23.6 (CH_3), 28.4 (CH), 29.5 (CH), 30.1 (CH_2), 30.7 (CH_2), 30.8 (CH_2), 31.0 (CH_2), 38.0 (CH_2), 40.4 (CH_2), 42.8 (CH_2), 50.1 (CH_2), 56.4 (CH_3), 113.2 (CH), 116.1 (CH), 119.9 (C), 121.7 (CH), 122.2 (C), 125.1 (CH), 126.1 (CH), 126.6 (CH), 127.4 (CH), 131.5 (C), 131.9 (CH), 133.6 (C), 133.9 (C), 135.7 (C), 145.8 (C), 148.5 (CH), 148.9 (C), 152.8 (C), 159.4 (C), 202.4 (C).

HRMS (ESI):

Calculated for ($C_{32}H_{35}{}^{35}ClN_2O_3 + H^+$): 531.2409

Found: 531.2405

Preparation of (±)-4-{[(3-chloro-6,7,10,11-tetrahydro-9-methyl-7,11-methanocyclooocta[*b*]quinolin-12-yl)imino]methyl}benzonitrile, (±)-34

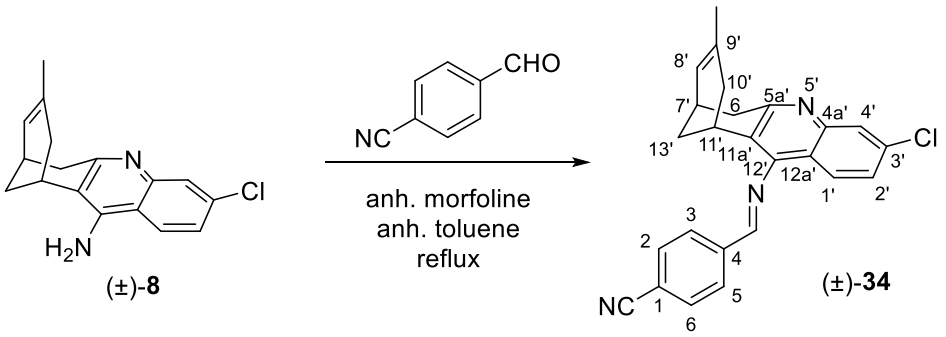

In a triple necked 50 mL round-bottomed flask provided with an inert atmosphere, a magnetic stirrer, a refrigerant, and 4 Å molecular sieves, a suspension of (±)-huprine Y, **8** (1.50 g, 5.27 mmol) in anhydrous toluene (10 mL) was prepared, then treated with a solution of anhydrous morfoline (0.69 mL, 7.91 mmol) and *p*-cyanobenzaldehyde (1.41 g, 10.54 mmol) in toluene (5 mL). The resulting suspension was stirred under reflux for 2 days, then concentrated under reduced pressure to give a brown oil (5.93 g), which was subjected to column chromatography purification [silica gel 35−70 μm (60 g); Ø = 5 cm; #1–104, 6.8 L, CH_2Cl_2 / 50% aq. NH_4OH 100:0.4; #105–108, 300 mL, CH_2Cl_2 / MeOH / 50% aq. NH_4OH 99.5:0.5:0.4; #109–111, 300 mL, CH_2Cl_2 / MeOH / 50% aq. NH_4OH 98.5:1.5:0.4], to provide the desired imine (±)-**34** (#20–109, 780 mg, 37% yield) as a clear brown solid.

R_f = 0.17 (silica gel, 10 cm, CH_2Cl_2).

Analytical sample of (±)-34

In a 25 mL round-bottomed flask, (±)-**34** (100 mg, 0.25 mmol) was dissolved in CH_2Cl_2 (6.6 mL), filtered with a PTFE filter (0.2 μm), evaporated *in vacuo*, and washed with pentane (3 × 2 mL), giving, after drying in standard conditions, (±)-**34** (94 mg) as a yellow solid.

Melting point: 208–210 °C (CH_2Cl_2).

IR (KBr) *v*: 2225 (CN st), 1721, 1639, 1600, 1570, 1553, 1500, 1479, 1455 (Ar–C–C and Ar–C–N st) cm^{-1}.

^{1}H NMR (400 MHz, $CDCl_3$) δ: 1.52 (s, 3H, 9'-CH_3), 1.85 (broad d, J = 17.2 Hz, 1H, 10'-H_{endo}), 1.95–1.97 (complex signal, 2H, 13'-H_{syn} and 13'-H_{anti}), 2.35 (dd, J = 17.2 Hz, J' = 4.6 Hz, 1H, 10'-H_{exo}), 2.78 (m, 1H, 7'-H), 3.12 (broad d, J = 18.0 Hz, 1H, 6'-H_{endo}), 3.21 (dd, J = 17.6 Hz, J' = 5.2 Hz, 1H, 6'-H_{exo}), 3.35 (m, 1H, 11'-H), 5.56 (broad d, J = 5.2 Hz, 1H, 8'-H), 7.31 (dd, J = 9.2 Hz, J' = 2.0 Hz, 1H, 2'-H), 7.47 (d, J = 9.2 Hz, 1H, 1'-H), 7.86 [dt, J = 8.0 Hz, J' = 1.6 Hz, 2H, 2(6)-H], 8.00 (d, J = 2.0 Hz, 2H, 4'-H), 8.12 [d, J = 8.4 Hz, 2H, 3(5)-H], 8.42 (s, 1H, C*H*N).

^{13}C NMR (100.6 MHz, $CDCl_3$) δ: 23.4 (CH_3, 9'-CH_3), 28.1 (CH, C11'), 28.3 (CH, C7'), 28.6 (CH_2, C13'), 37.1 (CH_2, C10'), 40.0 (CH_2, C6'), 115.8 (C, C1), 117.8 (C, C12a'), 118.1 (C, CN), 122.9 (C, C11a'), 123.9 (CH, C1'), 125.3 (CH, C8'), 126.4 (CH, C2'), 127.3 (CH, C4'), 129.4 [CH, C3(5)], 132.3 (C, C9'), 132.8 [CH, C2(6)], 134.9 (C, C3'), 138.5 (C, C4), 147.2 (C, C4a'), 153.4 (C, C12'), 159.8 (C, C5a'), 162.1 (CH, CHN).

HRMS (ESI):

Calculated for ($C_{25}H_{20}{}^{35}ClN_3 + H^+$):	398.1419
Found:	398.1426

Preparation of (±)-4-{[(3-chloro-6,7,10,11-tetrahydro-9-methyl-7,11-methanocyclooocta[*b*]quinolin-12-yl)amino]methyl}benzonitrile, (±)-35

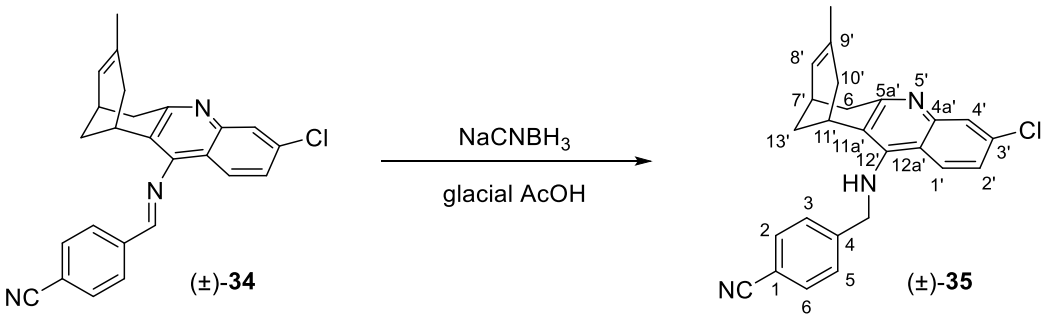

In a triple necked 50 mL round-bottomed flask provided with an inert atmosphere and a magnetic stirrer, a solution of imine (±)-**34** (743 mg, 1.87 mmol) in glacial AcOH (13 mL) was prepared, then treated portionwise for 1 hour with $NaCNBH_3$ (246 mg, 3.92 mmol). The reaction mixture was stirred at room temperature for 3 hours, then cooled to 0 °C with an ice bath, treated with 10 N NaOH aq. sol. (45 mL), and extracted with EtOAc (2 × 200 mL). The combined organic layers were washed with water (200 mL), dried over anhydrous Na_2SO_4, filtered and evaporated under reduced pressure to give a yellow solid (590 mg), which was subjected to column chromatography purification [silica gel 35−70 µm (60 g); Ø = 3 cm; #1–76, 3.4 L, CH_2Cl_2 / 50% aq. NH_4OH 100:0.4], to provide the desired amine (±)-**35** (#33–67, 337 mg, 45% yield) as a yellow solid.

R_f = 0.75 (silica gel, 10 cm, CH_2Cl_2 / MeOH / 50% aq. NH_4OH 90:10:1).

Analytical sample of (±)-35·HCl

In a 25 mL round-bottomed flask, (±)-**35** (60 mg, 0.15 mmol) was dissolved in CH_2Cl_2 (5 mL), filtered with a PTFE filter (0.2 µm), treated with HCl / MeOH (0.53 N, 0.85 mL), evaporated *in vacuo*, and washed with pentane (3 × 2 mL), giving, after drying in standard conditions, **35**·HCl (62 mg) as a yellow solid.

Melting point: 217–218 °C (CH_2Cl_2 / MeOH 85:15).

IR (KBr) *v*: 3500–2500 (max. at 3229, 3101, 3050, 2999, 2901, 2722, N–H, $^{+}$N–H and C–H st), 2226 (CN st), 1718, 1631, 1582, 1555, 1507 (Ar−C−C and Ar−C−N st) cm^{-1}.

^{1}H NMR (400 MHz, CD_3OD) *δ*: 1.61 (s, 3H, 9'-CH_3), 1.98 (broad d, *J* = 17.6 Hz, 1H, 10-H_{endo}), superimposed 2.00 (m, 1H, 13'-H_{syn}), 2.10 (dm, *J* = 12.4 Hz, 1H, 13'-H_{anti}), 2.57 (dd, *J* = 18.0 Hz, *J'* = 4.8 Hz, 1H, 10'-H_{exo}), 2.80 (m, 1H, 7'-H), 2.94 (broad d, *J* = 18.0 Hz, 1H, 6'-H_{endo}), 3.26 (dd, *J* = 18.0 Hz, *J'* = 5.4 Hz, 1H, 6'-H_{exo}), 3.53 (m, 1H, 11'-H), 4.85 (s, NH and $^{+}$NH), 5.28 (s, 2H, CH_2N), 5.61 (broad d, *J* = 4.8 Hz, 1H, 8'-H), 7.39, (dd, *J* = 9.2 Hz, *J'* = 2.0 Hz, 1H, 2'-H), 7.63 [d, *J* = 8.8 Hz, 2H, 3(5)-H], 7.79 [complex signal, 3H, 4'-H, 2(6)-H], 8.10 (d, *J* = 9.2 Hz, 1H, 1'-H).

^{13}C NMR (100.6 MHz, CD_3OD) δ: 23.4 (CH_3, 9'-CH_3), 27.6 (CH, C11'), 27.8 (CH, C7'), 29.2 (CH_2, C13'), 36.2 (CH_2), 36.4 (CH_2) (C6' and C10'), 51.9 (CH_2, *C*H_2N), 112.8 (C, C1), 115.7 (C, CN), 118.7 (C, C12a'), 119.4 (CH + C, C4' and C11a'), 125.1 (CH, C8'), 127.0 (CH, C2'), 128.7 [CH, C3(5)], 128.9 (CH, C1'), 134.0 [CH, C2(6)], 134.6 (C, C9'), 140.4 (C, C3'), 140.8 (C, C4a'), 144.6 (C, C4), 152.2 (C, C5a'), 157.4 (C, C12').

HRMS (ESI):

Calculated for ($C_{25}H_{22}{}^{35}ClN_3$ + H^+):	400.1575
Found:	400.1582

Preparation of (±)-4-{[(3-Chloro-6,7,10,11-tetrahydro-9-methyl-7,11-methanocycloocta[*b*]quinolin-12-yl)amino]methyl}benzaldehyde, (±)-21

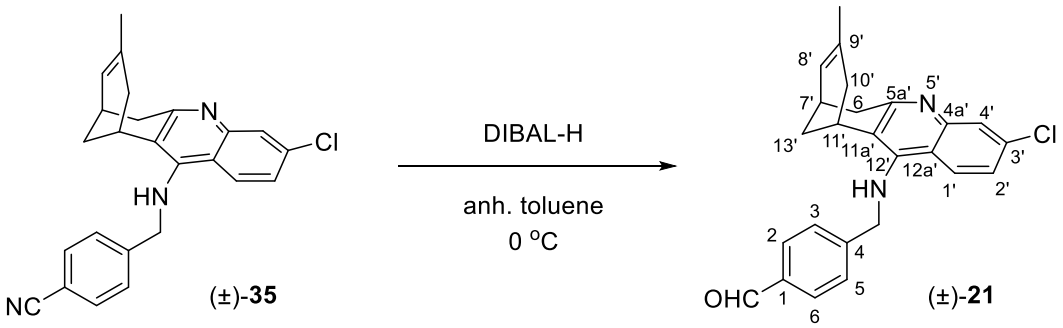

In a triple necked 50 mL round-bottomed flask provided with an inert atmosphere and a magnetic stirrer, a solution of nitrile (±)-**35** (337 mg, 0.84 mmol) in anhydrous toluene (14 mL) was prepared, then cooled to 0 °C and treated dropwise with diisobutylaluminum hydride (1.2 M in toluene, 1.05 mL, 1.26 mmol). The reaction mixture was stirred at 0 °C overnight, treated successively with 2 N HCl aq. sol. (5 mL) and 10 N NaOH aq. sol. (30 mL) at 0 °C, and extracted with CH_2Cl_2 (3 × 50 mL). The combined organic layers were washed with water (2 × 50 mL), dried over anhydrous Na_2SO_4, filtered and evaporated under reduced pressure to give the desired aldehyde (±)-**21** (354 mg, quantitative yield) as a yellow solid which was used in the next step without further purification.

R_f = 0.27 (silica gel, 10 cm, CH_2Cl_2 / MeOH 99:1).

Analytical data of (±)-21

^{1}H NMR (300 MHz, $CDCl_3$) δ: 1.50 (s, 3H, 9′-CH_3), 1.72 (broad d, J = 17.4 Hz, 1H, 10′-H_{endo}), 1.85 (dm, J = 12.6 Hz, 1H, 13′-H_{syn}), 1.98 (dm, J = 12.6 Hz, 1H, 13′-H_{anti}), 2.46 (dm, J = 17.4 Hz, 1H, 10′-H_{exo}), 2.73 (m, 1H, 7′-H), 3.02 (ddd, J = 17.7 Hz, J' = J'' = 2.1 Hz, 1H, 6′-H_{endo}), 3.16 (dd, J = 17.7 Hz, J' = 5.7 Hz, 1H, 6′-H_{exo}), superimposed 3.14–3.20 (m, 1H, 11′-H), 4.23 (t, J = 6.9 Hz, 1H, N*H*-CH_2-Ph), 4.68 (d, J = 6.9 Hz, 2H, NH-C*H*$_2$-Ph), 5.53 (m, 1H, 8′-H), 7.15–7.30 (complex signal), 7.56 (d, J = 8.1 Hz), and 7.80–8.00 (complex signal) [7H, 2(6)-H, 3(5)-H, 1′-H, 2′-H, 4′-H], 10.05 (s, 1H, Ph-C*H*O).

HRMS (ESI):

Calculated for ($C_{25}H_{23}{}^{35}ClN_2O + H^+$): 403.1571

Found: 403.1578

Preparation of (±)-{4-{[(3-chloro-6,7,10,11-tetrahydro-9-methyl-7,11-methanocyclooocta[*b*]quinolin-12-yl)amino]methyl}phenyl}-5-(4-hydroxy-3-methoxyphenyl)pent-1-en-3-one, (±)-27, and (±)-1-{4-{[(3-chloro-6,7,10,11-tetrahydro-9-methyl-7,11-methanocycloocta[*b*]quinolin-12-yl)amino]methyl}phenyl}-5-[3-(dimethylamino)methyl-4-hydroxy-5-methoxyphenyl]pent-1-en-3-one, (±)-36

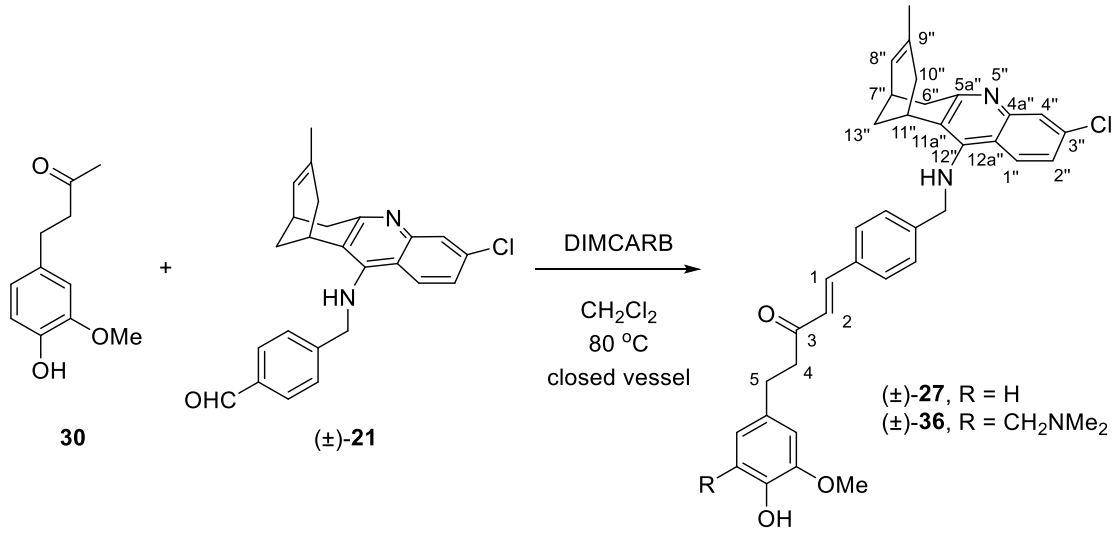

In a 25 mL closed vessel provided with a magnetic stirrer, a mixture of a solution of ketone **30** (86 mg, 0.44 mmol) in dimethylammonium dimethyl carbamate (DIMCARB, 29 µL, 30 mg, 0.23 mmol) and a solution of aldehyde (±)-**21** (178 mg, 0.44 mmol) in CH_2Cl_2 (1.2 mL) was prepared, then heated at 80 °C overnight. The resulting mixture was evaporated under reduced pressure to give a brown oil (262 mg), which was subjected to column chromatography [silica gel 35–70 µm (37 g); Ø = 3 cm; #1–6, 500 mL, CH_2Cl_2 / 50% aq. NH_4OH 100:0.4; #7–34, 2 L, CH_2Cl_2 / MeOH / 50% aq. NH_4OH 99.9:0.1:0.4; #35–37, 300 mL, CH_2Cl_2 / MeOH / 50% aq. NH_4OH 99.8:0.2:0.4; #38–41, 300 mL, CH_2Cl_2 / MeOH / 50% aq. NH_4OH 99.6:0.4:0.4; #42–45, 300 mL, CH_2Cl_2 / MeOH / 50% aq. NH_4OH 99.2:0.8:0.4; #46–48, 300 mL, CH_2Cl_2 / MeOH / 50% aq. NH_4OH 99:1:0.4; #49–54, 300 mL, CH_2Cl_2 / MeOH / 50% aq. NH_4OH 98.5:1.5:0.4; #55–63, 300 mL, CH_2Cl_2 / MeOH / 50% aq. NH_4OH 97:3:0.4; #64–72, 300 mL, CH_2Cl_2 / MeOH / 50% aq. NH_4OH 94:6:0.4], to provide the desired compound (±)-**27** (#13–15, 28 mg, 11% yield) as a yellow solid, and a mixture of compounds (±)-**27** and (±)-**36** (#16–22, 83 mg). The mixture was again subjected to column chromatography purification [silica gel 35–70 µm (10 g); Ø = 1 cm; #1–26, 430 mL, CH_2Cl_2 / 50% aq. NH_4OH 100:0.4; #27–30, 100 mL, CH_2Cl_2 / MeOH / 50% aq. NH_4OH 99.95:0.05:0.4; #31–41, 50 mL, CH_2Cl_2 / MeOH / 50% aq. NH_4OH 99.9:0.1:0.4; #42–44, 50 mL, CH_2Cl_2 / MeOH /

50% aq. NH_4OH 99.8:0.2:0.4; #45–47, 50 mL, CH_2Cl_2 / MeOH / 50% aq. NH_4OH 99.6:0.4:0.4; #48–50, 50 mL, CH_2Cl_2 / MeOH / 50% aq. NH_4OH 99:1:0.4; #51–53, 50 mL, CH_2Cl_2 / MeOH / 50% aq. NH_4OH 98:2:0.4; #54–57, 50 mL, CH_2Cl_2 / MeOH / 50% aq. NH_4OH 95:5:0.4], to provide a mixture of compounds (±)-**27** and (±)-**36** (#30–35, 45 mg), and byproduct (±)-**36** (#36–47, 11 mg, 4% yield). The mixture of compounds was subjected to one more column chromatography purification [silica gel 35–70 μm (6 g); Ø = 1 cm; #1–17, 250 mL, EtOAc / 50% aq. NH_4OH 100:0.4], to provide the desired compound (±)-**27** (#1, 4 mg, 2% yield), and byproduct (±)-**36** (#4–14, 32 mg, 11% yield). The overall yields for the desired compound (±)-**27** and byproduct (±)-**36** were 13% and 15%, respectively.

$R_{f(\mathbf{27})}$ = 0.73 (silica gel, 10 cm, CH_2Cl_2 / MeOH / 50% aq. NH_4OH 90:10:0.5).
$R_{f(\mathbf{36})}$ = 0.68 (silica gel, 10 cm, CH_2Cl_2 / MeOH / 50% aq. NH_4OH 90:10:0.5).

Analytical sample of (±)-27·HCl

In a 25 mL round-bottomed flask, (±)-**27** (13 mg, 0.05 mmol) was dissolved in CH_2Cl_2 (0.5 mL), filtered with a PTFE filter (0.2 μm), treated with HCl / MeOH (0.53 N, 0.24 mL), evaporated *in vacuo*, recrystallized from MeOH / EtOAc / hexane 1:2:0.5 (1.75 mL), and washed with pentane (3 × 2 mL), giving, after drying in standard conditions, (±)-**27**·HCl (19 mg) as a yellow solid.

Melting point: 140–142 °C (MeOH / EtOAc / hexane 1:2:0.5).

IR (ATR) *v*: 3500–2500 (max. at 3215, 2923, O–H, N–H, $^+$N–H, C–H st), 1631, 1600, 1582, 1563, 1513 (C=O, Ar–C–C, Ar–C–N st) cm^{-1}.

(±)-**27** (free base) ^{1}H NMR (400 MHz, $CDCl_3$) *δ*: 1.48 (s, 3H, 9″-CH_3), 1.70 (broad d, *J* = 16.8 Hz, 1H, 10″-H_{endo}), 1.83 (dm, *J* = 12.4 Hz, 1H, 13″-H_{syn}), 1.97 (dm, *J* = 12.4 Hz, 1H, 13″-H_{anti}), 2.43 (broad dd, *J* = 16.8 Hz, *J*′ = 3.6 Hz, 1H, 10″-H_{exo}), 2.72 (broad s, 1H, 7″-H), 2.92–3.01 (complex signal, 4H, 4-H_2, 5-H_2), 3.02 (broad d, *J* = 17.2 Hz, 1H, 6″-H_{endo}), 3.148 (dd, *J* = 17.2 Hz, *J*′ = 5.2 Hz, 1H, 6″-H_{exo}), superimposed 3.154 (m, 1H, 11″-H), 3.87 (s, 3H, 3′-OCH_3), 4.23 (broad signal, 2H, OH, NH), 4.63 (broad s, 2H, NH-CH_2-Ar), 5.52 (broad d, *J* = 4.4 Hz, 1H, 8″-H), 6.72 (dd, *J* = 8.0 Hz, *J*′ = 2.0 Hz, 1H, 6′-H), 6.74 (d, *J* = 16.4 Hz, 1H, 2-H), 6.75 (d, *J* = 2.0 Hz, 1H, 2′-H), 6.84 (d, *J* = 8.0 Hz, 1H, 5′-H),

7.27 (dd, *J* = 8.8 Hz, *J*′ = 2.0 Hz, 1H, 2″-H), 7.38 (dm, *J* = 8.0 Hz, 2H, *p*-phenylene-H_{meta}), 7.54 (d, *J* = 8.0 Hz, 2H, *p*-phenylene-H_{ortho}), 7.55 (d, *J* = 16.4 Hz, 1H, 1-H), 7.92 (d, *J* = 8.8 Hz, 1H, 1″-H), 7.93 (d, *J* = 2.0 Hz, 1H, 4″-H).

(±)-**27** (free base) ^{13}C NMR (100.6 MHz, $CDCl_3$) significant signals *δ*: 23.3 (CH_3), 27.5 (CH), 28.1 (CH), 28.9 (CH_2), 29.7 (CH_2), 37.1 (CH_2), 39.9 (CH_2), 42.9 (CH_2), 54.0 (CH_2), 55.9 (CH_3), 111.2 (CH), 114.4 (CH), 119.1 (C), 120.8 (CH), 122.5 (C), 124.8 (CH), 125.0 (CH), 125.5 (CH), 126.4 (CH), 127.7 (CH), 128.0 (2CH), 128.8 (2CH), 141.7 (C), 141.9 (CH), 144.0 (C), 146.4 (C), 148.4 (C), 149.7 (C), 158.9 (C), 199.4 (C).

HRMS (ESI):

Calculated for ($C_{36}H_{35}{}^{35}ClN_2O_3$ + H^+): 579.2409

Found: 579.2406

Analytical sample of (±)-36·2HCl

In a 25 mL round-bottomed flask, (±)-**36** (32 mg, 0.05 mmol) was dissolved in CH_2Cl_2 (0.5 mL), filtered with a PTFE filter (0.2 μm), treated with HCl / MeOH (0.53 N, 0.27 mL), evaporated *in vacuo*, recrystallized from MeOH / EtOAc / hexane 1:2:0.5 (1.75 mL), and washed with pentane (3 × 2 mL), giving, after drying in standard conditions, (±)-**36**·2HCl (34 mg) as a yellow solid.

Melting point: 163–167 °C (MeOH / EtOAc / hexane 1:2:0.5).

IR (ATR) *v*: 3500–2500 (max. at 3215, 3039, 2922, 2702, O–H, N–H, $^+$N–H, C–H st), 1630, 1600, 1582, 1566, 1504 (C=O, Ar–C–C, Ar–C–N st) cm^{-1}.

^{1}H NMR (500 MHz, CD_3OD) *δ*: 1.61 (s, 3H, 9″-CH_3), superimposed 1.95–2.00 (m, 1H, 13″-H_{syn}), 1.98 (broad d, *J* = 17.0 Hz, 1H, 10″-H_{endo}), 2.10 (dm, *J* = 11.0 Hz, 1H, 13″-H_{anti}), 2.56 (dm, *J* = 17.0 Hz, 1H, 10″-H_{exo}), 2.80 (m, 1H, 7″-H), 2.84 [s, 6H, 3′-CH_2-N(CH_3)$_2$], 2.91 (d, *J* = 18.0 Hz, 1H, 6″-H_{endo}), 2.93 (t, *J* = 7.0 Hz, 2H, 5-H_2), 3.07 (t, *J* = 7.0 Hz, 2H, 4-H_2), 3.25 (dd, *J* = 18.0 Hz, *J*′ = 5.5 Hz, 1H, 6″-H_{exo}), 3.51 (m, 1H, 11″-H), 3.89 (s, 3H, 5′-OCH_3), 4.27 [s, 2H, 3′-CH_2-N(CH_3)$_2$], 4.85 (s, OH, NH, and $^+$NH), 5.23 (s, 2H, NH-CH_2-Ar), 5.61 (dm, *J* = 4.5 Hz, 1H, 8″-H), 6.82 (s, 1H, 2′-H),

6.88 (d, *J* = 16.0 Hz, 1H, 2-H), 6.99 (s, 1H, 6'-H), 7.39 (dd, *J* = 9.0 Hz, *J*' = 2.0 Hz, 1H, 2''-H), 7.48 (broad d, *J* = 8.0 Hz, 2H, *p*-phenylene-H_{meta}), 7.65 (d, *J* = 16.0 Hz, 1H, 1-H), 7.71 (broad d, *J* = 8.0 Hz, 2H, *p*-phenylene-H_{ortho}), 7.77 (d, *J* = 2.0 Hz, 1H, 4''-H), 8.20 (d, *J* = 9.0 Hz, 1H, 1''-H).

^{13}C NMR (125.8 MHz, CD_3OD) δ: 23.5 (CH_3, 9''-CH_3), 27.6 (CH, C11''), 27.9 (CH, C7''), 29.3 (CH_2, C13''), 30.7 (CH_2, C5), 36.1 (CH_2, C6''), 36.3 (CH_2, C10''), 43.2 (CH_2, C4), 43.3 [$2CH_3$, 3'-CH_2-N(CH_3)$_2$], 52.1 (CH_2, NH-CH_2-Ph), 56.6 (CH_3, 5'-OCH_3), 57.9 [CH_2, 3'-CH_2-$N(CH_3)_2$], 114.7 (CH, C6'), 115.7 (C, C12a''), 117.1 (C, C3'), 118.4 (C, C11a''), 119.3 (CH, C4''), 124.3 (CH, C2'), 125.2 (CH, C8''), 126.8 (CH, C2''), 127.6 (CH, C2), 128.4 (2CH, *p*-phenylene-C_{meta}), 129.2 (CH, C1''), 130.3 (2CH, *p*-phenylene-C_{ortho}), 134.3 (C, C1'), 134.7 (C, C9''), 135.8 (C, *p*-phenylene-C_{ipso}), 140.4 (C, C3''), 140.9 (C, C4a''), 141.4 (C, *p*-phenylene-C_{para}), 143.7 (CH, C1), 145.4 (C, C4'), 149.1 (C, C5'), 152.0 (C, C5a''), 157.4 (C, C12''), 202.0 (C, C3).

HRMS (ESI):

Calculated for ($C_{39}H_{42}{}^{35}ClN_3O_3 + H^+$):	636.2987
Found:	636.2975

Preparation of tetramethyl 3,7-dihydroxybicyclo[3.3.1]nona-2,6-diene-2,4,6,8-tetracarboxylate, 44

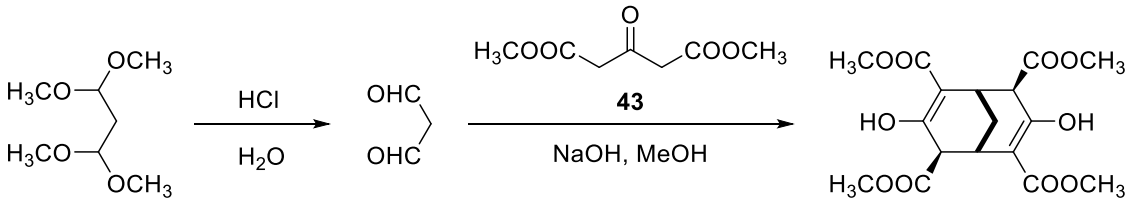

41 **42** **44**

In a triple necked 5 L reactor equipped with a magnetic stirrer and a pressure-equalizing dropping funnel, a suspension of 1,1,3,3-tetramethoxypropane, **41** (226 mL, 225 g, 1.37 mol) in 2 N HCl aq. sol. (690 mL, 1.38 mol) was prepared and stirred at room temperature for 1.5 hours, then cooled to 5 ^{o}C with an ice / water bath, treated dropwise with 5 N NaOH aq. sol. (480 mL, 2.40 mol), and diluted with MeOH (670 mL). To the resulting solution was added dimethyl-1,3-acetonedicarboxylate, **43** (396 mL, 477 g, 2.74 mol) and again diluted with MeOH (460 mL). The resulting mixture was stirred at room temperature for 3 days, cooled to 5 ^{o}C with an ice / water bath, acidified with concentrated HCl (84 mL), filtered under vacuum and the solid washed with water (2 × 100 mL), to afford the desired tetraester **44** (217 g, 41% yield) as a beige solid.

Preparation of bicyclo[3.3.1]nonane-3,7-dione, 45

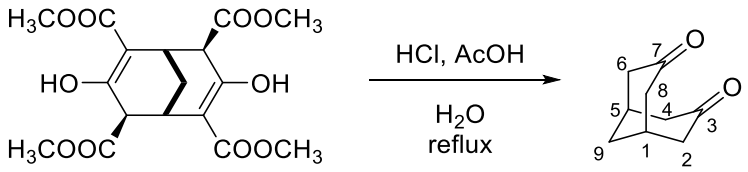

44 **45**

In a triple necked 5 L reactor provided with a magnetic stirrer and two refrigerants, a suspension of tetraester **44** (217 g, 566 mmol) in water (566 mL) was prepared and successively treated with concentrated HCl (566 mL) and AcOH (1.16 L). The reaction mixture was stirred under reflux for 1 day, then cooled to room temperature and extracted with CH_2Cl_2 (5 × 400 mL). The combined organic layers were washed with 5 N NaOH aq. sol. (2 × 650 mL), dried over anhydrous Na_2SO_4, filtered and evaporated under reduced pressure affording the desired diketone **45** (60.3 g, 70% yield) as a beige solid.

R_f = 0.14 (silica gel, 10 cm, hexane / EtOAc 1:1).

Analytical data of 45

Melting point: 240–242 ^oC (sublimated at 140 ºC and 0.8 Torr).

IR (KBr) *v*: 1706 (C=O st) cm^{-1}.

^1H NMR (200 MHz, $CDCl_3$) δ: 2.23 (s, 2H, 9-H_2), 2.38 [d, *J* = 15.4 Hz, 4H, 2(4,6,8)-H_{endo}], 2.62 [dd, *J* = 15.4 Hz, *J'* = 5.4 Hz, 4H, 2(4,6,8)-H_{exo}], 2.88 [broad s, 2H, 1(5)-H].

^{13}C NMR (50.4 MHz, $CDCl_3$) δ: 31.0 (CH_2, C9), 32.3 [CH, C1(5)], 47.5 [CH_2, C2(4,6,8)], 208.9 [C, C3(7)].

Preparation of 3-methyl-2-oxa-1-adamantanol, 46

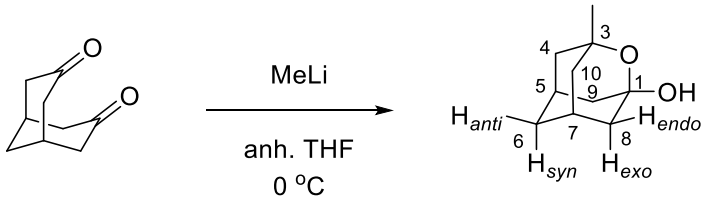

45 **46**

In a triple necked 2 L round-bottomed flask provided with an inert atmosphere, a magnetic stirrer and a pressure-equalizing dropping funnel, MeLi (1.6 N in Et_2O, 196 mL, 314 mmol) was placed, cooled to 0 °C with an ice bath and treated dropwise with a solution of diketone **45** (39.8 g, 262 mmol) in anhydrous THF (523 mL). The reaction mixture was stirred at 0 °C for 35 minutes, then treated dropwise with saturated aqueous NH_4Cl (500 mL) and extracted with Et_2O (3 × 400 mL). The combined organic layers were dried over anhydrous Na_2SO_4, filtered and concentrated *in* vacuo providing the desired oxaadamantanol **46** (43.4 g, 99% yield) as a yellow solid.

R_f = 0.36 (silica gel, 10 cm, hexane / EtOAc 1:1).

Analytical data of 46

Melting point: 87–90 °C (sublimated at 80 ºC and 0.5 Torr).

IR (KBr) *v*: 3327 (O–H st) cm^{-1}.

^{1}H NMR (500 MHz, $CDCl_3$) δ: 1.15 (s, 3H, 3-CH_3), 1.47 [ddd, J = 12.0 Hz, J' = 3.5 Hz, J'' = 2.0 Hz, 2H, 4(10)-H_{exo}], 1.62 [broad d, J = 12.0 Hz, 2H, 4(10)-H_{endo}], 1.65 (m, 2H, 6-H_{syn} and 6-H_{anti}), 1.68 [broad d, J = 12.0 Hz, 2 H, 8(9)-H_{endo}], 1.75 [ddd, J = 12.0 Hz, J' = 3.5 Hz, J'' = 2.0 Hz, 2H, 8(9)-H_{exo}], 2.30 [m, 2 H, 5(7)-H].

^{13}C NMR (50.4 MHz, $CDCl_3$) δ: 28.5 (CH_3, 3-CH_3), 29.2 [CH, C5(7)], 33.5 (CH_2, C6), 40.2 [CH_2, 4(10)], 40.7 [CH_2, C8(9)], 74.6 (C, C3), 94.7 (C, C1).

Preparation of 3-methyl-2-oxa-1-adamantyl methanesulfonate, 47

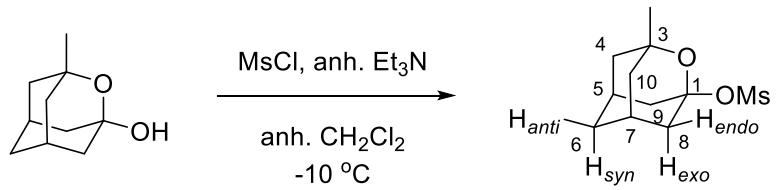

In a triple necked 2 L round-bottomed flask provided with an inert atmosphere and a magnetic stirrer, a solution of oxaadamantanol **46** (43.4 g, 260 mmol) and freshly distilled Et_3N (54.0 mL, 39.4 g, 390 mmol) in CH_2Cl_2 (1.22 L) was prepared, cooled to -10 °C with an ice / NaCl bath and treated dropwise with MsCl (31.9 mL, 47.7 g, 413 mmol). The reaction mixture was stirred at -10 °C for 30 minutes, then poured onto a mixture of 10% aq. HCl (320 mL) and ice (80 mL), and extracted with CH_2Cl_2 (2 × 330 mL). The combined organic layers were washed with sat. aq. $NaHCO_3$ (550 mL) and brine (550 mL), dried over anhydrous Na_2SO_4, filtered and concentrated under reduced pressure giving the desired mesylate **47** (67.7 g, quantitative yield) as a dark reddish solid.

Analytical data of 47

Melting point: 79–81 °C (CH_2Cl_2).

IR (KBr) *v*: 1345 (SO_2 st as), 1175 (SO_2 st si) cm^{-1}.

^1H NMR (500 MHz, $CDCl_3$) *δ*: 1.19 (s, 3H, 3-CH_3), 1.50 [broad d, *J* = 1.5 Hz, 2H, 4(10)-H_{exo}], 1.62–1.72 (complex signal, 2H, 6-H_{syn} and 6-H_{anti}), 1.69 [broad d, *J* = 12.5 Hz, 2H 4(10)-H_{endo}], 1.92 [broad d, *J* = 11.5 Hz, 2H, 8(9)-H_{exo}], 2.18 [broad d, *J* = 11.5 Hz, 2H, 8(9)-H_{endo}], 2.36 [broad s, 2H, 5(7)-H], 3.11 (s, 3H, CH_3SO_3).

^{13}C NMR (50.4 MHz, $CDCl_3$) *δ*: 28.3 (CH_3, 3-CH_3), 30.0 [CH, C5(7)], 33.2 (CH_2, C6), 39.7 [CH_2, C8(9)], 40.0 [CH_2, C4(10)], 42.0 (CH_3, CH_3SO_3), 77.4 (C, C3), 108.0 (C, C1).

Preparation of (±)-7-methylbicyclo[3.3.1]non-6-en-3-one, (±)-48

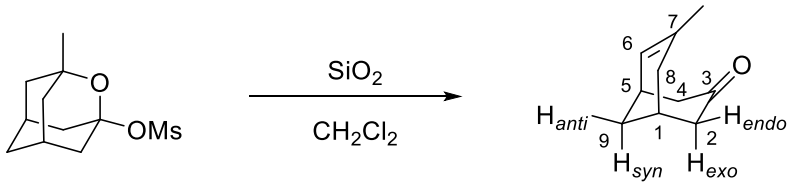

47 (±)-**48**

In a 250 mL round-bottomed flask provided with a magnetic stirrer, a suspension of mesylate **47** (4.70 g, 19.1 mmol) and SiO_2 (4.77 g) in CH_2Cl_2 (51 mL) was prepared, then stirred for 3 hours and concentrated *in vacuo* affording a dark reddish solid (9.48 g), which was purified through column chromatography [silica gel 35−70 μm (195 g); Ø = 8 cm; #1–10, 2 L, hexane; #11–39, 3 L, hexane / EtOAc 95:5], to provide the desired enone (±)-**48** (#22–38, 2.43 g, 85% yield) as a colourless oil.

R_f = 0.61 (silica gel, 10 cm, hexane / EtOAc 1:1).

Analytical data of (±)-48

IR (NaCl) *v*: 1709 (C=O st) cm^{-1}.

^{1}H NMR (500 MHz, $CDCl_3$) *δ*: 1.57 (s, 3H, 7-CH_3), 1.78 (broad d, *J* = 18.0 Hz, 1H, 8-H_{endo}), 1.90 (dm, *J* = 12.5 Hz, 1H, 9-H_{anti}), 1.97 (dm *J* = 12.5 Hz, 1H, 9-H_{syn}), 2.24 (dddd, *J* = 15.5 Hz, *J'* = *J''* = *J'''* = 2.0 Hz, 1H, 2-H_{endo}), 2.28 (dddd, *J* = 14.5 Hz, *J'* = *J''* = *J'''* = 2.0 Hz, 1H, 4-H_{endo}), 2.33 (broad dd, *J* = 18.0 Hz, *J'* = 6.0 Hz, 1H, 8-H_{exo}), 2.40 (dd, *J* = 14.5 Hz, *J'* = 4.5 Hz, 1H, 4-H_{exo}), 2.48 (broad dd, *J* = 15.5 Hz, *J'* = 6.5 Hz, 1H, 2-H_{exo}), 2.55 (m, 1H, 1-H), 2.63 (broad s, 1H, 5-H), 5.40 (dm, *J* = 6.0 Hz, 1H, 6-H).

^{13}C NMR (50.4 MHz, $CDCl_3$) *δ*: 23.1 (CH_3, 7-CH_3), 30.1 (CH, C1), 30.1 (CH_2, C9), 31.0 (CH, C5), 37.3 (CH_2, C8), 46.4 (CH_2, C4), 49.0 (CH_2, C2), 124.5 (CH, C6), 132.7 (C, C7), 212.2 (C, C3).

Preparation of 9-bromononanenitrile, 50c

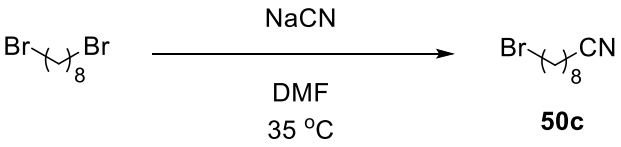

In a triple necked 250 mL round-bottomed flask provided with an inert atmosphere, a magnetic stirrer and a refrigerant, 1,8-dibromooctane (6.81 mL, 10.0 g, 36.8 mmol) and NaCN (1.80 g, 36.8 mmol) were dissolved in anhydrous DMF (55 mL). The reaction mixture was stirred at 35 °C for 2 hours, then treated with water (100 mL) and extracted with Et_2O (3 × 100 mL). The combined organic layers were washed with water (3 × 100 mL) and saturated NaCl aqueous solution (3 × 100 mL), dried with anhydrous Na_2SO_4, filtered and evaporated under reduced pressure to give a transparent oil (8.88 g), which was purified by several consecutive micro-distillations at 150 °C to provide the desired compound **50c** (7.17 g, 89% yield) as a transparent oil.

Preparation of (±)-12-amine-1,4-difluoro-6,7,10,11-tetrahydro-8-methyl-6,10-methanocycloocta[*b*]quinoline, (±)-39a

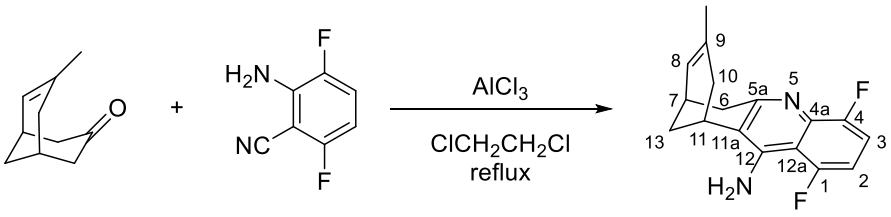

(±)-**48** **49a** (±)-**39a**

In a 50 mL closed vessel equipped with an inert atmosphere and a magnetic stirrer, a suspension of 2-amino-3,6-difluorobenzonitrile, **49a** (270 mg, 1.75 mmol), and $AlCl_3$ (292 mg, 2.19 mmol) in anhydrous 1,2-dichloroethane (3 mL) was prepared, then treated with a solution of enone (±)-**48** (219 mg, 1.46 mmol) in anhydrous 1,2-dichloroethane (12 mL). The reaction mixture was stirred at 100 °C for 2 days, then allowed to cool to room temperature, diluted with water (9 mL) and THF (9 mL), alkalinized with 5 N NaOH aq. sol. (4 mL), again stirred for 30 minutes at room temperature, and extracted with CH_2Cl_2 (6 × 12 mL). The combined organic layers were dried over anhydrous Na_2SO_4, filtered and evaporated under reduced pressure to afford a clear brown solid (437 mg), which was subjected to column chromatography purification [silica gel 35−70 µm (22 g); Ø = 1.8 cm; #1, 500 mL, hexane / Et_3N 100:0.2; #2–3, 500 mL, hexane / EtOAc / Et_3N 95:5:0.2; #4–12, 1 L, hexane / EtOAc / Et_3N 90:10:0.2; #13–14, 200 mL, hexane / EtOAc / Et_3N 80:20:0.2], to give the desired modified huprine (±)-**39a** (#5–9, 155 mg, 37% yield) as a pale yellow solid.

R_f = 0.78 (silica gel, 10 cm, hexane / EtOAc / Et_3N 50:50:0.5).

Analytical sample of (±)-39a·HCl

In a 25 mL round-bottomed flask, (±)-**39a** (44 mg, 0.15 mmol) was dissolved in CH_2Cl_2 (2 mL), filtered with a PTFE filter (0.2 µm), treated with HCl / Et_2O (3 N, 0.15 mL), evaporated *in vacuo*, and washed with pentane (3 × 2 mL), to provide, after drying in standard conditions, (±)-**39a**·HCl (58 mg) as a pale beige solid.

Melting point: 185–188 °C.

IR (ATR) *v*: 3500–2500 (max at 3354, 3312, 3198, 2914, N–H, $^{+}$N–H, C–H st), 1646, 1594 (Ar–C–C, Ar–C–N st) cm^{-1}.

^{1}H NMR (400 MHz, CD_3OD) *δ*: 1.60 (s, 3H, 9-CH_3), superimposed in part 1.96 (dm, *J* = 12.8 Hz, 1H, 13-H_{syn}), 1.99 (broad d, *J* = 18.0 Hz, 1H, 10-H_{endo}), 2.09 (dm, *J* = 12.8 Hz, 1H, 13'-H_{anti}), 2.53 (dd, *J* = 18.0 Hz, *J'* = 4.8 Hz, 1H, 10-H_{exo}), 2.79 (m, 1H, 7-H), 2.99 (ddd, *J* = 18.0 Hz, *J'* = *J''* = 1.6 Hz, 1H, 6-H_{endo}), 3.20 (dd, *J* = 18.0 Hz, *J'* = 5.6 Hz, 1H, 6-H_{exo}), 3.40 (m, 1H, 11-H), 4.85 (s, NH, $^{+}$NH), 5.58 (dm, *J* = 5.2 Hz, 1H, 8-H), 7.33 (ddd, *J* = 13.2 Hz, *J'* = 9.2 Hz, *J''* = 4.0 Hz, 1H, 2-H), 7.68 (ddd, *J* = 10.0 Hz, *J'* = 9.2 Hz, *J''* = 4.0 Hz, 1H, 3-H).

^{13}C NMR (100.6 MHz, CD_3OD) *δ*: 23.4 (CH_3, 9-CH_3), 27.3 (CH, C11), 28.0 (CH, C7), 29.0 (CH_2, C13), 35.5 (CH_2), 36.0 (CH_2) (C6 and C10), 108.5 (d, *J* = 14.3 Hz, C, C12a), 111.4 (dd, *J* = 26.4 Hz, *J'* = 7.4 Hz, CH, C2), 117.0 (C, C11a), 118.5 (dd, *J* = 19.6 Hz, *J'* = 10.8 Hz, CH, C3), 125.0 (CH, C8), 130.3 (d, *J* = 15.6 Hz, C, C4a), 134.9 (C, C9), 149.4 (d, *J* = 247.7 Hz, C, C1), 153.9 (C, C5a), 155.4 (C, C12), 157.1 (d, *J* = 249.0 Hz, C, C4).

HRMS (ESI):

Calculated for ($C_{17}H_{16}F_2N_2$ + H^+):	287.1354
Found:	287.1362

HPLC purity: 94.7%.

Preparation of (±)-9-[(1,4-difluoro-6,7,10,11-tetrahydro-8-methyl-6,10-methanocycloocta[*b*]quinolin-12-yl)amino]nonanenitrile, (±)-51a

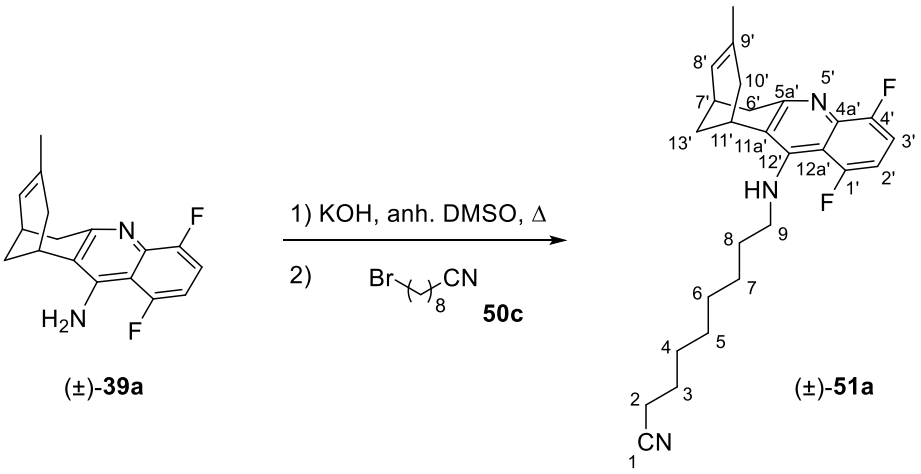

In a double necked 10 mL round-bottomed flask provided with an inert atmosphere, a magnetic stirrer and 4 Å molecular sieves, modified huprine (±)-**39a** (185 mg, 0.65 mmol) and finely powdered KOH (85% purity, 141 mg, 2.13 mmol) were suspended in anhydrous DMSO (2.8 mL). The resulting suspension was stirred, heating every 10 minutes with a heat gun for 1 hour, and at room temperature one more hour, then treated with 9-bromononanenitrile, **50c** (155 mg, 0.71 mmol). The reaction mixture was stirred at room temperature overnight, then diluted with 5 N NaOH aq. sol. (20 mL), and extracted with CH_2Cl_2 (3 × 17 mL). The combined organic layers were washed with water (5 × 17 mL), dried with anhydrous Na_2SO_4, filtered and evaporated under reduced pressure to afford a brown oil (269 mg), which was purified by column chromatography [silica gel 35−70 μm (15 g); Ø = 1.5 cm; #1, 250 mL, hexane / Et_3N 100:0.2; #2, 250 mL, hexane / EtOAc / Et_3N 95:5:0.2; #3–11, 250 mL, hexane / EtOAc / Et_3N 90:10:0.2, #12–50, 750 mL, hexane / EtOAc / Et_3N 85:15:0.2], to give the desired nitrile (±)-**51a** (#16–25, 225 mg, 82% yield) as a yellow oil.

R_f = 0.84 (silica gel, 10 cm, hexane / EtOAc / Et_3N 50:50:0.5).

Analytical sample of (±)-51a·HCl

In a 10 mL round-bottomed flask (±)-**51a** (31 mg, 0.07 mmol) was dissolved in CH_2Cl_2 (2 mL), filtered with a PTFE filter (0.2 μm), treated with HCl / Et_2O (3 N, 0.07 mL), evaporated *in*

vacuo, and washed with pentane (3 × 2 mL), providing, after drying in standard conditions, (±)-**51a**·HCl (33 mg) as a yellow solid.

Melting point: 58–62 °C.

IR (ATR) *v*: 3500–2500 (max at 3071, 2925, 2852, N–H, $^{+}$N–H, C–H st), 2255 (CN st), 1648, 1586, 1514 (Ar–C–C, Ar–C–N st) cm^{-1}.

^{1}H NMR (400 MHz, CD_3OD) *δ*: 1.30–1.46 (complex signal, 8H, 4-H_2, 5-H_2, 6-H_2 and 7-H_2), 1.60 (s, 3H, 9'-CH_3), superimposed in part 1.60 (tt, *J* = *J'* = 7.2 Hz, 2H, 3-H_2), 1.79 (tt, *J* = *J'* = 6.8 Hz, 2H, 8-H_2), 1.97 (broad d, *J* = 17.2 Hz, 1H, 10'-H_{endo}), superimposed 1.94–2.00 (m, 1H, 13'-H_{syn}), 2.09 (dm, *J* = 12.4 Hz, 1H, 13'-H_{anti}), 2.42 (t, *J* = 7.2 Hz, 2H, 2-H_2), 2.58 (dd, *J* = 17.2 Hz, *J'* = 4.0 Hz, 1H, 10'-H_{exo}), 2.78 (m, 1H, 7'-H), 2.99 (broad d, *J* = 18.0 Hz, 1H, 6'-H_{endo}), 3.19 (dd, *J* = 18.0 Hz, *J'* = 5.6 Hz, 1H, 6'-H_{exo}), 3.59 (m, 1H, 11'-H), 3.73 (dt, *J* = *J'* = 6.8 Hz, 2H, 9-H_2), 4.85 (s, NH, $^{+}$NH), 5.61 (broad d, *J* = 4.8 Hz, 1H, 8'-H), 7.30 (ddd, *J* = 12.8 Hz, *J'* = 8.8 Hz, *J''* = 4.0 Hz, 1H, 2'-H), 7.68 (ddd, *J* = 10.0 Hz, *J'* = 8.8 Hz, *J''* = 4.0 Hz, 1H, 3'-H).

^{13}C NMR (100.6 MHz, CD_3OD) *δ*: 17.3 (CH_2, C2), 23.4 (CH_3, 9'-CH_3), 26.4 (CH_2, C3), 27.5 (CH, C11'), 27.6 (CH_2, C7), 27.8 (CH, C7'), 29.0 (CH_2, C13'), 29.5 (CH_2), 29.6 (CH_2), 29.9 (CH_2) (C4, C5 and C6), 31.6 (CH_2, C8), 36.4 (CH_2, C6'), 37.0 (CH_2, C10'), 51.2 (d, *J* = 12.3 Hz, CH_2, C9), 109.4 (d, *J* = 13.9 Hz, C, C12a'), 111.2 (dd, *J* = 26.8 Hz, *J'* = 7.0 Hz, CH, C2'), 118.2 (m, CH, C3'), 119.0 (C, C11a'), 121.2 (C, C1), 125.5 (CH, C8'), 131.6 (m, C, C4a'), 134.1 (C, C9'), 149.5 (d, *J* = 249.2 Hz, C, C1'), 153.2 (C, C5a'), 156.1 (C, C12'), 155.6 (d, *J* = 247.4 Hz, C, C4').

HRMS (ESI):

Calculated for ($C_{26}H_{31}F_2N_3$ + H^+):	424.2559
Found:	424.2565

Preparation of (±)-*N*-(1,4-difluoro-6,7,10,11-tetrahydro-8-methyl-6,10-methanocycloocta[*b*]quinolin-12-yl)nonane-1,9-diamine, (±)-52a

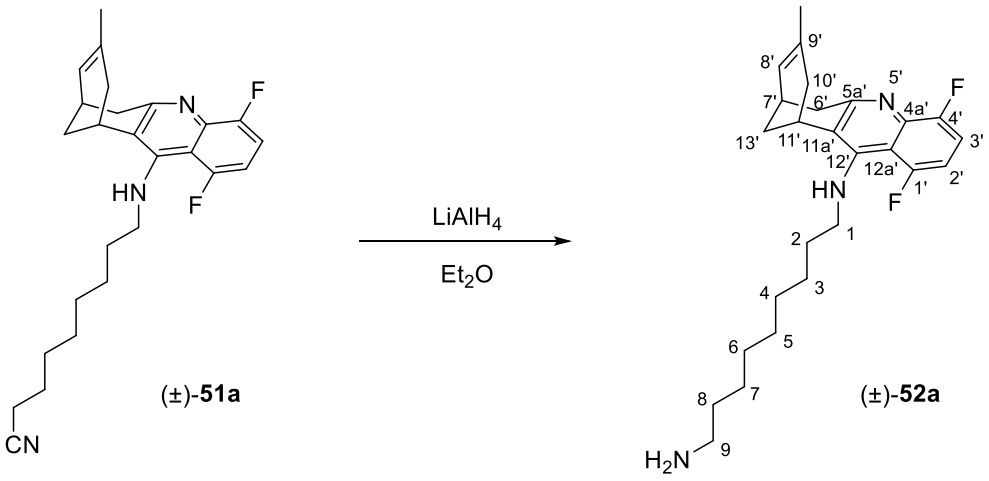

(±)-**51a** (±)-**52a**

In a triple neck 10 mL round-bottomed flask equipped with an inert atmosphere and a magnetic stirrer, nitrile (±)-**51a** (101 mg, 0.24 mmol) was dissolved in anhydrous Et_2O (4 mL), cooled to 0 °C with an ice bath and treated dropwise with $LiAlH_4$ (4 M in Et_2O, 0.19 mL, 0.74 mmol). The reaction mixture was stirred at room temperature overnight, then cooled to 0 °C with an ice bath, diluted dropwise with 1 N NaOH aq. sol. (12 mL) and water (15 mL), and extracted with CH_2Cl_2 (3 × 20 mL). The combined organic layers were dried over anhydrous Na_2SO_4, filtered and evaporated under reduced pressure to give the desired primary amine (±)-**52a** (100 mg, 98% yield) as a yellow oil.

R_f = 0.18 (silica gel, 10 cm, CH_2Cl_2 / MeOH / NH_4OH 50% 95:5:1).

Analytical sample of (±)-52a·2HCl

In a 25 mL round-bottomed flask (±)-**52a** (23 mg, 0.05 mmol) was dissolved in CH_2Cl_2 (2 mL), filtered with a PTFE filter (0.2 µm), treated with HCl / Et_2O (3 N, 0.15 mL), evaporated *in vacuo*, and washed with pentane (3 × 2 mL), providing, after drying in standard conditions, (±)-**52a**·2HCl (30 mg) as a yellow solid.

Melting point: 153–155 °C.

IR (ATR) *v*: 3500–2500 (max at 3369, 3214, 2919, 2852, N–H, $^{+}$N–H, C–H st), 1646, 1586, 1516 (Ar–C–C, Ar–C–N st) cm^{-1}.

^{1}H NMR (400 MHz, CD_3OD) *δ*: 1.28–1.42 (complex signal, 10H, 3-H_2, 4-H_2, 5-H_2, 6-H_2 and 7-H_2), 1.60 (s, 3H, 9'-CH_3), 1.64 (m, 2H, 8-H_2), 1.78 (tt, *J* = *J'* = 6.8 Hz, 2H, 2-H_2), 1.97 (broad d, *J* = 17.2 Hz, 1H, 10'-H_{endo}), superimposed 1.94–2.00 (m, 1H, 13'-H_{syn}), 2.08 (dm, *J* = 12.0 Hz, 1H, 13'-H_{anti}), 2.58 (dd, *J* = 17.2 Hz, *J'* = 4.8 Hz, 1H, 10'-H_{exo}), 2.77 (m, 1H, 7'-H), 2.90 (broad t, *J* = 7.6 Hz, 2H, 9-H_2), 2.99 (broad d, *J* = 18.0 Hz, 1H, 6'-H_{endo}), 3.19 (dd, *J* = 18.0 Hz, *J'* = 5.2 Hz, 1H, 6'-H_{exo}), 3.60 (m, 1H, 11'-H), 3.73 (dt, *J* = *J'* = 6.8 Hz, 2H, 1-H_2), 4.86 (s, NH, $^{+}$NH), 5.61 (broad d, *J* = 5.2 Hz, 1H, 8'-H), 7.29 (ddd, *J* = 12.8 Hz, *J'* = 8.8 Hz, *J''* = 4.0 Hz, 1H, 2'-H), 7.68 (ddd, *J* = 10.0 Hz, *J'* = 8.8 Hz, *J''* = 4.4 Hz, 1H, 3'-H).

^{13}C NMR (100.6 MHz, CD_3OD) *δ*: 23.4 (CH_3, 9'-CH_3), 27.4 (CH, C11'), 27.5 (CH_2, C3), 27.7 (CH + CH_2, C7' and C4), 28.6 (CH_2, C5), 29.0 (CH_2, C13'), 30.11 (CH_2), 30.14 (CH_2), 30.3 (CH_2) (C6, C7 and C8), 31.6 (CH_2, C2), 36.2 (CH_2, C6'), 37.0 (CH_2, C10'), 40.8 (CH_2, C9), 51.3 (d, *J* = 14.6 Hz, CH_2, C1), 109.3 (d, *J* = 14.6 Hz, C, C12a'), 111.3 (dd, *J* = 27.5 Hz, *J'* = 7.6 Hz, CH, C2'), 118.4 (dd, *J* = 18.6 Hz, *J'* = 12.3 Hz, CH, C3'), 118.8 (C, C11a'), 125.4 (CH, C8'), 131.1 (m, C, C4a'), 134.1 (C, C9'), 149.3 (d, *J* = 250.9 Hz, C, C1'), 152.9 (C, C5a'), 155.6 (d, *J* = 249.2 Hz, C, C4'), 156.3 (C, C12').

HRMS (ESI):

Calculated for ($C_{26}H_{35}F_2N_3$ + H^{+}):	428.2872
Found:	428.2880

Preparation of (±)-*N*-{9-[(1,4-difluoro-6,7,10,11-tetrahydro-8-methyl-6,10-methanocycloocta[*b*]quinolin-12-yl)amino]nonyl}-9,10-dihydro-4,5-dihydroxy-9,10-dioxoanthracene-2-carboxamide, (±)-40a

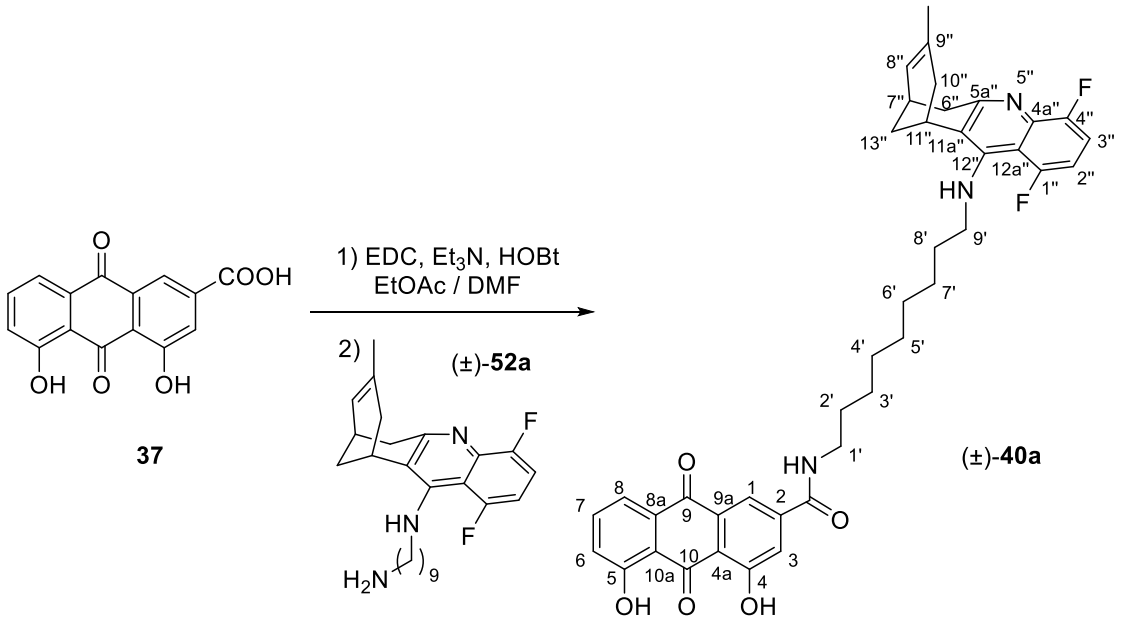

In a 25 mL round-bottomed flask equipped with a magnetic stirrer, rhein acid **37** (53.0 mg, 0.19 mmol) was suspended in a mixture of EtOAc (1.1 mL) and DMF (0.1 mL), and treated with *N*-(3-dimethylaminopropyl)-*N'*-ethylcarbodiimide hydrochloride (40 mg, 0.21 mmol), triethylamine (0.06 mL, 43 mg, 0.43 mmol), and 1-hydroxy-1*H*-benzotriazole (35 mg, 0.26 mmol). The resulting mixture was stirred at room temperature for 1 hour and treated with a suspension of the amine (±)-**52a** (73 mg, 0.17 mmol) in a mixture of EtOAc (4 mL) and DMF (0.4 mL). The reaction mixture was stirred at room temperature for 1 day and concentrated under reduced pressure to give a dark brown oil (295 mg), which was subjected to column chromatography purification [silica gel 35−70 µm (30 g); Ø = 2.5 cm; #1–14, 1.5 L, CH_2Cl_2 / 50% aq. NH_4OH 100:0.4; #15–19, 500 mL, CH_2Cl_2 / MeOH / 50% aq. NH_4OH 99.9:0.1:0.4; #20–24, 500 mL, CH_2Cl_2 / MeOH / 50% aq. NH_4OH 99.8:0.2:0.4; #25–39, 1.5 L, CH_2Cl_2 / MeOH / 50% aq. NH_4OH 99.7:0.3:0.4; #40–44, 500 mL, CH_2Cl_2 / MeOH / 50% aq. NH_4OH 99:1:0.4], to afford the desired amide (±)-**40a** (#27–44, 82 mg, 69% yield) as a yellow solid.

R_f = 0.87 (silica gel, 10 cm, CH_2Cl_2 / MeOH / 50% aq. NH_4OH 90:10:1).

Analytical sample of (±)-40a·HCl

In a 10 mL round-bottomed flask (±)-**40a** (56 mg, 0.08 mmol) was dissolved in CH_2Cl_2 (1 mL), filtered with a PTFE filter (0.2 µm), treated with HCl / Et_2O (3 N, 0.1 mL), concentrated *in vacuo*, and washed with pentane (3 × 2 mL), to give, after drying in standard conditions, (±)-**40a**·HCl (51 mg) as an orange solid.

Melting point: 145–150 °C.

IR (ATR) *v*: 3500−2500 (max at 3271, 2925, 2852, O–H, N–H, $^+$N–H, C–H st), 1622, 1591 (C=O, Ar–C–C, Ar–C–N st) cm^{-1}.

^{1}H NMR (400 MHz, CD_3OD) *δ*: 1.26−1.42 (complex signal, 10H, 3'-H_2, 4'-H_2, 5'-H_2, 6'-H_2 and 7'-H_2), 1.59 (s, 3H, 9"-CH_3), superimposed in part 1.64 (m, 2H, 2'-H_2), 1.76 (m, 2H, 8'-H_2), superimposed in part 1.95 (dm, *J* = 11.6 Hz, 1H, 13"-H_{syn}), 1.97 (broad d, *J* = 18.0 Hz, 1H, 10"-H_{endo}), 2.06 (dm, *J* = 11.6 Hz, 1H, 13"-H_{anti}), 2.56 (dm, *J* = 18.0 Hz, 1H, 10"-H_{exo}), 2.75 (m, 1H, 7"-H), 2.97 (broad d, *J* = 18.0 Hz, 1H, 6"-H_{endo}), 3.16 (dm, *J* = 18.0 Hz, 1H, 6"-H_{exo}), 3.39 (m, 2H, 1'-H_2), 3.58 (m, 1H, 11"-H), 3.70 (m, 2H, 9'-H_2), 4.86 (s, OH, NH, $^+$NH), 5.59 (broad d, *J* = 4.0 Hz, 1H, 8"-H), 7.22 (m, 1H, 2"-H), 7.32 (m, 1H, 6-H), 7.56−7.78 (complex signal, 3H, 7-H, 8-H and 3"-H), 7.64 (s, 1H, 3-H), 8.07 (s, 1H, 1-H).

^{13}C NMR (100.6 MHz, CD_3OD) *δ*: 23.4 (CH_3, 9"-CH_3), 27.5 (CH, C11"), 27.6 (CH_2), 27.7 (CH_2) (C6' and C7'), 27.8 (CH, C7"), 29.0 (CH_2, C13"), 29.9 (CH_2), 30.0 (CH_2), 30.2 (CH_2), 30.3 (CH_2) (C2', C3', C4' and C5'), 31.6 (CH_2, C8'), 36.2 (CH_2, C6"), 37.0 (CH_2, C10"), 41.1 (CH_2, C1'), 51.1 (d, *J* = 12.2 Hz, CH_2, C9'), 109.2 (d, *J* = 16.9 Hz, C, C12a"), 111.3 (broad d, *J* = 21.6 Hz, CH, C2"), 116.8 (C, C10a), 118.4 (CH + C, C3" and C4a), 118.7 (C, C11a"), 118.8 (CH, C1), 120.9 (CH, C8), 123.7 (CH, C3), 125.5 (CH, C8"), 125.8 (CH, C6), 130.9 (d, *J* = 18.3 Hz, C, C4a"), 134.1 (C, C9"), 134.6 (C, C8a), 135.0 (C, C9a), 138.7 (CH, C7), 143.6 (C, C2), 149.2 (d, *J* = 244.9 Hz, C, C1"), 153.0 (C, C5a"), 155.6 (d, *J* = 250.4 Hz, C, C4"), 156.1 (C, C12"), 163.3 (C, C4), 163.6 (C, C5), 167.1 (C, CONH), 181.9 (C, C9), 193.5 (C, C10).

HRMS (ESI):

Calculated for ($C_{41}H_{41}F_2N_3O_5$ + H^+): 694.3087

Found: 694.3089

HPLC purity: 99.3%.

Preparation of (±)-4-amine-5,6,9,10-tetrahydro-7-methyl-5,9-methanocycloocta[*b*]thieno[2,3-*e*]pyridine, (±)-39b

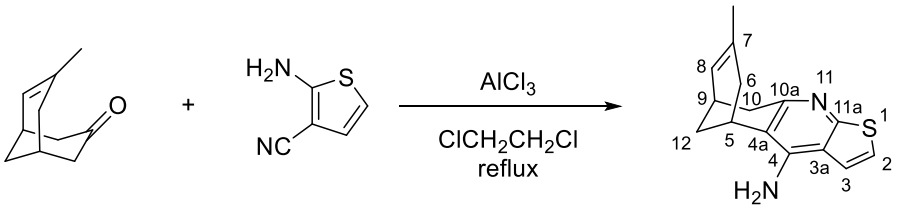

(±)-**48** **49b** (±)-**39b**

In a triple necked 250 mL round-bottomed flask equipped with an inert atmosphere, a magnetic stirrer and a pressure-equalizing dropping funnel, a suspension of 2-aminothiophene-3-carbonitrile, **49b** (1.00 g, 8.05 mmol), and $AlCl_3$ (1.34 g, 10.1 mmol) in anhydrous 1,2-dichloroethane (15 mL) was prepared, then treated with a solution of enone (±)-**48** (1.01 g, 6.71 mmol) in anhydrous 1,2-dichloroethane (61 mL). The reaction mixture was stirred under reflux overnight, then allowed to cool to room temperature, diluted with water (35 mL) and THF (35 mL), alkalinized with 5 N NaOH aq. sol. (15 mL), again stirred for 30 minutes at room temperature, and extracted with CH_2Cl_2 (6 × 50 mL). The combined organic layers were dried over anhydrous Na_2SO_4, filtered and evaporated under reduced pressure to afford a brown solid (1.92 g), which was subjected to column chromatography purification [silica gel 35−70 µm (200 g); Ø = 8 cm; #1–2, 500 mL, hexane / Et_3N 100:0.2; #3–4, 200 mL, hexane / EtOAc / Et_3N 90:10:0.2; #5–6, 200 mL, hexane / EtOAc / Et_3N 80:20:0.2; #7–8, 200 mL, hexane / EtOAc / Et_3N 70:30:0.2; #9–10, 200 mL, hexane / EtOAc / Et_3N 60:40:0.2; #11–22, 1.2 L, hexane / EtOAc / Et_3N 50:50:0.2], to afford the desired modified huprine (±)-**39b** (#10–15, 1.37 g, 80% yield) as a yellow solid.

R_f = 0.45 (silica gel, 10 cm, hexane / EtOAc / Et_3N 50:50:0.5).

Analytical sample of (±)-39b·HCl

In a 25 mL round-bottomed flask, (±)-**39b** (200 mg, 0.78 mmol) was dissolved in CH_2Cl_2 (4 mL), treated with HCl / Et_2O (3 N, 0.78 mL), concentrated *in vacuo*, and washed with pentane (3 × 2 mL), to provide, after drying in standard conditions, (±)-**39b**·HCl (230 mg) as a dark yellow solid.

Melting point: 227–228 °C.

IR (ATR) *v*: 3500–2500 (max at 3418, 3190, 2905, N–H, $^{+}$N–H, C–H st), 1651, 1584, 1520 (Ar–C–C, Ar–C–N st) cm^{-1}.

^{1}H NMR (400 MHz, CD_3OD) *δ*: 1.58 (s, 3H, 7-CH_3), superimposed in part 1.92 (dm, *J* = 12.4 Hz, 1H, 12-H_{syn}), 1.95 (broad d, *J* = 18.0 Hz, 1H, 6-H_{endo}), 2.05 (dm, *J* = 12.4 Hz, 1H, 12-H_{anti}), 2.50 (dd, *J* = 17.6 Hz, *J'* = 4.4 Hz, 1H, 6-H_{exo}), 2.76 (m, 1H, 9-H), 2.80 (broad d, *J* = 17.6 Hz, 1H, 10-H_{endo}), 3.17 (dd, *J* = 17.6 Hz, *J'* = 5.6 Hz, 1H, 10-H_{exo}), 3.34 (m, 1H, 5-H), 4.86 (s, NH, $^{+}$NH), 5.56 (broad d, *J* = 4.8 Hz, 1H, 8-H), 7.53 (d, *J* = 6.0 Hz, 1H, 3-H), 7.68 (d, *J* = 6.0 Hz, 1H, 2-H).

^{13}C NMR (100.6 MHz, CD_3OD) *δ*: 23.5 (CH_3, 7-CH_3), 27.4 (CH, C5), 28.3 (CH, C9), 29.2 (CH_2, C12), 35.5 (CH_2, C10), 35.9 (CH_2, C6), 116.2 (C, C4a), 120.8 (CH, C3), 121.7 (C, C3a), 123.8 (CH, C2), 125.0 (CH, C8), 134.7 (C, C7), 149.1 (C, C10a), 149.8 (C, C11a), 154.2 (C, C4).

HRMS (ESI):

Calculated for ($C_{15}H_{16}N_2S + H^+$):	257.1107
Found:	257.1107

HPLC purity: 98.0%.

Preparation of (±)-9-[(7-methyl-5,6,9,10-tetrahydro-5,9-methanocycloocta[*b*]thieno[3,2-*e*]pyridin-4-yl)amino]nonanenitrile, (±)-51b

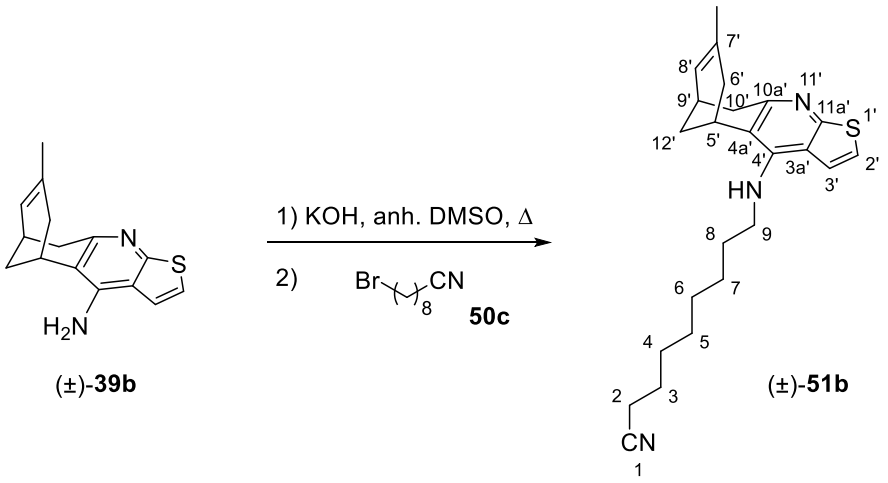

In a double necked 50 mL round-bottomed flask provided with an inert atmosphere, a magnetic stirrer and 4 Å molecular sieves, modified huprine (±)-**39b** (1.00 g, 3.90 mmol) and finely powdered KOH (85% purity, 850 mg, 12.9 mmol) were suspended in anhydrous DMSO (17 mL). The resulting suspension was stirred, heating every 10 minutes with a heat gun for 1 hour, and at room temperature one more hour, then treated with 9-bromononanenitrile, **50c** (935 mg, 4.29 mmol). The reaction mixture was stirred at room temperature overnight, then diluted with 2 N NaOH aq. sol. (120 mL), and extracted with CH_2Cl_2 (4 × 100 mL). The combined organic layers were washed with water (5 × 100 mL), dried over anhydrous Na_2SO_4, filtered and evaporated under reduced pressure to afford a brown oil (1.51 g), which was purified by column chromatography [silica gel 35−70 µm (110 g); Ø = 4 cm; #1, 300 mL, hexane / Et_3N 100:0.2; #2–4, 200 mL, hexane / EtOAc / Et_3N 90:10:0.2; #5–7, 200 mL, hexane / EtOAc / Et_3N 80:20:0.2, #8–10, 20 mL, hexane / EtOAc / Et_3N 70:30:0.2; #11–22, 800 mL], to give the desired nitrile (±)-**51b** (#14–17, 760 mg, 50% yield) as a yellow oil.

R_f = 0.56 (silica gel, 10 cm, hexane / EtOAc / Et_3N 50:50:0.5).

Analytical sample of (±)-51b·HCl

In a 10 mL round-bottomed flask (±)-**51b** (100 mg, 0.26 mmol) was dissolved in CH_2Cl_2 (2 mL), filtered with a PTFE filter (0.2 µm), treated with HCl / Et_2O (3 N, 0.25 mL), evaporated *in*

vacuo, and washed with pentane (3 × 2 mL), providing, after drying in standard conditions, (±)-**51b**·HCl (103 mg) as a yellow solid.

Melting point: 92–93 °C.

IR (ATR) *v*: 3500−2500 (max at 3404, 3252, 2928, 2855, N–H, $^{+}$N–H, C–H st), 2243 (CN st), 1580, 1553 (Ar–C–C, Ar–C–N st) cm^{-1}.

^{1}H NMR (400 MHz, CD_3OD) *δ*: 1.36−1.54 (complex signal, 8H, 4-H_2, 5-H_2, 6-H_2 and 7-H_2), 1.59 (s, 3H, 7'-CH_3), 1.64 (tt, *J* = *J'* = 7.2 Hz, 2H, 3-H_2), 1.81 (tt, *J* = *J'* = 7.2 Hz, 2H, 8-H_2), 1.89 (broad d, *J* = 17.2 Hz, 1H, 6'-H_{endo}), superimposed in part 1.91 (dm, *J* = 12.4 Hz, 1H, 12'-H_{syn}), 2.07 (dm, *J* = 12.4 Hz, 1H, 12'-H_{anti}), 2.43 (t, *J* = 7.2 Hz, 2H, 2-H_2), 2.52 (dd, *J* = 17.2 Hz, *J'* = 4.8 Hz, 1H, 6'-H_{exo}), superimposed in part 2.75 (m, 1H, 9'-H), 2.76 (broad d, *J* = 17.6 Hz, 1H, 10'-H_{endo}), 3.16 (dd, *J* = 17.6 Hz, *J'* = 5.6 Hz, 1H, 10'-H_{exo}), 3.33 (m, 1H, 5'-H), 3.86 (tm, *J* = 7.2 Hz, 2H, 9-H_2), 4.85 (s, NH, $^{+}$NH), 5.57 (broad d, *J* = 4.8 Hz, 1H, 8'-H), 7.54 (d, *J* = 5.6 Hz, 1H, 3'-H), 7.72 (d, *J* = 5.6 Hz, 1H, 2'-H).

^{13}C NMR (100.6 MHz, CD_3OD) *δ*: 17.4 (CH_2, C2), 23.6 (CH_3, 7'-CH_3), 26.4 (CH_2, C3), 27.1 (CH, C5'), 27.7 (CH_2, C7), 27.9 (CH, C9'), 29.5 (CH_2, C12'), 29.6 (CH_2), 29.7 (CH_2), 30.1 (CH_2) (C4, C5 and C6), 30.9 (CH_2, C8), 35.5 (CH_2, C10'), 35.9 (CH_2, C6'), 46.7 (CH_2, C9), 117.3 (C, C4a'), 119.1 (C, C3a'), 121.3 (C, C1), 122.7 (CH, C3'), 123.5 (CH, C2'), 125.0 (CH, C8'), 134.5 (C, C7'), 147.0 (C, C10a'), 152.4 (C, C11a'), 153.2 (C, C4').

HRMS (ESI):

Calculated for ($C_{24}H_{31}N_3S$ + H^+):	394.2311
Found:	394.2313

Preparation of (±)-*N*-(5,6,9,10-tetrahydro-7-methyl-5,9-methanocycloocta[*b*]thieno[3,2-*e*]pyridin-4-yl)nonane-1,9-diamine, (±)-52b

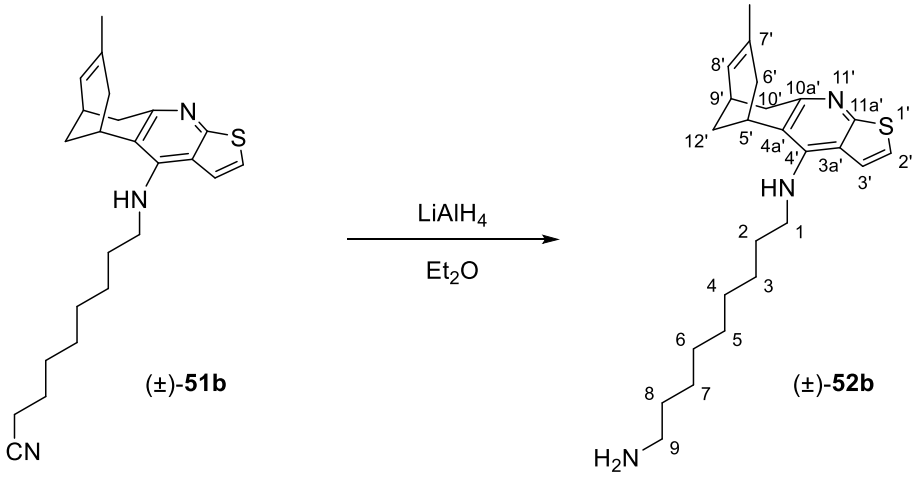

In a triple necked 50 mL round-bottomed flask equipped with an inert atmosphere and a magnetic stirrer, nitrile (±)-**51b** (585 mg, 1.49 mmol) was dissolved in anhydrous Et_2O (25 mL), cooled to 0 °C with an ice bath and treated dropwise with $LiAlH_4$ (4 M in Et_2O, 1.15 mL, 4.61 mmol). The reaction mixture was stirred at room temperature overnight, then cooled to 0 °C with an ice bath, diluted dropwise with 1 N NaOH aq. sol. (40 mL) and water (90 mL), and extracted with CH_2Cl_2 (3 × 100 mL). The combined organic layers were dried over anhydrous Na_2SO_4, filtered and evaporated under reduced pressure to give the desired primary amine (±)-**52b** (599 mg, quantitative yield) as a yellow oil.

R_f = 0.24 (silica gel, 10 cm, CH_2Cl_2 / MeOH / NH_4OH 50% 95:5:1).

Analytical sample of (±)-52b·2HCl

In a 25 mL round-bottomed flask (±)-**52b** (88 mg, 0.22 mmol) was dissolved in CH_2Cl_2 (5 mL), filtered with a PTFE filter (0.2 µm), treated with HCl / Et_2O (3 N, 0.2 mL), evaporated *in vacuo*, and washed with pentane (3 × 2 mL), providing, after drying in standard conditions, (±)-**52b**·2HCl (100 mg) as a yellow solid.

Melting point: 86–87 °C.

IR (ATR) *v*: 3500–2500 (max at 3441, 3291, 3198, 3003, 2855, N–H, $^{+}$N–H, C–H st), 1580, 1553 (Ar–C–C, Ar–C–N st) cm^{-1}.

^{1}H NMR (400 MHz, CD_3OD) δ: 1.36–1.54 (complex signal, 10H, 3-H_2, 4-H_2, 5-H_2, 6-H_2 and 7-H_2), 1.58 (s, 3H, 7'-CH_3), 1.66 (tt, $J = J' = 7.6$ Hz, 2H, 8-H_2), 1.81 (tt, $J = J' = 7.6$ Hz, 2H, 2-H_2), 1.89 (broad d, $J = 18.0$ Hz, 1H, 6'-H_{endo}), superimposed in part 1.91 (dm, $J = 12.8$ Hz, 1H, 12'-H_{syn}), 2.07 (dm, $J = 12.8$ Hz, 1H, 12'-H_{anti}), 2.52 (dd, $J = 18.0$ Hz, $J' = 4.8$ Hz, 1H, 6'-H_{exo}), superimposed in part 2.76 (m, 1H, 9'-H), 2.77 (broad d, $J = 17.6$ Hz, 1H, 10'-H_{endo}), 2.91 (t, $J = 7.6$ Hz, 2H, 9-H_2), 3.16 (dd, $J = 17.6$ Hz, $J' = 5.6$ Hz, 1H, 10'-H_{exo}), 3.34 (m, 1H, 5'-H), 3.86 (tm, $J = 7.6$ Hz, 2H, 1-H_2), 4.85 (s, NH, $^{+}$NH), 5.57 (broad d, $J = 4.8$ Hz, 1H, 8'-H), 7.54 (d, $J = 6.0$ Hz, 1H, 3'-H), 7.72 (d, $J = 6.0$ Hz, 1H, 2'-H).

^{13}C NMR (100.6 MHz, CD_3OD) δ: 23.5 (CH_3, 7'-CH_3), 27.2 (CH, C5'), 27.5 (CH_2, C3), 27.8 (CH_2, C4), 28.0 (CH, C9'), 28.6 (CH_2, C5), 29.4 (CH_2, C12'), 30.1 (CH_2), 30.3 (CH_2), 30.4 (CH_2) (C6, C7 and C8), 31.0 (CH_2, C2), 35.5 (CH_2, C10'), 35.9 (CH_2, C6'), 40.8 (CH_2, C9), 46.6 (CH_2, C1), 117.3 (C, C4a'), 119.2 (C, C3a'), 122.6 (CH, C3'), 123.5 (CH, C2'), 125.0 (CH, C8'), 134.6 (C, C7'), 147.1 (C, C10a'), 152.5 (C, C11a'), 153.3 (C, C4').

HRMS (ESI):

Calculated for ($C_{24}H_{35}N_3S + H^+$):	398.2624
Found:	398.2629

Preparation of (±)-9,10-dihydro-4,5-dihydroxy-9,10-dioxo-*N*-{9-[(5,6,9,10-tetrahydro-7-methyl-5,9-methanocycloocta[*b*]thieno[3,2-*e*]pyridin-4-yl)amino]nonyl}anthracene-2-carboxamide, (±)-40b

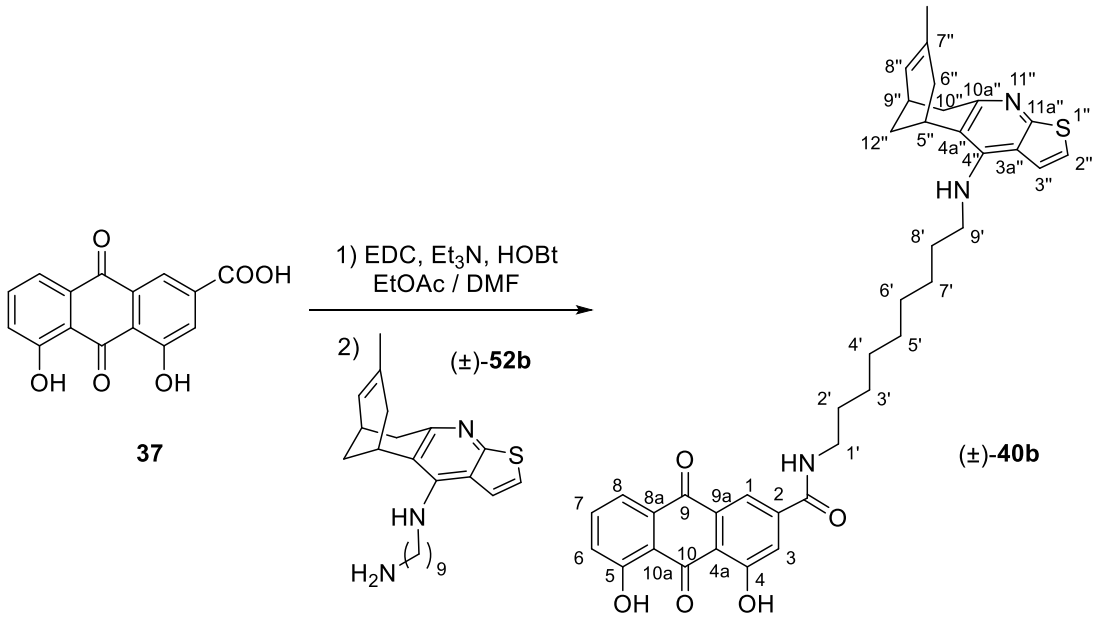

In a 50 mL round-bottomed flask equipped with a magnetic stirrer, rhein acid **37** (387 mg, 1.36 mmol) was suspended in a mixture of EtOAc (17 mL) and DMF (1.7 mL), and treated with *N*-(3-dimethylaminopropyl)-*N'*-ethylcarbodiimide hydrochloride (356 mg, 1.86 mmol), triethylamine (0.43 mL, 313 mg, 3.10 mmol), and 1-hydroxy-1*H*-benzotriazole (253 mg, 1.86 mmol). The resulting mixture was stirred at room temperature for 1 hour and treated with a suspension of the amine (±)-**52b** (493 mg, 1.24 mmol) in a mixture of EtOAc (20 mL) and DMF (2 mL). The reaction mixture was stirred at room temperature for 1 day and concentrated under reduced pressure to give a dark brown oily residue (1.53 g), which was subjected to column chromatography purification [silica gel 35−70 μm (45 g); Ø = 2.7 cm; #1–8, 500 mL, CH_2Cl_2 / 50% aq. NH_4OH 100:0.4; #9–15, 500 mL, CH_2Cl_2 / MeOH / 50% aq. NH_4OH 99.8:0.2:0.4; #16–36, 1.9 L, CH_2Cl_2 / MeOH / 50% aq. NH_4OH 99.5:0.5:0.4], to afford the desired amide (±)-**40b** (#19–24, 581 mg, 71% yield) as an orange solid.

R_f = 0.39 (silica gel, 10 cm, hexane / EtOAc / Et_3N 50:50:0.5).

Analytical sample of (±)-40b·HCl

In a 100 mL round-bottomed flask (±)-**40b** (581 mg, 0.88 mmol) was dissolved in CH_2Cl_2 (5 mL), filtered with a PTFE filter (0.2 µm), treated with HCl / Et_2O (3 N, 0.9 mL), concentrated *in vacuo*, and washed with pentane (3 × 2 mL), to give, after drying in standard conditions, (±)-**40b**·HCl (562 mg) as an orange solid.

Melting point: 174–175 °C.

IR (ATR) *v*: 3500–2500 (max at 3225, 3094, 2926, 2853, O–H, N–H, $^+$N–H, C–H st), 1674, 1628, 1609, 1553 (C=O, Ar–C–C, Ar–C–N st) cm^{-1}.

^{1}H NMR (400 MHz, CD_3OD) δ: 1.37–1.50 (complex signal, 10H, 3'-H_2, 4'-H_2, 5'-H_2, 6'-H_2 and 7'-H_2), 1.57 (s, 3H, 7"-CH_3), 1.66 (tt, $J = J' = 6.8$ Hz, 2H, 2'-H_2), 1.76 (tt, $J = J' = 7.2$ Hz, 2H, 8'-H_2), 1.86 (broad d, $J = 17.2$ Hz, 1H, 6"-H_{endo}), superimposed in part 1.87 (dm, $J = 11.6$ Hz, 1H, 12"-H_{syn}), 2.03 (dm, $J = 11.6$ Hz, 1H, 12"-H_{anti}), 2.49 (dm, $J = 17.2$ Hz, 1H, 6"-H_{exo}), superimposed in part 2.71 (broad d, $J = 17.6$ Hz, 1H, 10"-H_{endo}), 2.73 (m, 1H, 9"-H), 3.08 (dd, $J = 17.6$ Hz, $J' = 5.6$ Hz, 1H, 10"-H_{exo}), 3.26 (m, 1H, 5"-H), 3.41 (t, $J = 6.8$ Hz, 2H, 1'-H_2), 3.72 (tm, $J = 7.2$ Hz, 2H, 9'-H_2), 4.85 (s, OH, NH, $^+$NH), 5.54 (broad d, $J = 4.8$ Hz, 1H, 8"-H), 7.25 (d, $J = 8.0$ Hz, 1H, 6-H), 7.40 (d, $J = 6.0$ Hz, 1H, 3"-H), 7.52 (d, $J = 6.0$ Hz, 1H, 2"-H), 7.59 (broad s, 1H, 3-H), superimposed in part 7.60 (d, $J = 8.0$ Hz, 1H, 8-H), 7.68 (dd, $J = J' = 8.0$ Hz, 1H, 7-H), 7.99 (broad s, 1-H).

^{13}C NMR (100.6 MHz, CD_3OD) δ: 23.5 (CH_3, 7"-CH_3), 27.1 (CH, C5"), 27.7 (CH + CH_2), 28.0 (CH_2) (C9", C6' and C7'), 29.3 (CH_2, C12"), 29.9 (CH_2), 30.0 (CH_2), 30.1 (CH_2), 30.3 (CH_2) (C2', C3', C4' and C5'), 30.9 (CH_2, C8'), 35.4 (CH_2, C10"), 35.8 (CH_2, C6"), 41.1 (CH_2, C1'), 46.7 (CH_2, C9'), 116.8 (C, C10a), 117.2 (C, C4a"), 118.3 (C, C4a), 118.9 (CH, C1), 119.0 (C, C3a"), 120.9 (CH, C8), 122.5 (CH, C3"), 123.3 (CH, C2"), 123.7 (CH, C3), 125.0 (CH, C8"), 125.8 (CH, C6), 134.5 (C, C8a), 134.6 (C, C7"), 135.0 (C, C9a), 138.7 (CH, C7), 143.6 (C, C2), 147.0 (C, C10a"), 152.4 (C, C11a"), 153.2 (C, C4"), 163.3 (C, C4), 163.5 (C, C5), 167.1 (C, CONH), 181.8 (C, C9), 193.4 (C, C10).

HRMS (ESI):

Calculated for ($C_{39}H_{41}N_3O_5S + H^+$): 664.2840

Found: 664.2838

HPLC purity: 98.5%.

Preparation of (±)-5-amine-6,7,10,11-tetrahydro-8-methyl-6,10-methanocycloocta[*b*][1,8]naphthyridine, (±)-39c

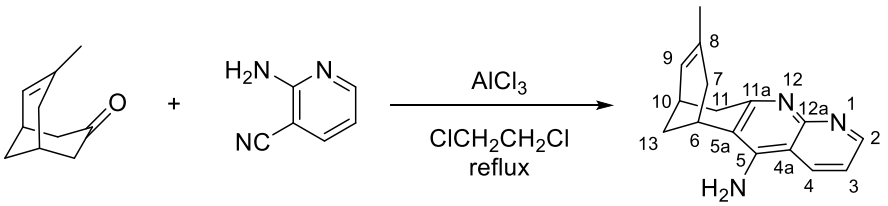

(±)-**48** **49c** (±)-**39c**

In a triple necked 250 mL round-bottomed flask equipped with an inert atmosphere, a magnetic stirrer, a pressure-equalizing dropping funnel and a condenser, a suspension of 2-amino-3-pyridinecarbonitrile, **49c** (1.05 g, 8.84 mmol), and $AlCl_3$ (1.18 g, 8.84 mmol) in anhydrous 1,2-dichloroethane (13.6 mL) was prepared, then treated with a solution of enone (±)-**48** (885 mg, 5.89 mmol) in anhydrous 1,2-dichloroethane (53 mL). The reaction mixture was stirred under reflux overnight, then allowed to cool to room temperature, diluted with water (30 mL) and THF (30 mL), alkalinized with 5 N NaOH aq. sol. (11 mL), again stirred for 30 minutes at room temperature, and extracted with CH_2Cl_2 (6 × 45 mL). The combined organic layers were dried over anhydrous Na_2SO_4, filtered and evaporated under reduced pressure to provide a brown solid (1.76 g), which was subjected to column chromatography purification [silica gel 35−70 µm (40 g); Ø = 3 cm; #1–2, 500 mL, CH_2Cl_2 / 50% aq. NH_4OH 100:0.4; #3, 500 mL, CH_2Cl_2 / MeOH / 50% aq. NH_4OH 99.5:0.5:0.4; #4–27, 2.5 L, CH_2Cl_2 / MeOH / 50% aq. NH_4OH 99:1:0.4], to afford the desired modified huprine (±)-**39c** (#5–23, 1.04 g, 70% yield) as a pale yellow solid.

R_f = 0.51 (silica gel, 10 cm, CH_2Cl_2 / MeOH / 50% aq. NH_4OH 95:5:1).

Analytical sample of (±)-39c·HCl

In a 25 mL round-bottomed flask, (±)-**39c** (47 mg, 0.19 mmol) was dissolved in a mixture CH_2Cl_2 / MeOH 9:1 (3 mL), filtered with a PTFE filter (0.2 µm), treated with HCl / Et_2O (3 N, 0.18 mL), evaporated *in vacuo*, and washed with pentane (3 × 2 mL), to provide, after drying in standard conditions, (±)-**39c**·HCl (55 mg) as a yellow solid.

Melting point: 240–244 °C.

Calculated logP: 3.95

IR (ATR) *v*: 3500–2500 (max at 3049, 2908, 2454, N–H, $^{+}$N–H, C–H st), 1669, 1635, 1624, 1604, 1586, 1535 (Ar–C–C, Ar–C–N st) cm^{-1}.

^{1}H NMR (400 MHz, CD_3OD) *δ*: 1.59 (s, 3H, 8-CH_3), superimposed in part 1.97 (dm, *J* = 12.4 Hz, 1H, 13-H_{syn}), 1.99 (d, *J* = 18.0 Hz, 1H, 7-H_{endo}), 2.08 (dm, *J* = 12.4 Hz, 1H, 13-H_{anti}), 2.52 (dd, *J* = 18.0 Hz, *J′* = 4.8 Hz, 1H, 7-H_{exo}), 2.79 (m, 1H, 10-H), 2.92 (ddd, *J* = 18.0 Hz, *J′* = 2.0 Hz, *J′′* = 1.2 Hz, 1H, 11-H_{endo}), 3.21 (dd, *J* = 18.0 Hz, *J′* = 5.6 Hz, 1H, 11-H_{exo}), 3.39 (m, 1H, 6-H), 4.91 (s, NH, $^{+}$NH), 5.59 (broad d, *J* = 4.8 Hz, 1H, 9-H), 7.64 (dd, *J* = 8.8 Hz, *J′* = 4.4 Hz, 1H, 3-H), 8.85 (dd, *J* = 8.8 Hz, *J′* = 1.6 Hz, 1H, 4-H), 8.95 (dd, *J* = 4.4 Hz, *J′* = 1.6 Hz, 1H, 2-H).

^{13}C NMR (100.6 MHz, CD_3OD) *δ*: 23.4 (CH_3, 8-CH_3), 27.6 (CH, C6), 28.1 (CH, C10), 29.1 (CH_2, C13), 35.8 (CH_2), 35.9 (CH_2) (C7 and C11), 111.9 (C, C4a), 115.8 (C, C5a), 123.0 (CH, C3), 125.1 (CH, C9), 134.3 (CH, C4), 134.9 (C, C8), 148.6 (C, C11a), 154.5 (C, C12a), 156.6 (CH, C2), 157.8 (C, C5).

HPLC purity: 100%.

Preparation of (±)-9-[(6,7,10,11-tetrahydro-8-methyl-6,10-methanocycloocta[*b*][1,8]naphthyridin-5-yl)amino]nonanenitrile, (±)-51c

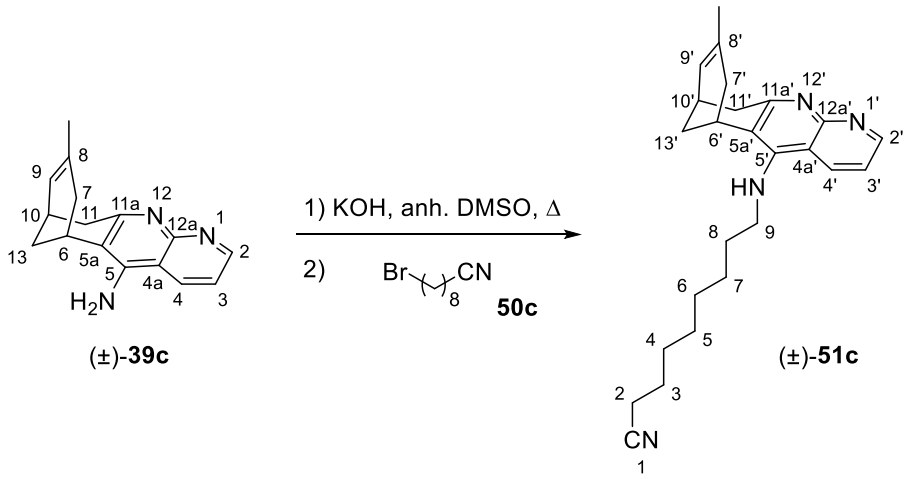

In a double necked 50 mL round-bottomed flask provided with an inert atmosphere, a magnetic stirrer and 4 Å molecular sieves, modified huprine (±)-**39c** (992 mg, 3.94 mmol) and finely powdered KOH (85% purity, 860 mg, 13.0 mmol) were suspended in anhydrous DMSO (16.8 mL). The resulting suspension was stirred, heating every 10 minutes with a heat gun for 1 hour, and at room temperature one more hour, then treated with 9-bromononanenitrile, **50c** (947 mg, 4.34 mmol). The reaction mixture was stirred at room temperature overnight, then diluted with 2 N NaOH aq. sol. (120 mL), and extracted with CH_2Cl_2 (3 × 100 mL). The combined organic layers were washed with water (5 × 100 mL), dried with anhydrous Na_2SO_4, filtered and evaporated under reduced pressure to afford a reddish oil (1.49 g), which was subjected to column chromatography purification [silica gel 35−70 µm (75 g); Ø = 3.5 cm; #1, 500 mL, CH_2Cl_2 / 50% aq. NH_4OH 100:0.4; #2, 500 mL, CH_2Cl_2 / MeOH / 50% aq. NH_4OH 99.8:0.2:0.4; #3–4, 500 mL, CH_2Cl_2 / MeOH / 50% aq. NH_4OH 99.6:0.4:0.4; #5–29, 3 L, CH_2Cl_2 / MeOH / 50% aq. NH_4OH 99.4:0.6:0.4; #30–34, 800 mL, CH_2Cl_2 / MeOH / 50% aq. NH_4OH 99:1:0.4; #35–38, 500 mL, CH_2Cl_2 / MeOH / 50% aq. NH_4OH 98:2:0.4; #39–43, 500 mL, CH_2Cl_2 / MeOH / 50% aq. NH_4OH 97:3:0.4; #43–48, 500 mL, CH_2Cl_2 / MeOH / 50% aq. NH_4OH 95:5:0.4], to afford the desired nitrile (±)-**51c** (#11–32, 618 mg, 40% yield) as a strong reddish oil.

R_f = 0.84 (gel de sílice, 10 cm, CH_2Cl_2 / MeOH / NH_4OH 50% 95:5:1).

Analytical sample of (±)-51c·HCl

In a 10 mL round-bottomed flask (±)-**51c** (25 mg, 0.06 mmol) was dissolved in CH_2Cl_2 (1 mL), treated with HCl / Et_2O (3 N, 0.06 mL), evaporated *in vacuo*, and washed with pentane (3 × 2 mL), providing, after drying in standard conditions, (±)-**51c** ·HCl (27 mg) as an orange solid.

Melting point: 110–113 °C.

IR (ATR) *v*: 3500–2500 (max at 3204, 2925, 2852, N–H, $^+$N–H, C–H st), 2245 (CN st), 1612, 1589, 1519 (Ar–C–C, Ar–C–N st) cm^{-1}.

^{1}H NMR (400 MHz, CD_3OD) *δ*: 1.36–1.52 (complex signal, 8H, 4-H_2, 5-H_2, 6-H_2 and 7-H_2), 1.59 (s, 3H, 8'-CH_3), 1.63 (tt, *J* = *J'* = 7.2 Hz, 2H, 3-H_2), superimposed in part 1.89 (tt, *J* = *J'* = 7.2 Hz, 2H, 8-H_2), 1.95 (broad d, *J* = 17.6 Hz, 1H, 7'-H_{endo}), superimposed in part 1.96 (dm, *J* = 12.8 Hz, 1H, 13'-H_{syn}), 2.09 (dm, *J* = 12.8 Hz, 1H, 13'-H_{anti}), 2.43 (t, *J* = 7.2 Hz, 2H, 2-H_2), 2.54 (dd, *J* = 17.6 Hz, *J'* = 4.4 Hz, 1H, 7'-H_{exo}), 2.78 (m, 1H, 10'-H), 2.91 (broad d, *J* = 18.0 Hz, 1H, 11'-H_{endo}), 3.21 (dd, *J* = 18.0 Hz, *J'* = 5.6 Hz, 1H, 11'-H_{exo}), 3.45 (m, 1H, 6'-H), 4.01 (t, *J* = 7.2 Hz, 2H, 9-H_2), 4.85 (s, NH, $^+$NH), 5.59 (broad d, *J* = 4.8 Hz, 1H, 9'-H), 7.60 (dd, *J* = 8.4 Hz, *J'* = 4.4 Hz, 1H, 3'-H), 8.86 (broad d, *J* = 8.4 Hz, 1H, 4'-H), 8.91 (dd, *J* = 4.4 Hz, *J'* = 1.2 Hz, 1H, 2'-H).

^{13}C NMR (100.6 MHz, CD_3OD) *δ*: 17.3 (CH_2, C2), 23.4 (CH_3, 8'-CH_3), 26.4 (CH_2, C3), 27.3 (CH, C6'), 27.7 (CH_2, C7), 27.8 (CH, C10'), 29.2 (CH_2, C13'), 29.6 (CH_2), 29.7 (CH_2), 30.0 (CH_2) (C4, C5 and C6), 30.9 (CH_2, C8), 35.9 (CH_2), 36.0 (CH_2) (C7' and C11'), 49.6 (CH_2, C9), 112.0 (C, C4a'), 117.6 (C, C5a'), 121.2 (C, C1), 121.9 (CH, C3'), 125.1 (CH, C9'), 134.6 (C, C8'), 137.4 (CH, C4'), 149.7 (C, C11a'), 152.3 (C, C12a'), 156.2 (CH, C2'), 157.4 (C, C5').

HRMS (ESI):

Calculated for ($C_{25}H_{32}N_4$ + H^+):	389.2700
Found:	389.2692

Preparation of (±)-*N*-(6,7,10,11-tetrahydro-8-methyl-6,10-methanocycloocta[*b*][1,8]naphthyridin-5-yl)-1,9-diaminononane, (±)-52c

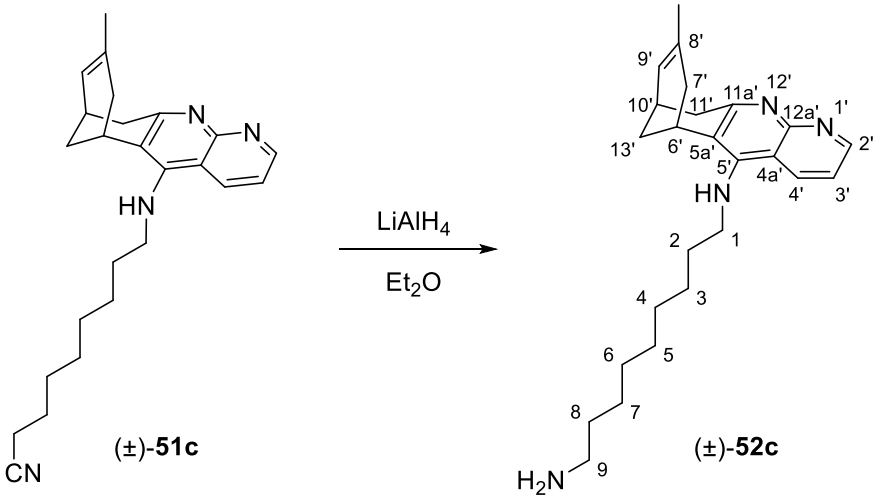

In a triple necked 50 mL round-bottomed flask equipped with an inert atmosphere and a magnetic stirrer, nitrile (±)-**51c** (608 mg, 1.57 mmol) was suspended in anhydrous Et_2O (26.6 mL), cooled to 0 °C with an ice bath and treated dropwise with $LiAlH_4$ (4 M in Et_2O, 1.21 mL, 4.85 mmol). The reaction mixture was stirred at room temperature overnight, then cooled to 0 °C with an ice bath, diluted dropwise with 1 N NaOH aq. sol. (40 mL) and water (95 mL), and extracted with CH_2Cl_2 (3 × 100 mL). The combined organic layers were with anhydrous Na_2SO_4, filtered and evaporated under reduced pressure to give a brown solid (584 mg), which was subjected to column chromatography purification [silica gel 35−70 μm (50 g); Ø = 3 cm; #1, 250 mL, CH_2Cl_2 / 50% aq. NH_4OH 100:0.4; #2, 250 mL, CH_2Cl_2 / MeOH / 50% aq. NH_4OH 99.8:0.2:0.4; #3, 250 mL, CH_2Cl_2 / MeOH / 50% aq. NH_4OH 99.6:0.4:0.4; #4, 500 mL, CH_2Cl_2 / MeOH / 50% aq. NH_4OH 99.4:0.6:0.4; #5, 500 mL, CH_2Cl_2 / MeOH / 50% aq. NH_4OH 99.2:0.8:0.4; #6–41, 3.5 L, CH_2Cl_2 / MeOH / 50% aq. NH_4OH 99:1:0.4; #42–66, 2.5 L, CH_2Cl_2 / MeOH / 50% aq. NH_4OH 98.5:1.5:0.4; #67–96, 2.5 L, CH_2Cl_2 / MeOH / 50% aq. NH_4OH 98:2:0.4; #97–98, 500 mL, CH_2Cl_2 / MeOH / 50% aq. NH_4OH 95:5:0.4], to afford the desired primary amine (±)-**52c** (#74–95, 189 mg, 31% yield) as a clear beige sticky solid.

R_f = 0.24 (gel de sílice, 10 cm, CH_2Cl_2 / MeOH / NH_4OH 50% 95:5:1).

Analytical sample of (±)-52c·HCl

In a 25 mL round-bottomed flask (±)-**52c** (19 mg, 0.05 mmol) was dissolved in CH_2Cl_2 (2 mL), filtered with a PTFE filter (0.2 µm), treated with HCl / Et_2O (3 N, 0.15 mL), evaporated *in vacuo*, and washed with pentane (3 × 2 mL), providing, after drying in standard conditions, (±)-**52c**·HCl (27 mg) as an orange solid.

Melting point: 173–176 °C.

IR (ATR) *v*: 3500–2500 (max at 3367, 3224, 2919, 2852, N–H, $^+$N–H, C–H st), 1609, 1589, 1519 (Ar–C–C, Ar–C–N st) cm^{-1}.

^{1}H NMR (400 MHz, CD_3OD) δ: 1.34–1.50 (complex signal, 10H, 3-H_2, 4-H_2, 5-H_2, 6-H_2 and 7-H_2), 1.59 (s, 3H, 8'-CH_3), 1.66 (m, 2H, 8-H_2), 1.88 (m, 2H, 2-H_2), 1.94 (broad d, *J* = 18.0 Hz, 1H, 7'-H_{endo}), superimposed in part 1.95 (dm, *J* = 12.4 Hz, 1H, 13'-H_{syn}), 2.09 (dm, *J* = 12.4 Hz, 1H, 13'-H_{anti}), 2.55 (dm, *J* = 18.0 Hz, 1H, 7'-H_{exo}), 2.77 (m, 1H, 10'-H), 2.84–2.94 (complex signal, 3H, 9-H_2 and 11'-H_{endo}), 3.20 (dd, *J* = 17.6 Hz, *J'* = 5.6 Hz, 1H, 11'-H_{exo}), 3.45 (m, 1H, 6'-H), 4.00 (m, 2H, 1-H_2), 4.86 (s, NH, $^+$NH), 5.59 (broad d, *J* = 4.4 Hz, 1H, 9'-H), 7.60 (m, 1H, 3'-H), 8.85 (broad d, *J* = 8.4 Hz, 1H, 4'-H), 8.91 (d, *J* = 2.0 Hz, 1H, 2'-H).

^{13}C NMR (100.6 MHz, CD_3OD) δ: 23.5 (CH_3, 8'-CH_3), 27.4 (CH, C6'), 27.5 (CH_2, C3), 27.8 (CH, C10'), 28.0 (CH_2, C4), 28.6 (CH_2, C5), 29.3 (CH_2, C13'), 30.2 (CH_2), 30.3 (CH_2), 30.5 (CH_2) (C6, C7 and C8), 31.2 (CH_2, C2), 36.0 (CH_2), 36.1 (CH_2) (C7' and C11'), 40.9 (CH_2, C9), 49.3 (CH_2, C1), 112.0 (C, C4a'), 117.6 (C, C5a'), 122.0 (CH, C3'), 125.2 (CH, C9'), 134.6 (C, C8'), 137.6 (CH, C4'), 149.7 (C, C11a'), 152.2 (C, C12a'), 156.2 (CH, C2'), 157.4 (C, C5').

HRMS (ESI):

Calculated for ($C_{25}H_{36}N_4$ + H^+):	393.3013
Found:	393.3022

Preparation of (±)-*N*-{9-[(6,7,10,11-tetrahydro-8-methyl-6,10-methanocycloocta[*b*][1,8]naphthyridin-5-yl)amino]nonyl}-9,10-dihydro-4,5-dihydroxy-9,10-dioxoanthracene-2-carboxamide, (±)-40c

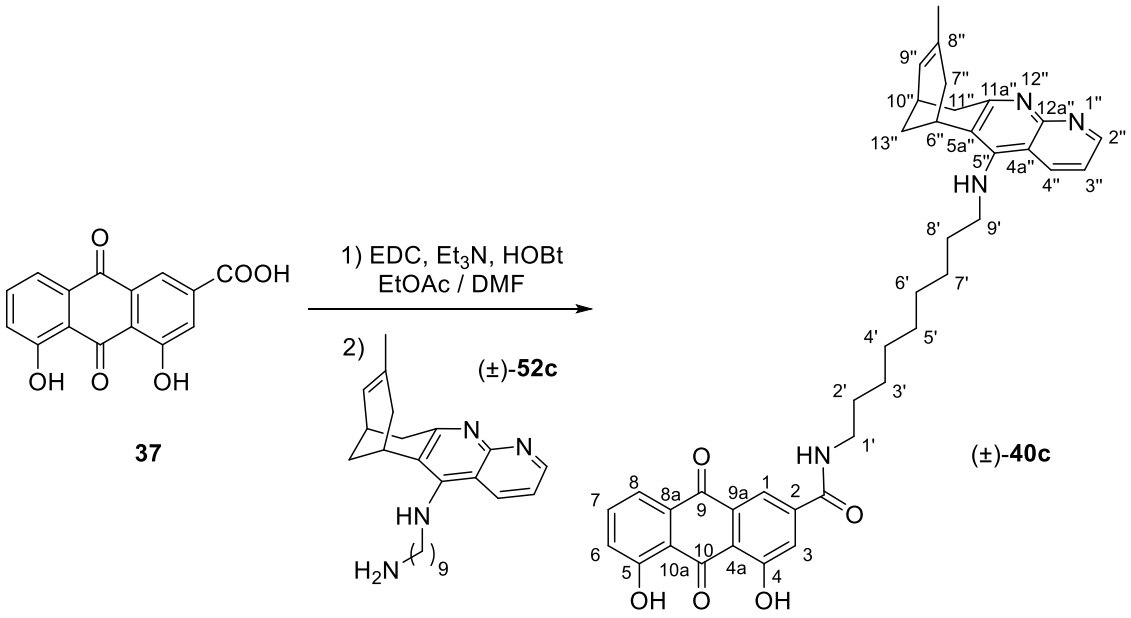

In a 25 mL round-bottomed flask equipped with a magnetic stirrer, rhein acid **37** (80 mg, 0.28 mmol) was suspended in a mixture of EtOAc (2.3 mL) and DMF (0.3 mL), and treated with *N*-(3-dimethylaminopropyl)-*N'*-ethylcarbodiimide hydrochloride (60 mg, 0.31 mmol), triethylamine (0.09 mL, 65 mg, 0.64 mmol), and 1-hydroxy-1*H*-benzotriazole (52 mg, 0.39 mmol). The resulting mixture was stirred at room temperature for 1 hour and treated with a suspension of the amine (±)-**52c** (101 mg, 0.26 mmol) in a mixture of EtOAc (5 mL) and DMF (2.5 mL). The reaction mixture was stirred at room temperature for 1 day and concentrated under reduced pressure to give a dark brown oil (447 mg), which was subjected to column chromatography purification [silica gel 35−70 μm (26 g); Ø = 2.5 cm; #1–2, 200 mL, CH_2Cl_2 / 50% aq. NH_4OH 100:0.4; #3–11, 1 L, CH_2Cl_2 / MeOH / 50% aq. NH_4OH 99.5:0.5:0.4; #12–45, 3.5 L, CH_2Cl_2 / MeOH / 50% aq. NH_4OH 99:1:0.4; #46–50, 500 mL, CH_2Cl_2 / MeOH / 50% aq. NH_4OH 95:5:0.4], to afford the desired amide (±)-**40c** (#24–45, 152 mg, 90% yield) as a dark reddish solid.

R_f = 0.75 (gel de sílice, 10 cm, CH_2Cl_2 / MeOH / NH_4OH 50% 95:5:1).

Analytical sample of (±)-40c·HCl

In a 25 mL round-bottomed flask (±)-**40c** (88 mg, 0.13 mmol) was dissolved in CH_2Cl_2 (3 mL), filtered with a PTFE filter (0.2 µm), treated with HCl / Et_2O (3 N, 0.13 mL), concentrated *in vacuo*, and washed with pentane (3 × 2 mL), to give, after drying in standard conditions, (±)-**40c**·HCl (89 mg) as an orange solid.

Melting point: 173–176 °C.

IR (ATR) *v*: 3500−2500 (max at 3214, 2919, 2852, O–H, N–H, $^+$N–H, C–H st), 1622, 1589 (C=O, Ar–C–C, Ar–C–N st) cm^{-1}.

^{1}H NMR (400 MHz, CD_3OD) *δ*: 1.38−1.50 (complex signal, 10H, 3'-H_2, 4'-H_2, 5'-H_2, 6'-H_2 and 7'-H_2), 1.59 (s, 3H, 8''-CH_3), 1.65 (m, 2H, 2'-H_2), 1.82−1.96 (complex signal, 3H, 8'-H_2, 13''-H_{syn}), 1.94 (broad d, *J* = 16.8 Hz, 1H, 7''-H_{endo}), 2.08 (dm, *J* = 12.4 Hz, 1H, 13''-H_{anti}), 2.53 (dm, *J* = 16.8 Hz, 1H, 7''-H_{exo}), 2.76 (m, 1H, 10''-H), 2.87 (broad d, *J* = 18.0 Hz, 1H, 11''-H_{endo}), 3.16 (dd, *J* = 18.0 Hz, *J'* = 5.6 Hz, 1H, 11''-H_{exo}), superimposed in part 3.38 (m, 1H, 6''-H), 3.41 (t, *J* = 6.8 Hz, 2H, 1'-H_2), 3.93 (broad t, *J* = 6.0 Hz, 2H, 9'-H_2), 4.85 (s, OH, NH, $^+$NH), 5.59 (broad d, *J* = 5.2 Hz, 1H, 9''-H), 7.37 (dd, *J* = 7.6 Hz, *J'* = 2.4 Hz, 1H, 6-H), 7.51 (dd, *J* = 8.8 Hz, *J'* = 4.0 Hz, 1H, 3''-H), 7.69 (d, *J* = 1.6 Hz, 1H, 3-H), 7.74−7.81 (complex signal, 2H, 7-H and 8-H), 8.14 (d, *J* = 1.6 Hz, 1H, 1-H), 8.74 (dd, *J* = 8.8 Hz, *J'* = 1.6 Hz, 1H, 4"-H), 8.84 (dd, *J* = 4.0 Hz, *J'* = 1.6 Hz, 1H, 2"-H).

^{13}C NMR (100.6 MHz, CD_3OD) *δ*: 23.5 (CH_3, 8"-CH_3), 27.2 (CH, C6"), 27.7 (CH, C10"), 27.78 (CH_2), 27.84 (CH_2) (C6', C7'), 29.2 (CH_2, C13"), 30.0 (CH_2), 30.1 (CH_2), 30.2 (CH_2), 30.4 (CH_2) (C2', C3', C4' and C5'), 31.0 (CH_2, C8'), 35.9 ($2CH_2$, C7" and C11"), 41.5 (CH_2, C1'), 49.3 (CH_2, C9'), 111.7 (C, C4a"), 116.6 (C, C10a), 117.5 (C, C5a"), 118.1 (C, C4a), 118.9 (CH, C1), 120.8 (CH, C8), 121.8 (CH, C3"), 123.7 (CH, C3), 125.1 (CH, C9"), 125.8 (CH, C6), 134.3 (C, C8"), 134.6 (C, C8a), 134.7 (C, C9a), 137.2 (CH, C4"), 138.7 (CH, C7), 143.5 (C, C2), 149.4 (C, C11a"), 152.1 (C, C12a"), 156.0 (CH, C2"), 157.1 (C, C5"), 163.2 (C, C4), 163.5 (C, C5), 166.9 (C, CONH), 181.6 (C, C9), 193.2 (C, C10).

HRMS (ESI):

Calculated for ($C_{40}H_{42}N_4O_5$ + H^+):	659.3228
Found:	659.3230

HPLC purity: 99.8%.

Preparation of (±)-6,7,10,11-tetrahydro-2-methoxy-9-methyl-7,11-methanocycloocta[*b*]quinolin-12-amine, (±)-39d

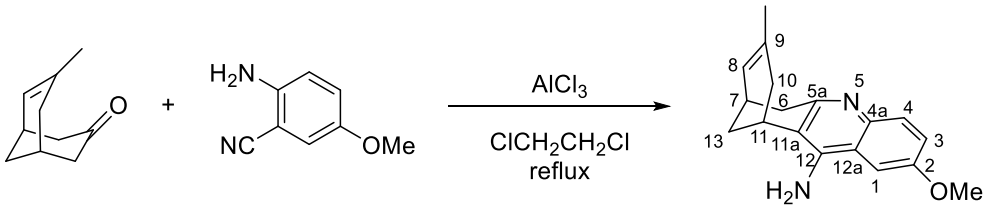

(±)-**48** **49d** (±)-**39d**

In a triple necked 50 mL round-bottomed flask equipped with an inert atmosphere, a magnetic stirrer and a pressure-equalizing dropping funnel, a suspension of 2-amino-5-methoxybenzonitrile, **49d** (223 mg, 1.51 mmol), and $AlCl_3$ (250 mg, 1.87 mmol) in anhydrous 1,2-dichloroethane (10 mL) was prepared, then treated with a solution of enone (±)-**48** (188 mg, 1.25 mmol) in anhydrous 1,2-dichloroethane (55 mL). The reaction mixture was stirred under reflux for 3 days, then allowed to cool to room temperature, diluted with water (8 mL) and THF (8 mL), alkalinized with 5 N NaOH aq. sol. (4 mL), again stirred for 30 minutes at room temperature, and extracted with CH_2Cl_2 (6 × 10 mL). The combined organic layers were dried over anhydrous Na_2SO_4, filtered and evaporated under reduced pressure to afford a yellow solid residue (300 mg), which was subjected to column chromatography purification [silica gel 35−70 µm (21 g); Ø = 2.5 cm; #1–19, 200 mL, CH_2Cl_2 / 50% aq. NH_4OH 100:0.4; #20–39, 200 mL, CH_2Cl_2 / MeOH / 50% aq. NH_4OH 99.8:0.2:0.4; #40–59, 200 mL, CH_2Cl_2 / MeOH / 50% aq. NH_4OH 99.6:0.4:0.4; #60–79, 200 mL, CH_2Cl_2 / MeOH / 50% aq. NH_4OH 99.4:0.6:0.4; #80–99, 200 mL, CH_2Cl_2 / MeOH / 50% aq. NH_4OH 99.2:0.8:0.4; #100–148, 500 mL, CH_2Cl_2 / MeOH / 50% aq. NH_4OH 99:1:0.4], to afford the desired modified huprine (±)-**39d** (#61–135, 150 mg, 43% yield) as a yellow solid.

R_f = 0.38 (silica gel, 10 cm, CH_2Cl_2 / MeOH / 50% aq. NH_4OH 90:10:1).

Analytical sample of (±)-**39d·HCl**

In a 25 mL round-bottomed flask, (±)-**39d** (100 mg, 0.36 mmol) was dissolved in CH_2Cl_2 (2 mL), treated with HCl / Et_2O (3 N, 0.36 mL), concentrated *in vacuo*, and washed with pentane (3 × 2 mL), to provide, after drying in standard conditions, (±)-**39d**·HCl (118 mg) as a yellow solid.

Melting point: 285–286 °C.

IR (ATR) *v*: 3500–2500 (max at 3325, 3177, 2963, 2893, 2835, N–H, $^+$N–H, C–H st), 1659, 1589 (Ar–C–C, Ar–C–N st) cm^{-1}.

^{1}H NMR (400 MHz, CD_3OD) *δ*: 1.58 (s, 3H, 9-CH_3), superimposed in part 1.95 (dm, *J* = 12.4 Hz, 1H, 13-H_{syn}), 1.99 (broad d, *J* = 17.6 Hz, 1H, 10-H_{endo}), 2.07 (dm, *J* = 12.4 Hz, 1H, 13-H_{anti}), 2.51 (dd, *J* = 17.6 Hz, *J'* = 4.0 Hz, 1H, 10-H_{exo}), 2.77 (m, 1H, 7-H), 2.87 (broad d, *J* = 17.6 Hz, 1H, 6-H_{endo}), 3.18 (dd, *J* = 17.6 Hz, *J'* = 5.6 Hz, 1H, 6-H_{exo}), 3.40 (m, 1H, 11-H), 3.97 (s, 3H, 2-OCH_3), 4.87 (s, NH, $^+$NH), 5.57 (broad d, *J* = 4.8 Hz, 1H, 8-H), 7.47 (dd, *J* = 9.2 Hz, *J'* = 2.4 Hz, 1H, 3-H), 7.67 (d, *J* = 9.2 Hz, 1H, 4-H), 7.70 (d, *J* = 2.4 Hz, 1H, 1-H).

^{13}C NMR (100.6 MHz, CD_3OD) *δ*: 23.5 (CH_3, 9-CH_3), 27.6 (CH, C11), 28.3 (CH, C7), 29.4 (CH_2, C13), 35.7 (CH_2), 36.0 (CH_2) (C6 and C10), 56.7 (CH_3, 2-OCH_3), 102.8 (CH, C1), 114.7 (C, C12a), 117.9 (C, C11a), 121.7 (CH), 126.1 (CH) (C3 and C4), 125.0 (CH, C8), 134.2 (C), 134.9 (C) (C4a, C9), 150.4 (C, C5a), 155.4 (C, C12), 159.3 (C, C2).

HRMS (ESI):

Calculated for ($C_{18}H_{20}N_2O$ + H^+):	281.1648
Found:	281.1650

HPLC purity: 98.0%.

Preparation of (±)-9-[(6,7,10,11-tetrahydro-2-methoxy-9-methyl-7,11-methanocycloocta[*b*]quinolin-12-yl)amino]nonanenitrile, (±)-51d

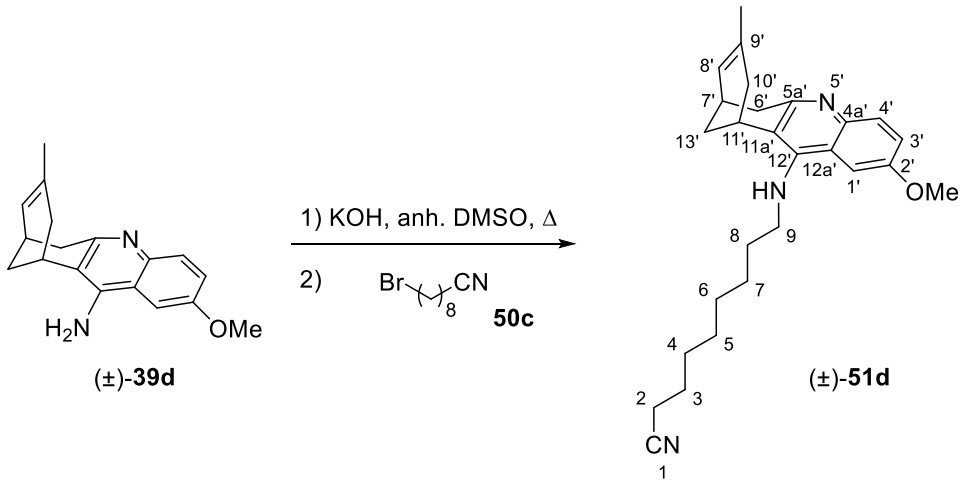

In a triple necked 25 mL round-bottomed flask equipped with an inert atmosphere, a magnetic stirrer and 4 Å molecular sieves, modified huprine (±)-**39d** (260 mg, 0.93 mmol) and finely powdered KOH (85% purity, 202 mg, 3.06 mmol) were suspended in anhydrous DMSO (4 mL). The resulting suspension was stirred, heating every 10 minutes with a heat gun for 1 hour, and at room temperature one more hour, then treated with 9-bromononanenitrile, **50c** (222 mg, 1.02 mmol). The reaction mixture was stirred at room temperature overnight, then diluted with 5 N NaOH aq. sol. (30 mL), and extracted with CH_2Cl_2 (4 × 25 mL). The combined organic layers were washed with water (5 × 25 mL), dried over anhydrous Na_2SO_4, filtered and evaporated under reduced pressure to afford a brown oil (450 mg), which was purified by column chromatography [silica gel 35−70 μm (31 g); Ø = 2.5 cm; #1, 200 mL, CH_2Cl_2 / 50% aq. NH_4OH 100:0.4; #2, 200 mL, CH_2Cl_2 / MeOH / 50% aq. NH_4OH 99.9:0.1:0.4; #2–78, 1.2 L, CH_2Cl_2 / MeOH / 50% aq. NH_4OH 99.8:0.2:0.4], to give the desired nitrile (±)-**51d** (#43–73, 114 mg, 29% yield) as a yellow oil.

R_f = 0.81 (silica gel, 10 cm, CH_2Cl_2 / MeOH / 50% aq. NH_4OH 90:10:1).

Analytical sample of (±)-51d·HCl

In a 10 mL round-bottomed flask (±)-**51d** (23 mg, 0.06 mmol) was dissolved in CH_2Cl_2 (2 mL), filtered with a PTFE filter (0.2 μm), treated with HCl / Et_2O (3 N, 0.06 mL), evaporated *in*

vacuo, and washed with pentane (3 × 2 mL), providing, after drying in standard conditions, (±)-**51d**·HCl (23 mg) as a yellow solid.

Melting point: 162–163 °C.

IR (ATR) *v*: 3500–2500 (max at 3474, 3412, 3258, 2930, 2859, N–H, $^{+}$N–H, C–H st), 2241 (CN st), 1622, 1582, 1524 (Ar–C–C, Ar–C–N st) cm^{-1}.

^{1}H NMR (400 MHz, CD_3OD) δ: 1.32−1.50 (complex signal, 8H, 4-H_2, 5-H_2, 6-H_2 and 7-H_2), 1.58 (s, 3H, 9'-CH_3), 1.62 (tt, $J = J' = 6.8$ Hz, 2H, 3-H_2), superimposed in part 1.88 (m, 2H, 8-H_2), 1.94 (broad d, $J = 17.6$ Hz, 1H, 10'-H_{endo}), superimposed in part 1.96 (dm, $J = 12.8$ Hz, 1H, 13'-H_{syn}), 2.09 (dm, $J = 12.8$ Hz, 1H, 13'-H_{anti}), 2.43 (m, 2H, 2-H_2), 2.56 (dm, $J = 17.6$ Hz, 1H, 10'-H_{exo}), 2.77 (m, 1H, 7'-H), 2.88 (broad d, $J = 17.6$ Hz, 1H, 6'-H_{endo}), 3.20 (dd, $J = 17.6$ Hz, $J' = 5.6$ Hz, 1H, 6'-H_{exo}), 3.48 (m, 1H, 11'-H), 3.96 (s, 3H, 2'-OCH_3), superimposed in part 3.98 (m, 2H, 9-H_2), 4.85 (s, NH, $^{+}$NH), 5.59 (broad d, $J = 4.4$ Hz, 1H, 8'-H), 7.53 (dd, $J = 9.2$ Hz, $J' = 2.4$ Hz, 1H, 3'-H), 7.66 (d, $J = 2.4$ Hz, 1H, 1'-H), 7.72 (d, $J = 9.2$ Hz, 1H, 4'-H).

^{13}C NMR (100.6 MHz, CD_3OD) δ: 17.1 (CH_2, C2), 23.3 (CH_3, 9'-CH_3), 26.2 (CH_2, C3), 27.3 (CH, C11'), 27.6 (CH_2, C7), 27.8 (CH, C7'), 29.3 (CH_2, C13'), 29.4 (CH_2), 29.6 (CH_2), 29.9 (CH_2) (C4, C5 and C6), 31.7 (CH_2, C8), 35.8 (CH_2, C6'), 36.4 (CH_2, C10'), 48.9 (CH_2, C9), 56.3 (CH_3, 2'-OCH_3), 105.9 (CH, C1'), 117.2 (C), 118.6 (C) (C11a' and C12a'), 121.1 (C, C1), 121.6 (CH), 125.4 (CH) (C3' and C4'), 125.0 (CH, C8'), 134.4 (C), 135.1 (C) (C4a' and C9'), 149.4 (C, C5a'), 156.1 (C, C12'), 158.1 (C, C2').

HRMS (ESI):

Calculated for ($C_{27}H_{35}N_3O + H^+$):	418.2853
Found:	418.2862

Preparation of (±)-*N*-(6,7,10,11-tetrahydro-2-methoxy-9-methyl-7,11-methanocycloocta[*b*]quinolin-12-yl)nonane-1,9-diamine, (±)-52d

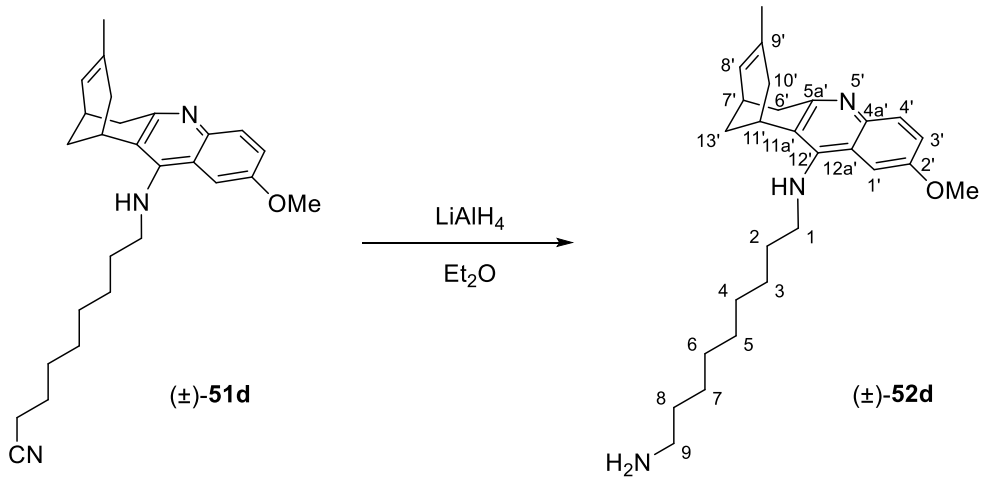

(±)-**51d** (±)-**52d**

In a double necked 10 mL round-bottomed flask equipped with an inert atmosphere and a magnetic stirrer, nitrile (±)-**51d** (60 mg, 0.14 mmol) was dissolved in anhydrous Et_2O (2.4 mL), cooled to 0 °C with an ice bath and treated dropwise with $LiAlH_4$ (4 M in Et_2O, 0.11 mL, 0.44 mmol). The reaction mixture was stirred at room temperature overnight, then cooled to 0 °C with an ice bath, diluted dropwise with 1 N NaOH aq. sol. (7 mL) and water (9 mL), and extracted with CH_2Cl_2 (3 × 15 mL). The combined organic layers were dried over anhydrous Na_2SO_4, filtered and evaporated under reduced pressure to give the desired primary amine (±)-**52d** (34 mg, 58% yield) as a yellow oil, without the need of further purification.

R_f = 0.41 (silica gel, 10 cm, CH_2Cl_2 / MeOH / NH_4OH 50% 90:10:1).

Analytical sample of (±)-52d·2HCl

In a 25 mL round-bottomed flask (±)-**52d** (34 mg, 0.08 mmol) was dissolved in CH_2Cl_2 (1 mL), filtered with a PTFE filter (0.2 µm), treated with HCl / Et_2O (3 N, 0.08 mL), evaporated *in vacuo*, and washed with pentane (3 × 2 mL), providing, after drying in standard conditions, (±)-**52d**·2HCl (37 mg) as a yellow solid.

^{1}H NMR (400 MHz, CD_3OD) δ: 1.28–1.48 (complex signal, 10H, 3-H_2, 4-H_2, 5-H_2, 6-H_2 and 7-H_2), 1.58 (s, 3H, 9'-CH_3), 1.66 (m, 2H, 8-H_2), 1.88 (m, 2H, 2-H_2), 1.93 (broad d, J = 17.6 Hz, 1H, 10'-

H_{endo}), superimposed in part 1.96 (dm, *J* = 12.8 Hz, 1H, 13'-H_{syn}), 2.09 (dm, *J* = 12.8 Hz, 1H, 13'-H_{anti}), 2.56 (dd, *J* = 17.6 Hz, *J'* = 4.0 Hz, 1H, 10'-H_{exo}), 2.77 (m, 1H, 7'-H), superimposed in part 2.89 (d, *J* = 18.0 Hz, 1H, 6'-H_{endo}), 2.91 (m, 2H, 9-H_2), 3.20 (dd, *J* = 18.0 Hz, *J'* = 5.6 Hz, 1H, 6'-H_{exo}), 3.49 (m, 1H, 11'-H), 3.96 (s, 3H, 2'-OCH_3), 3.97 (m, 2H, 1-H_2), 4.86 (s, NH, $^+$NH), 5.59 (broad d, *J* = 4.4 Hz, 1H, 8'-H), 7.53 (dd, *J* = 9.2 Hz, *J'* = 2.4 Hz, 1H, 3'-H), 7.66 (d, *J* = 2.4 Hz, 1H, 1'-H), 7.73 (d, *J* = 9.2 Hz, 1H, 4'-H).

^{13}C NMR (100.6 MHz, DMSO-d_6) δ: 23.1 (9'-CH_3), 25.4, 25.8, 26.0, 26.1, 26.9, 27.9, 28.4, 28.5, 28.7 (C3, C4, C5, C6, C7, C8, C7', C11' and C13'), 30.1 (C2), 34.5, 35.6 (C6' and C10'), 38.7 (C9), 47.0 (C1), 55.8 (2'-OCH_3), 104.7 (C1'), 115.4, 117.0 (C11a' and C12a'), 120.9, 123.9, 124.2 (C3', C4' and C8'), 132.6, 133.4 (C4a' and C9'), 148.1 (C5a'), 153.7 (C, C12'), 156.0 (C, C2').

HRMS (ESI):

Calculated for ($C_{27}H_{39}N_3O + H^+$): 422.3166

Found: 422.3181

Preparation of (±)-9,10-dihydro-4,5-dihydroxy-9,10-dioxo-*N*-{9-[(6,7,10,11-tetrahydro-2-methoxy-9-methyl-7,11-methanocycloocta[*b*]quinolin-12-yl)amino]nonyl}anthracene-2-carboxamide, (±)-40d

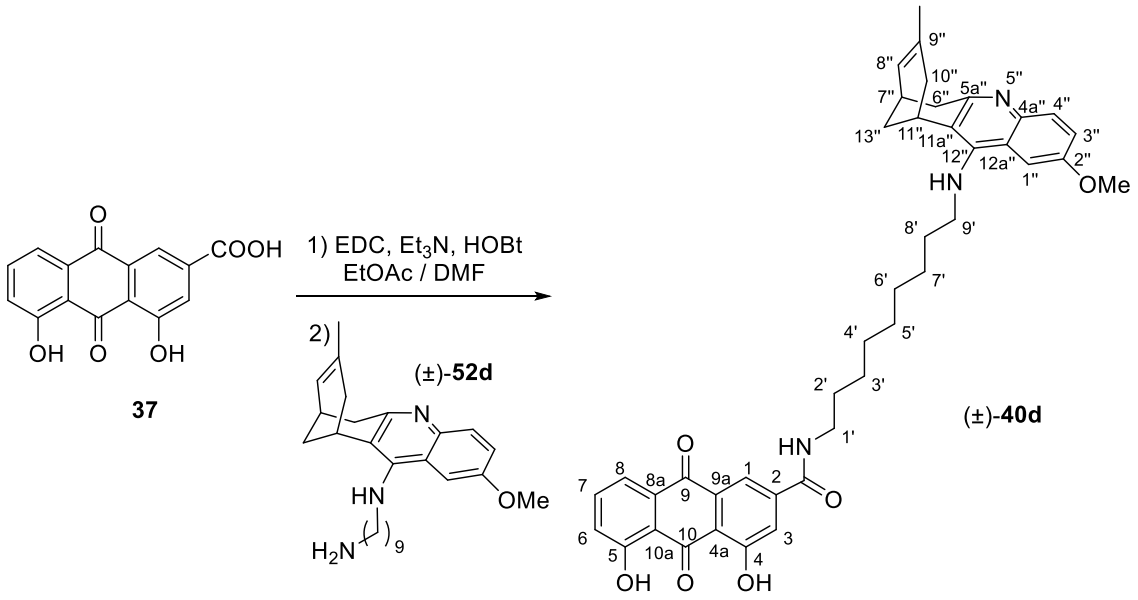

In a 25 mL round-bottomed flask equipped with a magnetic stirrer, rhein acid **37** (74 mg, 0.26 mmol) was suspended in a mixture of EtOAc (3 mL) and DMF (0.3 mL), and treated with *N*-(3-dimethylaminopropyl)-*N'*-ethylcarbodiimide hydrochloride (55 mg, 0.29 mmol), triethylamine (0.07 mL, 51 mg, 0.51 mmol), and 1-hydroxy-1*H*-benzotriazole (48 mg, 0.35 mmol). The resulting mixture was stirred at room temperature for 10 minutes and treated with a suspension of the amine (±)-**52d** (100 mg, 0.24 mmol) in a mixture of EtOAc (5 mL) and DMF (0.4 mL). The reaction mixture was stirred at room temperature for 1 day and concentrated under reduced pressure to give a dark brown oily residue (425 mg), which was subjected to column chromatography purification [silica gel 35−70 μm (34 g); Ø = 2.5 cm; #1, 100 mL, CH_2Cl_2 / 50% aq. NH_4OH 100:0.4; #2, 100 mL, CH_2Cl_2 / MeOH / 50% aq. NH_4OH 99.8:0.2:0.4; #3, 100 mL, CH_2Cl_2 / MeOH / 50% aq. NH_4OH 99.5:0.5:0.4; #4, 100 mL, CH_2Cl_2 / MeOH / 50% aq. NH_4OH 99:1:0.4; #5, 100 mL, CH_2Cl_2 / MeOH / 50% aq. NH_4OH 97:3:0.4; #6–142, 1.3 L, CH_2Cl_2 / MeOH / 50% aq. NH_4OH 95:5:0.4], to afford the desired amide (±)-**40d** (#112–131, 73 mg, 45% yield) as an orange solid.

R_f = 0.90 (silica gel, 10 cm, CH_2Cl_2 / MeOH / NH_4OH 50% 90:10:1).

Analytical sample of (±)-40d·HCl

In a 25 mL round-bottomed flask (±)-**40d** (73 mg, 0.11 mmol) was dissolved in CH_2Cl_2 (2 mL), filtered with a PTFE filter (0.2 μm), treated with HCl / Et_2O (3 N, 0.10 mL), concentrated *in vacuo*, and washed with pentane (3 × 2 mL), to give, after drying in standard conditions, (±)-**40d**·HCl (76 mg) as an orange solid.

Melting point: 137–138 °C.

IR (ATR) *v*: 3500−2500 (max at 3264, 3055, 2926, 2855, O–H, N–H, $^+$N–H, C–H st), 1674, 1628, 1585, 1558 (C=O, Ar–C–C, Ar–C–N st) cm^{-1}.

^{1}H NMR (400 MHz, CD_3OD) *δ*: 1.38–1.46 (complex signal, 10H, 3'-H_2, 4'-H_2, 5'-H_2, 6'-H_2 and 7'-H_2), 1.60 (s, 3H, 9"-CH_3), 1.67 (tt, *J* = *J'* = 6.4 Hz, 2H, 2'-H_2), 1.85 (tt, *J* = *J'* = 6.8 Hz, 2H, 8'-H_2), 1.93 (broad d, *J* = 18.0 Hz, 1H, 10"-H_{endo}), superimposed in part 1.94 (dm, *J* = 13.2 Hz, 1H, 13"-H_{syn}), 2.07 (dm, *J* = 13.2 Hz, 1H, 13"-H_{anti}), 2.53 (dd, *J* = 18.0 Hz, *J'* = 5.2 Hz, 1H, 10"-H_{exo}), 2.75 (m, 1H, 7"-H), 2.80 (broad d, *J* = 17.6 Hz, 1H, 6"-H_{endo}), 3.14 (dd, *J* = 17.6 Hz, *J'* = 5.6 Hz, 1H, 6"-H_{exo}), 3.39 (m, 1H, 11"-H), 3.43 (dt, *J* = *J'* = 6.4 Hz, 2H, 1'-H_2), 3.83 (s, 3H, 2"-OCH_3), superimposed in part 3.84 (m, 2H, 9'-H_2), 4.85 (s, OH, NH, $^+$NH), 5.59 (broad d, *J* = 5.2 Hz, 1H, 8"-H), 7.33 (dd, *J* = 8.0 Hz, *J'*=1.2 Hz, 1H, 6-H), 7.37 (dd, *J* = 9.2 Hz, *J'* = 2.4 Hz, 1H, 3"-H), 7.41 (d, *J* = 2.4 Hz, 1H, 1"-H), 7.50 (d, *J* = 9.2 Hz, 1H, 4"-H), 7.65 (dd, *J* = 7.6 Hz, *J'* = 1.2 Hz, 1H, 8-H), 7.69 (d, *J* = 1.6 Hz, 1H, 3-H), 7.73 (dd, *J* = 8.0 Hz, *J'* = 7.6 Hz, 1H, 7-H), 8.12 (d, *J* = 1.6 Hz, 1H, 1-H).

^{13}C NMR (100.6 MHz, CD_3OD) *δ*: 23.5 (CH_3, 9"-CH_3), 27.4 (CH, C11"), 27.5 (CH_2), 27.7 (CH_2) (C6' and C7'), 27.9 (CH, C7"), 29.4 (CH_2, C13"), 29.7 (CH_2), 29.9 (CH_2), 30.0 (CH_2), 30.1 (CH_2) (C2', C3', C4' and C5'), 32.0 (CH_2, C8'), 35.8 (CH_2, C6"), 36.3 (CH_2, C10"), 41.0 (CH_2, C1'), 49.1 (CH_2, C9'), 56.3 (CH_3, 2"-OCH_3), 105.8 (CH, C1"), 116.7 (C, C10a), 117.1 (C), 118.2 (C), 118.3 (C) (C4a, C11a" and C12a"), 118.8 (CH, C1), 120.7 (CH, C8), 121.6 (CH), 125.2 (2CH) (C3", C4" and C8"), 123.7 (CH, C3), 125.8 (CH, C6), 134.4 (C), 134.9 (2C) (C9a, C4a" and C9"), 134.6 (C, C8a), 138.7 (CH, C7), 143.6 (C, C2), 149.3 (C, C5a"), 155.7 (C, C12"), 157.9 (C, C2"), 163.3 (C, C4), 163.5 (C, C5), 167.1 (C, CONH), 181.8 (C, C9), 193.3 (C, C10).

HRMS (ESI):

Calculated for ($C_{42}H_{45}N_3O_6$ + H^+): 688.3381

Found: 688.3378

HPLC purity: 97.6%.

Preparation of 6,9-dichloro-1,2,3,4-tetrahydroacridine, 67

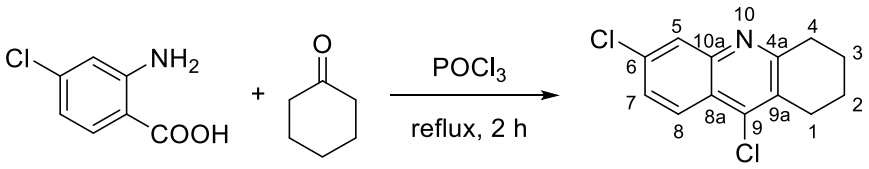

65 **66** **67**

In a triple necked 250 mL round-bottomed flask equipped with a magnetic stirrer, a condenser and cooled with an ice bath, a mixture of 4-chloroanthranilic acid, **65** (10.0 g, 58.3 mmol), cyclohexanone, **66** (5.73 mL, 5.43 g, 55.3 mmol) and $POCl_3$ (50 mL, 82.3 g, 0.54 mol) was prepared. The reaction mixture was heated under reflux for 2 h and the resulting suspension was allowed to cool to room temperature and evaporated under reduced pressure. The given solid was dissolved in CH_2Cl_2 (150 mL) and treated dropwise with 5 N aq. sol. NaOH until basic pH while cooled with an ice bath. The aqueous layers were extracted with CH_2Cl_2 (3 × 200 mL), and the combined organic layers were washed with 5 N aq. sol. NaOH (3 × 200 mL), dried with anhydrous Na_2SO_4, filtered and concentrated in vacuo to afford **67** (11.3 g, 81% yield) as a brown solid.

R_f = 0,92 (silica gel, 10 cm, CH_2Cl_2 / MeOH / 50% aq. NH_4OH 90:10:1).

Analytical sample of 67·HCl

In a 25 mL round-bottomed flask **67** (240 mg, 0.95 mmol) was dissolved in MeOH (10 mL), filtered with a PTFE filter (0.2 µm), treated with HCl / MeOH (1.7 N, 0.8 mL), and evaporated in vacuo. The obtained solid (276 mg) was crystallized with MeOH / EtOAc 1:2 (3 mL), giving, after drying in standard conditions, **67**·HCl (254 mg) as a beige solid.

Melting point: 170–171 °C (MeOH / AcOEt 6:1).

IR (KBr) *v*: 3500–2150 (max. at 3048, 3010, 2943, 2865, 2388, 2283 and 2145, C–H, N–H^+ st), 1964, 1888, 1641, 1602, 1574, 1526 (Ar–C–C, Ar–C–N st) cm^{-1}.

^{1}H NMR (300 MHz, CD_3OD) δ: 2.03–2.09 (complex signal, 4H, 2-H_2, 3-H_2), 3.15 (m, 2H), 3.37 (m, 2H) (1-H_2, 4-H_2), 4.87 (s, NH^+), 7.97 (dd, J = 9.0 Hz, J' = 2.0 Hz, 1H, 7-H), 8.10 (d, J = 2.0 Hz, 1H, 5-H), 8.52 (d, J = 9.0 Hz, 1H, 8-H).

^{13}C NMR (75.4 MHz, CD_3OD) δ: 21.5 (CH_2), 22.2 (CH_2) (C2, C3), 27.9 (CH_2), 30.5 (CH_2) (C1, C4), 120.4 (CH), 128.1 (CH), 132.0 (CH) (C5, C7, C8), 125.8 (C, C9a), 133.4 (C, C8a), 138.5 (C, C6), 141.8 (C, C4a), 152.7 (C, C10a), 160.6 (C, C9).

Preparation of *N*-(6-chloro-1,2,3,4-tetrahydroacridin-9-yl)hexane-1,6-diamine, 59a

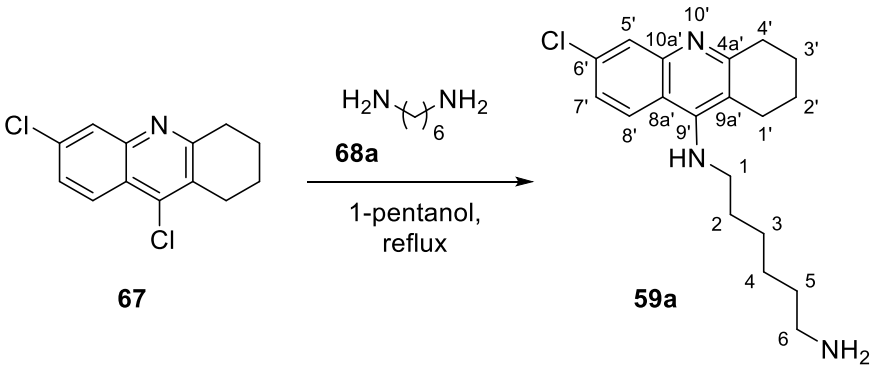

In a 10 mL round-bottomed flask provided with a magnetic stirrer and a condenser, a solution of compound **67** (1.00 g, 3.97 mmol) and hexane-1,6-diamine, **68a** (1.84 g, 15.8 mmol), in 1-pentanol (5 mL) was prepared, then stirred and heated under reflux for 24 h. The resulting solution was cooled to room temperature until a precipitate was formed, then dissolved in CH_2Cl_2 (25 mL), washed with 2 N aq. sol. NaOH (4 × 25mL) and water (25 mL), dried with anhydrous Na_2SO_4, filtered and evaporated under reduced pressure to give a brown oil (4.05 g), which was purified by column chromatography [silica gel 35−70 µm (100 g); Ø = 4.5 cm; #1–11, 1 L, CH_2Cl_2 / 50% aq. NH_4OH 100:0.4; #12–13, 250 mL, CH_2Cl_2 / MeOH / 50% aq. NH_4OH 97.7:0.3:0.4; #14–25, 1.5 L, CH_2Cl_2 / MeOH / 50% aq. NH_4OH 99:1:0.4; #26–27, 250 mL, CH_2Cl_2 / MeOH / 50% aq. NH_4OH 98.5:1.5:0.4; #28–34, 750 mL, CH_2Cl_2 / MeOH / 50% aq. NH_4OH 98:2:0.4; #35–39, 500 mL, CH_2Cl_2 / MeOH / 50% aq. NH_4OH 97:3:0.4; #40–42, 250 mL, CH_2Cl_2 / MeOH / 50% aq. NH_4OH 96:4:0.4; #43–60, 1.25 L, CH_2Cl_2 / MeOH / 50% aq. NH_4OH 95:5:0.4; #61–64, 750 mL, CH_2Cl_2 / MeOH / 50% aq. NH_4OH 95:5:30; #65, 300 mL, CH_2Cl_2 / MeOH / 50% aq. NH_4OH 90:10:30], to provide the starting material **67** (#4–9, 824 mg, 63% yield) as a yellow solid and the desired compound **59a** (#50–64, 424 mg, 32% yield) as a brown oil.

R_f = 0.39 (gel de sílice, 10 cm, CH_2Cl_2 / MeOH / 25% aq. NH_4OH 25% 90:10:0.1).

Analytical sample of 59a·2HCl

Melting point: 157–158 °C (MeOH).

IR (KBr) *v*: 3500–2500 (max. at 3413, 2935 and 2864, N–H, $^+$N–H and C–H st), 1630, 1573, and 1513 (Ar–C–C and Ar–C–N st) cm^{-1}.

^{1}H NMR (300 MHz, CD_3OD) δ: 1.39–1.52 (complex signal, 4H, 3-H_2 and 4-H_2), 1.66 (tt, $J \approx J' \approx 7.5$ Hz, 2H, 5-H_2), 1.80 (tt, $J \approx J' \approx 7.5$ Hz, 2H, 2-H_2), 1.88−1.98 (complex signal, 4H, 2'-H_2 and 3'-H_2), 2.69 (m, 2H, 1'-H_2), 2.90 (t, $J = 7.5$ Hz, 2H, 6-H_2), 2.98 (m, 2H, 4'-H_2), 3.83 (t, $J = 7.5$ Hz, 2H, 1-H_2), 7.48 (dd, $J = 9.3$ Hz, $J' = 2.1$ Hz, 1H, 7'-H), 7.75 (d, $J = 2.1$ Hz, 2H, 5'-H), 8.30 (d, $J = 9.3$ Hz, 1H, 8'-H).

^{13}C NMR (75,4 MHz, CD_3OD) δ: 22.3 (CH_2, C3'), 23.2 (CH_2, C2'), 25.2 (CH_2, C1'), 27.1 (CH_2) and 27.3 (CH_2) (C3 and C4), 28.5 (CH_2), 30.9 (CH_2) and 31.4 (CH_2) (C2, C5 and C4'), 40.6 (CH_2, C6), 49.1 (CH_2, C1), 114.3 (C, C9a'), 116.5 (C, C8a'), 121.3 (CH, C5'), 126.1 (CH, C7'), 128.0 (CH, C8'), 138.5 (C, C6'), 142.8 (C, C10a'), 154.5 (C, C4a'), 156.2 (C, C9').

Preparation of *N*-(6-chloro-1,2,3,4-tetrahydroacridin-9-yl)heptane-1,7-diamine, 59b

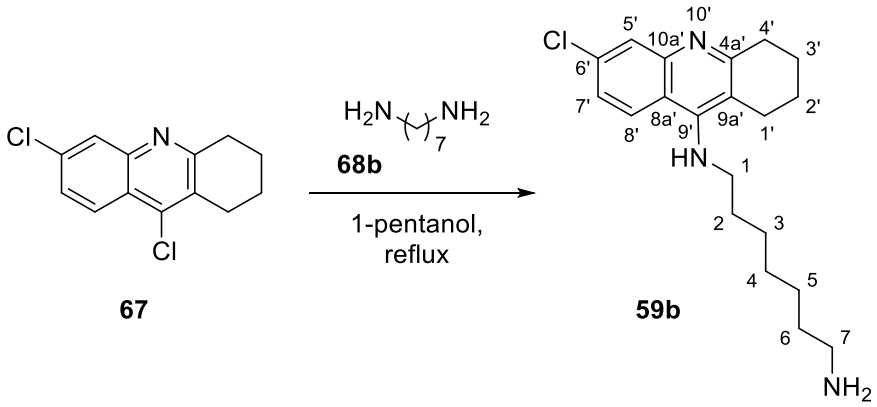

In a 10 mL round-bottomed flask provided with a magnetic stirrer and a condenser was prepared a solution of compound **67** (1.00 g, 3.97 mmol) and heptane-1,7-diamine, **68b** (2.07 g, 15.9 mmol), in 1-pentanol (5 mL). The reaction mixture was stirred and heated under reflux for 24 h. The resulting suspension was cooled to room temperature until a precipitate was formed, then dissolved in EtOAc (50 mL), washed with 2 N NaOH aq. sol. (4 × 25 mL) and water (2 × 25 mL), dried with anhydrous Na_2SO_4, filtered and evaporated under reduced pressure to give a brown oil (1.41 g), which was purified by column chromatography [silica gel 35−70 µm (80 g); Ø = 4 cm; #1–5, 200 mL, CH_2Cl_2 / 50% aq. NH_4OH 100:0.4; #6–9, 300 mL, CH_2Cl_2 / MeOH / 50% aq. NH_4OH 99.9:0.1:0.4; #10–14, 300 mL, CH_2Cl_2 / MeOH / 50% aq. NH_4OH 99.8:0.2:0.4; #15–18, 300 mL, CH_2Cl_2 / MeOH / 50% aq. NH_4OH 99.7:0.3:0.4; #19–21, 300 mL, CH_2Cl_2 / MeOH / 50% aq. NH_4OH 99.6:0.4:0.4; #22–26, 300 mL, CH_2Cl_2 / MeOH / 50% aq. NH_4OH 99.5:0.5:0.4; #27–29, 300 mL, CH_2Cl_2 / MeOH / 50% aq. NH_4OH 99.4:0.6:0.4; #30–32, 300 mL, CH_2Cl_2 / MeOH / NH_4OH 99.3:0.7:0.4; #33–35, 300 mL, CH_2Cl_2 / MeOH / 50% aq. NH_4OH 99.2:0.8:0.4; #36–38, 300 mL, CH_2Cl_2 / MeOH / 50% aq. NH_4OH 99.1:0.9:0.4; #39–52, 1.5 L, CH_2Cl_2 / MeOH / 50% aq. NH_4OH 99:1:0.4; #53–58, 500 mL, CH_2Cl_2 / MeOH / NH_4OH 98:2:0.4; #59–90, 3 L, CH_2Cl_2 / MeOH / 50% aq. NH_4OH 97:3:0.4; #91–100, 1 L, CH_2Cl_2 / MeOH / 50% aq. NH_4OH 95:5:0.4], to provide the desired compound **59b** (#63–94, 812 mg, 59% yield) as a brown oil.

R_f = 0.33 (gel de sílice, 10 cm, CH_2Cl_2 / MeOH / 25% aq. NH_4OH 25% 90:10:0.1).

Analytical sample of 59b·2HCl

Melting point: 164–165 °C (MeOH).

IR (KBr) *v*: 3500–2500 (max. at 3411, 3255, 2931 and 2859, N–H, $^{+}$N–H and C–H st), 1629, 1572, and 1514 (Ar–C–C and Ar–C–N st) cm^{-1}.

^{1}H NMR (300 MHz, CD_3OD) *δ*: 1.38–1.53 (complex signal, 6H, 3-H_2, 4-H_2, and 5-H_2), 1.66 (tt, *J* ≈ *J'* ≈ 7.5 Hz, 2H, 6-H_2), 1.85 (tt, *J* ≈ *J'* ≈ 7.5 Hz, 2H, 2-H_2), 1.92–1.99 (complex signal, 4H, 2'-H_2 and 3'-H_2), 2.68 (m, 2H, 1'-H_2), 2.91 (t, *J* = 7.5 Hz, 2H, 7-H_2), 3,00 (m, 2H, 4'-H_2), 3.94 (t, *J* ≈ 7.5 Hz, 2H, 1-H_2), 7.56 (dd, *J* = 9.3 Hz, *J'* = 2.1 Hz, 1H, 7'-H), 7.78 (d, *J* = 2.1 Hz, 1H, 5'-H), 8.39 (d, *J* = 9.3 Hz, 1H, 8'-H).

^{13}C NMR (75,4 MHz, CD_3OD) *δ*: 21.8 (CH_2, C3'), 22.9 (CH_2, C2'), 24.8 (CH_2, C1'), 27.3 (CH_2) and 27.5 (CH_2) (C3 and C5), 29.4 (CH_2, C4'), 28.5 (CH_2), 29.8 (CH_2) and 31.3 (CH_2) (C2, C4 and C6), 40.7 (CH_2, C7), 49.1 (CH_2, C1), 113.3 (C, C9a'), 115.3 (C, C8a'), 119.1 (CH, C5'), 126.7 (CH, C7'), 128.7 (CH, C8'), 139.9 (C, C6'), 140.4 (C, C10a'), 152.0 (C, C4a'), 157.6 (C, C9').

Preparation of *N*-(6-chloro-1,2,3,4-tetrahydroacridin-9-yl)octane-1,8-diamine, 59c

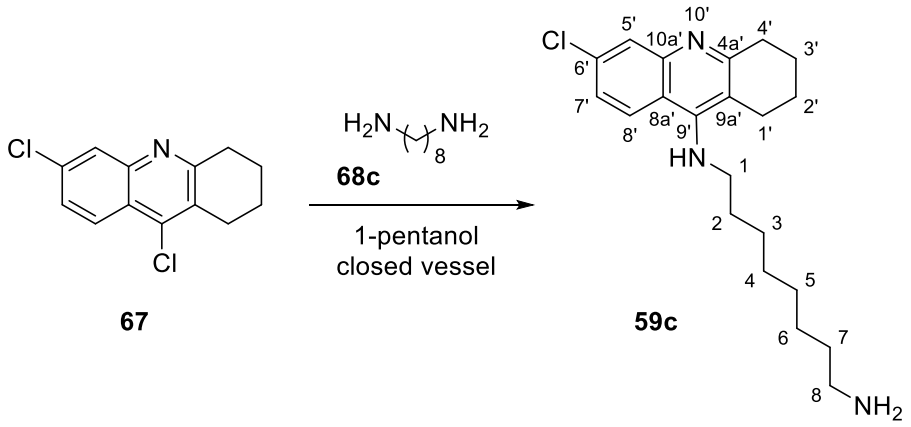

In a 25 mL closed vessel provided with a magnetic stirrer was prepared a solution of compound **67** (1.00 g, 3.97 mmol) and octane-1,8-diamine, **68c** (2.29 g, 15.9 mmol), in 1-pentanol (5 mL). The resulting solution was stirred and heated at 137 °C overnight. The resulting suspension was cooled to room temperature until a precipitate was formed, then dissolved in EtOAc (20 mL), washed with 2 N NaOH aq. sol. (4 × 20 mL) and water (20 mL), dried with anhydrous Na_2SO_4, filtered and evaporated under reduced pressure to give a dark brown oil (2.20 g), which was subjected to column chromatography purification [silica gel 35−70 μm (90 g); Ø = 4 cm; #1–58, 4 L, CH_2Cl_2 / 50% aq. NH_4OH 100:0.4; #59–79, 2 L, CH_2Cl_2 / MeOH / 50% aq. NH_4OH 99:1:0.4; #80–98, 2.3 L, CH_2Cl_2 / MeOH / 50% aq. NH_4OH 95:5:0.4], to provide the starting material **67** (#2–5, 111 mg, 8% yield) as a yellow solid and the desired compound **59c** (#80–96, 978 mg, 69% yield) as an orange-brown oil.

R_f = 0.33 (gel de sílice, 10 cm, CH_2Cl_2 / MeOH / NH_4OH 50% 90:10:0.5).

Analytical simple of 59c·2HCl

In a 25 mL round-bottomed flask **59c** (148 mg, 0.41 mmol) was dissolved in MeOH (5 mL), filtered with a PTFE filter (0.45 μm), treated with HCl / MeOH (1.81 N, 1.4 mL), and evaporated *in vacuo*. The resulting solid (168 mg) was crystallized with MeOH / EtOAc 1:1 (0.5 mL), giving, after drying in standard conditions, **59c**·2HCl (121 mg) as a yellowish solid.

Melting point: 109–110 °C (MeOH / EtOAc 1:1).

IR (KBr) *v*: 3500–2500 (max at 3344, 2929, 2855, N–H,$^{+}$N–H and C–H st), 1630, 1605, 1574, 1558 y 1512 (Ar–C–C and Ar–C–N st) cm^{-1}.

^{1}H NMR (300 MHz, CD_3OD) δ: 1.24–1.44 (complex signal, 8H, 3-H_2, 4-H_2, 5-H_2 and 6-H_2), 1.63 (tt, $J = J'$ = 7.5 Hz, 2H, 7-H_2), 1.71 (tt, $J = J'$ = 7.5 Hz, 2H, 2-H_2), 1.84–1.94 (complex signal, 4H, 2'-H_2 and 3'-H_2), 2.66 (m, 2H, 1'-H_2), 2.89 (t, J = 7.5 Hz, 2H, 8-H_2), 2.94 (m, 2H, 4'-H_2), 3.69 (t, J = 7.5 Hz, 2H, 1-H_2), 4.89 (s, NH, $^{+}$NH, $^{+}NH_3$), 7.36 (dd, J = 9.0 Hz, J' = 2.1 Hz, 1H, 7'-H), 7.71 (d, J = 2.1 Hz, 1H, 5'-H), 8.16 (d, J = 9.0 Hz, 1H, 8'-H).

^{13}C NMR (75,4 MHz, CD_3OD) δ: 22.8 (CH_2, C3'), 23.5 (CH_2, C2'), 25.5 (CH_2, C1'), 27.4 (CH_2) y 27.7 (CH_2) (C3 y C6), 28.6 (CH_2), 30.1 ($2CH_2$), 31.8 (CH_2), 32.1 (CH_2) (C2, C4, C5, C7 y C4'), 40.8 (CH_2, C8), 49.4 (CH_2, C1), 115.1 (C, C9a'), 117.6 (C, C8a'), 123.3 (CH, C5'), 125.6 (CH, C7'), 127.4 (CH, C8'), 137.3 (C, C6'), 144.9 (C, C10a'), 155.0 (C, C4a'), 156.6 (C, C9').

Preparation of *N*-(6-chloro-1,2,3,4-tetrahydroacridin-9-yl)nonane-1,9-diamine, 59d

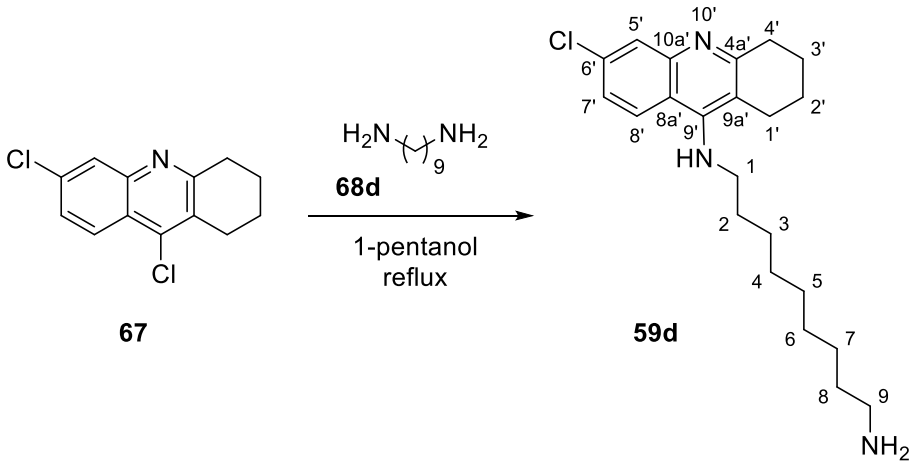

In a 10 mL round-bottomed flask equipped with a magnetic stirrer and a condenser was prepared a solution of compound **67** (1.00 g, 3.97 mmol) and nonane-1,9-diamine, **68d** (2.51 g, 15.9 mmol), in 1-pentanol (5 mL). The reaction mixture was stirred and heated under reflux for 18 h. The resulting suspension was cooled to room temperature and concentrated under reduced pressure. The resulting precipitate was dissolved in EtOAc (30 mL) and extracted with 1 N HCl aq. sol. (4 × 30 mL). The combined aqueous layers were washed with EtOAc (3 × 50 mL), then basified with 2 N NaOH aq. sol. (100 mL) and extracted with CH_2Cl_2 (4 × 60 mL). The combined organic layers were dried over anhydrous Na_2SO_4, filtered and evaporated *in vacuo* to give a brown oil (3.43 g), which was purified by column chromatography [silica gel 35−70 µm (60 g); Ø = 3 cm; #1–55, 5 L, CH_2Cl_2 / 50% aq. NH_4OH 100:0.4; #56–59, 500 mL, CH_2Cl_2 / MeOH / 50% aq. NH_4OH 95:5:0.4], to provide the desired compound **59d** (#18–58, 875 mg, 59% yield) as an orange oil.

R_f = 0.18 (gel de sílice, 10 cm, EtOAc / MeOH / Et_3N 90:10:0.1).

Analytical simple of 59d·2HCl

In a 25 mL round-bottomed flask **59c** (148 mg, 0.41 mmol) was dissolved in MeOH (5 mL), filtered with a PTFE filter (0.45 µm), treated with HCl / MeOH (1.81 N, 1.4 mL), and evaporated *in vacuo*. The resulting solid (168 mg) was crystallized with MeOH / EtOAc 1:1 (0.5 mL), giving, after drying in standard conditions, **59c**·2HCl (121 mg) as a yellowish solid.

Melting point: 179–180 °C (MeOH / EtOAc 3:8).

IR (KBr) *v*: 3500–2500 (max at 3405, 3253, 2926 and 2853, N–H,$^{+}$N–H and C–H st), 1629, 1570, and 1515 (Ar–C–C and Ar–C–N st) cm^{-1}.

^{1}H NMR (300 MHz, CD_3OD) δ: 1.28–1.48 (complex signal, 10H, 3-H_2, 4-H_2, 5-H_2, 6-H_2 and 7-H_2), 1.65 (tt, $J \approx J' \approx 7.5$ Hz, 2H, 8-H_2), 1.83 (tt, $J \approx J' \approx 7.5$ Hz, 2H, 2-H_2), 1.90–2.00 (complex signal, 4H, 2'-H_2 and 3'-H_2), 2.67 (m, 2H, 1'-H_2), 2.91 (t, $J = 7.5$ Hz, 2H, 9-H_2), 3.00 (m, 2H, 4'-H_2), 3.94 (t, $J = 7.5$ Hz, 2H, 1-H_2), 4.84 (s, NH, $^{+}$NH and $^{+}NH_3$), 7.55 (dd, $J = 9.3$ Hz, $J' = 2.1$ Hz, 1H, 7'-H), 7.79 (d, $J \approx 2.1$ Hz, 5'-H), 8.38 (d, $J = 9.3$ Hz, 1H, 8'-H).

^{13}C NMR (75,4 MHz, CD_3OD) δ: 21.8 (CH_2, C3'), 22.9 (CH_2, C2'), 24.8 (CH_2, C1'), 27.4 (CH_2) and 27.7 (CH_2) (C3 and C7), 29.3 (CH_2, C4'), 28.6 (CH_2), 30.1 (CH_2), 30.2 (CH_2), 30.4 (CH_2) and 31.4 (CH_2) (C2, C4, C5, C6 and C8), 40.8 (CH_2, C9), 113.3 (C, C9a'), 115.4 (C, C8a'), 119.1 (CH, C5'), 126.7 (CH, C7'), 128.8 (CH, C8'), 140.1 (C, C6'), 140.5 (C, C10a'), 152.1 (C, C4a'), 157.8 (C, C9'), the signal corresponding to C1', probably superimposed to those of CD_3OD, was not observed.

Preparation of *N*-(6-chloro-1,2,3,4-tetrahydroacridin-9-yl)-3,6-dioxaoctane-1,8-diamine, 59e

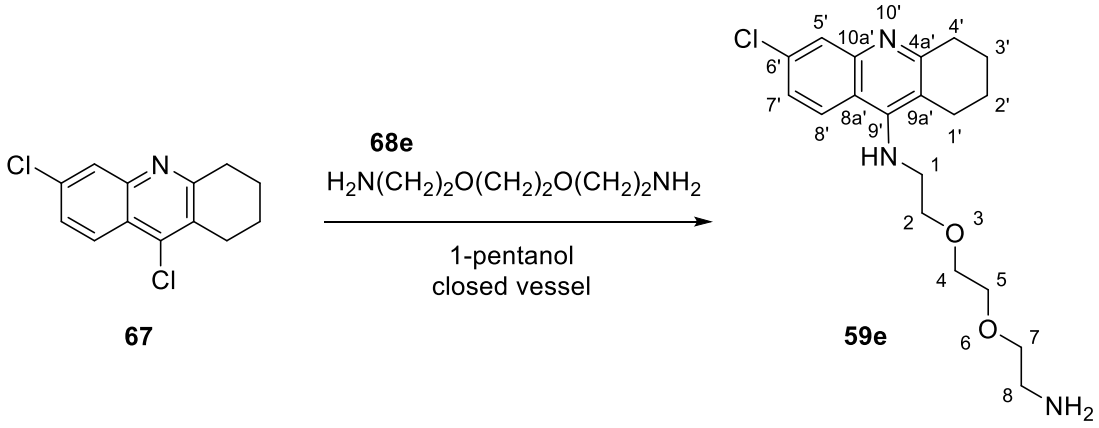

In a 25 mL closed vessel provided with a magnetic stirrer was prepared a solution of compound **67** (1.50 g, 5.95 mmol) and 3,6-dioxaoctane-1,8-diamine, **68e** (4.34 mL, 4.41 g, 29.8 mmol), in 1-pentanol (5.9 mL), then stirred at 137 °C overnight. The resulting suspension was concentrated under reduced pressure to give a dark brown oil (6.10 g), which was subjected to column chromatography purification [silica gel 35−70 µm (92 g); Ø = 4 cm; #1–5, 250 mL, hexane; #6–8, 250 mL, hexane / CH_2Cl_2 70:30; #9–10, 250 mL, hexane / CH_2Cl_2 30:70; #11–13, 250 mL, CH_2Cl_2; #14–15, 250 mL, CH_2Cl_2 / 50% aq. NH_4OH 100:2; #16–18, 250 mL, CH_2Cl_2 / 50% aq. NH_4OH 100:0.4; #19–20, 250 mL, CH_2Cl_2 / MeOH / 50% aq. NH_4OH 99.9:0.1:0.4; #21–23, 250 mL, CH_2Cl_2 / MeOH / 50% aq. NH_4OH 99.8:0.2:0.4; #24–25, 250 mL, CH_2Cl_2 / MeOH / 50% aq. NH_4OH 99.6:0.4:0.4; #26–30, 500 mL, CH_2Cl_2 / MeOH / 50% aq. NH_4OH 99.2:0.8:0.4; #31–35, 500 mL, CH_2Cl_2 / MeOH / 50% aq. NH_4OH 99:1:0.4; #36–50, 1.5 L, CH_2Cl_2 / MeOH / 50% aq. NH_4OH 98.5:1.5:0.4; #51–67, 1.5 L, CH_2Cl_2 / MeOH / NH_4OH 98:2:0.4; #68–72, 500 mL, CH_2Cl_2 / MeOH / 50% aq. NH_4OH 97:3:0.4; #73–74, 250 mL, CH_2Cl_2 / MeOH / 50% aq. NH_4OH 96.5:3.5:0.4; #75–79, 500 mL, CH_2Cl_2 / MeOH / 50% aq. NH_4OH 96:4:0.4; #80–81, 400 mL, CH_2Cl_2 / MeOH / NH_4OH 95:5:0.4], to provide the starting material **67** (#14–17, 305 mg, 14% yield) and the desired compound **59e** (#46–74, 1.66 g, 77% yield) as a yellow oil.

R_f = 0.69 (gel de sílice, 10 cm, CH_2Cl_2 / MeOH / NH_4OH 50% 90:10:1).

Analytical sample of 59e·2HCl

In a 25 mL round-bottomed flask **59e** (70 mg; 0.19 mmol) was dissolved in CH_2Cl_2 (2 mL), filtered with a PTFE filter (0.2 µm), treated with HCl / Et_2O (1.35 N, 1.28 mL), concentrated under

reduced pressure, and washed with pentane (3 × 2 mL), giving, after drying in standard conditions, **59e**·2HCl (91 mg) as a yellow sticky solid.

IR (ATR) ν: 3600–2400 (max. at 3351, 3048, 2870, N–H, $^{+}$N–H, C–H st), 1630, 1572, 1512 (Ar–C–C and Ar–C–N st) cm^{-1}.

^{1}H NMR (400 MHz, CD_3OD) δ: 1.92–2.03 (complex signal, 4H, 2'-H_2 and 3'-H_2), 2.72 (t, J = 5.6 Hz, 2H, 1'-H_2), 3.04 (t, J = 5.6 Hz, 2H, 4'-H_2), 3.10 (t, J = 5.2 Hz, 2H, 8-H_2), superimposed 3.68 (dt, J = 5.2 Hz, J' = 1.2 Hz, 2H, 4-H_A and 5-H_A), 3.71 (t, J = 8.0 Hz, 2H, 7-H_2), 3.74 (dt, J = 5.2 Hz, J' = 1.2 Hz, 2H, 4-H_B and 5-H_B), 3.89 (t, J = 5.6 Hz, 2H, 2-H_2), 4.17 (t, J = 5.6 Hz, 2H, 1-H_2), 4.85 (s, NH, $^{+}$NH), 7.57 (dd, J = 9.2 Hz, J' = 2.0 Hz, 1H, 7'-H), 7.83 (d, J = 2.0 Hz, 1H, 5'-H), 8.51 (d, J = 8.8 Hz, 1H, 8'-H).

^{13}C NMR (100.6 MHz, CD_3OD) δ: 21.8 (CH_2, C2'), 22.8 (CH_2, C3'), 24.7 (CH_2, C1'), 29.4 (CH_2, C4'), 40.6 (CH_2, C8), 49.3 (CH_2, C1), 67.9 (CH_2, C7), 70.5 (CH_2, C2), 71.4 ($2CH_2$, C4 and C5), 113.8 (C, C9a'), 115.7 (C, C8a'), 119.2 (CH, C5'), 126.9 (CH, C7'), 128.8 (CH, C8'), 140.2 (C, C6'), 140.4 (C, C10a'), 152.6 (C, C4a'), 158.4 (C, C9').

HRMS (ESI):

Calculated for ($C_{19}H_{26}{}^{35}ClN_3O_2$ + H^+):	364.1786
Found:	364.1797

Preparation of (±)-*N*-{6-[(6-chloro-1,2,3,4-tetrahydroacridin-9-yl)amino]hexyl}-2-(6-benzyloxy-7-methoxy-2-methylchroman-2-yl)acetamide, (±)-70a

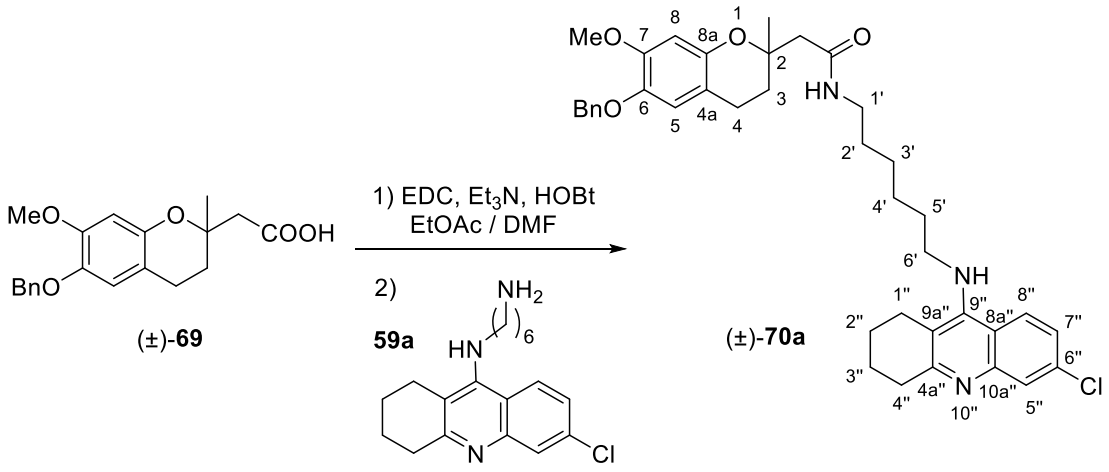

In a 25 mL round-bottomed flask equipped with a magnetic stirrer, the acid (±)-**69** (100 mg, 0.29 mmol) was dissolved in a mixture of EtOAc (5 mL) and DMF (0.4 mL), and treated with *N*-(3-dimethylaminopropyl)-*N'*-ethylcarbodiimide hydrochloride (68 mg, 0.35 mmol), triethylamine (0.09 mL, 66 mg, 0.65 mmol), and 1-hydroxy-1*H*-benzotriazole (60 mg, 0.44 mmol). The resulting mixture was stirred at room temperature for 15 minutes and then treated with a suspension of the amine **59a** (107 mg, 0.32 mmol) in a mixture of EtOAc (3 mL) and DMF (0.4 mL). The reaction mixture was stirred at room temperature for 1 day and concentrated under reduced pressure to give a brown solid (463 mg), which was subjected to column chromatography purification [silica gel 35−70 μm (20 g); Ø = 2 cm; #1–47, 800 mL, CH_2Cl_2 / 50% aq. NH_4OH 100:0.4; #48–60, 200 mL, CH_2Cl_2 / MeOH / 50% aq. NH_4OH 95:5:0.4], to provide the desired benzylated amide (±)-**70a** (#25–37, 191 mg, quantitative yield) as a pale yellow solid.

R_f = 0.73 (silica gel, 10 cm, CH_2Cl_2 / MeOH / 50% aq. NH_4OH 90:10:1).

Analytical sample of (±)-70a·HCl

In a 25 mL round-bottomed flask (±)-**70a** (59 mg, 0.09 mmol) was dissolved in CH_2Cl_2 (4 mL), filtered with a PTFE filter (0.2 μm), treated with HCl / MeOH (0.5 N, 0.54 mL), evaporated *in vacuo*, and washed with pentane (3 × 2 mL), to give, after drying in standard conditions, (±)-**70a**·HCl (68 mg) as a pale yellow solid.

Melting point: 126–128 °C

Calculated logP: 8.62

IR (ATR) ν: 3600–2200 (max. at 3250, 3048, 2928, 2852, N–H, $^{+}$N–H, C–H st), 1632, 1573, 1510 (C=O, Ar–C–C and Ar–C–N st) cm^{-1}.

^{1}H NMR (400 MHz, CD_3OD) δ: 1.31 (s, 3H, 2-CH_3), 1.34–1.44 (complex signal, 4H, 3'-H_2 and 4'-H_2), 1.51 (tt, $J = J' = 6.8$ Hz, 2H, 2'-H_2), 1.70 (tt, $J = 7.2$ Hz, $J' = 6.8$ Hz, 2H, 5'-H_2), 1.80 (dt, $J = 13.6$ Hz, $J' = 6.0$ Hz, 1H, 3-H_A), superimposed 1.93 (dt, $J = 13.6$ Hz, $J' = 6.0$ Hz, 1H, 3-H_B), 1.85–1.96 (complex signal, 4H, 2"-H_2 and 3"-H_2), 2.45 (d, $J = 13.6$ Hz, 1H, 2-CH_A-CO), 2.53 (d, $J = 13.2$ Hz, 1H, 2-CH_B-CO), superimposed in part 2.61 (t, $J = 6.8$ Hz, 2H, 1"-H_2), 2.65 (dt, $J = 8.8$ Hz, $J' = 6.4$ Hz, 2H, 4-H_2), 2.90 (t, $J = 5.6$ Hz, 2H, 4"-H_2), 3.14 (dt, $J = 13.6$ Hz, $J' = 6.8$ Hz, 1H, 1'-H_A), 3.28 (dt, $J = 13.2$ Hz, $J' = 6.4$ Hz, 1H, 1'-H_B), 3.75 (s, 3H, 7-OCH_3), 3.80 (t, $J = 7.6$ Hz, 2H, 6'-H_2), 4.83 (d, $J = 11.6$ Hz, 1H, 6-OCH_A), 4.85 (s, NH, $^{+}$NH), 4.91 (d, $J = 12.0$ Hz, 1H, 6-OCH_B), 6.40 (s, 1H, 8-H), 6.62 (s, 1H, 5-H), 7.25 (dddd, $J = J' = 7.2$ Hz, $J'' = J''' = 2.8$ Hz, 1H, 4-H benzyl), 7.29 (ddd, $J = J' = 6.8$ Hz, $J'' = 1.6$ Hz, 2H, 3(5)-H benzyl), 7.35 (dd, $J = 8.0$ Hz, $J' = 1.2$ Hz, 2H, 2(6)-H benzyl), 7.52 (dd, $J = 8.8$ Hz, $J' = 2.0$ Hz, 1H, 7"-H), 7.71 (d, $J = 2.0$ Hz, 1H, 5"-H), 8.28 (d, $J = 9.6$ Hz, 1H, 8"-H).

^{13}C NMR (100.6 MHz, CD_3OD) δ: 21.7 (CH_2, C2"), 22.4 (CH_2, C4), 22.8 (CH_2, C3"), 24.56 (CH_2, C1"), 24.64 (CH_3, 2-CH_3), 27.36 (CH_2, C4'), 27.39 (CH_2, C3'), 29.2 (CH_2, C4"), 30.3 (CH_2, C2'), 31.3 (CH_2, C5'), 31.9 (CH_2, C3), 40.0 (CH_2, C1'), 47.8 (CH_2, 2-CH_2-CO), 49.3 (CH_2, C6'), 56.5 (CH_3, 7-OCH_3), 73.5 (CH_2, 6-OCH_2), 75.9 (C, C2), 103.1 (CH, C8), overlapped 113.2 (2C, C9a" and C4a), 115.3 (C, C8a"), 117.7 (CH, C5), 119.1 (CH, C5"), 126.7 (CH, C7"), 128.7 [3CH, C2(4 and 6) benzyl], 128.8 (CH, C8"), 129.3 [2CH, C3(5) benzyl], 138.9 (C, C1 benzyl), 140.0 (C, C6"), 140.4 (C, C10a"), 143.3 (C, C6), 149.3 (C, C8a), 150.9 (C, C7), 151.9 (C, C4a"), 157.5 (C, C9"), 172.3 (C, CONH).

HRMS (ESI):

Calculated for ($C_{41}H_{50}{}^{35}ClN_3O_4 + H^+$): 684.3562

Found: 684.3563

Preparation of (±)-*N*-{7-[(6-chloro-1,2,3,4-tetrahydroacridin-9-yl)amino]heptyl}-2-(6-benzyloxy-7-methoxy-2-methylchroman-2-yl)acetamide, (±)-70b

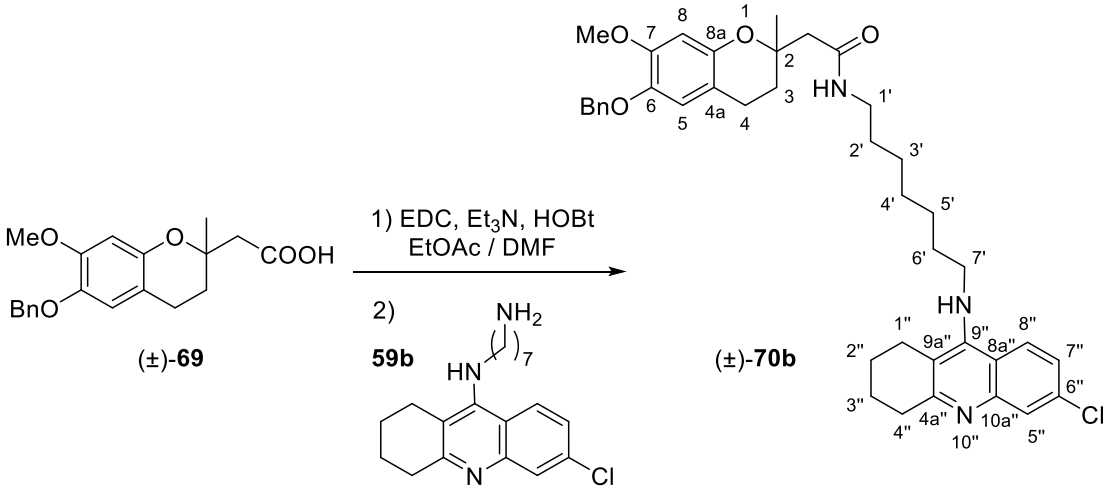

In a 50 mL round-bottomed flask provided with a magnetic stirrer, the acid (±)-**69** (200 mg, 0.58 mmol) was dissolved in a mixture of EtOAc (7.5 mL) and DMF (0.8 mL), and treated with *N*-(3-dimethylaminopropyl)-*N'*-ethylcarbodiimide hydrochloride (136 mg, 0.71 mmol), triethylamine (0.18 mL, 131 mg, 1.30 mmol), and 1-hydroxy-1*H*-benzotriazole (119 mg, 0.88 mmol). The resulting mixture was stirred at room temperature for 15 minutes and then treated with a suspension of the amine **59b** (222 mg, 0.64 mmol) in a mixture of EtOAc (10 mL) and DMF (1 mL). The reaction mixture was stirred at room temperature for 1 day and concentrated *in vacuo* to give a dark brown solid (784 mg), which was purified by column chromatography [silica gel 35−70 μm (31 g); Ø = 2.8 cm; #1–128, 2.25 L, CH_2Cl_2 / 50% aq. NH_4OH 100:0.4; #129–133, 100 mL, CH_2Cl_2 / MeOH / 50% aq. NH_4OH 99:1:0.4; #134–144, 200 mL, CH_2Cl_2 / MeOH / 50% aq. NH_4OH 95:5:0.4], to provide the desired benzylated amide (±)-**70b** (#89–136, 326 mg, 83% yield) as a pale yellow solid.

R_f = 0.73 (silica gel, 10 cm, CH_2Cl_2 / MeOH / 50% aq. NH_4OH 90:10:1).

Analytical sample of (±)-70b·HCl

In a 25 mL round-bottomed flask (±)-**70b** (83 mg, 0.12 mmol) was dissolved in CH_2Cl_2 (1.5 mL), filtered with a PTFE filter (0.2 μm), treated with HCl / dioxane (4 M, 0.09 mL), evaporated

in vacuo, and washed with pentane (3 × 2 mL), to give, after drying in standard conditions, (±)-**70b**·HCl (85 mg) as a white-yellow solid.

Melting point: 107–109 °C

Calculated logP: 8.86

IR (ATR) ν: 3600–2200 (max. at 3255, 3053, 2929, 2852, N–H, $^{+}$N–H, C–H st), 1632, 1568, 1512 (C=O, Ar–C–C and Ar–C–N st) cm^{-1}.

^{1}H NMR (400 MHz, CD_3OD) δ: 1.27–1.38 (complex signal, 6H, 3'-H_2, 4'-H_2 and 5'-H_2), 1.33 (s, 3H, 2-CH_3), 1.48 (tt, J = J' = 6.8 Hz, 2H, 2'-H_2), superimposed in part 1.75 (tt, J = J' = 6.4 Hz, 2H, 6'-H_2), 1.80 (dt, J = 13.6 Hz, J' = 5.6 Hz, 1H, 3-H_A), superimposed 1.90 (dt, J = 13.6 Hz, J' = 5.6 Hz, 1H, 3-H_B), 1.88–1.98 (complex signal, 4H, 2"-H_2 and 3"-H_2), 2.45 (d, J = 13.6 Hz, 1H, 2-CH_A-CO), 2.53 (d, J = 13.2 Hz, 1H, 2-CH_B-CO), 2.61 (t, J = 6.0 Hz, 2H, 1"-H_2), 2.67 (dt, J = 8.4 Hz, J' = 5.6 Hz, 2H, 4-H_2), 2.94 (t, J = 5.6 Hz, 2H, 4"-H_2), 3.14 (dt, J = 13.6 Hz, J' = 6.4 Hz, 1H, 1'-H_A), 3.25 (dt, J = 13.2 Hz, J' = 6.4 Hz, 1H, 1'-H_B), 3.76 (s, 3H, 7-OCH_3), 3.86 (t, J = 7.6 Hz, 2H, 7'-H_2), 4.85 (s, NH, $^{+}$NH), 4.89 (d, J = 11.6 Hz, 1H, 6-OCH_A), 4.93 (d, J = 11.6 Hz, 1H, 6-OCH_B), 6.41 (s, 1H, 8-H), 6.67 (s, 1H, 5-H), 7.25 (tt, J = 7.2 Hz, J' = 2.8 Hz, 1H, 4-H benzyl), 7.28 (ddd, J = J' = 6.8 Hz, J'' = 1.6 Hz, 2H, 3(5)-H benzyl), 7.35 (dd, J = 8.4 Hz, J' = 1.6 Hz, 2H, 2(6)-H benzyl), 7.53 (dd, J = 9.2 Hz, J' = 2.0 Hz, 1H, 7"-H), 7.71 (d, J = 2.4 Hz, 1H, 5"-H), 8.33 (d, J = 9.6 Hz, 1H, 8"-H).

^{13}C NMR (100.6 MHz, CD_3OD) δ: 21.7 (CH_2, C2"), 22.4 (CH_2, C4), 22.8 (CH_2, C3"), 24.63 (CH_2, C1"), 24.64 (CH_3, 2-CH_3), 27.7 (CH_2, C5'), 27.8 (CH_2, C3'), 29.3 (CH_2, C4"), 30.0 (CH_2, C4'), 30.3 (CH_2, C2'), 31.3 (CH_2, C6'), 32.0 (CH_2, C3), 40.1 (CH_2, C1'), 47.7 (CH_2, 2-CH_2-CO), 49.3 (CH_2, C7'), 56.5 (CH_3, 7-OCH_3), 73.5 (CH_2, 6-OCH_2), 75.9 (C, C2), 103.1 (CH, C8), overlapped 113.2 (2C, C9a" and C4a), 115.4 (C, C8a"), 117.7 (CH, C5), 119.1 (CH, C5"), 126.7 (CH, C7"), 128.7 [3CH, C2(4 and 6) benzyl], 128.8 (CH, C8"), 129.3 [2CH, C3(5) benzyl], 138.9 (C, C1 benzyl), 140.1 (C, C6"), 140.5 (C, C10a"), 143.3 (C, C6), 149.3 (C, C8a), 151.0 (C, C7), 151.9 (C, C4a"), 157.6 (C, C9"), 172.3 (C, CONH).

HRMS (ESI):

Calculated for ($C_{40}H_{48}{}^{35}ClN_3O_4$ + H^+): 670.3406

Found: 670.3400

Preparation of (±)-*N*-{8-[(6-chloro-1,2,3,4-tetrahydroacridin-9-yl)amino]octyl}-2-(6-benzyloxy-7-methoxy-2-methylchroman-2-yl)acetamide, (±)-70c

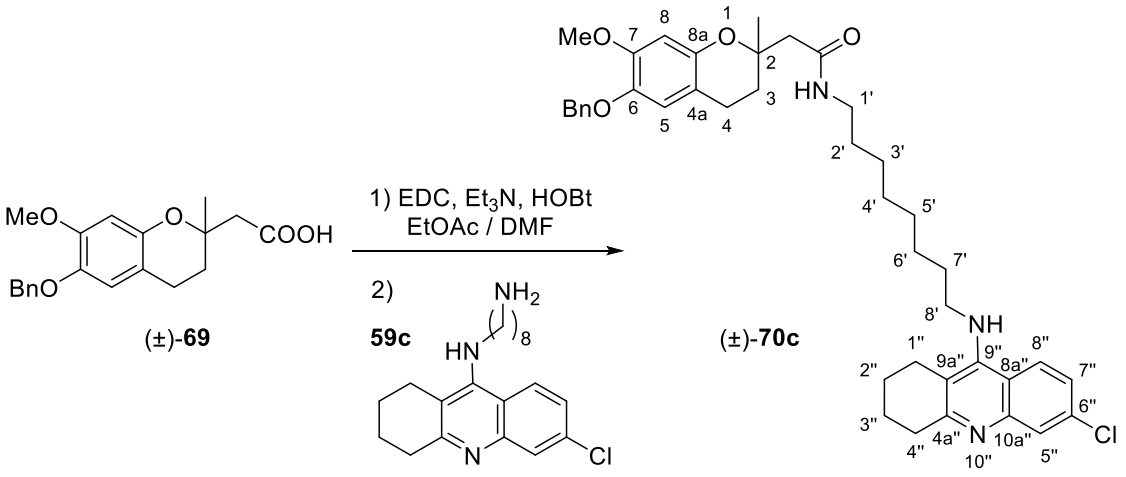

In a 25 mL round-bottomed flask provided with a magnetic stirrer, the acid (±)-**69** (100 mg, 0.29 mmol) was dissolved in a mixture of EtOAc (5 mL) and DMF (0.4 mL), and treated with *N*-(3-dimethylaminopropyl)-*N'*-ethylcarbodiimide hydrochloride (68 mg, 0.35 mmol), triethylamine (0.09 mL, 66 mg, 0.65 mmol), and 1-hydroxy-1*H*-benzotriazole (60 mg, 0.44 mmol). The resulting mixture was stirred at room temperature for 15 minutes and then treated with a suspension of the amine **59c** (116 mg, 0.32 mmol) in a mixture of EtOAc (3 mL) and DMF (0.4 mL). The reaction mixture was stirred at room temperature for 1 day and concentrated under reduced pressure to give a brown solid (462 mg), which was subjected to column chromatography purification [silica gel 35−70 μm (20.5 g); Ø = 2 cm; #1–47, 900 mL, CH_2Cl_2 / 50% aq. NH_4OH 100:0.4; #48–57, 200 mL, CH_2Cl_2 / MeOH / 50% aq. NH_4OH 95:5:0.4], to provide the desired benzylated amide (±)-**70c** (#26–34, 183 mg, 92% yield) as a yellow solid.

R_f = 0.73 (silica gel, 10 cm, CH_2Cl_2 / MeOH / 50% aq. NH_4OH 90:10:1).

Analytical sample of (±)-70c·HCl

In a 25 mL round-bottomed flask (±)-**70c** (51 mg, 0.08 mmol) was dissolved in CH_2Cl_2 (4 mL), filtered with a PTFE filter (0.2 μm), treated with HCl / MeOH (0.5 N, 0.45 mL), evaporated *in vacuo*, and washed with pentane (3 × 2 mL), to give, after drying in standard conditions, (±)-**70c**·HCl (58 mg) as a pale yellow solid.

Melting point: 127–129 °C

Calculated logP: 9.05

IR (ATR) ν: 3600–2200 (max. at 3261, 3053, 2924, 2852, N–H, $^{+}$N–H, C–H st), 1632, 1571, 1510 (C=O, Ar–C–C and Ar–C–N st) cm^{-1}.

^{1}H NMR (400 MHz, CD_3OD) δ: 1.20–1.34 (complex signal, 6H, 3'-H_2, 4'-H_2 and 5'-H_2), 1.33 (s, 3H, 2-CH_3), 1.37 (tt, J = J' = 6.8 Hz, 2H, 6'-H_2), 1.48 (tt, J = J' = 6.8 Hz, 2H, 2'-H_2), superimposed in part 1.77 (tt, J = 7.2 Hz, J' = 6.8 Hz, 2H, 7'-H_2), 1.79 (dt, J = 13.6 Hz, J' = 6.8 Hz, 1H, 3-H_A), superimposed 1.90 (dt, J = 13.6 Hz, J' = 6.8 Hz, 1H, 3-H_B), 1.87–1.99 (complex signal, 4H, 2"-H_2 and 3"-H_2), 2.45 (d, J = 13.6 Hz, 1H, 2-CH_A-CO), 2.53 (d, J = 13.2 Hz, 1H, 2-CH_B-CO), 2.61 (t, J = 5.6 Hz, 2H, 1"-H_2), 2.67 (dt, J = 6.0 Hz, J' = 5.2 Hz, 2H, 4-H_2), 2.94 (t, J = 6.0 Hz, 2H, 4"-H_2), 3.14 (dt, J = 13.6 Hz, J' = 6.8 Hz, 1H, 1'-H_A), 3.25 (dt, J = 13.2 Hz, J' = 6.8 Hz, 1H, 1'-H_B), 3.77 (s, 3H, 7-OCH_3), 3.85 (t, J = 7.2 Hz, 2H, 8'-H_2), 4.85 (s, NH, $^{+}$NH), 4.89 (d, J = 12.0 Hz, 1H, 6-OCH_A), 4.93 (d, J = 12.0 Hz, 1H, 6-OCH_B), 6.42 (s, 1H, 8-H), 6.67 (s, 1H, 5-H), 7.22 (dddd, J = J' = 7.2 Hz, J'' = J''' = 2.8 Hz, 1H, 4-H benzyl), 7.27 (ddd, J = J' = 6.8 Hz, J'' = 1.6 Hz, 2H, 3(5)-H benzyl), 7.35 (dd, J = 8.0 Hz, J' = 1.2 Hz, 2H, 2(6)-H benzyl), 7.52 (dd, J = 9.2 Hz, J' = 2.0 Hz, 1H, 7"-H), 7.72 (d, J = 2.0 Hz, 1H, 5"-H), 8.33 (d, J = 9.2 Hz, 1H, 8"-H).

^{13}C NMR (100.6 MHz, CD_3OD) δ: 21.7 (CH_2, C2"), 22.4 (CH_2, C4), 22.8 (CH_2, C3"), 24.62 (CH_2, C1"), 24.63 (CH_3, 2-CH_3), 27.6 (CH_2, C6'), 27.8 (CH_2, C5'), 29.3 (CH_2, C4"), 30.2 (CH_2), 30.3 (CH_2) (C3' and C4'), 30.4 (CH_2, C2'), 31.4 (CH_2, C7'), 32.0 (CH_2, C3), 40.2 (CH_2, C1'), 47.7 (CH_2, 2-CH_2-CO), 49.3 (CH_2, C8'), 56.5 (CH_3, 7-OCH_3), 73.4 (CH_2, 6-OCH_2), 75.9 (C, C2), 103.0 (CH, C8), 113.17 (C, C9a"), 113.20 (C, C4a), 115.3 (C, C8a"), 117.5 (CH, C5), 119.1 (CH, C5"), 126.7 (CH, C7"), 128.7 [3CH, C2(4 and 6) benzyl], 128.8 (CH, C8"), 129.3 [2CH, C3(5) benzyl], 138.9 (C, C1 benzyl), 140.0 (C, C6"), 140.5 (C, C10a"), 143.3 (C, C6), 149.3 (C, C8a), 150.9 (C, C7), 151.9 (C, C4a"), 157.6 (C, C9"), 172.3 (C, CONH).

HRMS (ESI):

Calculated for ($C_{41}H_{50}{}^{35}ClN_3O_4$ + H^{+}): 684.3562

Found: 684.3563

Preparation of (±)-*N*-{9-[(6-chloro-1,2,3,4-tetrahydroacridin-9-yl)amino]nonyl}-2-(6-benzyloxy-7-methoxy-2-methylchroman-2-yl)acetamide, (±)-70d

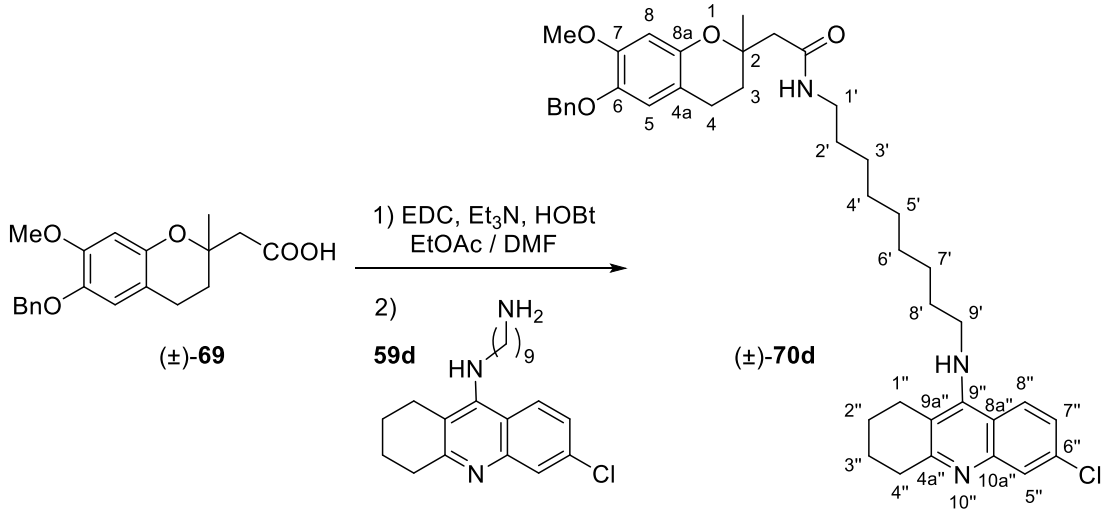

In a 25 mL round-bottomed flask provided with a magnetic stirrer, the acid (±)-**69** (128 mg, 0.37 mmol) was dissolved in a mixture of EtOAc (5 mL) and DMF (0.5 mL), and treated with *N*-(3-dimethylaminopropyl)-*N'*-ethylcarbodiimide hydrochloride (87 mg, 0.45 mmol), triethylamine (0.11 mL, 80 mg, 0.79 mmol), and 1-hydroxy-1*H*-benzotriazole (76 mg, 0.56 mmol). The resulting mixture was stirred at room temperature for 15 minutes and then treated with a suspension of the amine **59d** (154 mg, 0.41 mmol) in a mixture of EtOAc (6 mL) and DMF (0.6 mL). The reaction mixture was stirred at room temperature for 1 day and concentrated under reduced pressure to give a brown oil (521 mg), which was subjected to column chromatography purification [silica gel 35−70 μm (20 g); Ø = 2 cm; #1–92, 1.6 L, CH_2Cl_2 / 50% aq. NH_4OH 100:0.4; #93–95, 100 mL, CH_2Cl_2 / MeOH / 50% aq. NH_4OH 99:1:0.4], to provide the desired benzylated amide (±)-**70d** (#57–95, 236 mg, 90% yield) as a pale yellow oil.

R_f = 0.74 (silica gel, 10 cm, CH_2Cl_2 / MeOH / 50% aq. NH_4OH 90:10:1).

Analytical sample of (±)-70d·HCl

In a 25 mL round-bottomed flask (±)-**70d** (32 mg, 0.05 mmol) was dissolved in CH_2Cl_2 (1 mL), filtered with a PTFE filter (0.2 μm), treated with HCl / dioxane (4 M, 0.04 mL), evaporated *in vacuo*, and washed with pentane (3 × 2 mL), to give, after drying in standard conditions, (±)-**70d**·HCl (33 mg) as a white-yellow solid.

Melting point: 107–109 °C

Calculated logP: 9.21

IR (ATR) ν: 3600–2200 (max. at 3244, 3053, 2924, 2852, N–H, $^{+}$N–H, C–H st), 1633, 1573, 1510 (C=O, Ar–C–C and Ar–C–N st) cm^{-1}.

^{1}H NMR (400 MHz, CD_3OD) δ: 1.18–1.36 (complex signal, 8H, 3'-H_2, 4'-H_2, 5'-H_2 and 6'-H_2), 1.33 (s, 3H, 2-CH_3), 1.39 (tt, J = 8.0 Hz, J' = 6.8 Hz, 2H, 7'-H_2), 1.48 (tt, J = 6.8 Hz, J' = 6.4 Hz, 2H, 2'-H_2), superimposed in part 1.77 (tt, J = 7.6 Hz, J' = 7.2 Hz, 2H, 8'-H_2), 1.80 (dt, J = 13.2 Hz, J' = 6.0 Hz, 1H, 3-H_A), superimposed 1.90 (dt, J = 13.2 Hz, J' = 6.0 Hz, 1H, 3-H_B), 1.87–1.98 (complex signal, 4H, 2"-H_2 and 3"-H_2), 2.45 (d, J = 13.6 Hz, 1H, 2-CH_A-CO), 2.52 (d, J = 13.6 Hz, 1H, 2-CH_B-CO), 2.63 (t, J = 5.2 Hz, 2H, 1"-H_2), 2.69 (dt, J = 6.4 Hz, J' = 2.4 Hz, 2H, 4-H_2), 2.95 (t, J = 6.0 Hz, 2H, 4"-H_2), 3.14 (dt, J = 13.2 Hz, J' = 6.8 Hz, 1H, 1'-H_A), 3.23 (dt, J = 13.2 Hz, J' = 6.8 Hz, 1H, 1'-H_B), 3.77 (s, 3H, 7-OCH_3), 3.87 (t, J = 7.2 Hz, 2H, 9'-H_2), 4.85 (s, NH, $^{+}$NH), 4.91 (s, J = 12.4 Hz, 1H, 6-OCH_A), 4.94 (d, J = 12.4 Hz, 1H, 6-OCH_B), 6.42 (s, 1H, 8-H), 6.68 (s, 1H, 5-H), 7.22 (dddd, J = J' = 6.8 Hz, J'' = J''' = 2.4 Hz, 1H, 4-H benzyl), 7.27 (ddd, J = J' = 7.2 Hz, J'' = 1.6 Hz, 2H, 3(5)-H benzyl), 7.36 (dd, J = 7.2 Hz, J' = 1.2 Hz, 2H, 2(6)-H benzyl), 7.53 (dd, J = 9.2 Hz, J' = 2.0 Hz, 1H, 7"-H), 7.73 (d, J = 2.0 Hz, 1H, 5"-H), 8.34 (d, J = 9.2 Hz, 1H, 8"-H).

^{13}C NMR (100.6 MHz, CD_3OD) δ: 21.8 (CH_2, C2"), 22.5 (CH_2, C4), 22.8 (CH_2, C3"), 24.56 (CH_3, 2-CH_3), 24.63 (CH_2, C1"), 27.7 (CH_2, C7'), 27.9 (CH_2, C3'), 29.32 (CH_2, C4"), 30.2 (CH_2), 30.3 (CH_2), 30.4 (CH_2), 30.5 (CH_2) (C2', C4', C5' and C6'), 31.3 (CH_2, C8'), 32.1 (CH_2, C3'), 40.2 (CH_2, C1'), 47.7 (CH_2, 2-CH_2-CO), 49.3 (CH_2, C9'), 56.4 (CH_3, 7-OCH_3), 73.5 (CH_2, 6-OCH_2), 75.9 (C, C2), 103.0 (CH, C8), 113.2 (C, C9a"), 113.3 (C, C4a), 115.4 (C, C8a"), 117.6 (CH, C5'), 119.2 (CH, C5"), 126.7 (CH, C7"), 128.78 (CH, C8"), 128.81 [3CH, C2(4 and 6) benzyl], 129.3 [2CH, C3(5) benzyl], 139.0 (C, C1 benzyl), 140.1 (C, C6"), 140.6 (C, C10a"), 143.4 (C, C6), 149.3 (C, C8a), 150.9 (C, C7), 152.0 (C, C4a"), 157.7 (C, C9"), 172.3 (C, CONH).

HRMS (ESI):

Calculated for ($C_{42}H_{52}{}^{35}ClN_3O_4$ + H^+): 698.3719

Found: 698.3714

Preparation of (±)-*N*-{7-[(6-chloro-1,2,3,4-tetrahydroacridin-9-yl)amino]heptyl}-2-(6-hydroxy-7-methoxy-2-methylchroman-2-yl)acetamide, (±)-57b

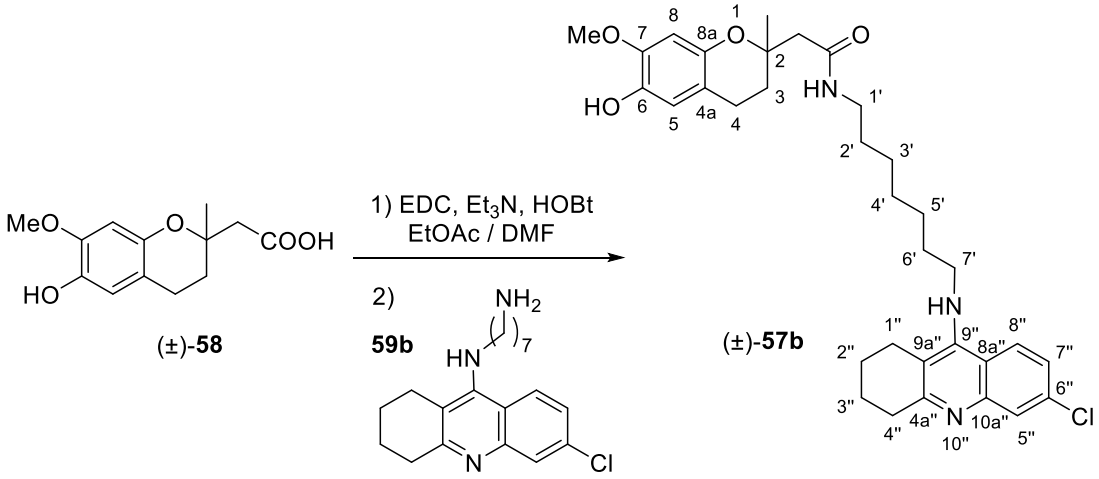

In a 50 mL round-bottomed flask equipped with a magnetic stirrer, the acid (±)-**58** (166 mg, 0.66 mmol) was dissolved in a mixture of EtOAc (9.7 mL) and DMF (0.5 mL), and treated with *N*-(3-dimethylaminopropyl)-*N'*-ethylcarbodiimide hydrochloride (153 mg, 0.80 mmol), triethylamine (0.18 mL, 131 mg, 1.30 mmol), and 1-hydroxy-1*H*-benzotriazole (134 mg, 0.99 mmol). The resulting mixture was stirred at room temperature for 15 minutes and then treated with a suspension of the amine **59b** (250 mg, 0.72 mmol) in a mixture of EtOAc (10 mL) and DMF (1.5 mL). The reaction mixture was stirred at room temperature for 1 day and concentrated *in vacuo* to give a dark brown solid (763 mg), which was purified by column chromatography [silica gel 35−70 μm (76 g); Ø = 4 cm; #1–4, 250 mL, hexane / Et_3N 100:0.2; #5–7, 250 mL, hexane / EtOAc / Et_3N 90:10:0.2; #8–9, 250 mL, hexane / EtOAc / Et_3N 80:20:0.2; #10–11, 250 mL, hexane / EtOAc / Et_3N 70:30:0.2; #12–14, 250 mL, hexane / EtOAc / Et_3N 60:40:0.2; #15–19, 500 mL, hexane / EtOAc / Et_3N 50:50:0.2; #20–24, 500 mL, hexane / EtOAc / Et_3N 40:60:0.2; #25–32, 750 mL, hexane / EtOAc / Et_3N 30:70:0.2; #33–131, 2 L, hexane / EtOAc / Et_3N 20:80:0.2; #132–135, 250 mL, EtOAc / Et_3N 100:0.2], to provide the desired amide (±)-**57b** (#34–100, 254 mg, 67% yield) as a white solid, and a mixture of (±)-**57b** / an unknown byproduct in a ratio of 1:0.4 (^{1}H-NMR) (#101–133, 72 mg, 11% yield of (±)-**57b**). The overall yield for the desired amide (±)-**57b** was 78%.

R_f = 0.62 (silica gel, 10 cm, CH_2Cl_2 / MeOH / 50% aq. NH_4OH 95:5:1).

Analytical sample of (±)-57b·HCl

In a 50 mL round-bottomed flask (±)-**57b** (237 mg, 0.41 mmol) was dissolved in CH_2Cl_2 (2 mL), filtered with a PVDF filter (0.22 μm), treated with HCl / Et_2O (1.35 N, 0.91 mL), evaporated *in vacuo*, and washed with pentane (3 × 2 mL), to give, after drying in standard conditions, (±)-**57b**·HCl (232 mg) as a white-yellow solid.

Melting point: 122–126 °C

Calculated logP: 7.45

IR (ATR) ν: 3600–2200 (max. at 3244, 3065, 2927, 2852, N–H, $^{+}$N–H, O–H, C–H st), 1632, 1573, 1509 (C=O, Ar–C–C and Ar–C–N st) cm^{-1}.

^{1}H NMR (400 MHz, CD_3OD) δ: 1.31 (s, 3H, 2-CH_3), 1.31–1.41 (complex signal, 6H, 3'-H_2, 4'-H_2 and 5'-H_2), 1.49 (tt, J = J' = 6.8 Hz, 2H, 2'-H_2), superimposed in part 1.77 (dt, J = 13.2 Hz, J' = 6.8 Hz, 1H, 3-H_A), 1.79 (tt, J = J' = 6.0 Hz, 2H, 6'-H_2), 1.89 (dt, J = 13.6 Hz, J' = 7.2 Hz, 1H, 3-H_B), 1.91–2.00 (complex signal, 4H, 2"-H_2 and 3"-H_2), 2.44 (d, J = 13.6 Hz, 1H, 2-CH_A-CO), 2.48 (d, J = 13.6 Hz, 1H, 2-CH_B-CO), 2.61 (t, J = 6.4 Hz, 2H, 4-H_2), 2.65 (t, J = 6.4 Hz, 2H, 1"-H_2), 2.99 (t, J = 5.6 Hz, 2H, 4"-H_2), 3.16 (dt, J = 13.6 Hz, J' = 6.8 Hz, 1H, 1'-H_A), 3.20 (dt, J = 13.6 Hz, J' = 6.8 Hz, 1H, 1'-H_B), 3.73 (s, 3H, 7-OCH_3), 3.89 (t, J = 7.2 Hz, 2H, 7'-H_2), 4.85 (s, NH, $^{+}$NH, OH), 6.31 (s, 1H, 8-H), 6.44 (s, 1H, 5-H), 7.55 (dd, J = 9.2 Hz, J' = 2.0 Hz, 1H, 7"-H), 7.77 (d, J = 2.4 Hz, 1H, 5"-H), 8.36 (d, J = 9.2 Hz, 1H, 8"-H).

^{13}C NMR (100.6 MHz, CD_3OD) δ: 21.7 (CH_2, C3"), 22.4 (CH_2, C4), 22.8 (CH_2, C2"), 24.5 (CH_3, 2-CH_3), 24.7 (CH_2, C1"), 27.6 (CH_2, C5'), 27.7 (CH_2, C4'), 29.3 (CH_2, C4"), 29.9 (CH_2, C3'), 30.3 (CH_2, C2'), 31.3 (CH_2, C6'), 32.3 (CH_2, C3), 40.1 (CH_2, C1'), 47.5 (CH_2, 2-CH_2-CO), 49.3 (CH_2, C7'), 56.4 (CH_3, 7-OCH_3), 75.6 (C, C2), 102.2 (CH, C8), 113.3 (C, C9a"), 113.4 (C, C4a), 115.4 (C, C8a"), 116.1 (CH, C5), 119.1 (CH, C5"), 126.8 (CH, C7"), 128.7 (CH, C8"), 140.1 (C, C6"), 140.5 (C, C10a"), 141.1 (C, C6), 147.4 (C, C8a), 148.3 (C, C7), 152.1 (C, C4a"), 157.8 (C, C9"), 172.4 (C, CONH).

HRMS (ESI):

Calculated for ($C_{33}H_{42}{}^{35}ClN_3O_4$ + H^+): 580.2937

Found: 580.2927

Preparation of (±)-*N*-{8-[(6-chloro-1,2,3,4-tetrahydroacridin-9-yl)amino]octyl}-2-(6-hydroxy-7-methoxy-2-methylchroman-2-yl)acetamide, (±)-57c

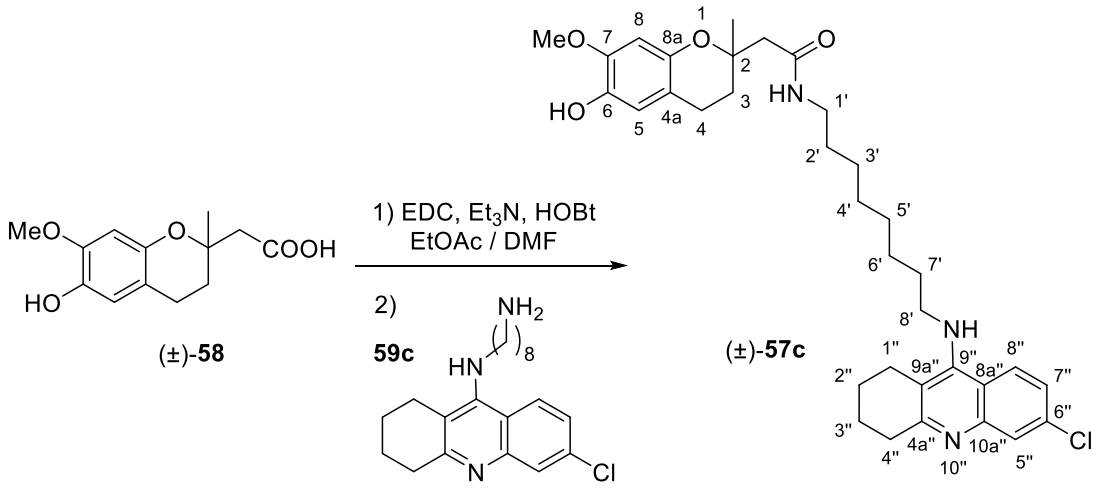

In a 25 mL round-bottomed flask equipped with a magnetic stirrer, the acid (±)-**58** (120 mg, 0.48 mmol) was dissolved in a mixture of EtOAc (10 mL) and DMF (1 mL), and treated with *N*-(3-dimethylaminopropyl)-*N'*-ethylcarbodiimide hydrochloride (111 mg, 0.58 mmol), triethylamine (0.13 mL, 95 mg, 0.94 mmol), and 1-hydroxy-1*H*-benzotriazole (97 mg, 0.71 mmol). The resulting mixture was stirred at room temperature for 15 minutes and then treated with a suspension of the amine **59c** (188 mg, 0.52 mmol) in a mixture of EtOAc (4.3 mL) and DMF (0.4 mL). The reaction mixture was stirred at room temperature for 1 day and concentrated under reduced pressure to give a dark brown sticky solid (624 mg), which was subjected to column chromatography purification [silica gel 35−70 μm (30 g); Ø = 2.8 cm; #1–67, 800 mL, CH_2Cl_2 / 50% aq. NH_4OH 100:0.4; #68–87, 250 mL, CH_2Cl_2 / MeOH / 50% aq. NH_4OH 99.8:0.2:0.4; #88–173, 1 L, CH_2Cl_2 / MeOH / 50% aq. NH_4OH 99.5:0.5:0.4; #174–191, 250 mL, CH_2Cl_2 / MeOH / 50% aq. NH_4OH 95:5:0.4], to provide a mixture that included the desired amide **57c** / byproduct structurally related with tacrine moiety in proportion 1:0.17 (^{1}H-NMR) (#113–181, 219 mg, 77 % yield) as a pale yellow solid, which was again subjected to column chromatography purification [silica gel 35−70 μm (21 g); Ø = 2 cm; #1–5, 100 mL, hexane / Et_3N 100:0.2; #6–8, 100 mL, hexane / EtOAc / Et_3N 90:10:0.2; #9–16, 100 mL, hexane / EtOAc / Et_3N 80:20:0.2; #17–24, 100 mL, hexane / EtOAc / Et_3N 70:30:0.2; #25–33, 100 mL, hexane / EtOAc / Et_3N 60:40:0.2; #34–58, 100 mL, hexane / EtOAc / Et_3N 50:50:0.2; #59–67, 100 mL, hexane / EtOAc / Et_3N 40:60:0.2; #68–85, 200 mL, hexane / EtOAc / Et_3N 30:70:0.2; #83–145, 700 mL, hexane / EtOAc / Et_3N 20:80:0.2; #146–155, 100 mL, EtOAc / Et_3N 100:0.2], to provide the pure desired amide (±)-**57c** (#85–127, 189 mg, 67% yield) as a white-yellow solid.

R_f = 0.63 (silica gel, 10 cm, CH_2Cl_2 / MeOH / 50% aq. NH_4OH 95:5:1).

Analytical sample of (±)-57c·HCl

In a 25 mL round-bottomed flask (±)-**57c** (170 mg, 0.29 mmol) was dissolved in CH_2Cl_2 (2 mL), filtered with a PVDF filter (0.22 µm), treated with HCl / Et_2O (1.35 N, 0.64 mL) and MeOH (1 mL), evaporated *in vacuo*, and washed with pentane (3 × 2 mL), to give, after drying in standard conditions, (±)-**57c**·HCl (162 mg) as a beige solid.

Melting point: 127–130 °C

Calculated logP: 7.96

IR (ATR) ν: 3600–2200 (max. at 3244, 3059, 2927, 2854, N–H, $^+$N–H, O–H, C–H st), 1632, 1573, 1510 (C=O, Ar–C–C and Ar–C–N st) cm^{-1}.

^{1}H NMR (400 MHz, CD_3OD) δ: 1.27–1.34 (complex signal, 6H, 3'-H_2, 4'-H_2 and 5'-H_2), 1.31 (s, 3H, 2-CH_3), 1.39 (tt, J = J' = 6.8 Hz, 2H, 6'-H_2), 1.48 (tt, J = J' = 6.8 Hz, 2H, 2'-H_2), superimposed in part 1.75 (dt, J = 13.6 Hz, J' = 6.8 Hz, 1H, 3-H_A), 1.80 (tt, J = 7.2 Hz, J' = 6.8 Hz, 2H, 7'-H_2), 1.89 (dt, J = 13.6 Hz, J' = 6.8 Hz, 1H, 3-H_B), 1.92–2.00 (complex signal, 4H, 2"-H_2 and 3"-H_2), 2.44 (d, J = 13.6 Hz, 1H, 2-CH_A-CO), 2.48 (d, J = 13.6 Hz, 1H, 2-CH_B-CO), 2.62 (t, J = 6.8 Hz, 2H, 4-H_2), 2.66 (t, J = 5.6 Hz, 2H, 1"-H_2), 2.99 (t, J = 6.0 Hz, 2H, 4"-H_2), 3.16 (dt, J = 13.6 Hz, J' = 6.8 Hz, 1H, 1'-H_A), 3.20 (dt, J = 13.6 Hz, J' = 6.8 Hz, 1H, 1'-H_B), 3.75 (s, 3H, 7-OCH_3), 3.90 (t, J = 7.2 Hz, 2H, 8'-H_2), 4.85 (s, NH, $^+$NH, OH), 6.32 (s, 1H, 8-H), 6.44 (s, 1H, 5-H), 7.55 (dd, J = 9.2 Hz, J' = 2.4 Hz, 1H, 7"-H), 7.76 (d, J = 2.4 Hz, 1H, 5"-H), 8.36 (d, J = 9.2 Hz, 1H, 8"-H).

^{13}C NMR (100.6 MHz, CD_3OD) δ: 21.8 (CH_2, C3"), 22.4 (CH_2, C4), 22.8 (CH_2, C2"), 24.62 (CH_3, 2-CH_3), 24.64 (CH_2, C1"), 27.5 (CH_2, C6'), 27.7 (CH_2, C5'), 29.3 (CH_2, C4"), 30.1 (CH_2), 30.2 (CH_2) (C3' and C4'), 30.4 (CH_2, C2'), 31.3 (CH_2, C7'), 32.3 (CH_2, C3), 40.2 (CH_2, C1'), 47.4 (CH_2, 2-CH_2-CO), 49.3 (CH_2, C8'), 56.4 (CH_3, 7-OCH_3), 75.6 (C, C2), 102.2 (CH, C8), 113.3 (C, C9a"), 113.4 (C, C4a), 115.4 (C, C8a"), 116.1 (CH, C5), 119.1 (CH, C5"), 126.7 (CH, C7"), 128.8 (CH, C8"), 140.1 (C, C6"), 140.5 (C, C10a"), 141.1 (C, C6), 147.4 (C, C8a), 148.3 (C, C7), 152.0 (C, C4a"), 157.8 (C, C9"), 172.4 (C, CONH).

HRMS (ESI):

Calculated for ($C_{34}H_{44}{}^{35}ClN_3O_4 + H^+$): 594.3093

Found: 594.3096

Preparation of (±)-*N*-{9-[(6-chloro-1,2,3,4-tetrahydroacridin-9-yl)amino]nonyl}-2-(6-hydroxy-7-methoxy-2-methylchroman-2-yl)acetamide, (±)-57d

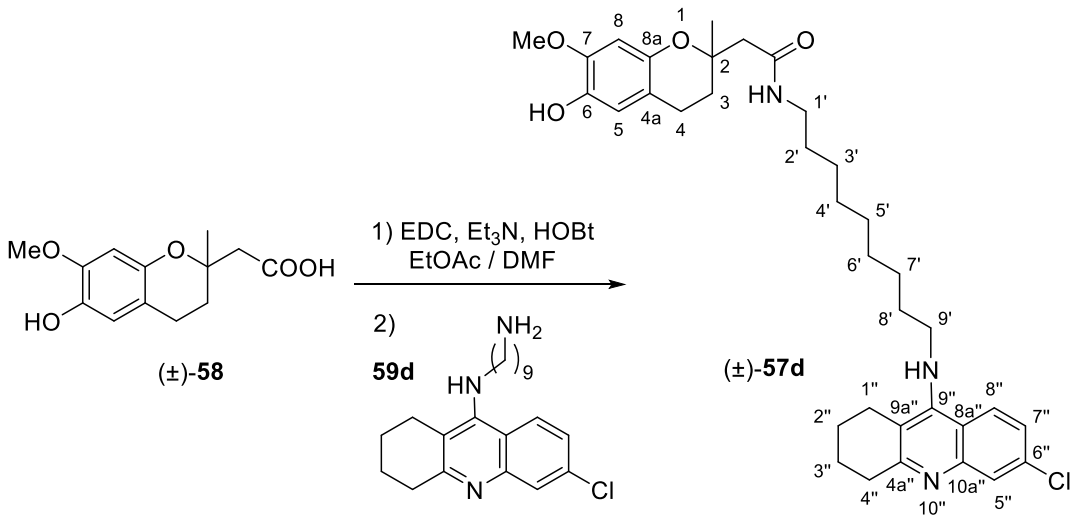

In a 50 mL round-bottomed flask provided with a magnetic stirrer, the acid (±)-**58** (163 mg, 0.65 mmol) was dissolved in a mixture of EtOAc (9.4 mL) and DMF (0.4 mL), and treated with *N*-(3-dimethylaminopropyl)-*N'*-ethylcarbodiimide hydrochloride (150 mg, 0.78 mmol), triethylamine (0.18 mL, 131 mg, 1.30 mmol), and 1-hydroxy-1*H*-benzotriazole (132 mg, 0.97 mmol). The resulting mixture was stirred at room temperature for 15 minutes and then treated with a suspension of the amine **59d** (266 mg, 0.71 mmol) in a mixture of EtOAc (10 mL) and DMF (1.5 mL). The reaction mixture was stirred at room temperature for 1 day and concentrated under reduced pressure to give a dark brown sticky solid (828 mg), which was subjected to column chromatography purification [silica gel 35−70 µm (83 g); Ø = 4 cm; #1–4, 200 mL, hexane / Et_3N 100:0.2; #5–6, 200 mL, hexane / EtOAc / Et_3N 90:10:0.2; #7–10, 300 mL, hexane / EtOAc / Et_3N 80:20:0.2; #11–15, 300 mL, hexane / EtOAc / Et_3N 70:30:0.2; #16–19, 300 mL, hexane / EtOAc / Et_3N 60:40:0.2; #20–24, 500 mL, hexane / EtOAc / Et_3N 50:50:0.2; #25–27, 300 mL, hexane / EtOAc / Et_3N 40:60:0.2; #28–32, 500 mL, hexane / EtOAc / Et_3N 30:70:0.2; #33–52, 2 L, hexane / EtOAc / Et_3N 20:80:0.2; #53–54, 200 mL, EtOAc / Et_3N 100:0.2], to provide the desired amide (±)-**57d** (#35–52, 338 mg, 86% yield) as a white solid.

R_f = 0.66 (silica gel, 10 cm, CH_2Cl_2 / MeOH / 50% aq. NH_4OH 95:5:1).

Analytical sample of (±)-57d·HCl

In a 50 mL round-bottomed flask (±)-**57d** (234 mg, 0.39 mmol) was dissolved in CH_2Cl_2 (2 mL), filtered with a PTFE filter (0.45 μm), treated with HCl / Et_2O (1.35 N, 0.86 mL), evaporated *in vacuo*, and washed with pentane (3 × 2 mL), to give, after drying in standard conditions, (±)-**57d**·HCl (228 mg) as a pale yellow solid.

Melting point: 104–106 °C

Calculated logP: 8.38

IR (ATR) ν: 3600–2200 (max. at 3244, 3065, 2924, 2852, N–H, $^+$N–H, O–H, C–H st), 1632, 1573, 1510 (C=O, Ar–C–C and Ar–C–N st) cm^{-1}.

^{1}H NMR (400 MHz, CD_3OD) δ: 1.23–1.33 (complex signal, 8H, 3'-H_2, 4'-H_2, 5'-H_2 and 6'-H_2), 1.32 (s, 3H, 2-CH_3), 1.40 (tt, J = J' = 7.2 Hz, 2H, 7'-H_2), 1.48 (tt, J = J' = 6.8 Hz, 2H, 2'-H_2), superimposed in part 1.77 (dt, J = 13.6 Hz, J' = 6.0 Hz, 1H, 3-H_A), 1.80 (tt, J = 7.6 Hz, J' = 6.8 Hz, 2H, 8'-H_2), 1.90 (dt, J = 13.6 Hz, J' = 7.6 Hz, 1H, 3-H_B), 1.92–2.00 (complex signal, 4H, 2"-H_2 and 3"-H_2), 2.44 (d, J = 13.2 Hz, 1H, 2-CH_A-CO), 2.49 (d, J = 13.6 Hz, 1H, 2-CH_B-CO), 2.63 (t, J = 6.8 Hz, 2H, 4-H_2), 2.67 (t, J = 5.2 Hz, 2H, 1"-H_2), 2.99 (t, J = 5.2 Hz, 2H, 4"-H_2), 3.16 (dt, J = 13.6 Hz, J' = 6.8 Hz, 1H, 1'-H_A), 3.20 (dt, J = 13.6 Hz, J' = 6.8 Hz, 1H, 1'-H_B), 3.75 (s, 3H, 7-OCH_3), 3.92 (t, J = 7.2 Hz, 2H, 9'-H_2), 4.85 (s, NH, $^+$NH, OH), 6.34 (s, 1H, 8-H), 6.45 (s, 1H, 5-H), 7.56 (dd, J = 9.2 Hz, J' = 2.0 Hz, 1H, 7"-H), 7.76 (d, J = 2.4 Hz, 1H, 5"-H), 8.38 (d, J = 9.2 Hz, 1H, 8"-H).

^{13}C NMR (100.6 MHz, CD_3OD) δ: 21.7 (CH_2, C3"), 22.4 (CH_2, C4), 22.8 (CH_2, C2"), 24.6 (CH_3, 2-CH_3), 24.7 (CH_2, C1"), 27.6 (CH_2, C7'), 27.8 (CH_2, C6'), 29.3 (CH_2, C4"), 30.1 (CH_2), 30.2 (CH_2) (C3' and C4'), 30.38 (CH_2), 30.42 (CH_2) (C2' and C5'), 31.3 (CH_2, C8'), 32.3 (CH_2, C3), 40.2 (CH_2, C1'), 47.4 (CH_2, 2-CH_2-CO), 49.3 (CH_2, C9'), 56.4 (CH_3, 7-OCH_3), 75.6 (C, C2), 102.2 (CH, C8), 113.31 (C, C9a"), 113.35 (C, C4a), 115.4 (C, C8a"), 116.1 (CH, C5), 119.1 (CH, C5"), 126.7 (CH, C7"), 128.8 (CH, C8"), 140.1 (C, C6"), 140.5 (C, C10a"), 141.1 (C, C6), 147.4 (C, C8a), 148.3 (C, C7), 152.0 (C, C4a"), 157.8 (C, C9"), 172.4 (C, CONH).

HRMS (ESI):

Calculated for ($C_{34}H_{44}{}^{35}ClN_3O_4 + H^+$): 594.3093

Found: 594.3096

Preparation of (±)-*N*-{8-[(6-chloro-1,2,3,4-tetrahydroacridin-9-yl)amino]-3,6-dioxaoctyl}-2-(6-hydroxy-7-methoxy-2-methylchroman-2-yl)acetamide, (±)-57e

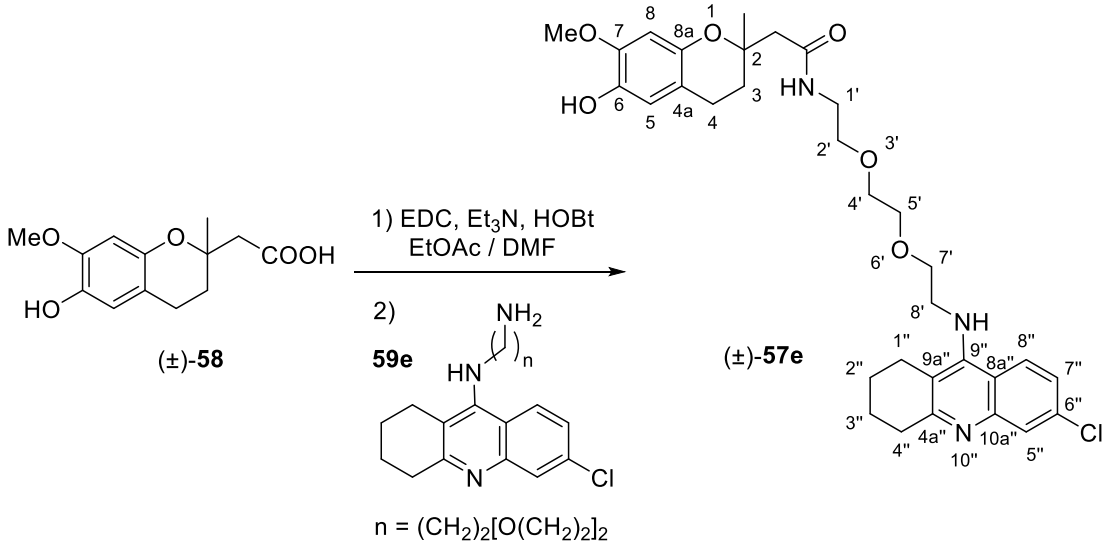

In a 25 mL round-bottomed flask equipped with a magnetic stirrer, the acid (±)-**58** (130 mg, 0.52 mmol) was dissolved in a mixture of EtOAc (7.5 mL) and DMF (0.8 mL), and treated with *N*-(3-dimethylaminopropyl)-*N'*-ethylcarbodiimide hydrochloride (120 mg, 0.63 mmol), triethylamine (0.14 mL, 102 mg, 1.01 mmol), and 1-hydroxy-1*H*-benzotriazole (105 mg, 0.77 mmol). The resulting mixture was stirred at room temperature for 15 minutes and then treated with a suspension of the amine **59e** (206 mg, 0.57 mmol) in a mixture of EtOAc (8 mL) and DMF (0.8 mL). The reaction mixture was stirred at room temperature for 1 day and concentrated under reduced pressure to give a dark brown sticky solid (617 mg), which was subjected to column chromatography purification [silica gel 35−70 μm (52 g); Ø = 3 cm; #1, 250 mL, hexane / Et_3N 100:0.2; #2, 250 mL, hexane / EtOAc / Et_3N 90:10:0.2; #3, 250 mL, hexane / EtOAc / Et_3N 80:20:0.2; #4, 250 mL, hexane / EtOAc / Et_3N 70:30:0.2; #5, 250 mL, hexane / EtOAc / Et_3N 60:40:0.2; #6, 250 mL, hexane / EtOAc / Et_3N 50:50:0.2; #7, 250 mL, hexane / EtOAc / Et_3N 40:60:0.2; #8–11, 500 mL, hexane / EtOAc / Et_3N 30:70:0.2; #12–21, 1 L, hexane / EtOAc / Et_3N 20:80:0.2; #22–41, 2 L, hexane / EtOAc / Et_3N 10:90:0.2; #42–55, 1.25 L, EtOAc / Et_3N 100:0.2], to provide the desired amide (±)-**57e** (#28–52, 281 mg, 91% yield) as a brown-yellow sticky solid.

R_f = 0.79 (silica gel, 10 cm, CH_2Cl_2 / MeOH / 50% aq. NH_4OH 95:5:1).

Analytical sample of (±)-57e·HCl

In a 50 mL round-bottomed flask (±)-**57e** (195 mg, 0.33 mmol) was dissolved in CH_2Cl_2 (2 mL), filtered with a PTFE filter (0.2 µm), treated with HCl / Et_2O (1.35 N, 0.72 mL), evaporated *in vacuo*, and washed with pentane (3 × 2 mL), to give, after drying in standard conditions, (±)-**57e**·HCl (175 mg) as a brown solid.

Melting point: 55–57 °C

Calculated logP: 5.18

IR (ATR) ν: 3600–2400 (max. at 3362, 3250, 3068, 2921, 2860, N–H, $^+$N–H, O–H, C–H st), 1630, 1572, 1509 (C=O, Ar–C–C and Ar–C–N st) cm^{-1}.

^{1}H NMR (400 MHz, CD_3OD) δ: 1.28 (s, 3H, 2-CH_3), 1.68 (dt, J = 13.6 Hz, J' = 6.8 Hz, 1H, 3-H_A), 1.81 (dt, J = 13.6 Hz, J' = 6.8 Hz, 1H, 3-H_B), 1.89–2.00 (complex signal, 4H, 2"-H_2 and 3"-H_2), 2.36 (d, J = 13.6 Hz, 1H, 2-CH_A-CO), 2.46 (d, J = 14.0 Hz, 1H, 2-CH_B-CO), 2.53 (t, J = 6.8 Hz, 2H, 4-H_2), 2.63 (t, J = 6.0 Hz, 2H, 1"-H_2), 2.98 (t, J = 5.6 Hz, 2H, 4"-H_2), 3.33 (dt, J = 14.0 Hz, J' = 5.2 Hz, 1H, 1'-H_A), 3.38 (dt, J = 14.0 Hz, J' = 5.2 Hz, 1H, 1'-H_B), 3.53 (t, J = 5.6 Hz, 2H, 2-H_2), 3.62 (dt, J = 5.2 Hz, J' = 4.0 Hz, 2H, 4'-H_A and 5'-H_A), 3.66 (complex signal, 2H, 4'-H_B and 5'-H_B), 3.71 (s, 3H, 7-OCH_3), 3.84 (t, J = 4.8 Hz, 2H, 7'-H_2), 4.10 (t, J = 4.8 Hz, 2H, 8'-H_2), 4.85 (s, NH, $^+$NH, OH), 6.33 (s, 1H, 8-H), 6.35 (s, 1H, 5-H), 7.52 (dd, J = 9.2 Hz, J' = 2.0 Hz, 1H, 7"-H), 7.74 (d, J = 2.0 Hz, 1H, 5"-H), 8.41 (d, J = 9.2 Hz, 1H, 8"-H).

^{13}C NMR (100.6 MHz, CD_3OD) δ: 21.7 (CH_2, C3"), 22.2 (CH_2, C4), 22.7 (CH_2, C2"), overlapped 24.4 (CH_3, 2-CH_3, and CH_2, C1"), 29.3 (CH_2, C4"), 32.6 (CH_2, C3), 40.2 (CH_2, C1'), 46.7 (CH_2, 2-CH_2-CO), 49.3 (CH_2, C8'), 56.5 (CH_3, 7-OCH_3), 70.2 (CH_2, C7'), 70.4 (CH_2, C2'), 71.0 (CH_2), 71.3 (CH_2) (C4 and C5), 75.4 (C, C2), 102.5 (CH, C8), 113.4 (C, C4a), 113.6 (C, C9a"), 115.6 (C, C8a"), 116.0 (CH, C5), 119.1 (CH, C5"), 126.7 (CH, C7"), 128.9 (CH, C8"), 140.0 (C, C6"), 140.4 (C, C10a"), 141.2 (C, C6), 146.9 (C, C8a), 148.2 (C, C7), 152.3 (C, C4a"), 158.3 (C, C9"), 172.7 (C, CONH).

HRMS (ESI):

Calculated for ($C_{32}H_{40}{}^{35}ClN_3O_6$ + H^+): 598.2678

Found: 598.2692

Preparation of 6-chloro-1,2,3,4-tetrahydro-9-acridinamine, 13

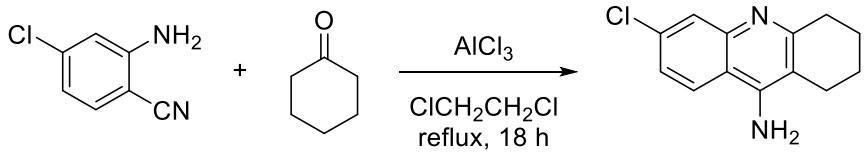

72 **66** **13**

In a triple necked 2 L round-bottomed flask equipped with a magnetic stirrer, a condenser and an anhydrous atmosphere, a suspension of $AlCl_3$ (16.2 g, 122 mmol) and 2-amino-4-chlorobenzonitrile, **72** (14.0 g, 91.8 mmol), in anhydrous 1,2-dichloroethane (140 mL) was prepared, then treated with a solution of cyclohexanone, **66** (8.4 mL, 9.95 g, 85.4 mmol), in anhydrous 1,2-dichloroethane (600 mL). The resulting mixture was stirred under reflux for 18 hours, then cooled to room temperature, diluted with THF (500 mL) and water (400 mL), and stirred at room temperature for 30 minutes. The organic solvents were evaporated under reduced pressure and the residue was filtered off. The resulting yellow solid was crystallized in EtOAc (300 mL) to obtain the desired compound **13** (18.9 g, quantitative yield) as a yellow solid.

R_f = 0.29 (silica gel, 10 cm, CH_2Cl_2 / MeOH / NH_4OH 95:5:1).

Preparation of 7-[(6-chloro-1,2,3,4-tetrahydroacridin-9-yl)amino]heptanenitrile, 73a

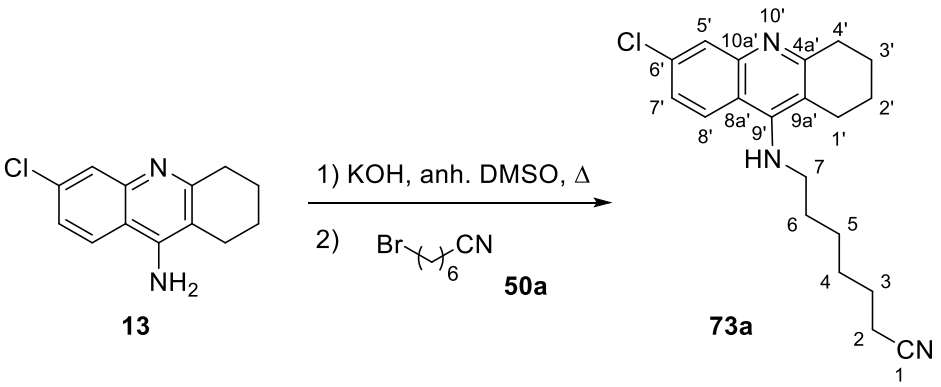

In a double necked 50 mL round-bottomed flask provided with an inert atmosphere, a magnetic stirrer and 4 Å molecular sieves, tacrine **13** (1.00 g, 4.23 mmol) and finely powdered KOH (85% purity, 567 mg, 8.59 mmol) were suspended in anhydrous DMSO (18 mL). The resulting suspension was stirred, heating every 10 minutes with a heat gun for 1 hour, and at room temperature one more hour, then treated with 7-bromoheptanenitrile, **50a** (0.74 mL, 936 mg, 4.92 mmol). The reaction mixture was stirred at room temperature overnight, then diluted with 5 N NaOH aq. sol. (100 mL), and extracted with EtOAc (3 × 80 mL). The combined organic layers were washed with water (4 × 80 mL) and brine (50 mL), dried with anhydrous Na_2SO_4, filtered and evaporated under reduced pressure to give a clear brown oil (1.54 g), which was purified by column chromatography [silica gel 35−70 µm (54 g); Ø = 3.2 cm; #1–42, 3.75 L, CH_2Cl_2 / 50% aq. NH_4OH 100:0.4; #43–45, 250 mL, CH_2Cl_2 / MeOH / 50% aq. NH_4OH 95:5:0.4], to provide the desired nitrile **73a** (#23–32, 1.27 g, 86% yield) as a clear yellow oil.

R_f = 0.80 (gel de sílice, 10 cm, CH_2Cl_2 / MeOH / NH_4OH 50% 90:10:1).

Analytical sample of 73a·HCl

In a 25 mL round-bottomed flask **73a** (34 mg, 0.10 mmol) was dissolved in CH_2Cl_2 (1 mL), filtered with a PTFE filter (0.2 µm), treated with HCl / dioxane (4 M, 0.07 mL), evaporated *in vacuo*, and washed with pentane (3 × 2 mL), giving, after drying in standard conditions, **73a**·HCl (37 mg) as a yellow solid.

Melting point: 86–87 °C.

IR (ATR) *v*: 3500–2500 (max at 3347, 3138, 3059, 2949, 2928, 2858, 2744, $^{+}$NH, NH, CH st), 2245 (CN st), 1639, 1605, 1573, 1524 (Ar–C–C and Ar–C–N st) cm^{-1}.

^{1}H NMR (400 MHz, CD_3OD) *δ*: 1.46–1.54 (complex signal, 4H, 4-H_2 and 5-H_2), 1.66 (tt, *J* = 7.2 Hz, *J'* = 6.8 Hz, 2H, 3-H_2), 1.87 (tt, *J* = *J'* = 7.2 Hz, 2H, 6-H_2), 1.92–2.02 (complex signal, 4H, 2'-H_2 and 3'-H_2), 2.45 (t, *J* = 7.2 Hz, 2H, 2-H_2), 2.69 (broad t, *J* = 6.0 Hz, 2H, 1'-H_2), 3.01 (broad t, *J* = 5.6 Hz, 2H, 4'-H_2), 3.96 (t, *J* = 7.2 Hz, 2H, 7-H_2), 4.84 (s, $^{+}$NH, NH), 7.56 (dd, *J* = 9.2 Hz, *J'* = 2.4 Hz, 1H, 7'-H), 7.79 (d, *J* = 2.4 Hz, 1H, 5'-H), 8.39 (d, *J* = 9.2 Hz, 1H, 8'-H).

^{13}C NMR (100.6 MHz, CD_3OD) *δ*: 17.2 (CH_2, C2), 21.7 (CH_2, C3'), 22.9 (CH_2, C2'), 24.8 (CH_2, C1'), 26.3 (CH_2, C3), 26.9 (CH_2, C5), 29.29 (CH_2), 29.34 (CH_2) (C4 and C4'), 31.1 (CH_2, C6), 49.1 (CH_2, C7), 113.4 (C), 115.4 (C) (C8a' and C9a'), 119.1 (CH, C5'), 121.2 (C, C1), 126.8 (CH, C7'), 128.8 (CH, C8'), 140.1 (CH, C6'), 140.5 (C, C10a'), 152.2 (C, C4a'), 157.8 (C, C9').

HRMS (ESI):

Calculated for ($C_{20}H_{24}{}^{35}ClN_3 + H^+$):	342.1732
Found:	342.1737

Preparation of 8-bromooctanenitrile, 50b

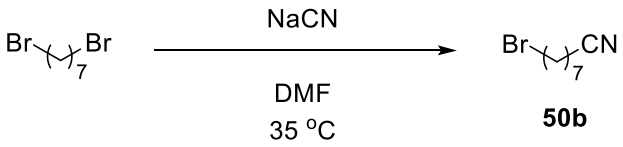

In a triple necked 100 mL round-bottomed flask provided with an inert atmosphere, a magnetic stirrer and a condenser, 1,7-dibromoheptane (3.31 mL, 5.00 g, 19.4 mmol) and NaCN (950 mg, 19.4 mmol) were dissolved in anhydrous DMF (30 mL). The reaction mixture was stirred at 35 °C for 2 hours, then treated with water (50 mL) and extracted with Et_2O (3 × 50 mL). The combined organic layers were washed with water (3 × 50 mL) and saturated NaCl aqueous solution (3 × 50 mL), dried with anhydrous Na_2SO_4, filtered and evaporated under reduced pressure to give a colourless oil (4.29 g), which was purified by micro-distillation at 150 °C to provide the desired compound **50b** (4.172 g, quantitative yield) as a colourless oil.

Preparation of 8-[(6-chloro-1,2,3,4-tetrahydroacridin-9-yl)amino]octanenitrile, 73b

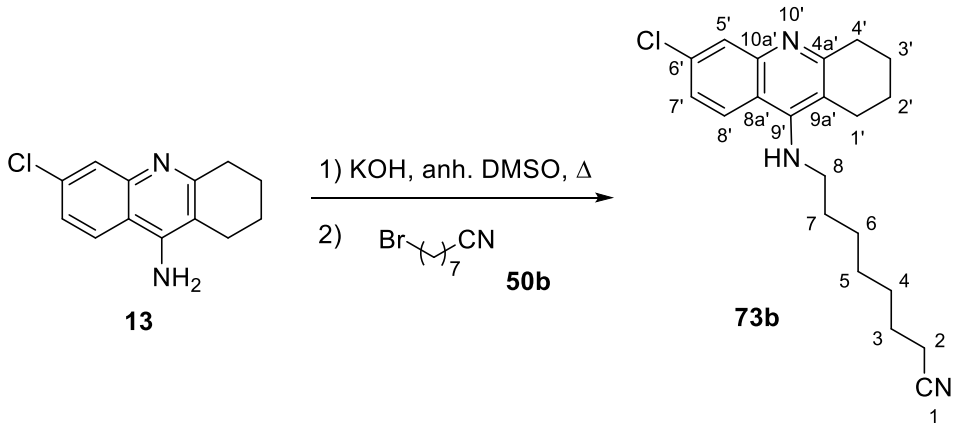

In a double necked 50 mL round-bottomed flask equipped with an inert atmosphere, a magnetic stirrer and 4 Å molecular sieves, tacrine **13** (1.00 g, 4.23 mmol) and finely powdered KOH (85% purity, 567 mg, 8.59 mmol) were suspended in anhydrous DMSO (18 mL). The resulting suspension was stirred, heating every 10 minutes with a heat gun for 1 hour, and at room temperature one more hour, then treated with 8-bromooctanenitrile, **50b** (1.01 g, 4.94 mmol). The reaction mixture was stirred at room temperature overnight, then diluted with 5 N NaOH aq. sol. (100 mL), and extracted with EtOAc (3 × 80 mL). The combined organic layers were washed with water (4 × 80 mL) and brine (50 mL), dried with anhydrous Na_2SO_4, filtered and evaporated under reduced pressure to give a clear brown oil (1.63 g), which was purified by column chromatography [silica gel 35−70 μm (65 g); Ø = 4 cm; #1–4, 250 mL, hexane / Et_3N 100:0.2; #5–8, 250 mL, hexane / EtOAc / Et_3N 95:5:0.2; #9–11, 250 mL, hexane / EtOAc / Et_3N 90:10:0.2, #12–22, 1 L, hexane / EtOAc / Et_3N 85:15:0.2; #23–30, 750 mL, hexane / EtOAc / Et_3N 80:20:0.2; #31–45, 1.5 L, hexane / EtOAc / Et_3N 75:25:0.2; #46–49, 500 mL, EtOAc / Et_3N 100:0.2], to provide the desired nitrile **73b** (#32–48, 993 g, 65% yield) as a yellow oil.

R_f = 0.80 (gel de sílice, 10 cm, CH_2Cl_2 / MeOH / NH_4OH 50% 90:10:1).

Analytical sample of 73b·HCl

In a 25 mL round-bottomed flask **73b** (34 mg, 0.10 mmol) was dissolved in CH_2Cl_2 (1.5 mL), filtered with a PTFE filter (0.2 μm), treated with HCl / dioxane (4 M, 0.07 mL), evaporated *in vacuo*, and washed with pentane (3 × 2 mL), giving, after drying in standard conditions, **73b**·HCl (40 mg) as a yellow solid.

Melting point: 210–213 °C.

IR (ATR) *v*: 3500–2500 (max at 3251, 3052, 2934, 2853, 2711, $^{+}$NH, NH, CH st), 2246 (CN st), 1633, 1616, 1588, 1567, 1542, 1517 (Ar–C–C and Ar–C–N st) cm^{-1}.

^{1}H NMR (400 MHz, CD_3OD) *δ*: 1.40–1.52 (complex signal, 6H, 4-H_2, 5-H_2 and 6-H_2), 1.64 (tt, *J* = *J'* = 7.2 Hz, 2H, 3-H_2), 1.85 (tt, *J* = *J'* = 7.2 Hz, 2H, 7-H_2), 1.92–2.00 (complex signal, 4H, 2'-H_2 and 3'-H_2), 2.43 (t, *J* = 7.2 Hz, 2H, 2-H_2), 2.68 (broad t, *J* = 6.0 Hz, 2H, 1'-H_2), 3.00 (broad t, *J* = 6.0 Hz, 2H, 4'-H_2), 3.95 (t, *J* = 7.2 Hz, 2H, 8-H_2), 4.85 (s, $^{+}$NH, NH), 7.57 (dd, *J* = 9.2 Hz, *J'* = 2.0 Hz, 1H, 7'-H), 7.77 (d, *J* = 2.0 Hz, 1H, 5'-H), 8.39 (d, *J* = 9.2 Hz, 1H, 8'-H).

^{13}C NMR (100.6 MHz, CD_3OD) *δ*: 17.2 (CH_2, C2), 21.8 (CH_2, C3'), 22.9 (CH_2, C2'), 24.7 (CH_2, C1'), 26.3 (CH_2, C3), 27.4 (CH_2, C6), 29.36 (CH_2), 29.40 (CH_2) (C4 and C4'), 29.6 (CH_2, C5), 31.2 (CH_2, C7), 49.2 (CH_2, C8), 113.4 (C), 115.5 (C) (C8a' and C9a'), 119.2 (CH, C5'), 121.2 (C, C1), 126.8 (CH, C7'), 128.8 (CH, C8'), 140.1 (CH, C6'), 140.6 (C, C10a'), 152.2 (C, C4a'), 157.8 (C, C9').

HRMS (ESI):

Calculated for ($C_{21}H_{26}{}^{35}ClN_3 + H^+$):	356.1888
Found:	356.1878

Preparation of 9-[(6-chloro-1,2,3,4-tetrahydroacridin-9-yl)amino]nonanenitrile, 73c

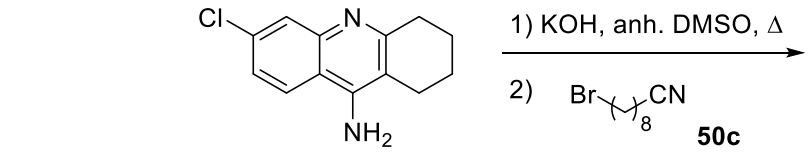

13

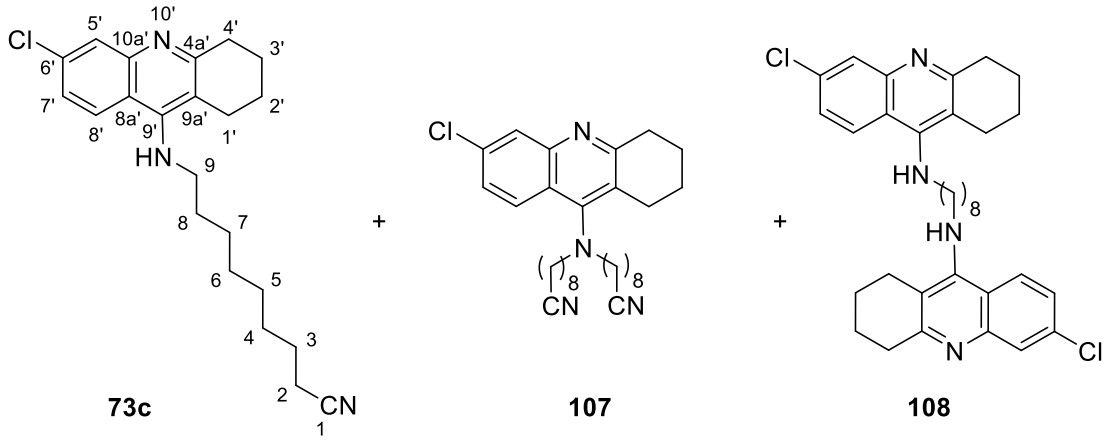

73c **107** **108**

In a double necked 50 mL round-bottomed flask equipped with an inert atmosphere, a magnetic stirrer and 4 Å molecular sieves, tacrine **13** (1 g, 4.23 mmol) and finely powdered KOH (85% purity, 567 mg, 8.59 mmol) were suspended in anhydrous DMSO (18 mL). The resulting suspension was stirred, heating every 10 minutes with a heat gun for 1 hour, and at room temperature one more hour, then treated with 9-bromononanenitrile, **50c** (1.078 g, 4.94 mmol). The reaction mixture was stirred at room temperature overnight, then diluted with 5 N NaOH aq. sol. (100 mL), and extracted with EtOAc (3 × 80 mL). The combined organic layers were washed with water (4 × 80 mL) and brine (50 mL), dried with anhydrous Na_2SO_4, filtered and evaporated under reduced pressure to give a dark brown oil (1.70 g), which was subjected to column chromatography purification [silica gel 35−70 μm (60 g); Ø = 3.2 cm; #1–50, 4.5 L, CH_2Cl_2 / 50% aq. NH_4OH 100:0.4; #51–56, 500 mL, CH_2Cl_2 / MeOH / 50% aq. NH_4OH 95:5:0.4], to provide a mixture of desired compound **73c** / dialkylated tacrine **107** in a ratio 1:0.07 (^{1}H-NMR) (#27–31, 217 mg, 13% yield of the desired nitrile) as a yellow oil, the desired nitrile **73c** (#32–38, 524 mg, 33% yield) as a yellow oil, and a mixture desired compound **73c** / bis-tacrine **108**[211] in a ratio 1:0.09 (^{1}H-NMR) (#39–47, 477 mg, 27% yield of the desired nitrile) as a yellow oil. The overall yield for the desired nitrile **73c** was 73% yield.

[211] M.-K. Hu, C.-F. Lu. *Tetrahedron Lett.* **2000**, *41*, 1815.

R_f = 0.82 (gel de sílice, 10 cm, CH_2Cl_2 / MeOH / NH_4OH 50% 90:10:1).

Analytical sample of 73c·HCl

In a 25 mL round-bottomed flask **73c** (30 mg, 0.08 mmol) was dissolved in CH_2Cl_2 (1 mL), filtered with a PTFE filter (0.2 µm), treated with HCl / dioxane (4 M, 0.06 mL), evaporated *in vacuo*, and washed with pentane (3 × 2 mL), giving, after drying in standard conditions, **73c**·HCl (32 mg) as a yellow solid.

Melting point: 176–177 °C.

IR (ATR) *v*: 3500–2500 (max at 3248, 3048, 2931, 2852, 2714, $^+$NH, NH, CH st), 2246 (CN st), 1632, 1589, 1566, 1523 (Ar–C–C and Ar–C–N st) cm^{-1}.

^{1}H NMR (400 MHz, CD_3OD) *δ*: 1.36–1.50 (complex signal, 8H, 4-H_2, 5-H_2, 6-H_2 and 7-H_2), 1.62 (tt, *J* = *J'* = 7.2 Hz, 2H, 3-H_2), 1.85 (tt, *J* = *J'* = 7.2 Hz, 2H, 8-H_2), 1.91–2.02 (complex signal, 4H, 2'-H_2 and 3'-H_2), 2.43 (t, *J* = 7.2 Hz, 2H, 2-H_2), 2.68 (broad t, *J* = 6.0 Hz, 2H, 1'-H_2), 3.00 (broad t, *J* = 6.4 Hz, 2H, 4'-H_2), 3.95 (t, *J* = 7.2 Hz, 2H, 9-H_2), 4.85 (s, $^+$NH, NH), 7.56 (dd, *J* = 9.2 Hz, *J'* = 2.0 Hz, 1H, 7'-H), 7.78 (d, *J* = 2.0 Hz, 1H, 5'-H), 8.39 (d, *J* = 9.2 Hz, 1H, 8'-H).

^{13}C NMR (100.6 MHz, CD_3OD) *δ*: 17.3 (CH_2, C2), 21.8 (CH_2, C3'), 22.9 (CH_2, C2'), 24.7 (CH_2, C1'), 26.4 (CH_2, C3), 27.6 (CH_2, C7), 29.3 (CH_2, C4'), 29.6 (CH_2), 29.7 (CH_2), 30.0 (CH_2) (C4, C5 and C6), 31.3 (CH_2, C8), 49.3 (CH_2, C9), 113.4 (C), 115.5 (C) (C8a' and C9a'), 119.2 (CH, C5'), 121.2 (C, C1), 126.8 (CH, C7'), 128.8 (CH, C8'), 140.1 (CH, C6'), 140.5 (C, C10a'), 152.1 (C, C4a'), 157.9 (C, C9').

HRMS (ESI):

Calculated for ($C_{22}H_{28}{}^{35}ClN_3$ + H^+):	370.2045
Found:	370.2037

Preparation of (±)-7-[(6-chloro-1,2,3,4-tetrahydroacridin-9-yl)amino]-*N*-[2-(6-hydroxy-7-methoxy-2-methylchroman-2-yl)ethyl]heptanamide, (±)-60a

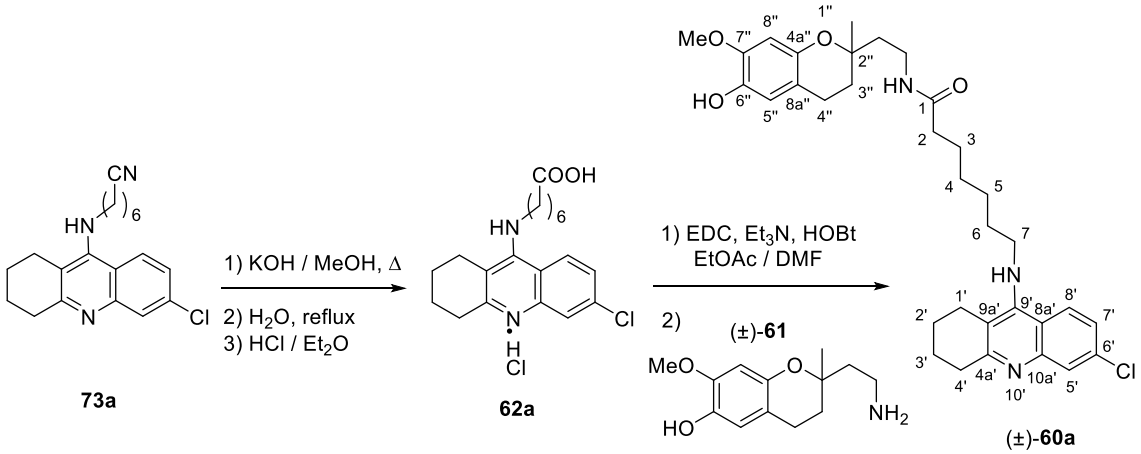

In a 50 mL round-bottomed flask equipped with a magnetic stirrer and a condenser, nitrile **73a** (462 mg, 1.35 mmol) was dissolved in MeOH (2 mL) and treated with a 40% solution of KOH in MeOH (3.7 mL). The resulting suspension was stirred under reflux for 3 hours, then treated with water (4.7 mL), and again stirred under reflux overnight. The resulting solution was cooled to room temperature, evaporated under reduced pressure, and treated with HCl / dioxane (4 M, 6.8 mL), and concentrated *in vacuo* to give a yellow solid (2.46 g), whose ^{1}H-NMR spectra was consistent with that expected for the desired acid, **62a**·HCl, and was used as a crude in the next step.

In a 50 mL round-bottomed flask provided with a magnetic stirrer, the acid **62a**·HCl (2.46 g of a crude that could contain a maximum of 1.35 mmol of the desired acid) was suspended in a mixture of EtOAc (10.3 mL) and DMF (4 mL), and treated with *N*-(3-dimethylaminopropyl)-*N'*-ethylcarbodiimide hydrochloride (157 mg, 0.82 mmol), triethylamine (0.28 mL, 204 mg, 2.02 mmol), and 1-hydroxy-1*H*-benzotriazole (138 mg, 1.01 mmol). The resulting mixture was stirred at room temperature for 15 minutes, then treated with a suspension of the amine (±)-**61** (159 mg, 0.68 mmol) in a mixture of EtOAc (10 mL) and DMF (1 mL), stirred at room temperature for 1 day, and concentrated *in vacuo* to give a brown sticky solid (3.30 g), which was subjected to column chromatography purification [silica gel 35−70 μm (100 g); Ø = 4 cm; #1–4, 250 mL, hexane / Et_3N 100:0.2; #5–7, 250 mL, hexane / EtOAc / Et_3N 90:10:0.2; #8–10, 250 mL, hexane / EtOAc / Et_3N 80:20:0.2; #11–13, 250 mL, hexane / EtOAc / Et_3N 70:30:0.2; #14–15, 250 mL, hexane / EtOAc / Et_3N 60:40:0.2; #16–20, 500 mL, hexane / EtOAc / Et_3N 50:50:0.2; #21–25, 500

mL, hexane / EtOAc / Et_3N 40:60:0.2; #26–30, 500 mL, hexane / EtOAc / Et_3N 30:70:0.2; #31–35, 500 mL, hexane / EtOAc / Et_3N 20:80:0.2; #36–40, 500 mL, hexane / EtOAc / Et_3N 10:90:0.2; #41–70, 2.75 L, EtOAc / Et_3N 100:0.2], to provide the desired amide (±)-**60a** (#42–65, 337 mg, 87% overall yield) as a white-yellow solid.

R_f = 0.57 (silica gel, 10 cm, CH_2Cl_2 / MeOH / 50% aq. NH_4OH 95:5:1).

Analytical sample of (±)-60a·HCl

In a 50 mL round-bottomed flask (±)-**60a** (220 mg, 0.36 mmol) was dissolved in CH_2Cl_2 (2 mL), filtered with a PTFE filter (0.2 μm), treated with HCl / Et_2O (1.35 N, 0.8 mL), evaporated *in vacuo*, and washed with pentane (3 × 2 mL), to give, after drying in standard conditions, (±)-**60a**·HCl (209 mg) as a yellow solid.

Melting point: 121–123 °C

Calculated logP: 7.45

IR (ATR) ν: 3600–2400 (max. at 3245, 3068, 2926, 2850, N–H, $^+$N–H, O–H, C–H st), 1630, 1572, 1509 (C=O, Ar–C–C and Ar–C–N st) cm^{-1}.

^{1}H NMR (400 MHz, CD_3OD) δ: 1.25 (s, 3H, 2”-CH_3), superimposed in part 1.35 (tt, J = J' = 6.4 Hz, 2H, 4-H_2), 1.43 (tt, J = J' = 7.2 Hz, 2H, 5-H_2), 1.59 (tt, J = J' = 7.2 Hz, 2H, 3-H_2), 1.70 (dt, J = 13.6 Hz, J' = 6.8 Hz, 1H, 3”-H_A), 1.73 (dt, J = 13.6 Hz, J' = 6.0 Hz, 1H, 2”-CH_A-CH_2-NHCO), 1.78 (dt, J = 13.6 Hz, J' = 6.8 Hz, 1H, 3”-H_B), 1.79 (tt, J = J' = 6.8 Hz, 2H, 6-H_2), 1.82 (dt, J = 13.6 Hz, J' = 6.4 Hz, 1H, 2”-CH_B-CH_2-NHCO), 1.90–2.00 (complex signal, 4H, 2”-H_2 and 3”-H_2), 2.16 (t, J = 7.2 Hz, 2H, 2-H_2), 2.60 (t, J = 6.8 Hz, 2H, 4”-H_2), 2.66 (broad t, J = 5.6 Hz, 2H, 1’-H_2), 2.99 (broad t, J = 5.6 Hz, 2H, 4’-H_2), 3.27 (ddd, J = 13.2 Hz, J' = 9.2 Hz, J'' = 6.0 Hz, 1H, CH_A-NHCO), 3.39 (ddd, J = 13.2 Hz, J' = 9.2 Hz, J'' = 6.0 Hz, 1H, CH_B-NHCO), 3.74 (s, 3H, 7”-OCH_3), 3.90 (t, J = 7.2 Hz, 2H, 7-H_2), 4.86 (s, NH, $^+$NH, OH), 6.30 (s, 1H, 8”-H), 6.42 (s, 1H, 5”-H), 7.55 (dd, J = 9.2 Hz, J' = 2.0 Hz, 1H, 7’-H), 7.76 (d, J = 2.0 Hz, 1H, 5’-H), 8.36 (d, J = 9.2 Hz, 1H, 8’-H).

^{13}C NMR (100.6 MHz, CD_3OD) δ: 21.7 (CH_2, C3’), 22.3 (CH_2, C4”), 22.8 (CH_2, C2’), 24.3 (CH_3, 2”-CH_3), 24.7 (CH_2, C1’, 26.7 (CH_2, C3), 27.4 (CH_2, C5), 29.3 (CH_2, C4’), 29.7 (CH_2, C4), 31.1 (CH_2, C6),

32.6 (CH_2, C3”), 35.9 (CH_2, CH_2-NHCO), 36.9 (CH_2, C2), 39.4 (CH_2, C2”-*C*H_2-CH_2-NHCO), 49.1 (CH_2, C7), 56.3 (CH_3, 7”-OCH_3), 75.8 (C, C2”), 102.2 (CH, C8”), 113.3 (C, C9a’), 113.4 (C, C4a”), 115.4 (C, C8a’), 116.1 (CH, C5”), 119.1 (CH, C5’), 126.8 (CH, C7’), 128.8 (CH, C8’), 140.1 (C, C6’), 140.5 (C, C10a’), 140.8 (C, C6”), 147.7 (C, C8a”), 148.3 (C, C7”), 152.0 (C, C4a’), 157.8 (C, C9’), 175.9 (C, CONH).

HRMS (ESI):

Calculated for ($C_{33}H_{42}{}^{35}ClN_3O_4 + H^+$): 580.2937

Found: 580.2946

Preparation of (±)-8-[(6-chloro-1,2,3,4-tetrahydroacridin-9-yl)amino]-*N*-[2-(6-hydroxy-7-methoxy-2-methylchroman-2-yl)ethyl]octanamide, (±)-60b

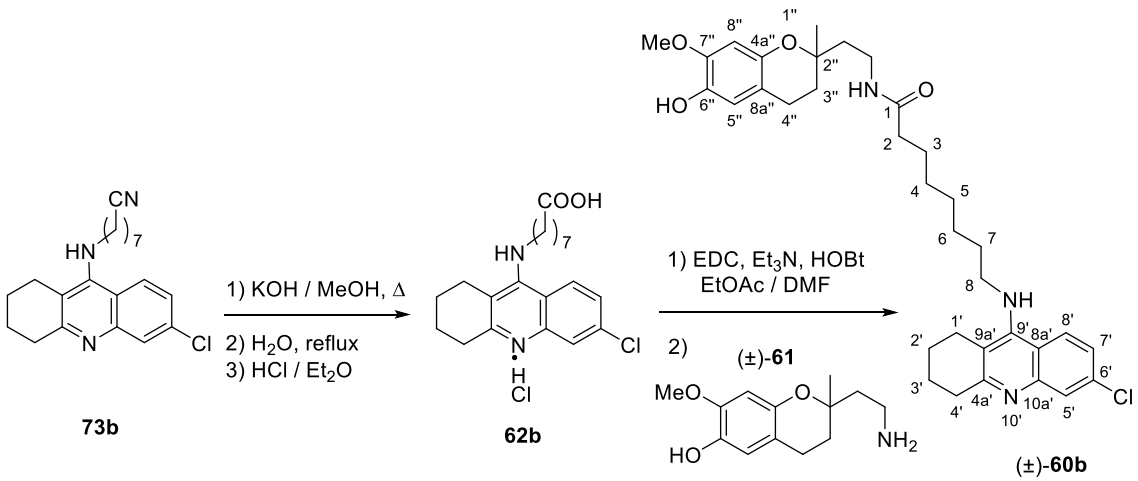

In a 25 mL round-bottomed flask equipped with a magnetic stirrer and a refrigerant, nitrile **73b** (367 mg, 1.03 mmol) was dissolved in MeOH (1.6 mL) and treated with a 40% solution of KOH in MeOH (2.8 mL). The resulting suspension was stirred under reflux for 3 hours, then treated with water (3.6 mL), and again stirred under reflux overnight. The resulting solution was cooled to room temperature, evaporated under reduced pressure, and treated with HCl / Et_2O (2.35 N, 8.8 mL), and concentrated *in vacuo* to give a yellow solid (1.93 g), whose ^{1}H-NMR spectra was consistent with that expected for the desired acid, **62b**·HCl, and was used as a crude in the next step.

In a 25 mL round-bottomed flask provided with a magnetic stirrer, the acid **62b**·HCl (1.93 g of a crude that could contain a maximum of 1.03 mmol of the desired acid) was suspended in a mixture of EtOAc (6.8 mL) and DMF (0.8 mL), and treated with *N*-(3-dimethylaminopropyl)-*N'*-ethylcarbodiimide hydrochloride (99 mg, 0.52 mmol), triethylamine (0.18 mL, 131 mg, 1.30 mmol), and 1-hydroxy-1*H*-benzotriazole (87 mg, 0.64 mmol). The resulting mixture was stirred at room temperature for 15 minutes, then treated with a suspension of the amine (±)-**61** (100 mg, 0.43 mmol) in a mixture of EtOAc (6 mL) and DMF (0.5 mL), stirred at room temperature for 1 day, and concentrated *in vacuo* to give a brown sticky solid (2.29 g), which was subjected to column chromatography purification [silica gel 35−70 μm (97 g); Ø = 4 cm; #1–3, 300 mL, hexane / Et_3N 100:0.2; #4–6, 300 mL, hexane / EtOAc / Et_3N 90:10:0.2; #7–9, 300 mL, hexane / EtOAc / Et_3N 80:20:0.2; #10–12, 300 mL, hexane / EtOAc / Et_3N 70:30:0.2; #13–15, 300 mL, hexane / EtOAc / Et_3N 60:40:0.2; #16–20, 500 mL, hexane / EtOAc / Et_3N 50:50:0.2; #21–25, 500 mL,

hexane / EtOAc / Et_3N 40:60:0.2; #26–29, 500 mL, hexane / EtOAc / Et_3N 30:70:0.2; #30–59, 2.5 L, hexane / EtOAc / Et_3N 20:80:0.2; #60–71, 1.3 L, EtOAc / Et_3N 100:0.2], to provide the desired amide (±)-**60b** (#40–53, 139 mg, 55% overall yield) as a yellow solid.

R_f = 0.67 (silica gel, 10 cm, CH_2Cl_2 / MeOH / 50% aq. NH_4OH 95:5:1).

Analytical sample of (±)-60b·HCl

In a 25 mL round-bottomed flask (±)-**60b** (63 mg, 0.10 mmol) was dissolved in CH_2Cl_2 (1 mL), filtered with a PTFE filter (0.2 μm), treated with HCl / Et_2O (1.35 N, 0.22 mL), evaporated *in vacuo*, and washed with pentane (3 × 2 mL), to give, after drying in standard conditions, (±)-**60b**·HCl (64 mg) as a yellow solid.

Melting point: 72–74 °C

Calculated logP: 7.96

IR (ATR) ν: 3600–2200 (max. at 3245, 3063, 2921, 2850, N–H, $^+$N–H, O–H, C–H st), 1630, 1572, 1509 (C=O, Ar–C–C and Ar–C–N st) cm^{-1}.

^{1}H NMR (400 MHz, CD_3OD) δ: 1.25 (s, 3H, 2”-CH_3), 1.28–1.40 (complex signal, 4H, 4-H_2 and 5-H_2), superimposed 1.39 (tt, J = J' = 6.8 Hz, 2H, 6-H_2), 1.57 (tt, J = J' = 7.2 Hz, 2H, 3-H_2), 1.71 (dt, J = 13.6 Hz, J' = 6.8 Hz, 1H, 3”-H_A), 1.73 (dt, J = 13.6 Hz, J' = 6.0 Hz, 1H, 2”-CH_A-CH_2-NHCO), 1.80 (dt, J = 13.6 Hz, J' = 6.8 Hz, 1H, 3”-H_B), 1.81 (tt, J = J' = 6.8 Hz, 2H, 7-H_2), 1.83 (dt, J = 13.6 Hz, J' = 6.0 Hz, 1H, 2”-CH_B-CH_2-NHCO), 1.92–2.00 (complex signal, 4H, 2’-H_2 and 3’-H_2), 2.16 (t, J = 7.2 Hz, 2H, 2-H_2), 2.61 (t, J = 6.4 Hz, 2H, 4”-H_2), 2.66 (broad t, J = 5.6 Hz, 2H, 1’-H_2), 2.99 (broad t, J = 5.6 Hz, 2H, 4’-H_2), 3.29 (ddd, J = 13.2 Hz, J' = 9.2 Hz, J'' = 6.0 Hz, 1H, CH_A-NHCO), 3.40 (ddd, J = 13.2 Hz, J' = 9.2 Hz, J'' = 6.0 Hz, 1H, CH_B-NHCO), 3.75 (s, 3H, 7”-OCH_3), 3.91 (t, J = 7.2 Hz, 2H, 8-H_2), 4.87 (s, NH, $^+$NH, OH), 6.30 (s, 1H, 8”-H), 6.43 (s, 1H, 5”-H), 7.56 (dd, J = 9.2 Hz, J' = 2.0 Hz, 1H, 7’-H), 7.77 (d, J = 2.0 Hz, 1H, 5’-H), 8.37 (d, J = 9.2 Hz, 1H, 8’-H).

^{13}C NMR (100.6 MHz, CD_3OD) δ: 21.8 (CH_2, C3’), 22.3 (CH_2, C4”), 22.8 (CH_2, C2’), 24.2 (CH_3, 2”-CH_3), 24.7 (CH_2, C1’), 26.7 (CH_2, C3), 27.5 (CH_2, C6), 29.3 (CH_2, C4’), 29.9 (CH_2), 30.0 (CH_2) (C4 and C5), 31.4 (CH_2, C7), 32.6 (CH_2, C3”), 36.0 (CH_2, CH_2-NHCO), 37.0 (CH_2, C2), 39.4 (CH_2, C2”-*C*H_2-

CH_2-NHCO), 49.3 (CH_2, C8), 56.3 (CH_3, 7”-OCH_3), 75.8 (C, C2”), 102.2 (CH, C8”), 113.3 (C, C9a’), 113.4 (C, C4a”), 115.4 (C, C8a’), 116.1 (CH, C5”), 119.1 (CH, C5’), 126.8 (CH, C7’), 128.8 (CH, C8’), 140.1 (C, C6’), 140.5 (C, C10a’), 140.8 (C, C6”), 147.7 (C, C8a”), 148.3 (C, C7”), 152.1 (C, C4a’), 157.8 (C, C9’), 176.1 (C, CONH).

HRMS (ESI):

Calculated for ($C_{34}H_{44}{}^{35}ClN_3O_4 + H^+$): 594.3093

Found: 594.3092

Preparation of (±)-9-[(6-chloro-1,2,3,4-tetrahydroacridin-9-yl)amino]-*N*-[2-(6-hydroxy-7-methoxy-2-methylchroman-2-yl)ethyl]nonanamide, (±)-60c

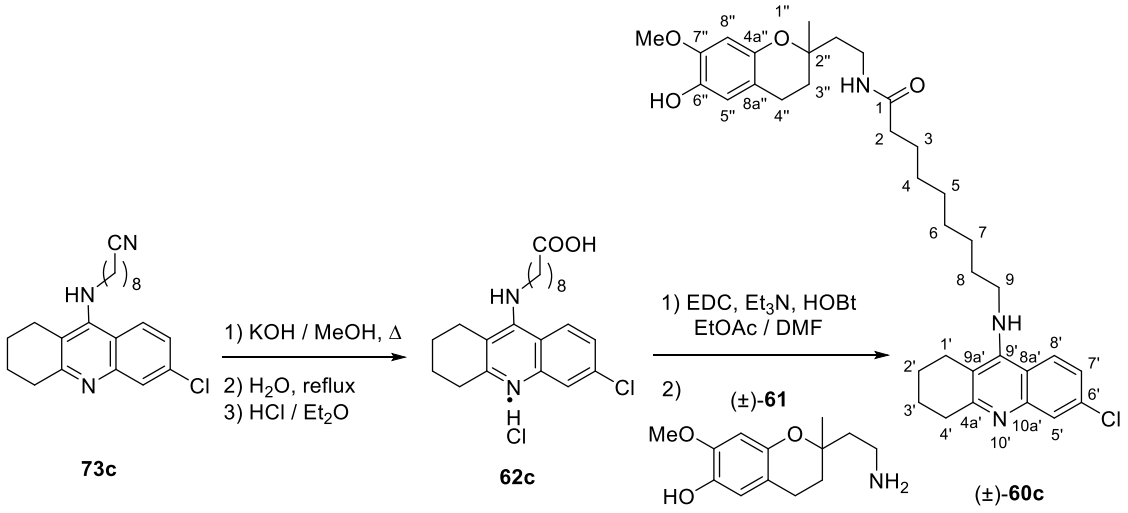

73c **62c** (±)-**60c**

In a 50 mL round-bottomed flask provided with a magnetic stirrer and a condenser, nitrile **73c** (315 mg, 0.85 mmol) was dissolved in MeOH (1.3 mL) and treated with a 40% solution of KOH in MeOH (2.3 mL). The resulting suspension was stirred under reflux for 3 hours, then treated with water (3 mL), and again stirred under reflux overnight. The resulting solution was cooled to room temperature, evaporated under reduced pressure, and treated with HCl / Et_2O (2.35 N, 7.3 mL), and concentrated *in vacuo* to give a pale yellow solid (1.55 g), whose ^{1}H-NMR spectra was consistent with that expected for the desired acid, **62c**·HCl, and was used as a crude in the next step.

In a 50 mL round-bottomed flask equipped with a magnetic stirrer, the acid **62c**·HCl (1.55 g of a crude that could contain a maximum of 0.85 mmol of the desired acid) was suspended in a mixture of EtOAc (10 mL) and DMF (1 mL), and treated with *N*-(3-dimethylaminopropyl)-*N'*-ethylcarbodiimide hydrochloride (132 mg, 0.69 mmol), triethylamine (0.24 mL, 175 mg, 1.73 mmol), and 1-hydroxy-1*H*-benzotriazole (116 mg, 0.85 mmol). The resulting mixture was stirred at room temperature for 15 minutes, then treated with a suspension of the amine (±)-**61** (133 mg, 0.57 mmol) in a mixture of EtOAc (7 mL) and DMF (0.7 mL), stirred at room temperature for 1 day, and concentrated *in vacuo* to give a brown oil (2.21 g), which was subjected to column chromatography purification [silica gel 35−70 µm (100 g); Ø = 4 cm; #1, 250 mL, hexane / Et_3N 100:0.2; #2, 250 mL, hexane / EtOAc / Et_3N 90:10:0.2; #3, 250 mL, hexane / EtOAc / Et_3N 80:20:0.2; #4, 250 mL, hexane / EtOAc / Et_3N 70:30:0.2; #5, 250 mL, hexane / EtOAc / Et_3N

60:40:0.2; #6, 250 mL, hexane / EtOAc / Et_3N 50:50:0.2; #7, 500 mL, hexane / EtOAc / Et_3N 40:60:0.2; #8, 500 mL, hexane / EtOAc / Et_3N 30:70:0.2; #9–15, 500 mL, hexane / EtOAc / Et_3N 20:80:0.2; #16–36, 2 L, hexane / EtOAc / Et_3N 10:90:0.2; #37–45, 1 L, EtOAc / Et_3N 100:0.2], to provide the desired amide (±)-**60c** (#20–25, 189 mg, 52% overall yield) as a pale yellow solid.

R_f = 0.69 (silica gel, 10 cm, CH_2Cl_2 / MeOH / 50% aq. NH_4OH 95:5:1).

Analytical sample of (±)-60c·HCl

In a 25 mL round-bottomed flask (±)-**60c** (88 mg, 0.14 mmol) was dissolved in CH_2Cl_2 (1 mL), filtered with a PTFE filter (0.2 μm), treated with HCl / Et_2O (1.35 N, 0.3 mL), evaporated *in vacuo*, and washed with pentane (3 × 2 mL), to give, after drying in standard conditions, (±)-**60c**·HCl (88 mg) as a yellow solid.

Melting point: 107–111 °C

Calculated logP: 8.38

IR (ATR) ν: 3600–2200 (max. at 3314, 3242, 3057, 2921, 2849, N–H, $^+$N–H, O–H, C–H st), 1625, 1571, 1518 (C=O, Ar–C–C and Ar–C–N st) cm^{-1}.

^{1}H NMR (400 MHz, CD_3OD) δ: 1.26 (s, 3H, 2”-CH_3), 1.26–1.38 (complex signal, 6H, 4-H_2, 5-H_2, and 6-H_2), superimposed in part 1.42 (tt, J = J' = 7.6 Hz, 2H, 7-H_2), 1.57 (tt, J = J' = 7.2 Hz, 2H, 3-H_2), 1.72 (dt, J = 13.6 Hz, J' = 6.8 Hz, 1H, 3”-H_A), 1.75 (dt, J = 13.6 Hz, J' = 6.0 Hz, 1H, 2”-CH_A-CH_2-NHCO), 1.79 (dt, J = 13.6 Hz, J' = 6.8 Hz, 1H, 3”-H_B), 1.82 (tt, J = J' = 6.8 Hz, 2H, 8-H_2), 1.84 (dt, J = 13.6 Hz, J' = 6.0 Hz, 1H, 2”-CH_B-CH_2-NHCO), 1.91–2.00 (complex signal, 4H, 2’-H_2 and 3’-H_2), 2.16 (t, J = 7.2 Hz, 2H, 2-H_2), 2.61 (t, J = 6.8 Hz, 2H, 4”-H_2), 2.66 (broad t, J = 6.0 Hz, 2H, 1’-H_2), 2.99 (broad t, J = 6.0 Hz, 2H, 4’-H_2), 3.29 (ddd, J = 13.2 Hz, J' = 9.2 Hz, J'' = 6.4 Hz, 1H, CH_A-NHCO), 3.41 (ddd, J = 13.2 Hz, J' = 9.2 Hz, J'' = 6.4 Hz, 1H, CH_B-NHCO), 3.75 (s, 3H, 7”-OCH_3), 3.91 (t, J = 7.2 Hz, 2H, 9-H_2), 4.87 (s, NH, $^+$NH, OH), 6.30 (s, 1H, 8”-H), 6.44 (s, 1H, 5”-H), 7.56 (dd, J = 9.6 Hz, J' = 2.4 Hz, 1H, 7’-H), 7.77 (d, J = 2.4 Hz, 1H, 5’-H), 8.37 (d, J = 9.2 Hz, 1H, 8’-H).

^{13}C NMR (100.6 MHz, CD_3OD) δ: 21.8 (CH_2, C3’), 22.3 (CH_2, C4”), 22.8 (CH_2, C2’), 24.2 (CH_3, 2”-CH_3), 24.7 (CH_2, C1’), 26.8 (CH_2, C3), 27.6 (CH_2, C7), 29.3 (CH_2, C4’), 30.00 (CH_2), 30.02 (CH_2), 30.1

(CH_2) (C4, C5 and C6), 31.3 (CH_2, C8), 32.6 (CH_2, C3”), 36.1 (CH_2, CH_2-NHCO), 37.0 (CH_2, C2), 39.4 (CH_2, C2”-*C*H_2-CH_2-NHCO), 49.3 (CH_2, C9), 56.3 (CH_3, 7”-OCH_3), 75.8 (C, C2”), 102.2 (CH, C8”), 113.3 (C, C9a’), 113.4 (C, C4a”), 115.4 (C, C8a’), 116.1 (CH, C5”), 119.1 (CH, C5’), 126.8 (CH, C7’), 128.8 (CH, C8’), 140.1 (C, C6’), 140.5 (C, C10a’), 140.8 (C, C6”), 147.7 (C, C8a”), 148.3 (C, C7”), 152.0 (C, C4a’), 157.8 (C, C9’), 176.2 (C, CONH).

HRMS (ESI):

Calculated for ($C_{35}H_{46}{}^{35}ClN_3O_4 + H^+$): 608.3250

Found: 608.3259

Preparation of (±)-*N*-(6-chloro-1,2,3,4-tetrahydroacridin-9-yl)-*N'*-[2-(6-hydroxy-7-methoxy-2-methylchroman-2-yl)ethyl]heptane-1,7-diamine, (±)-63b

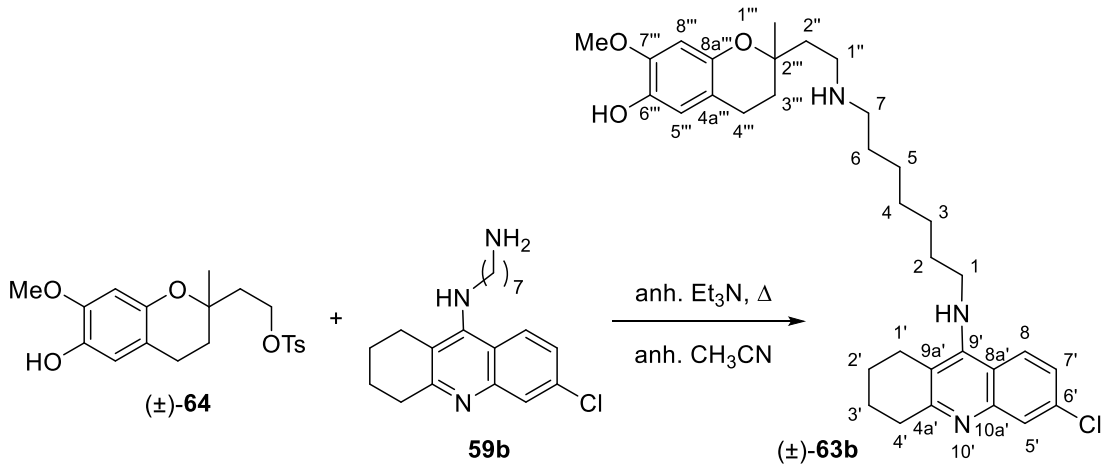

In a double necked 10 mL round-bottomed flask equipped with an inert atmosphere, a magnetic stirrer and a condenser, a suspension of amine **59b** (461 mg, 1.33 mmol), and anhydrous triethylamine (0.07 mL, 51 mg, 0.50 mmol) in a mixture of anhydrous CH_3CN (2 mL) and anhydrous THF (1.5 mL) was prepared. Then a solution of tosylate (±)-**64** (175 mg, 0.44 mmol) in anhydrous CH_3CN (1.5 mL) was added, and the reaction mixture was stirred at 80 °C for 48 hours, then concentrated *in vacuo* to give a dark brown oil (789 mg), which was purified by column chromatography [silica gel 35−70 μm (15 g); Ø = 1.5 cm; #1–37, 500 mL, CH_2Cl_2 / 50% aq. NH_4OH 100:0.4; #38–45, 100 mL, CH_2Cl_2 / MeOH / 50% aq. NH_4OH 99.8:0.2:0.4; #46–54, 100 mL, CH_2Cl_2 / MeOH / 50% aq. NH_4OH 99.5:0.5:0.4; #55–97, 450 mL, CH_2Cl_2 / MeOH / 50% aq. NH_4OH 99:1:0.4; #98–106, 100 mL, CH_2Cl_2 / MeOH / 50% aq. NH_4OH 98:2:0.4; #107, 250 mL, CH_2Cl_2 / MeOH / 50% aq. NH_4OH 95:5:0.4], to provide the desired secondary amine (±)-**63b** (#72–106, 61 mg, 24% yield) as a beige solid.

R_f = 0.76 (silica gel, 10 cm, CH_2Cl_2 / MeOH / 50% aq. NH_4OH 90:10:1).

Analytical sample of (±)-63b·2HCl

In a 25 mL round-bottomed flask (±)-**63b** (37 mg, 0.07 mmol) was dissolved in CH_2Cl_2 (1 mL), filtered with a PTFE filter (0.2 μm), treated with HCl / Et_2O (1.35 N, 0.43 mL), evaporated *in vacuo*, and washed with pentane (3 × 2 mL), to give, after drying in standard conditions, (±)-**63b**·2HCl (34 mg) as a beige solid.

Melting point: 160–163 °C

Calculated logP: 7.78

IR (ATR) ν: 3600–2200 (max. at 3240, 2930, 2852, 2780, 2604, 2496, N–H, $^{+}$N–H, O–H, C–H st), 1628, 1573, 1509 (C=O, Ar–C–C and Ar–C–N st) cm^{-1}.

^{1}H NMR (400 MHz, CD_3OD) δ: 1.30 (s, 3H, 2'''-CH_3), 1.39–1.51 (complex signal, 6H, 3-H_2, 4-H_2, and 5-H_2), 1.71 (m, 2H, 6-H_2), superimposed in part 1.80 (ddd, J = 13.6 Hz, J' = J'' = 6.8 Hz, 2H, 3'''-H_2), superimposed in part 1.84 (m, 2H, 2-H_2), overlapped 1.90–2.00 (complex signal, 4H, 2'-H_2 and 3'-H_2), superimposed 1.96 (dt, 1H, 2''-H_A), 2.07 (dt, J = 14.4 Hz, J' = 6.8 Hz , 1H, 2''-H_B), superimposed 2.67 (t, 2H, 4'''-H_2), superimposed 2.68 (broad t, 2H, 1'-CH_2), 2.97–3.05 (complex signal, 4H, 7-H_2 and 4'-H_2), 3.21 (t, J = 7.6 Hz, 2H, 1''-H_2), 3.76 (s, 3H, 7'''-OCH_3), 3.94 (t, J = 7.6 Hz, 2H, 1-H_2), 4.86 (s, NH, $^{+}$NH, $^{+}NH_2$, OH), 6.35 (s, 1H, 8'''-H), 6.48 (s, 1H, 5'''-H), 7.56 (dd, J = 9.2 Hz, J' = 1.6 Hz, 1H, 7'-H), 7.79 (d, J = 1.6 Hz, 1H, 5'-H), 8.39 (d, J = 9.2 Hz, 1H, 8'-H).

^{13}C NMR (100.6 MHz, CD_3OD) δ: 21.7 (CH_2, C2'), 22.2 (CH_2, C4'''), 22.9 (CH_2, C3'), 23.7 (CH_2, 2'''-CH_3), 27.2 (CH_2, C6), 27.4 (CH_2, C3), 27.5 (CH_2, C5), 29.3 (CH_2, C4'), 29.7 (CH_2, C4), 31.3 (CH_2, C2), 32.6 (CH_2, C3'''), 36.4 (CH_2, C2''), 44.7 (CH_2, C1''), 48.9 (CH_2, C7), 49.1 (CH_2, C1), 56.4 (CH_3, 7'''-OCH_3), 75.3 (C, C2'''), 102.2 (CH, C8'''), 113.32 (C, C9a'), 113.34 (C, C4a'''), 115.4 (C, C8a'), 116.2 (CH, C5'''), 119.1 (CH, C5'), 126.8 (CH, C7'), 128.8 (CH, C8'), 140.0 (C, C6'), 140.5 (C, C10a'), 141.3 (C, C6'''), 147.2 (C, C8a'''), 148.4 (C, C7'''), 152.1 (C, C4a'), 157.8 (C, C9').

HRMS (ESI):

Calculated for ($C_{33}H_{44}{}^{35}ClN_3O_3$ + H^{+}): 566.3144

Found: 566.3138

Preparation of (±)-*N*-(6-chloro-1,2,3,4-tetrahydroacridin-9-yl)-*N'*-[2-(6-hydroxy-7-methoxy-2-methylchroman-2-yl)ethyl]octane-1,8-diamine, (±)-63c

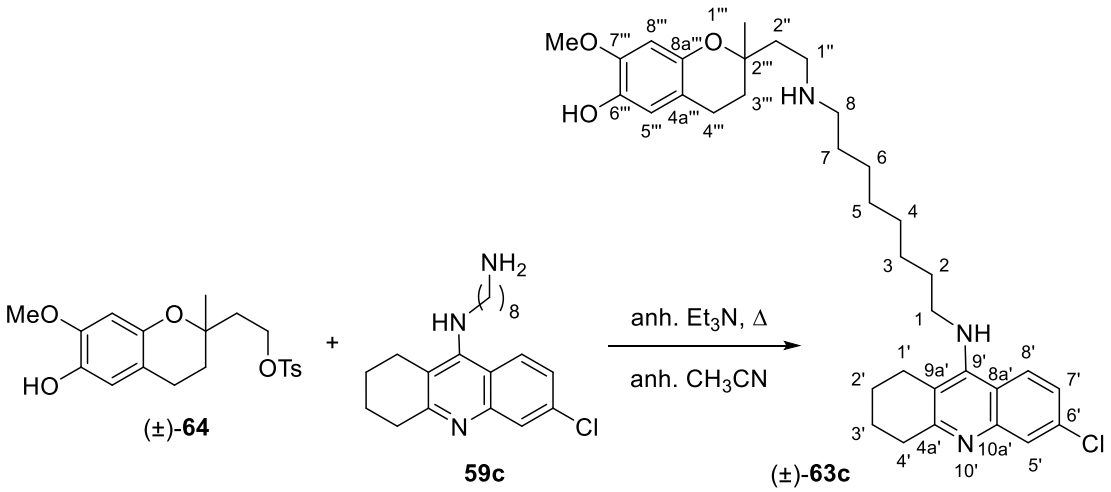

In a double necked 10 mL round-bottomed flask equipped with an inert atmosphere, a magnetic stirrer and a condenser, amine **59c** (467 mg, 1.30 mmol) was placed, then treated with anhydrous triethylamine (0.07 mL, 51 mg, 0.50 mmol) and a solution of tosylate (±)-**64** (170 mg, 0.43 mmol) in anhydrous CH_3CN (4.3 mL). The reaction mixture was stirred under reflux for 48 hours, then concentrated *in vacuo* to give a brown oil (678 mg), which was subjected to column chromatography purification [silica gel 35−70 µm (54 g); Ø = 3.5 cm; #1, 500 mL, CH_2Cl_2 / 50% aq. NH_4OH 100:0.4; #2–22, 4 L, CH_2Cl_2 / MeOH / 50% aq. NH_4OH 99.5:0.5:0.4; #23–26, 500 mL, CH_2Cl_2 / MeOH / 50% aq. NH_4OH 99.2:0.8:0.4; #27–47, 2 L, CH_2Cl_2 / MeOH / 50% aq. NH_4OH 99:1:0.4], to provide the desired secondary amine (±)-**63c** (#29–46, 143 mg, 57% yield) as a beige solid.

R_f = 0.74 (silica gel, 10 cm, CH_2Cl_2 / MeOH / 50% aq. NH_4OH 90:10:1).

Analytical sample of (±)-63c·2HCl

In a 25 mL round-bottomed flask (±)-**63c** (100 mg, 0.17 mmol) was dissolved in CH_2Cl_2 (1 mL), filtered with a PTFE filter (0.2 µm), treated with HCl / Et_2O (1.35 N, 1.15 mL), evaporated *in vacuo*, and washed with pentane (3 × 2 mL), to give, after drying in standard conditions, (±)-**63c**·2HCl (130 mg) as a pale yellow solid.

Melting point: 147–149 °C

Calculated logP: 8.25

IR (ATR) ν: 3600–2200 (max. at 3240, 2930, 2852, 2780, N–H, $^{+}$N–H, O–H, C–H st), 1630, 1573, 1511 (C=O, Ar–C–C and Ar–C–N st) cm^{-1}.

^{1}H NMR (400 MHz, CD_3OD) δ: 1.30 (s, 3H, 2'''-CH_3), overlapped 1.36–1.44 (complex signal, 6H, 3-H_2, 4-H_2, and 5-H_2), partially overlapped 1.42–1.50 (complex signal, 2H, 3-H_2), 1.69 (m, 2H, 7-H_2), superimposed in part 1.78 (ddd, J = 13.6 Hz, J' = J'' = 6.4 Hz, 2H, 3'''-H_2), superimposed in part 1.85 (m, 2H, 2-H_2), overlapped 1.91–2.01 (complex signal, 4H, 2'-H_2 and 3'-H_2), superimposed 1.96 (dt, 1H, 2''-H_A), 2.07 (dt, J = 14.0 Hz, J' = 7.2 Hz , 1H, 2''-H_B), superimposed 2.67 (t, 2H, 4'''-H_2), superimposed 2.68 (broad t, 2H, 1'-CH_2), superimposed 3.00 (broad t, 2H, 4'-H_2), superimposed 3.02 (t, 2H, 8-H_2), 3.21 (t, J = 8.0 Hz, 2H, 1''-H_2), 3.76 (s, 3H, 7'''-OCH_3), 3.94 (t, J = 7.2 Hz, 2H, 1-H_2), 4.86 (s, NH, $^{+}$NH, $^{+}NH_2$, OH), 6.36 (s, 1H, 8'''-H), 6.49 (s, 1H, 5'''-H), 7.56 (dd, J = 9.6 Hz, J' = 2.4 Hz, 1H, 7'-H), 7.79 (d, J = 2.4 Hz, 1H, 5'-H), 8.39 (d, J = 9.6 Hz, 1H, 8'-H).

^{13}C NMR (100.6 MHz, CD_3OD) δ: 21.8 (CH_2, C2'), 22.2 (CH_2, C4'''), 22.9 (CH_2, C3'), 23.7 (CH_2, 2'''-CH_3), 24.8 (CH_2, C1'), 27.2 (CH_2, C7), 27.5 (CH_2, C3), 27.6 (CH_2, C6), 29.3 (CH_2, C4'), 30.05 (CH_2) and 30.08 (CH_2) (C4 and C5), 31.4 (CH_2, C2), 32.6 (CH_2, C3'''), 36.4 (CH_2, C2''), 44.7 (CH_2, C1''), 49.2 (CH_2) and 49.3 (CH_2) (C1 and C8), 56.4 (CH_3, 7'''-OCH_3), 75.4 (C, C2'''), 102.2 (CH, C8'''), 113.32 (C, C9a'), 113.34 (C, C4a'''), 115.4 (C, C8a'), 116.2 (CH, C5'''), 119.1 (CH, C5'), 126.8 (CH, C7'), 128.8 (CH, C8'), 140.1 (C, C6'), 140.5 (C, C10a'), 141.3 (C, C6'''), 147.2 (C, C8a'''), 148.4 (C, C7'''), 152.1 (C, C4a'), 157.8 (C, C9').

HRMS (ESI):

Calculated for ($C_{34}H_{46}{}^{35}ClN_3O_3$ + H^+):	580.3300
Found:	580.3302

Preparation of (±)-*N*-(6-chloro-1,2,3,4-tetrahydroacridin-9-yl)-*N'*-[2-(6-hydroxy-7-methoxy-2-methylchroman-2-yl)ethyl]nonane-1,9-diamine, (±)-63d

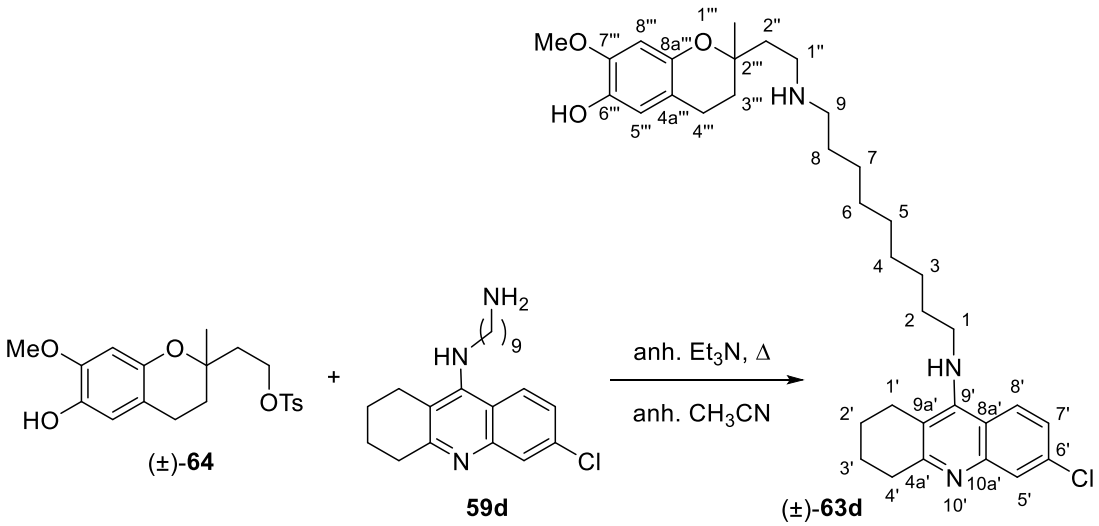

In a double necked 10 mL round-bottomed flask provided with an inert atmosphere, a magnetic stirrer and a condenser, amine **59d** (403 mg, 1.08 mmol) was placed, then treated with anhydrous triethylamine (0.05 mL, 40 mg, 0.40 mmol) and a solution of tosylate (±)-**64** (142 mg, 0.36 mmol) in anhydrous CH_3CN (3.6 mL). The reaction mixture was stirred under reflux for 48 hours, then concentrated *in vacuo* to give a brown oil (544 mg), which was subjected to column chromatography purification [silica gel 35−70 µm (55 g); Ø = 3.5 cm; #1, 300 mL, CH_2Cl_2 / 50% aq. NH_4OH 100:0.4; #2–22, 3 L, CH_2Cl_2 / MeOH / 50% aq. NH_4OH 99.5:0.5:0.4; #23–25, 300 mL, CH_2Cl_2 / MeOH / 50% aq. NH_4OH 99.3:0.7:0.4; #26–40, 1.5 L, CH_2Cl_2 / MeOH / 50% aq. NH_4OH 99:1:0.4; #41–43, 500 mL, CH_2Cl_2 / MeOH / 50% aq. NH_4OH 95:5:0.4], to provide the desired secondary amine (±)-**63d** (#24–33, 125 mg, 59% yield) as a beige sticky solid.

R_f = 0.76 (silica gel, 10 cm, CH_2Cl_2 / MeOH / 50% aq. NH_4OH 90:10:1).

Analytical sample of (±)-63d·2HCl

In a 25 mL round-bottomed flask (±)-**63d** (120 mg, 0.20 mmol) was dissolved in CH_2Cl_2 (1 mL), filtered with a PTFE filter (0.2 µm), treated with HCl / Et_2O (1.35 N, 1.35 mL), evaporated *in vacuo*, and washed with pentane (3 × 2 mL), to give, after drying in standard conditions, (±)-**63d**·2HCl (104 mg) as a beige solid.

Melting point: 153–157 °C

Calculated logP: 5.58

IR (ATR) ν: 3600–2200 (max. at 3229, 2925, 2852, 2785, N–H, $^{+}$N–H, O–H, C–H st), 1628, 1571, 1509 (C=O, Ar–C–C and Ar–C–N st) cm^{-1}.

^{1}H NMR (400 MHz, CD_3OD) δ: 1.30 (s, 3H, 2'''-CH_3), 1.32–1.44 (complex signal, 8H, 4-H_2, 5-H_2, 6-H_2 and 7-H_2), partially overlapped 1.40–1.52 (complex signal, 2H, 3-H_2), 1.68 (m, 2H, 8-H_2), superimposed in part 1.79 (ddd, J = 13.2 Hz, J' = J'' = 6.4 Hz, 2H, 3'''-H_2), superimposed in part 1.83 (m, 2H, 2-H_2), overlapped 1.90–2.01 (complex signal, 4H, 2'-H_2 and 3'-H_2), superimposed 1.95 (dt, 1H, 2''-H_A), 2.06 (dt, J = 13.6 Hz, J' = 7.6 Hz , 1H, 2''-H_B), overlapped 2.68 (broad t, 2H, 1'-CH_2), overlapped 2.69 (t, J = 6.0 Hz, 2H, 4'''-H_2), 2.97–3.03 (complex signal, 4H, 8-H_2 and 4'-H_2), 3.22 (t, J = 7.6 Hz, 2H, 1''-H_2), 3.77 (s, 3H, 7'''-OCH_3), 3.94 (t, J = 7.6 Hz, 2H, 1-H_2), 4.85 (s, NH, $^{+}$NH, $^{+}NH_2$, OH), 6.36 (s, 1H, 8'''-H), 6.50 (s, 1H, 5'''-H), 7.56 (dd, J = 9.2 Hz, J' = 2.0 Hz, 1H, 7'-H), 7.79 (d, J = 2.0 Hz, 1H, 5'-H), 8.39 (d, J = 9.2 Hz, 1H, 8'-H).

^{13}C NMR (100.6 MHz, CD_3OD) δ: 21.8 (CH_2, C2'), 22.2 (CH_2, C4'''), 22.9 (CH_2, C3'), 23.7 (CH_2, 2'''-CH_3), 24.7 (CH_2, C1'), 27.3 (CH_2, C8), 27.5 (CH_2, C3), 27.7 (CH_2, C7), 29.3 (CH_2, C4'), 30.1 (CH_2), 30.2 (CH_2) and 30.4 (CH_2) (C4, C5 and C6), 31.4 (CH_2, C2), 32.6 (CH_2, C3'''), 36.5 (CH_2, C2''), 44.7 (CH_2, C1''), 48.9 (CH_2) and 49.1 (CH_2) (C1 and C9), 56.4 (CH_3, 7'''-OCH_3), 75.4 (C, C2'''), 102.2 (CH, C8'''), 113.4 (2C, C9a' and C4a'''), 115.5 (C, C8a'), 116.2 (CH, C5'''), 119.2 (CH, C5'), 126.8 (CH, C7'), 128.8 (CH, C8'), 140.1 (C, C6'), 140.6 (C, C10a'), 141.3 (C, C6'''), 147.2 (C, C8a'''), 148.4 (C, C7'''), 152.2 (C, C4a'), 157.8 (C, C9').

HRMS (ESI):

Calculated for ($C_{35}H_{48}{}^{35}ClN_3O_3$ + H^+):	594.3457
Found:	594.3461

Preparation of (±)-*N*-(6-chloro-1,2,3,4-tetrahydroacridin-9-yl)-*N'*-[2-(6-hydroxy-7-methoxy-2-methylchroman-2-yl)ethyl]-3,6-dioxaoctane-1,8-diamine, (±)-63e

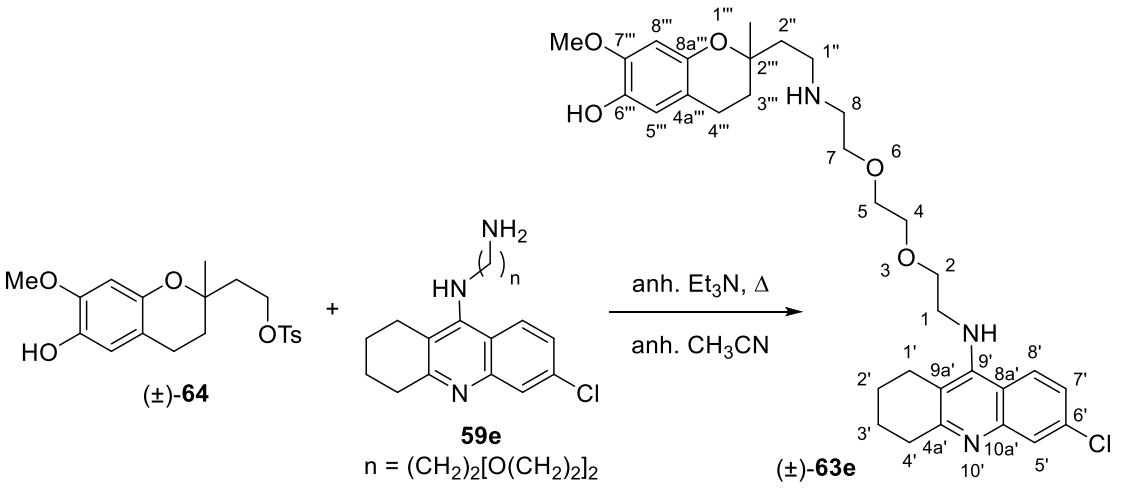

In a double necked 10 mL round-bottomed flask equipped with an inert atmosphere, a magnetic stirrer and a condenser, amine **59e** (553 mg, 1.52 mmol) was placed, then treated with anhydrous triethylamine (0.08 mL, 58 mg, 0.57 mmol) and a solution of tosylate (±)-**64** (200 mg, 0.51 mmol) in anhydrous CH_3CN (5.1 mL). The reaction mixture was stirred under reflux for 48 hours, then concentrated *in vacuo* to give a dark brown sticky solid (763 mg), which was subjected to column chromatography purification [silica gel 35−70 µm (63 g); Ø = 3.5 cm; #1–2, 500 mL, CH_2Cl_2 / 50% aq. NH_4OH 100:0.4; #3–8, 2 L, CH_2Cl_2 / MeOH / 50% aq. NH_4OH 99.5:0.5:0.4; #9–23, 1.5 L, CH_2Cl_2 / MeOH / 50% aq. NH_4OH 99.3:0.7:0.4; #24–33, 1 L, CH_2Cl_2 / MeOH / 50% aq. NH_4OH 95:5:0.4], to provide the impure secondary amine (±)-**63e** (#26–28, 223 mg) as a clear brown oil, which was subjected to a second column chromatography purification [silica gel 35−70 µm (40 g); Ø = 3.5 cm; #1, 300 mL, CH_2Cl_2 / 50% aq. NH_4OH 100:0.4; #2–20, 2.5 L, CH_2Cl_2 / MeOH / 50% aq. NH_4OH 99.8:0.2:0.4; #21–41, 3 L, CH_2Cl_2 / MeOH / 50% aq. NH_4OH 99.5:0.5:0.4; #42–46, 500 mL, CH_2Cl_2 / MeOH / 50% aq. NH_4OH 99.3:0.7:0.4; #47–60, 2 L, CH_2Cl_2 / MeOH / 50% aq. NH_4OH 99:1:0.4; #61–64, 500 mL, CH_2Cl_2 / MeOH / 50% aq. NH_4OH 90:10:0.4], to provide the pure desired amine (±)-**63e** (#45–52, 90 mg, 30% yield) as a brown solid.

R_f = 0.77 (silica gel, 10 cm, CH_2Cl_2 / MeOH / 50% aq. NH_4OH 90:10:1).

Analytical sample of (±)-63e·2HCl

In a 25 mL round-bottomed flask (±)-**63e** (90 mg, 0.15 mmol) was dissolved in CH_2Cl_2 (1 mL), filtered with a PTFE filter (0.2 μm), treated with HCl / Et_2O (1.35 N, 1 mL), evaporated *in vacuo*, and washed with pentane (3 × 2 mL), to give, after drying in standard conditions, (±)-**63e**·2HCl (86 mg) as a brown sticky solid.

Calculated logP: 5.50

IR (ATR) ν: 3600–2200 (max. at 3369, 3250, 2919, 2857, 2790, N–H, $^{+}$N–H, O–H, C–H st), 1630, 1576, 1509 (C=O, Ar–C–C and Ar–C–N st) cm^{-1}.

^{1}H NMR (400 MHz, CD_3OD) δ: 1.27 (s, 3H, 2'''-CH_3), 1.73 (dt, J = 13.6 Hz, J' = 6.4 Hz, 1H, 3'''-H_A), 1.79 (dt, J = 13.6 Hz, J' = 6.4 Hz, 1H, 3'''-H_B), 1.90–2.05 (complex signal, 5H, 2'-H_2, 3'-H_2 and 2''-H_A), 2.07 (dt, J = 14.0 Hz, J' = 7.2 Hz, 1H, 2''-H_B), 2.56 (dt, J = 16.0 Hz, J' = 6.0 Hz, 1H, 4'''-H_A), 2.60 (dt, J = 16.0 Hz, J' = 6.0 Hz, 1H, 4'''-H_B), 2.66 (t, J = 6.4 Hz, 2H, 1'-H_2), 3.01 (t, J = 5.6 Hz, 2H, 4'-H_2), 3.26 (t, J = 4.8 Hz, 2H, 8-H_2), overlapped 3.26–3.31 (t, 2H, 1''-H_2), overlapped 3.67–3.74 (complex signal, 4H, 4-H_2 and 5-H_2), 3.71 (s, 3H, 7'''-OCH_3), 3.77 (t, J = 4.8 Hz, 2H, 7-H_2), 3.88 (t, J = 4.8 Hz, 2H, 2-H_2), 4.12 (t, J = 4.8 Hz, 2H, 1-H_2), 4.85 (s, NH, $^{+}$NH, $^{+}NH_2$, OH), 6.32 (s, 1H, 8'''-H), 6.40 (s, 1H, 5'''-H), 7.54 (dd, J = 9.2 Hz, J' = 2.0 Hz, 1H, 7'-H), 7.78 (d, J = 2.0 Hz, 1H, 5'-H), 8.43 (d, J = 9.2 Hz, 1H, 8'-H).

^{13}C NMR (100.6 MHz, CD_3OD) δ: 21.7 (CH_2, C2'), 22.1 (CH_2, C4'''), 22.8 (CH_2, C3'),23.4 (CH_3, 2'''-CH_3), 24.6 (CH_2, C1'), 29.3 (CH_2, C4'), 32.6 (CH_2, C3'''), 36.4 (CH_2, C2''), 44.8 (CH_2, C1''), 48.5 (CH_2, C8), 49.1 (CH_2, C1), 56.5 (CH_3, 7'''-OCH_3), 66.8 (CH_2, C7), 70.4 (CH_2, C2), 71.3 (CH_2) and 71.4 (CH_2) (C4 and C5), 75.9 (C, C2'''), 102.4 (CH, C8'''), 113.4 (C, C4a'''), 113.7 (C, C9a'), 115.6 (C, C8a'), 116.1 (CH, C5'''), 119.2 (CH, C5'), 126.8 (CH, C7'), 128.8 (CH, C8'), 140.1 (C, C6'), 140.4 (C, C10a'), 141.4 (C, C6'''), 146.8 (C, C8a'''), 148.3 (C, C7'''), 152.4 (C, C4a'''), 158.2 (C, C9').

HRMS (ESI):

Calculated for ($C_{32}H_{42}{}^{35}ClN_3O_5$ + H^+): 584.2886

Found: 584.2879

Preparation of tetramethyl 7,11-dihydroxy-5*H*-6,9-dihydro-5,9-prop-1-enobenzo[7]annulene-6,8,10,12-tetracarboxylate, 82

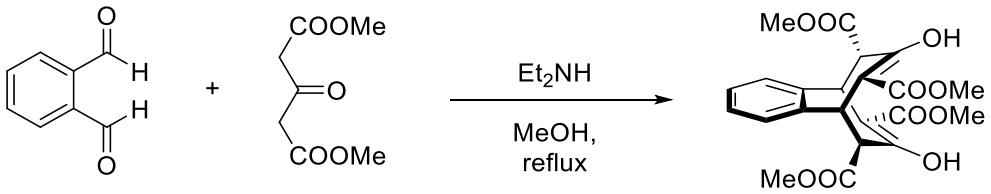

81 **43** **82**

In a 500 mL round-bottomed flask equipped with a magnetic stirrer and a condenser, a solution of phthaldialdehyde, **81** (9.8 g, 73.1 mmol), and dimethyl-1,3-acetonedicarboxylate, **43** (21.5 mL, 25.9 g, 149 mmol), in MeOH (200 mL) was prepared, then treated with diethylamine (0.7 mL) and stirred under reflux for 1.5 hours. The resulting mixture was treated again with diethylamine (0.83 mL) and allowed to cool to 4 ^{o}C overnight, and the precipitated formed was filtered off and washed with cold MeOH (25 mL) to give the desired tetraester **82** (21.3 g, 65% yield) as a white solid, which was directly used for the next step.

Preparation of 5,6,8,9-tetrahydro-5,9-propanebenzocycloheptane-7,11-dione, 83 and 7,11-epoxi-6,7,8,9-tetrahydro-5,9-propane-5*H*-benzocycloheptane-7,11-diol, 84

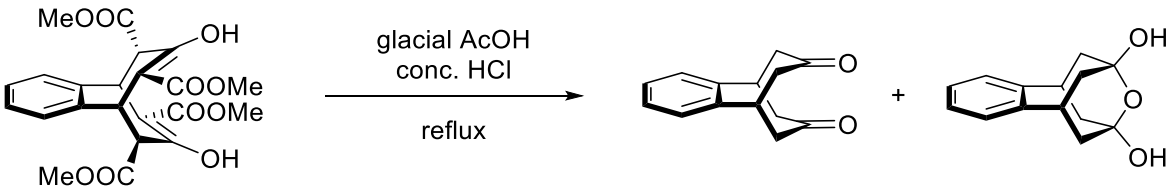

82 **83** **84**

In a 500 mL round-bottomed flask equipped with a magnetic stirrer and a condenser, tetraester **82** (21.3 g, 47.7 mmol) was dissolved in glacial AcOH (112 mL) and concentrated HCl (30 mL), then stirred under reflux for 12 hours. Acidic mixture was removed under reduced pressure and the resulting residue was digested with Et_2O (140 mL) for 15 minutes and allowed to cool to 4 ^oC overnight, then filtered off providing a mixture of diketone **83** and its hydrate **84** with a 1:3 ratio as a white solid (10.4 g). Dehydration of the mixture was carried out by a Dean-Stark system with toluene (250 mL), affording the pure diketone **83** (9.08 g, 89% yield).

Preparation of methyltriphenylphosphonium iodide, 85

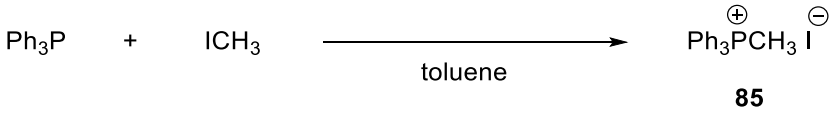

85

In a triple necked 500 mL round-bottomed flask equipped with a magnetic stirrer, a solution of triphenylphosphine (50.0 g, 190 mmol) in toluene (300 mL) was prepared and treated with methyl iodide (11.8 mL, 26.9 g, 190 mmol) and stirred at room temperature overnight. The resulting mixture was filtered off to provide the desired compound **85** (70.8 g, 92% yield) as a white solid.

Preparation of 5,6,8,9-tetrahydro-5,9-propanebenzocyclohept-11-en-7-one, 86

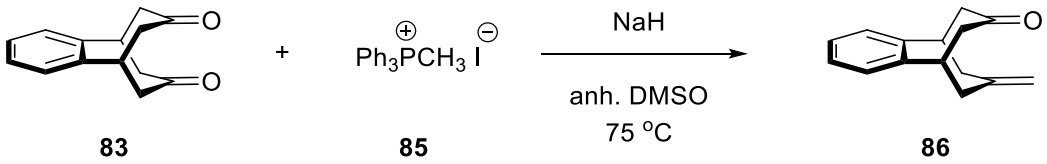

83 **85** **86**

In a triple necked 250 mL round-bottomed flask equipped with an inert atmosphere, a magnetic stirrer and a condenser, a suspension of sodium hydride (60% dispersion in mineral oil, 940 mg, 23.5 mmol) in anhydrous DMSO (45 mL) was prepared and heated to 75 °C for 45 minutes. After the reaction mixture was tempered, a solution of methyltriphenylphosphonium iodide, **85** (9.17 g, 21.9 mmol), in anhydrous DMSO (54 mL) was added and the resulting solution was stirred at room temperature for 20 minutes. Then treated with a suspension of diketone **83** (4.79 g, 22.4 mmol) in anhydrous DMSO (56 mL) and stirred at 75 °C overnight. The resulting solution was allowed to cool to room temperature, poured onto water (150 mL) and extracted with hexane (3 × 75 mL). The combined organic layers were washed with brine (2 × 100 mL), dried over anhydrous Na_2SO_4, filtered and concentrated *in vacuo* to provide a mixture mono-Wittig / di-Wittig products in ratio 1:0.18 (^{1}H NMR) (3.83 g) as a white solid, which was purified by packing in silica gel and extracting with 10% petroleum ether / diethylether mixture to afford monoketone **86** (2.93 g, 62% yield) as a white solid.

Preparation of 2-chloro-*N*-(9-hydroxy-7*H*-5,6,8,9,10,11-hexahydro-5,9:7,11-dimethanobenzo[9]annulen-7-yl)acetamide, 87

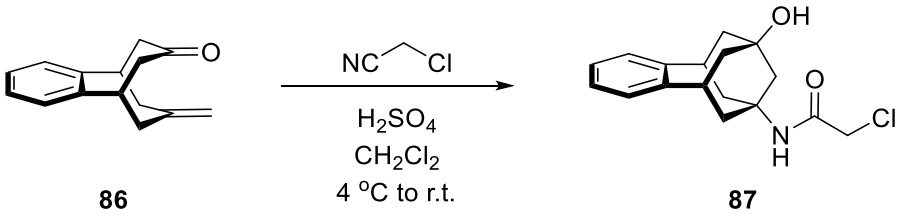

86 **87**

In a 50 mL round-bottomed flask equipped with a magnetic stirrer, a solution of enone **86** (7.81 g, 36.8 mmol) in CH_2Cl_2 (55 mL) was prepared and treated with chloroacetonitrile (2.31 mL, 2.76 g, 36.6 mmol). The resulting mixture was cooled with an ice bath, treated dropwise with concentrated H_2SO_4 (2.95 mL, 5.42 g, 55.3 mmol), then allowed to reach room temperature and stirred overnight. To the resulting solution ice (95 g) was added, and the mixture was stirred at room temperature for a few minutes, then extracted with CH_2Cl_2 (3 × 110 mL). The combined organic layers were dried over anhydrous Na_2SO_4, filtered and concentrated *in vacuo* to provide a white solid (6.30 g), which was subjected to column chromatography purification [Al_2O_3 (250 g); Ø = 5 cm; #1–7, 500 mL, hexane; #8–35, 2 L, hexane / EtOAc 90:10; #36–39, 250 mL, hexane / EtOAc 80:20; #40–43, 250 mL, hexane / EtOAc 70:30; #44–47, 300 mL, hexane / EtOAc 60:40; #48–52, 400 mL, hexane / EtOAc 50:50; #53–55, 250 mL, hexane / EtOAc 40:60; #56–59, 250 mL, hexane / EtOAc 30:70; #60–65, 1.2 L, EtOAc; #66–67, 1 L, CH_2Cl_2 / MeOH 90:10], to provide a mixture of desired cloracetamide **87** / starting material **86** in ratio 1:0.7 (#24–65, 2.72 g, 16% yield of desired compound) as a white solid, and the desired cloracetamide **87** (#66, 2.72 g, 24% yield) as a white solid. The overall yield of desired cloracetamide **87** was 40%.

Preparation of 2-chloro-*N*-(9-fluoro-7*H*-5,6,8,9,10,11-hexahydro-5,9:7,11-dimethanobenzo[9]annulen-7-yl)acetamide, 88

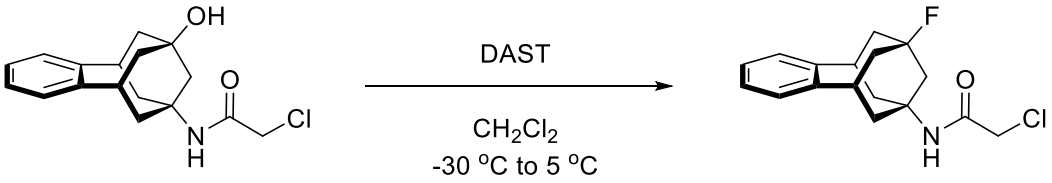

87 **88**

In a triple necked 100 mL round-bottomed flask equipped with an inert atmosphere, a magnetic stirrer and a dry ice acetone bath, a solution of alcohol **87** (1.56 g, 5.13 mmol) in CH_2Cl_2 (42 mL) was prepared, cooled to -30 °C, and treated with (diethylamino)sulfur trifluoride (DAST, 1.01 mL, 1.23 g, 7.63 mmol). The resulting mixture was stirred at the same temperature overnight, then treated dropwise with water (30 mL) and alkalinized with 5 N NaOH (15 mL), and extracted with CH_2Cl_2 (3 × 50 mL). The combined organic layers were dried over anhydrous Na_2SO_4, filtered and concentrated *in vacuo* to provide the desired compound **88** (1.56 g, quantitative yield) as a yellow solid that was used in the next step without further purification.

Preparation of 9-fluoro-7*H*-5,6,8,9,10,11-hexahydro-5,9:7,11-dimethanobenzo[9]annulen-7-amine, 18

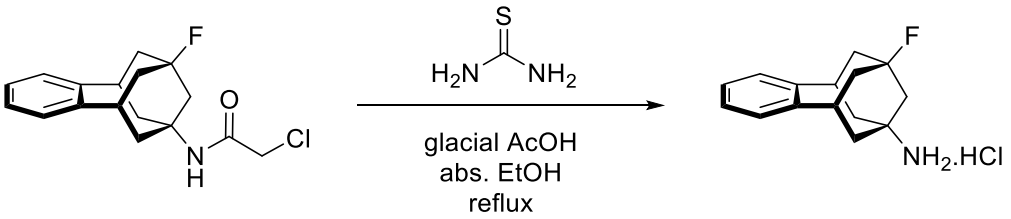

88 **18**

In a 250 mL round-bottomed flask equipped with a magnetic stirrer and a condenser, a suspension of cloracetamide **88** (1 g, 4.53 mmol) and thiourea (410 mg, 5.43 mmol) in absolute EtOH (91 mL) was prepared, then treated with glacial AcOH (4.52 mL) and stirred under reflux overnight. The resulting mixture was cooled to room temperature, evaporated under reduced pressure, then diluted with 1 N NaOH (100 mL) and extracted with CH_2Cl_2 (3 × 100 mL). The combined organic layers were dried over anhydrous Na_2SO_4, filtered and evaporated *in vacuo* to give a brown oil (703 mg), which was treated with HCl / Et_2O (1.35 N, 11 mL) to provide the desired primary amine **18**·HCl (880 mg, 73% yield) as a clear yellow solid.

Attempted preparation of 4-[(6-chloro-1,2,3,4-tetrahydroacridin-9-yl)amino]butanenitrile, 90a

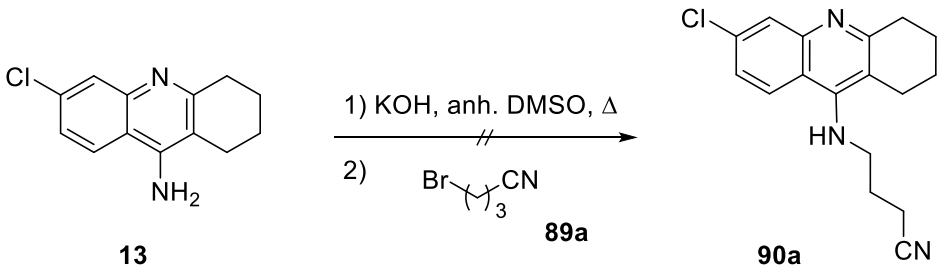

13 **89a** **90a**

In a triple necked 100 mL round-bottomed flask equipped with an inert atmosphere, a magnetic stirrer and 4 Å molecular sieves, 6-chlorotacrine **13** (1.50 g, 6.45 mmol) and finely powdered KOH (85% purity, 851 mg, 12.9 mmol) were suspended in anhydrous DMSO (20 mL). The resulting suspension was stirred, heating every 10 minutes with a heat gun for 1 hour, and at room temperature one more hour, then treated with 4-bromobutyronitrile, **89a** (0.77 mL, 1.15 g, 7.77 mmol). The reaction mixture was stirred at room temperature overnight, then diluted with 5 N NaOH aq. sol. (400 mL), and extracted with EtOAc (3 × 200 mL). The combined organic layers were washed with water (3 × 150 mL), dried over anhydrous Na_2SO_4, filtered and evaporated under reduced pressure to give a yellow solid (1.59 g), which resulted to be starting material **13**.

Attempted preparation of 4-[(6-chloro-1,2,3,4-tetrahydroacridin-9-yl)amino]butanenitrile, 90a

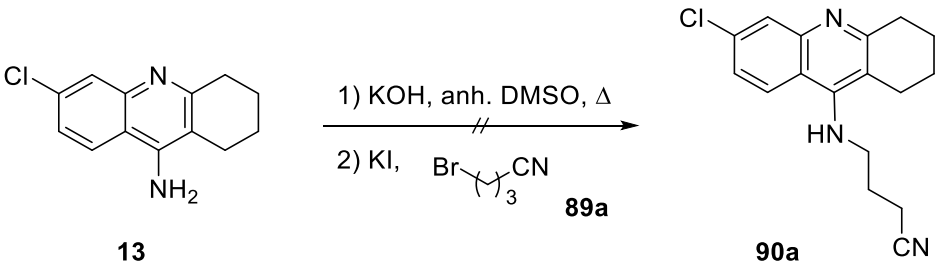

13 **90a**

In a triple necked 100 mL round-bottomed flask equipped with an inert atmosphere, a magnetic stirrer and 4 Å molecular sieves, 6-chlorotacrine **13** (1.50 g, 6.45 mmol) and finely powdered KOH (85% purity, 851 mg, 12.9 mmol) were suspended in anhydrous DMSO (20 mL). The resulting suspension was stirred, heating every 10 minutes with a heat gun for 1 hour, and at room temperature one more hour, then treated with potassium iodide (107 mg, 0.64 mmol) and dropwise with 4-bromobutyronitrile, **89a** (0.77 mL, 1.15 g, 7.77mmol). The reaction mixture was stirred at room temperature overnight, then diluted with 5 N NaOH aq. sol. (300 mL), and extracted with EtOAc (3 × 200 mL). The combined organic layers were washed with water (3 × 250 mL), dried over anhydrous Na_2SO_4, filtered and evaporated under reduced pressure to give a yellow solid (1.39 g), which resulted to be starting material **13**.

Attempted preparation of 4-[(6-chloro-1,2,3,4-tetrahydroacridin-9-yl)amino]butanenitrile, 90a

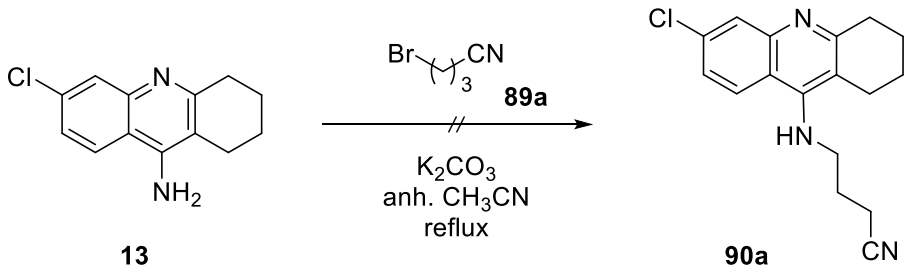

13 **90a**

In a triple necked 100 mL round-bottomed flask equipped with an inert atmosphere, a magnetic stirrer, 4 Å molecular sieves and a condenser, 6-chlorotacrine **13** (1.50 g, 6.45 mmol) was suspended in anhydrous CH_3CN (33 mL). The resulting suspension was treated with potassium carbonate (3.29 g, 23.9 mmol), stirred at room temperature for 10 minutes, treated with a solution of 4-bromobutyronitrile, **89a** (0.77 mL, 1.15 g, 7.77 mmol) in anhydrous CH_3CN (16 mL), and stirred again for 2 days. A control TLC of the reaction showed only starting material.

Preparation of 6-chloro-9-[(3-hydroxypropyl)amino]-1,2,3,4-tetrahydroacridine, 92

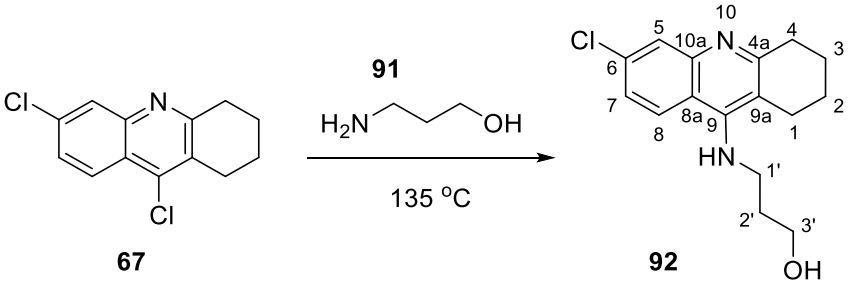

In a 25 mL round-bottomed flask equipped with a magnetic stirrer and a condenser, a mixture of 6,9-dichlo-1,2,3,4-tetrahydroacridine, **67** (1.50 g, 5.95 mmol), and 3-amino-1-propanol, **91** (5.46 mL, 5.36 g, 71.4 mmol) was prepared, and stirred at 135 °C for 1 day. After cooling to room temperature, the mixture was poured onto water (100 mL), filtered off, and the solid residue was dried and boiled in EtOAc (100 mL) to afford the desired alcohol **92** (1.62 g, 94% yield) as a white solid.

R_f = 0.32 (gel de sílice, 10 cm, CH_2Cl_2 / MeOH / NH_4OH 25% 90:10:1).

Analytical sample of 92·HCl

In a 25 mL round-bottomed flask **92** (25 mg, 0.09 mmol) was dissolved in CH_2Cl_2 (1 mL), filtered with a PTFE filter (0.2 µm), treated with HCl / MeOH (0.5 M, 0.54 mL), evaporated *in vacuo*, and washed with pentane (3 × 2 mL), giving, after drying in standard conditions, **92**·HCl (27 mg) as a yellow solid.

Melting point: 164–165 °C (MeOH / EtOAc 1:4).

IR (ATR) *v*: 3500–2400 (max. at 3353, 3314, 3263, 3131, 3051, 3014, 2936, 2907, 2875, 2845, 2803, C–H, O–H, N–H and $N–H^+$ st), 1630, 1572, 1526 (Ar–C–C and Ar–C–N st) cm^{-1}.

^{1}H NMR (500 MHz, CD_3OD) δ: 1.92–2.00 (complex signal, 4H, 2-H_2 and 3-H_2), 2.03 (m, 2H, 2'-H_2), 2.64 (m, 2H, 1-H_2), 2.99 (m, 2H, 4-H_2), 3.83 (t, J = 5.5 Hz, 2H, 3'-H_2), 4.14 (t, J = 6.0 Hz, 2H, 1'-H_2),

4.85 (s, OH, NH and $^{+}$NH), 7.54 (dd, *J* = 9.0 Hz, *J'* = 2.0 Hz, 1H, 7-H), 7.76 (d, *J* = 2.0 Hz, 1H, 5-H), 8.46 (d, *J* = 9.0 Hz, 1H, 8-H).

^{13}C NMR (75,4 MHz, CD_3OD) *δ*: 21.8 (CH_2, C3), 22.8 (CH_2, C2), 24.6 (CH_2, C1), 29.3 (CH_2, C4), 33.0 (CH_2, C2'), 48.6 (CH_2, C1'), 61.5 (CH_2, C3'), 113.1 (C, C9a), 115.1 (C, C8a), 118.9 (CH, C5), 126.1 (CH, C7), 129.0 (CH, C8), 139.9 (C, C6), 140.5 (C, C10a), 151.6 (C, C4a), 157.5 (C, C9).

Preparation of 3-[(6-chloro-1,2,3,4-tetrahydroacridin-9-yl)amino]propyl methanesulfonate, 93

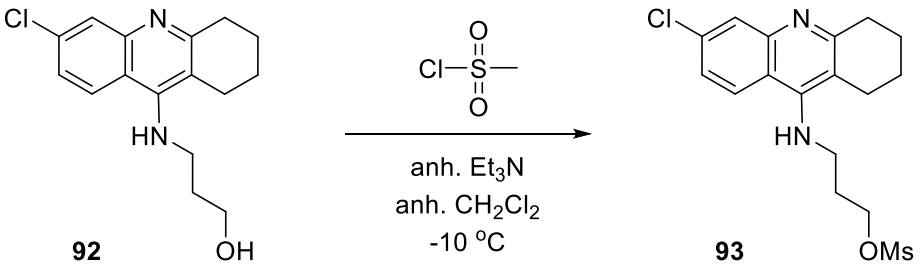

In double necked 100 mL round-bottomed flask provided with a magnetic stirrer, an inert atmosphere and an ice / NaCl bath (-10 °C), a solution of alcohol **92** (1.62 g, 5.58 mmol) and anhydrous Et_3N (1.31 mL, 0.95 g, 9.41 mmol) in anhydrous CH_2Cl_2 (33.5 mL) was prepared, then treated dropwise with methanesulfonyl chloride (0.65 mL, 0.96 g, 8.38 mmol) and stirred for 30 minutes at -10 °C. The resulting mixture was concentrated in vacuo and the residue was dissolved in CH_2Cl_2 (25 mL), then washed with 2 N NaOH aq. sol. (3 × 20 mL), dried over anhydrous Na_2SO_4, filtered and concentrated under vacuum to afford the desired mesylate **93** (2.32 g, quantitative yield) as a brown dark oil.

R_f = 0.70 (gel de sílice, 10 cm, CH_2Cl_2 / MeOH / NH_4OH 25% 90:10:1).

Preparation of 4-[(6-chloro-1,2,3,4-tetrahydroacridin-9-yl)amino]butanenitrile, 90a

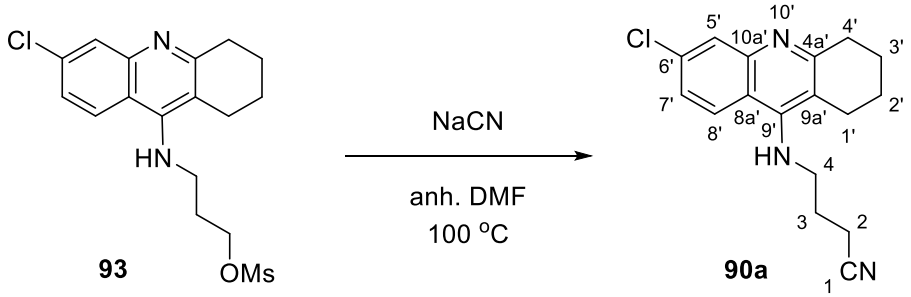

In triple necked 50 mL round-bottomed flask provided with a magnetic stirrer, an inert atmosphere and a condenser, a mixture of mesylate **93** (2.32 g of a crude that could contain a maximum of 5.58 mmol of the desired mesylate) and sodium cyanide (1.64 g, 33.5 mmol) in anhydrous DMF (5 mL) was prepared, then stirred at 100 °C for 1 hour, neutralized with 1 N NaOH aq. sol. (50 mL), and extracted with CH_2Cl_2 (4 × 30 mL). The combined organic layers were washed with water (6 × 40 mL), dried over anhydrous Na_2SO_4, filtered and evaporated under reduced pressure to give the desired nitrile **90a** (1.61 g, 98% yield) as a brown dark oil.

R_f = 0.68 (gel de sílice, 10 cm, CH_2Cl_2 / MeOH / NH_4OH 50% 95:5:1).

Analytical sample of 90a·HCl

In a 25 mL round-bottomed flask, desired nitrile **90a** (142 mg) was dissolved in CH_2Cl_2 (1 mL), filtered with a PTFE filter (0.2 µm), treated with HCl / MeOH (0.53 M, 0.77 mL), concentrated *in vacuo*, and washed with pentane (3 × 2 mL), giving, after drying in standard conditions, **90a**·HCl (154 mg) as a dark brown solid.

Melting point: 114–116 °C.

IR (ATR) *v*: 3500–2500 (max at 3050, 2930, 2861, 2761, N–H, $^+$N–H, C–H st), 2232 (CN st), 1629, 1567, 1514 (Ar–C–C, Ar–C–N st) cm^{-1}.

^{1}H NMR (400 MHz, CD_3OD) δ: 1.92–2.02 (complex signal, 4H, 2'-H_2 and 3'-H_2), 2.18 (dt, J = J' = 7.0 Hz, 2H, 3-H_2), 2.62 (t, J = 7.2 Hz, 2H, 2-H_2), 2.73 (broad t, J = 6.0 Hz, 2H, 1'-H_2), 3.02 (broad t,

J = 5.6 Hz, 2H, 4'-H_2), 4.08 (t, *J* = 7.2 Hz, 2H, 4-H_2), 4.85 (s, $^+$NH, NH), 7.58 (dd, *J* = 9.2 Hz, *J'* = 2.0 Hz, 1H, 7'-H), 7.80 (d, *J* = 1.6 Hz, 1H, 5'-H), 8.39 (d, *J* = 9.2 Hz, 1H, 8'-H).

^{13}C NMR (100.6 MHz, CD_3OD) *δ*: 15.1 (CH_2, C2), 21.7 (CH_2, C3'), 22.9 (CH_2, C2'), 25.0 (CH_2, C1'), 27.1 (CH_2, C3), 29.4 (CH_2, C4'), 47.8 (CH_2, C4), 113.9 (C), 115.5 (C) (C8a' and C9a'), 119.2 (CH, C5'), 120.5 (C, C1), 127.1 (CH, C7'), 128.6 (CH, C8'), 140.2 (CH, C6'), 140.4 (C, C10a'), 152.6 (C, C4a'), 157.9 (C, C9').

HRMS (ESI):

Calculated for ($C_{17}H_{18}{}^{35}ClN_3 + H^+$): 300.1262

Found: 300.1265

Preparation of 5-[(6-chloro-1,2,3,4-tetrahydroacridin-9-yl)amino]pentanenitrile, 90b

In a double necked 100 mL round-bottomed flask equipped with an inert atmosphere, a magnetic stirrer and 4 Å molecular sieves, 6-chlorotacrine **13** (1.50 g, 6.45 mmol) and finely powdered KOH (85% purity, 851 mg, 12.9 mmol) were suspended in anhydrous DMSO (20 mL). The resulting suspension was stirred, heating every 10 minutes with a heat gun for 1 hour, and at room temperature one more hour, then treated with 5-bromovaleronitrile, **89b** (0.9 mL, 1.25 g, 7.71 mmol). The reaction mixture was stirred at room temperature overnight, then diluted with 5 N NaOH aq. sol. (350 mL), and extracted with EtOAc (3 × 150 mL). The combined organic layers were washed with water (3 × 200 mL), dried over anhydrous Na_2SO_4, filtered and evaporated under reduced pressure to give a yellow oil (2.28 g), which was subjected to column chromatography purification [silica gel 35−70 µm (60 g); Ø = 4 cm; #1–38, 3 L, CH_2Cl_2 / 50% aq. NH_4OH 100:0.4], to afford the desired nitrile **90b** (#10–28, 1.30 g, 64% yield) as a clear yellow solid.

R_f = 0.73 (gel de sílice, 10 cm, CH_2Cl_2 / MeOH / NH_4OH 50% 95:5:1).

Analytical sample of 90b·HCl

In a 25 mL round-bottomed flask **90b** (21 mg, 0.07 mmol) was dissolved in CH_2Cl_2 (1 mL), filtered with a PTFE filter (0.2 µm), treated with HCl / MeOH (0.5 M, 0.41 mL), evaporated *in vacuo*, and washed with pentane (3 × 2 mL), giving, after drying in standard conditions, **90b**·HCl (35 mg) as a yellow solid.

Melting point: 73–75 °C.

IR (ATR) *v*: 3500–2500 (max at 3126, 3043, 2920, 2857, N–H, $^{+}$N–H, C–H st), 2236 (CN st), 1631, 1573, 1515 (Ar–C–C, Ar–C–N st) cm^{-1}.

^{1}H NMR (400 MHz, CD_3OD) *δ*: 1.78 (broad m, 2H, 3-H_2), 1.92–2.02 (complex signal, 6H, 4-H_2, 2'-H_2 and 3'-H_2), 2.54 (t, *J* = 6.0 Hz, 2H, 2-H_2), 2.70 (broad t, 2H, 1'-H_2), 3.00 (broad t, 2H, 4'-H_2), 4.00 (t, *J* = 7.2 Hz, 2H, 5-H_2), 4.85 (s, $^{+}$NH, NH), 7.57 (dd, *J* = 9.2 Hz, *J'* = 2.0 Hz, 1H, 7'-H), 7.78 (d, *J* = 1.6 Hz, 1H, 5'-H), 8.39 (d, *J* = 9.2 Hz, 1H, 8'-H).

^{13}C NMR (100.6 MHz, CD_3OD) *δ*: 17.5 (CH_2, C2), 21.9 (CH_2, C3'), 23.0 (CH_2, C2'), 24.1 (CH_2, C1'), 25.2 (CH_2, C3), 29.6 (CH_2, C4'), 30.6 (CH_2, C4), 49.9 (CH_2, C5), 113.7 (C), 115.6 (C) (C8a' and C9a'), 119.3 (CH, C5'), 120.9 (C, C1), 127.1 (CH, C7'), 128.9 (CH, C8'), 140.1 (CH, C6'), 140.5 (C, C10a'), 152.4 (C, C4a'), 157.9 (C, C9').

HRMS (ESI):

Calculated for ($C_{18}H_{20}{}^{35}ClN_3$ + H^+):	314.1419
Found:	300.1416

Preparation of 4-[(6-chloro-1,2,3,4-tetrahydroacridin-9-yl)amino]-*N*-(9-fluoro-7*H*-5,6,8,9,10,11-hexahydro-5,9:7,11-dimethanobenzo[9]annulen-7-yl)butanamide, 76a

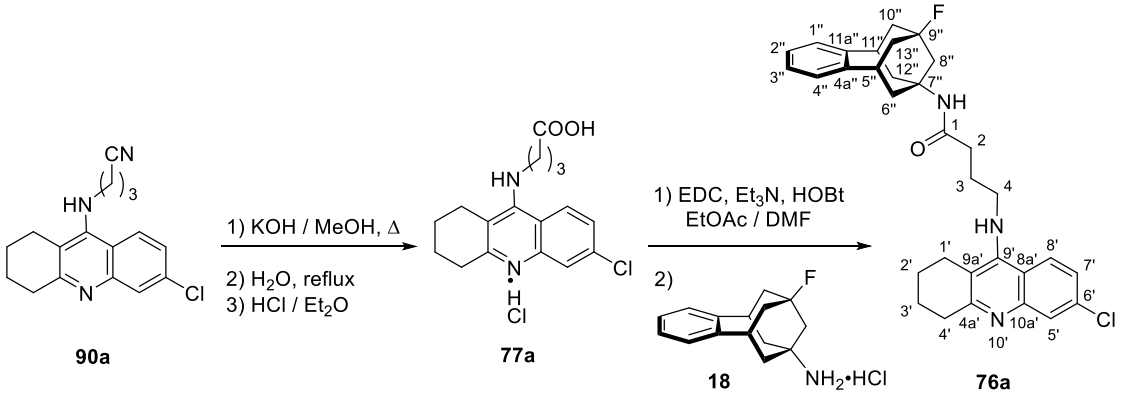

In a 100 mL round-bottomed flask supplied with a magnetic stirrer and a condenser, nitrile **90a** (1.53 g, 5.20mmol) was dissolved in MeOH (6.5 mL) and treated with a 40% solution of KOH in MeOH (13 mL). The resulting suspension was stirred under reflux for 3 hours, then treated with water (20.8 mL), and again stirred under reflux overnight. The resulting solution was cooled to room temperature, evaporated under reduced pressure, and treated with HCl / Et_2O (0.734 N, 142 mL), and concentrated *in vacuo* to give a white solid (7.42 g), whose ^{1}H-NMR spectrum was consistent with that expected for the desired acid, **77a**·HCl, and was used as a crude without further purification in the next step.

In a 100 mL round-bottomed flask provided with a magnetic stirrer, the acid **77a**·HCl (1.94 g of a crude that could contain a maximum of 1.36 mmol of the desired acid) was suspended in a mixture of EtOAc (25 mL) and DMF (2 mL), and treated with *N*-(3-dimethylaminopropyl)-*N'*-ethylcarbodiimide hydrochloride (316 mg, 1.65 mmol), triethylamine (0.94 mL, 685 mg, 6.78 mmol), and 1-hydroxy-1*H*-benzotriazole (185 mg, 1.36 mmol). The resulting mixture was stirred at room temperature for 15 minutes, then treated with a suspension of the amine **18** (346 mg, 1.50 mmol) in a mixture of EtOAc (16 mL) and DMF (2.1 mL), stirred at room temperature for 2 days, then concentrated *in vacuo* and diluted with 1 N NaOH aq. sol. (200 mL), and extracted with CH_2Cl_2 (2 × 150 mL). The combined organic layers were washed with water (5 × 100 mL), dried over anhydrous Na_2SO_4, filtered and evaporated under reduced pressure to give a brown oil (696 mg), which was subjected to column chromatography purification [silica gel 35−70 μm (50 g); Ø = 3 cm; #1–7, 1.1 L, CH_2Cl_2 / 50% aq.

NH_4OH 100:0.4; #8–15, 600 mL, CH_2Cl_2 / MeOH / 50% aq. NH_4OH 99.9:0.1:0.4; #16–47, 2 L, CH_2Cl_2 / MeOH / 50% aq. NH_4OH 99.8:0.2:0.4; #48–50, 200 mL, CH_2Cl_2 / MeOH / 50% aq. NH_4OH 99.5:0.5:0.4; #51–53, 200 mL, CH_2Cl_2 / MeOH / 50% aq. NH_4OH 99:1:0.4], to afford the desired amide **76a** with some unknown impurities (#31–40, 262 mg, 36% yield) as a yellow brown oil, and the pure desired compound **76a** (#41–48, 26 mg, 4% yield) as yellow-brown oil. The overall yield for the coupling reaction was 40%.

R_f = 0.53 (silica gel, 10 cm, CH_2Cl_2 / MeOH / 50% aq. NH_4OH 95:5:1).

Analytical sample of 76a·HCl

In a 25 mL round-bottomed flask, amide **76a** (26 mg, 0.05 mmol) was dissolved in CH_2Cl_2 (1 mL), filtered with a PTFE filter (0.2 μm), treated with HCl / MeOH (0.5 M, 0.3 mL), evaporated *in vacuo*, and washed with pentane (3 × 2 mL), to give, after drying in standard conditions, **76a**·HCl (27 mg) as a yellow solid.

Melting point: 169–173 °C.

Calculated logP: 6.59.

IR (ATR) *v*: 3500–2400 (max at 3246, 3054, 2917, 2852, 2795, N–H, $^+$N–H, C–H st), 1631, 1584, 1574, 1494 (Ar–C–C, Ar–C–N st) cm^{-1}.

^{1}H NMR (400 MHz, CD_3OD) δ: 1.80 [broad d, J = 10.8 Hz, 2H, 10''(13'')-H_B], 1.93 (complex signal, 4H, 2'-H_2 and 3'-H_2), 1.98–2.17 [complex signal, 10H, 3-H_2, 6''(12'')-H_A, 6''(12'')-H_B, 10''(13'')-H_A, 8''-H_2], 2.37 (t, J = 6.4 Hz, 2H, 2-H_2), 2.69 (broad t, 2H, 1'-H_2), 2.98 (broad t, 2H, 4'-H_2), 3.21 [m, 2H, 5''(11'')-H], 3.97 (t, J = 6.4 Hz, 2H, 4-H_2), 4.86 (s, $^+$NH, NH), 7.06–7.14 (complex signal, 4H, 1''-H, 2''-H, 3''-H and 4''-H), 7.49 (dd, J = 9.2 Hz, J' = 2.0 Hz, 1H, 7'-H), 7.75 (d, J = 2.4 Hz, 1H, 5'-H), 8.41 (d, J = 9.6 Hz, 1H, 8'-H).

^{13}C NMR (100.6 MHz, CD_3OD) δ: 21.8 (CH_2, C3'), 22.8 (CH_2, C2'), 25.0 (CH_2, C1'), 26.5 (CH_2, C3), 29.3 (CH_2, C4'), 34.8 (CH_2, C2), 39.3 [CH_2, d, $J_{C\text{-}F}$ = 1.3 Hz, C6''(12'')], 40.9 [CH, d, $J_{C\text{-}F}$ = 12.9 Hz, C5''(11'')], 41.3 [CH_2, d, $J_{C\text{-}F}$ = 20.0 Hz, C10''(13'')], 46.9 (CH_2, d, $J_{C\text{-}F}$ = 18.1 Hz, C8''), 49.3 (CH_2, C4),

58.8 (C, d, J_{C-F} = 11.0 Hz, C7''), 94.7 (C, d, J_{C-F} = 176.8 Hz, C9''), 113.4 (C, C9a'), 115.4 (C, C8a'), 119.0 (CH, C5'), 126.7 (CH, C7'), 128.0 [CH, C2''(3'')], 129.0 (CH, C8'), 129.2 [CH, C1"(C4''], 140.1 (C, C6'), 140.5 (C, C10a'), 146.2 [C, C4a''(C11a'')], 151.9 (C, C4a'), 157.9 (C, C9'), 174.3 (C, CONH).

HRMS (ESI):

Calculated for ($C_{32}H_{35}{}^{35}ClFN_3O + H^+$): 532.2525

Found: 532.2525

Preparation of 5-[(6-chloro-1,2,3,4-tetrahydroacridin-9-yl)amino]-*N*-(9-fluoro-7*H*-5,6,8,9,10,11-hexahydro-5,9:7,11-dimethanobenzo[9]annulen-7-yl)pentanamide, 76b

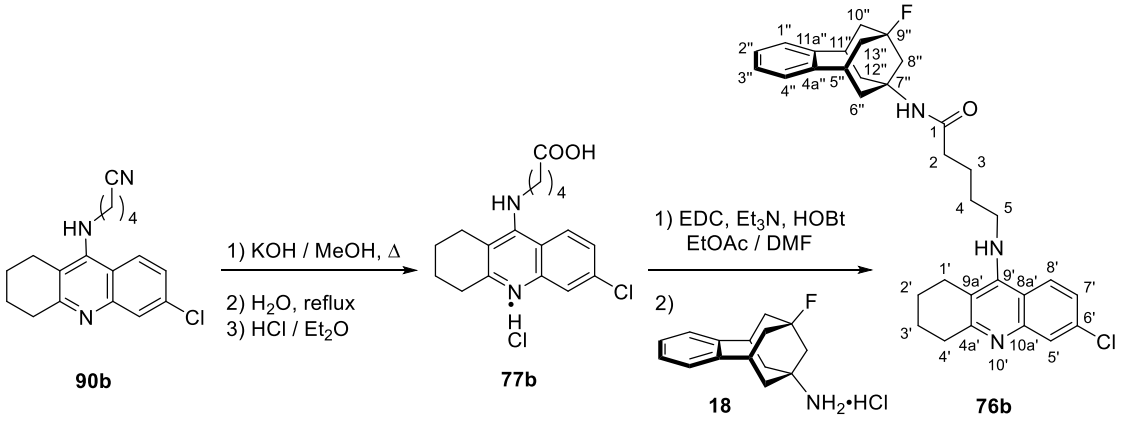

In a 100 mL round-bottomed flask equipped with a magnetic stirrer and a condenser, nitrile **90b** (1.24 g, 4.04 mmol) was dissolved in MeOH (5 mL) and treated with a 40% solution of KOH in MeOH (10 mL). The resulting suspension was stirred under reflux for 3 hours, then treated with water (16 mL), and again stirred under reflux overnight. The resulting solution was cooled to room temperature, evaporated under reduced pressure, and treated with HCl / Et_2O (0.734 N, 110 mL), and concentrated *in vacuo* to give a white solid (6.17 g), whose ^{1}H-NMR spectrum was consistent with that expected for the desired acid, **77b**·HCl, and was used as a crude without further purification in the next step.

In a 100 mL round-bottomed flask provided with a magnetic stirrer, the acid **77b**·HCl (1.21 g of a crude that could contain a maximum of 0.793 mmol of the desired acid) was suspended in a mixture of EtOAc (13.8 mL) and DMF (2.4 mL), and treated with *N*-(3-dimethylaminopropyl)-*N'*-ethylcarbodiimide hydrochloride (184 mg, 0.96 mmol), triethylamine (0.55 mL, 401 mg, 3.97 mmol), and 1-hydroxy-1*H*-benzotriazole (162 mg, 1.19 mmol). The resulting mixture was stirred at room temperature for 15 minutes, then treated with a suspension of the amine **18** (200 mg, 0.87 mmol) in a mixture of EtOAc (10 mL) and DMF (5 mL), stirred at room temperature for 2 days, and concentrated *in vacuo* to give a brown solid (1.87 g), which was subjected to column chromatography purification [silica gel 35−70 μm (120 g); Ø = 5 cm; #1–9, 800 mL, CH_2Cl_2 / 50% aq. NH_4OH 100:0.4; #10–12, 300 mL, CH_2Cl_2 / MeOH / 50% aq. NH_4OH 99.9:0.1:0.4; #13–15, 300 mL, CH_2Cl_2 / MeOH / 50% aq. NH_4OH 99.8:0.2:0.4; #16–18, 300 mL, CH_2Cl_2 / MeOH / 50% aq. NH_4OH 99.7:0.3:0.4; #19–21, 300 mL, CH_2Cl_2 / MeOH / 50%

aq. NH_4OH 99.5:0.5:0.4; #22–24, 300 mL, CH_2Cl_2 / MeOH / 50% aq. NH_4OH 99.3:0.7:0.4; #25–57, 3.2 L, CH_2Cl_2 / MeOH / 50% aq. NH_4OH 99:1:0.4; #58–60, 300 mL, CH_2Cl_2 / MeOH / 50% aq. NH_4OH 98.5:1.5:0.4; #61–63, 300 mL, CH_2Cl_2 / MeOH / 50% aq. NH_4OH 98:2:0.4], to afford the desired amide **76b** (#45–49, 120 mg, 28% yield) as a yellow oil, and the desired amide **76b** with some unknown impurities (#50–60, 204 mg, 47% yield) as a yellow oil. The overall yield for the coupling reaction was 75%.

R_f = 0.61 (silica gel, 10 cm, CH_2Cl_2 / MeOH / 50% aq. NH_4OH 95:5:1).

Analytical sample of 76b·HCl

In a 25 mL round-bottomed flask **76b** (36 mg, 0.07 mmol) was dissolved in CH_2Cl_2 (1 mL), filtered with a PTFE filter (0.45 µm), treated with HCl / MeOH (0.5 M, 0.4 mL), evaporated *in vacuo*, and washed with pentane (3 × 2 mL), to give, after drying in standard conditions, **76b**·HCl (38 mg) as a yellow solid.

Melting point: 181–185 °C.

Calculated logP: 7.10.

IR (ATR) *v*: 3500–2500 (max at 3193, 3126, 3043, 2915, 2857, N–H, $^+$N–H, C–H st), 1632, 1589, 1571 (Ar–C–C, Ar–C–N st) cm^{-1}.

^{1}H NMR (400 MHz, CD_3OD) *δ*: 1.68 (dt, *J* = 8.0 Hz, 2H, 3-H_2), 1.77–1.82 [complex signal, 2H, 10''(13'')-H_B], overlapped 1.83 (broad dt, 2H, 4-H_2), 1.93 (complex signal, 4H, 2'-H_2 and 3'-H_2), 2.00–2.15 [complex signal, 8H, 6''(12'')-H_A, 6''(12'')-H_B, 10''(13'')-H_A and 8''-H_2], 2.20 (t, *J* = 6.4 Hz, 2H, 2-H_2), 2.67 (broad t, 2H, 1'-H_2), 2.98 (broad t, 2H, 4'-H_2), 3.20 [broad m, 2H, 5''(11'')-H], 3.94 (t, *J* = 6.4 Hz, 2H, 5-H_2), 4.85 (s, $^+$NH, NH), 7.06–7.13 (complex signal, 4H, 1''-H, 2''-H, 3''-H and 4''-H), 7.54 (dd, *J* = 9.2 Hz, *J*' = 2.0 Hz, 1H, 7'-H), 7.76 (d, *J* = 2.4 Hz, 1H, 5'-H), 8.39 (d, *J* = 9.2 Hz, 1H, 8'-H).

^{13}C NMR (100.6 MHz, CD_3OD) *δ*: 21.7 (CH_2, C3'), 22.8 (CH_2, C2'), 23.6 (CH_2, C3), 24.8 (CH_2, C1'), 29.3 (CH_2, C4'), 30.5 (CH_2, C4), 36.7 (CH_2, C2), 39.3 [CH_2, d, $J_{C\text{-}F}$ = 2.0 Hz, C6''(12'')], 40.9 [CH, d,

$J_{C\text{-}F}$ = 12.9 Hz, C5''(11'')], 41.3 [CH_2, d, $J_{C\text{-}F}$ = 20.0 Hz, C10''(13'')], 46.8 (CH_2, d, $J_{C\text{-}F}$ = 18.1 Hz, C8''), 48.7 (CH_2, C5), 58.7 (C, d, $J_{C\text{-}F}$ = 11.6 Hz, C7''), 94.7 (C, d, $J_{C\text{-}F}$ = 176.8 Hz, C9''), 113.5 (C, C9a'), 115.5 (C, C8a'), 119.1 (CH, C5'), 126.8 (CH, C7'), 128.0 [CH, C2''(3'')], 128.8 (CH, C8'), 129.1 [CH, C1"(C4''], 140.1 (C, C6'), 140.5 (C, C10a'), 146.2 [C, C4a''(C11a'')], 152.1 (C, C4a'), 157.8 (C, C9'), 174.8 (C, CONH).

HRMS (ESI):

Calculated for ($C_{33}H_{37}{}^{35}ClFN_3O + H^+$): 546.2682

Found: 546.2685

Preparation of *N*-(6-chloro-1,2,3,4-tetrahydroacridin-9-yl)-*N'*-(9-fluoro-7*H*-5,6,8,9,10,11-hexahydro-5,9:7,11-dimethanobenzo[9]annulen-7-yl)butane-1,4-diamine, 75a

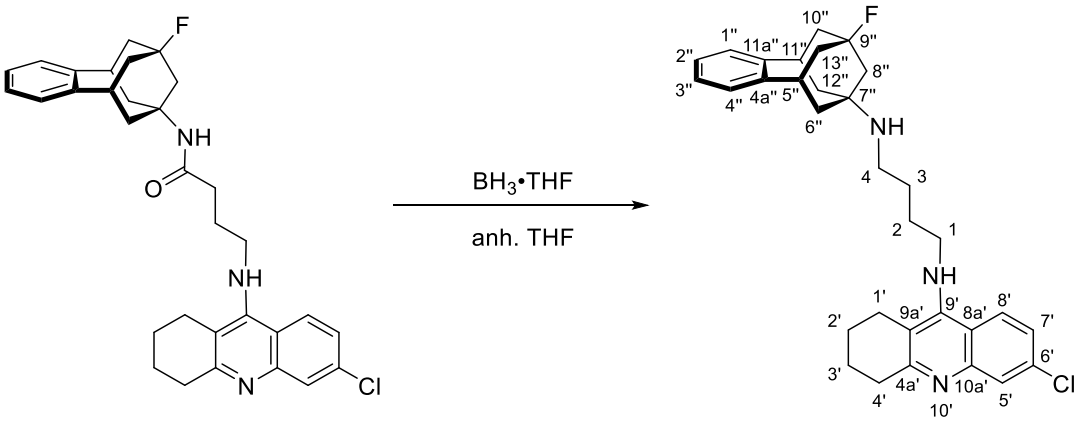

76a **75a**

In a double necked 5 mL round-bottomed flask equipped with an inert atmosphere and a magnetic stirrer, a solution of amide **76a** (124 mg, 0.22 mmol) in anhydrous THF (5 mL) was prepared, cooled to 0 °C with an ice bath, then treated dropwise with BH_3·THF (1 M in THF, 0.87 mL, 0.87 mmol) and stirred at room temperature overnight. The resulting mixture was cooled to 0 °C, and treated dropwise with MeOH (3 mL) and water (3 mL). The organic phase was evaporated under reduced pressure, the aqueous phase was diluted with 1 N NaOH aq. sol. (10 mL) and extracted with CH_2Cl_2 (3 × 10 mL). The combined organic layers were dried over anhydrous Na_2SO_4, filtered and evaporated *in vacuo* to give a beige solid (111 mg), which was subjected to column chromatography purification [silica gel 35−70 µm (12 g); Ø = 1.5 cm; #1–42, 700 mL, hexane / EtOAc / 50% aq. NH_4OH 50:50:0.4; #43–80, 800 mL, hexane / EtOAc / 50% aq. NH_4OH 40:60:0.4], to afford starting material **76a** (#9–42, 41 mg) as a yellow oil, and the desired amine **75a** (#45–70, 27 mg, 24% yield) as a yellow sticky solid.

R_f = 0.45 (silica gel, 10 cm, CH_2Cl_2 / MeOH / 50% aq. NH_4OH 95:5:1).

Analytical sample of 75a·2HCl

In a 25 mL round-bottomed flask **75a** (27 mg, 0.05 mmol) was dissolved in CH_2Cl_2 (1 mL), filtered with a PTFE filter (0.22 µm), treated with HCl / MeOH (0.5 M, 0.26 mL), evaporated *in vacuo*, washed with pentane (3 × 2 mL), then dissolved in a mixture MeOH / EtOAc 1:1 (1 mL),

and after 10 days at 4 °C, filtered off to give, after drying in standard conditions, **75a**·2HCl (7 mg) as a pale yellow solid.

Calculated logP: 7.27.

^{1}H NMR (400 MHz, CD_3OD) δ: 1.81 (broad m, 2H, 3-H_2), 1.86–2.03 (complex signal, 10H, 2-H_2, 2'-H_2, 3'-H_2, 6''(12'')-H_B and 10''(13'')-H_B], 2.14–2.26 [complex signal, 6H, 6''(12'')-H_A, 10''(13'')-H_A and 8''-H_2], 2.71 (broad t, J = 5.2 Hz, 2H, 1'-H_2), 3.00 (broad t, 2H, 4'-H_2), 3.08 (t, J = 7.6 Hz, 2H, 4-H_2), 3.42 [m, 2H, 5''(11'')-H], 4.01 (t, J = 7.2 Hz, 2H, 1-H_2), 4.86 (s, $^{+}$NH, NH), 7.16 (broad s, 4H, 1''-H, 2''-H, 3''-H and 4''-H), 7.58 (dd, J = 8.8 Hz, J' = 2.0 Hz, 1H, 7'-H), 7.77 (d, J = 2.0 Hz, 1H, 5'-H), 8.41 (d, J = 8.8 Hz, 1H, 8'-H).

^{13}C NMR (125.8 MHz, CD_3OD) δ: 21.8 (CH_2, C2'), 22.9 (CH_2, C3'), overlapped 24.9 (CH_2, C1'), 25.1, C3), 28.5 (CH_2, C2), 29.4 (CH_2, C4'), 36.6 [CH_2, C6''(12'')], 40.0 [CH, d, $J_{C\text{-}F}$ = 16.4 Hz, C5''(11'')], 40.7 [CH_2, d, $J_{C\text{-}F}$ = 25.2 Hz, C10''(13'')], 41.2 (CH_2, C4), 43.0 (CH_2, d, $J_{C\text{-}F}$ = 26.4 Hz, C8''), 49.7 (CH_2, C1), 63.8 (C, d, $J_{C\text{-}F}$ = 13.8 Hz, C7''), 94.2 (C, d, $J_{C\text{-}F}$ = 225.182 Hz, C9''), 113.8 (C, C9a'), 115.6 (C, C8a'), 119.3 (CH, C5'), 127.0 (CH, C7'), 128.6 [CH, C2''(3'')], 128.8 (CH, C8'), 129.4 [CH, C1"(C4''], 140.1 (C, C6'), 140.6 (C, C10a'), 145.1 [C, C4a''(C11a'')], 152.5 (C, C4a'), 157.9 (C, C9').

HRMS (ESI):

Calculated for ($C_{32}H_{37}{}^{35}ClFN_3 + H^+$): 518.2733

Found: 518.2738

Preparation of *N*-(6-chloro-1,2,3,4-tetrahydroacridin-9-yl)-*N'*-(9-fluoro-7*H*-5,6,8,9,10,11-hexahydro-5,9:7,11-dimethanobenzo[9]annulen-7-yl)pentane-1,5-diamine, 75b

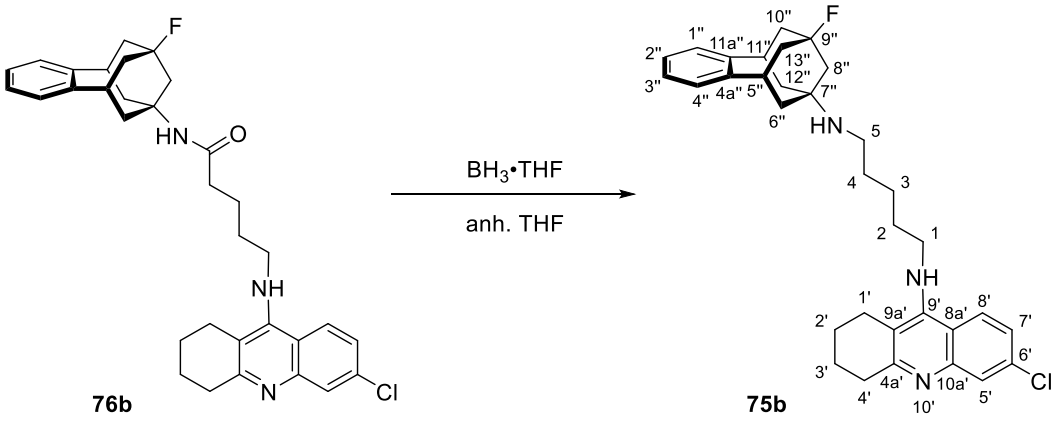

In a double necked 10 mL round-bottomed flask equipped with an inert atmosphere and a magnetic stirrer, a solution of amide **76b** (100 mg, 0.18 mmol) in anhydrous THF (1.5 mL) was prepared, cooled to 0 °C with an ice bath, then treated dropwise with BH_3·THF (1 M in THF, 0.73 mL, 0.73 mmol) and stirred at room temperature overnight. The resulting mixture was cooled to 0 °C, and treated dropwise with MeOH (2 mL) and water (2 mL). The organic phase was evaporated under reduced pressure, and the aqueous phase diluted with 1 N NaOH aq. sol. (10 mL), and extracted with CH_2Cl_2 (3 × 10 mL). The combined organic layers were dried over anhydrous Na_2SO_4, filtered and evaporated *in vacuo* to give an orange solid (79 mg), which was subjected to column chromatography purification [silica gel 35−70 μm (16 g); Ø = 1.5 cm; #1–9, 100 mL, hexane / Et_3N 100:0.2; #10–21, 150 mL, hexane / EtOAc / Et_3N 90:10:0.2; #22–28, 100 mL, hexane / EtOAc / Et_3N 80:20:0.2; #29–40, 150 mL, hexane / EtOAc / Et_3N 70:30:0.2; #41–48, 100 mL, hexane / EtOAc / Et_3N 60:40:0.2; #49–62, 200 mL, hexane / EtOAc / Et_3N 50:50:0.2; #63–70, 100 mL, hexane / EtOAc / Et_3N 40:60:0.2; #71–110, 300 mL, hexane / EtOAc / Et_3N 30:70:0.2; #100–115, 100 mL, EtOAc / Et_3N 100:0.2], to afford the desired amine **75b** (#82–92, 10 mg, 10% yield) as a yellow solid.

R_f = 0.45 (silica gel, 10 cm, CH_2Cl_2 / MeOH / 50% aq. NH_4OH 95:5:1).

Analytical sample of 75b·2HCl

In a 10 mL round-bottomed flask, **75b** (10 mg, 0.02 mmol) was dissolved in CH_2Cl_2 (1 mL), filtered with a PTFE filter (0.2 µm), treated with HCl / Et_2O (1.35 N, 0.13 mL), evaporated *in vacuo*, and washed with pentane (3 × 2 mL), to give, after drying in standard conditions, **75b**·2HCl (12 mg) as a yellow solid.

Calculated logP: 7.78.

^{1}H NMR (400 MHz, CD_3OD) δ: 1.55 (dt, J = J' = 7.6Hz, 2H, 3-H_2), 1.77 (broad dt, 2H, 4-H_2), 1.85–1.97 (complex signal, 6H, 2-H_2, 6''(12'')-H_B and 10''(13'')-H_B], overlapped 1.92–2.00 (complex signal, 4H, 2'-H_2 and 3'-H_2), 2.16–2.26 [complex signal, 6H, 6''(12'')-H_A, 10''(13'')-H_A and 8''-H_2], 2.70 (broad t, J = 6.0 Hz, 2H, 1'-H_2), 3.00 (broad t, 2H, 4'-H_2), 3.04 (t, J = 8.0 Hz, 2H, 5-H_2), 3.42 [m, 2H, 5''(11'')-H], 3.97 (t, J = 7.6 Hz, 2H, 1-H_2), 4.85 (s, $^+$NH, NH), 7.15 (broad s, 4H, 1''-H, 2''-H, 3''-H and 4''-H), 7.57 (dd, J = 9.2 Hz, J' = 2.0 Hz, 1H, 7'-H), 7.78 (d, J = 2.0 Hz, 1H, 5'-H), 8.41 (d, J = 9.6 Hz, 1H, 8'-H).

^{13}C NMR (100.6 MHz, CD_3OD) δ: 21.7 (CH_2, C2'), 22.9 (CH_2, C3'), overlapped 24.8 (CH_2, C1' and C3), 27.4 (CH_2, C4), 29.3 (CH_2, C4'), 30.8 (CH_2, C2), 36.5 [CH_2, C6''(12'')], 40.0 [CH, d, $J_{C\text{-}F}$ = 13.0 Hz, C5''(11'')], 40.7 [CH_2, d, $J_{C\text{-}F}$ = 20.6 Hz, C10''(13'')], 41.3 (CH_2, C5), 44.3 (CH_2, d, $J_{C\text{-}F}$ = 20.7 Hz, C8''), overlapped 48.8 (CH_2, C1), 63.7 (C, d, $J_{C\text{-}F}$ = 11.0 Hz, C7''), 94.2 (C, d, $J_{C\text{-}F}$ = 180.0 Hz, C9''), 113.5 (C, C9a'), 115.5 (C, C8a'), 119.1 (CH, C5'), 126.9 (CH, C7'), 128.5 [CH, C2''(3'')], 128.8 (CH, C8'), 129.4 [CH, C1"(C4''], 140.1 (C, C6'), 140.5 (C, C10a'), 145.2 [C, C4a''(C11a'')], 152.2 (C, C4a'), 157.9 (C, C9').

HRMS (ESI):

Calculated for ($C_{33}H_{39}{}^{35}ClFN_3$ + H^+):	532.2889
Found:	532.2906

Attempted preparation of *N*-[(6-chloro-1,2,3,4-tetrahydroacridin-9-yl)amino]-*N'*-(9-fluoro-7*H*-5,6,8,9,10,11-hexahydro-5,9:7,11-dimethanobenzo[9]annulen-7-yl)pentane-1,5-diamine, 75b

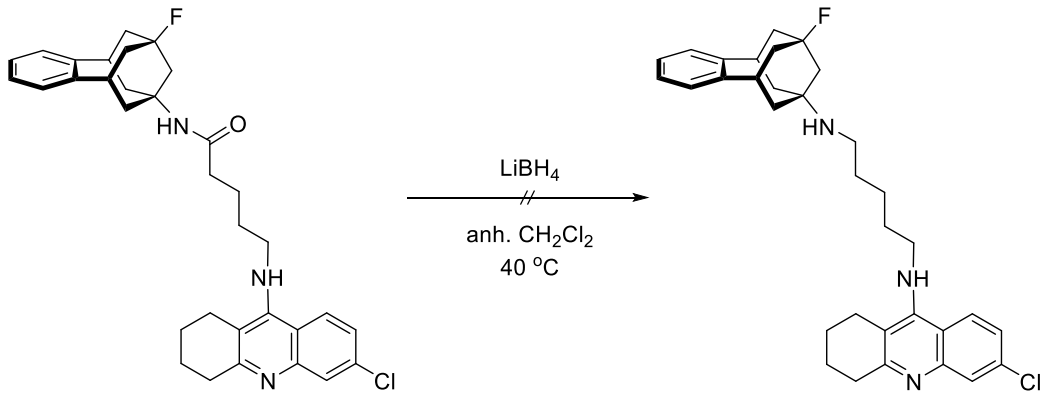

76b **75b**

In a double necked 25 mL round-bottomed flask equipped with an inert atmosphere, a magnetic stirrer and a condenser, lithium borohydride (17 mg, 0.78 mmol) was suspended in anhydrous CH_2Cl_2 (2 mL), then treated with a solution of amide **76b** (148 mg, 0.26 mmol) in anhydrous CH_2Cl_2 (6.2 mL). The resulting suspension was stirred at 40 °C for 2 hours, then treated dropwise with MeOH (3.9 mL) and water (3.9 mL), and alkalinized with 1 N NaOH aq. sol. (50 mL). The organic layer was evaporated under reduced pressure and the aqueous layer was extracted with EtOAc (3 × 40 mL). The combined organic layers were dried over anhydrous Na_2SO_4, filtered and concentrated *in vacuo* to provide starting material (128 mg) as a yellow oil.

Attempted preparation of *N*-[(6-chloro-1,2,3,4-tetrahydroacridin-9-yl)amino]-*N'*-(9-fluoro-7*H*-5,6,8,9,10,11-hexahydro-5,9:7,11-dimethanobenzo[9]annulen-7-yl)pentane-1,5-diamine, 75b

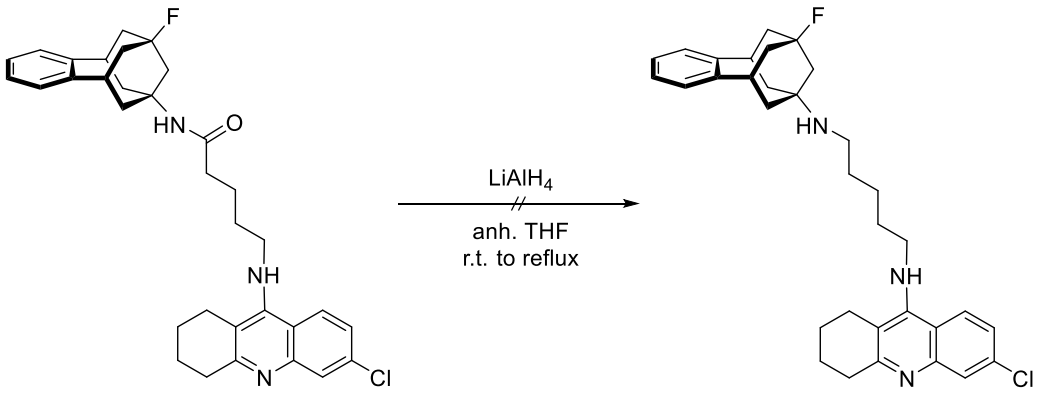

76b **75b**

In a double necked 5 mL round-bottomed flask equipped with an inert atmosphere, a magnetic stirrer and a condenser, $LiAlH_4$ (18 mg, 0.46 mmol) was placed, then treated dropwise with a solution of amide **76b** (90 mg, 0.17 mmol) in anhydrous THF (0.9 mL), and the resulting mixture was stirred at room temperature for 1 hour, and for 30 more minutes under reflux. The reaction mixture was cooled to 0 ^{o}C with an ice bath, then treated with water (0.5 mL), diluted with EtOAc (20 mL), dried over anhydrous Na_2SO_4, filtered and evaporated *in vacuo* to give a yellow oil (92 mg), which was identified as starting material **76b**.

Attempted preparation of *N*-[(6-chloro-1,2,3,4-tetrahydroacridin-9-yl)amino]-*N'*-(9-fluoro-7*H*-5,6,8,9,10,11-hexahydro-5,9:7,11-dimethanobenzo[9]annulen-7-yl)pentane-1,5-diamine, 75b

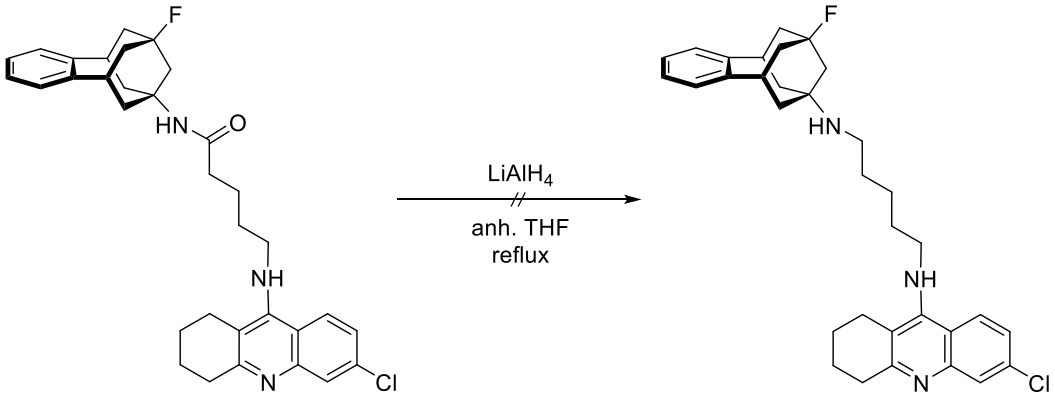

76b **75b**

In a double necked 10 mL round-bottomed flask equipped with an inert atmosphere, a magnetic stirrer and a condenser, a solution of amide **76b** (32 mg, 0.06 mmol) in anhydrous THF (5 mL) was prepared, cooled to 0 °C with an ice bath, then treated portionwise with lithium aluminum hydride (6.7 mg, 0.18 mmol) and stirred under reflux overnight. The resulting mixture was cooled to 0 °C, treated with 1 N NaOH aq. sol. (3 mL), diluted with water (8 mL), and extracted with EtOAc (3 × 10 mL). The combined organic layers were dried over anhydrous Na_2SO_4, filtered and evaporated *in vacuo* to give a pale yellow oil (32 mg), which was purified by preparative thin-layer chromatography [20 × 20 cm, silica gel 60 F_{25} 0.5 mm, eluent CH_2Cl_2 / MeOH / 50% aq. NH_4OH 95:5:1], nevertheless only byproducts were found.

Attempted preparation of *N*-[(6-chloro-1,2,3,4-tetrahydroacridin-9-yl)amino]-*N'*-(9-fluoro-7*H*-5,6,8,9,10,11-hexahydro-5,9:7,11-dimethanobenzo[9]annulen-7-yl)pentane-1,5-diamine, 75b

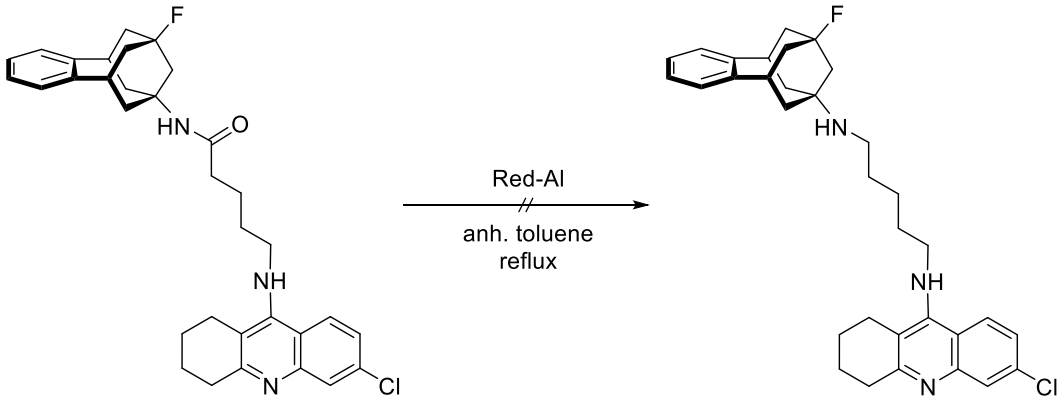

76b **75b**

In a double necked 10 mL round-bottomed flask equipped with an inert atmosphere, a magnetic stirrer and a condenser, a solution of amide **76b** (92 mg, 0.17 mmol) in anhydrous toluene (2.5 mL) was prepared, cooled to 0 °C with an ice bath, then treated dropwise with sodium bis(2-methoxyethoxy)aluminum hydride (65% purity, 209 mg, 0.67 mmol) and stirred under reflux overnight. The resulting mixture was cooled to room temperature, treated with 1 N NaOH aq. sol. (3 mL), and extracted with CH_2Cl_2 (4 × 12 mL). The combined organic layers were dried over anhydrous Na_2SO_4, filtered and evaporated *in vacuo* to give a brown oil (81 mg), which was found to be starting material.

Preparation of 4-[(6-chloro-1,2,3,4-tetrahydroacridin-9-yl)amino]butan-1-ol, 96a

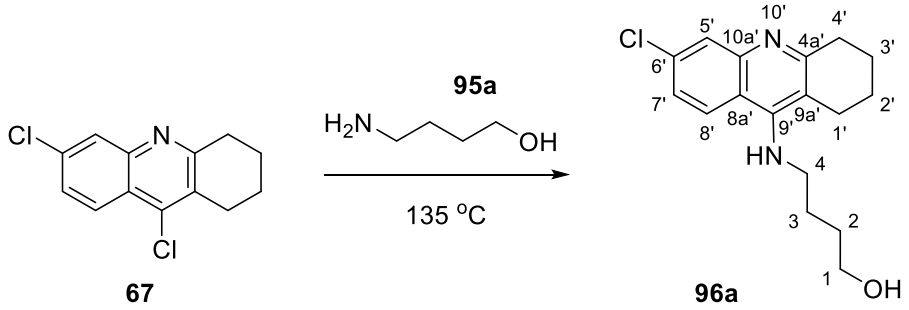

In a 25 mL round-bottomed flask equipped with a magnetic stirrer and a refrigerant, a mixture of 6,9-dichlo-1,2,3,4-tetrahydroacridine, **67** (1.50 g, 5.95 mmol), and 4-amino-1-butanol, **95a** (2.39 mL, 2.31 g, 25.9 mmol), was prepared, and stirred at 135 °C for 1 day. The reaction mixture was cooled to room temperature, poured onto water (150 mL) and filtered off, to give the desired alcohol **96a** (1.81 g, quantitative yield) as a brown solid.

R_f = 0.28 (gel de sílice, 10 cm, CH_2Cl_2 / MeOH / NH_4OH 50% 95:5:1).

Analytical sample of 96a·HCl

In a 25 mL round-bottomed flask, alcohol **96a** (66 mg, 0.22 mmol) was dissolved in CH_2Cl_2 (1 mL), filtered with a PTFE filter (0.2 µm), treated with HCl / MeOH (0.5 M, 1.3 mL), evaporated *in vacuo*, and washed with pentane (3 × 2 mL), giving, after drying in standard conditions, **96a**·HCl (80 mg) as a white solid.

Melting point: 203–205 °C

IR (ATR) *v*: 3241 (O–H), 3500–2400 (max at 2930, 2781, N–H, $^+$N–H, C–H st), 1632, 1590, 1567, 1524 (Ar–C–C, Ar–C–N st) cm^{-1}.

^{1}H NMR (400 MHz, CD_3OD) δ: 1.67 (m, 2H, 2-H_2), 1.89–2.20 (complex signal, 6H, 3-H_2, 2'-H_2 and 3'-H_2), 2.68 (broad t, J = 5.6 Hz, 2H, 1'-H_2), 3.00 (broad t, J = 6.4 Hz, 2H, 4'-H_2), 3.63 (t, J = 6.4 Hz, 2H, 1-H_2), 3.99 (t, J = 7.6 Hz, 2H, 4-H_2), 4.88 (s, $^+$NH, NH, OH), 7.56 (dd, J = 9.2 Hz, J' = 2.0 Hz, 1H, 7'-H), 7.77 (d, J = 2.4 Hz, 1H, 5'-H), 8.42 (d, J = 9.6 Hz, 1H, 8'-H).

^{13}C NMR (100.6 MHz, CD_3OD) δ: 21.8 (CH_2, C3'), 22.9 (CH_2, C2'), 24.8 (CH_2, C1'), 28.0 (CH_2, C2), 29.3 (CH_2, C4'), 30.5 (CH_2, C3), 49.1 (CH_2, C4), 62.2 (CH_2, C1), 113.3 (C, C9a'), 115.4 (C, C8a'), 119.1 (CH, C5'), 126.7 (CH, C7'), 128.9 (CH, C8'), 140.0 (C, C6'), 140.5 (C, C10a'), 152.0 (C, C4a'), 157.8 (C, C9').

HRMS (ESI):

Calculated for ($C_{17}H_{21}{}^{35}ClN_2O + H^+$): 305.1415

Found: 305.1421

Preparation of 5-[(6-chloro-1,2,3,4-tetrahydroacridin-9-yl)amino]pentan-1-ol, 96b

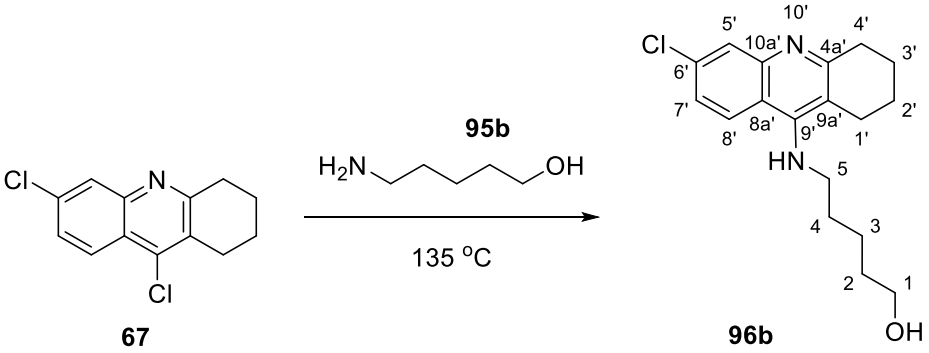

In a 50 mL round-bottomed flask equipped with a magnetic stirrer and a refrigerant, a mixture of 6,9-dichlo-1,2,3,4-tetrahydroacridine, **67** (1.50 g, 5.95 mmol), and 5-amino-1-pentanol, **95b** (7.76 mL, 7.36 g, 71.3 mmol), was prepared, and stirred at 135 °C for 1 day. The reaction mixture was cooled to room temperature, poured onto water (200 mL), diluted with 5 N NaOH aq. sol. (50 mL), and extracted with EtOAc (3 × 100 mL). The combined organic layers were dried over anhydrous Na_2SO_4, filtered and evaporated under reduced pressure, to give a dark brown oil (2.50 g), which was subjected to column chromatography purification [silica gel 35−70 µm (100 g); Ø = 4.5 cm; #1–9, 700 mL, CH_2Cl_2 / 50% aq. NH_4OH 100:0.4; #10–12, 300 mL, CH_2Cl_2 / MeOH / 50% aq. NH_4OH 99:1:0.4; #13–15, 300 mL, CH_2Cl_2 / MeOH / 50% aq. NH_4OH 98:2:0.4; #16–29, 1.3 L, CH_2Cl_2 / MeOH / 50% aq. NH_4OH 97:3:0.4; #30–31, 200 mL, CH_2Cl_2 / MeOH / 50% aq. NH_4OH 95:5:0.4], to afford starting material **67** (#4–7, 943 mg) as a white solid, and desired compound **96b** (#19–24, 767 mg, 40% yield).

R_f = 0.32 (gel de sílice, 10 cm, CH_2Cl_2 / MeOH / NH_4OH 50% 95:5:1).

Analytical sample of 96b·HCl

In a 25 mL round-bottomed flask, alcohol **96b** (55 mg, 0.17 mmol) was dissolved in CH_2Cl_2 (1 mL), filtered with a PTFE filter (0.2 µm), treated with HCl / MeOH (0.5 M, 1.0 mL), evaporated *in vacuo*, and washed with pentane (3 × 2 mL), giving, after drying in standard conditions, **96b**·HCl (61 mg) as a beige solid.

Melting point: 148–150 °C

IR (ATR) *v*: 3250 (O–H), 3100–2400 (max at 2924, 2859, 2702, N–H, $^{+}$N–H, C–H st), 1629, 1567, 1513 (Ar–C–C, Ar–C–N st) cm^{-1}.

^{1}H NMR (400 MHz, CD_3OD) *δ*: 1.51 (m, 2H, 3-H_2), 1.67 (m, 2H, 2-H_2), 1.88 (m, 2H 4-H_2), 1.92–2.20 (complex signal, 4H, 2'-H_2 and 3'-H_2), 2.68 (broad t, *J* = 6.0 Hz, 2H, 1'-H_2), 3.00 (broad t, *J* = 6.0 Hz, 2H, 4'-H_2), 3.57 (t, *J* = 6.4 Hz, 2H, 1-H_2), 3.96 (t, *J* = 7.2 Hz, 2H, 5-H_2), 4.85 (s, $^{+}$NH, NH, OH), 7.57 (dd, *J* = 9.2 Hz, *J*' = 2.0 Hz, 1H, 7'-H), 7.77 (d, *J* = 2.0 Hz, 1H, 5'-H), 8.40 (d, *J* = 9.2 Hz, 1H, 8'-H).

^{13}C NMR (100.6 MHz, CD_3OD) *δ*: 21.8 (CH_2, C3'), 22.9 (CH_2, C2'), 24.1 (CH_2, C3), 24.7 (CH_2, C1'), 29.3 (CH_2, C4'), 31.1 (CH_2, C4), 33.0 (CH_2, C2), 48.8 (CH_2, C5), 62.6 (CH_2, C1), 113.4 (C, C9a'), 115.4 (C, C8a'), 119.1 (CH, C5'), 126.8 (CH, C7'), 128.8 (CH, C8'), 140.1 (C, C6'), 140.5 (C, C10a'), 152.1 (C, C4a'), 157.9 (C, C9').

HRMS (ESI):

Calculated for ($C_{18}H_{23}{}^{35}ClN_2O + H^{+}$):	319.1578
Found:	319.1585

Attempted preparation of 4-[(6-chloro-1,2,3,4-tetrahydroacridin-9-yl)amino]butyl methanesulfonate, 94a

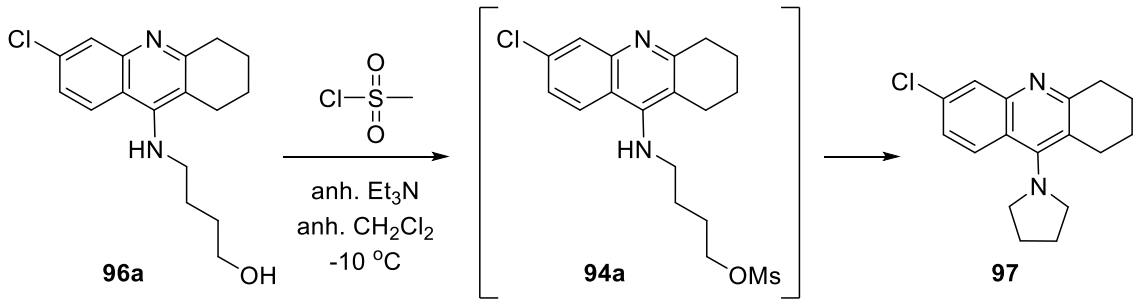

In double necked 25 mL round-bottomed flask provided with a magnetic stirrer, an inert atmosphere and an ice / NaCl bath (-10 °C), a solution of alcohol **96a** (400 mg, 1.31 mmol) and anhydrous Et_3N (0.31 mL, 225 mg, 2.23 mmol) in anhydrous CH_2Cl_2 (8 mL) was prepared, then treated dropwise with methanesulfonyl chloride (0.15 mL, 225 mg, 1.97 mmol) and stirred for 30 minutes at -10 °C. The resulting mixture was concentrated *in vacuo* and the residue was dissolved in CH_2Cl_2 (20 mL), then washed with 2 N NaOH aq. sol. (3 × 15 mL), dried over anhydrous Na_2SO_4, filtered and concentrated under vacuum, to afford the cyclization compound **97** (497 mg) as a dark brown oil.

Preparation of 5-[(6-chloro-1,2,3,4-tetrahydroacridin-9-yl)amino]pentyl methanesulfonate, 94b

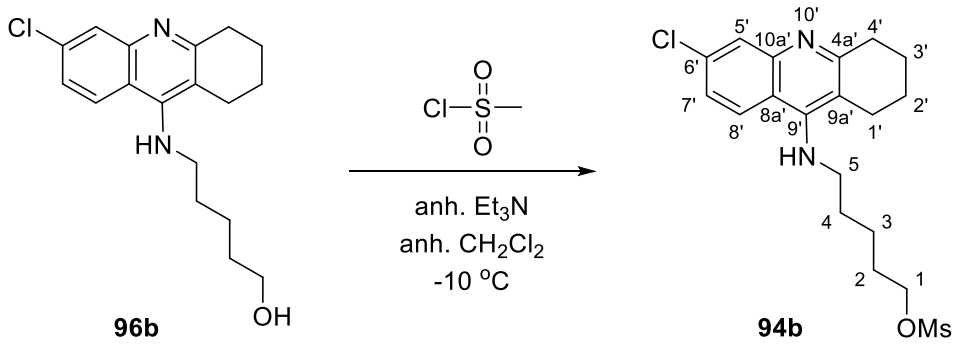

In double necked 25 mL round-bottomed flask provided with a magnetic stirrer, an inert atmosphere and an ice / NaCl bath (-10 °C), a solution of alcohol **96b** (368 mg, 1.15 mmol) and anhydrous Et_3N (0.27 mL, 197 mg, 1.95 mmol) in anhydrous CH_2Cl_2 (6.9 mL) was prepared, then treated dropwise with methanesulfonyl chloride (0.13 mL, 192 mg, 1.68 mmol) and stirred for 30 minutes at -10 °C. The resulting mixture was concentrated *in vacuo* and the residue was dissolved in CH_2Cl_2 (20 mL), then washed with 2 N NaOH aq. sol. (3 × 15 mL), dried over anhydrous Na_2SO_4, filtered and concentrated under vacuum to afford the desired mesylate **94b** (461 mg; quantitative yield) as a dark brown oil.

R_f = 0.72 (gel de sílice, 10 cm, CH_2Cl_2 / MeOH / NH_4OH 50% 95:5:1).

Analytical sample of 94b

In a 25 mL round-bottomed flask, **94b** (25 mg, 0.06 mmol) was dissolved in CH_2Cl_2 (1 mL), filtered with a PTFE filter (0.2 µm), evaporated *in vacuo*, and washed with pentane (3 × 2 mL), giving, after drying in standard conditions, **94b** (24 mg) as a dark brown oil.

IR (ATR) *v*: 3100–2800 (max at 2932, 2860, N–H, $^+$N–H, C–H st), 1634, 1604, 1574, 1555 (Ar–C–C, Ar–C–N st) cm^{-1}.

^{1}H NMR (400 MHz, $CDCl_3$) *δ*: 1.54 (m, 2H, 3-H_2), 1.74 (dt, *J* = 13.6 Hz, *J* = 6.8 Hz, 2H, 2-H_2), partially overlapped 1.80 (m, 2H 4-H_2), 1.86–1.93 (complex signal, 4H, 2'-H_2 and 3'-H_2), 2.67 (broad t, 2H,

1'-H_2), 2.99 (s, 3H, 1-SO_3CH_3), 3.03 (broad t, 2H, 4'-H_2), 3.58 (broad t, 2H, 5-H_2), 4.24 (t, *J* = 6.4 Hz, 2H, 1-H_2), 7.25 (dd, *J* = 9.2 Hz, *J*' = 2.0 Hz, 1H, 7'-H), 7.88 (d, *J* = 2.0 Hz, 1H, 5'-H), 7.93 (d, *J* = 9.2 Hz, 1H, 8'-H).

HRMS (ESI):

Calculated for ($C_{19}H_{25}{}^{35}ClN_2O_3 + H^+$): 397.1347

Found: 397.1353

Attempted preparation of *N*-[(6-chloro-1,2,3,4-tetrahydroacridin-9-yl)amino]-*N'*-(9-fluoro-7*H*-5,6,8,9,10,11-hexahydro-5,9:7,11-dimethanobenzo[9]annulen-7-yl)pentane-1,5-diamine, 75b

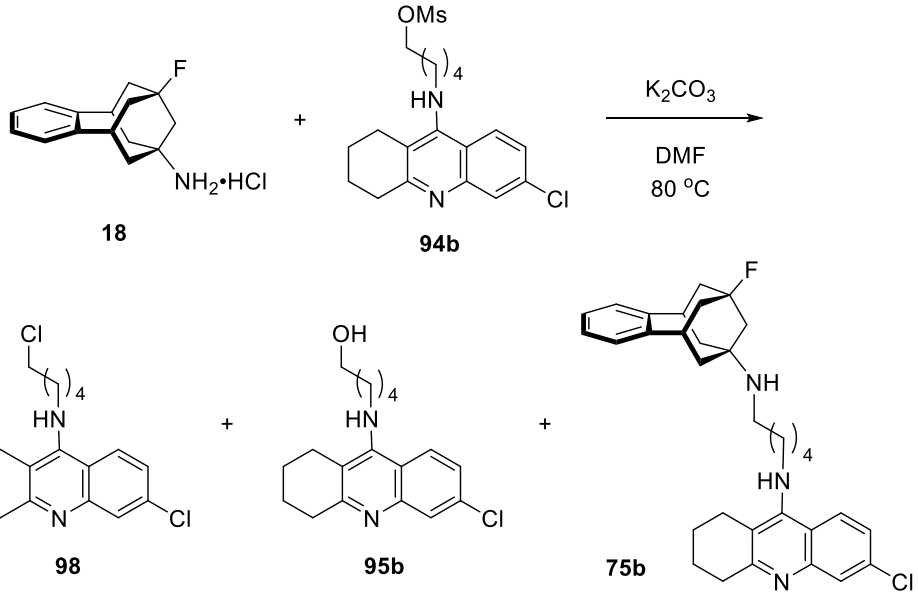

In a 25 mL closed vessel equipped with a magnetic stirrer, a suspension of amine **18** (115 mg, 0.43 mmol) and K_2CO_3 (130 mg, 0.94 mmol) in DMF (1 mL) was prepared. To this suspension vigorously stirred a solution of mesylate **94b** (237 mg, 0.60 mmol) in DMF (1.5 mL) was added, then stirred at 80 °C for 2 days. The reaction mixture was evaporated *in vacuo*, and the resulting residue taken up with water (15 mL) and 2 N NaOH aq. sol. (15 mL), then extracted with CH_2Cl_2 (3 × 20 mL). The combined organic layers were dried over anhydrous Na_2SO_4, filtered and evaporated under vacuum to give a dark brown oil (309 mg), which was subjected to column chromatography purification [silica gel 35−70 μm (30 g); Ø = 5 cm; #1–5, 500 mL, CH_2Cl_2 / 50% aq. NH_4OH 100:0.4; #6–7, 250 mL, CH_2Cl_2 / MeOH / 50% aq. NH_4OH 99.9:0.1:0.4; #8–10, 250 mL, CH_2Cl_2 / MeOH / 50% aq. NH_4OH 99.8:0.2:0.4; #11–12, 250 mL, CH_2Cl_2 / MeOH / 50% aq. NH_4OH 99.7:0.3:0.4; #13–15, 250 mL, CH_2Cl_2 / MeOH / 50% aq. NH_4OH 99.6:0.4:0.4; #16–19, 500 mL, CH_2Cl_2 / MeOH / 50% aq. NH_4OH 99.5:0.5:0.4; #20–22, 250 mL, CH_2Cl_2 / MeOH / 50% aq. NH_4OH 99.4:0.6:0.4; #23–24, 250 mL, CH_2Cl_2 / MeOH / 50% aq. NH_4OH 99.2:0.8:0.4; #25–27, 250 mL, CH_2Cl_2 / MeOH / 50% aq. NH_4OH 99:1:0.4; #28–37, 1 L, CH_2Cl_2 / MeOH / 50% aq. NH_4OH 98.6:1.4:0.4; #38–41, 500 mL, CH_2Cl_2 / MeOH / 50% aq. NH_4OH 98:2:0.4; #42–50, 900 mL, CH_2Cl_2 / MeOH / 50% aq. NH_4OH 97:3:0.4; #51, 250 mL, CH_2Cl_2 / MeOH / 50% aq. NH_4OH 95:5:0.4; #52, 500 mL, CH_2Cl_2 / MeOH / 50% aq. NH_4OH 90:10:0.4], to afford the byproduct **98** (#28–32, 38 mg,

26% yield) as a white-grey solid, and a mixture of desired amide **75b** / alcohol **95b** in ratio 1.5:1 (#43–49, 86 mg, 27% yield of the desired amide) as a clear brown oil, which we were not able to separate by neither crystallization nor two more column chromatography purifications.

$R_{f\,(\mathbf{98})}$ = 0.68 (gel de sílice, 10 cm, CH_2Cl_2 / MeOH / NH_4OH 50% 95:5:1).

Analytical sample of 98

In a 25 mL round-bottomed flask, **98** (38 mg, 0.11 mmol) was dissolved in CH_2Cl_2 (0.5 mL), filtered with a PTFE filter (0.2 µm), evaporated *in vacuo*, and washed with pentane (3 × 2 mL), giving, after drying in standard conditions, **98** (24 mg) as a white-grey solid.

IR (ATR) *v*: 3500–2500 (max at 3136, 2922, 2857, N–H, C–H st), 1604, 1575, 1554 (Ar–C–C, Ar–C–N st) cm^{-1}.

^1H NMR (400 MHz, $CDCl_3$) *δ*: 1.56 (m, 2H, 3'-H_2), 1.69 (dt, *J* = *J'* = 6.8 Hz, 2H, 4'-H_2), 1.81 (dt, *J* = *J* = 6.4 Hz, 2H, 2'-H_2), 1.87–1.96 (complex signal, 4H, 2-H_2 and 3-H_2), 2.68 (broad t, 2H, 1-H_2), 3.03 (broad t, 2H, 4-H_2), 3.49 (t, *J* = 7.2 Hz, 2H, 5'-H_2), 3.54 (t, *J* = 6.8 Hz, 2H, 1'-H_2), 7.27 (dd, *J* = 8.8 Hz, *J'* = 2.0 Hz, 1H, 7-H), 7.88 (d, *J* = 9.2 Hz, 1H, 8'-H), 7.89 (d, *J* = 1.6 Hz, 1H, 5'-H).

^{13}C NMR (100.6 MHz, $CDCl_3$) *δ*: 22.6, 22.9, 24.1, 24.6, 29.7, 31.0, 32.1, 34.0, 44.7, 49.3, 116.0, 118.5, 124.35, 124.44, 127.6, 134.0, 148.1, 150.7, 159.6.

HRMS (ESI):

Calculated for ($C_{18}H_{22}{}^{35}Cl_2N_2 + H^+$):	337.1233
Found:	337.1240

Preparation of 5-[(9-fluoro-7*H*-5,6,8,9,10,11-hexahydro-5,9:7,11-dimethanobenzo[9]annulen-7-yl)amino]pentanenitrile, 100b

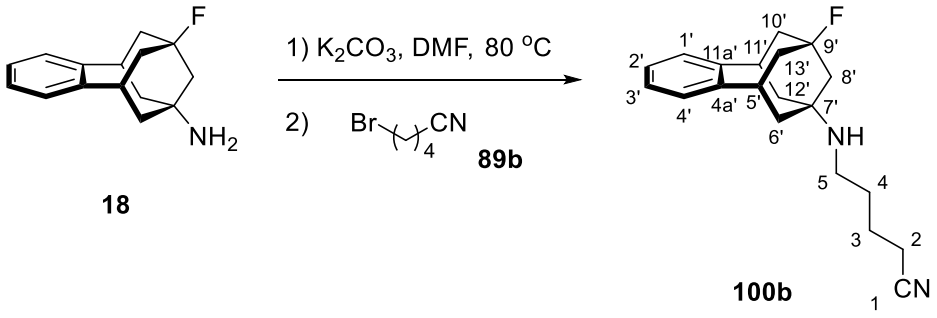

In a 25 mL closed vessel equipped with a magnetic stirrer, amine **18** (400 mg, 1.73 mmol) and K_2CO_3 (287 mg, 2.08 mmol) were suspended in DMF (8.7 mL). To this suspension vigorously stirred 5-bromovaleronitrile, **89b** (0.24 mL, 333 mg, 2.06 mmol), was added, and the reaction mixture was stirred at 80 °C for 2 days, then concentrated under reduced pressure, and the residue was taken up with water (30 mL) and extracted with CH_2Cl_2 (3 × 15 mL). The combined organic layers were dried over anhydrous Na_2SO_4, filtered and evaporated *in vacuo* to give a brown oil (588 mg), which was subjected to column chromatography purification [silica gel 35−70 µm (30 g); Ø = 3 cm; #1–14, 800 mL, CH_2Cl_2 / 50% aq. NH_4OH 100:0.4; #15–18, 200 mL, CH_2Cl_2 / MeOH / 50% aq. NH_4OH 99.9:0.1:0.4; #19–41, 600 mL, CH_2Cl_2 / MeOH / 50% aq. NH_4OH 99.8:0.2:0.4; #42–45, 150 mL, CH_2Cl_2 / MeOH / 50% aq. NH_4OH 99:1:0.4; #46–54, 300 mL, CH_2Cl_2 / MeOH / 50% aq. NH_4OH 97:3:0.4], to afford the desired nitrile **100b** (#25–51, mg, 61% yield) as an orange oil.

R_f = 0.72 (gel de sílice, 10 cm, CH_2Cl_2 / MeOH / NH_4OH 50% 90:10:1).

Analytical sample of 100b·HCl

In a 25 mL round-bottomed flask, nitrile **100b** (23 mg, 0.07 mmol) was dissolved in CH_2Cl_2 (1 mL), filtered with a PTFE filter (0.2 µm), treated with HCl / MeOH (0.5 M, 0.44 mL), evaporated *in vacuo*, and washed with pentane (3 × 2 mL), giving, after drying in standard conditions, **100b**·HCl (27 mg) as a yellow solid.

Melting point: 229–233 °C.

IR (ATR) *v*: 3600–2400 (max at 3511, 2935, 2675, 2359, N–H, $^{+}$N–H, C–H st), 3259 (CN st), 1584, 1495, 1444 (Ar–C–C, Ar–C–N st) cm^{-1}.

^{1}H NMR (400 MHz, CD_3OD) *δ*: 1.70–1.87 (complex signal, 4H, 6'(12')-H_B and 10'(13')-H_B], 1.88–1.95 (complex signal, 4H, 3-H_2 and 4-H_2), 2.14–2.26 [complex signal, 6H, 6'(12')-H_A, 10'(13')-H_A and 8'-H_2], 2.55 (t, *J* = 6.8 Hz, 2H, 2-H_2), 3.08 (t, *J* = 8.0 Hz, 2H, 5-H_2), 3.43 [broad m, 2H, 5'(11')-H], 4.85 (s, $^{+}$NH), 7.16 (broad s, 4H, 1'-H, 2'-H, 3'-H and 4'-H).

^{13}C NMR (100.6 MHz, CD_3OD) *δ*: 17.0 (CH_2, C2), 23.7 (CH_2, C3), 26.9 (CH_2, C4), 36.5 [CH_2, C6'(12')], 40.0 [CH, d, J_{C-F} = 13.3 Hz, C5'(11')], 40.7 [CH_2, d, J_{C-F} = 20.2 Hz, C10'(13')], 40.8 (CH_2, C5), 44.3 (CH_2, d, J_{C-F} = 21.1 Hz, C8'), 63.7 (C, d, J_{C-F} = 11.0 Hz, C7'), 94.2 (C, d, J_{C-F} = 180.0 Hz, C9'), 120.6 (C, C1), 128.6 [CH, C2'(3')], 129.4 [CH, C1'(C4'], 145.1 [C, C4a'(C11a')].

HRMS (ESI):

Calculated for ($C_{20}H_{25}{}^{35}ClFN_2 + H^+$):	313.2075
Found:	313.2080

Attempted preparation of *N*-(9-fluoro-7*H*-5,6,8,9,10,11-hexahydro-5,9:7,11-dimethanobenzo[9]annulen-7-yl)pentane-1,5-diamine, 99b

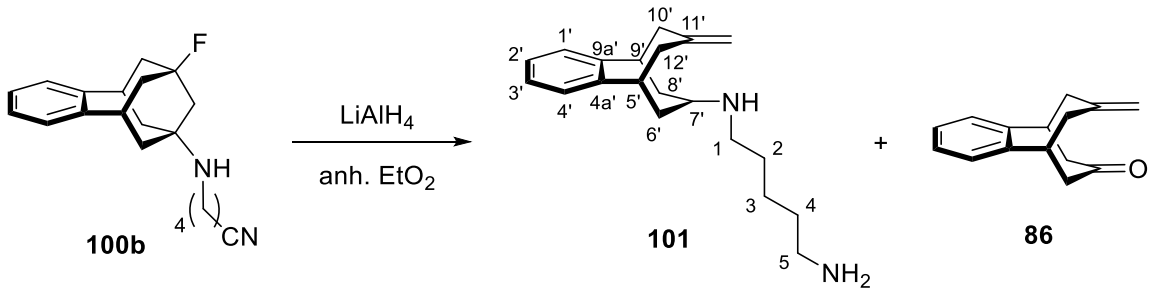

In a 25 mL round-bottomed flask provided with an inert atmosphere and a magnetic stirrer, nitrile **100b** (174 mg, 0.56 mmol) was suspended in anhydrous Et_2O (8.4 mL), cooled to 0 °C with an ice bath, and treated dropwise with a solution of $LiAlH_4$ / Et_2O (4 M, 0.42 mL, 1.67 mmol). The reaction mixture was stirred at room temperature overnight, then cooled to 0 °C with an ice bath, diluted with 1 N NaOH aq. sol. (15 mL) and water (7 mL), and extracted with EtOAc (3 × 20 mL). The combined organic layers were dried over anhydrous Na_2SO_4, filtered and evaporated *in vacuo* to give a yellow oil (169 mg), which was subjected to column chromatography purification [silica gel 35−70 µm (5 g); Ø = 1 cm; #1–4, 50 mL, CH_2Cl_2 / 50% aq. NH_4OH 100:0.4; #5–7, 50 mL, CH_2Cl_2 / MeOH / 50% aq. NH_4OH 99.5:0.5:0.4; #8–18, 200 mL, CH_2Cl_2 / MeOH / 50% aq. NH_4OH 99:1:0.4; #19–24, 100 mL, CH_2Cl_2 / MeOH / 50% aq. NH_4OH 98:2:0.4; #25–36, 200 mL, CH_2Cl_2 / MeOH / 50% aq. NH_4OH 95:5:0.4; #37–44, 100 mL, CH_2Cl_2 / MeOH / 50% aq. NH_4OH 90:10:0.4], to afford two byproducts of degradation of the benzoadamantane scaffold, the monoketone **86** (#1–2, 31 mg, 26% yield) as a pale yellow solid, and the primary amine **101** (#24–40, 119 mg, 72% yield) as a yellow oil.

$R_{f\,(\mathbf{101})}$ = 0.01 (silica gel, 10 cm, CH_2Cl_2 / MeOH / 50% aq. NH_4OH 90:10:1).

Analytical sample of 101

In a 25 mL round-bottomed flask, **101** (29 mg, 0.01 mmol) was dissolved in CH_2Cl_2 (0.5 mL), filtered with a PTFE filter (0.2 µm), evaporated *in vacuo*, and washed with pentane (3 × 2 mL), giving, after drying in standard conditions, **101** (29 mg) as a yellow oil.

IR (ATR) *v*: 3500–2500 (max. at 3359, 3064, 2923, 2853 C–H, N–H, N–H^+ st), 1731, 1632, 1492, 1453 (Ar–C–C st) cm^{-1}.

^{1}H NMR (400 MHz, $CDCl_3$) *δ*: 1.24–1.36 [complex signal, 4H, 3-H_2 and 6'(8')-H_B], 1.37–1.51 [complex signal, 6H, 2-H_2, 4-H_2 and 6'(8')-H_A], 2.32 [complex signal, 2H, 10'(12')-H_B], overlapped 2.58 (broad d, 2H, 7'-H_2), 2.60 (t, 2H, *J* = 7.2 Hz, 1'-H_2), 2.67 (t, 2H, *J* = 6.4 Hz, 5'-H_2), 2.75 [complex signal, 2H, 10'(12')-H_A], 3.10 [m, 2H, 5'(9')-H], 3.89 (m, 1H, NH), 4.72 (t, *J* = 1.6 Hz, 2H, 11'-C*H*$_2$), 7.72 [m, 4H, 1'(4')-H and 2'(3')-H].

^{13}C NMR (100.6 MHz, $CDCl_3$) *δ*: 24.6 (CH_2), 30.3 (CH_2), 33.6 (CH_2) (C2, C3 and C4), 23.7 (CH_2, C3), 39.6 (CH_2) and 40.3 (CH_2) [C6'(8') and C10'(12')], 42.0 [CH, C5'(9')], 42.1 (CH_2), 46.7 (CH_2) (C1 and C5), 51.5 (CH, C7'), 112.9 (CH_2, 11'-*C*H_2), 126.5 [CH, C2'(3')], 128.0 [CH, C1'(C4')], 145.8 [C, C4a'(C9a')], 150.5 (C, 11').

HRMS (ESI):

Calculated for ($C_{20}H_{30}N_2$ + H^+):	299.2485
Found:	299.2486

Preparation of (±)-2-chloro-*N*-(9-fluoro-2-nitro-7*H*-5,6,8,9,10,11-hexahydro-5,9:7,11-dimethanobenzo[9]annulen-7-yl)acetamide, (±)-102

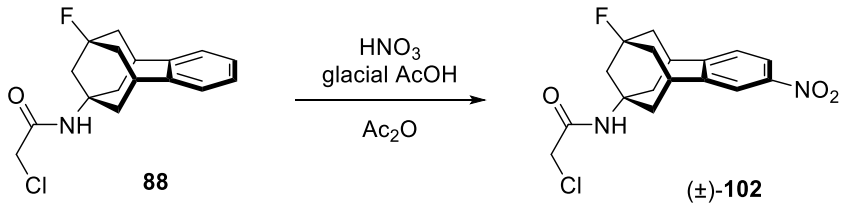

In a 25 mL round-bottomed flask provided with a magnetic stirrer, a solution of compound **88** (1.53 g, 5.00 mmol) in acetic anhydride (5.31 mL) was prepared and cooled to 0 ^{o}C with an ice bath. Then treated dropwise with glacial acetic acid (0.86 mL) and HNO_3 (65% purity, 1.02 mL), and stirred at room temperature for 24 hours. The resulting mixture was poured onto a mixture ice / water (28 mL) and extracted with CH_2Cl_2 (3 × 30 mL). The combined organic layers were washed with water (50 mL) and brine (30 mL), dried over anhydrous Na_2SO_4, filtered and evaporated under reduced pressure to give the desired nitrated compound (±)-**102** (1.36 g, 77% yield), which was used in the next step without further purification.

Attempted preparation of (±)-2-chloro-*N*-(2-amino-9-fluoro-7*H*-5,6,8,9,10,11-hexahydro-5,9:7,11-dimethanobenzo[9]annulen-7-yl)acetamide, (±)-80

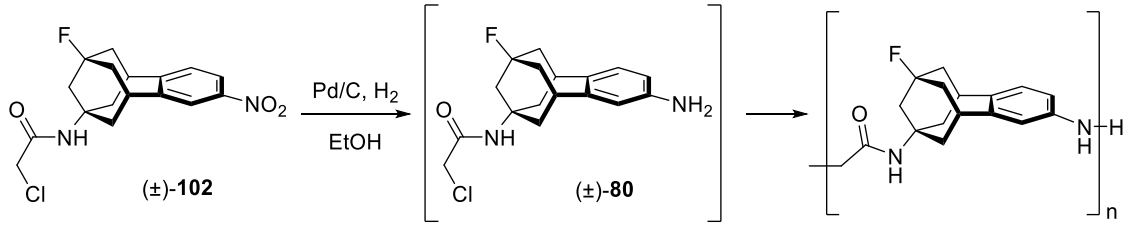

In a 250 mL round-bottomed flask provided with an inert atmosphere and a magnetic stirrer, a suspension of compound (±)-**102** (2.79 g, 7.91 mmol) and Pd/C 10% wt. (428 mg) in EtOH (106 mL) was prepared, then subjected to 1 atmosphere of H_2 at room temperature for 1 day. The resulting suspension was filtered off and evaporated under reduced pressure to give a polymerized derivative of (±)-**80** (2.47g) as a brown solid, but no desired compound was clearly observed.

Preparation of (±)-*N*-{7-[(*tert*-butyloxycarbonyl)amino]-9-fluoro-7*H*-5,6,8,9,10,11-hexahydro-5,9:7,11-dimethanobenzo[9]annulen-2-yl}-4-[(6-chloro-1,2,3,4-tetrahydroacridin-9-yl)amino]butanamide, (±)-106a

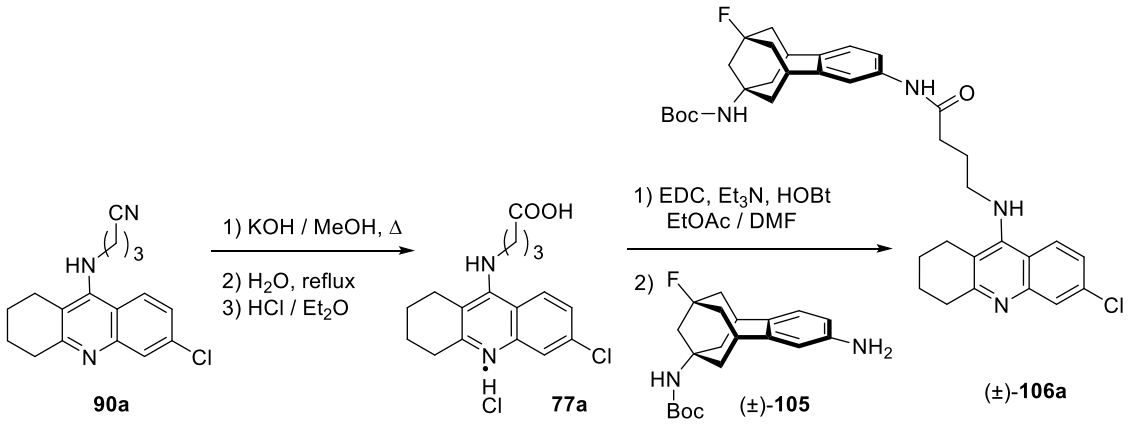

In a 100 mL round-bottomed flask equipped with a magnetic stirrer and a condenser, nitrile **90a** (369 mg, 1.23 mmol) was dissolved in MeOH (1.6 mL) and treated with a 40% solution of KOH in MeOH (3.1 mL). The resulting suspension was stirred under reflux for 3 hours, then treated with water (5 mL), and again stirred under reflux overnight. The resulting solution was cooled to room temperature, evaporated under reduced pressure, and treated with HCl / Et_2O (3 N, 14 mL, 42.0 mmol), and concentrated *in vacuo* to give a yellow solid (2.55 g), whose ^{1}H-NMR spectrum was consistent with that expected for the desired acid, **77a**·HCl, and was used as a crude without further purification in the next step.

In a 100 mL round-bottomed flask provided with a magnetic stirrer, the acid **77a**·HCl (2.55 g of a crude that could contain a maximum of 1.23 mmol of the desired acid) was suspended in a mixture of EtOAc (17 mL) and DMF (1.7 mL), and treated with *N*-(3-dimethylaminopropyl)-*N*′-ethylcarbodiimide hydrochloride (366 mg, 1.91 mmol), triethylamine (0.55 mL, 401 mg, 3.97 mmol), and 1-hydroxy-1*H*-benzotriazole (261 mg, 1.92 mmol). The resulting mixture was stirred at room temperature for 15 minutes, then treated with a suspension of the amine (±)-**105** (302 mg, 0.87 mmol) in a mixture of EtOAc (9 mL) and DMF (0.9 mL), stirred at room temperature for 1 day, and concentrated *in vacuo* to give a brown sticky solid (3.11 g), which was subjected to column chromatography purification [silica gel 35−70 μm (170 g); Ø = 4.5 cm; #1, 500 mL, hexane / EtOAc / Et_3N 50:50:0.2; #2, 500 mL, hexane / EtOAc / Et_3N 40:60:0.2; #3, 500 mL, hexane / EtOAc / Et_3N 30:70:0.2; #4–5, 1 L, hexane / EtOAc / Et_3N

20:80:0.2; #6–19, 1.5 L, hexane / EtOAc / Et_3N 10:90:0.2; #20–29, 1 L, EtOAc / Et_3N 100:0.2], to afford a mixture of desired amide (±)-**106a** / methyl ester of tacrine moiety in a ratio 1:2.51 (#5–6, 235 mg, 18% yield of desired compound) as a yellow oil.

R_f = 0.72 (silica gel, 10 cm, CH_2Cl_2 / MeOH / 50% aq. NH_4OH 95:5:1).

Analytical data of (±)-106a

LRMS (ESI): 647.3159 ($M + H^+$)

Preparation of (±)-*N*-{7-[(*tert*-butyloxycarbonyl)amino]-9-fluoro-7*H*-5,6,8,9,10,11-hexahydro-5,9:7,11-dimethanobenzo[9]annulen-2-yl}-5-[(6-chloro-1,2,3,4-tetrahydroacridin-9-yl)amino]pentanamide, (±)-106b

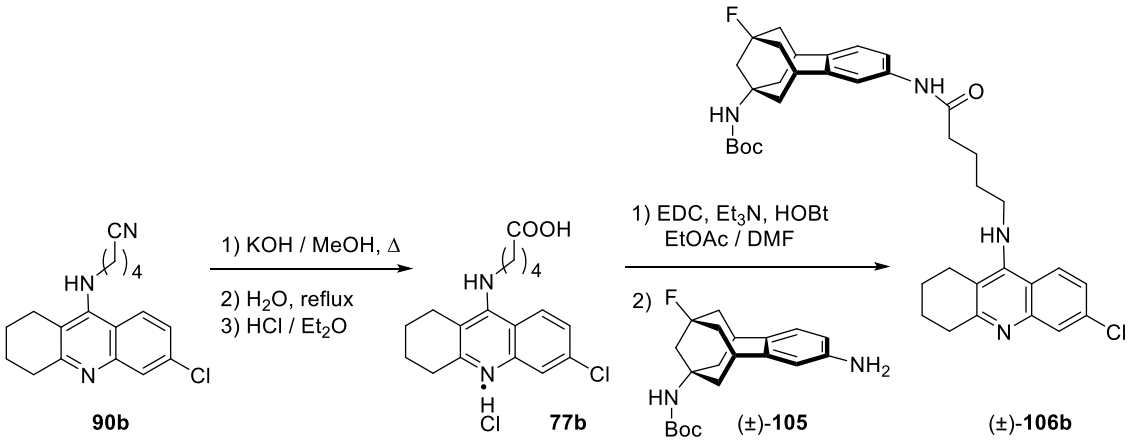

In a 100 mL round-bottomed flask equipped with a magnetic stirrer and a condenser, nitrile **90b** (1.10 g, 3.51 mmol) was dissolved in MeOH (5.3 mL) and treated with a 40% solution of KOH in MeOH (9.6 mL). The resulting suspension was stirred under reflux for 3 hours, then treated with water (12.3 mL), and again stirred under reflux overnight. The resulting solution was cooled to room temperature, evaporated under reduced pressure, and treated with HCl / Et_2O (3 N, 23.4 mL, 70.1 mmol), and concentrated *in vacuo* to give a yellow solid (5.80 g), whose ^{1}H-NMR spectrum was consistent with that expected for the desired acid, **77b**·HCl, and was used as a crude without further purification in the next step.

In a 100 mL round-bottomed flask provided with a magnetic stirrer, the acid **77b**·HCl (5.80 g of a crude that could contain a maximum of 3.51 mmol of the desired acid) was suspended in a mixture of EtOAc (30 mL) and DMF (3 mL), and treated with *N*-(3-dimethylaminopropyl)-*N'*-ethylcarbodiimide hydrochloride (698 mg, 3.65 mmol), triethylamine (1.22 mL, 889 mg, 8.80 mmol), and 1-hydroxy-1*H*-benzotriazole (497 mg, 3.65 mmol). The resulting mixture was stirred at room temperature for 15 minutes, then treated with a suspension of the amine (±)-**105** (575 mg, 1.66 mmol) in a mixture of EtOAc (20 mL) and DMF (2 mL), stirred at room temperature for 1 day, and concentrated *in vacuo* to give a brown sticky solid (9.84 g), which was subjected to column chromatography purification [silica gel 35−70 µm (320 g); Ø = 8.5 cm; #1, 500 mL, hexane / EtOAc / Et_3N 50:50:0.2; #2–3, 1.1 L, hexane / EtOAc /

Et_3N 40:60:0.2; #4–11, 500 mL, hexane / EtOAc / Et_3N 30:70:0.2; #12–18, 500 mL, hexane / EtOAc / Et_3N 20:80:0.2; #19–33, 1.5 L, hexane / EtOAc / Et_3N 10:90:0.2; #34–58, 2.5 L, EtOAc / Et_3N 100:0.2], to afford a mixture of desired amide (±)-**106b** / methyl ester of tacrine moiety 1:0.55 (#32–39, 312 mg, 22% yield of desired compound) as a brown oil, and the desired amide (±)-**106b** with some unknown impurities (#40–48, 235 mg, 21% yield) as a brown oil. The overall yield for the coupling reaction was 43%.

R_f = 0.72 (silica gel, 10 cm, CH_2Cl_2 / MeOH / 50% aq. NH_4OH 95:5:1).

Analytical data of (±)-106b

LRMS (ESI): 661.3323 ($M + H^+$)

Preparation of (±)-*N*-(7-amino-9-fluoro-7*H*-5,6,8,9,10,11-hexahydro-5,9:7,11-dimethanobenzo[9]annulen-2-yl)-4-[(6-chloro-1,2,3,4-tetrahydroacridin-9-yl)amino]butanamide, (±)-78a

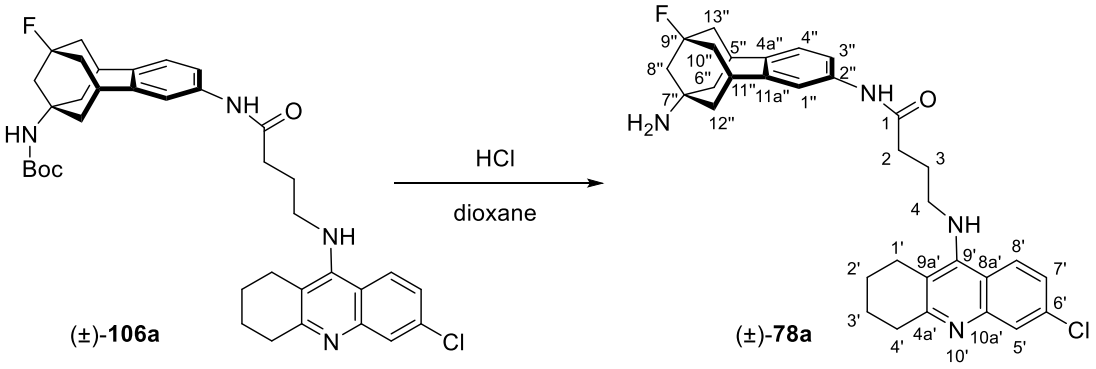

In a 10 mL round-bottomed flask equipped with a magnetic stirrer and an ice bath, protected amine (±)-**106a** (218 mg, maximum of 0.34 mmol) was placed and treated with HCl / dioxane (4 M, 2.4 mL. 9.61 mmol), then stirred at room temperature for 18 hours. The resulting mixture was evaporated under reduced pressure, providing a brown solid which was dissolved with water (3 mL), alkalinized with 10% Na_2CO_3 aq. sol. (15 mL), and extracted with a mixture 10% MeOH / $CHCl_3$ (4 × 10 mL). The combined organic layers were dried over anhydrous Na_2SO_4, filtered and concentrated *in vacuo* to give a clear brown oil (213 mg), which was subjected to column chromatography purification [silica gel 35−70 μm (11 g); Ø = 1.5 cm; #1–20, 1.25 L, CH_2Cl_2 / 50% aq. NH_4OH 100:0.4; #21–23, 250 mL, CH_2Cl_2 / MeOH / 50% aq. NH_4OH 99.5:0.5:0.4; #24–26, 250 mL, CH_2Cl_2 / MeOH / 50% aq. NH_4OH 99:1:0.4; #27–37, 1 L, CH_2Cl_2 / MeOH / 50% aq. NH_4OH 98.5:1.5:0.4; #38–39, 250 mL, CH_2Cl_2 / MeOH / 50% aq. NH_4OH 98:2:0.4; #40–41, 250 mL, CH_2Cl_2 / MeOH / 50% aq. NH_4OH 95:5:0.4], to afford the desired primary amine (±)-**78a** (#27–40, 91 mg, 49% yield) as a white solid.

R_f = 0.22 (silica gel, 10 cm, CH_2Cl_2 / MeOH / 50% aq. NH_4OH 95:5:1).

Analytical sample of (±)-78a·2HCl

In a 25 mL round-bottomed flask (±)-**78a** (50 mg, 0.09 mmol) was dissolved in CH_2Cl_2 (2 mL), treated with HCl / Et_2O (3 N, 0.27 mL), evaporated *in vacuo*, and washed with pentane (3 × 2 mL), to give, after drying in standard conditions, (±)-**78a**·2HCl (49 mg) as a white solid.

Calculated logP: 6.05.

^{1}H NMR (400 MHz, CD_3OD) δ: 1.80–1.96 [complex signal, 8H, 2'-H_2, 3'-H_2, 6''(12'')-H_B and 10''(13'')-H_B], 2.06–2.15 [complex signal, 4H, 6''(12'')-H_A and 8''-H_2], 2.16–2.26 [complex signal, 2H, 3-H_2 and 10''(13'')-H_A], 2.58 (t, J = 6.4 Hz, 2H, 2-H_2), 2.69 (broad t, J = 6.0 Hz, 2H, 1'-H_2), 2.94 (broad t, 2H, J = 6.4 Hz, 4'-H_2), overlapped 3.32 (broad t, 1H, 5''-H), 3.38 (broad t, 1H, 11''-H), 4.07 (t, J = 6.8 Hz, 2H, 4-H_2), 4.85 (s, $^{+}$NH, NH), 7.10 (d, J = 8.4 Hz, 1H, 4''-H), 7.27 (dd, J = 8.0 Hz, J' = 2.4 Hz, 1H, 3''-H), 7.36 (d, J = 2.0 Hz, 1H, 1''-H), 7.52 (dd, J = 9.2 Hz, J' = 2.4 Hz, 1H, 7'-H), 7.76 (d, J = 2.4 Hz, 1H, 5'-H), 8.47 (d, J = 9.6 Hz, 1H, 8'-H).

^{13}C NMR (100.6 MHz, CD_3OD) δ: 21.7 (CH_2, C2'), 22.8 (CH_2, C3'), 24.8 (CH_2, C1'), 26.5 (CH_2, C3), 29.3 (CH_2, C4'), 35.1 (CH_2, C2), 38.7 [CH_2, d, $J_{C\text{-}F}$ = 19.3 Hz, C6''(12'')], 39.5 (CH, d, $J_{C\text{-}F}$ = 13.5 Hz, C11''), 40.4 (CH, d, $J_{C\text{-}F}$ = 12.9 Hz, C5''), 40.7 [CH_2, d, $J_{C\text{-}F}$ = 19.4 Hz, C10''(13'')], 45.9 (CH_2, d, $J_{C\text{-}F}$ = 20.7 Hz, C8''), 49.1 (CH_2, C4), 58.1 (C, d, $J_{C\text{-}F}$ = 10.3 Hz, C7''), 94.0 (C, d, $J_{C\text{-}F}$ = 179.3 Hz, C9''), 113.4 (C, C9a'), 115.4 (C, C8a'), 119.0 (CH, C5'), 119.6 (CH, C3''), 120.9 (CH, C1''), 126.7 (CH, C7'), 129.0 (CH, C8'), 130.0 (CH, C4''), 138.9 (C, C2''), 140.0 (C, C6'), 140.5 (C, C10a'), 141.0 (C, C4a''), 145.8 (C, C11a''), 151.9 (C, C4a'), 157.9 (C, C9'), 173.5 (C, CONH).

HRMS (ESI):

Calculated for ($C_{32}H_{37}{}^{35}ClFN_4O + H^{+}$): 547.2634

Found: 547.2632

Preparation of (±)-*N*-(7-amino-9-fluoro-7*H*-5,6,8,9,10,11-hexahydro-5,9:7,11-dimethanobenzo[9]annulen-2-yl)-5-[(6-chloro-1,2,3,4-tetrahydroacridin-9-yl)amino]pentanamide, (±)-78b

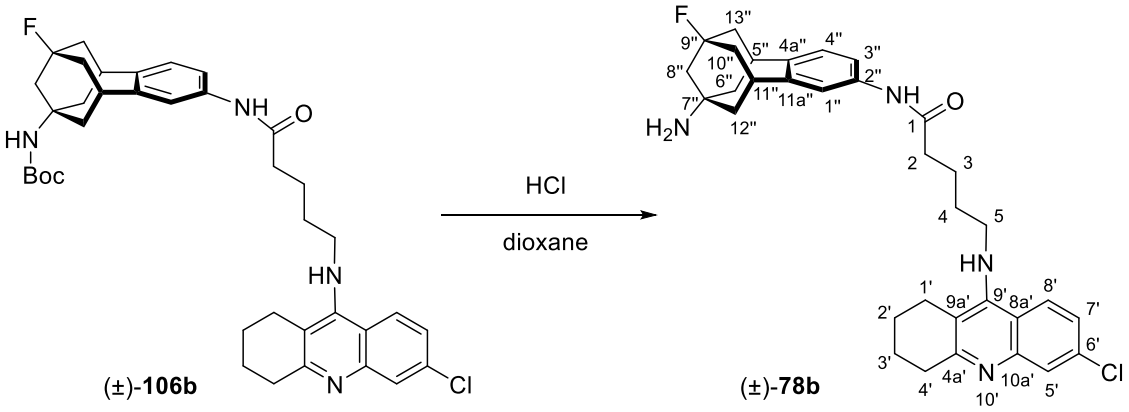

(±)-**106b** (±)-**78b**

In a 5 mL round-bottomed flask equipped with a magnetic stirrer and an ice bath, mixture of desired amide (±)-**106b** / tacrine-derived byproduct (303 mg, maximum of 0.46 mmol) was placed and treated with HCl / dioxane (4 M, 3.26 mL. 13.05 mmol), then stirred at room temperature for 18 hours, and the resulting suspension evaporated under reduced pressure, giving a brown solid which was dissolved with water (3 mL), alkalinized with 10% Na_2CO_3 aq. sol. (20 mL), and extracted with a mixture 10% MeOH / $CHCl_3$ (4 × 12 mL). The combined organic layers were dried over anhydrous Na_2SO_4, filtered and concentrated *in vacuo* to give a clear brown oil (261 mg), which was subjected to column chromatography purification [silica gel 35−70 µm (13 g); Ø = 1.5 cm; #1–5, 500 mL, CH_2Cl_2 / 50% aq. NH_4OH 100:0.4; #6–33, 400 mL, CH_2Cl_2 / MeOH / 50% aq. NH_4OH 99.8:0.2:0.4; #34–49, 150 mL, CH_2Cl_2 / MeOH / 50% aq. NH_4OH 99.5:0.5:0.4; #50–58, 150 mL, CH_2Cl_2 / MeOH / 50% aq. NH_4OH 99:1:0.4; #59–79, 500 mL, CH_2Cl_2 / MeOH / 50% aq. NH_4OH 98:2:0.4], to afford the desired primary amine (±)-**78b** (#67–75, 94 mg, 37% yield) as a white solid.

R_f = 0.45 (silica gel, 10 cm, CH_2Cl_2 / MeOH / 50% aq. NH_4OH 95:5:1).

Analytical sample of (±)-78b·2HCl

In a 25 mL round-bottomed flask (±)-**78b** (19 mg, 0.03 mmol) was dissolved in CH_2Cl_2 (1 mL), treated with HCl / Et_2O (3 N, 0.03 mL), evaporated *in vacuo*, and washed with pentane (3 × 2 mL), to give, after drying in standard conditions, (±)-**78b**·2HCl (22 mg) as a yellow solid.

Calculated logP: 6.56.

^{1}H NMR (400 MHz, CD_3OD) δ: 1.78–1.86 [complex signal, 4H, 3-H_2 and 6''(12'')-H_B], 1.85–1.95 [complex signal, 4H, 4-H_2 and 10''(13'')-H_B], partially overlapped 1.92–2.00 (complex signal, 4H, 2'-H_2 and 3'-H_2), 2.05–2.14 [complex signal, 4H, 6''(12'')-H_A and 8''-H_2], 2.19 [broad m, 2H, 10''(13'')-H_A], 2.45 (t, J = 7.2 Hz, 2H, 2-H_2), 2.70 (broad t, J = 5.2 Hz, 2H, 1'-H_2), 2.99 (broad t, 2H, J = 6.0 Hz, 4'-H_2), overlapped 3.31 (broad t, 1H, 5''-H), 3.37 (broad t, 1H, 11''-H), 4.00 (t, J = 6.4 Hz, 2H, 5-H_2), 4.86 (s, $^+$NH, NH), 7.10 (d, J = 8.4 Hz, 1H, 4''-H), 7.29 (dd, J = 8.0 Hz, J' = 2.4 Hz, 1H, 3''-H), 7.38 (d, J = 2.0 Hz, 1H, 1''-H), 7.53 (dd, J = 9.2 Hz, J' = 2.0 Hz, 1H, 7'-H), 7.76 (d, J = 2.0 Hz, 1H, 5'-H), 8.40 (d, J = 9.2 Hz, 1H, 8'-H).

^{13}C NMR (100.6 MHz, CD_3OD) δ: 21.8 (CH_2, C2'), 22.8 (CH_2, C3'), 23.5 (CH_2, C3), 24.8 (CH_2, C1'), 29.4 (CH_2, C4'), 30.7 (CH_2, C4), 36.9 (CH_2, C2), 38.7 [CH_2, d, $J_{C\text{-}F}$ = 20.0 Hz, C6''(12'')], 39.5 (CH, d, $J_{C\text{-}F}$ = 13.0 Hz, C11''), 40.4 (CH, d, $J_{C\text{-}F}$ = 13.1 Hz, C5''), 40.7 [CH_2, d, $J_{C\text{-}F}$ = 19.9 Hz, C10''(13'')], 45.9 (CH_2, d, $J_{C\text{-}F}$ = 20.6 Hz, C8''), 48.8 (CH_2, C5), 58.1 (C, d, $J_{C\text{-}F}$ = 10.7 Hz, C7''), 94.0 (C, d, $J_{C\text{-}F}$ = 180.2 Hz, C9''), 113.5 (C, C9a'), 115.5 (C, C8a'), 119.1 (CH, C5'), 119.7 (CH, C3''), 121.0 (CH, C1''), 126.8 (CH, C7'), 128.8 (CH, C8'), 129.9 (CH, C4''), 138.9 (C, C2''), 140.0 (C, C6'), 140.5 (C, C10a'), 141.0 (C, C4a''), 145.7 (C, C11a''), 152.1 (C, C4a'), 157.9 (C, C9'), 174.0 (C, CONH).

HRMS (ESI):

Calculated for ($C_{33}H_{38}{}^{35}ClFN_4O$ + H^+):	561.2791
Found:	561.2796

CHAPTER 9

Bibliography

Image source: Atlas Technologies (*www.atlasuhv.com/Technology/Bibliography*)

1. M. Prince, A. Comas-Herrera, M. Knapp, M. Guerchet, M. Karagiannidou. *World Alzheimer Report 2016: Improving healthcare for people living with dementia.* A*lzheimer's Disease International* **2016**.
2. M. Prince, R. Bryce, E. Albanese, A. Wimo, W. Ribeiro, C. P. Ferri. *Alzheimer's & Dementia* **2013**, *9*, 63.
3. a) Alzheimer's Association. *Alzheimer's & Dementia* **2015**, *11*, 332. b) Alzheimer's Association. *Alzheimer's & Dementia* **2013**, *9*, 208.
4. D. Avramopoulos. *Genome Medicine* **2009**, *1*, 3.
5. K. Blennow, M. J. de Leon, H. Zetterberg. *Lancet* **2006**, *368*, 387.
6. L. Bertram, M. B. McQueen, K. Mullin, D. Blacker, R. E. Tanzi. *Nat. Genet.* **2007**, *39*, 17.
7. D. Harold, R. Abraham, P. Hollingworth, R. Sims, A. Gerrish, M. L. Hamshere, J. S. Pahwa, V. Moskvina, K. Dowzell, A. Williams, N. Jones, C. Thomas, A. Stretton, A. R. Morgan, S. Lovestone, J. Powell, P. Proitsi, M. K. Lupton, C. Brayne, D. C. Rubinsztein *et al. Nat. Genet.* **2009**, *41*, 1088.
8. a) A. Alzheimer. *Allgemeine Zeitschrift für Psychiatrie and Psychisch-Gerichtliche Medizin* **1907**, *64*, 146. b) A. Rainulf, H. Stelzma, N. Schnitzlein, F. R. Murtagh. *Clin. Anat.* **1995**, *8*, 429.
9. R. Katzman. *Arch. Neurol.* **1976**, *33*, 217.
10. P. Nelson, I. Alafuzoff, E. Bigio, C. Bouras, H. Braak, N. Cairns, R. Castellani, B. Crain, P. Davies. *J. Neuropathol. Exp. Neurol.* **2012**, *71*, 362.
11. J. Hardy, D. Allsop. *Trends Pharm. Sci.* **1991**, *12*, 383.
12. D. J. Selkoe. *Neuron.* **1991**, *6*, 487.
13. J. Hardy, D. J. Selkoe. *Science* **2002**, *297*, 353.
14. D. J. Selkoe, J. Hardy. *EMBO Mol. Med.* **2016**, *8*, 595.
15. K. G. Mawuenyega, W. Sigurdson, V. Ovod, L. Munsell, T. Kasten, J. C. Morris, K. E. Yarasheski, R. J. Bateman. *Science* **2010**, *330*, 1774.
16. C. Priller, T. Bauer, G. Mitteregger, B. Krebs, H. A. Kretzschmar, J. Herms. *J. Neurosci.* **2006**, *26*, 7212.
17. P. R. Turner, K. O'Connor, W. P. Tate, W. C. Abraham. *Prog. Neurobiol.* **2003**, *70*, 1.
18. J. Näslund, A. Schierhorn, U. Hellman, L. Lannfelt, D. Roses, L. O. Tjernberg, J. Silberring, S. E. Gandy, B. Winblad, P. Greengard. *PNAS* **1994**, *91*, 8378.
19. H. F. Kung. *ACS Med. Chem. Lett.* **2012**, *3*, 265.
20. I. W. Hamley. *Chem. Rev.* **2012**, *112*, 5147.
21. S. T. Ferreira, W. L. Klein. *Neurobiol. Learn Mem.* **2011**, *96*, 529.

22. M. T. Heneka, M. J. Carson, J. El Khoury, G. E. Landreth, F. Brosseron, D. L. Feinstein, A. H. Jacobs, T. Wyss-Coray, J. Vitorica, R. M. Ransohoff, K. Herrup, S. A. Frautschy, B. Finsen, G. C. Brown, A. Verkhratsky, K. Yamanaka, J. Koistinaho, E. Latz, A. Halle, G. C. Petzold *et al. Lancet Neurol.* **2015**, *14*, 388.
23. C. Haass, D. J. Selkoe. *Nat. Rev. Mol. Cell Biol.* **2007**, *8*, 101.
24. E. S. Musiek, D. M. Holtzman. *Nat. Neurosci.* **2015**, *18*, 800.
25. E. Giacobini, G. Gold. *Nat. Rev. Neurol*. **2013**, *9*, 677.
26. A. Serrano-Pozo, M. P. Frosch, E. Masliah, B. T. Hyman. *Cold Spring Harb. Perspect. Med.* **2011**, *1*, a006189.
27. L. Buée, T. Bussière, V. Buée-Scherrer, A. Delacourte, P. R. Hof. *Brain Res. Rev.* **2000**, *33*, 95.
28. a) V. M.-Y. Lee, M. Goedert, J. Q. Trojanowski. *Annu. Rev. Neurosci.* **2001**, *24*, 1121. b) K. Iqbal, A. del C. Alonso, S. Chen, M. O. Chohan, E. El-Akkad, C.-X. Gong, S. Khatoon, B. Li, F. Liu, A. Rahman, H. Tanimukai, I. Grundke-Iqbal. *Biochim. Biophys. Acta* **2005**, *1739*, 198.
29. D. A. Drachman, J. Leavitt. *Arch. Neurol.* **1974**, *30*, 113.
30. a) P. Davies, A. J. F. Maloney. *Lancet* **1976**, *2*, 1403. b) D. M. Bowen, C.B. Smith, P. White, A. N. Davison. *Brain* **1976**, *99*, 459.
31. R. Bartus, R. Dean, B. Beer, A. Lippa. *Science* **1982**, *217*, 408.
32. P. Francis, A. Palmer, M. Snape, G. Wilcock. *J. Neurol. Neurosurg. Psychiatry* **1999**, *66*, 137.
33. G. Benzi, A. Moretti. *Eur. J. Pharmacol.* **1998**, *346*, 1.
34. B. Halliwell. *Drug & Aging* **2001**, *18*, 685.
35. M. Ansari, S. Scheff. *J. Neuropathol. Exp. Neurol.* **2010**, *69*, 155.
36. P. Moreira, M. Santos, C. Oliveira, J. Shenk, A. Nunomura, M. Smith, X. Zhu, G. Perry. *CNS Neurol. Disord. – Drug Targets* **2008**, *7*, 3.
37. F. Gu, M. Zhu, J. Shi, Y. Hu, Z. Zhao. *Neurosci. Lett.* **2008**, *440*, 44.
38. M. Rosini, E. Simoni, A. Milelli, A. Minarini, C. Melchiorre. *J. Med. Chem.* **2014**, *57*, 2821.
39. B. Moghaddam, D. Javitt. *Neuropsychopharmacology Rev.* **2012**, *37*, 4.
40. T. Takeuchi, A. Duszkiewicz, R. Morris. *Phil. Trans. R. Soc. B* **2014**, *369*, 20130288.
41. C. Tabone, M. Ramaswami. *Neuron* **2012**, *74*, 767.
42. H. Wei, C. Dobkin, A. Sheikh, M. Malik, W. T. Brown, X. Li. *PLoS ONE* **2012**, *7*, e36981.
43. M. Parsons, L. Raymond. *Neuron* **2014**, *82*, 279.

44. I. Morales, L. Guzmán-Martínez, C. Cerda-Troncoso, G. A. Farías, R. B. Maccioni. *Front. Cell. Neurosci.* **2014**, *8*, 112.
45. M. Kitazawa, D. Cheng, F. LaFerla. *J. Neurochem.* **2009**, *108*, 1550.
46. L. Bojarski, J. Herms, J. Kuznicki. *Neurochem. Int.* **2008**, *52*, 621.
47. M. Khalil, C. Teunissen, C. Langkammer. *Mult. Scler. Int.* **2011**, 606807.
48. J. Duce, A. Tsatsanis, M. Cater, S. James, E. Robb, K. Wikhe, S. L. Leong, K. Perez, T. Johanssen, M. Greenough, H.-H. Cho, D. Galatis, R. Moir, C. Masters, C. McLean, R. Tanzi, R. Cappai, K. Barnham, G. Ciccotosto, J. Rogers, A. Bush. *Cell* **2010**, *142*, 857.
49. X. Huang, M. Cuajungco, C. Atwood, M. Hartshorn, J. Tyndall, G. Hanson, K. Stokes, M. Leopold, G. Multhaup, L. Goldstein, R. Scarpa, A. Saunders, J. Lim, R. Moir, C. Glabe, E. Bowden, C. Masters, D. Fairlie, R. Tanzi, A. Bush. *J. Biol. Chem.* **1999**, *274*, 37111.
50. A. Yamamoto, R.-W. Shin, K. Hasegawa, H. Naiki, H. Sato, F. Yoshimasu, T. Kitamoto. *J. Neurochem.* **2002**, *82*, 1137.
51. R. Swerdlow, S. Khan. *Med. Hypotheses* **2004**, *63*, 8.
52. R. Swerdlow, J. Burns, S. Khan. *Biochim. Biophys. Acta* **2014**, *1842*, 1219.
53. B. Zlokovic. *Nat. Rev. Neurosci*. **2014**, *12*, 723.
54. B. Zlokovic. *Trends Neurosci.* **2005**, *28*, 202.
55. J. Lustbader, M. Cirilli, C. Lin, H. W. Xu, K. Takuma, N. Wang, C. Caspersen, X. Chen, S. Pollak, M. Chaney, F. Trinchese, S. Liu, F. Gunn-Moore, L.-F. Lue, D. Walker, P. Kuppusamy, Z. Zewier, O. Arancio, D. Stern, S. S. Yan,H. Wu. *Science* **2004**, *304*, 448.
56. A. Caricasole, A. Copani, A. Caruso, F. Caraci, L. Iacovelli, M. A. Sortino, G. C. Terstappen, F. Nicoletti. *Trends Pharm. Sci.* **2003**, *24*, 233.
57. L. Xie, E. Helmerhorst, K. Taddei, B. Plewright, W. v. Bronswijk, R. Martins. *J. Neurosci.* **2002**, *22*, RC221.
58. B. Kagana, Y. Hirakura, R. Azimov, R. Azimova, M.-C. Lin. *Peptides* **2002**, *23*, 1311.
59. E. Tamagno, M. Parola, M. Guglielmotto, G. Santoro, P. Bardini, L. Marra, M. Tabaton, O. Danni. *Free Radic. Biol. Med.* **2003**, *35*, 45.
60. M. Bamberger, G. Landreth. *Microsc. Res. Tech.* **2001**, *54*, 59.
61. T. Maas, J. Eidenmüller, R. Brandt. *J. Biol. Chem.* **2000**, *275*, 15733.
62. X. Li, Y. Kumar, H. Zempel, E.-M. Mandelkow, J. Biernat, E. Mandelkow. *EMBO J.* **2011**, *30*, 4825.
63. F. Hernández, J. Avila. *Cell. Mol. Life Sci.* **2007**, *64*, 2219.
64. R. Schliebs. *Neurochem. Res.* **2005**, *30*, 895.
65. M. A. Moran, E. J. Mufson, P. Gomez-Ramos. *Acta Neuropathol.* **1993**, *85*, 362.

66. N. Inestrosa, A. Alvarez, C. Pérez, R. Moreno, M. Vicente, C. Linker, O. Casanueva, C. Soto, J. Garrido. *Neuron* **1996**, *16*, 881.
67. A. Alvarez, R. Alarcón, C. Opazo, E. O. Campos, F. J. Muñoz, F. H. Calderón, F. Dajas, M. K. Gentry, B. P. Doctor, F. G. De Mello, N. Inestrosa. *J. Neurosci.* **1998**, *18*, 3213.
68. A. Reyes, M. Chacon, M. Dinamarca, W. Cerpa, C. Morgan, N. Inestrosa. *Am. J. Pathol.* **2004**, *164*, 2163.
69. N. Inestrosa, R. Alarcón. *J. Physiol.-Paris* **1998**, *92*, 341.
70. A. Alvarez, C. Opazo, R. Alarcón, J. Garrido, N. Inestrosa. *J. Mol. Biol.* **1997**, *272*, 348.
71. J. L. Sussman, M. Harel, F. Frolow, C. Oefner, A. Goldman, L. Toker, I. Silman. *Science* **1991**, *253*, 872.
72. R. Fuentealba, G. Farias, J. Scheu, M. Bronfman, M. Marzolo, N. Inestrosa. *Brain Res. Rev.* **2004**, *47*, 275.
73. L. Fodero, S. Mok, D. Losic, L. Martin, M. Aguilar, C. Barrow, B. Livett, D. Small. *J. Neurochem.* **2004**, *88*, 1186.
74. D. Venkitaramani, J. Chin, W. Netzer, G. Gouras, S. Lesne, R. Malinow, P. Lombroso. *J. Neurosci.* **2007**, *27*, 11832.
75. F. De Felice, P. Velasco, M. Lambert, K. Viola, S. Fernandez, S. Ferreira, L. Klein. *J. Biol. Chem.* **2007**, *282*, 11590.
76. W. Danysz, C. G. Parsons. *Br. J. Pharmacol.* **2012**, *167*, 324.
77. R. Malinow. *Curr Opin Neurobiol.* **2012**, *22*, 559.
78. D. Verges, J. Restivo, W. Goebel, D. Holtzman, J. Cirrito. *J. Neurosci.* **2011**, *31*, 11328.
79. P. Anand, B. Singh. *Arch. Pharm. Res.* **2013**, *36*, 375.
80. J. Kemp, R. McKernan. *Nat. Neurosci.* **2002**, *5*, 1039.
81. H. Dvir, I. Silman, M. Harel, T. L. Rosenberry, J. Sussman. *Chem. Biol. Interact.* **2010**, *187*, 10.
82. W. Krall, J. Sramek, N. Cutler. *Ann. Pharmacother.* **1999**, *33*, 441.
83. L. Savini, A. Gaeta, C. Fattorusso, B. Catalanotti, G. Campiani, L. Chiasserini, C. Pellerano, E. Novellino, D. McKissic, A. Saxena. *J. Med. Chem.* **2003**, *46*, 1.
84. G. Reid, N. Chilukuri, S. Darvesh. *Neuroscience* **2013**, *234*, 53.
85. K. Davis, L. Thai, E. Gamzu, C. Davis, R. Woolson, S. Gracon, D. Drachman, L. Schneider, P. Whitehouse, T. Hoover *et al. N. Engl. J. Med.* **1992**, *327*, 1253.
86. M. Knapp, D. Knopman, P. Solomon, W. Pendlebury, C. Davis, S. Gracon. *JAMA* **1994**, *271*, 985.
87. H. Sugimoto, Y. Iimura, Y. Yamanishi, K. Yamatsu. *J. Med. Chem.* **1996**, *38*, 4821.

88. R. Polinsky. *Clin. Therap.* **1998**, *20*, 634.
89. J. Sramek, E. Frackiewicz, N. Cutler. *Exp. Opin. Invest. Drugs* **2000**, *9*, 2393.
90. P. Camps, D. Muñoz-Torrero. *Mini Rev. Med. Chem.* **2002**, *2*, 11.
91. E. Giacobini. *Pharmacol. Res.* **2004**, *50*, 433.
92. P. Connelly, N. Prentice, K. Fowler. *J. Neurol. Neurosurg. Psychiatry* **2005**, *76*, 320.
93. J. Waring, Q. Tang, W. Robieson, D. King, U. Das, J. Dubow, S. Dutta, G. Marek, L. M. Gault. *J. Alzheimers Dis.* **2015**, *47*, 137.
94. E. Giacobini. *Neurochem. Res.* **2000**, *25*, 1185.
95. S. Buckingham, A. Jones, L. Brown, D. Sattelle. *Pharmacol. Rev.* **2009**, *61*, 39.
96. D. Muñoz-Torrero. *Curr. Med. Chem.* **2008**, *15*, 2433.
97. C.H. Lee, W. Lü, J. C. Michel, A. Goehring, J. Du, X. Song, E. Gouaux. *Nature* **2014**, *511*, 191.
98. E. Karakas, H. Furukawa. *Science* **2014**, *344*, 992.
99. H. Yuan, K. Hansen, K. Vance, K. Ogden, S. Traynelis. *J. Neurosci.* **2009**, *29*, 12045.
100. S. Lipton. *Nature* **2004**, *428*, 473.
101. C. Parsons, A. Stöffler, W. Danysz. *Neuropharmacol.* **2007**, *53*, 699.
102. J. Johnson, N. Glasgow, N. Povysheva. *Curr. Opin. Pharmacol.* **2015**, *20*, 54.
103. W. Limapichat, W. Yu, E. Branigan, H. Lester, D. Dougherty. *ACS Chem. Neurosci.* **2013**, *4*, 255.
104. R. Doody, R. Raman, M. Farlow, T. Iwatsubo, B. Vellas, S. Joffe, K. Kieburtz, F. He, X. Sun, R. G. Thomas, P. S. Aisen *et al. N. Engl. J. Med.* **2013**, *369*, 341.
105. V. Coric, C. v. Dyck, S. Salloway, N. Andreasen, M. Brody, R. Richter, H. Soininen, S. Thein, T. Shiovitz, G. Pilcher, S. Colby, L. Rollin, R. Dockens, C. Pachai, E. Portelius, U. Andreasson, K. Blennow, H. Soares, C. Albright, H. Feldman, R. Berman. *Arch. Neurol.* **2012**, *69*, 1430.
106. A. Ghosh, H. Osswald. *Chem. Soc. Rev.* **2014**, *43*, 6765.
107. L. Hong, J. Tang. *Biochemistry* **2004**, *43*, 4689.
108. B. Winblad, P. Amouyel, S. Andrieu, C. Ballard, C. Brayne, H. Brodaty, A. Cedazo-Minguez, B. Dubois, D. Edvardsson, H. Feldman, L. Fratiglioni, G. B. Frisoni, S. Gauthier, J. Georges, C. Graff, K. Iqbal, F. Jessen, G. Johansson, L. Jönsson, M. Kivipelto *et al. Lancet Neurol.* **2016**, *15*, 455.
109. V. Graham, A. Bonito-Oliva, T. Sakmar. *Annu. Rev. Med.* **2017**, *68*, 413.
110. D. Selkoe. *Neuron* **2001**, *32*, 177.
111. D. Frenkel, O. Katz, B. Solomon. *PNAS* **2000**, *97*, 11455.

112. J. Legleiter, D. Czilli, B. Gitter, R. DeMattos, D. Holtzman, T. Kowalewski. *J. Mol. Biol.* **2004**, *335*, 997.

113. B. Bohrmann, K. Baumann, J. Benz, F. Gerber, W. Huber, F. Knoflach, J. Messer, K. Oroszlan, R. Rauchenberger, W.F. Richter, C. Rothe, M. Urban, M. Bardroff, M. Winter, C. Nordstedt, H. Loetscher. *J. Alzheimers Dis.* **2012**, *28*, 49.

114. J. Sevigny, P. Chiao, T. Bussière, P. H. Weinreb, L. Williams, M. Maier, R. Dunstan, S. Salloway, T. Chen, Y. Ling, J. O'Gorman, F. Qian, M. Arastu, M. Li, S. Chollate, M. Brennan, O. Quintero-Monzon, R. Scannevin, M. Arnold, T. Engber. *Nature* **2016**, *537*, 50.

115. M. v. Bergen, P. Friedhoff, J. Biernat, J. Heberle, E.-M. Mandelkow, E. Mandelkow. *PNAS* **2000**, *97*, 5129.

116. F. Clavaguera, J. Hench, I. Lavenir, G. Schweighauser, S. Frank, M. Goedert, M. Tolnay. *Acta Neuropathol.* **2014**, *127*, 299.

117. D. Sanders, S. Kaufman, S. DeVos, A. Sharma, H. Mirbaha, A. Li, S. Barker, A. Foley, J. Thorpe, L. Serpell, T. Miller, L. Grinberg, W. Seeley, M. Diamond. *Neuron* **2014**, *82*, 1271.

118. K. Hochgräfe, A. Sydow, D. Matenia, D. Cadinu, S. Könen, O. Petrova, M. Pickhardt, P. Goll, F. Morellini, E. Mandelkow, E.-M. Mandelkow. *Acta Neuropathol. Commun.* **2015**, *3*, 25.

119. T. Baddeley, J. McCaffrey, J. Storey, J. Cheung, V. Melis, D. Horsley, C. Harrington, C. Wischik. *J. Pharmacol. Exp. Ther.* **2015**, *352*, 110.

120. C. Theunis, N. Crespo-Biel, V. Gafner, M. Pihlgren, M. P. López-Deber, P. Reis, D. Hickman, O. Adolfsson, N. Chuard, D. M. Ndao, P. Borghgraef, H. Devijver, F. v. Leuven, A. Pfeifer, A. Muhs. *PLoS ONE* **2013**, *8*, e72301.

121. E. Kontsekova, N. Zilka, B. Kovacech, P. Novak, M. Novak. *Alzheimers Res. Ther.* **2014**, *6*, 44.

122. J. T. Pedersen, E. Sigurdsson. *Trends Mol. Med.* **2015**, *21*, 394.

123. M. Valko, D. Leibfritz, J. Moncola, M. Cronin, M. Mazura, J. Telser. *Int. J. Biochem. Cell. Biol.* **2007**, *39*, 44.

124. M. Dysken, P. Guarino, J. Vertrees, S. Asthana, M. Sano, M. Llorente, M. Pallaki, S. Love, G. Schellenberg, R. McCarten, J. Malphurs, S. Prieto, P. Chen, D. Loreck, S. Carney, G. Trapp, R. Bakshi, J. Mintzer, J. Heidebrink, A. Vidal-Cardona. *Alzheimers Dement.* **2014**, *10*, 36.

125. H. Javed, M. M. Khan, A. Ahmad, K. Vaibhav, M. E. Ahmad, A. Khan, M. Ashafaq, F. Islam, M. S. Siddiqui, M. M. Safhi. *Neuroscience* **2012**, *210*, 340.

126. D. Cardinali, A. Furio, L. Brusco. *Curr. Neuropharmacol.* **2010**, *8*, 218.

127. M. She, X. Deng, Z. Guo, M. Laudon, Z. Hu, D. Liao, X. Hu, Y. Luo, Q. Shen, Z. Su, W. Yin. *Pharmacol. Res.* **2009**, *59*, 248.

128. A. Cavalli, M. L. Bolognesi, A. Minarini, M. Rosini, V. Tumiatti, M. Recanatini, C. Melchiorre. *J. Med. Chem.* **2008**, *51*, 347.

129. B. Schmitt, T. Bernhardt, H.-J. Moeller, I. Heuser, L. Frölich. *CNS Drugs* **2004**, *18*, 827.

130. R. Morphy, Z. Rankovic. *J. Med. Chem.* **2005**, *48*, 6523.

131. D. Muñoz-Torrero. *Curr. Med. Chem.* **2013**, *20*, 1621.

132. E. Viayna, I. Sola, O. Di Pietro, D. Muñoz-Torrero. **2013**, *20*, 1623.

133. A. Anighoro, J. Bajorath, G. Rastelli. *J. Med. Chem.* **2014**, *57*, 7874.

134. T. Kihara, H. Sawada, T. Nakamizo, R. Kanki, H. Yamashita, A. Maelicke, S. Shimohama. *Biochem. Biophys. Res. Commun.* **2004**, *325*, 976.

135. M. Decker. *Curr. Med. Chem.* **2011**, *18*, 1464.

136. I. Sola, E. Aso, D. Frattini, I. López-González, A. Espargaró, R. Sabaté, O. Di Pietro, F. J. Luque, M. V. Clos, I. Ferrer, D. Muñoz-Torrero. *J. Med. Chem.* **2015**, *58*, 6018.

137. D. d. C. Miranda, S. M. D. Brucki. *Dement. Neuropsychol.* **2014**, *8*, 66.

138. J.-Q. Shi, B.-R. Wang, Y.-Y. Tian, J. Xu, L. Gao, S.-L. Zhao, T. Jiang, H.-G. Xie, Y.-D. Zhang. *CNS Neurosci. Ther.* **2013**, *19*, 871.

139. O. Di Pietro, E. Viayna, E. Vicente-García, M. Bartolini, R. Ramón, J. Juárez-Jiménez, M. V. Clos, B. Pérez, V. Andrisano, F. J. Luque, R. Lavilla, D. Muñoz-Torrero. *Eur. J. Med. Chem.* **2014**, *73*, 141.

140. O. Di Pietro, F. J. Pérez-Areales, J. Juárez-Jiménez, A. Espargaró, M. V. Clos, B. Pérez, R. Lavilla, R. Sabaté, F. J. Luque, D. Muñoz-Torrero. *Eur. J. Med. Chem.* **2014**, *84*, 107.

141. E. Viayna, I. Sola, M. Bartolini, A. De Simone, C. Tapia-Rojas, F. G. Serrano, R. Sabaté, J. Juárez-Jiménez, B. Pérez, F. J. Luque, V. Andrisano, M. V. Clos, N. C. Inestrosa, D. Muñoz-Torrero. *J. Med. Chem.* **2014**, *57*, 2549.

142. P. Camps, R. El Achab, M. Font-Bardia, D. Görbig, J. Morral, D. Muñoz-Torrero, X. Solans, M. Simon. *Tetrahedron* **1996**, *52*, 5867.

143. L. Vázquez-Jiménez, M. Garrido, M. Miceli, E. Prats, A. Ferrer-Montiel, M. Teixidó, C. Jimeno, A. Messeguer. *Eur. J. Med. Chem.* **2016**, *123*, 788.

144. E. Valverde, F. X. Sureda, S. Vázquez. *Bioorg. Med. Chem.* **2014**, *22*, 2678.

145. M. Barniol-Xicota, A. Escandell, E. Valverde, E. Julián, E. Torrents, S. Vázquez. *Bioorg. Med. Chem.* **2015**, *23*, 290.

146. A. Badia, J. E. Baños, P. Camps, J. Contreras, D. M. Görbig, D. Muñoz-Torrero, M. Simón, N. M. Vivas. *Bioorg. Med. Chem.* **1998**, *6*, 427.

147. P. Camps, R. El Achab, D. Görbig, J. Morral, D. Muñoz-Torrero, A. Badia, J. E. Baños, N. M. Vivas, X. Barril, M. Orozco, F. J. Luque. *J. Med. Chem.* **1999**, *42*, 3227.

148. D. Muñoz-Torrero, P. Camps. *Exp. Op. Drug Disc.* **2008**, *3*, 65.

149. S. Dugasani, M. R. Pichika, V. D. Nadarajah, M. K. Balijepalli, S. Tandra, J. N. Korlakunta. *J. Ethnopharmacol.* **2010**, *127*, 515.

150. M.-J. Bak, S. Ok, M. Jun, W.-S. Jeong. *Molecules* **2012**, *17*, 8037.

151. S. Shim, J. Kwon. *Food Chem. Toxicol.* **2012**, *50*, 1454.

152. N. Mase, N. Kitagawa, K. Takabe. *Synlett* **2010**, *1*, 93.

153. G. L. Ellman, K. D. Courtney, V. Andres Jr., R. M. Featherstone. *Biochem. Pharmacol.* **1961**, *7*, 88.

154. C. Galdeano, E. Viayna, I. Sola, X. Formosa, P. Camps, A. Badia, M. V. Clos, J. Relat, M. Ratia, M. Bartolini, F. Mancini, V. Andrisano, M. Salmona, C. Minguillón, G. C. González-Muñoz, M. I. Rodríguez-Franco, A. Bidon-Chanal, F. J. Luque, D. Muñoz-Torrero. *J. Med. Chem.* **2012**, *55*, 661.

155. P. Masson, W. Xie, M. T. Froment, V. Levitsky, P. L. Fortier, C. Albaret, O. Lockridge. *Biochim. Biophys. Acta* **1999**, 1433, 281.

156. R. L. Prior, X. Wu, K. Schaich. *J. Agric. Food Chem.* **2005**, *53*, 4290.

157. E. Viayna, R. Sabaté, D. Muñoz-Torrero. *Curr. Top. Med. Chem.* **2013**, *13*, 1820.

158. S. Pouplana, A. Espargaró, C. Galdeano, E. Viayna, I. Sola, S. Ventura, D. Muñoz-Torrero, R. Sabaté. *Curr. Med. Chem.* **2014**, *21*, 1152.

159. H.-Y. Zhang. *Biochem. Biophys. Res. Commun.* **2006**, *351*, 578.

160. L. Di, E. Kerns, K. Fan, O. McConnell, G. Carter. *Eur. J. Med. Chem.* **2003**, *38*, 223.

161. P. Camps, R. El Achab, J. Morral, D. Muñoz-Torrero, A. Badia, J. E. Baños, N. M. Vivas, X. Barril, M. Orozco, F. Javier Luque. *J. Med. Chem.* **2000**, *43*, 4657.

162. M. Hedberg, M. V. Clos, M. Ratia, D. Gonzalez, C. U. Lithner, P. Camps, D. Muñoz-Torrero, A. Badia, L. Giménez-Llort, A. Nordberg. *Neurodegener. Dis.* **2010**, *7*, 379.

163. J. Teixeira, T. Silva, P. B. Andrade, F. Borges. *Curr. Med. Chem.* **2013**, *20*, 2939.

164. A. Mattarei, M. Azzolini, M. Carraro, N. Sassi, M. Zoratti, C. Paradisi, L. Biasutto. *Mol. Pharmaceutics* **2013**, *10*, 2781.

165. S. Barnes, J. Prasain, T. D'Alessandro, A. Arabshahi, N. Botting, M. A. Lila, G. Jackson, E. M. Janleb, C. M. Weaver. *Food Funct.* **2011**, *2*, 235.

166. M. Pickhardt, Z. Gazova, M. v. Bergen, I. Khlistunova, Y. Wang, A. Hascher, E.-M. Mandelkow, J. Biernat, E. Mandelkow. *J. Biol. Chem.* **2005**, *280*, 3628.

167. B. Bulic, M. Pickhardt, B. Schmidt, E.-M. Mandelkow, H. Waldmann, E. Mandelkow. *Angew. Chem. Int. Ed.* **2009**, *48*, 1740.

168. X. Yang, G. Sun, C. Yang, B. Wang. *ChemMedChem* **2011**, *6*, 2294.

169. F. G. Serrano, C. Tapia-Rojas, F. J. Carvajal, P. Cisternas, E. Viayna, I. Sola, D. Muñoz-Torrero, N. C. Inestrosa. *Curr. Alzheimer Res.* **2016**, *13*, 1017.

170. S. Patel, L. Vuillard, A. Cleasby, C. Murray, J. Yon. *J. Mol. Biol.* **2004**, *343*, 407.

171. Z. Rankovic. *J. Med. Chem.* **2015**, *58*, 2584.

172. T. Ginman, J. Viklund, J. Malmström, J. Blid, R. Emond, R. Forsblom, A. Johansson, A. Kers, F. Lake, F. Sehgelmeble, K. J. Sterky, M. Bergh, A. Lindgren, P. Johansson, F. Jeppsson, J. Fälting, Y. Gravenfors, F. Rahm. *J. Med. Chem.* **2013**, *56*, 4181.

173. F. Rombouts, G. Tresadern, O. Delgado, C. Martínez-Lamenca, M. v. Gool, A. García-Molina, S. Alonso de Diego, D. Oehlrich, H. Prokopcova, J. M. Alonso, N. Austin, H. Borghys, S. v Brandt, M Surkyn, M De Cleyn, A. Vos, R. Alexander, G. Macdonald, D. Moechars, H. Gijsen, A. Trabanco. *J. Med. Chem.* **2015**, *58*, 8216.

174. P. Camps, B. Cusack, W. D. Mallender, R. El Achab, J. Morral, D. Muñoz-Torrero, T. L. Rosenberry. *Mol. Pharmacol.* **2000**, *57*, 409.

175. A. Lerchner, R. Machauer, C. Betschart, S. Veenstra, H. Rueeger, C. McCarthy, M. Tintelnot-Blomley, A.-L. Jaton, S. Rabe, S. Desrayaud, A. Enz, M. Staufenbiel, P. Paganetti, J.-M. Rondeau, U. Neumann. *Bioorg. Med. Chem. Lett.* **2010**, *20*, 603.

176. A. Sorkin, M. von Zastrow. *Nat. Rev. Mol. Cell Biol.* **2002**, *3*, 600.

177. X. Zhang, W. Song. *Alzheimers Res. Ther.* **2013**, *5*, 46.

178. V. Hook, T. Toneff, W. Aaron, S. Yasothornsrikul, R. Bundey, T. Reisine. *J. Neurochem.* **2002**, *81*, 237.

179. C. Ronco, G. Sorin, F. Nachon, R. Foucault, L. Jean, A. Romieu, P.-Y. Renard. *Bioorg. Med. Chem.* **2009**, *17*, 4523.

180. S.-Y. Li, N. Jiang, S.-S. Xie, K. Wang, X.-B. Wang, L.-Y. Kong. *Org. Biomol. Chem.* **2014**, *12*, 801.

181. F. J. Pérez-Areales, O. Di Pietro, A. Espargaró, A. Vallverdú-Queralt, C. Galdeano, I. M. Ragusa, E. Viayna, C. Guillou, M. V. Clos, B. Pérez, R. Sabaté, R. M. Lamuela-Raventós, F. J. Luque, D. Muñoz-Torrero. *Bioorg. Med. Chem.* **2014**, *22*, 5298.

182. Y. Wang, X. Fan, T. Tang, R. Fan, C. Zhang, Z. Huang, W. Peng, P. Gan, X. Xiong, W. Huang, X. Huang. *Sci Rep.* **2016**, *30*, 37098.

183. F. Vargas, Y. Díaz, K. Carbonell. *Pharm. Biol.* **2004**, *42*, 342.

184. R. Brigelius-Flohé, M. G. Traber. *FASEB J.* **1999**, *13*, 1145.

185. J. Irurre, J. Casas, I. Ramos, A. Messeguer. *Bioorg. Med. Chem.* **1993**, *1*, 219.

186. J. Casas, G. Gorchs, F. Sánchez-Baeza, P. Teixidor, A. Messeguer. *J. Agric. Food Chem.* **1992**, *40*, 585.

187. S. Yenes, J. Commandeur, N. Vermeulen, A. Messeguer. *Chem. Res. Toxicol.* **2004**, *17*, 904.

188. G. W. Burton, K. U. Ingold. *Acc. Chem. Res.* **1986**, *19*, 194.

189. C. Montoliu, M. Llansola, R. Sáez, S. Yenes, A. Messeguer, V. Felipo. *Biochem. Pharmacol.* **1999**, *58*, 255.

190. N. Sanvicens, V. Gómez-Vicente, A. Messeguer, T. G. Cotter. *J. Neurochem.* **2006**, *98*, 735.

191. F. Jiménez-Altayó, L. Caracuel, F. J. Pérez-Asensio, S. Martínez-Revelles, A. Messeguer, A. M. Planas, E. Vila. *J. Pharm. Exp. Ther.* **2009**, *331*, 429.

192. F. Pérez-Asensio, X. de la Rosa, F. Jiménez-Altayó, R. Gorina, E. Martínez, À. Messeguer, E. Vila, À. Chamorro, A. M. Planas. *J. Cereb. Blood Flow Metab.* **2010**, *30*, 638.

193. P. Camps, X. Formosa, C. Galdeano, T. Gómez, D. Muñoz-Torrero, L. Ramírez, E. Viayna, E. Gómez, N. Isambert, R. Lavilla, A. Badia, M. V. Clos, M. Bartolini, F. Mancini, V. Andrisano, A. Bidon-Chanal, Ó. Huertas, T. Dafni, F. J. Luque. *Chem. Biol. Interact.* **2010**, *187*, 411.

194. P. Camps, X. Formosa, C. Galdeano, D. Muñoz-Torrero, L. Ramírez, E. Gómez, N. Isambert, R. Lavilla, A. Badia, M. V. Clos, M. Bartolini, F. Mancini, V. Andrisano, M. P. Arce, M. I. Rodríguez-Franco, O. Huertas, T. Dafni, F. J. Luque. *J. Med. Chem.* **2009**, *52*, 5365.

195. P. Camps, X. Formosa, C. Galdeano, T. Gómez, D. Muñoz-Torrero, M. Scarpellini, E. Viayna, A. Badia, M. V. Clos, A. Camins, M. Pallàs, M. Bartolini, F. Mancini, V. Andrisano, J. Estelrich, M. Lizondo, A. Bidon-Chanal, F. J. Luque. *J. Med. Chem.* **2008**, *51*, 3588.

196. P. Carlier, Y. F. Han, E. Chow, C. Li, H. Wang, T. X. Lieu, H. S. Wong, Y.-P. Pang. *Bioorg. Med. Chem.* **1999**, *7*, 351.

197. I. Sola, A. Artigas, M. C. Taylor, F. J. Pérez-Areales, E. Viayna, M. V. Clos, B. Pérez, C. Wright, J. Kelly, D. Muñoz-Torrero. *Bioorg. Med. Chem.* **2016**, *24*, 5162.

198. a) V. Tumiatti, A. Minarini, M. L. Bolognesi, A. Milelli, M. Rosini, C. Melchiorre. *Curr. Med. Chem.* **2010**, *17,* 1825. b) A. Minarini, A. Milelli, E. Simoni, M. Rosini, M. L. Bolognesi, C. Marchetti, V. Tumiatti. *Curr. Top. Med. Chem.* **2013**, *13*, 1771.

199. M. Rosini, E. Simoni, A. Minarini, C. Melchiorre. *Neurochem. Res.* **2014**, *39*, 1914.

200. E. Simoni, S. Daniele, G. Bottegoni, D. Pizzirani, M. L. Trincavelli, L. Goldoni, G. Tarozzo, A. Reggiani, C. Martini, D. Piomelli, C. Melchiorre, M. Rosini, A. Cavalli. *J. Med. Chem.* **2012**, *55*, 9708.

201. V. N. Devegowda, S. H. Seo, A. N. Pae, G. Nam, K. Il Choi. *Bull. Korean Chem. Soc.* **2012**, *33*, 647.

202. R. A. Gardner, M. Belting, K. Svensson, O. Phanstiel, *J. Med. Chem.* **2007**, *50,* 308.

203. S. J. Burgess, A. Selzer, J. X. Kelly, M. J. Smilkstein, M. K. Riscoe, D. H. Peyton. *J. Med. Chem.* **2006**, *49,* 5623.

204. K. Starčević, D. Pešić, A. Toplak, G. Landek, S. Alihodžić, E. Herreros, S. Ferrer, R. Spaventi, M. Perć. *Eur. J. Med. Chem.* **2012**, *49*, 365.

205. M. de Souza, K. Pais, C. Kaiser, M. Peralta, M. Ferreira, M. Lourenço. *Bioorg. Med. Chem.* **2009**, *17*, 1474.

206. U. Larsen, M, Begtrup, L. Martiny. *J. Labelled Comp. Radiopharm.* **2005**, *48*, 429.

207. S. Seto, K. Yumoto, K. Okada, Y. Asahina, A. Iwane, M. Iwago, R. Terasawa, K. Shreder, K. Murakami, Y. Kohno. *Bioorg. Med. Chem.* **2012**, *20*, 1188.

208. T. Eckroat, K. Green, R. Reed, J. Bornstein, S. Garneau-Tsodikova. *Bioorg. Med. Chem.* **2013**, *21*, 3614.

209. E. Torres, M. D. Duque, M. López-Querol, M. Taylor, L. Naesens, C. Mae, L. Pinto, F. Sureda, J. Kelly, S. Vázquez. *Bioorg. Med. Chem.* **2012**, *20*, 942.

210. F. J. Pérez-Areales, N. Betari, A. Viayna, C. Pont, A. Espargaró, M. Bartolini, A. De Simone, J. F. Rinaldi Alvarenga, B. Pérez, R. Sabate, R. M. Lamuela-Raventós, V. Andrisano, F. J. Luque, D. Muñoz-Torrero. *Fut. Med. Chem.* **2017**, in press.

211. M.-K. Hu, C.-F. Lu. *Tetrahedron Lett.* **2000**, *41*, 1815.

CHAPTER 10

Communication of results

Image source: Canadian Association of Petroleum Producers (*www.capp.ca/publications-and-statistics*)

Journal publications

F. J. Pérez-Areales, N. Betari, A. Viayna, C. Pont, A. Espargaró, M. Bartolini, A. De Simone, J. F. Rinaldi de Alvarenga, B. Pérez, R. Sabate, R. M. Lamuela-Raventós, V. Andrisano, F. J. Luque, D. Muñoz-Torrero. Design, synthesis, and multitarget biological profiling of a second generation of anti-Alzheimer rhein–huprine hybrids. *Fut. Med. Chem.* **2017**, in press.

J. E. Prinston, J. R. Emlaw, M. F. Dextraze, C. J. G. Tessier, **F. J. Pérez-Areales**, M. S. McNulty, C. J. B. daCosta. Ancestral reconstruction approach to acetylcholine receptor structure and function. *Structure* **2017**, in press.

I. Sola, A. Artigas, M. C. Taylor, **F. J. Pérez-Areales**, E. Viayna, M. V. Clos, B. Pérez, C. W. Wright, J. M. Kelly, D. Muñoz-Torrero. Synthesis and biological evaluation of *N*-cyanoalkyl-, *N*-aminoalkyl-, and *N*-guanidinoalkyl-substituted 4-aminoquinoline derivatives as potent, selective, brain permeable antitrypanosomal agents. *Bioorg. Med. Chem.* **2016**, *24*, 5162.

F. J. Pérez-Areales, O. Di Pietro, A. Espargaró, A. Vallverdú-Queralt, C. Galdeano, I. M. Ragusa, E. Viayna, C. Guillou, M. V. Clos, B. Pérez, R. Sabaté, R. M. Lamuela-Raventós, F. J. Luque, D. Muñoz-Torrero. Shogaol–huprine hybrids: Dual antioxidant and anticholinesterase agents with beta-amyloid and tau anti-aggregating properties. *Bioorg. Med. Chem.* **2014**, *22*, 5298.

O. Di Pietro, **F. J. Pérez-Areales**, J. Juárez-Jiménez, A. Espargaró, M. V. Clos, B. Pérez, R. Lavilla, R. Sabaté, F. J. Luque, D. Muñoz-Torrero. Tetrahydrobenzo[*h*][1,6]naphthyridine–6-chlorotacrine hybrids as a new family of anti-Alzheimer agents targeting beta-amyloid, tau, and cholinesterase pathologies. *Eur. J. Med. Chem.* **2014**, *84*, 107.

Presentations in scientific meetings

Poster presentation. **F. J. Pérez-Areales**, N. Betari, A. Viayna, C. Pont, A. Espargaró, M. Bartolini, A. De Simone, J. F. Rinaldi de Alvarenga, B. Pérez, R. Sabate, R. M. Lamuela-Raventós, V. Andrisano, F. J. Luque, D. Muñoz-Torrero. "Exploring the effect of basicity in MTDL therapies against Alzheimer's disease". *IV Simposio de Jóvenes Investigadores de la Sociedad Española de Química Terapéutica*. May **2017**, Barcelona (Spain).

Poster presentation. **F. J. Pérez-Areales**, M. Garrido, M. Bartolini, A. De Simone, A. Espargaró, R. Sabaté, B. Pérez, V. Andrisano, F. J. Luque, À. Messeguer, D. Muñoz-Torrero. "A new structural family for the multitarget therapy of Alzheimer's disease". *52nd International Conference on Medicinal Chemistry (RICT)*. July **2016**, Caen (France).

Oral communication. **F. J. Pérez-Areales**, M. Garrido, M. Bartolini, A. De Simone, A. Espargaró, R. Sabaté, B. Pérez, V. Andrisano, F. J. Luque, À. Messeguer, D. Muñoz-Torrero. "Design, synthesis and biological profiling of a promising new family of multitarget directed ligands for the treatment of Alzheimer's Disease". *III Simposio de Jóvenes Investigadores de la Sociedad Española de Química Terapéutica*. June **2016**, Barcelona (Spain).

Poster presentation. **F. J. Pérez-Areales**, O. Di Pietro, A. Espargaró, A. Vallverdú-Queralt, C. Galdeano, I. M. Ragusa, E. Viayna, C. Guillou, M. V. Clos, B. Pérez, R. Sabaté, R. M. Lamuela-Raventós, F. J. Luque, D. Muñoz-Torrero. "Shogaol-huprine hybrids as a new family of anti-Alzheimer agents targeting β-amyloid, tau, cholinesterase, and oxidative stress pathologies". *Barcelona BioMed Conference Amyloid-beta and Alzheimer's disease: From fundamental principles to therapeutic strategies*. July **2014**, Barcelona (Spain).

Poster presentation. O. Di Pietro, **F. J. Pérez-Areales**, E. Viayna, E. Vicente-García, A. Espargaró, J. Juárez-Jiménez, M. V. Clos, B. Pérez, M. Bartolini, V. Andrisano, R. Sabaté, F. J. Luque, R. Lavilla, D. Muñoz-Torrero. "Tetrahydrobenzo[*h*][1,6]naphthyridine-6-chlorotacrine hybrids as a new family of anticholinesterasic agents with dual β-amyloid and tau anti-aggregating properties". *Barcelona BioMed Conference Amyloid-beta and Alzheimer's disease: From fundamental principles to therapeutic strategies*. July **2014**, Barcelona (Spain).

Poster presentation. **F. J. Pérez-Areales**, O. Di Pietro, A. Espargaró, A. Vallverdú-Queralt, C. Galdeano, I. M. Ragusa, E. Viayna, C. Guillou, M. V. Clos, B. Pérez, R. Sabaté, R. M. Lamuela-Raventós, F. J. Luque, D. Muñoz-Torrero. "Synthesis, molecular modeling, and pharmacological evaluation of huprine-based multitarget anti-Alzheimer hybrids bearing a polyphenol moiety". *I Simposio de Jóvenes Investigadores de la Sociedad Española de Química Terapéutica*. June **2014**, Madrid (Spain).

Poster presentation. O. Di Pietro, **F. J. Pérez-Areales**, E. Viayna, E. Vicente-García, A. Espargaró, J. Juárez-Jiménez, M. V. Clos, B. Pérez, M. Bartolini, V. Andrisano, R. Sabaté, F. J. Luque, R. Lavilla, D. Muñoz-Torrero. "Hit-to-lead optimization from an inactive to a picomolar inhibitor of acetylcholinesterase". *I Simposio de Jóvenes Investigadores de la Sociedad Española de Química Terapéutica*. June **2014**, Madrid (Spain).

Research stays

University of Ottawa (uOttawa), Department of Chemistry and Biomolecular Sciences. Supervisor: Dr. Corrie J. B. daCosta. Research topic: Molecular biology and electrophysiology studies of nicotinic acetylcholine receptors. 01/10/2016 - 31/03/2017. This research stay was possible thanks to a *NOVADOMUS – CHEMEDPHO scholarship* (*Erasmus Mundus – Action 2 Programme*).